NASA SP-302

28

SECOND CONFERENCE ON

PORTABLE LIFE SUPPORT SYSTEMS

Held at
AMES RESEARCH CENTER
Moffett Field, California
May 11-13, 1971

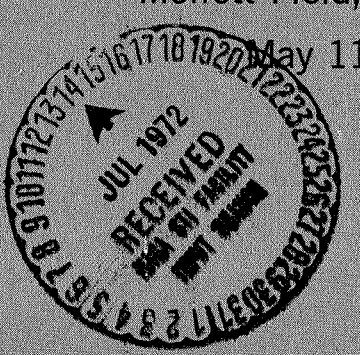

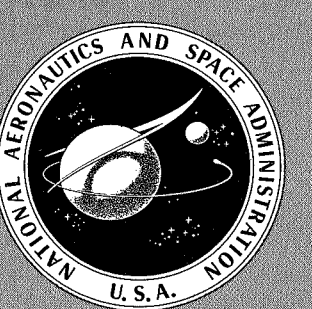

NATIONAL AERONAUTICS AND SPACE ADMINISTRATION

NASA SP-302

SECOND CONFERENCE ON

PORTABLE LIFE SUPPORT SYSTEMS

The proceedings of a conference sponsored by NASA and the U.S. Bureau of Mines and held at NASA Ames Research Center, Moffett Field, California, May 11–13, 1971

Prepared at Ames Research Center

Scientific and Technical Information Office 1972
NATIONAL AERONAUTICS AND SPACE ADMINISTRATION
Washington, D.C.

For sale by the National Technical Information Service, Springfield, Virginia 22151 — Price $[redacted]
$6.00

PREFACE

The second conference on Portable Life Support Systems was held at Ames Research Center on May 11-13, 1971 under the sponsorship of NASA and the U.S. Bureau of Mines. The conference gave people interested in these systems a second opportunity to meet and exchange information on current research and development efforts. Prior to the first conference, held two years earlier at Ames Research Center, the exchange of information on these life support systems had been limited to papers scattered throughout many journals and conferences, with no attempt to integrate them into a meaningful dialogue.

The first conference was followed by numerous requests for another meeting. The intent of the resulting second conference was similar to that of the first and participation was as widespread, with representation from the Army, Navy, Air Force, industry, Bureau of Mines, NASA, and the academic community. If the second conference proves as successful as the first in creating new exchanges of information and providing a common place for old ones, then our efforts will again have been worthwhile.

Alan Chambers
Conference Chairman

N72-21

PRECEDING PAGE BLANK NOT FILMED

CONTENTS

1 PORTABLE BREATHING APPARATUS FOR COAL MINES

Robert W. Van Dolah
Bureau of Mines
Pittsburgh, Pennsylvania

Although recent emphasis has been on breathing apparatus for space and deep underwater applications, the earliest interest in breathing apparatus was prompted by the need to protect miners engaged in mine rescue operations and underground firefighting. The first self-contained oxygen breathing apparatus for use in mines appears to have been developed in 1853 by Prof. Schwann (ref. 1); however, a really satisfactory oxygen breathing apparatus was not developed until 1906, by Draeger of Germany. By 1908, the Draeger apparatus had been introduced in U.S. coal mines, and the Technological Branch of the U.S. Geological Survey had purchased several. The Bureau of Mines inherited these upon its creation in 1910, and by 1911 it had acquired 150 self-contained oxygen breathing apparatus, including a second German model, the Westphalia, and the "Pronto" produced in England by Fluess. In 1912, the Bureau-sponsored Second National Mine Rescue and First Aid Conference (ref. 2) reported that instruction and training in the use of breathing apparatus had penetrated to every coal field and to several metal mining areas in the United States. At this conference also, it was resolved that "breathing apparatus used for mine rescue and mine recovery work should be of such types as passed the test of the Bureau of Mines" and that "the keeping of birds and mice at rescue stations for the purpose of detecting carbon monoxide is desirable." This last resolution was prompted by consideration for those older miners who preferred to wait until a bird or mouse toppled over before encumbering themselves with breathing apparatus.

Prior to World War I, only foreign-made oxygen breathing apparatus were used in this country, but by 1915, the Bureau was engaged in developing an apparatus that would be free of the "well-defined limitations" (ref. 3) of the imported models. Specifically, the new design was to meet the oxygen requirements of a man exerting himself to full physical capacity, to be lighter, to furnish more air, and to leave hands and arms free. This effort resulted in the Gibbs apparatus in 1916, the Paul apparatus in 1920, and the McCaa in 1926 (ref. 4). A somewhat improved version of the McCaa apparatus is still widely used in U.S. coal mines. These and similar self-contained oxygen breathing apparatus subsequently developed in this country and in Europe are based on the use of compressed oxygen.

From time to time, various other types of oxygen breathing apparatus have been developed. In the early 1940s a self-contained breathing apparatus supplied with chemically generated oxygen and giving 45-min protection (Chemox, ref. 4) was developed by the Navy. Used for firefighting in World War II, it was subsequently made available to industry and introduced into coal mines as auxiliary rescue equipment. A 2-hr liquid oxygen apparatus (ref. 5) and a 2-hr liquid air apparatus are also available (ref. 6). Nevertheless, most of the self-contained oxygen breathing apparatus used today in U.S. coal mines are but updated versions of a 45-year-old compressed oxygen design. Although heavy, bulky, and expensive, they have proved to be reasonably adequate for team rescue work.

In environments with sufficient (16 percent or more) oxygen, the universal gas mask (refs. 1,4,7) developed by the Bureau of Mines soon after World War I, has been widely used in mines, especially for recovery work. Although designed primarily to protect against carbon monoxide, universal gas masks, also known as Type N masks, afford protection against other toxic and noxious gases and vapors in concentrations up to 2 and 3 percent, and against smoke. They were approved for use in coal mines in 1925. Although gas masks are less cumbersome than the oxygen breathing apparatus, their dependence on an adequate oxygen concentration and their limited capacity for any one contaminant reduce their usefulness. The Federal Coal Mine Health and Safety Act of 1969 established a minimum oxygen concentration of 19.5 percent, further limiting the conditions for acceptable use of the universal gas masks. The National Fire Protection Association Subcommittee on Protective Equipment recently adopted a strong recommendation against the use of Type N gas masks by firefighters.

Another type of portable breathing apparatus, the one with which we are most immediately concerned, is the apparatus used under emergency conditions by miners escaping from a toxic environment. These are the carbon monoxide self-rescue respirators, more generally known as self-rescuers, which were first approved by the Bureau of Mines in 1924 (refs. 2,8). The self-rescuers are compact enough to be worn on the miner's belt; they are designed exclusively for protection against carbon monoxide, and like the universal gas mask are not intended for use in air containing less than 16 percent oxygen. Their operation is based on the catalytic conversion of carbon monoxide to carbon dioxide by hopcalite, which was first developed in the early 1920s at the University of California and Johns Hopkins University under a Bureau of Mines grant. A model providing at least 1 hr of protection is available. The use of self-rescuers is limited to reasonably low carbon monoxide concentrations because the heat generated by catalytic conversion to carbon dioxide increases with the carbon monoxide content of the intake air. With high concentrations, the inhaled air may become intolerably hot and dry, and since the mouthpiece is simply clamped between the wearer's lips and teeth, the urge to open the mouth for a breath of relatively cool but lethal air can be a very real hazard.

Certain other design features also limit the effectiveness of the self-rescuer. Moisture and organic vapors impair the activity of the catalyst, and the wearer has no way of determining whether it is functioning properly. Protection for face and eyes against dust and smoke is also lacking. All forms of voice communication by the wearer are precluded.

In a recent survey of disasters in U.S. coal mines from 1950 to 1969, a National Academy of Engineering committee (ref. 5) estimated that at least 20 percent of those who died could have been saved if adequate postdisaster survival systems had been available. Of 451 fatalities in 28 major mine disasters (disasters resulting in five or more deaths), 83 were attributed to asphyxiation by smoke or carbon monoxide or both, and five to suffocation by carbon dioxide. In the same period 115 men died in so-called "minor disasters" (involving fewer than five deaths); 35 of these deaths were attributed to carbon monoxide and smoke, and three to carbon dioxide.

These findings demonstrate what has been known for many years—that the hazards of a mine disaster are not limited to its violent phase. They underline the importance of postdisaster procedures. As early as 1928, S. H. Katz and J. J. Forbes (ref. 8) wrote: "More miners have probably been killed by carbon monoxide than by fires or the violence of explosions . . . it seems that the half-hour of protection given by a self-rescuer would in most instances have assured their escape."

The Federal Coal Mine Health and Safety Act of 1969 requires that mine operators provide every miner with a self-rescue device offering 1 hr or more of protection; at present, only the

hopcalite self-rescuers are available. The Act also established a greatly expanded program of research and development in all phases of coal mine health and safety. Clearly, improved breathing apparatus should be a part of this program.

The National Academy of Engineering report (ref. 5) proposed a complete system for postdisaster mine survival and rescue. One element of the survival subsystem was to be a portable breathing apparatus (PBA), light enough and small enough to be carried by the miners, to replace the present self-rescuers. The Bureau of Mines funded a contract with Westinghouse Electric Corporation for the entire system, and required, as part of the survival subsystem, a 1-hr PBA. Frank Martin describes the development of the PBA in paper 6. However, problems still remain. The PBA developed under the hurried contractual effort required by the Bureau is so bulky and so heavy that it is unrealistic to expect the miner to wear or carry it constantly.

The requirements for PBAs in coal mines have much in common with those for other hostile environments, such as space or underwater. In all cases oxygen must be supplied and carbon dioxide removed at rates appropriate to the metabolic load. However, there are important differences. For a lunar backpack, bulk is a nuisance in egressing the lunar module, but in the lunar environment the bulk and the weight of the backpack become less significant. Underwater, bulk can again cause inconvenience but weight is relatively unimportant. In a coal mine, bulk and weight assume commanding importance, probably in that order, but there are other special requirements that must be imposed on any PBA designed for self-rescue. The apparatus must be capable of easy and rapid donning because a toxic atmosphere may descend on the miner with little warning. Eye protection against smoke and dust is very desirable, and because visibility may be reduced, voice communication should be possible without exposing the wearer to a toxic atmosphere. Further, in the United States, some 50 percent of coal is mined from seams 4 ft thick or less. Except in a few locations, the height of the work space is the height of the coal seam, sometimes less. Under this low roof, the miner must carry out arduous work, operate machinery, or drive a shuttle car, while already encumbered by a caplamp battery and at times by a respirable dust sampling pump and battery. Some miners also carry other instruments or equipment.

As Dr. Alan Chambers has pointed out (ref. 9), the probability of success for a surface-stationed rescue device is just the probability of its proper functioning. On the other hand, the probability of success for a self-rescue device is the product of probability of its proper functioning and the probability of its timely use by the miner. The probability of timely use will approach unity only if the device is worn by all miners constantly; this means providing the miner with a small and lightweight PBA that he will accept as one more thing to wear on his belt.

Existing technology does not seem capable of producing such a PBA that will function for 1 hr at a high metabolic rate. According to the 1969 Act, a 1-hr self-rescue device "shall be made available to each miner ..."; wearing is not required. As a result, the Bureau has recently published its search for R&D sources for a 10-min device that is believed feasible within reasonable constraints of bulk and weight. Ten minutes should provide ample time for miners to reach a fresh air base or a cache of longer duration PBAs, or to escape from a small mine or even a large one if they are near a portal or shaft. The cache of longer life PBAs in each section could be moved as the mine workings advance or retreat. Even in a large section, miners should not be more than a few hundred feet from a conveniently located cache.

The longer duration PBA could provide 1 hr of protection, which should allow escape from most mines under most circumstances. However, a 2-hr device might be necessary if the distance to an exit is great, if injured miners are to be assisted, or if progress is impeded by detours

necessitated by fires, roof falls, and the like. With a certain percentage of the weight and cost fixed, perhaps a 2-hr PBA might not be an unrealistic goal.

A study of the time required to rescue survivors or locate fatalities from carbon monoxide asphyxiation revealed an interesting breakpoint. Of 87 that were rescued, 82 were rescued in 6 hrs or less after the fire or explosion, and the bodies of about 20 percent of those who succumbed from asphyxiation were recovered within the same elapsed time. The other miners were rescued or recovered one to many days later. Although they represent a rather small sample, these data suggest the desirability of a 6-to 8-hr PBA (with a corresponding loss in portability).

Bureau personnel with experience in mine rescue and recovery, or in reopening operations, believe that rescue apparatus of longer duration than the most common 2-hr apparatus would be extremely valuable. Along with increased duration, a reduction in bulk and weight made possible by improved technology would be welcome.

For the necessary improvements in rescue and self-rescue portable breathing apparatus, the Bureau of Mines seeks to take advantage of the expertise of the members of this conference and their colleagues to advance life support technology and provide greater protection to miners in underground "space."

REFERENCES

1. Forbes, J. J.; and Grove, G. W.: Protection Against Mine Gases. Bur. Mines Miners' Circ. 35, 1937.
2. Wilson, H. E.: National Mine-Rescue and First-Aid Conference. Bur. Mines Bull. 62, 1913.
3. Paul, J. W.; and Wolflin, H. M.: Rescue and Recovery Operations in Mines after Fires and Explosions. Bur. Mines Handbook, Washington, D.C., 1916.
4. Morrow, A. E.; Demkowiscz, W. M.; and Chastain, G. W.: Mine Rescue and Auxiliary Equipment. A Handbook for Miners. Washington, D.C., 1961.
5. National Academy of Engineering, Committee on Mine Rescue and Survival Techniques: Mine Rescue and Survival. Final Report, March 1970.
6. Schutz, R. H.; and Kloos, E. J.: Respiratory Protective Devices Approved by the Bureau of Mines as of Dec. 31, 1968. Bur. Mines Info. Circ. 8436, 1969, p. 4.
7. Katz, S. H.; and McCaa, G. S.: Use of Type N, Miners' Gas Mask. Bur. Mines Miners' Circ. 32, 1929.
8. Katz, S. H.; and Forbes, J. J.: Use of the Miners' Self-Rescuer. Bur. Mines Miners' Circ. 30, 1928.
9. Chambers, A.: Oral communication. Safety Research Center Seminar, Bruceton, Pa., Feb. 10, 1971.

2 DESIGN CONSIDERATIONS FOR DIVERS' BREATHING GAS SYSTEMS

O. R. Hansen
Office of the U.S. Navy Supervisor of Diving
Naval Ships Systems Command

INTRODUCTION

The advent of deep dive systems and saturation diving has necessitated the careful planning and design of breathing gas systems. For saturation diving, the divers' enclosures must be pressurized to, and sustained at, a pressure equivalent to the depth at which the mission operations are to be performed. Thus, the flow rate itself is not a significant design parameter. The initial pressurization is normally conducted at a relatively low rate, and the mission duration can be up to 10 days.

Breathing gas, normally a helium-oxygen mixture, must be available to effect the required pressurization. There also must be sufficient gas to supply the breathing apparatus used by the deployed divers, as well as a reserve supply for treating decompression sickness.

This paper discusses some of the design methods used to establish the gas storage, mixing, and transfer requirements for existing deep dive systems.

DEEP DIVE SYSTEMS

Table 2.1 *Design parameters for gas requirements in Mark I and II deep dive systems.*

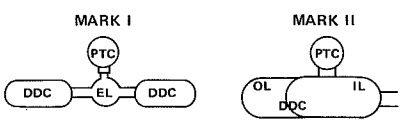

ENCLOSURE	VOLUME – FT^3	VOLUME – FT^3
Deck Decompression Chamber (DDC)	321.0 (1 chbr)	765.0
Personnel Transfer Capsule (PTC)	144.0	227.0
Entrance Lock (EL)	103.79	235.0
Supply Lock (SL)	1.61	3.0
MARK I		
EL to DDC Trunk	3.00	—
EL to PTC Trunk	9.28	—
PTC Trunk	8.15	—
MARK II		
DDC Transfer Trunk		16.0
PTC Transfer Trunk		13.0
PTC FLASKS		
Helium	20.0	30.0
Oxygen	6.0	6.0
Mixed Gas	10.0	24.0
Scrubber – DDC	2.90	3.00
OTHER PARAMETERS	**MARK I**	**MARK II**
Design Depth of Diving Mission	850 feet	1000 feet
Diving Man-Hours	4*	8**

*The Mark I PTC is normally used with a three-man crew: a capsule operator (tender), a diver and a standby diver. One descent of PTC for a diving mission normally includes 4 hours of bottom time, 4 hours handling time and 2 hours for recharging PTC flasks. Two alternating crews are employed on a saturation mission with one crew being maintained at pressure in the DDC.

**The Mark II PTC can accommodate a four-man crew: a capsule operator (tender), a standby diver and 2 working divers. The 2 working divers provide an eight man-hour diving capability for one deployment of the PTC.

The U.S. Navy has two major deep dive systems (DDS), the Mark I and Mark II. These systems differ in the number of divers they will support, in enclosure volume, and in system arrangement. These differences reflect intended system application and installation: The Mark I was designed primarily to support the large object salvage system (LOSS), and the Mark II was designed to support submarine rescue operations. Table 2.1 provides the design parameters for establishing the gas requirements of these two systems.

The gas required to support missions of maximum duration must be stored aboard the diving platform or mother ship and must be available in a readily transferable state to permit performance of any mission within the design capability of the system.

The usual gas supply is a mixture of helium and oxygen, with a small quantity of nitrogen present in the system atmosphere prior to pressurization. The enclosure environment is maintained at ∿0.3 atm oxygen partial pressure throughout the mission, and the oxygen required to replace that consumed by the divers in the enclosures is only about 1 SCF[1] hr. Thus, analysis of helium requirements receives the most attention.

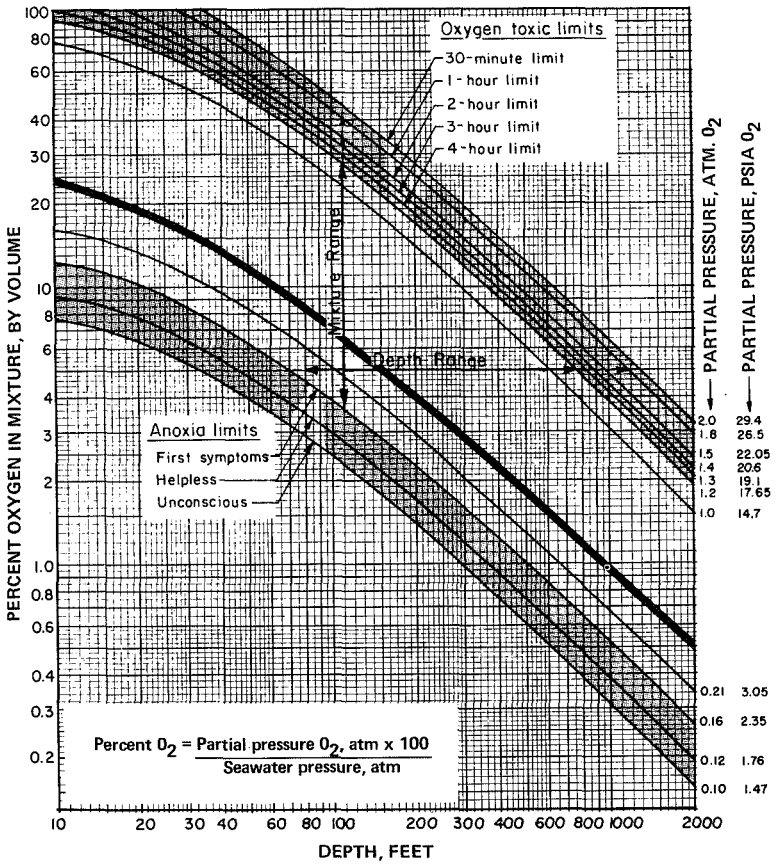

Figure 2.1 *Percentage of* O_2 *in breathing mixture as a function of depth and* O_2 *partial pressure.*

Systems that use a semiclosed diver breathing apparatus are an exception, however, and demand a more extensive analysis of oxygen requirements. Figure 2.1 relates the percentage of oxygen in the breathing mixture to depth, and to oxygen partial pressure in both psia and atm. The curves show a large area within which mixtures are physiologically acceptable. The oxygen concentration must be maintained within the concentration range shown in this figure. In the semiclosed apparatus, mixtures must provide an adequate liter flow through the system to supply metabolic oxygen for the diver as well as maintain an oxygen concentration within tolerable limits. This system was adequately described in the initial life support systems conference but the definition of gas mixture oxygen concentration and liter flow (fig. 2.2) was developed later. It is again evident, however, that for deep diving, the availability of helium is of paramount importance. To avoid toxicity, the oxygen percentage must decrease as depth increases so that the quantity of helium supplied with the oxygen will increase with depth.

The Mark 10 closed-circuit breathing apparatus (see paper 8), appears to be an optimum system in which essentially only the oxygen to support the diver's metabolic requirements must be provided. This will simplify the establishment of gas storage system requirements.

GAS STORAGE SYSTEMS

High Pressure Storage Systems

Utilizing design principals applied in nuclear submarines, the original diving gas storage systems were designed as high pressure stored gas systems. Recognizing that the submarine environment is at one atmosphere and that the diving system is at the diving depth pressure the significance of storage pressure and volume are not readily apparent. Pressure and volume effects both space and weight of the system and a method to relate these parameters is presented in this section.

[1]SCF = standard cubic ft; helium at 70° F and 14.7 psia.

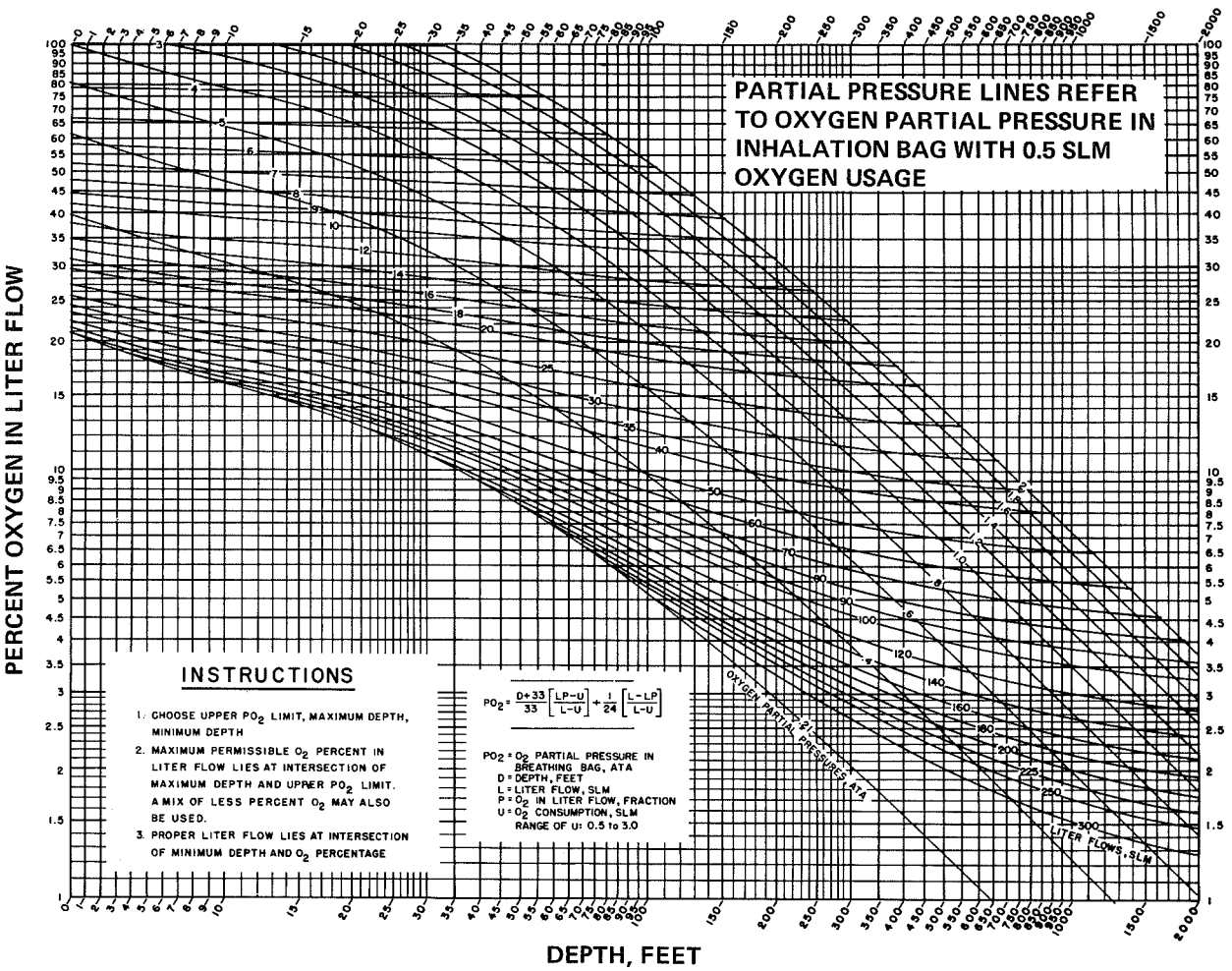

Figure 2.2 *Liter flow and* O_2 *percentage for semiclosed circuit breathing apparatus.*

An adequate supply of gas must provide for the maximum mission as well as gas reserves needed in emergency. Unless provision is made for gas transfer, the storage volume will contain gas at equilibrium pressure with the depth of the diving mission. A second consideration is that helium, oxygen, and mixtures thereof deviate significantly from ideal gas, thus precluding application of simple gas laws. Figure 2.3 indicates that less than 90 percent of the helium predicted by ideal gas laws will be stored in a 3000 psi volume where real gas properties exist. This deviation has prompted the application of various techniques to account for real gas characteristics in the design of gas storage systems.

The importance of this deviation in maintaining the permissible mixtures was the subject of considerable study leading to the publication of a U.S. Navy Diving-Gas Manual (ref. 1), which has been invaluable in the design of breathing gas systems.

The use of a single virial coefficient (ref. 2) for determining helium storage requirements has been expedient in developing computer analyses of the many systems being designed. The helium properties established by means of this coefficient, have been compared to those in the manual, which were obtained with the use of additional virial coefficients. Properties obtained with the

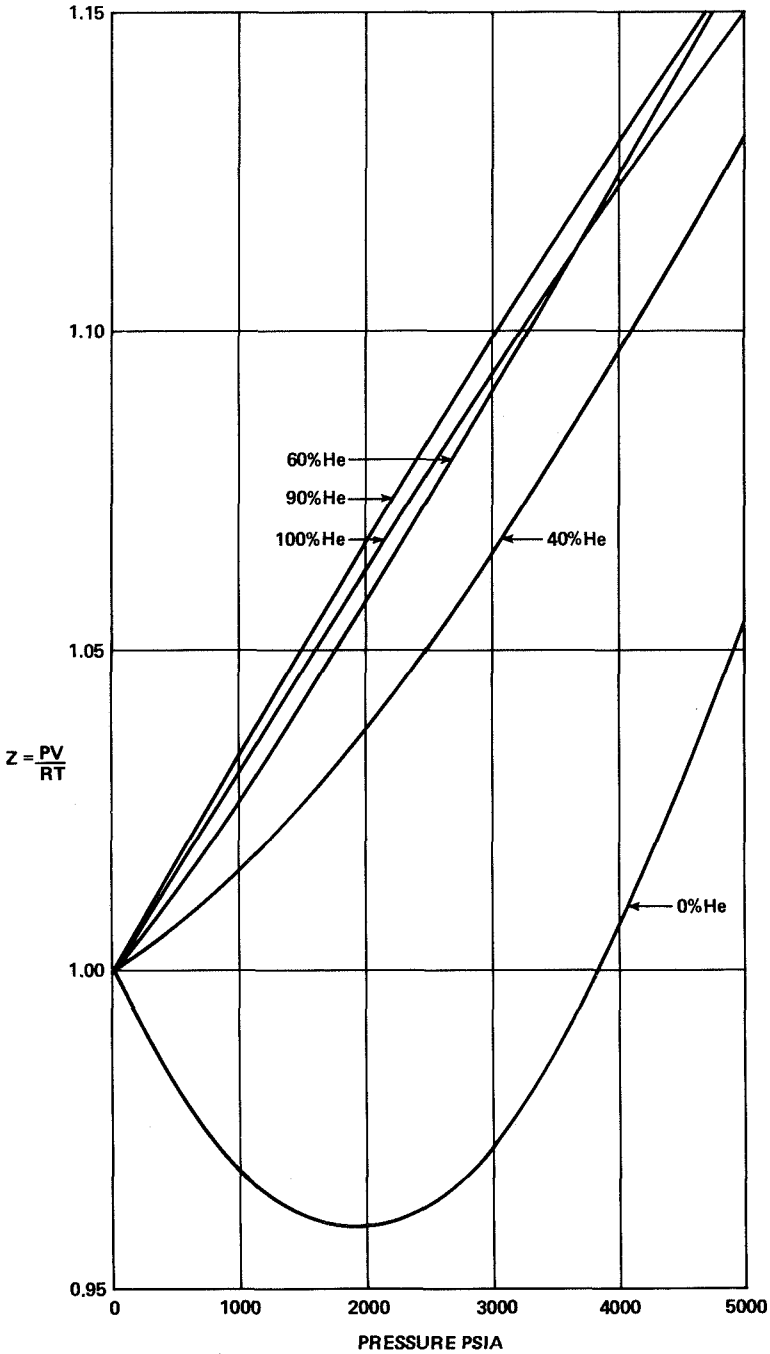

Figure 2.3 *Deviation of* HeO_2 *mixtures from ideal gas laws.*

single coefficient show a maximum variation of 0.12 percent from those in the manual. The computer program used for this analysis and the resulting output data are given in appendix A.

The application of this single coefficient established the compressibility factor that can be introduced into the ideal gas equation

$$PV = WRT$$

The compressibility factor is related to the pressure times B for any isotherm as follows. The real gas compressibility factor is

$$Z = \frac{PV}{RT}$$

where

$$Z = (1 + BP)$$

and

$$B = \textit{virial coefficient}$$

The density is then

$$\lambda = \frac{P}{(1 + BP)RT}$$

and the pressure will be

$$P = \frac{\lambda TR}{1 - B\lambda RT}$$

which, applied in analyses, provides helium properties approaching real properties.

Once the gas property data have been determined for various state points existing within the diving system, effort can be directed toward establishing the system requirements.

Mark II DDS specifications dictate that 306,000 SCF of helium be available from the storage system at pressures above 200 psig. This gas supply is intended to support the two systems installed in the submarine rescue ships, ASR 21 and ASR 22. These are catamaran type ships, and half of the gas would be available to support a 10-day saturation mission in a single Mark II DDS installed in one hull.

Numerous studies were conducted to find the best method of storing this gas. Desired storage pressure, individual flask capacity, and storage bank arrangements were analyzed to arrive at the storage system as currently defined. In general, stored gas is contained in seamless steel pressure vessels designed according to Department of Transportation regulations.

The criteria for flasks used by the U.S. Navy are contained in a military specification (ref. 3); the pressure vessels are restricted to 3000 and 5000 psi working pressures and geometry defined by type. Investigation indicated alternative configurations and rated pressures could be obtained, and a limited optimization was performed within the capability.

To optimize the design of the cylinders it is necessary to define the stresses due to internal pressure in closed cylinders. Thus, an analysis for this study to obtain the stress in the cylinder wall was based on the fact that for a cylinder with other than very thin walls under internal pressure, the stress varies from a maximum at the inner surface to a minimum at the outer surface. The analysis also took into account the axial deformations, which affect the load capability of the material.

The following equations, known as Clavarino's equations, will provide the wall thickness to attain 67 percent of the material's ultimate strength at a test pressure equal to 5/3 the design pressure. The design pressure is equal to the pressure of the gas stored in the flask at standard conditions.

$$S_t' = (1 - 2m)\, a + \frac{(1 + m)\, b}{r^2}$$

$$S_r' = (1 - 2m)\, a - \frac{(1 + m) b}{r^2}$$

where

s_t' tangential stress, psi
s_r' radial stress, psi
m Poisson's ratio of lateral contraction
r radius at any point in the wall, in.
a,b constraints for any given values of pressures and diameters such that

$$a = \frac{P_i d_i^2 - P_O d_O^2}{d_O^2 - d_i^2}$$

$$b = \frac{d_i^2 d_O^2}{4} \left(\frac{P_i - P_O}{d_O^2 - d_i^2} \right)$$

where

d_i inside diam, in.
d_O outside diam, in.
P_i internal pressure, psi
P_O external pressure, psi

When a and b are evaluated, and when $d_i/2$ is substituted for r the equation of the thickness is

$$t = \frac{d_i}{2}\left[\sqrt{\frac{s_t' + (1 - 2m)\ P_i}{s_t' - (1 + m)\ P_i}} - 1\right]$$

where

s_t' = permissible working (tangential) stress in tension, psi

If, the end closure is assumed equivalent in thickness to the cylindrical walls and the normal corrosion allowance of 0.065 in. is added to wall thickness, the weight can be determined from the external volume less the internal volume times the density of the material used in fabrication. In the analyses, the outer diameter was maintained constant at 18, 20, 22, and 24 in. The cylinder configuration is shown in figure 2.4.

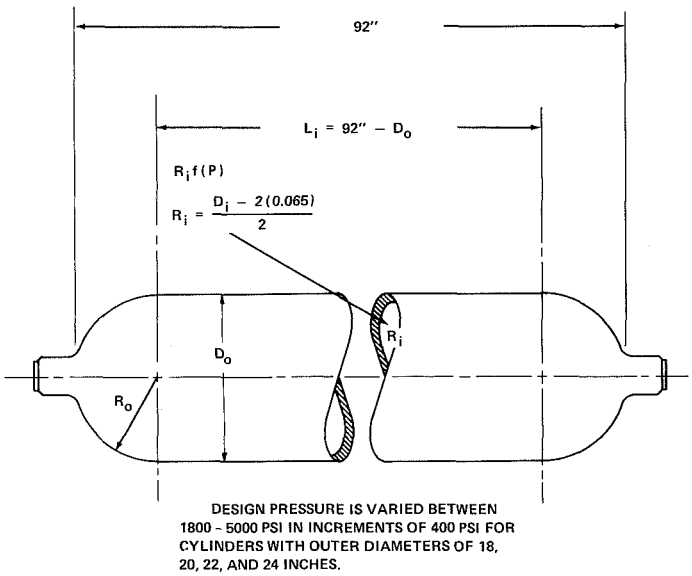

Figure 2.4 *Gas storage flask configuration used for* He *capacity and weight.*

The results of the analyses provide the wall thickness, internal volume, and weight for cylinders for each of the four diameters and the various design pressures.

These results are incorporated in the computer program for determining the total gas available above an equilibrium pressure equivalent to a given operating depth, established as 1000 ft. A ratio of available helium (in SCF) to each pound of metal in the storage system was obtained, which relates the gas storage pressure, diameter of the storage vessel, and gas contained at equilibrium pressure for each of the four outer diameters.

From the real gas properties for helium, one normally would expect less helium per pound of metal to be stored at higher pressures because of the increasing compressibility factor. This is correct, but the influence of reduced flask volume and diameter relative to the residual gas quantity is not immediately evident, although it becomes more apparent when the ratio is plotted versus storage pressure. The results are shown in figure 2.5, and the analytical data are given in appendix B.

The results indicate that the 24-in. diameter flask, with a design pressure ranging from 3400 to 3800 psi, is of optimum weight for helium storage in the system.

In general, this technique was applied in the selection of the gas flasks for the Mark II deep dive system aboard the ASR 21/22. Other factors in gas flask selection were the maximum available tooling capacity at the steel mill, which limited the outside diameter to 24 in. and the design pressure to 3800 psi, and the deck height, which restricted flask length to 8 ft (table 2.2).

Oxygen flasks were restricted to 3000 psi design pressures; the helium flasks had design pressures of 3800 psi. The helium available if filled to an equilibrium temperature of 100° F is 164,150 SCF; the quantity available above the minimum specified pressure is 153,860 SCF.

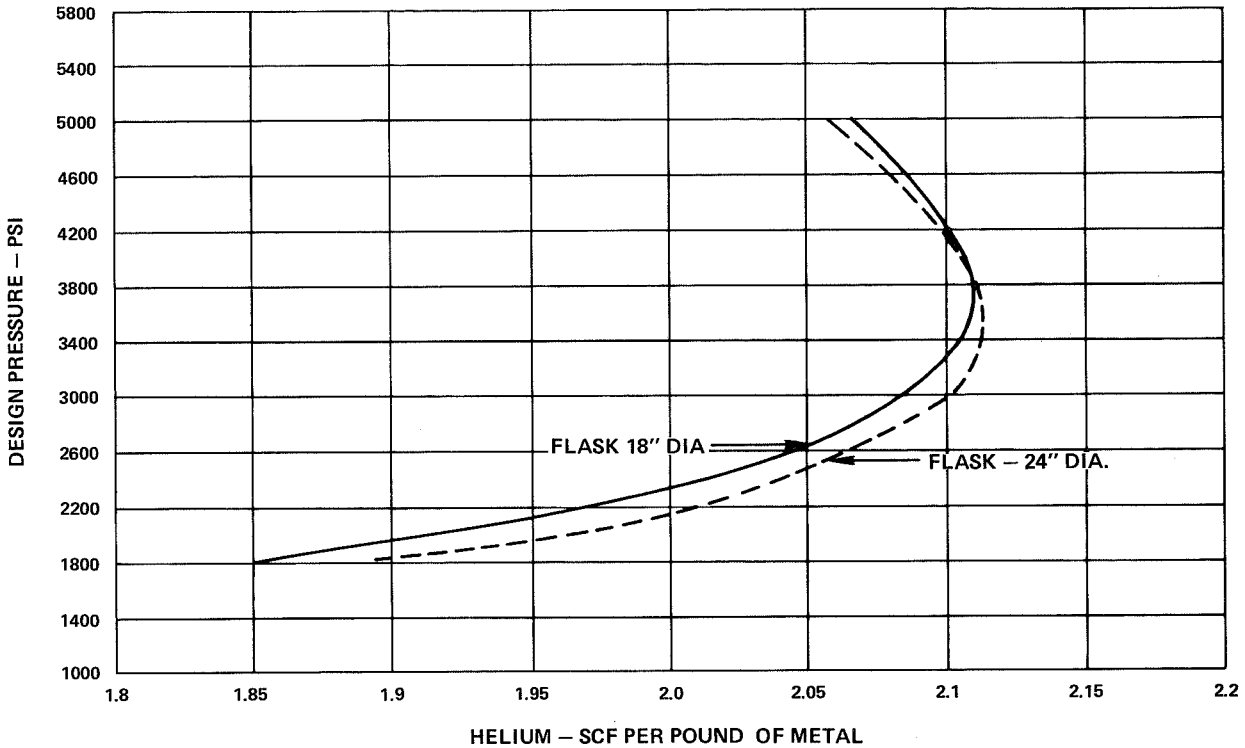

Figure 2.5 *Available* He/*lb of metal versus design pressure for flasks of 18- and 24-in. outer diam.*

Table 2.2 *System data for Mark II deep dive system aboard ASR 21/22.*

COMPRESSORS

USE	CAPACITY	QUANTITY	DISCH. PRESSURE	TYPE
Helium	0.45 CFM	2 per ship - 1 per hull	3800 PSIG max.	Diaphragm
Oxygen	Min. Displacement	2 per ship - 1 per hull	3800 PSIG max.	Booster

FLASKS

USE	VOLUME	QUANTITY	SIZE
Helium	16.88 cu. ft.	84 per ship - 42 per hull	8'0" Lg. x 24" O.D.
Oxygen	16.81 cu. ft.	24 per ship - 12 per hull	7'0" Lg. x 24" O.D.
Mixed Gases	16.88 cu. ft.	12 per ship - 6 per hull	8'0" Lg. x 24" O.D.
High Pressure Air	10.0 cu. ft.	20 per ship - 10 per hull	7'10" Lg. x 18" O.D.

Figure 2.6 illustrates the use of helium over a 10-day period in a saturation diving mission, relating the gas available for required events to that stored in the system. The analytical data resulting from these analyses are presented in appendix C. The results indicate that the helium stored is not quite sufficient to maintain the required reserve, and that flask filling and topping must be accomplished during replenishment.

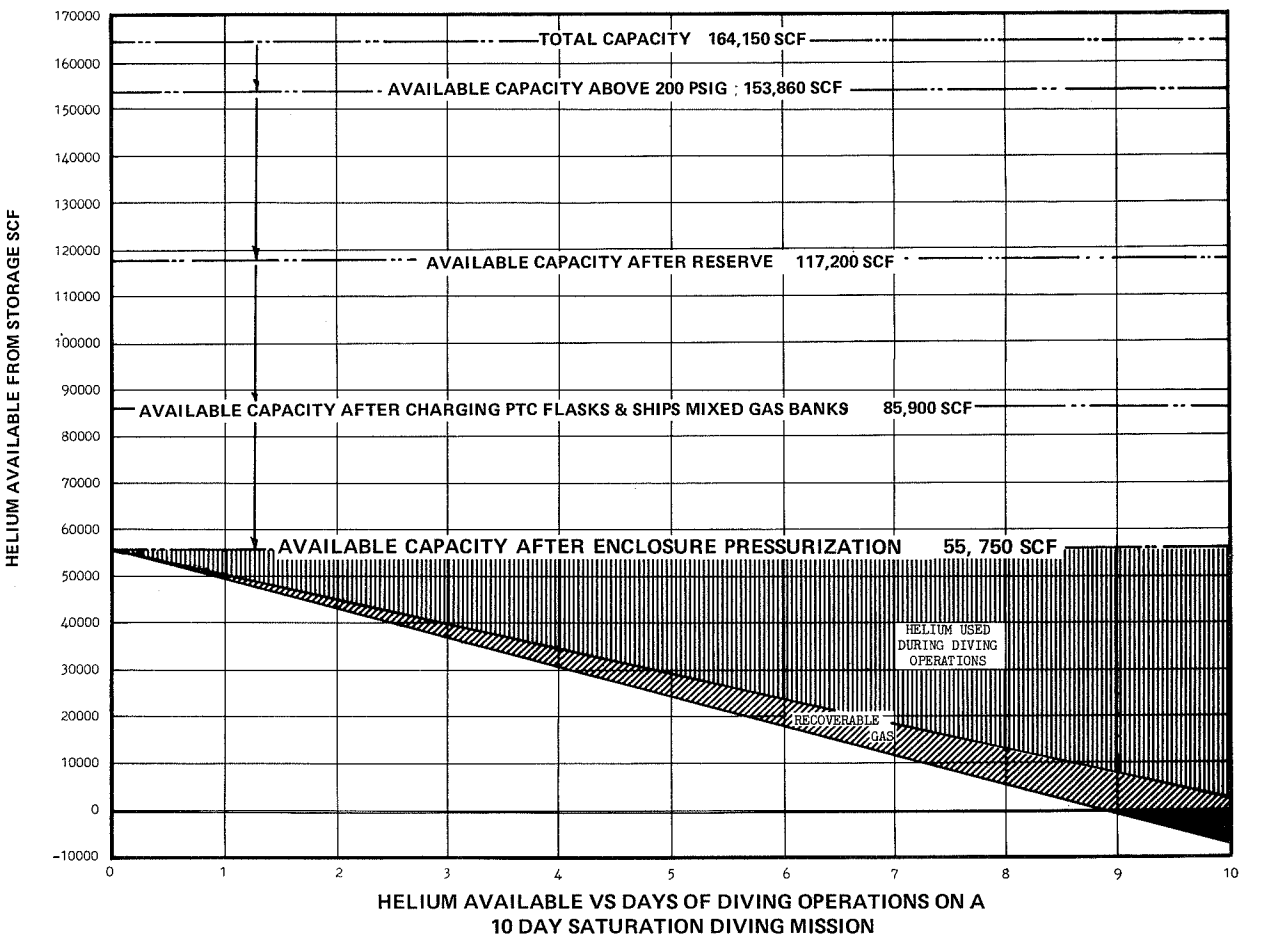

Figure 2.6 *Helium available versus days of diving operation on a 10-day saturation diving mission.*

Figure 2.7 shows the general arrangement of the Mark II system aboard an ASR 21/22 type platform.

Supercritical Storage Systems

One means of reducing gas storage system weight and volume is to convert the gas to liquid by cryogenic processes. It has been found that the low latent heat of vaporization and the high ΔT between the operational environment and liquid helium ($\sim\Delta T = 532^\circ R$) preclude the long term storage of supercritical helium; however, its properties are such that lighter weight and lesser volume transport systems can be designed, particularly since the development of super insulations.

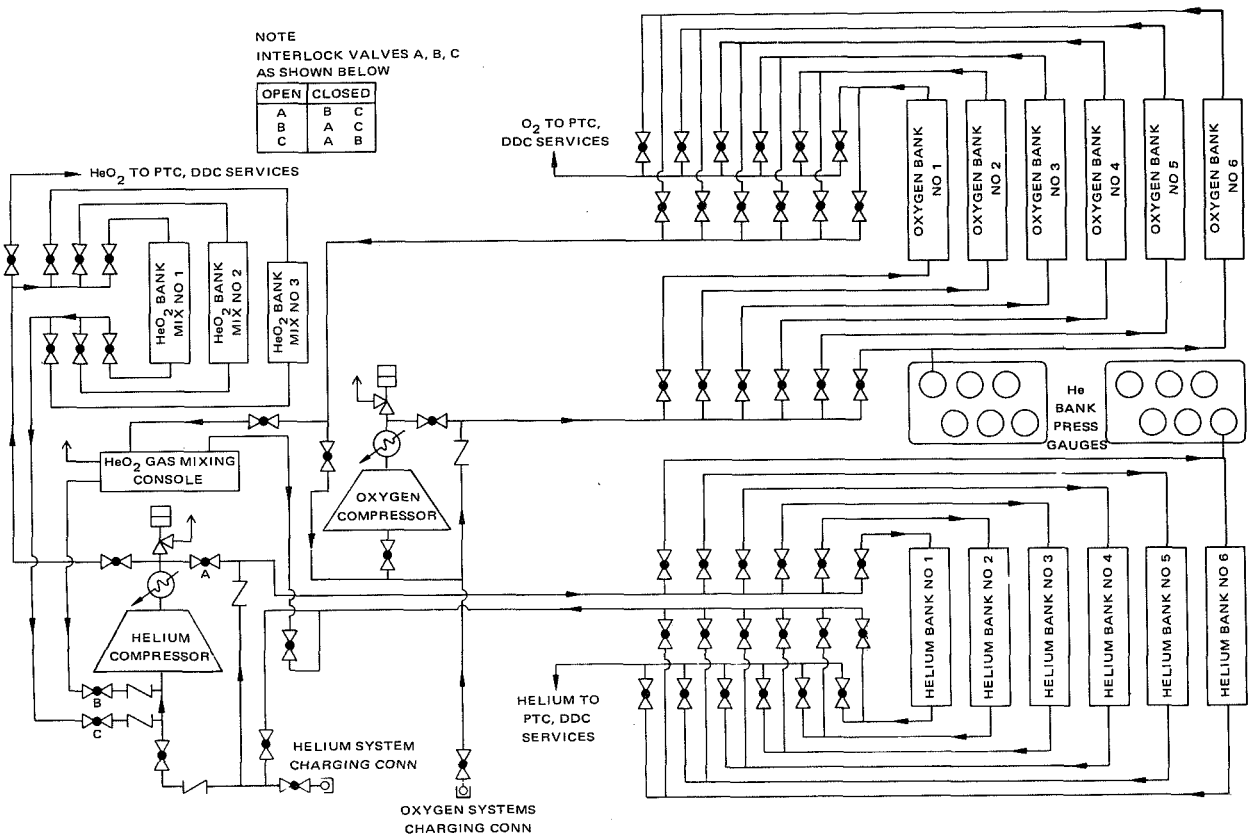

Figure 2.7 *Mark II deep dive system aboard ASR 21/22.*

The system concept is that a pressure vessel (fig. 2.8) is thermally insulated and filled with liquid helium at atmospheric pressure. The liquid inlet and gaseous vent are closed upon reaching the design capacity (in pounds of liquid); pressure then increases within the constant volume of the system in response to "heat leak" through the thermal insulation.

Then the pressure increase can be related as follows. From the first law of thermodynamics,

$$\Delta U = Q - W_k$$

and the definition of enthalpy

$$H = U + pv$$

where

Q heat added to the system
U internal energy function
W_k work done, by the system
P pressure
v specific volume = $\dfrac{\text{container volume}}{\text{total mass of liquid and vapor}}$

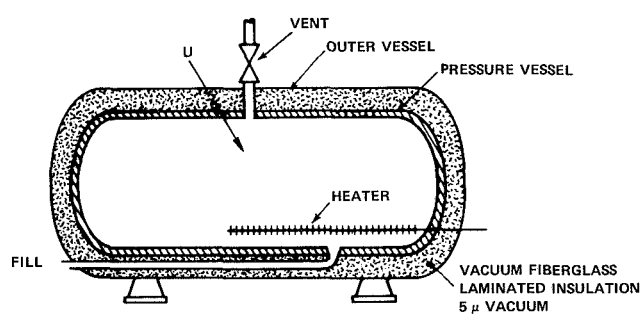

Figure 2.8 *Supercritical Dewar.*

Since the process is one of constant volume

$$W_k = 0$$

$$\Delta U = Q$$

or

$$Q = \Delta U = \Delta H + v\Delta p$$

Then the pressure rise is the result of the heat leak into the system, and the time for the system to reach the permissible working pressure is related to the thermal conductivity of the insulation. These principles were applied to a recently developed flyaway system to support the diving systems (fig. 2.9).

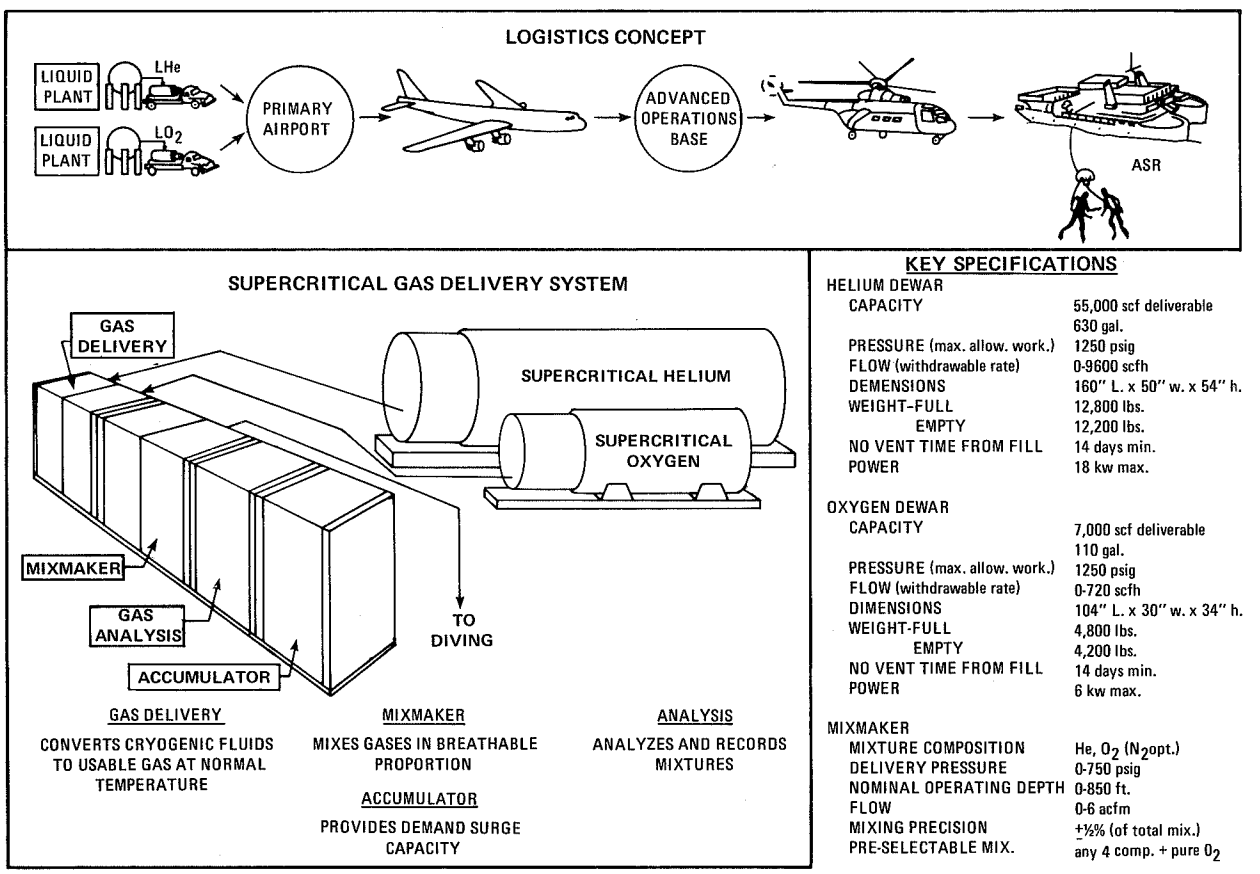

Figure 2.9 *Supercritical gas system for diving.*

Performance curves relating days to pressure increase are shown in figure 2.10.

When the previously stated relationship and helium property data from ref. 5 are applied, the helium temperature when the Dewar is at 1250 psi will be ~44° R. (Relationships of temperature and internal energy to pressure in a closed Dewar are shown in figure 2.11.) Therefore, any helium to be used in the diving system must be heated to a usable temperature. This is done in the gas delivery console. System weight is then full Dewar weight plus the delivery console or ~(12800 + 1300) = 14,100 and, based on their delivery criteria, there are ~4 SCF helium available per lb of metal in the system.

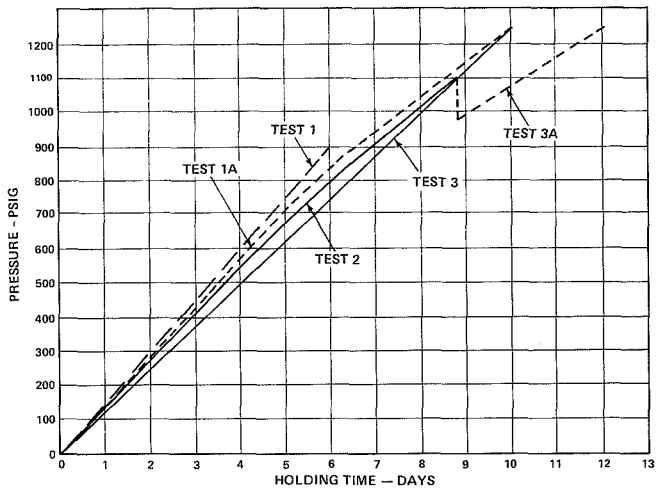

Figure 2.10 *Test results of pressure buildup versus time in one supercritical* He *Dewar.*

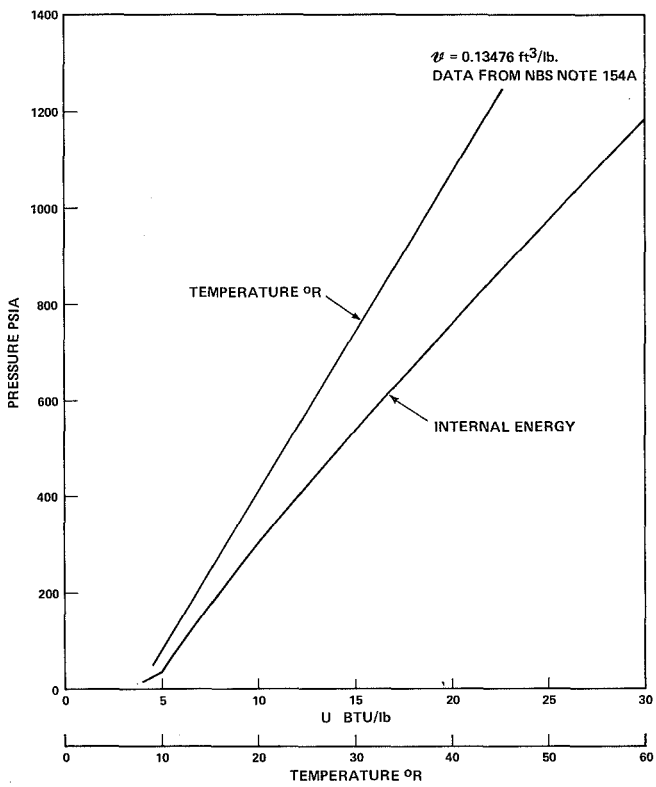

Figure 2.11 *Internal energy and temperature of He versus pressure in a closed Dewar.*

Refrigerated Cryogenic Storage

Another method for reducing weight and volume of the helium storage would be pressurized storage at liquid oxygen temperature (-297° F); at 1250 psi and 100 atm, the density is ~4.20 lb/ft^3. Using the same Dewar as designed for the supercritical system, which was 84.5 ft^3 in volume, this system would contain [(4.20 × 1250)/0.01034] = 50,600 SCF, and that available above 1000 psi would be ~46,000 SCF. Assuming that the delivery system would be no greater in weight than the one used in the supercritical system, we would obtain a ratio of 3.26 SCF/lb of metal in the system.

This system is promising in that the gas can be converted to a usable form, as required, and will not require helium transfer relative to thermal insulation characteristics. The use of liquid oxygen as a refrigerant appears logical in that the liquid produced and stored can be converted to gas to supply the system oxygen requirements.

The U.S. Navy currently uses cryogenic processes in small Joule-Thompson type liquefiers installed aboard aircraft carriers to generate breathing oxygen for fliers. The cryogenic refrigerated storage concept could be developed on the basis of experience and available technology.

GAS MIXING SYSTEMS

There are three basic methods of preparing breathing gas mixtures. The first two are mixing by weight and mixing by partial pressures. These are batch processes, and they introduce significant error in mix ratios because of deviation from ideal gas laws (ref. 1). Diffusion of oxygen into helium is a slow process; in some instances, it takes several days to obtain stabilized concentrations when the storage vessels are large.

The third technique, normally required for sustained large-scale diving operations, is a continuous flow method that consists of metering and controlling separate streams of oxygen, helium, and air or nitrogen and mixing them at high turbulence downstream from the metering system. To be effective this method requires a simple, easy-to-operate mixing system and a reliable analyzer to detect malfunctions quickly enough to permit adjustments to the gas mixture. The gas mixture may be fed directly to the diver through hose and regulators, introduced into a chamber such as a habitat or personnel transfer capsule, or recompressed and stored for later use.

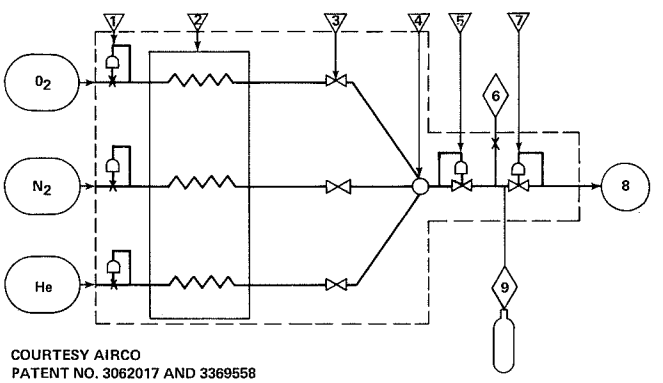

COURTESY AIRCO
PATENT NO. 3062017 AND 3369558

1	REGULATOR	6	ANALYZER
2	HEAT EXCHANGES	7	REGULATOR
3	METERING VALVES	8	SUPPLY TO DIVERS
4	MIXING CHAMBER	9	ACCUMULATOR
5	REGULATOR		

Figure 2.12 *AIRCO gas mixing system.*

Figure 2.12 shows the principles of the system, an Airco Mixmaker (TM), that is presently in use at the Navy Experimental Diving Unit. Stored, pure gases are supplied to the system at approximately 1100 psi through a regulator (1). At a constant, regulated pressure, the gases are passed through a heat exchanger (2) to reach a preset constant temperature. The system utilizes sonic flow characteristics through calibrated metering valves (3). The gases are mixed in a turbulent mixing chamber (4) and then sent through a regulator controlling flow-meter-outlet pressure at ~750 psi. The gas is sampled by bleeding from the main flow and routed to a gas chromatograph or other recording gas analyzer (6). The main gas stream passes through a final regulator (7) to be supplied directly to the divers (8). An accumulator (9) should be added to prevent high concentrations of oxygen from reaching the divers in the event of system malfunction. The mixed gas could be fed to storage cylinders or into a high-pressure diaphragm compressor for additional pressurization prior to storage.

The accuracy of mixing claimed for this system is as follows:

Amount of oxygen in mixture	*Precision of oxygen content*
0 - 10%	±0.15% O_2
10 - 15%	±0.25% O_2
15 - 100%	±0.50% O_2

For example, mixed gas prepared at the 9 percent setting would contain between 8.85 and 9.15 percent of pure oxygen.

Continuous-flow breathing-gas mixture systems, such as the system described above, can be fed to high-pressure compressors for filling UBA tanks or compressed-gas storage banks, as desired.

The oxygen content of the mixture would depend on the type of breathing apparatus to be used and the range of diving depths anticipated.

The Airco Mixmaker represents a fairly recent concept in gas mixing for underwater breathing applications. Since the only outside resources required are pure gas and electrical power, both binary and ternary mixtures of any predetermined requirement can be mixed on site, a significant advantage over "batch basis" mixing. Another version of a gas mixing system is shown in figure 2.13. This system uses calibrated turbine-type flowmeters and two-stage motor-operated needle valves.

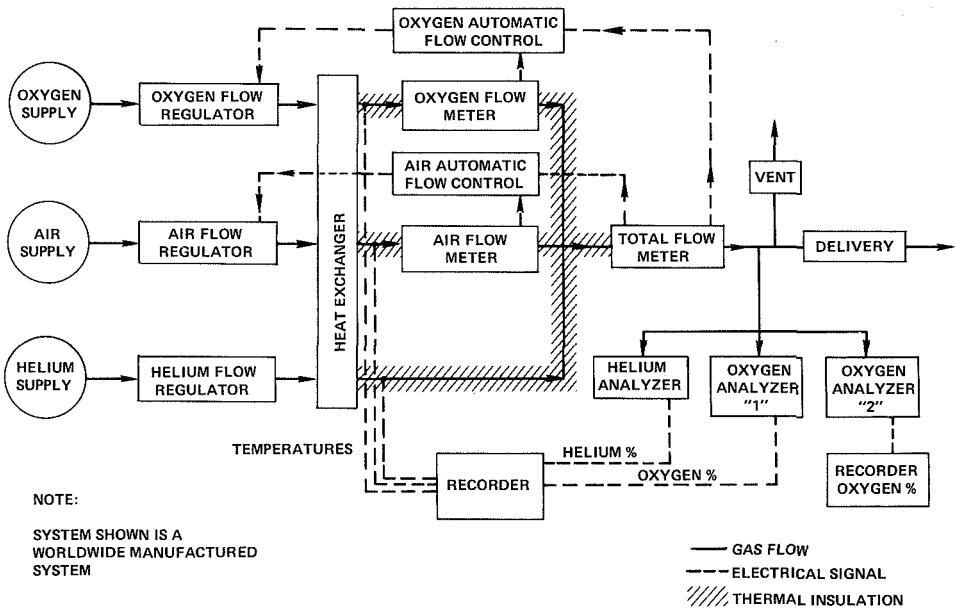

Figure 2.13. *Worldwide gas mixing system.*

GAS TRANSFER SYSTEMS

Transfer systems consisting of suitable noncontaminating compressors are desirable for helium, oxygen, and mixed gas systems. They enhance the performance ratio of SCF of helium available per pound of metal, but their operation requires a relatively high inlet pressure, as much as 200 to 400 psig for some of the smaller units. Figure 2.14 illustrates a transfer system utilizing an A5C250 compressor.

Application of these pumps in a system requires some knowledge of their performance characteristics. The only known parameters that can be applied are the displacement volume and rpm, from which the displacement per unit time and the flow capacity as related to the inlet pressure, outlet pressure, volumetric efficiency, and real gas properties can be obtained. The volumetric efficiency can be established theoretically if clearance volume is known, but more frequently, it is determined experimentally for each type of compressor. The volumetric efficiency for one model of a diaphragm type compressor is shown in figure 2.15. When the displacement and the volumetric efficiency are known, a simple computation relating the flow through the compressor with varying upstream-downstream pressure conditions, which are normally present in gas transfer operations, can be performed.

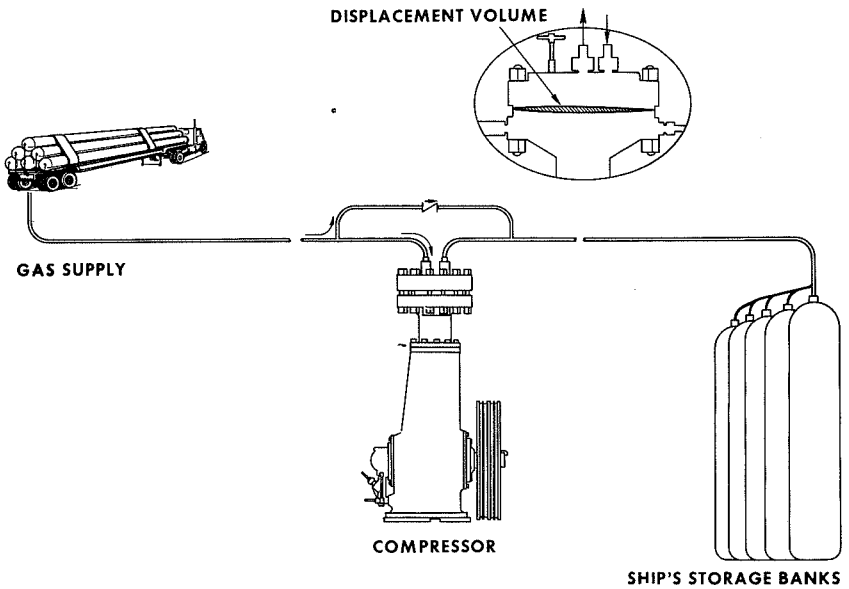

Figure 2.14 *A5C250 compressor unit.*

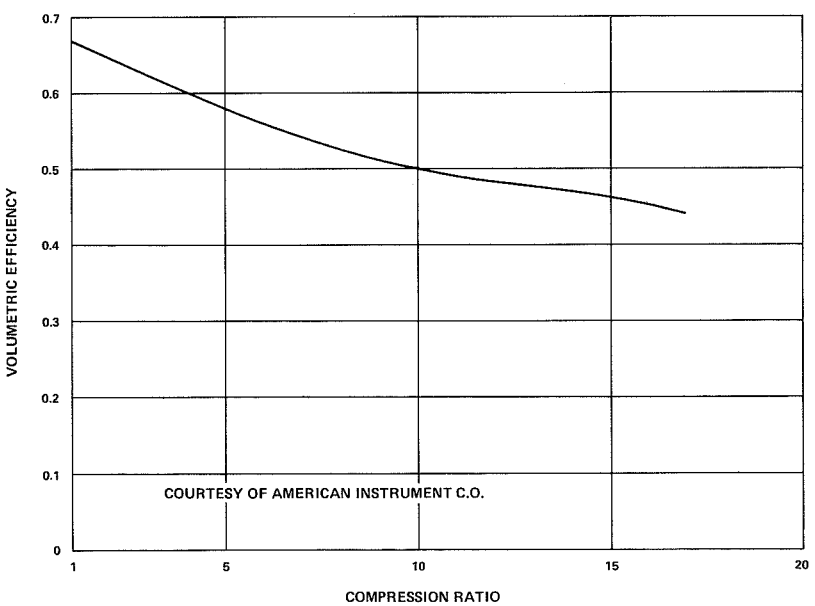

Figure 2.15 *Volumetric efficiency curve A5C250 compressor.*

A program was developed (appendix D), in which the data input permits variation in the input parameters (table 2.3). The program progressively reduces the pressure in the supply volume relative to the compressor displacement as affected by clearance, which is related to downstream pressure. It follows conventional compressor principles where a lb_{in} is a lb_{out} but takes into account the effect of the upstream-downstream condition on the flow capacity.

Table 2.3 *Input data constants for calculating* He *transfer time*

INPUT DATA

VOLUME OF ON BOARD STORAGE BANK	24.0 CU FEET
DESIGN PRESSURE OF STORAGE BANK	3000.0 PSIG
MINIMUM PRESSURE OF STORAGE BANK BEFORE PUMPING MAY BE INITIATED	200.0 PSIG
VOLUME OF SUPPLY BANK (100 BOTTLES)	60.0 CU FEET
INITIAL DELIVERY PRESSURE OF SUPPLY BANK	3000.0 PSIG
MINIMUM (RETURN) PRESSURE OF SUPPLY BANK	200.0 PSIG
PUMP CLEARANCE VOLUME	5.0 PERCENT
DURATION OF ONE PUMPING CYCLE	9.0 MINUTE(S)
VOLUME DISPLACED BY PUMP IN ONE MINUTE	0.6 CU FEET
POLYTROPIC PROCESS EXPONENT	1.6
TEMPERATURE OF GAS (ASSUMED CONSTANT)	70.0 DEG-F
HELIUM GAS CONSTANT (R)	386.3 FT-LBF/LBM-R

See Appendix D for the complete program and data concerning calculation of helium transfer time.

Although in our application of the program the polytropic exponent was near that of conventional compressors, in practice it more nearly approaches isothermal compression. Results obtained have provided transfer time for various shipboard applications, establishing constraints on time-related application of the compressor (e.g., the transfer of helium from a tube trailer into the nearby gas storage system).

COMPRESSED AIR CONSIDERATIONS

Although compressed air has limited application in DDS, it is the most common breathing gas used by divers. In deep diving systems compressed air is only for pressurizing the enclosures to an equivalent pressure to 14 ft of seawater to increase the oxygen partial pressure to 228 mm Hg so that the monitoring instrumentation can be zeroed and performance can be verified. Compressed air is used to support conventional surface-supplied systems and the more common scuba gear.

Purity Standards and Monitoring Techniques

Current purity standards for breathing air are:

Oxygen	20 to 22 percent by volume
Carbon dioxide	300 to 500 ppm (0.03 to 0.05 percent) by volume
Carbon monoxide	20 ppm maximum
Oil, mist, and vapor	5 mg/m^3 maximum
Solid and liquid particles	not detectable except as noted above under oil, mist, and vapor
Odor	not objectionable

Efforts to provide appropriate equipment for meeting these standards have been extensive. Filter testing at both the manufacturer's facility and another laboratory, together with a short-term test on one of the ARS-type ships, has verified the performance of an oil- and particulate-removal filter system. Procurement has been initiated for sufficient units to supply each existing salvage ship (ARS) and submarine rescue ship (ASR) with a portable unit, and an adequate number was included for salvage equipment pools, for supporting HCU and ATF surface-supplied diving.

Other projects include definition of compressor lubricating oils and their additives, with recommendations to exclude the use of oils containing phosphate esters. The commonly used 2190 TEP will be replaced with a 2135 TH type oil.

Proposed projects for monitoring techniques that will permit air sampling from the shipboard systems are being reviewed. These projects fall into two categories. The first is a technique for adapting coal dust monitoring equipment, under development as required by a recently established public law, for use in determining, on a periodic basis, the oil and particulate matter in diver air systems. This work involves the development of sampling techniques and adaptation of the coal dust sampler cassette for the sampling of air in diver breathing systems.

Currently under study are selective permeable membranes, incorporated into cassettes, that collect oil aerosols and particulate matter as the sample air passes through them. Once calibrated to provide representative quantities, these membranes will indicate the quantities of these

contaminants in an air stream. The contaminant levels established for the coal dust monitoring equipment are strikingly similar to diver system requirements: 2 mg/m^3 and 5 mg/m^3, respectively.

A second category comprises techniques for establishing the gaseous contaminants. A proposal in this area is under consideration that would refine current practice and hopefully provide acceptable techniques for periodically analyzing the air from divers' breathing gas systems.

Systems cleaning presents a major problem particularly in existing systems that do not permit in-place cleaning. Future installations, where practicable, will permit in-place cleaning.

CONCLUSION

The analytical approach to the design of compressed gas systems for supporting deep diving systems offers a method of effectively determining gas requirements and storage system definition. Although shipboard installations are not normally weight sensitive, the magnitude of these installations requires some optimization to reduce the weight.

Gas mixing systems also appear essential to provide the low concentration mixtures within the converging tolerance range dictated by applications to ever-increasing depths.

Time-related use of gas together with the performance of the gas transfer system is another significant consideration to ensure transfer within a reasonable time frame for systems application.

REFERENCES

1. U.S. Navy Diving Gas Manual, Oct. 1, 1969. U.S. Navy Supervisor of Diving Research Report 3-69.
2. Journal of Chemical Engineering Data, vol. 5, no. 1, Jan. 1960.
3. Anon.: Flask, Compressed Gas and End Plugs for Air, Oxygen, and Nitrogen. Military Spec. Mil-F-22606B (Ships).

APPENDIX A

PROGRAM - VIRIAL

```
PRØGRAM   VIRIAL

00100 READ R,T,T1,T2,T3,T4,T5,T9,B,B1,B2,B3,B4,B5
00110 DIM A(7),A1(7),A2(7),A3(7),A4(7),A5(7),A6(7)
00120 FØR C = 1 TØ 7
00130 READ A(C)
00140 NEXT C
00150 FØR C1 = 1 TØ 7
00160 READ A1(C1)
00170 NEXT C1
00180 FØR C2 = 1 TØ 7
00190 READ A2(C2)
00200 NEXT C2
00210 FØR C3 = 1 TØ 7
00220 READ A3(C3)
00230 NEXT C3
00240 FØR C4 = 1 TØ 7
00250 READ A4(C4)
00260 NEXT C4
00270 FØR C5 = 1 TØ 7
00280 READ A5(C5)
00290 NEXT C5
00300 FØR C6 = 1 TØ 7
00310 READ A6(C6)
00320 NEXT C6
00330 PRINT"TEMPERATURE DEG F    "T
00340 GØSUB 01380
00350 PRINT
00360 FØR I = 1 TØ 7
00370 LET P = A6(I)
00380 LET D = A(I)
00390 LET D1 = P/((1+B*P)*R*(T9+T))
00400 LET D2 = D1*1728
00410 LET V = ((D2-D)/D)*100
00420 LET V1 = 100*V
00430 LET V2 = INT(V1*10↑3 + .5)/10↑3
00440 LET V3 = V2/100
00450 PRINT TAB(1),P,TAB(13),D,TAB(30),D2,TAB(52),V3
00460 NEXT I
00470 PRINT
00480 PRINT
00490 PRINT"TEMPERATURE DEG F"T1
00500 GØ SUB 01380
00510 PRINT
00520 FØR I1 = 1 TØ 7
00530 LET P = A6(I1)
00540 LET D = A1(I1)
00550 LET D1 = P/((1+B1*P)*R*(T9+T1))
00560 LET D2 = D1*1728
00570 LET V = ((D2-D)/D)*100
00580 LET V1 = 100*V
00590 LET V2 = INT(V1*10↑3 + .5)/10↑3
00600 LET V3 = V2/100
00610 PRINT TAB(Q),P,TAB(13),D,TAB(30),D2,TAB(52),V3
00620 NEXT I1
00630 PRINT
00640 PRINT
00650 PRINT"TEMPERATURE DEG F"T2
00660 GØSUB 01380
00670 PRINT
00680 FØR I2 = 1 TØ 7
00690 LET P = A6(I2)
00700 LET D = A2(I2)
00710 LET D1 = P/((1+B2*P)*R*(T9+T2))
00720 LET D2 = D1*1728
00730 LET V = ((D2-D)/D)*100
00740 LET V1 = 100*V
00750 LET V2 = INT(V1*10↑3 +.5)/10↑3
00760 LET V3 = V2/100
00770 PRINT TAB(1),P,TAB(13),D,TAB(30),D2,TAB(52),V3
00780 NEXT I2
00790 PRINT
00800 PRINT
00810 PRINT"TEMPERATURE DEG F"T3
00820 GØ SUB 01380
00830 PRINT
00840 FØR I3 = 1 TØ 7
00850 LET P = A6(I3)
00860 LET D = A3(I3)
00870 LET D1 = P/((1+B3*P)*R*(T9+T3))
00880 LET D2 = D1*1728
00890 LET V = ((D2-D)/D)*100
00900 LET V1 = 100*V
00910 LET V2 = INT(V1*10↑3 + .5)/10↑3
00920 LET V3 = V2/100
00930 PRINT TAB(1),P,TAB(13),D,TAB(30),D2,TAB(52),V3
00940 NEXT I3
00950 PRINT
00960 PRINT
00970 PRINT"TEMPERATURE DEG F"T4
00980 GØSUB 01380
00990 PRINT
01000 FØR I4 = 1 TØ 7
01010 LET P = A6(I4)
01020 LET D = A4(I4)
01030 LET D1 = P/((1+B4*P)*R*(T9+T4))
01040 LET D2 = D1*1728
01050 LET V = ((D2-D)/D)*100
01060 LET V1 = 100*V
01070 LET V2 = INT(V1*10↑3 + .5)/10↑3
01080 LET V3 = V2/100
01090 PRINT TAB(1),P,TAB(13),D,TAB(30),D2,TAB(52),V3
01100 NEXT I4
01110 PRINT
01120 PRINT
01130 PRINT"TEMPERATURE DEG F"T5
01140 GØSUB 01380
01150 PRINT
01160 FØR I5 = 1 TØ 7
01170 LET P = A6(I5)
01180 LET D = A5(I5)
01190 LET D1 = P/((1+B5*P)*R*(T9+T5))
01200 LET D2 = D1*1728
01210 LET V = ((D2-D)/D)*100
01220 LET V1 = 100*V
01230 LET V2 = INT(V1*10↑3 +.5)/10↑3
01240 LET V3 = V2/100
01250 PRINT TAB(1),P,TAB(13),D,TAB(30),D2,TAB(52),V3
01260 IF I5 = 7 THEN 01470
01270 NEXT I5
01280 DATA 4636, 30, 50, 70, 90, 110, 130, 459.6
01290 DATA 3.4480E-5, 3.29277E-5, 3.16830E-5, 3.02923E-5, 2.90253E-5
01300 DATA 2.78820E-5
01310 DATA .01119, .37416, .73545, 1.08472, 1.4227, 1.7501, 2.0676
01320 DATA .01075, .35975, .70764, 1.04443, 1.3708, 1.6873, 1.9945
01330 DATA .01034, .34641, .68186, 1.00703, 1.3225, 1.6288, 1.9265
01340 DATA .00997, .33402, .65790,  .97223, 1.2775, 1.5743, 1.8631
01350 DATA .00962, .32249, .63557,  .93976, 1.2356, 1.5234, 1.8037
01360 DATA .00929, .31174, .61471,  .90941, 1.1963, 1.4756, 1.7480
01370 DATA 14.7, 500, 1000, 1500, 2000, 2500, 3000
01380 PRINT
01390 PRINT TAB(15),"USN DIVING",TAB(29),"VIRIAL CØEFF.",
01400 PRINT TAB(51),"DIFFERENCE"
01410 PRINT"PRESSURE",TAB(15),"GAS MANUAL",TAB(30),"CØMPUTATIØN",
01420 PRINT TAB(53),"PERCENT"
01430 PRINT TAB(16),"DENSITY",TAB(32),"DENSITY"
01440 PRINT TAB(2),"PSIA",TAB(16),"LBS/FT3",TAB(32),"LBS/FT3",
01450 PRINT
01460 RETURN
01470 END
```

PROGRAM VIRIAL - OUTPUT DATA

PRØGRAM VIRIAL

TEMPERATURE DEG F 30

PRESSURE PSIA	USN DIVING GAS MANUAL DENSITY LBS/FT3	VIRIAL CØEFF CØMPUTATIØN DENSITY LBS/FT3	DIFFERENCE PERCENT
14.7	.01119	1.11855 E-2	-.04004
500	.37416	.374201	.01108
1000	.73545	.735931	.06533
1500	1.08472	1.0858	.09961
2000	1.4227	1.42439	.11845
2500	1.7501	1.75222	.12125
3000	2.0676	2.06981	.10711

TEMPERATURE DEG F 50

PRESSURE PSIA	USN DIVING GAS MANUAL DENSITY LBS/FT3	VIRIAL CØEFF. CØMPUTATIØN DENSITY LBS/FT3	DIFFERENCE PERCENT
14.7	.01075	1.07468 E-2	-.03002
500	.35975	.35979	.01109
1000	.70764	.70811	.06647
1500	1.04443	1.0455	.10258
2000	1.3708	1.37247	.12177
2500	1.6873	1.68949	.12977
3000	1.9945	1.99701	.12583

TEMPERATURE DEG F 70

PRESSURE PSIA	USN DIVING GAS MANUAL DENSITY LBS/FT3	VIRIAL CØEFF. CØMPUTATIØN DENSITY LBS/FT3	DIFFERENCE PERCENT
14.7	.01034	1.03411 E-2	.0108
500	.34641	.346415	.00137
1000	.68186	.682191	.04856
1500	1.00703	1.00781	.07763
2000	1.3225	1.32373	.09304
2500	1.6288	1.63037	.09667
3000	1.9265	1.92815	.08547

TEMPERATURE DEG F 90

PRESSURE PSIA	USN DIVING GAS MANUAL DENSITY LBS/FT3	VIRIAL CØEFF. CØMPUTATIØN DENSITY LBS/FT3	DIFFERENCE PERCENT
14.7	00997	9.96501 E-3	-.05009
500	.33402	.334037	.00519
1000	.6579	.658253	.05372
1500	.97223	.973075	.08693
2000	1.2775	1.2789	.10998
2500	1.5743	1.57612	.11578
3000	1.8631	1.86509	.10665

TEMPERATURE DEG F 110

PRESSURE PSIA	USN DIVING GAS MANUAL DENSITY LBS/FT3	VIRIAL CØEFF. CØMPUTATIØN DENSITY LBS/FT3	DIFFERENCE PERCENT
14.7	.00962	9.61529 E-3	-.04896
500	.32249	.32251	.00613
1000	.63557	.635923	.05548
1500	.93976	.940618	.09131
2000	1.2356	1.23695	.10966
2500	1.5234	1.52527	.12291
3000	1.8037	1.80589	.12151

TEMPERATURE DEG F 130

PRESSURE PSIA	USN DIVING GAS MANUAL DENSITY LBS/FT3	VIRIAL CØEFF. CØMPUTATIØN DENSITY LBS/FT3	DIFFERENCE PERCENT
14.7	.00929	9.28928 E-3	-.00772
500	.31174	.311745	.00176
1000	.61471	.615035	.05281
1500	.90941	.910207	.08764
2000	1.1963	1.19758	.10733
2500	1.4756	1.47747	.12676
3000	1.748	1.75016	.12332

APPENDIX B

PROGRAM - HELIUM CAPACITY

```
10 PRINT"    TOTAL HELIUM CAPACITY OF FLASKS AT RATED DESIGN PRESSURE"
20 PRINT"                  CONSIDERING VARIOUS DIAMETERS"
30 PRINT
40 DIM V3(4,9),W(4,9),C(4,9),C1(4,9),S1(9)
50 DIM C2(4,9)
60 FOR A = 1 TO 9
70 READ S1(A)
80 NEXT A
90 LET S2 = .31851
100 FOR D0 = 18 TO 24 STEP 2
110 LET K = (D0/2)-8
120 LET L = 92
130 LET L1 = 92 - D0
140 LET R0 = D0/2
150 LET V = (4/3)*3.1416*R0↑3 + L1*3.1416*R0↑2
160 LET S = 0.67*110000
170 PRINT
180 PRINT"  FLASK DIAMETER",D0" INCHES"
190 PRINT
200 PRINT TAB(7),"DESIGN",TAB(20),"WALL",TAB(34),"INTERNAL"
210 PRINT TAB(7),"PRESS.",TAB(18),"THICKNESS",TAB(35),"VOLUME",
220 PRINT TAB(50),"WEIGHT"
230 PRINT TAB(9),"PSI",TAB(20),"INCH",TAB(37),"FT3",TAB(51),"LBS"
240 PRINT
250 FOR I = 1 TO 9
260 LET P = 1400 + I*400
270 LET P1 = (5/3)*P
280 LET D1 = D0*((S - 1.3*P1)/(S + 0.4*P1))↑0.5
290 LET D2 = D1 - 2*0.065
300 LET R1 = D2/2
310 LET V1 = (4/3)*3.1416*R1↑3 + L1*3.1416*R1↑2
320 LET V3(K,I) = V1/1728
330 LET V2 = (V-V1)/1728
340 LET W(K,I) = V2*485
350 LET T = (D0-D2)/2
360 LET C(K,I) = V3(K,I)*(S1(I) - S2)/0.01034
370 LET C1(K,I) = C(K,I)/W(K,I)
380 LET C2(K,I) = V3(K,I)*(S1(I)/0.01034)
390 PRINT P,T,V3(K,I),W(K,I)
400 NEXT I
410 NEXT D0
417 PRINT
418 PRINT
419 PRINT
420 PRINT"    TOTAL HELIUM CAPACITY OF FLASKS AT RATED DESIGN PRESS."
430 PRINT"       - AND - HELIUM AVAILABLE TO AN EQUILIBRIUM DEPTH"
440 PRINT"             EQUIVALENT TO 1000 FEET OF SEA-WATER"
450 PRINT
460 PRINT
470 FOR K3 = 1 TO 4
480 LET D0 = 16 + 2*K3
490 PRINT
500 PRINT"  FLASK DIAMETER",D0" INCHES"
510 PRINT
520 PRINT TAB(7),"DESIGN",TAB(20),"TOTAL",TAB(34),"AVAIL. HE",
530 PRINT TAB(48),"SCF HELIUM"
540 PRINT TAB(7),"PRESS.",TAB(19),"STORAGE",TAB(33),"FOR 1000 FT",
550 PRINT TAB(48),"AVAIL. PER"
560 PRINT TAB(8),"PSI",TAB(21),"SCF",TAB(33),"DIVE - SCF",
562 PRINT TAB(48),"LB OF METAL"
565 PRINT
570 FOR I1 = 1 TO 9
580 LET P = 1400 + I1*400
590 PRINT P,C2(K3,I1),C(K3,I1),C1(K3,I1)
600 NEXT I1
610 NEXT K3
620 DATA 1.206632, 1.455111, 1.697805, 1.935114, 2.167208, 2.394232
630 DATA 2.616470, 2.834094, 3.047276
640 END
```

OUTPUT DATA

TOTAL HELIUM CAPACITY OF FLASKS AT RATED DESIGN PRESS.
- AND - HELIUM AVAILABLE TO AN EQUILIBRIUM DEPTH
EQUIVALENT TO 1000 FEET OF SEA-WATER

FLASK DIAMETER 18 INCHES

DESIGN PRESS. PSI	TOTAL STORAGE SCF	AVAIL. HE FOR 1000 FT DIVE - SCF	SCF HELIUM AVAIL. PER LB OF METAL
1800	1348.811	992.7708	1.85044
2200	1598.746	1248.796	1.974715
2600	1833.215	1489.302	2.047285
3000	2053.086	1715.158	2.087352
3400	2256.954	1926.96	2.105693
3800	2451.367	2125.256	2.108922
4200	2630.996	2310.717	2.101459
4600	2798.374	2483.878	2.086196
5000	2954.016	2645.254	2.065158

FLASK DIAMETER 20 INCHES

DESIGN PRESS. PSI	TOTAL STORAGE SCF	AVAIL. HE FOR 1000 FT DIVE - SCF	SCF HELIUM AVAIL. PER LB OF METAL
1800	1653.805	1217.257	1.870051
2200	1960.024	1530.993	1.990134
2600	2247.21	1825.631	2.059095
3000	2516.436	2102.243	2.096135
3400	2768.436	2361.565	2.111953
3800	3003.887	2604.273	2.113074
4200	3223.618	2831.198	2.103843
4600	3428.286	3042.998	2.087091
5000	3618.529	3240.31	2.064793

FLASK DIAMETER 22 INCHES

DESIGN PRESS. PSI	TOTAL STORAGE SCF	AVAIL. HE FOR 1000 FT DIVE - SCF	SCF HELIUM AVAIL. PER LB OF METAL
1800	1986.726	1462.298	1.883806
2200	2354.299	1838.965	2.000091
2600	2698.922	2192.602	2.06586
3000	3021.893	2524.504	2.100271
3400	3324.098	2835.562	2.113927
3800	3606.36	3126.598	2.113264
4200	3869.679	3398.613	2.102553
4600	4114.853	3652.405	2.084569
5000	4342.652	3888.746	2.061239

FLASK DIAMETER 24 INCHES

DESIGN PRESS. PSI	TOTAL STORAGE SCF	AVAIL. HE FOR 1000 FT DIVE - SCF	SCF HELIUM AVAIL. PER LB OF METAL
1800	2346.727	1727.271	1.892969
2200	2780.553	2171.916	2.005791
2600	3187.166	2599.251	2.068714
3000	3568.108	2980.815	2.100817
3400	3924.436	3347.67	2.112598
3800	4257.129	3690.793	2.110407
4200	4567.376	4011 377	2.098443
4600	4856.127	4310.37	2.079425
5000	5124.298	4588.692	2.055241

OUTPUT DATA

TOTAL HELIUM CAPACITY OF FLASKS AT RATED DESIGN PRESSURE CONSIDERING VARIOUS DIAMETERS

FLASK DIAMETER 18 INCHES

DESIGN PRESS. PSI	WALL THICKNESS INCH	INTERNAL VOLUME FT3	WEIGHT LBS
1800	.3768101	11.55838	536.5054
2200	.4462458	11.36067	632.3931
2600	.5157485	11.16467	727.452
3000	.5853251	10.97037	821.691
3400	.6549829	10.77773	915.1192
3800	.7247291	10.58675	1007.745
4200	.7945708	10.3974	1099.578
4600	.8645161	10.20968	1190.625
5000	.9345727	10.02355	1280.896

FLASK DIAMETER 20 INCHES

DESIGN PRESS. PSI	WALL THICKNESS INCH	INTERNAL VOLUME FT3	WEIGHT LBS
1800	.4114556	14.17197	650.9219
2200	.4886065	13.92791	769.2914
2600	.5658317	13.68599	886.6183
3000	.643139	13.44621	1002.914
3400	.7205366	13.20853	1118.19
3800	.7980322	12.97292	1232.457
4200	.8756342	12.73938	1345.727
4600	.9533513	12.50787	1458.009
5000	1.031192	12.27837	1569.315

FLASK DIAMETER 22 INCHES

DESIGN PRESS. PSI	WALL THICKNESS INCH	INTERNAL VOLUME FT3	WEIGHT LBS
1800	.4461012	17.02487	776.2464
2200	.530967	16.72962	919.4408
2600	.6159148	16.43702	1061.351
3000	.7009529	16.14704	1201.99
3400	.7860903	15.85966	1341.372
3800	.8713354	15.57483	1479.512
4200	.9566977	15.29254	1616.422
4600	1.042186	15.01276	1752.116
5000	1.127811	14.73546	1886.606

FLASK DIAMETER 24 INCHES

DESIGN PRESS. PSI	WALL THICKNESS INCH	INTERNAL VOLUME FT3	WEIGHT LBS
1800	.4807467	20.10983	912.4662
2200	.5733277	19.75857	1082.823
2600	.665998	19.41053	1251.623
3000	.7587668	19.06567	1418.884
3400	.8516439	18 72394	1584.622
3800	9446386	18.38532	1748.854
4200	1.037761	18.04976	1911.597
4600	1.131021	17.71725	2072.866
5000	1.22443	17.38774	2232.678

APPENDIX C

PROGRAM - HELIUM AVAILABLE FOR SATURATION DIVING MISSION

```
10 READ U,V,Y,D
15 LET P = 0.44444*D
20 LET P1 = 0.44444*D - 0.5*0.44444
25 LET P2 = 3000
30 LET Z = 1 + U*P
35 LET Z1 = 1 + V*P
40 LET Z2 = 1 + Y*P
45 LET Z3 = 1 + U*P1
50 LET Z4 = 1 + V*P1
55 LET Z5 = 1 + Y*P1
60 LET Z6 = 1 + U*P2
65 LET Z7 = 1 + V*P2
70 LET Z8 = 1 + Y*P2
75 LET Z9 = 1 + V*3814.7
80 LET K = 4.0026*144/(1546*495)
85 LET K1 = 4.0026*144/(1546*548)
90 LET K2 = 4.0026*144/(1546*570)
95 LET W = K*P/Z
100 LET W1 = K*P1/Z3
105 LET W2 = K*P2/Z6
110 LET W3 = K1*P/Z1
115 LET W4 = K1*P1/Z4
120 LET W5 = K1*P2/Z7
125 LET W6 = K2*P/Z2
130 LET W7 = K2*P1/Z5
135 LET W8 = K2*P2/Z8
140 LET W9 = K1*3814.7/Z9
145 LET R1 = 1000*W3/0.01034
150 LET R2 = 235*W3/0.01034
155 LET R3 = (227 + 29)*W3/0.01034
160 LET A = 153860.5 - R1 - R2 - R3
165 LET H = 1 - (1.2/((0.44444*D + 14.7)/14.7))
170 LET M = H*2*16.88*W9/0.01034
175 LET M1 = M
180 LET M2 = M
185 LET M3 = H*4*6*W5/0.01034
190 LET M4 = 5*6*W5/0.01034
195 LET A1 = A - M - M1 - M2 - M3 - M4
200 LET C = 235*W3/0.01034
205 LET C1 = 765*W3/0.01034
210 LET C2 = 227*W3/0.01034
213 LET A2 = A1 - C - C1 - C2
215 LET C3 = 2*16*W3/0.01034
220 LET C4 = 2*13*W3/0.01034
225 LET C5 = 4*3*W3/0.01034
230 LET C6 = 2*227*(W3 - W6)/0.01034
232 LET C7 = 2*16*W/0.01034
235 LET C8 = (476.43*1.5)*2*2
240 LET C9 = 0.5*3*W3/0.01034
245 LET L = 24*1000*(W3 - W4)/0.01034
250 LET L1 = 24*227*(W3 - W4)/0.01034
255 LET L2 = L + L1
257 LET R4 = C3 + C4 + C5 + C9
260 LET B = C3 + C4 + C5 + C6 + C7 + C8 + C9
265 FOR X = 1 TO 10 STEP 1
267 LET L3 = X*L2
268 LET R5 = X*R4
270 LET A3 = A2 - X)(B + L2)
280 PRINT A;A1;A2;A3;L3;R5
290 NEXT X
300 DATA 3.3979E-5,3.0431E-5,2.9025E-5,850
305 PRINT
306 PRINT
307 PRINT
308 PRINT "DEFINITION OF SYMBOLS"
309 PRINT
310 PRINT "PRESSURE EQUIV. TO 850FT. S.W.                    PSIA" P
311 PRINT "                 TO 850FT. S.W. MINUS 0.5FT.      PSIA" P1
312 PRINT "PTC FLASK WP P2 = " P2
313 PRINT "COMPRESSIBILITY FOR P  AT  35 DEGREES F, Z =" Z
314 PRINT "                    P  AT  88 DEGREES F, Z1 =" Z1
315 PRINT "                    P  AT 110 DEGREES F, Z2 =" Z2
316 PRINT "                    P1 AT  35 DEGREES F, Z3 =" Z3
317 PRINT "                    P1 AT  88 DEGREES F, Z4 =" Z4
318 PRINT "                    P1 AT 110 DEGREES F, Z5 =" Z5
319 PRINT "                    P2 AT  35 DEGREES F, Z6 =" Z6
320 PRINT "                    P2 AT  88 DEGREES F, Z7 =" Z7
321 PRINT "                    P2 AT 110 DEGREES F, Z8 =" Z8
322 PRINT "                 3814.7 AT  88 DEGREES F, Z9 =" Z9
323 PRINT "HELIUM DENSITY AT     P  AND  35F, LB/FT3 W  =" W
324 PRINT "                      P1 AND  35F, LB/FT3 W1 =" W1
325 PRINT "                      P2 AND  35F, LB/FT3 W2 =" W2
326 PRINT "                      P  AND  88F, LB/FT3 W3 =" W3
327 PRINT "                      P1 AND  88F, LB/FT3 W4 =" W4
328 PRINT "                      P2 AND  88F, LB/FT3 W5 =" W5
329 PRINT "                      P  AND 110F, LB/FT3 W6 =" W6
330 PRINT "                      P1 AND 110F, LB/FT3 W7 =" W7
331 PRINT "                      P2 AND 110F, LB/FT3 W8 =" W8
332 PRINT "                   3814.7 AND  88F, LB/FT3 W9 =" W9
333 PRINT "RESERVE FOR HYPERBARIC TREATMENT IN DDC, SCF" R1
334 PRINT "RESERVE FOR OUTER LOCK OPERATION ONCE,   SCF" R2
335 PRINT "RESERVE FOR PTC MAINTENANCE ONCE,        SCF" R3
336 PRINT "*******QUANTITY AVAILABLE FOR DIVING MISSION SCF"A
337 PRINT "HELIUM FRACTION IN MIXED GAS" H
338 PRINT "HELIUM FOR SHIP'S MIXED GAS BANK PER BANK SCF" M
339 PRINT " HELIUM FOR PTC MIXED GAS FLASKS SCF" M3
340 PRINT " HELIUM FOR PTC HELIUM FLASKS SCF" M4
341 PRINT "*******QUANTITY AVAILABLE FOR DIVING MISSION SCF"A1
342 PRINT "HELIUM FOR PRESSURIZATION DDC OUTER LOCK SCF" C
343 PRINT "HELIUM FOR PRESSURIZATION DDC INNER LOCK SCF" C1
344 PRINT "HELIUM FOR PTC PRESSURIZATION SCF" C2
345 PRINT "*******QUANTITY AVAILABLE FOR DAILY OPERATIONS SCF"A2
346 PRINT " DAILY OPERATIONS "
347 PRINT "DDC TRUNK PRESS. TWICE DAILY SCF" C3
348 PRINT "PTC TRUNK PRESS. TWICE DAILY SCF" C4
349 PRINT " MEDICAL LOCK FOUR DAILY SCF" C5
350 PRINT " PTC DELTA T EQUALIZATION,TWICE DAILY SCF" C6
351 PRINT"PTC TRUNK BLOW AT DEPTH TWICE DAILY SCF" C7
352 PRINT " DIVERS USE WITH 0.008 IL.ORIFICE MANI) 11 SCF" C8
353 PRINT " LOSS IN PTC SCRUBBER CHANGE ONCE EVERY TWO DAYS SCF" C9
354 PRINT "DAILY LEAKAGE DDC, INNER & OUTER LOCK    SCF" L
355 PRINT "DAILY LEAKAGE PTC,                      SCF" L1
356 PRINT "TOTAL DAILY LEAKAGE DDC AND PTC         SCF" L2
357 PRINT "HELIUM USE DAILY FOR DIVING OPS       SCF" B
358 PRINT "HELIUM RECOVERABLE DURING DIVING OPS  SCF/DAY" R4
360 END
```

DATA

COLUMNS:

- A AVAILABLE TO OPERATE SYSTEM
- B AVAILABLE AFTER CHARGING PTC FLASKS AND SHIP'S MIXED GAS FLASKS
- C AVAILABLE AFTER ENCLOSURE PRESSURIZATION
- D AVAILABLE AFTER DAILY OPERATION
- E CUMULATIVE DDC AND PTC LEAKAGE
- F CUMULATIVE RECOVERABLE HELIUM

A	B	C	D	E	F
117221.8	85897.31	55745.98	49415.24	420.8263	1756.985
117221.8	85897.31	55745.98	43084.51	841.6525	3513.97
117221.8	85897.31	55745.98	36753.78	1262.479	5270.954
117221.8	85897.31	55745.98	30423.05	1683.305	7027.939
117221.8	85897.31	55745.98	24092.31	2104.131	8784.924
117221.8	85897.31	55745.98	17761.58	2524.958	10541.91
117221.8	85897.31	55745.98	11430.85	2945.784	12298.89
117221.8	85897.31	55745.98	5100.116	3366.61	14055.88
117221.8	85897.31	55745.98	-1230.617	3787.436	15812.86
117221.8	85897.31	55745.98	-7561.35	4208.263	17569.85

DEFINITION OF SYMBOLS

```
PRESSURE EQUIV. TO 850FT. S.W.                    PSIA 377.774
                TO 850FT. S.W. MINUS 0.5FT.       PSIA  377.5518
PTC FLASK WP P2 =  3000
COMPRESSIBILITY FOR P  AT  35 DEGREES F, Z =   1.012836
                    P  AT  88 DEGREES F, Z1 =  1.011496
                    P  AT 110 DEGREES F, Z2 =  1.010965
                   P1 AT  35 DEGREES F, Z3 =   1.012829
                   P1 AT  88 DEGREES F, Z4 =   1.011489
                   P1 AT 110 DEGREES F, Z5 =   1.010958
                   P2 AT  35 DEGREES F, Z6 =   1.101937
                   P2 AT  88 DEGREES F, Z7 =   1.091293
                   P2 AT 110 DEGREES F, Z8 =   1.087075
                 3814.7 AT  88 DEGREES F, Z9 =  1.116085
HELIUM DENSITY AT     P  AND  35F, LB/FT3 W  =  0.2809201
                      P1 AND  35F, LB/FT3 W1 =  0.2807569
                      P2 AND  35F, LB/FT3 W2 =   2.050475
                      P  AND  88F, LB/FT3 W3 =   0.254087
                      P1 AND  88F, LB/FT3 W4 =  0.2539393
                      P2 AND  88F, LB/FT3 W5 =   1.870228
                      P  AND 110F, LB/FT3 W6 =  0.2444085
                      P1 AND 110F, LB/FT3 W7 =  0.2442663
                      P2 AND 110F, LB/FT3 W8 = 1.80502
                   3814.7 AND  88F, LB/FT3 W9 =   2.325293
RESERVE FOR HYPERBARIC TREATMENT IN DDC, SCF   24573.21
RESERVE FOR OUTER LOCK OPERATION ONCE,   SCF   5774.705
RESERVE FOR PTC MAINTENANCE ONCE,        SCF   6290.743
*******QUANTITY AVAILABLE FOR DIVING MISSION SCF   117221.8
HELIUM FRACTION IN MIXED GAS  0.9550543
HELIUM FOR SHIP'S MIXED GAS BANK PER BANK SCF   7250.829
 HELIUM FOR PTC MIXED GAS FLASKS SCF   4145.847
 HELIUM FOR PTC HELIUM FLASKS SCF   5426.193
*******QUANTITY AVAILABLE FOR DIVING MISSION SCF   85897.31
HELIUM FOR PRESSURIZATION DDC OUTER LOCK SCF   5774.705
HELIUM FOR PRESSURIZATION DDC INNER LOCK SCF   18798.51
HELIUM FOR PTC PRESSURIZATION SCF 5578.12
*******QUANTITY AVAILABLE FOR DAILY OPERATIONS SCF   55745.98
 DAILY OPERATIONS
DDC TRUNK PRESS. TWICE DAILY SCF   786.3428
PTC TRUNK PRESS. TWICE DAILY SCF   638.9036
 MEDICAL LOCK FOUR DAILY SCF   294.8786
 PTC DELTA T EQUALIZATION,TWICE DAILY SCF   424.9565
PTC TRUNK BLOW AT DEPTH TWICE DAILY SCF   869.3851
 DIVERS USE WITH 0.008 IN.ORIFICE MARK 11 SCF 2858.58
 LOSS IN PTC SCRUBBER CHANGE ONCE EVERY TWO DAYS SCF   36.85982
DAILY LEAKAGE DDC, INNER & OUTER LOCK     SCF   342.9717
DAILY LEAKAGE PTC,                        SCF   77.85457
TOTAL DAILY LEAKAGE DDC AND PTC           SCF   420.8263
HELIUM USE DAILY FOR DIVING OPS         SCF   5909.906
HELIUM RECOVERABLE DURING DIVING OPS  SCF/DAY   1756.985
```

APPENDIX D

PROGRAM - HELIUM TRANSFER TIME CALCULATION

```
          MTAS       - EFN   SOURCE STATEMENT  - IFN(S)  -

C  HELIUM TRANSFER TIME CALCULATION   T. BRINKER  CODE 6432   X68002
C*       CASDAC 242053 MTAS        HANSEN 6154E 62434
      DIMENSION ITYPE(50),  PRESS1(50),  PRESS2(50),  P(2)
      DIMENSION DENSTY(2),   ATIME(50),  PTANK(50),  WTRANS(50)
      DIMENSION PHOLD1(2), PHOLD2(2)
      EQUIVALENCE (PHOLD1(2),PRESS1(1)), (PHOLD2(2),PRESS2(1))
   10 FORMAT(8F10.2)
   11 FORMAT( 4F10.2)
  111 FORMAT(/1X25HTOTAL TIME OF TRANSFER = , F9.2,2X,7HMINUTES)
  130 FORMAT(1X,5HOPER.,6X,15HBOTTLE PRESSURE,5X,4HMASS,6X,4HTANK,4X,9HO
     /PERATION,4X,4HTIME)
  140 FORMAT(1X,5HCOUNT,7X,4HFROM,5X,2HTO,5X,19HTRANSFERED PRESSURE/)
  200 FORMAT(///30X,10HINPUT DATA//)
  201 FORMAT(10X,31HVOLUME OF ON BOARD STORAGE BANK,11X,1H=,F8.1,2X,7HCU
     1 FEET/10X,31HDESIGN PRESSURE OF STORAGE BANK,11X,1H=,F8.1,2X,4HPSI
     2G/10X32HMINIMUM PRESSURE OF STORAGE BANK/  12X,31HBEFORE PUMPING M
     3AY BE INITIATED,9X,1H=,F8.1,2X,4HPSIG)
  204 FORMAT(10X,35HVOLUME OF SUPPLY BANK (100 BOTTLES),7X,1H=,F8.1,2X,7
     1HCU FEET/10X,43HINITIAL DELIVERY PRESSURE OF SUPPLY BANK =,F8.1,2X
     2,4HPSIG/10X,43HMINIMUM (RETURN) PRESSURE OF SUPPLY BANK =,F8.1,2X,
     34HPSIG/10X,21HPUMP CLEARANCE VOLUME,21X,1H=,F8.1,2X,7HPERCENT)
  205 FORMAT(10X,29HDURATION OF ONE PUMPING CYCLE,13X,1H=,F8.1,2X,9HMINU
     1TE(S))
  202 FORMAT(10X,38HVOLUME DISPLACED BY PUMP IN ONE MINUTE,4X,1H=,F8.1,
     12X,7HCU FEET/10X,27HPOLYTROPIC PROCESS EXPONENT,15X,1H=,F8.1/10X,
     237HTEMPERATURE OF GAS (ASSUMED CONSTANT),5X,1H=,F8.1,2X,5HDEG-F/
     310X,23HHELIUM GAS CONSTANT (R),19X,1H=,F8.1,2X,12HFT-LBF/LBM-R//)
  203 FORMAT(30X,13HGENERAL NOTES/ 17X,36HPRESSURES EXPRESSED IN PSI(ABS
     1OLUTE)/17X,39HMASS TRANSFERS EXPRESSED IN MASS POUNDS/17X,33HTIME
     2PERIODS EXPRESSED IN MINUTES//)
  777 READ(5,10)  VSTOR,VSUPLY,T,PBOTIN,PBOTFI,PSTORF,PSTORM,R                1
      READ(5,11)  CLEAR,POLY,DISPL,TIME                                       2
      WRITE(6,200)                                                            3
      WRITE(6,201) VSTOR,PSTORF,PSTORM                                        4
      WRITE(6,204) VSUPLY,PBOTIN,PBOTFI,CLEAR                                 5
      WRITE(6,205)  TIME                                                      6
      WRITE(6,202) DISPL,POLY,T,R                                             7
      WRITE(6,203)                                                            8
      WRITE(6,130)                                                            9
      WRITE(6,140)                                                           10
      TOTVOL=VSTOR+VSUPLY
      CLEAR=CLEAR/100.
      TIMSUM=0.0
      TR=T+460.
      PFINAL=PSTORF+14.7
      PTEST=PBOTIN+14.7
      ICOUNT=1
      Z=1. +3.25*10.**(-5)*(PSTORM+14.7)                                      12
      WTMIN=((PSTORM+14.7)*144.*VSTOR)/(Z*R*TR)
      ATIME(ICOUNT)=0.0
      ITYPE(ICOUNT)=0
      Z=1.+3.25*10.**(-5)*P(1)                                                16
      DENSTY(1)=(P(1)*144.)/(Z*R*TR)
      WBOTLE=DENSTY(1)*VSUPLY
      WRESDU=DENSTY(2)*VSUPLY
      WTEQU=WBOTLE-WRESDU
   50 WT2=WT2+WTEQU
      IF(WTMIN-WT2) 30,30,40
   40 PRESS1(ICOUNT)=P(1)
      PRESS2(ICOUNT)=P(2)
      PTANK(ICOUNT)=(WT2*R*TR)/(144.*VSTOR-3.25*10.**(-5)*WT2*R*TR)           22
      WTRANS(ICOUNT)=WTEQU
      ICOUNT=ICOUNT+1
      GO TO 50
C  INITIALIZATION FOR OPERATIONS.
   30 PRESS1(ICOUNT)=P(1)
      ICOUNT=ICOUNT-1
      WT2=WT2-WTEQU
      ICHECK=0
      IPRINT=0
      LOGIC=0
      ILAST=0
      WTSUM=WT2+WBOTLE
C  EQUALIZING OPERATION.
   90 ICOUNT=ICOUNT+1
      ATIME(ICOUNT)=0.0
      ITYPE(ICOUNT)=0
      P(1)=(WTSUM*R*TR)/(144.*TOTVOL-3.25*10.**(-5)*WTSUM*R*TR)               37
      PRESS2(ICOUNT)=P(1)
      PTANK(ICOUNT)=P(1)
      ZA=1.+3.25*10.**(-5)*P(1)                                               40
      WT1=(P(1)*144.*VSUPLY)/(ZA*R*TR)
      WTRANS(ICOUNT)=WBOTLE-WT1
      WT2=WT2+WTRANS(ICOUNT)
      P(2)=P(1)
```

```
C  PUMPING OPERATION.
   70 ICOUNT=ICOUNT+1
      IF(ICOUNT-51) 300,301,302
  301 CALL OUTPUT(ICOUNT,ILAST,ITYPE,PRESS1,PRESS2,WTRANS,PTANK,ATIME,TI
     1MSUM,PHOLD1,PHOLD2)                                                47
      ICOUNT=1
      GO TO 71
  300 CONTINUE
      IF(IPRINT) 302,71,304
  304 CALL OUTPUT(ICOUNT,ILAST,ITYPE,PRESS1,PRESS2,WTRANS,PTANK,ATIME,TI
     1MSUM,PHOLD1,PHOLD2)                                                53
      GO TO 305
   71 CONTINUE
      PRESS1(ICOUNT)=P(1)
      A=.67+CLEAR-CLEAR*(P(2)/P(1))**(1./PDLY)                            57
      B=(DISPL*TIME*P(1)*144.)/(ZA*R*TR)
      WTRANS(ICOUNT)=A*B
      WT1=WT1-WTRANS(ICOUNT)
      PTEMP=(WT1*R*TR)/(144.*VSUPLY-WT1*R*TR*(3.25*10.**(-5)))            60
      IF(PTEMP-PBOTFI-14.7) 20,60,60
   60 P(1)=PTEMP
      ATIME(ICOUNT)=TIME
      ITYPE(ICOUNT)=1
   61 WT2=WT2+WTRANS(ICOUNT)
      P(2)=(WT2*R*TR)/(144.*VSTOR -WT2*R*TR*(3.25*10.**(-5)))             67
      IF(P(2)-PFINAL) 99,100,100
  100 IPRINT=1
   99 CONTINUE
      IF(P(2)-PTEST) 80,81,81
   81 ICHECK=-1
   80 IF(LOGIC) 73,72,9999
   73 PTANK(ICOUNT)=P(2)
      LOGIC=0
      GO TO 62
   72 CONTINUE
      IF(ICHECK) 63,64,9999
   64 PRESS1(ICOUNT)=PRESS2(ICOUNT-1)
   63 PRESS2(ICOUNT)=P(1)
      PTANK(ICOUNT)=P(2)
      GO TO 70
   20 LOGIC=-1
      PRESS2(ICOUNT)=PBOTFI+14.7
      P(1)=PBOTIN+14.7
      PDIFF=PRESS1(ICOUNT-1)-PRESS2(ICOUNT-1)
      PDELTA=PRESS1(ICOUNT)-PRESS2(ICOUNT)
      ATIME(ICOUNT)=(PDELTA/PDIFF)*TIME
      ITYPE(ICOUNT)=1
      Z=1.+3.25*10.**(-5)*PRESS1(ICOUNT)                                  96
      WTRANS(ICOUNT)=(PRESS1(ICOUNT)*VSUPLY*144.)/(R*TR*Z)-WRESDU
      GO TO 61
   62 WTSUM=WT2+WBOTLE
      PRESS1(ICOUNT+1)=P(1)
      IF(ICHECK) 86,90,9999
   86 ZA=1.+3.25*10.**(-5)*P(1)                                           105
      WT1=(P(1)*144.*VSUPLY)/(ZA*R*TR)
      GO TO 70
  305 WRITE(6,111) TIMSUM                                                 107
      GO TO 9999
  302 WRITE(6,303)                                                        109
  303 FORMAT(/25HPROGRAM ERROR TERMINATION/)
 9999 GO TO 777
      END
```

04/23/68

OUTPUT - EFN SOURCE STATEMENT - IFN(S) -

```
      SUBROUTINE OUTPUT(ICOUNT,ILAST,ITYPE,PRESS1,PRESS2,WTRANS,PTANK,AT
     1IME,TIMSUM,PHOLD1,PHOLD2)
  121 FORMAT(I5,5X,2F8.2,2X,F8.3,2X,F10.3,2X,10HEQUALIZING,2X,F5.2)
  122 FORMAT(I5,5X,2F8.2,2X,F8.3,2X,F10.3,2X,7HPUMPING,5X,F5.2)
      DIMENSION ITYPE(50), PRESS1(50),PRESS2(50), WTRANS(50),PTANK(50)
      DIMENSION ATIME(50),PHOLD1(2),PHOLD2(2)
      ICOUNT=ICOUNT-1
      DO 120 I=1,ICOUNT
      KCOUNT=ILAST+I
      IF(ITYPE(I)) 2,2,3
    2 WRITE(6,121)KCOUNT,PRESS1(I),PRESS2(I),WTRANS(I),PTANK(I),ATIME(I)   9
      GO TO 119
    3 WRITE(6,122)KCOUNT,PRESS1(I),PRESS2(I),WTRANS(I),PTANK(I),ATIME(I)  16
  119 TIMSUM=TIMSUM+ATIME(I)
  120 CONTINUE
      ILAST=ILAST+ICOUNT
      PHOLD1(1)=PRESS1(ICOUNT)
      PHOLD2(1)=PRESS2(ICOUNT)
      RETURN
      END
```

DATA

IBLDR

UNUSED CORE 76654 THRU 77014

INPUT DATA

VOLUME OF ON BOARD STORAGE BANK	=	24.0	CU FEET
DESIGN PRESSURE OF STORAGE BANK	=	3000.0	PSIG
MINIMUM PRESSURE OF STORAGE BANK BEFORE PUMPING MAY BE INITIATED	=	200.0	PSIG
VOLUME OF SUPPLY BANK (100 BOTTLES)	=	60.0	CU FEET
INITIAL DELIVERY PRESSURE OF SUPPLY BANK	=,	3000.0	PSIG
MINIMUM (RETURN) PRESSURE OF SUPPLY BANK	=,	200.0	PSIG
PUMP CLEARANCE VOLUME	=	5.0	PERCENT
DURATION OF ONE PUMPING CYCLE	=	9.0	MINUTE(S)
VOLUME DISPLACED BY PUMP IN ONE MINUTE	=	0.6	CU FEET
POLYTROPIC PROCESS EXPONENT	=	1.6	
TEMPERATURE OF GAS (ASSUMED CONSTANT)	=	70.0	DEG-F
HELIUM GAS CONSTANT (R)	=	386.3	FT-LBF/LBM-R

GENERAL NOTES
PRESSURES EXPRESSED IN PSI(ABSOLUTE)
MASS TRANSFERS EXPRESSED IN MASS POUNDS
TIME PERIODS EXPRESSED IN MINUTES

OPER. COUNT	BOTTLE PRESSURE FROM	TO	MASS TRANSFERED	TANK PRESSURE	OPERATION	TIME
1	3014.70	2094.72	33.105	2094.718	EQUALIZING	0.
2	2094.72	1970.17	4.625	2410.262	PUMPING	9.00
3	1970.17	1855.06	4.306	2709.567	PUMPING	9.00
4	1855.06	1748.48	4.014	2993.465	PUMPING	9.00
5	1748.48	1649.66	3.745	3262.734	PUMPING	9.00

TOTAL TIME OF TRANSFER = 36.00 MINUTES

INPUT DATA

VOLUME OF ON BOARD STORAGE BANK	=	24.0	CU FEET
DESIGN PRESSURE OF STORAGE BANK	=	3000.0	PSIG
MINIMUM PRESSURE OF STORAGE BANK BEFORE PUMPING MAY BE INITIATED	=	200.0	PSIG
VOLUME OF SUPPLY BANK (100 BOTTLES)	=	50.0	CU FEET
INITIAL DELIVERY PRESSURE OF SUPPLY BANK	=,	3000.0	PSIG
MINIMUM (RETURN) PRESSURE OF SUPPLY BANK	=,	200.0	PSIG
PUMP CLEARANCE VOLUME	=	5.0	PERCENT
DURATION OF ONE PUMPING CYCLE	=	9.0	MINUTE(S)
VOLUME DISPLACED BY PUMP IN ONE MINUTE	=	0.6	CU FEET
POLYTROPIC PROCESS EXPONENT	=	1.6	
TEMPERATURE OF GAS (ASSUMED CONSTANT)	=	70.0	DEG-F
HELIUM GAS CONSTANT (R)	=	386.3	FT-LBF/LBM-R

GENERAL NOTES
PRESSURES EXPRESSED IN PSI(ABSOLUTE)
MASS TRANSFERS EXPRESSED IN MASS POUNDS
TIME PERIODS EXPRESSED IN MINUTES

OPER. COUNT	BOTTLE PRESSURE FROM	TO	MASS TRANSFERED	TANK PRESSURE	OPERATION	TIME
1	3014.70	1974.23	31.316	1974.225	EQUALIZING	0.
2	1974.23	1833.96	4.375	2270.364	PUMPING	9.00
3	1833.96	1706.10	4.021	2547.296	PUMPING	9.00
4	1706.10	1589.31	3.700	2806.296	PUMPING	9.00
5	1589.31	1482.43	3.410	3048.545	PUMPING	9.00

TOTAL TIME OF TRANSFER = 36.00 MINUTES

INPUT DATA

VOLUME OF ON BOARD STORAGE BANK	=	24.0	CU FEET
DESIGN PRESSURE OF STORAGE BANK	=	3000.0	PSIG
MINIMUM PRESSURE OF STORAGE BANK BEFORE PUMPING MAY BE INITIATED	=	200.0	PSIG
VOLUME OF SUPPLY BANK (100 BOTTLES)	=	80.0	CU FEET
INITIAL DELIVERY PRESSURE OF SUPPLY BANK	=,	3000.0	PSIG
MINIMUM (RETURN) PRESSURE OF SUPPLY BANK	=,	200.0	PSIG
PUMP CLEARANCE VOLUME	=	5.0	PERCENT
DURATION OF ONE PUMPING CYCLE	=	9.0	MINUTE(S)
VOLUME DISPLACED BY PUMP IN ONE MINUTE	=	0.6	CU FEET
POLYTROPIC PROCESS EXPONENT	=	1.6	
TEMPERATURE OF GAS (ASSUMED CONSTANT)	=	70.0	DEG-F
HELIUM GAS CONSTANT (R)	=	386.3	FT-LBF/LBM-R

GENERAL NOTES
PRESSURES EXPRESSED IN PSI(ABSOLUTE)
MASS TRANSFERS EXPRESSED IN MASS POUNDS
TIME PERIODS EXPRESSED IN MINUTES

OPER. COUNT	BOTTLE PRESSURE FROM	TO	MASS TRANSFERED	TANK PRESSURE	OPERATION	TIME
1	3014.70	2267.73	35.652	2267.726	EQUALIZING	0.
2	2267.73	2166.00	4.980	2611.402	PUMPING	9.00
3	2166.00	2070.31	4.713	2943.275	PUMPING	9.00
4	2070.31	1980.20	4.463	3263.713	PUMPING	9.00

TOTAL TIME OF TRANSFER = 27.00 MINUTES

3 APOLLO PLSS – ENVIRONMENTAL CONTROL OF THE "SMALLEST MANNED SPACE VEHICLE"

John C. Beggs and Fred H. Goodwin
Space Systems Department, Hamilton Standard,
Windsor Locks, Conn.

INTRODUCTION

The environmental control system for the "smallest manned space vehicle" had its beginning in October 1962 when NASA awarded Hamilton Standard a contract for development and production of a portable life support system (PLSS) and associated backup equipment for supporting an astronaut working outside of the lunar module (LM) either in space or on the lunar surface. This paper describes the system, outlines the philosophy behind its design, covers the basic requirements imposed on the system, and discusses some of the evolutionary process that led to the present configuration.

DESIGN PHILOSOPHY

Aside from obvious size, weight, and capacity differences of the equipment, the most significant difference between the PLSS and the aircraft environmental control systems with which Hamilton Standard has been involved for many years is the extreme emphasis on system reliability. The very nature of the lunar mission with the attendant hazards to the astronauts, worldwide attention, and involvement of national prestige produced an unprecedented emphasis on achieving a highly reliable system.

Thus, the design philosophy was to devise a system of utmost simplicity using ample performance margins with built-in redundancy, where required, to achieve the desired high system reliability. At the beginning of the design program, reliability targets of 0.99956 for the mission success, and 0.99995 for crew safety were established. To appreciate these numbers, consider that no more than 440 failures of a type that compromises complete accomplishment of mission objectives are allowed per million missions; only 50 failures of a type that would compromise the safety of the astronaut are permitted per million missions. Mathematical models were established and, on the basis of statistical data on the various components required to fabricate the system, a predicted reliability was calculated as an aid to component selection and system design.

These demanding reliability objectives required the basic environmental control system concept to be as simple as possible. A very deliberate attempt was made to reduce the number of moving parts as well as minimize the total number of parts. Where possible, processes were accomplished with static devices.

Examples of this are the components used for heat rejection and removal of excess water from the ventilation loop. The sublimator, which is a special type of boiler described in greater detail in the last section, is free of any moving parts and automatically reacts to a wide range of heat loads. It replaced the original plate-fin wick-fed boiler and back pressure control valve used in the first PLSS. The water separator is likewise free from any moving parts; an elbow in the flow

path induces an artificial gravity field and capillary action principles are used in trapping the water and pumping it to a storage area outside the ventilation loop.

Except for a few cases in electrical or electronic devices, redundancy is not employed within the PLSS. Overall redundancy is provided by the oxygen purge system (OPS) and buddy secondary life support system (BSLSS), which substitute for the functions normally provided by a PLSS in case of a significant malfunction. Great emphasis was placed on conservative design of the primary system components so that there is high confidence in the structural integrity of the unit and the margin of performance is great relative to absolute performance requirements.

BASIC REQUIREMENTS

To provide a suitable protective environment outside the LM during lunar surface excursions, the astronaut carries on his back a compact assembly of various environmental control devices that, when joined together, form the PLSS (see fig. 3.1). This package supplies the man with breathing oxygen, controls suit pressure, reprocesses the recirculated gas by removing carbon dioxide, odors, some trace contaminant gasses, and excess moisture, controls system temperature by rejecting excess heat, and provides for warnings of certain malfunctions, voice communication, and telemetry of essential data. The heat rejection system must accommodate, in addition to the metabolic load and heat generated by the functioning PLSS components, heat gained from or lost to the lunar environment through the system insulation. Table 3.1 presents a comparison of the initial requirements, requirements for the PLSS used on Apollo 11 through 14, and requirements for an extended life version of the PLSS that will be used for Apollo 15, 16, and 17.

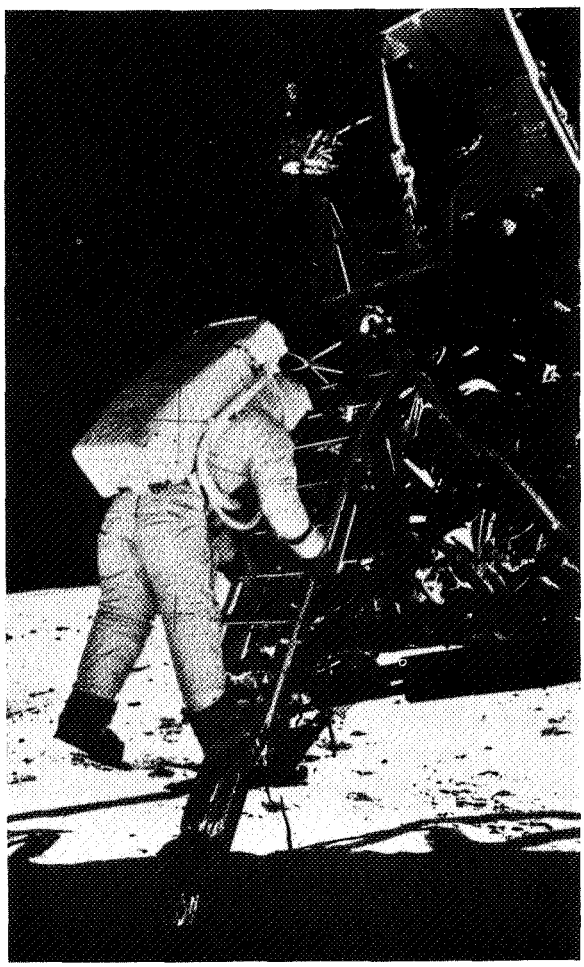

Figure 3.1 *Apollo 11 using -6 PLSS and OPS.*

An emergency oxygen supply, currently the OPS, can be manually actuated to supply breathing oxygen, control suit pressure, remove contaminants, and cool the astronaut in the event these functions in the PLSS are impaired. A high oxygen flow is introduced directly into the oro-nasal area and dumped overboard through a suit-mounted purge valve.

An umbilical assembly called the BSLSS enables two astronauts to share the liquid cooling capacity of a single PLSS should the other become disabled.

Multiple extravehicular activities (EVAs) are planned for each mission. Therefore, provisions for recharging PLSS expendables such as oxygen, water, contaminant removal cartridges, and power supplies from the LM are made. There is no requirement to recharge the OPS.

Table 3.1 *System requirements.*

Requirement	*Gas-cooled PLSS*	*Liquid Cooled PLSS* -5^a *and* -6^b	-7^c
Average metabolic load	930 Btu/hr	1600 Btu/hr	1600 Btu/hr
Peak metabolic load	1600 Btu/hr	2000 Btu/hr	2000 Btu/hr
Maximum heat leak in	250 Btu/hr	250 Btu/hr	300 Btu/hr
Maximum heat leak out	250 Btu/hr	250 Btu/hr	350 Btu/hr
Maximum CO_2 partial pressure	7.6 mm Hg	15 mm Hg	15 mm Hg
PGA pressure	3.5 and 5.0 psia	3.85 psia	3.85 psia
Ventilation flow	18 cfm	5.5 cfm	5.5 cfm
Duration	4 hr at 930 Btu/hr	4 hr at 1200 Btu/hr 3 hr at 1600 Btu/hr	6 hr at 1200 Btu/hr 5 hr at 1600 Btu/hr
O_2 Charge pressure at 70° F	950 psia	1020 psia	1410 psia
Battery capacity	290 W - hr	279 W - hr	360 W - hr
Emergency O_2	*EOS*	*OPS*	
Duration	5 min	30 min	
Maximum flow	2 lb/hr	8 lb/hr	
PGA pressure	3.45 psia	3.7 psia	

[a]Configuration used on Apollo 9 and 10
[b]Configuration used on Apollo 11 through 14
[c]Configuration to be used on Apollo 15 through 17

The combination of these major subsystems with the pressure garment assembly (PGA), or suit as it is commonly called, creates, in effect, a miniature personalized space vehicle that has basically all of the elements for sustenance of life that are found in the Command Module or LM. In fact, for short mission durations, one would merely have to add some form of propulsion and a guidance and stabilization system to have a space vehicle in every sense of the word.

SYSTEM DESCRIPTION

Figure 3.2 is a schematic of the liquid transport PLSS. Gas enters the suit ventilation distribution system and picks up heat, moisture, and metabolic byproduct contaminants as it passes through the suit adjacent to the man's body. This warm, moist, contaminated gas is then transported to a contaminant control package, which consists of an activated charcoal bed for absorption of trace contaminant gasses, and a lithium hydroxide bed, which reacts with carbon dioxide to form lithium carbonate. Byproducts of this chemical reaction are heat and moisture, which are added to that already carried by the recirculating gas stream. The gas stream then enters a heat exchanger where the heat is given up, and the excess moisture in the stream is condensed. Upon leaving the heat exchanger, or sublimator, as it is called, free water is removed from the gas stream by an elbow water separator, and transferred to the backside of the sublimator feedwater reservoir diaphragm. The stream then goes to a centrifugal fan that supplies the energy for overcoming the pressure drop in the PGA-PLSS system. The fan is driven by an electric motor that draws its power from a silver-zinc battery. Some heat is added to the stream because of fan

inefficiency. After passing through a back flow check valve, the cooled, dried, decontaminated gas is returned to the suit for recycling.

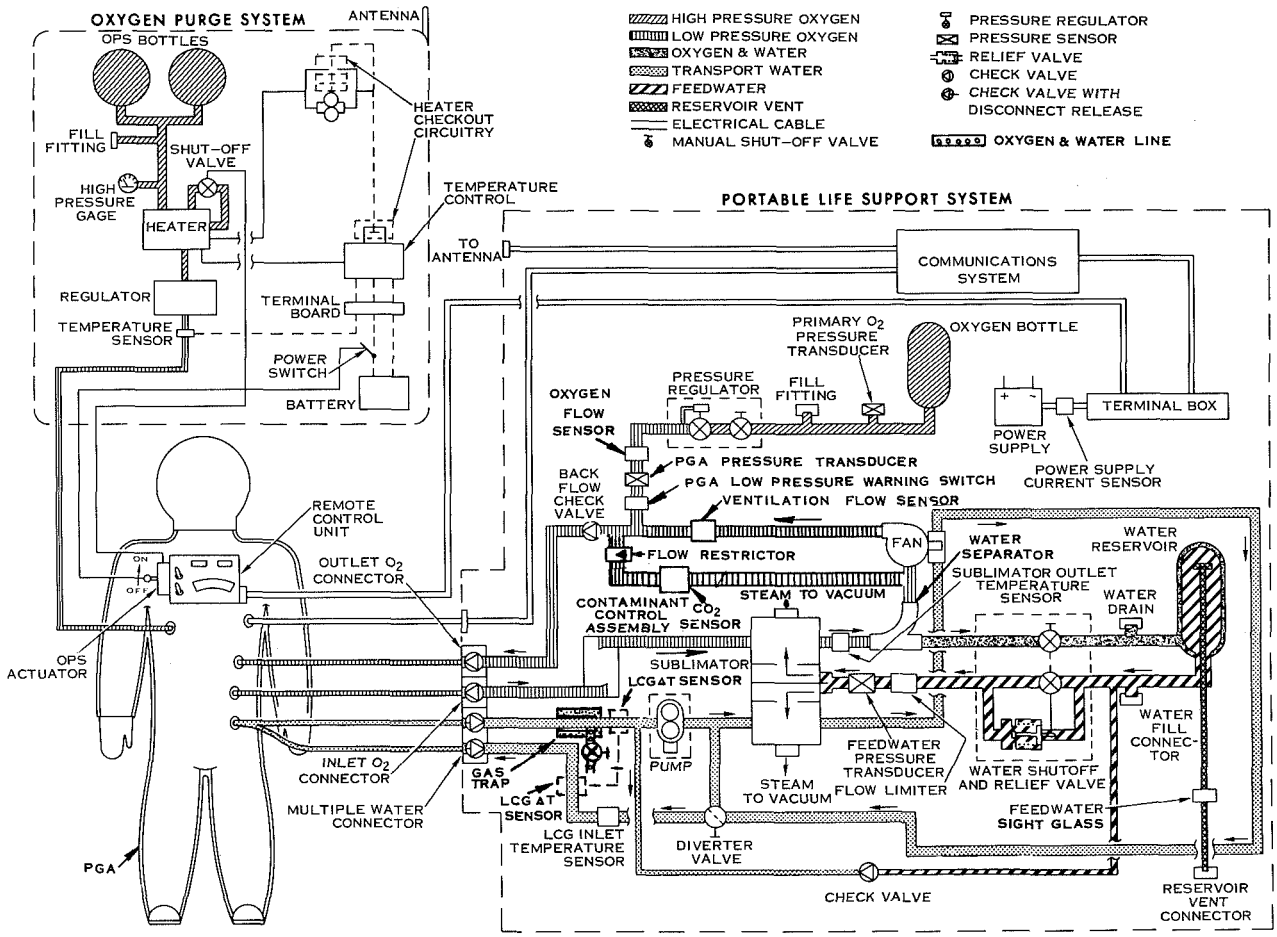

Figure 3.2 *Schematic of –6 PLSS and OPS (with heater).*

Pure gaseous oxygen is stored in a tank and admitted to the suit to make up for leakage losses and metabolic consumption. The single-stage in-flow pressure regulator maintains a suit pressure level of approximately 0.25 atm. Recirculation of oxygen is limited to that required for proper carbon dioxide purging from the helmet and defogging of the visor.

The liquid transport loop is very simple, consisting of a small pump, a set of heat exchange passages within the sublimator, a manually positioned diverter valve for controlling the temperature of the transport water circulated through the suit, and a gas separator to ensure that only water is circulated through the system. Water is circulated through a special plastic tubing heat exchanger/undergarment called the liquid cooling garment (LCG) for transporting heat from the man to the sublimator.

A communications system provides for voice communication and telemetry transmission of performance parameters. Instrumentation is limited to essential parameters that it is felt must be monitored during actual use by either Mission Control at the Manned Spacecraft Center (MSC) or by the astronaut himself. Ten channels of data are telemetered back to earth via a relay

system aboard the LM. These data permit comparison of real time mission performance of the PLSS with performance previously recorded during manned simulation tests conducted at MSC during preparations for the flight. The parameters telemetered are: primary oxygen tank pressure; PGA pressure; sublimator outlet temperature; LCG inlet temperature; LCG ΔT (inlet to outlet of transport water); feedwater pressure; carbon dioxide partial pressure; and battery voltage and battery current drain. In addition to the above nine, electrocardiogram (EKG) signals are telemetered, permitting monitoring of the physiological state of the astronaut.

The remote control unit (RCU), which is mounted on the chest of the PGA, houses electrical controls for the PLSS, primary oxygen quantity indicator, and visual warning devices; it also serves as an anchor point for a camera bracket and the OPS actuator mechanism. The controls are: fan on-off switch, pump on-off switch, push-to-talk switch (which can override the voice-operated switch normally used in the communication system), communication system volume control, and a communication system mode selector switch. An audible warning signal is given to the astronaut if certain parameters fall outside desired limits, and visual identification of the problem is given by small "flags" or indicators on the RCU. Warnings are sounded for low feedwater pressure, low ventilation flow, low PGA pressure and high oxygen flow.

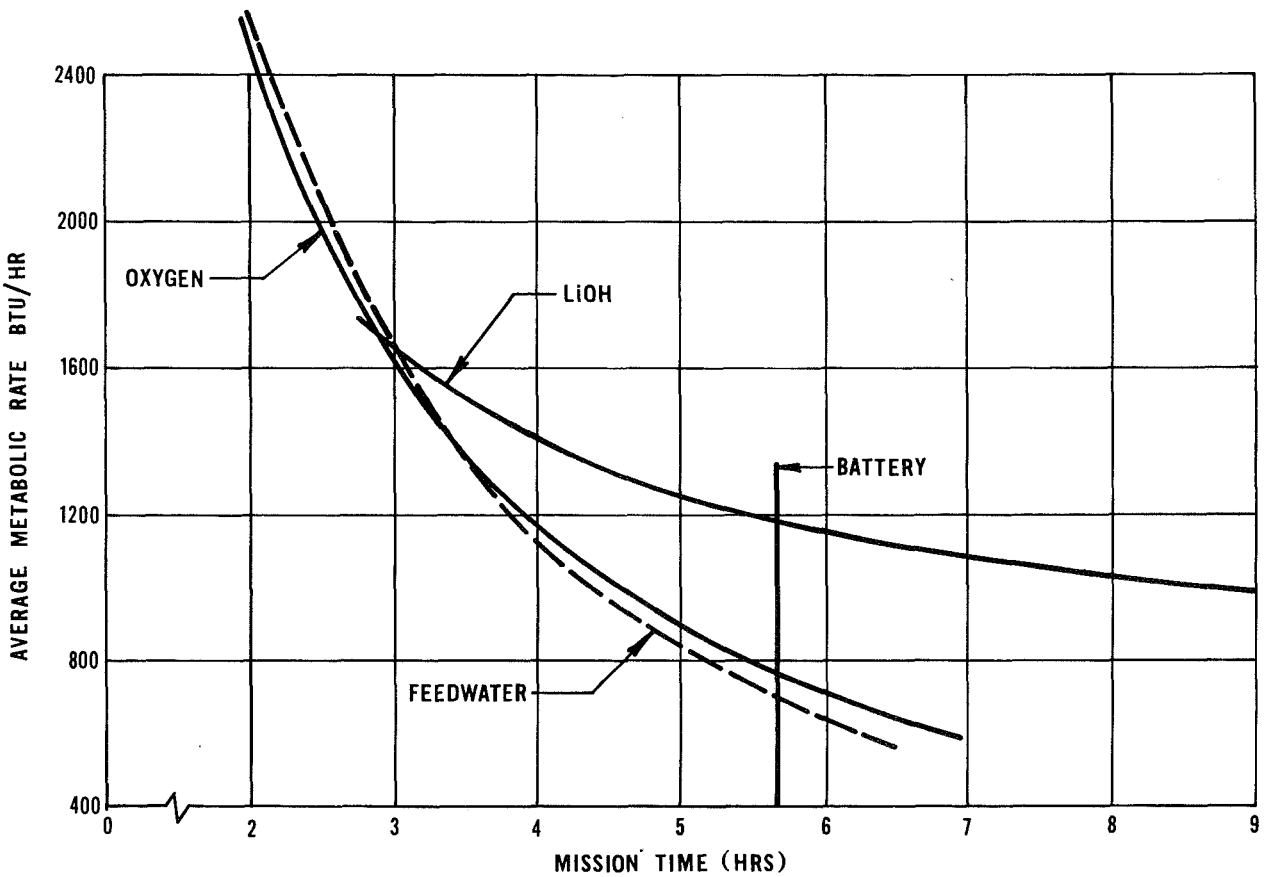

Figure 3.3 *Expendable duration of -6 PLSS.*

Figure 3.3 shows the performance of the -6 PLSS, which was used for all lunar surface missions through Apollo 14, in terms of the duration of the various expendables as affected by

the average metabolic rate of the astronaut. All curves shown are based on worst case conditions (suit leakage, thermal environment, etc.) and represent the duration left after all pre-egress checkouts have been completed. Under conditions normally encountered in actual missions, the curves are displaced to the right. For example, if the specified PLSS/PGA gas leakage was reduced to zero, the duration of the oxygen supply at an average metabolic rate of 1200 Btu/hr would increase by about 0.8 hr. Similarly, if the external heat leak was eliminated the feedwater saved would also increase the EVA duration at an average metabolic rate of 1200 Btu/hr by about 0.8 hr. In the -6 PLSS, these two expendables, oxygen and feedwater, have the most limited duration.

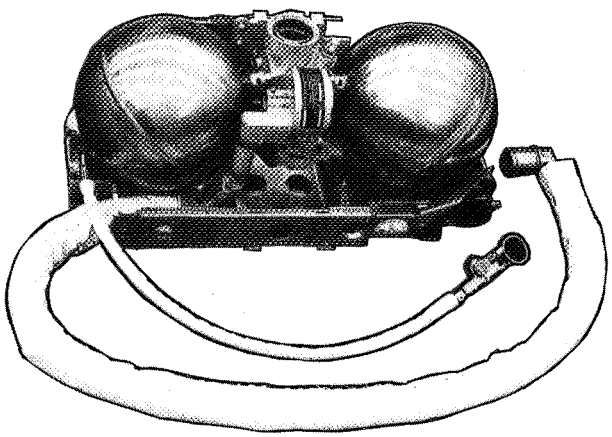

Figure 3.4 *OPS without protective cover and insulation.*

The OPS, shown in figure 3.4 without the protective fiberglas cover and insulation, consists of a pair of spherical tanks that hold 5.8 lb of pure gaseous oxygen at 5800 psi, a shut-off valve that is manually operated by means of a flexible cable and actuator lever assembly, and a single-stage in-flow pressure regulator that regulates PGA pressure to approximately 1/4 atm. A gage indicates the tank pressure level. A second low-range gage, along with a fixed orifice, is used to test for proper regulator performance. Both tank pressure and regulator performance are checked before committing to an EVA. The fold-down ribbon antenna for the communications system is mounted on top of the OPS.

The OPS can be utilized in three ways:

1. It can serve as a replacement for the primary oxygen supply with the remaining PLSS functions continuing normally.
2. With the "purge" valve in the PGA set on "low," 4 lb/hr of oxygen can be passed through the PGA to remove carbon dioxide and humidity with liquid cooling supplied by the BSLSS or PLSS.
3. With the "purge" valve in the PGA set on "high," 8 lb/hr can be passed through the PGA to remove carbon dioxide and provide cooling when completely independent of the PLSS.

Although normally mounted on top of the PLSS, the OPS can be mounted independently against the back of the helmet or against the abdomen for special zero G missions where the PLSS is not required.

The BSLSS (fig. 3.5) consists of a pair of water umbilical hoses with a standard connector on one end and a special divider connector at the other. A tether strap, two snap hooks, and an insulation sheath complete the assembly. If one crewman's PLSS water cooling capacity is impaired or lost, he disconnects the normal PLSS water umbilical and connects the standard connector end of the BSLSS to his suit. The other crewman, whose PLSS is still functioning normally, disconnects his PLSS water umbilical, attaches the divider connector to his PGA, and reconnects the PLSS water umbilical to the other side of the divider connector. The transport water flow from the functioning PLSS is now shared by the two crewmen. The tether hooks are attached to the PGA walls so that the tether relieves the water hoses of any strain.

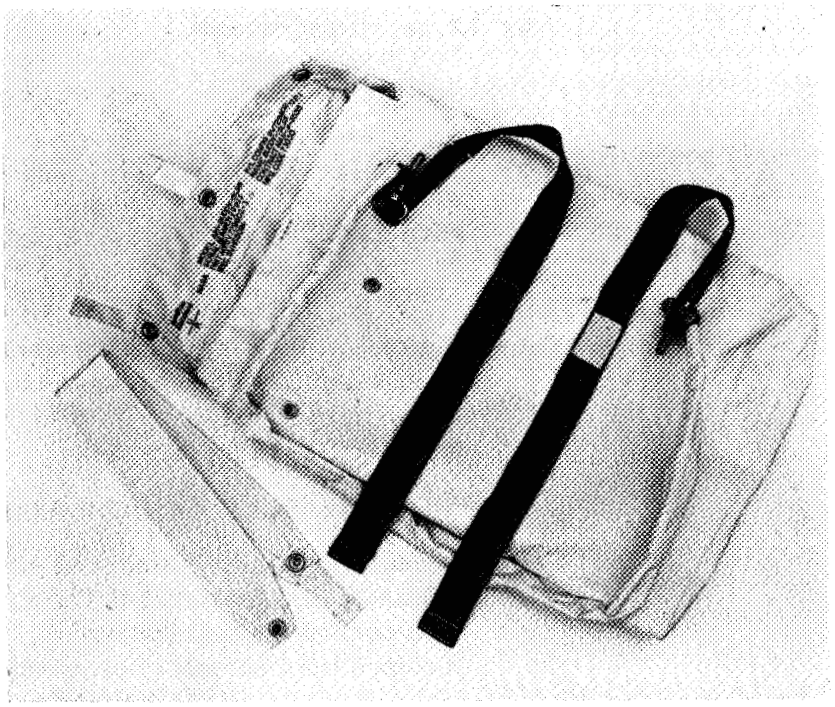

Figure 3.5(a) *BSLSS container.*

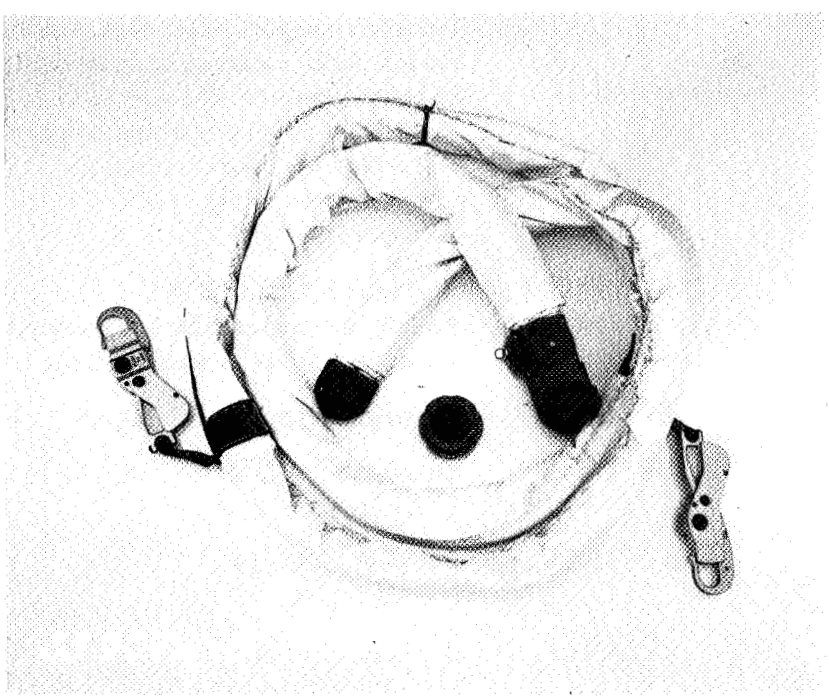

Figure 3.5(b) *BSLSS umbilical hoses.*

Table 3.2 *System configurations.*

Hardware Item	*Part Number*	*Configuration or Changes*
Gas-cooled PLSS	SV585200	n/a
Liquid-cooled PLSS	SV594750	First prototype water cooled system
	SV706100-1	Revised envelope for vehicle stowage Increased duration and heat rejection specification Added instrumentation Incorporated arde oxygen tank
	SV706100-2	Altered complete PLSS electrical system
	SV706100-3	Added H_2O quantity sensor and other instrumentation Relocated EOS from PGA to PLSS Incorporated Whittaker pump Incorporated space suit communications
	SV706100-4	Enlarged H_2O separator Deleted H_2O quantity sensor Incorporated blade antenna
	SV706100-5	Added back flow check valve to vent loop Deleted transport water accumulator Added check valves to Gas connectors Extensive material changes Changed to hi-rel electronic components Added further instrumentation Changed from EOS to OPS Incorporated RCU
	SV706100-6	Replaced SSC with EVCS Added instrumentation and controls Incorporated visual warning flags
	SV706100-7	Increased expendable duration
EOS	SV585115	Two-stage regulator Spherical tank
	SV594200	One-stage regulator Toroidal tank
OPS	SV730101-1	One-stage regulator Two large spherical tanks Heater, battery, and electronic controller
	SV730101-3	Deleted heater, battery, and electronic controller

SYSTEM EVOLUTION

Evolution of the PLSS and emergency oxygen provisions was marked by several changes that resulted from a better appreciation of equipment capability, significant changes in the state-of-art of available equipment, revised mission performance requirements, additional or revised instrumentation and warning system requirements, revised fire safety standards for materials in the presence of oxygen, and improved knowledge of man's requirements and physical limitations. Implementation of the above resulted in eight major configuration changes of the PLSS and three major configuration changes of emergency oxygen systems. Table 3.2 identifies these configurations and their significant differences.

Revisions in the specified metabolic heat rejection rate had the greatest amount of influence on changing the physical makeup of the PLSS. The original requirement for metabolic heat rejection was an average rate of 930 Btu/hr and a peak rate of 1600 Btu/hr. It has been traditional to cool personnel in aircraft by means of gas ventilation systems that carry heat from the generating source to the rejection device by means of a rise in temperature of the ventilating gas (sensible means) or an increase in the absolute humidity of the ventilating gas due to evaporation of available moisture (latent means). This approach was used on the Mercury, Gemini, Apollo command module, and Apollo lunar module vehicles, and was considered appropriate for the original PLSS (figs. 3.6 and 3.7). A limitation of this approach is that the sensible capacity of the ventilating gas is quite small, because of limited flow due to fan power considerations and the small differential between the minimum practical heat exchanger outlet temperature and the allowable maximum skin surface temperature. Assuming the oxygen pressure level to be approximately 3.7 psia and a maximum temperature rise of 45° F, the sensible capacity of the ventilating stream is approximately 9.9 Btu/lb-hr. The original specification allowed a maximum heat leak into the system through suit and PLSS walls of 250 Btu/hr. Since the practical ventilation rate was limited to about 18 lb/hr, the sensible capacity is only about 180 Btu/hr; it is apparent that the bulk of the metabolic heat transport relied on the latent capacity of the ventilation stream. Thus, the average heat rejection of 930 Btu/hr would require a sweat production of at least 3.5 lb for a 4-hr mission. Practically speaking, even more sweat would have to be produced since it is extremely difficult to get distribution of ventilation flow within the suit in such a manner that all of the sweat produced by the body is actually evaporated and carried by the ventilation gas. Sweat not evaporated contributes to dehydration without accomplishing any cooling. Dehydration in excess of 2 percent of body weight is a significant physiological strain on the astronaut.

Since studies indicated that the lunar surface EVA metabolic load might average 1200 Btu/hr over a 4-hr span or 1600 Btu/hr over a 3-hr span with peaks of 2000 Btu/hr, it was apparent that the capacity of the gas ventilation system, considering the limitations of the man, would be exceeded. Therefore, NASA directed that the system be revised to handle the above average loads. Subsequent experience showed just such difficulties were encountered in Gemini EVAs where the rate of metabolic heat generated in zero G maneuvers severely tested the ability of the umbilical ventilation system to carry away the heat produced. Studies were made of new heat transport techniques and new heat rejection devices. In the earlier system, the ventilation gas carried heat from the point of generation to the heat rejection device, which was a plate-fin wick-filled boiler. All of the water required for rejecting heat to space by boiling was carried in the wick reservoir. The temperature at which boiling occurred was controlled by a back pressure valve in the steam duct leading overboard to space vacuum. This valve was actuated by the expansion and contraction of a small quantity of a special wax mixed with metal particles that exhibited a very high rate of volume change with temperature. The valve was adjusted so that

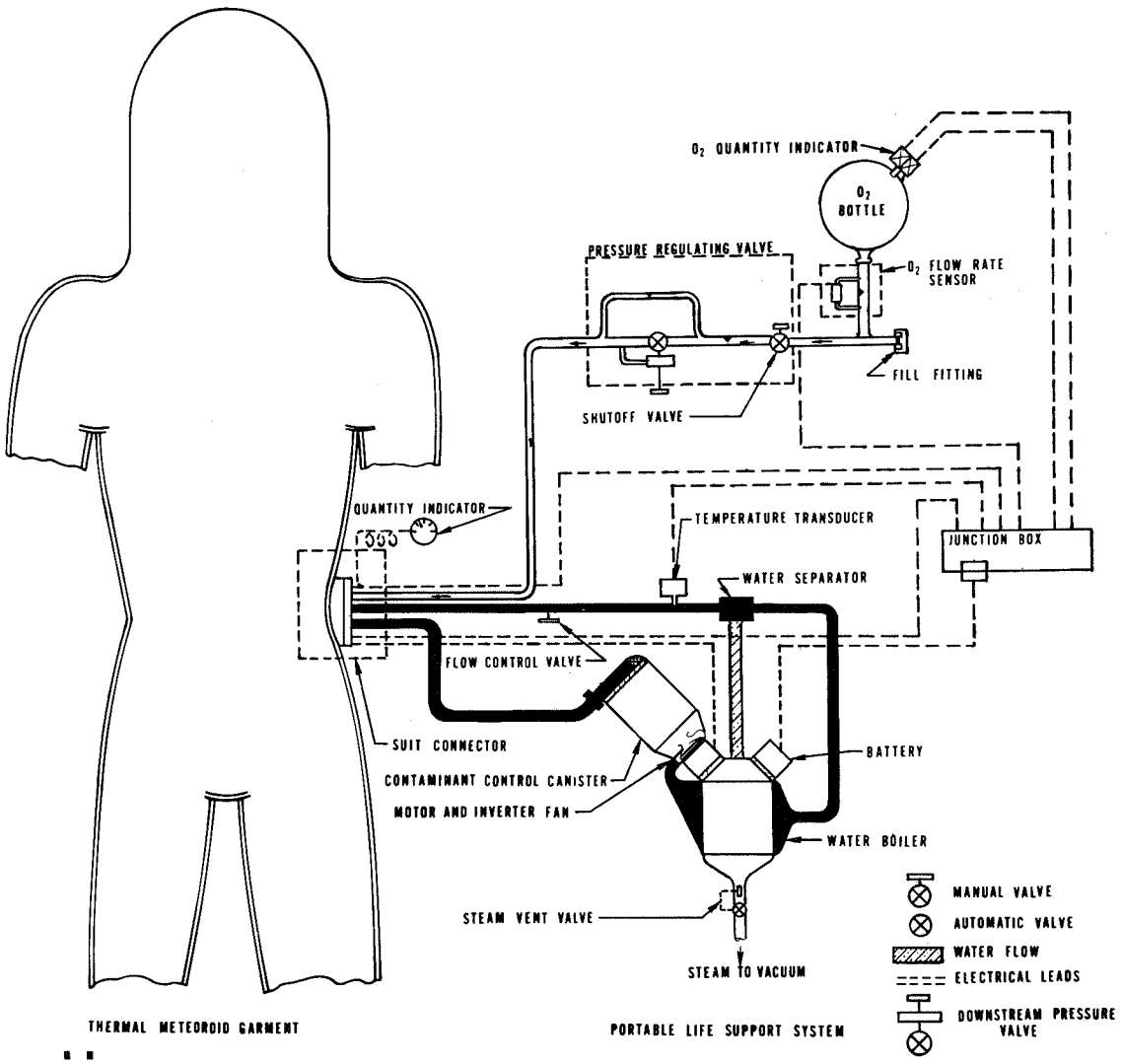

Figure 3.6 *Original PLSS.*

the temperature at which boiling occurred was maintained in the 35° to 50° F range. If the rate of heat rejection increased, the rate of steam production would increase and cause a rise in pressure and consequently elevate the boiling temperature. The temperature-sensitive valve would then respond by opening. The reverse would be true for a reduction in heat rejection rate.

In the system used at present, the ventilating gas still serves to transport a limited amount of heat, but a water loop is introduced for the express purpose of transporting metabolic heat sensibly rather than latently. A special undergarment, called the liquid cooling garment, was devised to form, in effect, a plastic tubing heat exchanger. It is worn against the astronaut's body surface. Water is recirculated at about 4 lb/min through a network of tubing distributed over the body surface roughly in proportion to the body mass, from the wrist and ankle of the limbs, to the neck on the upper torso. Heat is transferred from the astronaut's skin through the tubing wall into the water, which carries it to the sublimator in the PLSS. The large sensible capacity of water permits the 4-lb/min flow to carry the maximum design load of 2000 Btu/hr with a temperature rise of only 8.3° F. The astronaut's skin temperature can be held sufficiently low to inhibit sweating.

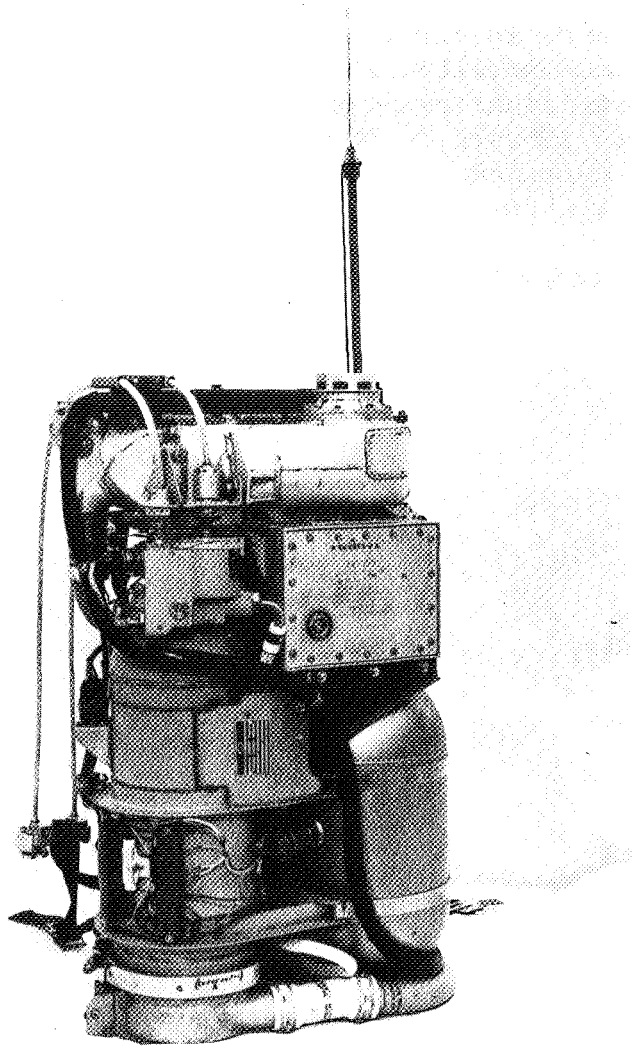

Figure 3.7 *Gas-cooled PLSS without protective cover and insulation.*

Hamilton Standard's independent development work on a new type of space heat exchanger called a sublimator showed improvements of about 30 percent more Btu/hr heat rejection per pound of equipment and about 40 percent greater Btu/hr heat rejection per unit of volume over the earlier wick-fed, plate-fin boiler. The first application of this new concept was its very successful use in cooling Saturn 1B and Saturn 5 booster vehicle instrumentation packages. Since the original PLSS boiler only had a ventilating gas loop, the addition of the water transport loop made redesign of the heat rejection device mandatory. Therefore, it was decided to take advantage of the improved performance offered by the sublimator. It contains flow paths for both the ventilating gas and the transport water. Adjacent to the plates that form the walls of these passages are sintered nickel plates having very fine pores. One side of the porous plate is exposed to vacuum; the cavity between the other side of the porous plate and the transport fluid

passage plate is filled with water under slight pressure. The slight pressurization is derived from internal suit pressure. This "feedwater" is carried in a reservoir in sufficient quantity to satisfy all heat rejection requirements. As the feedwater exudes through the pores of the sintered plate it freezes when coming to the vacuum side and forms, in effect, a seal against feedwater loss. Heat, transferred from the gas path, or transport water path, is carried via fins and through the feedwater to the porous metal plate. The rate of sublimation of the ice formed on the porous plate is a direct function of the amount of heat carried to the sublimator by the transport fluids. This system is entirely self-regulating. It requires no valving to control the amount of feedwater admitted to the sublimation section, nor does it require a temperature-sensitive or pressure-sensitive valve to maintain a controlled pressure in the boiling chamber for temperature control.

The prototype of the new PLSS, utilizing the water transport and sublimator concept is shown in figure 3.8.

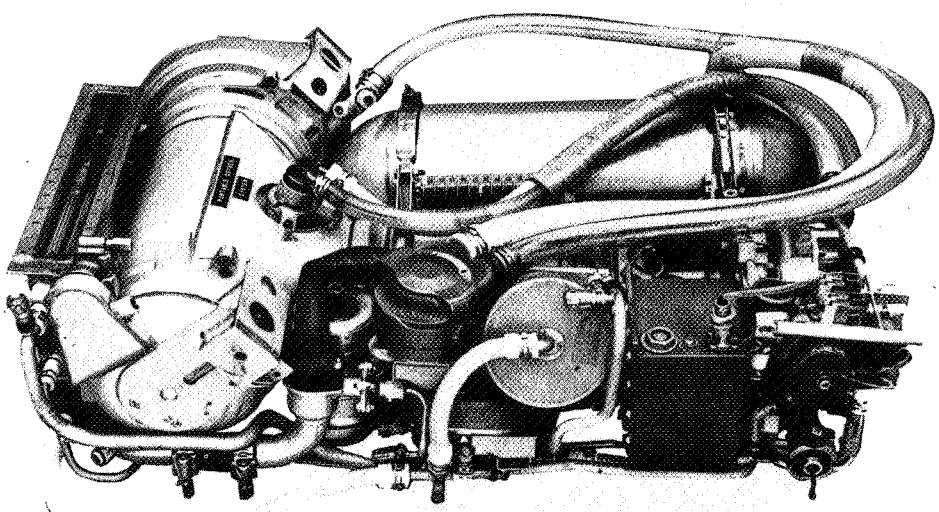

Figure 3.8 *Prototype liquid-cooled PLSS.*

The state-of-art in high-pressure oxygen tanks was advanced in the PLSS program. Tanks used on the first PLSS, built in 1963, were constructed of heat-treated AISI 4130 alloy steel with a protective coating of electroless nickel to prevent corrosion. Considerable difficulty was encountered in obtaining a satisfactory protective coating on the inside tank surface. Inspection techniques were quite difficult and, because of the lack of assurance of a satisfactory continuous coating of electroless nickel, frequent inspection was necessary to ensure that no degradation of the inner surface occurred in the presence of small amounts of moisture and pure oxygen.

At that time, the Ardé Corporation was engaged in developing a process that showed promise of achieving excellent high strength characteristics in a material having inherently high corrosion resistance in the presence of pure oxygen. Consequently, a subcontract was awarded to them for development of a tank for the PLSS.

Basically, the Ardé manufacturing process involves stretch forming a semifinished tank of a special grade of AISI 301 stainless steel to a finish die by pressurizing it with liquid nitrogen.

The resultant work hardening of the material at the very low temperature gives excellent unaged physical properties; for example, the ultimate tensile strength for design purposes is 240 KSI compared to about 180 KSI for the heat treated AISI 4130.

Recent work indicates that still higher design strengths could be safely used if the material is aged after cryogenically stretching, although unaged material is used in PLSS tanks for conservatism. With proper design, tanks could be based on an ultimate tensile strength of 290 KSI.

Another interesting example of state-of-art advancement in the PLSS is the small pump used to recirculate coolant water through the LCG and PLSS. This development was aimed at minimizing the amount of power consumed so that the battery, which is one of the heavier and more bulky of the components, could be reduced in both size and weight. The initial concepts for pumping the coolant flow were based on centrifugal pumping principles. The basic difficulty was that the efficiency of a centrifugal machine for the small flow and low head requirement was unacceptably low. When it was determined that the Whittaker Corporation was in the process of developing a small diaphragm pump, they were contracted to develop a model meeting PLSS requirements. The concept of the pump is quite interesting. Two small diaphragms are located at the end of a walking beam which is supported by a torsion rod. Inlet and outlet valves are provided for each diaphragm chamber. Part of the walking beam structure is a magnetic armature that can be moved in one or the other direction by an electromagnetic field causing the walking beam to displace the diaphragms. The electromagnetic field polarity can be reversed by an electronic control at a frequency chosen to nearly coincide with the natural frequency of the spring mass system supported by the torsion bars. Properly tuning the driving frequency to that of the resonance of the system, significantly reduces electrical input power for a given pumping load. This pump requires about 10 W input power to pump 4 lb/min with a head of 5.65 lb/sq in. Equivalent performance by the centrifugal machine required 30 W of input power.

The original liquid PLSS was designed to accommodate one extravehicular astronaut. Early in 1967, NASA established the requirement for two extravehicular astronauts. For a dual EVA, the communications system that existed at that time [space suit communications (SSC) system] provided for voice communications of both astronauts plus telemetry transmission of either astronaut but not both simultaneously. Furthermore, extravehicular activity was limited to line of sight between the LM and the astronauts if communications with earth were to be maintained. Consequently, a new communications system, named the extravehicular communications system (EVCS), was designed and incorporated into the PLSS. The EVCS provides the following additional capability: continuous telemetry data relayed to earth simultaneously from both astronauts; additional telemetry channels; line of sight limitation for extravehicular exploration eliminated for one astronaut (the other astronaut's communication system serves as a relay station to the LM); and greater output power to increase the operating range from the LM.

Three emergency oxygen systems were developed or qualified during the program. The first and second configurations, called the emergency oxygen system (EOS) shown on figure 3.9, are extremely simple schematically (see fig. 3.10) and performed identical functions. Both units provided for a 5-min emergency flow at 2 lb/hr but the later configuration, which used a single-stage pressure regulator nested in a toroidal tank rather than a 2-stage regulator and sperical tank, reduced the volume to one-third, and the weight to two-thirds of the original configuration.

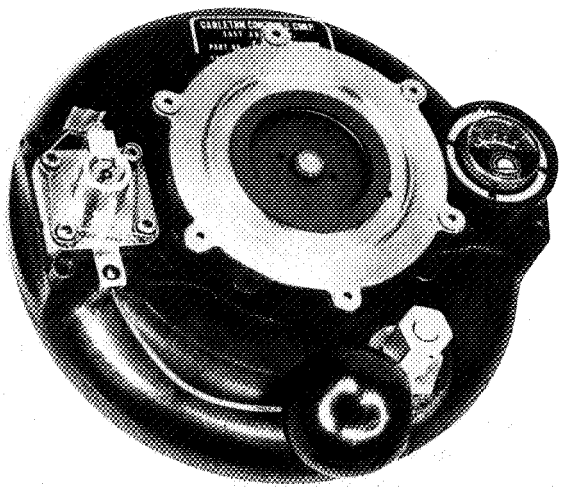

Figure 3.9(a) *EOS single-stage configuration.*

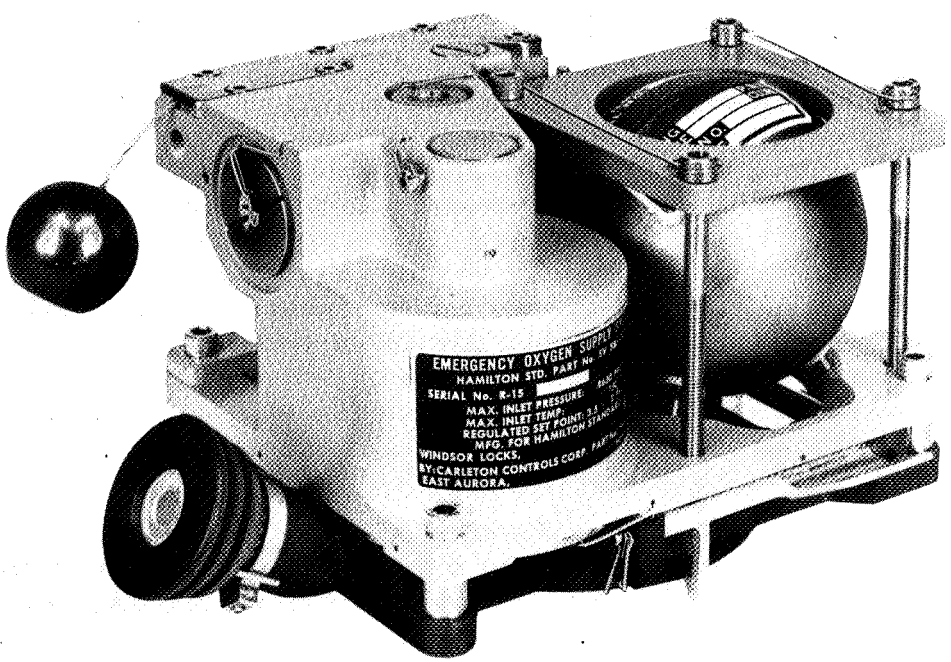

Figure 3.9(b) *EOS two-stage configuration.*

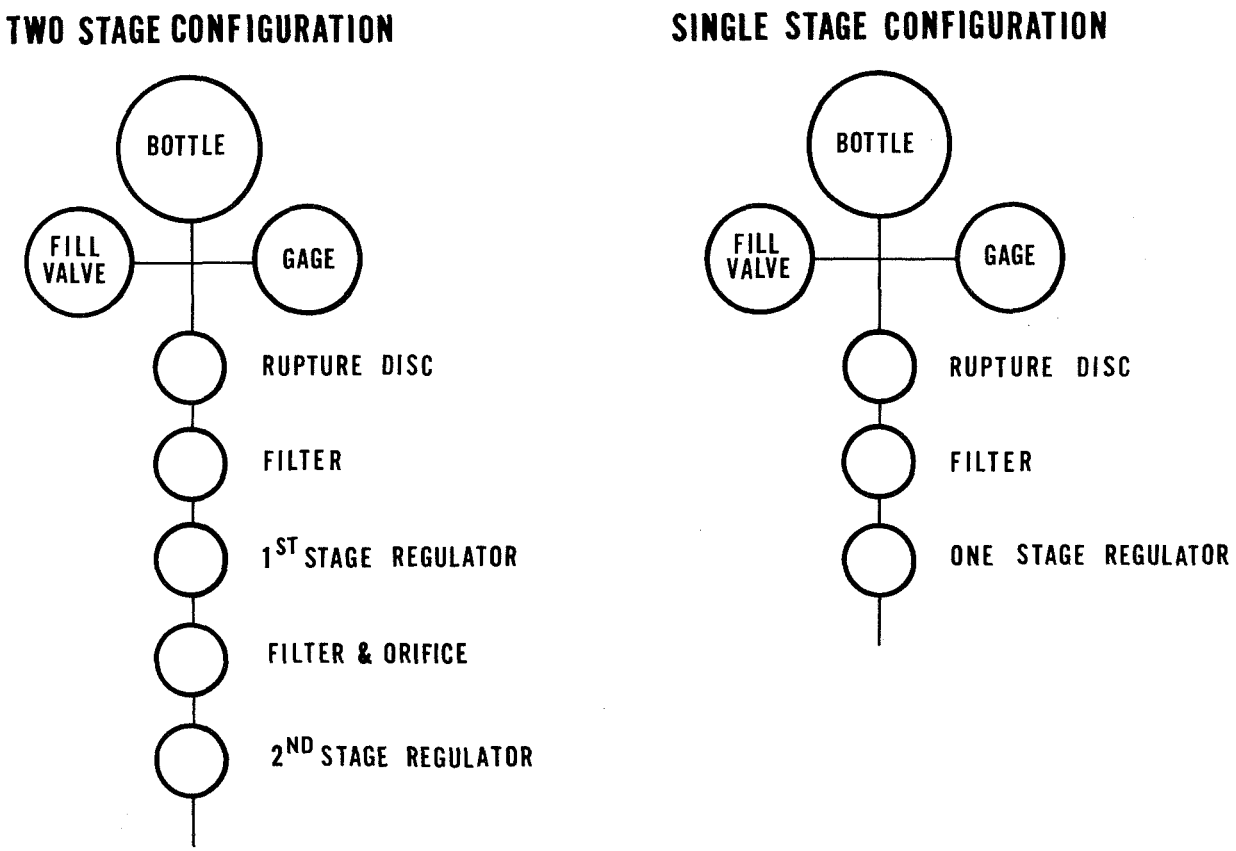

Figure 3.10 *EOS configuration.*

In mid-1967 NASA reviewed and revised mission requirements to establish the need for additional emergency oxygen to permit extravehicular excursions to greater distances from the LM. The oxygen purge system, which was designed for the new requirement, performs the same function as the EOS; however, it provides a minimum of 30 min of flow at 8 lb/hr (for increased metabolic heat rejection) and extends the safe EVA range. The rate of flow is determined by a purge valve located on the PGA. Full open valve position creates an 8 lb/hr deliberate "leak" in the system; a second valve setting creates a 4 lb/hr flow that can be used to conserve oxygen and provide at least 1 hr of emergency "get-back" capability when the BSLSS is used to handle the majority of heat removal.

The fill valve, regulator, and pressure gage designs were direct derivations from the EOS system. The EOS was sealed by a rupture disc, which was punctured by an actuation system to allow the release of the gas when needed. This concept was dropped in the OPS in favor of a multicycle shut-off valve as field experience gained with the EOS revealed that training and preflight acceptance testing was excessively limited by the one-cycle feature of the EOS. The original OPS incorporated a heater to preheat the gas introduced to the regulator and to maintain gas temperature delivered to the suit above 30° F. Subsequent OPS and manned testing revealed that flow, pressure regulation, and astronaut thermal conform could be maintained without the OPS heater. A schematic of the current OPS, which does not use a heater, is shown in figure 3.11.

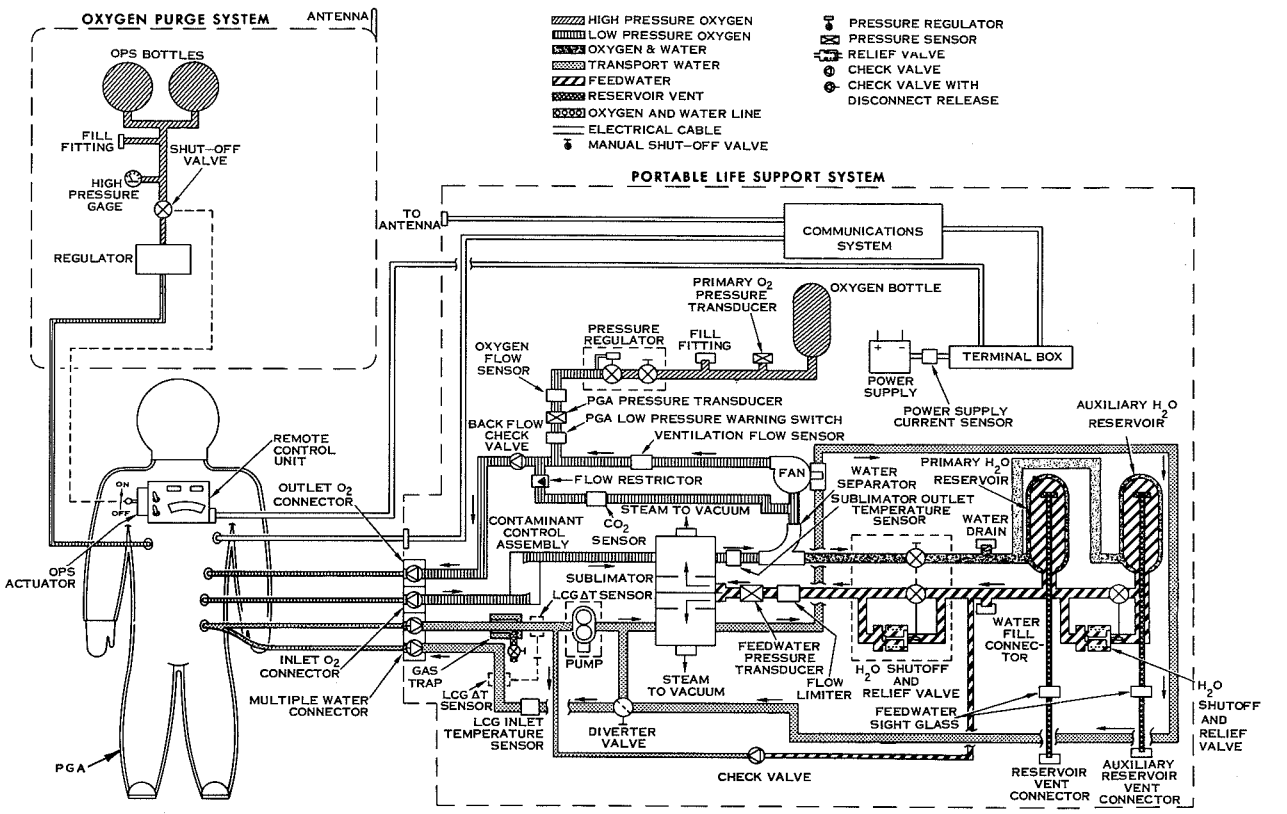

Figure 3.11 *Schematic of –7 PLSS and OPS (without heater).*

The -7 PLSS, which is to be used on the Apollo 15, 16, and 17 missions, is shown in figure 3.12. The PLSS has been modified to support longer lunar surface missions of up to 8-hr duration. The schematic of the modified system is shown in figure 3.11 and is the same as the -6 PLSS schematic except that an auxiliary water tank with associated valving and recharge system has been added. The metabolic rate versus mission duration relationship for this configuration under worst case conditions is shown in figure 3.13. The extended capability was achieved by increasing the operating pressure level in the high pressure oxygen subsystem with corresponding redesign of the subsystem components' incorporating an auxiliary water tank for storage of additional feedwater; increasing the size of the power supply with corresponding mounting provisions redesigned to support the increased weight; and increasing the amount of lithium hydroxide by using revised cartridge packing techniques.

CONCLUSION

The PLSS and associated Apollo life support equipment, having benefited from a thorough design period, extensive development through a number of stages, complete qualification, and repeated successful mission use, now represent the state-of-art in portable equipment for environmental control of man in space. The system has now evolved to the point where it can support an astronaut for any reasonable work-time cycle that can be expected of a man, with an ample margin of safety.

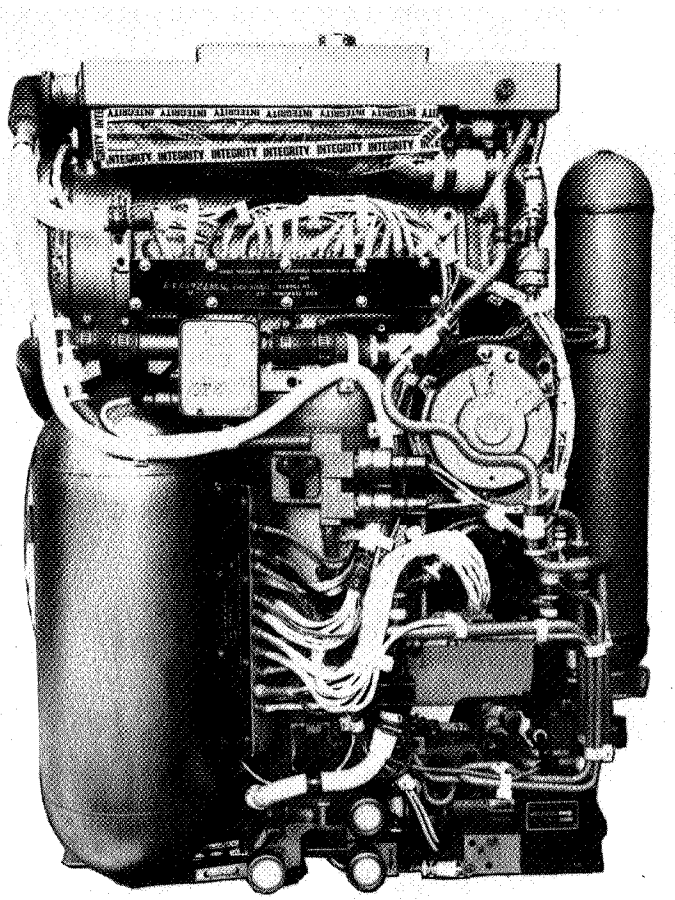

Figure 3.12 *–7 PLSS without protective cover and insulation.*

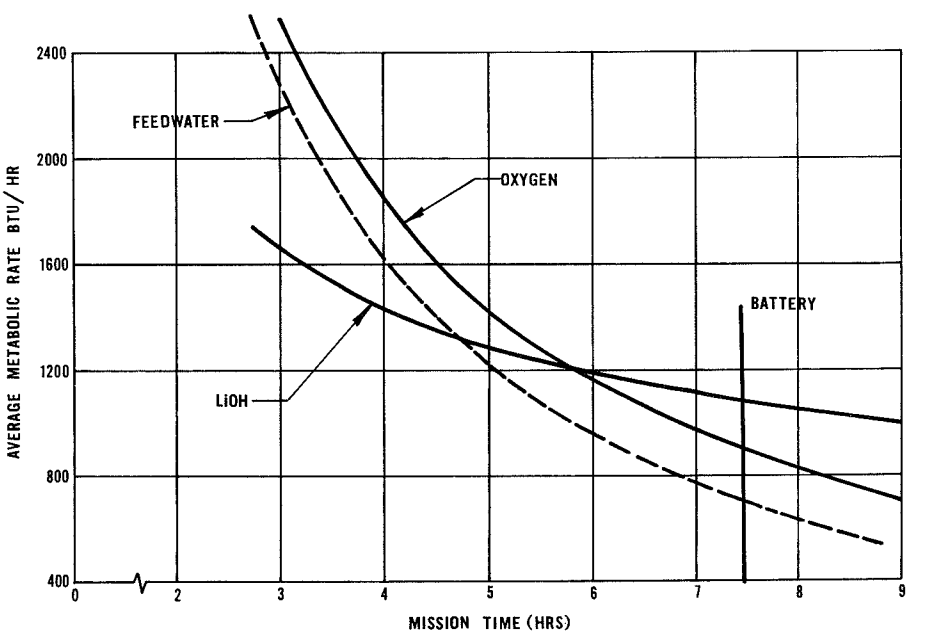

Figure 3.13 *Expendable duration of –7 PLSS.*

4 APOLLO PORTABLE LIFE SUPPORT SYSTEM PERFORMANCE REPORT

Maurice A. Carson
NASA Manned Spacecraft Center

INTRODUCTION

This paper discusses the performance of the Apollo portable life support system (PLSS) on actual lunar missions. Both subjective comments by the crewmen and recorded telemetry data are discussed although emphasis is on the telemetry data. Because the most important information yielded by the PLSS deals with determination of crewman metabolic rates, these data and their interpretation are explained in detail. System requirements are compared with actual performance, and the effect of performance margins on mission planning are described. Mission preparation testing is described to demonstrate how the mission readiness of the PLSS and the crewmen is verified, and to show how the PLSS and the crewmen are calibrated for mission evaluation. Finally, mission plans for extended lunar exploration are discussed, and the effect on PLSS design and performance is explained.

SYSTEM REQUIREMENTS

A system schematic of the Apollo 11 to 14 PLSS is shown in figure 4.1. The major subsystems of the PLSS and their functions are:

1. The primary oxygen subsystem, which supplies breathable oxygen at a regulated pressure of 3.85 psid.
2. The oxygen ventilation subsystem, which recirculates cooled oxygen and removes contaminants at a nominal rate of 5.5 absolute cubic ft/min (ACFM).
3. The feedwater subsystem, which supplies water to the porous plates of the sublimator for heat removal by means of sublimation to space vacuum.
4. The liquid-transport subsystem, which recirculates coolant water at a fixed rate of 4.0 lb/min.
5. The extravehicular communications subsystem (EVCS), which provides communications and instrumentation for the crewman and equipment.

One of the major planning and design problems before the lunar-surface missions was the prediction of crewman metabolic rate. Of course, this is the major parameter affecting PLSS duration and crewman comfort. As a man works harder, he generates more metabolic heat (which must be removed by the PLSS), he consumes more oxygen, and he generates more carbon dioxide and water vapor. Metabolic rates could be predicted for given tasks in earth gravity; however, it was not known whether metabolic rates in lunar gravity would be lower or higher than those on earth. The reduced weight of the man, suit, PLSS, and so forth on the moon would lead one to suspect that metabolic rate would be lower. However, reduced weight would mean reduced traction for walking. This, combined with the possibility of a loose or slippery lunar soil and a potential crewman/equipment balance problem, could lead to a net increase in metabolic rate.

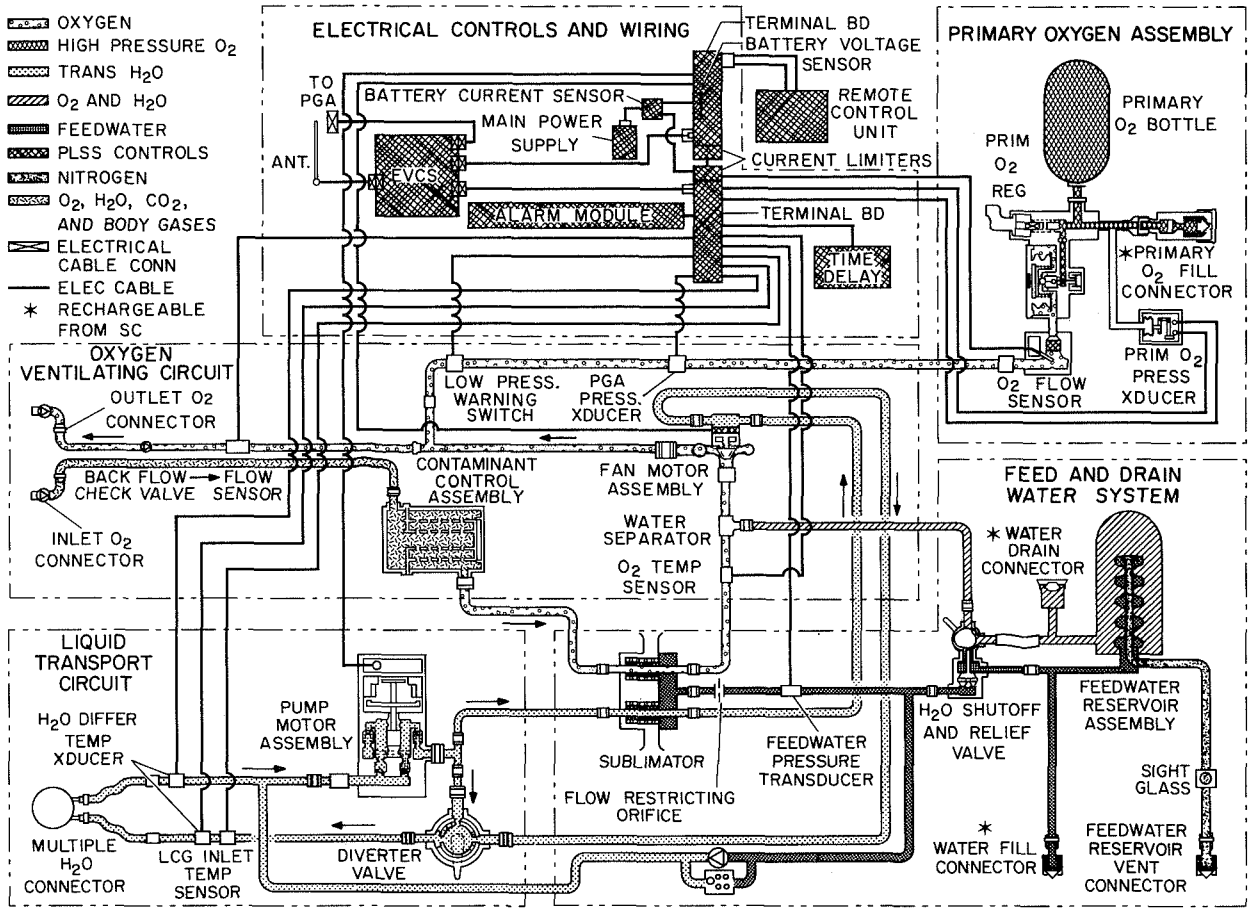

Figure 4.1 *The Apollo PLSS.*

Based on the best estimates of test data and analysis available at the time, the PLSS was designed for a 4-hr lunar exploration mission and an average crewman metabolic rate of 1200 Btu/hr. The requirement for two extravehicular activity (EVA) periods dictated that the PLSS be capable of being recharged with the consumable items (oxygen, water, lithium hydroxide, and battery) in the lunar module (LM) between EVA. The duration of each PLSS consumable as a function of a crewman metabolic rate is summarized in figure 4.2.

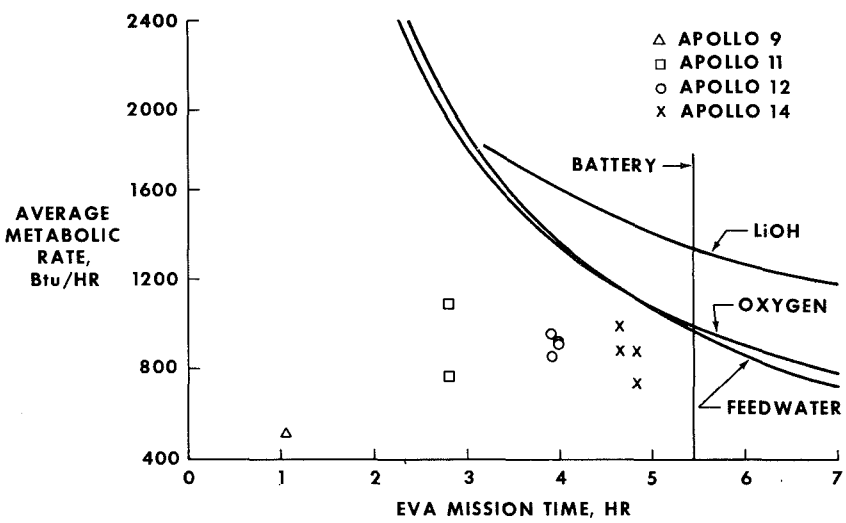

Figure 4.2 *The PLSS expendables duration compared with metabolic rate.*

In the event of a PLSS failure, a completely independent backup system, the oxygen purge system

(OPS), is provided. This system supplies sufficient breathing oxygen for a minimum of 0.5 hr. Carbon dioxide control is provided by purging suit gas overboard. The OPS neither provides recirculation of suit gas nor liquid cooling.

MISSION PREPARATION

Because the proper functioning of the PLSS is absolutely necessary to sustain the life of the astronaut during lunar traverse, each PLSS must be tested thoroughly before the mission to which it is assigned. Almost as important, each crewman must be trained thoroughly in the use of the PLSS, and each PLSS must be tested to obtain calibration points for later use in metabolic-rate and expendables-status determinations.

Each PLSS, upon receipt at the Manned Spacecraft Center, undergoes an acceptance test that includes detailed visual examination and leakage, proof-pressure, and basic functional tests. The PLSS then undergoes a "canned man" test, which is an unmanned performance test in a vacuum chamber wherein all human metabolic products are simulated. Specifically, carbon dioxide, water vapor, and some metabolic heat are introduced into the oxygen vent subsystem while oxygen is removed. Also, metabolic heat is introduced into the liquid-transport subsystem. Rates of heat input, carbon dioxide and water-vapor generation, and oxygen removal are keyed to a metabolic-rate profile for the test. Having passed this test, the PLSS next undergoes a crew altitude-training test. This is a manned test performed in a vacuum chamber for the basic purpose of familiarizing the crewman with the operation, performance, and response of the PLSS (and OPS) under actual space-vacuum conditions. Controls actuation, PLSS and OPS operation, and warning tones are checked at this point. Then, the PLSS is acceptance tested both before and after shipment to Kennedy Space Center. Next, a spacecraft-interface test is performed in which the fit of the PLSS and OPS into their respective stowage locations in the flight LM is checked. In addition, recharge of the PLSS and communications checkout with the LM electrical systems are performed during this test.

Subsequent to successful completion of these tests, a final preinstallation acceptance test is conducted. After preflight charging, the PLSS and OPS are installed in the flight vehicle.

MISSION RESULTS

Mission data from the Apollo 9, 11, 12, and 14 missions were indicative that the PLSS meets or exceeds its system requirements. This conclusion is based on subjective comments from the crewmen and on telemetered data received during the missions. Extravehicular activity durations and the average metabolic rate calculated from telemetered data are given in table 4.1, which shows that the metabolic rate has been consistently lower than the 1200 Btu/hr design point. Hence, the question of whether metabolic rate would be lower or higher for tasks on the moon than for the same tasks on earth appears to be answered. As a result of the lower rates encountered on the Apollo 11 and 12 missions, it was possible to extend the EVA duration for the Apollo 14 mission beyond the 4-hr limit imposed previously.

Telemetry data for all missions indicate that a reserve of consumables existed in all cases. The amount of oxygen, feedwater, lithium hydroxide, and electric power remaining for each Apollo 11, 12, and 14 crewman at the end of each EVA are shown in tables 4.2 to 4.4.

Table 4.1 *Extravehicular activity times and metabolic rates.*

Mission	*Crewman*	*EVA time, min (a)*	*Average metabolic rate, Btu/hr (b)*
Apollo 11	Armstrong	168	777
Apollo 11	Aldrin	168	1118
Apollo 12	Conrad (EVA-1)	241	925
Apollo 12	Bean (EVA-1)	241	930
Apollo 12	Conrad (EVA-2)	235	840
Apollo 12	Bean (EVA-2)	235	950
Apollo 14	Shepard (EVA-1)	288	750
Apollo 14	Mitchell (EVA-1)	288	900
Apollo 14	Shepard (EVA-2)	275	900
Apollo 14	Mitchell (EVA-2)	275	1050

(a) The official EVA times listed here begin with LM cabin pressure at 3.5 psia during depressurization and end with LM cabin pressure at 3.5 psia during repressurization. The EVA time interval used in the Apollo 12 EVA-1 Conrad sample calculations (tables 4.5, 4.7, and 4.9) is based on PLSS expendables usage, and thus is slightly less than the EVA time listed here.

(b) Average of metabolic rates calculated by the thermal-balance, feedwater-consumption, and oxygen-consumption methods (see text).

Table 4.2 *Extravehicular time remaining for indicated consumables – Apollo 11.*

Consumables	*Armstrong, hr*	*Aldrin, hr*
Oxygen	3.88	2.97
Feedwater	5.00	2.50
LiOH	2.34+	2.34+
Electric power	3.43	3.27

Table 4.3 *Extravehicular time remaining for indicated consumables – Apollo 12.*

Consumables	*EVA-1*		*EVA-2*	
	Conrad, hr	*Bean, hr*	*Conrad, hr*	*Bean, hr*
Oxygen	2.21	2.29	1.74	1.52
Feedwater	2.42	2.44	3.58	2.35
LiOH	2.06+	2.06+	2.19+	2.19+
Electric power	2.29	2.29	2.59	2.51

Table 4.4 *Extravehicular time remaining for indicated consumables – Apollo 14.*

Consumables	*EVA-1*		*EVA-2*	
	Shepard, hr	*Mitchell, hr*	*Shepard, hr*	*Mitchell, hr*
Oxygen	2.92	0.64	1.44	0.74
Feedwater	3.14	1.88	1.70	.96
LiOH	1.10+	1.10+	1.50+	1.50+
Electric power	.72	.43	1.38	1.20

Some typical PLSS telemetry data are shown in figures 4.3 to 4.9. These time plots are of liquid cooling garment (LCG) inlet temperature, liquid cooling garment temperature differential (LCG ΔT), oxygen pressure, feedwater pressure, sublimator-outlet gas temperature, suit pressure, battery current, battery voltage, and carbon dioxide partial pressure. All curves, except carbon dioxide partial pressure as a function of time, are for the Apollo 12 commander during the first EVA. No carbon dioxide data exist for missions before Apollo 14 because the PLSS for these misssions did not have carbon dioxide sensors.

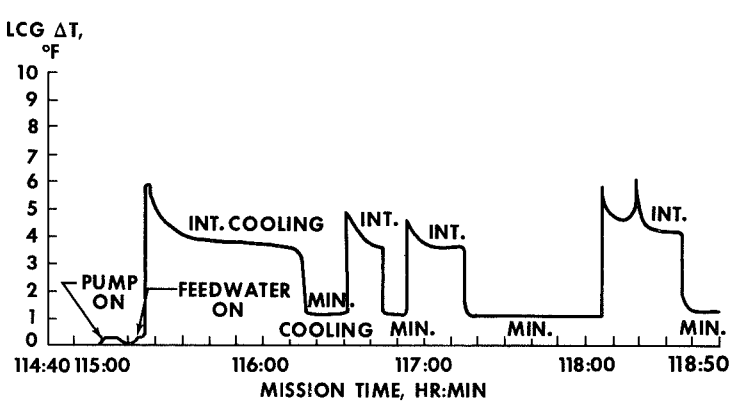

Figure 4.3 *Apollo 12 telemetry data on* H_2O *temperature differential for commander's LCG during first EVA.*

Switching from the minimum cooling to the intermediate cooling position of the diverter valve is indicated clearly by the step change in the delta temperatures (figs. 4.3 and 4.4). In some cases, the time interval between changes in diverter-valve position is too short to allow LCG inlet temperature to stabilize. Hence, some changes in valve position appear as spikes on the LCG inlet temperature curves of figure 4.4. Switch-on of the pump is shown by the sudden jump in LCG inlet temperature at mission time 115 hr 00 min.

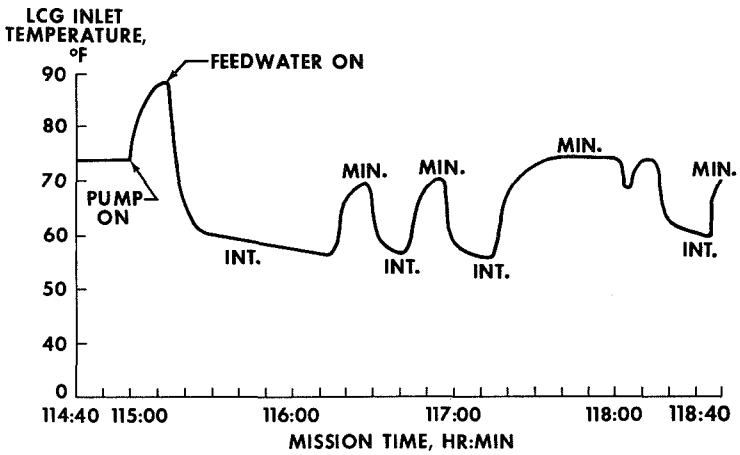

Figure 4.4 *Apollo 12 telemetry data on* H_2O *inlet temperature for commander's LCG during first EVA.*

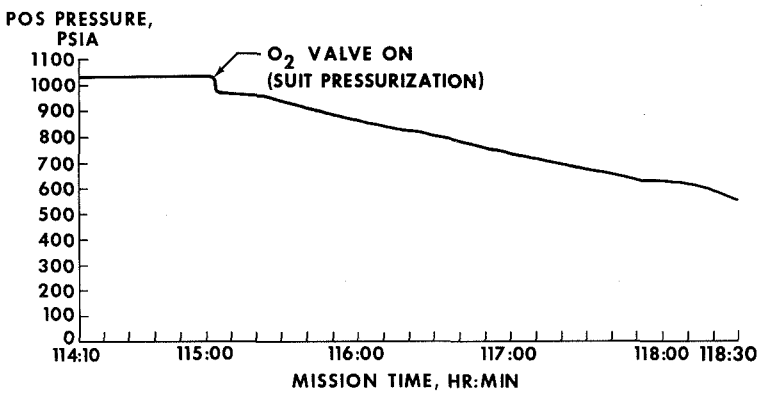

Figure 4.5 *Apollo 12 telemetry data on PLSS POS (*O_2 *supply bottle) for commander during first EVA.*

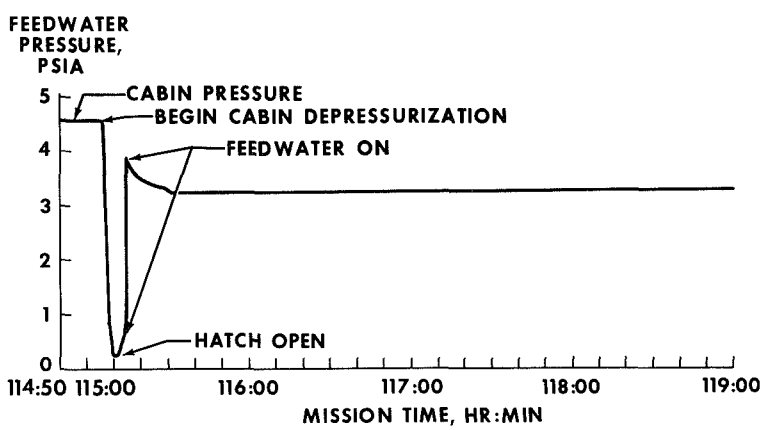

Figure 4.6 *Apollo 12 PLSS telemetry data on feedwater-pressure for commander during first EVA.*

The sudden dip in primary oxygen system (POS) pressure at 115 hr 02 min (fig. 4.5) occurred at the initiation of PLSS oxygen flow, and the dip represents the amount of oxygen needed to pressurize the commander's space suit. From that point on, steady pressure decay results from metabolic oxygen consumption and leakage from the suit.

The feedwater pressure curve of figure 4.6 is indicative of LM cabin pressure up to time 115 hr 10 min, because the empty sublimator is exposed to cabin ambient conditions. Feedwater pressure holds steady at 4.5 psia until cabin depressurization, at which time it drops off sharply, indicating the falling cabin pressure. When the feedwater valve is opened, the pressure rises to within its design range of 2.7 to 3.3 psia, where it remains for the duration of the EVA. If the EVA had been run to the point of feedwater depletion or if sublimator breakthrough had occurred, these conditions would have been indicated by falling feedwater pressure (and actuation of the low feedwater warning tone and flag).

Sublimator-outlet gas temperature (fig. 4.7) climbs steadily after fan switch-on because of the body heat of the crewman. This increase continues until the cabin is depressurized fully (hatch open) and the feedwater is turned on (to begin sublimator cooling). Then, the temperature drops off to about 44° F and remains steady for the duration of EVA. Suit pressure (fig. 4.7) increases suddenly to 3.9 psid as the oxygen valve is opened, then climbs to 5.0 psid as cabin depressurization proceeds. This increase reflects a decrease in cabin pressure rather

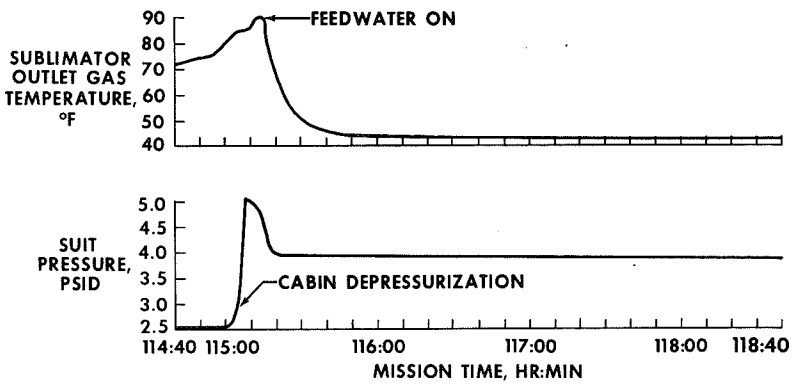

Figure 4.7 *Apollo 12 telemetry data on sublimator-outlet gas temperature and suit pressure for commander during first EVA.*

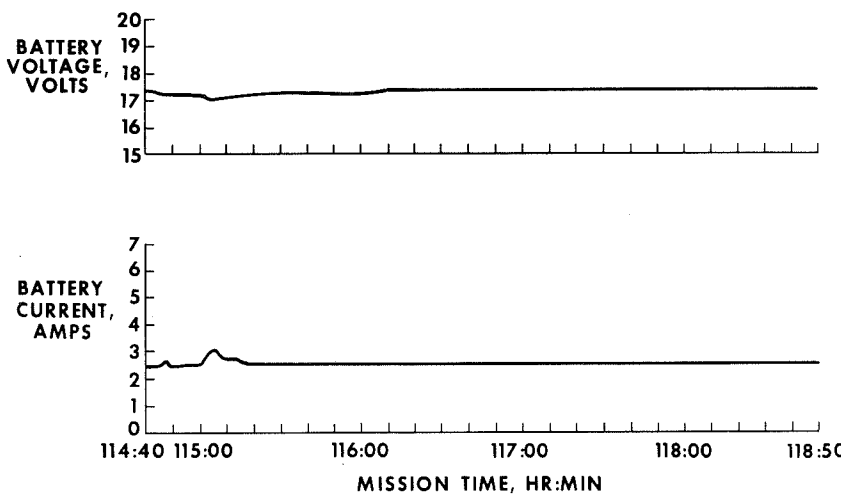

Figure 4.8 *Apollo 12 PLSS telemetry data on battery voltage and current for commander during first EVA.*

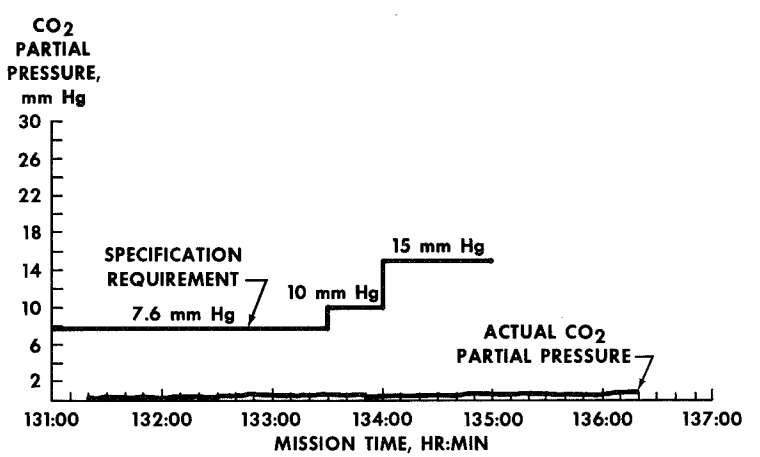

Figure 4.9 *Apollo 14 PLSS telemetry data on CO_2 partial pressure for commander during second EVA.*

than an increase in suit total pressure. Suit pressure decreases to 3.9 psid because of metabolic oxygen consumption and remains steady at that value.

After switch-on of fan and pump, the PLSS battery current and voltage (fig. 4.8) remain steady for the duration of EVA. Fan and pump switch-on show up as transients in the voltage curve and as step changes in the current curve. Telemetry data of carbon dioxide partial pressure for the commander during EVA-2 of the Apollo 14 mission are shown in figure 4.9. Specification requirements also are plotted on the same curve. It can be seen that the carbon dioxide removal capability of the PLSS is well within the requirements. Although Apollo 14 is the only mission to date for which carbon dioxide telemetry data are available, the performance shown in figure 4.9 is typical of test data. Because the most valuable information derived from PLSS data is the crewman metabolic rate, the procedures used for this derivation are discussed in detail. Determination of actual crewman metabolic rates during lunar mission enables mission planners to predict metabolic rates for future missions with good accuracy and is useful for understanding crewman limitations and equipment limitations in the planning of lunar excursions.

Metabolic rate is determined from telemetry data by use of four different methods: thermal balance, oxygen consumption, feedwater usage, and heart rate. These methods, with the

exception of heart rate, are explained below; sample calculations are included and a discussion of the errors and uncertainties associated with each is presented. The sample calculations shown are also for the Apollo 12 commander on EVA-1.

Thermal-Balance Method

The thermal-balance method involves calculation of the total heat removed by the liquid-transport loop and the latent heat removed by the oxygen-ventilation loop. This total is equated to the sum of metabolic heat, heat leakage into the suit, and heat stored by the crewman. The sensible heat removed by the ventilation loop is considered to be negligible and is disregarded.

The basic equations (fig. 4.10) are

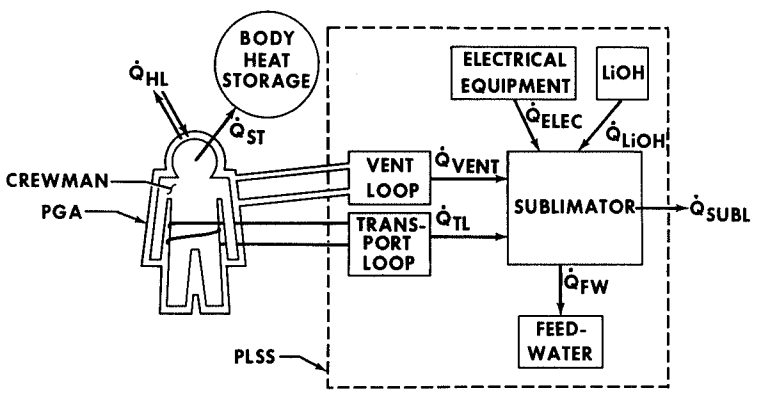

Figure 4.10 *Heat-balance diagram.*

$$\dot{Q}_{TL} + \dot{Q}_{VENT} = \dot{Q}_{MET} + \dot{Q}_{HL} - \dot{Q}_{ST}$$

$$\dot{Q}_{TL} = \dot{m}_{TL}\, C\, \Delta T$$

$$\dot{Q}_{VENT} = \dot{m}_{O_2}\, \Delta h$$

where

$\dot{Q}$	heat transfer, storage, or generation, Btu/hr
$\dot{m}$	mass flow rate, lb/hr
C	specific heat, Btu/lb-°F
ΔT	delta temperature across LCG, °F
Δh	delta enthalpy, Btu/lb

subscripts are defined

TL	transport loop
VENT	ventilation loop
MET	metabolic
HL	heat leak
O_2	dry oxygen
ST	stored

Liquid cooling garment ΔT values are taken directly from telemetry. Transport-loop flow rates are found from preflight test data by using pump-pressure rise compared with flow-rate curves

2-6

and LCG pressure drop compared with flow-rate curves for the various diverter-valve positions. Flow rates thus obtained are corrected for flow variations resulting from changes in LCG inlet temperatures by using experimentally determined correction factors.

Latent heat removal by the ventilation flow is calculated by multiplying the enthalpy change of the ventilating gas by the actual flow rate of dry oxygen. The enthalpy can be determined from psychrometric charts for oxygen at suit pressure if the inlet and outlet dewpoints are known. The PLSS outlet dewpoint is equal to sublimator-outlet gas temperature. The PLSS inlet dewpoints are assumed based on preflight manned-test data. Then, ventilation-loop flow rate is determined by using fan-pressure rise compared with flow curves and suit-pressure drop compared with flow curves. Dry oxygen flow rate is found by subtracting water-vapor flow rate from ventilation flow rate.

The sample calculations of table 4.5 are indicative of a metabolic rate ranging from 915 to 1060 Btu/hr for the Apollo 12 commander during EVA-1. This method has the disadvantages of having to assume PLSS inlet dewpoint and of having several other error sources, among which are uncertainties in determination of the transport and ventilation flows, LCG ΔT, and heat leak. Error sources and their effects are tabulated in table 4.6.

Table 4.5 *Sample calculations for the thermal-balance method.*

With reference to figure 4.10.

$$\dot{Q}_{MET} = \frac{Q_{TL} + Q_{VENT} - Q_{HL} + Q_{ST}}{t}$$

$$Q_{TL} = \dot{m}_{TL} C \, \Delta T(t)$$

$$Q_{VENT} = \dot{m}_{O_2} C \, \Delta h(t)$$

where

Q	heat transferred, stored, or generated, Btu/hr	ΔT	delta temperature across LCG, °F
t	EVA time, hr	C	specific heat, Btu/lb–°F
$\dot{m}$	mass flow rate, lb/hr	Δh	delta enthalpy, Btu/lb

Subscripts are defined

MET	metabolic	HL	heat leak
TL	transport loop	ST	stored
$VENT$	ventilation loop	O_2	dry oxygen

$Q_{HL} = 0$; $Q_{ST} = 0$ for Conrad's first EVA

(EVA time for this and other sample calculations is defined as the interval from PLSS regulator take-over to cabin repressurization.)

$$t = 3.85$$

$$\dot{Q}_{MET} = \frac{Q_{TL} + Q_{VENT}}{3.85} = \frac{Q_{TL}}{3.85} + \dot{Q}_{VENT}$$

Table 4.5 *Sample calculations for the thermal-balance method.(Continued)*

(1) Transport loop

Duration, hr	*LCG ΔT °F*	*Flow rate, lb/min*
2.30	3.8	[a] 240
1.55	1.2	[a] 273
3.85 (total)		

[a]Based on preflight PLSS pump test data corrected for the effects of varying LCG inlet temperature.

$$Q_1 = (240)\,(1.0)\,(3.8)\,(2.30) = 2208.5 \text{ Btu}$$

$$Q_2 = (273)\,(1.0)\,(1.2)\,(1.55) = 507.8 \text{ Btu}$$

$$Q_{TL} = Q_1 + Q_2 = 2710.3 \text{ Btu}$$

$$\dot{Q}_{TL} = \frac{Q_{TL}}{3.85} = 704 \text{ Btu/hr}$$

(2) O_2 ventilation loop

$$Q_{VENT} = \dot{m}_{O_2}\,\Delta h\,t$$

From test data, m_m = 7.695 lb/hr (flow rate of oxygen/water-vapor mixture in veltilation loop) PLSS outlet dewpoint = 42° F (from telemetry data, fig. 4.7); at this dewpoint, absolute humidity w is

$$w = 0.022 \text{ lb } H_2O \text{ vapor/lb dry } O_2$$

Because $m_m = m_{O_2} + m_v$ (where m_v is mass flow rate of water vapor)

$$\dot{m}_v = 0.022\,\dot{m}_{O_2}$$

$$\dot{m}_m = \dot{m}_{O_2} + 0.022\,\dot{m}_{O_2}$$

$$\dot{m}_{O_2} = \frac{\dot{m}_m}{1.022} = 7.500$$

$\dot{Q}_{VENT}$ is found from various PLSS inlet dewpoints (assumed) and $\dot{Q}_{MET}$ is found by summing $\dot{Q}_{VENT}$ and $\dot{Q}_{TL}$

$$\dot{Q}_{VENT} = \dot{m}_{O_2}\Delta h$$

Table 4.5 *Sample calculations for the thermal-balance method. (Concluded)*

The enthalpy change Δh across the sublimator is per pound of dry oxygen flow and is found from psychrometric charts fro oxygen at suit pressure

PLSS inlet dewpoint, °F	Δh, Btu/hr	$\dot{Q}_{VENT}$, Btu/hr	$\dot{Q}_{TL}$, Btu/hr	$\dot{Q}_{MET}$, Btu/hr
68	47.5	356.3	704.0	1060.3
64	37.1	278.3	704.0	982.3
60	28.1	210.7	704.0	914.7

The tabulation above shows values of Q_{VENT} and corresponding values of Q_{MET} for various values of PLSS inlet dewpoint. As there is no instrumentation in the PLSS that provides an indication of actual PLSS dewpoint versus time, it is necessary to assume a range of dewpoints and calculate a range of metabolic rates. Dewpoints shown above were estimated based on results of extensive manned testing on earth.

Table 4.6 *Possible errors for the thermal-balance method.*

Parameter	*Variation*	*Error, Btu/hr*
Heat storage	100 Btu	25
Transport loop flow	0.1 lb/min	6
LCG ΔT	0.1°F	25
Ventilation flow	0.1 lb/hr	4
Dewpoint	1° F	20

Feedwater-Consumption Method

The amount of feedwater sublimated to space vacuum is a measure of the total heat load on the PLSS during EVA. This heat load consists of crewman metabolic-heat generation, heat generated by electrical equipment, heat generated by the reaction of carbon dioxide with lithium hydroxide in the lithium hydroxide canister, heat leak into the suit, crewman heat storage just before EVA, and heat storage in the feedwater (i.e., temperature difference between feedwater at start of EVA and 32° F at which sublimation occurs). Feedwater remaining in the PLSS at the end of the EVA is drained and weighed. This weight, plus an allowance for water remaining in the PLSS, is subtracted from the total weight of water with which the PLSS is charged before EVA. The difference is the weight of feedwater sublimated into space. The water usage is multiplied by the heat of conversion (from liquid to solid to vapor at 32° F) of water to obtain

the total heat removed. To obtain metabolic rate, factors are included to account for heat storage in the feedwater, electrical heat load, and heat load caused by reaction of carbon dioxide with lithium hydroxide. The overall equation is

$$\dot{Q}_{MET} = \frac{m_{FW}\left[h_c - C\left(T_{FW} - 32\right)\right] - Q_{ELEC}}{1.276t}$$

where

Q_{MET}	metabolic rate, Btu/hr
m_{FW}	mass feedwater sublimated, lb
h_C	heat of conversion, Btu/lb
T_{FW}	feedwater temperature at start of EVA, °F
Q_{ELEC}	electrical heat load, Btu
t	EVA time, hr
C	specific heat of water, Btu/lb–°F

This equation is derived and a sample calculation is performed (table 4.7). For the Apollo 12 commander's first EVA, this method yields a metabolic rate of 894.4 Btu/hr. As with the thermal-balance method, this procedure does not take into account crewman heat storage. Other sources of error are scale reading (during weighing of feedwater on lunar surface) and amount of residual feedwater remaining in the sublimator porous plate after the EVA. These possible errors and their effect are summarized in table 4.8.

Table 4.7 *Sample calculation for the feedwater-consumption method.*

Heat balance (see figure 4.10)

$$\dot{Q}_{MET} + Q_{\text{LiOH}} + \frac{Q_{ELEC}}{t} + \frac{Q_{FW}}{t} + \dot{Q}_{HL} - \frac{Q_{ST}}{t} = \frac{m_{FW}\, h_c}{t}$$

where

$\dot{Q}_{ST}$	heat storage, Btu = 0
$\dot{Q}_{MET}$	metabolic rate Btu/hr
$\dot{Q}_{\text{LiOH}}$	heat generation rate of $LiOH/CO_2$ reaction, Btu/hr
Q_{ELEC}	electrical heat load, Btu
Q_{FW}	heat load of PLSS required to reduce feedwater temperature to 32° F, Btu
$\dot{Q}_{HL}$	heat leak, Btu/hr
t	EVA duration, hr
m_{FW}	mass of feedwater sublimated, lb
h_c	heat of conversion, Btu/hr

Table 4.7 *Sample calculation for the feedwater-consumption method. (Continued)*

From test data

$$\dot{Q}_{\mathrm{LiOH}} = 0.276\ \dot{Q}_{MET}$$

$$Q_{ELEC} = 545 \text{ Btu, from test data}$$

$$Q_{FW} = m_{FW} C_P \left(T_{FW} - 32\right);\ C_P = 1.0 \text{ Btu/lb-}^\circ \text{ F}$$

$$T_{FW} = T_{cabin} \quad \text{(assumed)}$$

$$T_{cabin} = 68^\circ \text{F}$$

$$Q_{FW} = m_{FW}(68 - 32) = 36 m_{FW}$$

$$t = 3.85 \text{ hr}$$

$$Q_{HL} = 0$$

$$\dot{Q}_{MET} = \frac{m_{FW}\left[h_c - C_P\left(T_{FW} - 32\right)\right] - Q_{ELEC}}{1.276t}$$

Feedwater collected	2.98 lb (earth weight)
Residual feedwater	0.83 lb (after collection)
Total unsublimated feedwater	3.81 lb

Initial feedwater charge	8.56 lb
	3.81 lb
Feedwater sublimated	4.75 lb

Table 4.7 *Sample calculation for the feedwater-consumption method. (Concluded)*

$$h_c = h\,(liquid\ to\ ice) + h\,(ice\ to\ solid)$$

$$h_c = 143.3 + 1219.1 = 1075.8\ \text{Btu/lb}$$

From reference 1

$$\dot{Q}_{MET} = \frac{(4.75)\,(1075.8 - 36.0) - 545}{1.276\,(3.85)}$$

$$\dot{Q}_{MET} = 894.4\ \text{Btu/hr}$$

Table 4.8 *Possible errors for the feedwater-consumption method.*

Parameter	*Variation*	*Error, Btu/hr*
Scale reading	0 to 0.6 lb H_2O remaining in sublimator	0 to 130
Heat leak	±100 Btu/hr	±75
Heat storage	0 to 100 Btu	0 to 25

Oxygen-Consumption Method

Primarily, oxygen consumption is a function of metabolic rate only. Hence, this method is the most direct measure of metabolic rate available from PLSS telemetry data. The relationship between oxygen consumption and metabolic rate has been known quantitatively for many years (ref. 2). The basic equation is

$$Q_{MET} = \frac{m_{O_2}}{0.0001708 - \left[\left(\frac{RQ - 0.707}{0.293}\right) 0.0000123\right]}$$

where

Q_{MET} metabolic load, Btu

m_{O_2} mass of oxygen consumed, lb

RQ respiratory quotient, defined as the ratio of volume of carbon dioxide produced to the volume of oxygen consumed.

The mass of oxygen supplied by the PLSS is calculated from the pressure decay of the bottle (telemetered data) using compressibility factors to account for the deviation of the oxygen from the ideal-gas law. The mass of oxygen consumed is found by subtracting suit leakage from the mass of oxygen supplied by the PLSS. The respiratory quotient is assumed based on ground-test data.

A sample calculation is shown in table 4.9 where a metabolic rate for the Apollo 12 commander's first EVA is 846 Btu/hr. Error sources for this method are determination of suit leakage, error in POS pressure reading, and assumption of respiratory quotient (table 4.10). Suit leakage of 0.0044 lb/hr of oxygen during the EVA was based on preflight data. Postflight leakage tests on the suit were indicative of a leakage of 0.0169 lb/hr. This value was used in calculating the metabolic rate for EVA-2.

Table 4.9 *Sample calculation for the oxygen-consumption method.*

$$Q_{MET} = \frac{m_{O_2}}{0.0001708 - \left[\left(\frac{RQ - 0.707}{0.293}\right) 0.0000123\right]}$$

where

Q_{MET} metabolic load, Btu

m_{O_2} mass of oxygen consumed, lb

RQ respiratory quotient (dimensionless) = volume of CO_2 produced divided by volume of O_2 consumed

but

$$m_{O_2} = m_{POS} - m_{LEAK}$$

where

m_{POS} mass of oxygen supplied by POS bottle

m_{LEAK} mass of oxygen leaked overboard.

Hence

$$Q_{MET} = \frac{m_{POS} - m_{LEAK}}{0.0001708 - \left[\left(\frac{RQ - 0.707}{0.293}\right) 0.0000123\right]}$$

Table 4.9 *Sample calculation for the oxygen-consumption method. (Continued).*

First, calculate m_{POS}

$$m_{POS} = m_i - m_f$$

where subscripts i and f refer to initial and final conditions, respectively.

$$m_i = \frac{P_i V}{Z_i R T}$$

Z_i = compressibility factor = 0.974

P_i = 960 psia; T = 530° R

V = 378 in.^{3}; R = 48.28 ft lb/lb–° R

$$m_i = \frac{(960)\,(144)\,(378)}{(0.974)\,(48.28)\,(5.30)\,(1728)} = 1.21 \text{ lb}$$

$$m_f = \frac{P_i V}{Z_f R T}$$

Z_f = 0.987

P_f = 475 psia; T_f = 530° R

V = 378 in.^{3}; R = 48.28 ft lb/lb–° R

$$m_f = \frac{(475)\,(144)\,(378)}{(0.987)\,(48128)\,(530)\,(1728)} = 0.582 \text{ lb}$$

and

$$m_{POS} = 1.210 - 0.582 = 0.622 \text{ lb}$$

From preflight test data m_{LEAK} = 0.017

Table 4.9 *Sample calculation for the oxygen-consumption method. (Concluded)*

Based on manned test experience and analysis, $RQ = 0.85$ and

$$Q_{MET} = \frac{0.622 - 0.017}{0.0001708 - \left[\left(\frac{0.85 - 0.707}{0.293}\right) 0.0000123\right]}$$

$$Q_{MET} = 3670 \text{ Btu}$$

$$\dot{Q}_{MET} = \frac{3670 \text{ Btu}}{3.85 \text{ hr}} = 953 \text{ Btu/hr (average)}$$

Table 4.10 *Possible errors for the oxygen-consumption method.*

Parameter	*Variation*	*Error, Btu/hr*
PGA leakage	1 cc/min	1
RQ change	0.01	2
Cr pressure	1 psi	2

Heart-rate Method

The heart-rate method is the least accurate of the methods used, and, for that reason, it is not included in the average metabolic-rate tabulation of table 4.1. However, it does offer the advantage of a real-time update of approximate metabolic rate during the mission. It also allows the estimation of metabolic rates for specific tasks on the lunar surface that have durations too short to be determined by other methods. It may be used as a backup method in the event of a data loss that prevents the use of one of the other methods.

Primarily, the heart-rate method involves preflight calibration curves (heart rate as a function of work rate) generated for the crewman in question; these data are compared with telemetered heart-rate data received on the mission. Because physiological parameters are involved (which require interpretation by medically trained personnel), the details of this method will not be discussed in this paper.

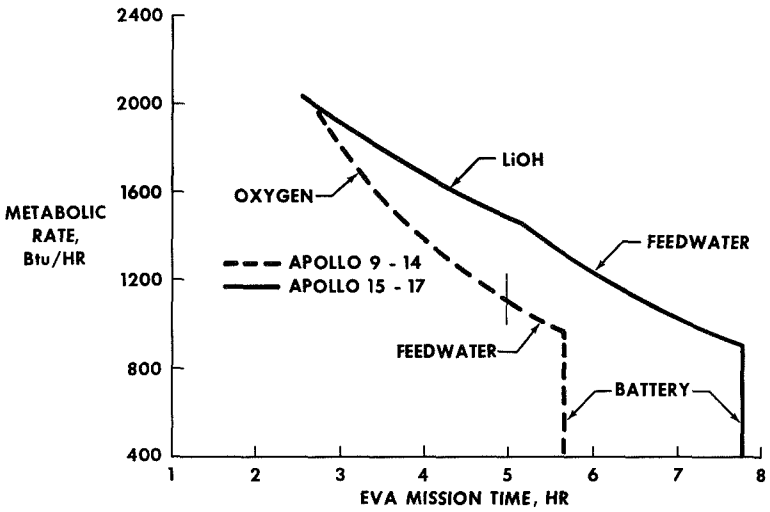

Figure 4.11 *Apollo 9 to 14 missions compared with Apollo 15 to 17 missions with respect to PLSS-limiting expandables.*

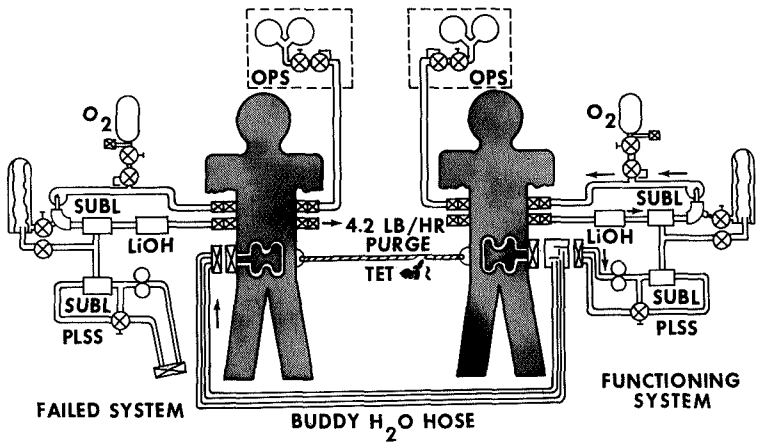

Figure 4.12 *The BSLSS/EMU schematic.*

FUTURE MISSIONS

Requirements for more and longer EVAs on Apollo missions have necessitated several design changes to the PLSS. Among these changes are a higher pressure oxygen bottle, an auxiliary feedwater tank, a lithium hydroxide canister that has increased capacity, and a larger battery. These changes have increased the PLSS performance to the levels shown in figure 4.11. Because of the increased EVA duration and the use of the lunar-roving vehicle, the range of lunar exploration has increased significantly. This capability has required increased emergency return capability in the event of a failure of one of the PLSSs. On the early Apollo missions, the OPS functioned as a backup system in the event of a PLSS failure. The OPS provided a 0.5-hr flow of oxygen that was dumped overboard through a purge valve in the suit. This purge flow provided breathing oxygen, carbon dioxide removal, and some cooling. For later Apollo missions, the buddy secondary life support system (BSLSS), (fig. 4.12), supplements the OPS. The BSLSS consists of two water hoses with a PLSS water connector at one end and a water-flow-dividing connector on the other. In the event of a failure of one PLSS, the flow-divider connector is connected to the suit water connector of the crewman with the working PLSS. The connector at the other end of the BSLSS hoses is attached to the suit-water connector of the crewman that has the failed PLSS. The water connector of the operating PLSS is installed in the BSLSS water-divider connector. Thus, both crewmen share the cooling capability of the operating PLSS. The crewman with the failed PLSS receives oxygen for breathing and has carbon dioxide removed by his OPS. For use with the BSLSS where gas cooling from the OPS is not required, the crewmen have two-position purge valves, allowing them to select two purge flow rates. During this operation, the purge valve would be set in the low-flow position for which the OPS would provide a 1.25-hr supply of oxygen.

Although EVA durations will increase, the telemetry data transmitted during the mission will be the same. Hence, the PLSS on future missions will continue to provide both complete environmental control for the crewman and vital PLSS performance data that can be used to determine crewmember metabolic rates for scientific purposes.

REFERENCES

1. Keenan, Joseph Henry; and Keyes, Frederick G.: Thermodynamic Properties of Steam. J. Wiley and Sons, Inc., New York; and Chapman and Hall, limited, London, 1936.
2. Lusk, Graham: Animal Calorimetry – Twenty-Fourth Paper – Analysis of the Oxidation of Mixtures of Carbohydrate and Fat, A Correction. J. Biol. Chem., vol. 59, 1924.

5 NAVY-DEVELOPED LIFE SUPPORT SYSTEMS FOR FULLY ENCLOSED PROTECTIVE SUITS

G. M. Orner and N. F. Audet
Navy Clothing and Textile Research Unit
Natick, Mass.

INTRODUCTION

The Navy has long had an interest in fully enclosed protective clothing. Early work by the Navy Clothing and Textile Research Unit (NAVYCLOTEXTRSCHU) using forced ventilation in a protective impermeable suit dates back more than 15 years (ref. 1). The Navy research unit is now interested in developing a life support system primarily for shipboard use where many situations exist requiring protection of this kind. For example, engine room environments are often severe, particularly during shutdown periods. Temperatures as high as 140° F are frequently encountered, which when coupled with high humidity preclude the entry of engine room personnel, even to perform such light duties as standing watch. Other shipboard uses include damage control and rescue operations in which personnel may be required to enter spaces filled with smoke or toxic gases.

Previous work at NAVCLOTEXTRSCHU includes the development and testing, under actual shipboard conditions, of an insulated impermeable suit supplied with compressed air for ventilation, cooling, and breathing (ref. 2); the evaluation of a thermoelectric cooled suit (ref. 3); and the physiological evaluation of a liquid air suit (ref. 4).

It was shown that the tolerance time of personnel under elevated temperature conditions can be appreciably extended when compressed air is used. The thermoelectric approach was unsatisfactory because of the weight and bulk of thermoelectric devices available at that time. The liquid air approach, attractive because the liquid air provides cooling, air for breathing, and power for its own circulation, is not generally suitable for shipboard use because liquid air is not usually available aboard ships.

The environmental control unit (ECU), the life support system currently under development by the Navy Clothing and Textile Research Unit, uses wet ice for a coolant. The purpose of this system is to control the environment within a fully enclosed impermeable suit (damage control suit or DCS), also being developed at the Unit's laboratory. The ECU is designed to circulate and cool the air within the suit, remove excess moisture and carbon dioxide, and maintain a safe oxygen level, thus providing maximum personnel protection against hostile environments, such as toxic gases, low oxygen levels, high relative humidities, and temperature extremes.

Although additional work is required on the ECU and modifications are being considered, it appears that the system is well able to fulfill its intended objectives. Tests have shown that a man can be maintained for periods up to 90 min in 130° F environments and for about 2 hr at atmospheric temperatures not greater than 100° F.

The main modification contemplated at this time is a redesign of the ECU to allow it to be carried like a suitcase, rather than worn as a backpack as was originally intended. This change will reduce the bulk of the suit and facilitate entry through the small hatches and passageways found aboard ship, particularly on the smaller vessels. Furthermore, this modification will add

flexibility to the system by allowing either the suit or the ECU component to be used separately as a part of another system if desired.

In another Navy development, the Naval Explosive Ordnance Disposal Facility uses liquid air as a refrigerant in the backpack. Appendix A updates their paper, presented at the 1969 conference on Portable Life Support Systems (ref. 5).

In this report the design and performance of the NAVCLOTEXTRSCHU system are discussed. Data are presented showing the rate of heat absorption under a wide variety of inlet air temperature and relative humidity conditions.

DESCRIPTION OF ECU

There are three basic requirements for the support of a man in a fully enclosed space: (1) temperature control (the removal of excess metabolic heat); (2) oxygen supply; and (3) the removal of carbon dioxide. In the NAVCLOTEXTRSCHU system, as with most life support systems, metabolic heat is dissipated from the man's body by evaporation and conduction into the air within the suit, which must be continually cooled and dried. Several methods for cooling the air are available and have been tried, such as simple circulation of external air, evaporation of liquids, and sublimation of solids. Other methods include thermoelectric cooling and melting of solids, such as plain ice. Each approach has its own advantages and disadvantages, but the wet ice method appears to be most suitable for shipboard use. Wet ice is easily produced and is a desirable refrigerant. It is safe and nontoxic, and pound-for-pound it absorbs as much heat as liquid air (between 0° and 70° F for ice and -314° and 70° F for air).

The ice for the NAVCLOTEXTRSCHU ECU is contained in two finned canisters, each containing 6 lb of ice. Fins formed from deeply corrugated aluminum sheeting are brazed to the four vertical sides of the canisters, as illustrated in figure 5.1, which shows the assembled ECU and its component parts.

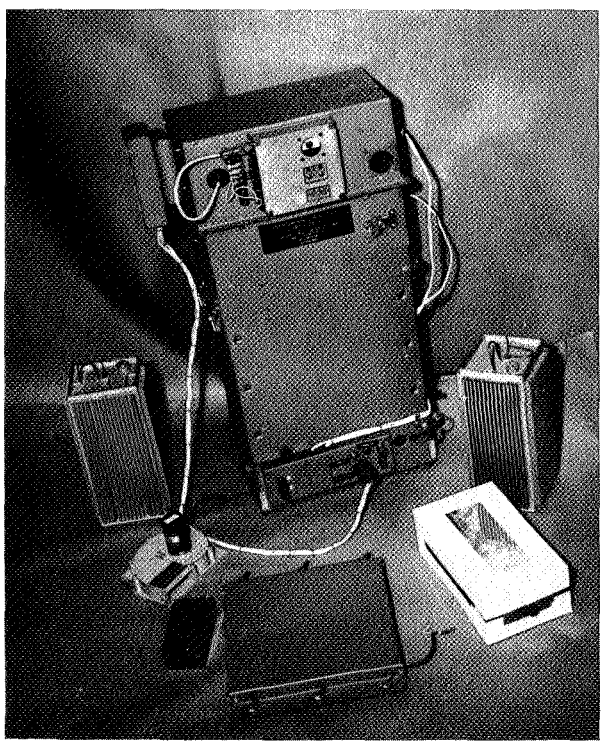

Figure 5.1 *Environmental control unit backpack and component parts.*

The ECU case and the freeze canisters were made by the Frigivest Company under contract to NAVCLOTEXTRSCHU. The case is constructed of PVC plastic with a double outer wall sandwiching 3/8 in. thick polyurethane foam core for insulation. The upper section of the ECU comprising the plenum, contains the blower and the compartment for the chemical pack. It attaches to the lower section with quick-release fasteners to expedite replacement of the freeze canisters. A tank is provided below the freeze canister compartment to contain the condensate. Check valves prevent the condensate from flowing back into the freeze canister compartment should the ECU become inverted. The ECU is designed so that both the cooling canisters and the chemical pack can be quickly and readily replaced when the suit is being used on an extended mission.

The ECU is worn inside a pouch, which is attached to the upper back of the suit (fig. 5.2).

Figure 5.2 *Side view of model 11 prototype damage control suit.*

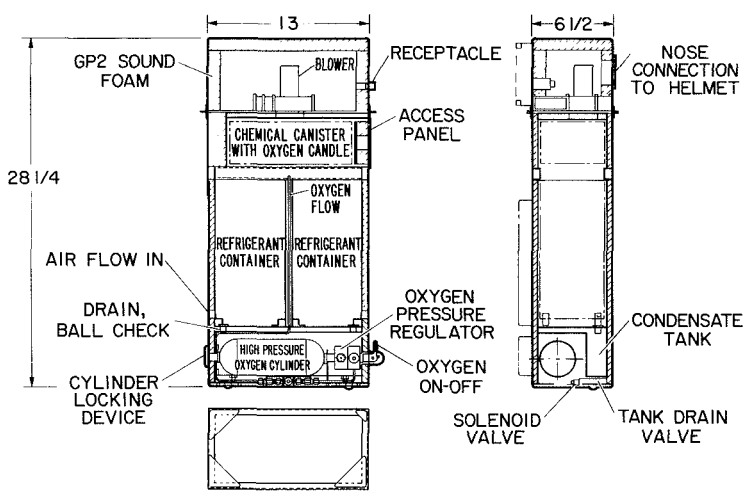

Figure 5.3 *Environmental control unit.*

An aluminum frame support strapped to the wearer supports the backpack as well as the polycarbonate plastic dome helmet.

The approximate overall dimensions of the ECU are 28 X 14 X 18 in. The backpack, fully loaded with ice and chemical packs weighs approximately 40 lb.

Figure 5.3 is a schematic of the backpack. Air enters through the inlet at the lower end of the freeze canisters and passes upwards through the canister fins, giving off heat and moisture as it cools. Passing through the chemical canister, the air gives off additional moisture, oxygen is produced and carbon dioxide is removed. The chemical canister measures 10 in. long, 5-5/8 in. wide and 3-1/2 in. deep. It weighs 4-3/4 lb when filled with lithium hydroxide for the removal of carbon dioxide, and potassium superoxide for the replenishment of the oxygen. The canister bodies are made of stainless steel sheet and contain 12 troughs made from metal screening, 3-1/2 in. deep, running along the length of the canister. The troughs hold the coarsely granular chemicals in layers to allow a free, well-distributed flow of air through the pack. Seven troughs are filled with potassium superoxide for the production of oxygen according to the equation.

$$2\,KO_2 + H_2O \rightarrow 2KOH + 3/2\,O_2 + \textit{heat}$$

The remaining five troughs are filled with lithium hydroxide for the removal of carbon dioxide according to this equation

$$2\,LiOH + CO_2 \rightarrow Li_2CO_3 + H_2O + \textit{heat}$$

Since the moisture in the air greatly exceeds that required for the production of oxygen, a perforated baffle is placed over the side of the chemical pack that contains the potassium superoxide to divert most of the air through the lithium hydroxide. A sodium chlorate candle is incorporated within the chemical pack for emergency use. The candle is fired electrically and produces enough oxygen to support a man for 10 min. Provision was made for an alternate oxygen supply, using oxygen under high pressure from a cylinder below the condensate tank. The alternate system, however, will be eliminated because the chemical system appears to be well able to handle the oxygen requirements. The development, construction and testing of the chemical canisters was done by the MSA Corporation under contract to NAVCLOTEXTRSCHU (ref. 6).

After passing through the chemical pack, the air is drawn into the plenum and exhausted through the outlet into the suit helmet. Air circulation is accomplished by an electrically driven blower made by the Torrington Company. This is a centrifugal-type blower driven by a 12 V Globe dc motor running at about 12,000 rpm. It is designed to produce 27 cu ft of air flow at a head of 3 in. of water. Extensive testing at NAVCLOTEXTRSCHU has shown that it will meet that requirement drawing 2.65 A at 12 V. The blower exhausts into a GP 2 sound foam-lined plenum and, from there, directly into the helmet where the noise level is about 70 dB.

Power is obtained for the system from a 12-V, 10-ah silver-zinc battery (Silvercell) made by the Yardney Company. The battery, which provides ample power for a 2-hr run, weighs only 5 lb including the case, which is attached externally to the ECU with quick-release fasteners. The silver-zinc battery is a low-resistance storage cell that can be discharged up to 30 times its amp-hr capacity rating. Its life is claimed by the manufacturer to be 1 to 2 years after activation, but tests conducted at NAVCLOTEXTRSCHU have indicated a considerably longer life expectancy. Each cell contains a small quantity of an alkaline electrolyte (potassium hydroxide) that is largely absorbed by the plates and separators, resulting in an almost unspillable battery. Charging may be accomplished by an inexpensive, constant potential charger requiring approximately 24 hr for a full charge, from the fully discharged condition.

A novel and highly functional innovation, from a safety standpoint, is the oxygen sensing and warning device shown attached to the backpack in figure 5.1. This instrument, developed by the Beckman Instrument Company, Inc., under contract to the Navy, monitors oxygen from a polargraphic sensor mounted in the plenum and warns the wearer by a red light whenever the oxygen level falls below or rises above safe values. This unit draws very little current (the maximum is about 125 mA). Tests have shown that it responds very quickly to changes in oxygen partial pressure, is essentially insensitive to changes in temperature and relative humidity, and is a highly reliable and apparently nearly maintenance-free device. The entire unit weighs approximately 1 lb.

A low-profile communications headset compatible with existing sound-powered Navy gear has been developed by Dyna-Magnetic Devices, Inc., under contract to NAVCLOTEXTRSCHU, for use with this suit. The headset uses a bone-conduction-type microphone mounted at the rear of the head. All the electronics required for this system are contained within the headset, which weighs approximately 1 lb.

TESTING

Exhaustive tests have been conducted on the backpack to determine airflow rates, cooling rates, and the cooling capacity of the freeze canisters. These tests were held in an environmentally controlled chamber with the use of an "open circuit" configuration (i.e., inlet air was drawn from, but exhausted outside of, the chamber). The outlet air was not allowed to return to the

backpack as it does when the backpack is used with the suit. Testing in this manner allowed accurate control over both inlet temperature and relative humidity. Airflow was measured directly with a hot-wire air-velocity meter (Flowtronic model 55A1). A sensor was mounted in a special flow tube, made and calibrated by Flow Corp., to read directly in ft/min. Exhaust air from the backpack was passed through the flow tube and the flow rate continually monitored. Electrical power for these tests was supplied from a filtered adjustable dc-power supply.

Temperature and relative humidity measurements were made with wet and dry thermocouples. Some difficulty was experienced by the drying out of the wet couples; however, in most tests the humidity was high enough to prevent this happening during the test periods. Signals from the thermocouples were recorded on a multipoint Honeywell temperature recorder.

The rate of water extraction, airflow, and the temperature difference between incoming and outgoing air were used to calculate the rate of heat absorption by the backpack. Since heat absorption rates were generally decreasing and data were taken *at the end* of every 15-min period, conservative values were obtained.

RESULTS AND DISCUSSION

Water versus Sodium Thiosulphate Solution

The finned aluminum canisters used for holding the refrigerant solutions were supplied by the manufacturer filled with 6 lb of a solution reported to be water with 10 percent sodium thiosulphate and 6 percent alcohol added. The use of a frozen salt solution instead of plain ice for cooling purposes has been advocated to take advantage of the negative heat of solution found in some salts and also to lower the temperature of the melting ice and thereby enhance the transfer rate of heat from the air to the canister fins.

The initial tests were conducted on the backpack, with the cooling canisters in place, in a room at 90° F and 65 percent RH. Inlet air was drawn directly into the backpack from the chamber while exhausted air was passed through an instrumented flow tube used for measuring the flow rate. Tests were run using both the salt-alcohol-water solution and plain water frozen in the canisters to determine the relative performance of both liquids.

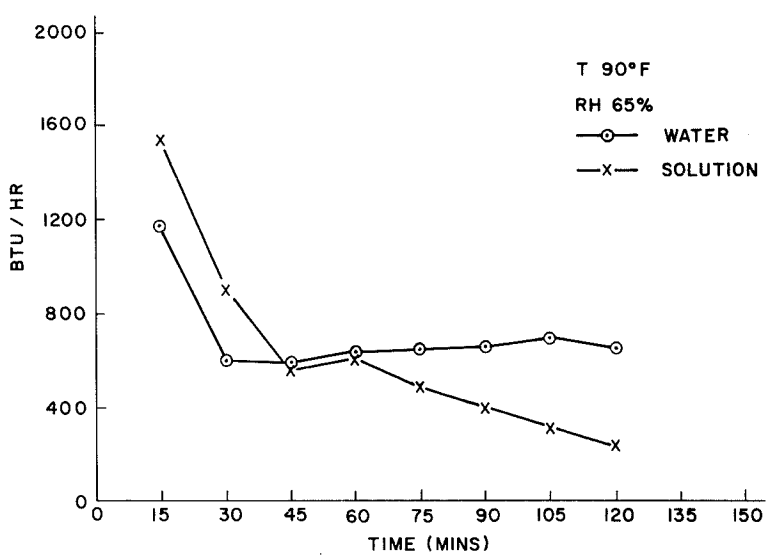

Figure 5.4 *Comparison of heat absorption rates versus time for water and for sodium thiosulphate-alcohol solution in canisters.*

Results from the tests using the solution-filled canisters showed a very high initial rate of heat absorption but, after about 1 hr, the rate of heat absorption fell to an unacceptably low level though ice remained in the canisters (fig. 5.4). In the tests run with water-filled canisters, on the other hand, the rate of heat absorption, after an initial drop during the first half hour or so, typically increased during the next half hour and thereafter maintained a relatively high level until all of the ice was melted. In these tests the total Btu

outputs from the water and solution filled canisters did not appear to be materially different and, thus, from a performance point of view, plain ice appeared to be the better choice.

The initial high rate of heat absorption for both the water- and solution-filled canisters apparently occurs before the supercooled ice starts to melt. Once melting begins, the insulation afforded by the layer of water between the ice and the can retards the heat flow. Apparently once this layer becomes thick enough, convection currents form that increase the rate of heat transfer. Hence the recovery noted in the rate of heat absorption in all the tests using plain ice. Melting of the frozen sodium thiosulphate solution, on the other hand, results in the formation of a viscous slush that presumably inhibits convection. Consequently, the rate of heat transfer continues to decline.

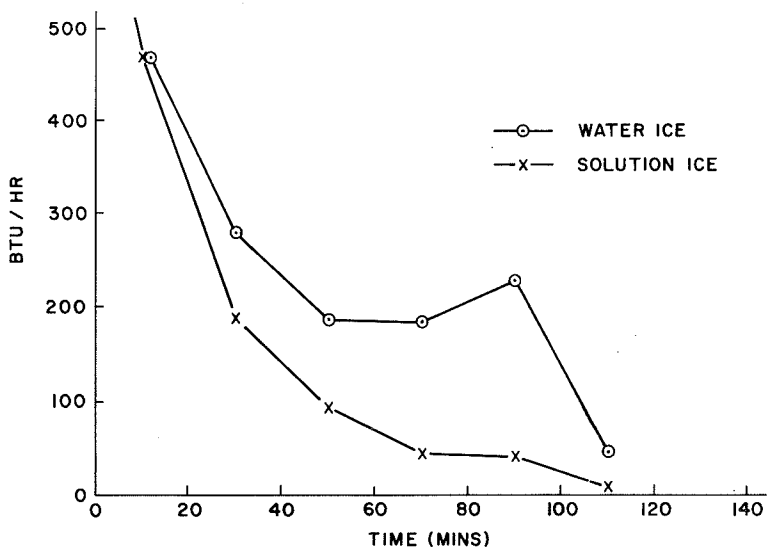

Figure 5.5 *Comparison of heat absorption rates versus time for water and for sodium thiosulphate-alcohol solution in a calorimeter.*

Additional experiments were conducted to investigate further the low rate of heat absorption noted for the solution-filled canisters. A cylindrical aluminum can containing 4 lb of the sodium thiosulphate-alcohol solution was placed in an insulated calorimeter containing 31 lb of water at ambient temperature. Provision was made for continually agitating the water and recording its temperature. The experiment was duplicated using plain-water ice in the can and the results (illustrated in fig. 5.5, where rate of heat loss is plotted against time) confirm the previous findings that heat is more readily absorbed in plain ice than in ice made from the sodium thiosulphate solution. Furthermore, measurements made in a vacuum insulated calorimeter, where ice was melted directly in water, showed that plain-water ice absorbs about 5 percent more heat in melting than ice made from the solution. Thus, since plain-water ice appeared to be an all-around better performer, it was used exclusively for the remainder of the tests.

Effect of Variables on Rate of Heat Extraction

In general, tests were conducted at the relatively high temperatures and humidity levels expected to occur at the outlet of an impermeable suit containing a working man. Test temperatures ranged from 80° to 100° F and relative humidities from 80 to nearly 100 percent. Three rates of air flow through the pack were used (15, 22, and 35 cfm).

Effect of Temperature and RH

The effect of inlet air temperature on the rate of heat absorption is illustrated in figure 5.6. Relative humidity was held at 80 percent for these tests and each data point represents the average of two, and in some cases three, tests; the airflow rate was 35 cfm.

Note that, in general, heat absorption rates are well above the 1000 Btu level that is considered to be the practical minimum required for comfort at the activity levels of interest.

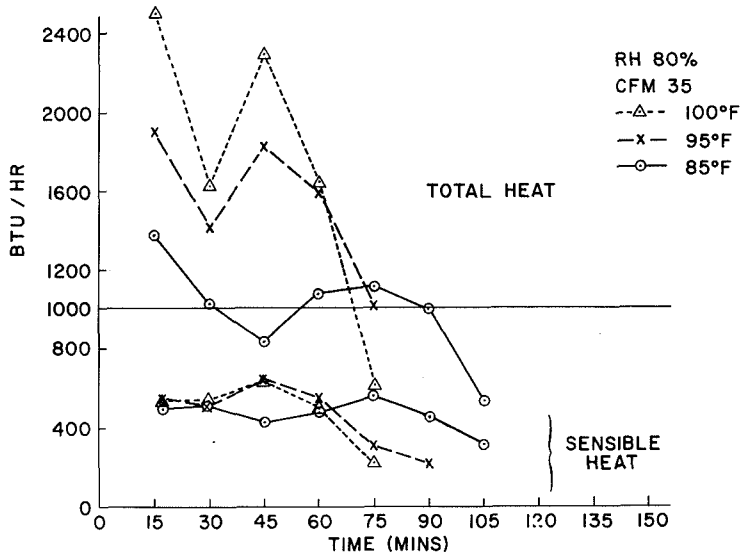

Figure 5.6 *Effect of inlet air temperature on heat absorption rates of canisters in ECU.*

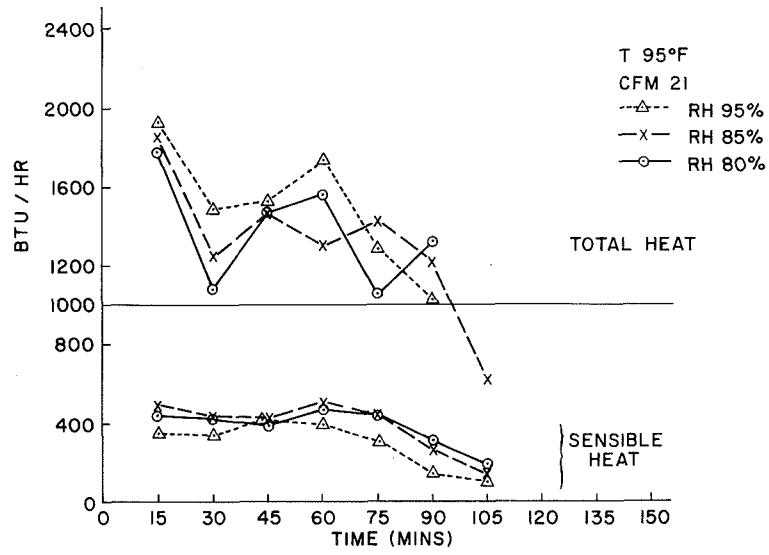

Figure 5.7 *Effect of relative humidity of inlet air on heat absorption rate of canisters in ECU.*

While temperature has a very significant effect on the total rate of heat absorption, its effect on sensible heat extraction (lower set of curves) is almost insignificant.

The effect of relative humidity on heat extraction is shown in figure 5.7 for an airflow of 21 cfm and a temperature of 95° F. The effect on the rate of heat extraction of humidity between 85 and 95 percent is quite small. It is the result of a change of only about 12 percent in water content of the air compared with the almost 60 percent change resulting from the temperature change from 85° to 100° F at 80 percent RH in the previous illustration.

Effect of Rate of Air Flow

In figure 5.8, the effect of the rate of air flow through the backpack on the rate at which heat is extracted is illustrated. The effect, although apparently quite small between 21 and 35 cfm, is to reduce the rate of heat extraction very significantly at 15 cfm.

Several graphs (figs. 5.9 and 5.10) are presented from ref. 6 showing the performance of the chemical pack (breathing canister) under conditions using a simulated man to absorb oxygen and expel carbon dioxide and water vapor. Details covering the development, construction, and testing of the canisters are documented in reference 6. These data demonstrate that, under the conditions of test, the breathing canisters were able to maintain the ambient oxygen level and hold the carbon dioxide level below 0.4 percent.

Tests of the ECU-DCS System

Some tests were run with the ECU attached to a dummy inside the DCS. These tests were run to determine airflow rates within the suit itself and to determine environmental heat loads on the

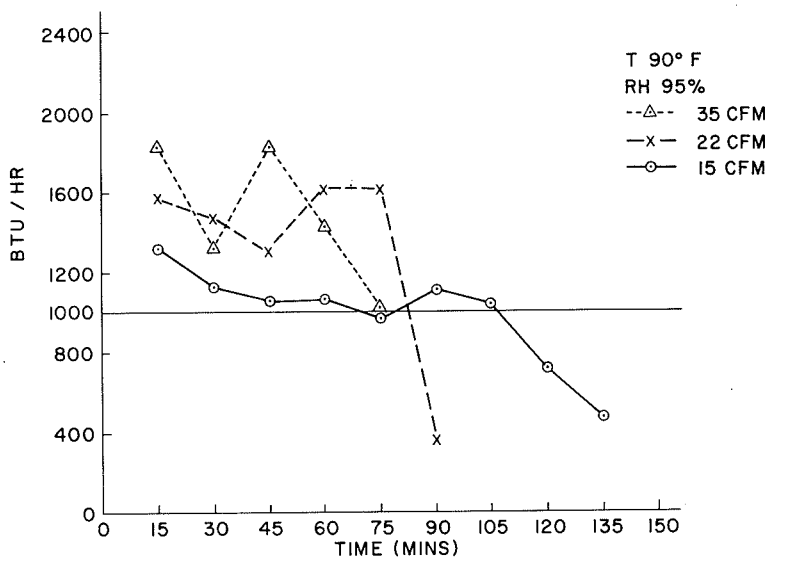

Figure 5.8 *Effect of rate of air flow through ECU on heat absorption rate.*

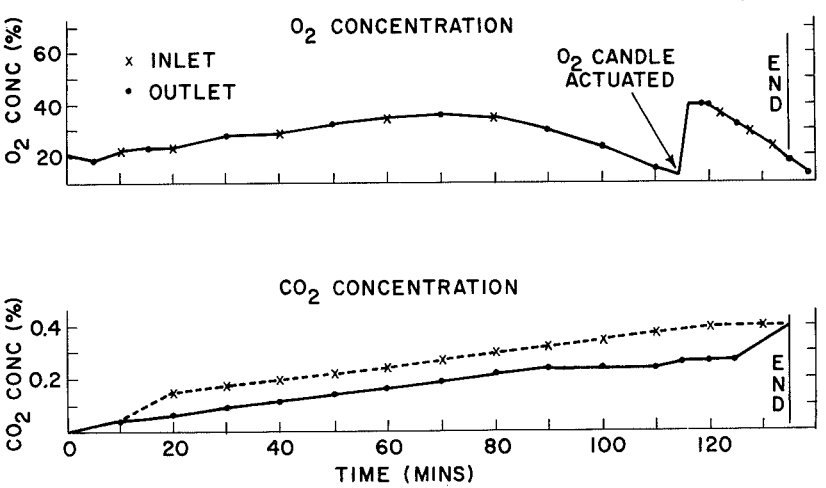

Figure 5.9 *Performance of chemical breathing canister.*

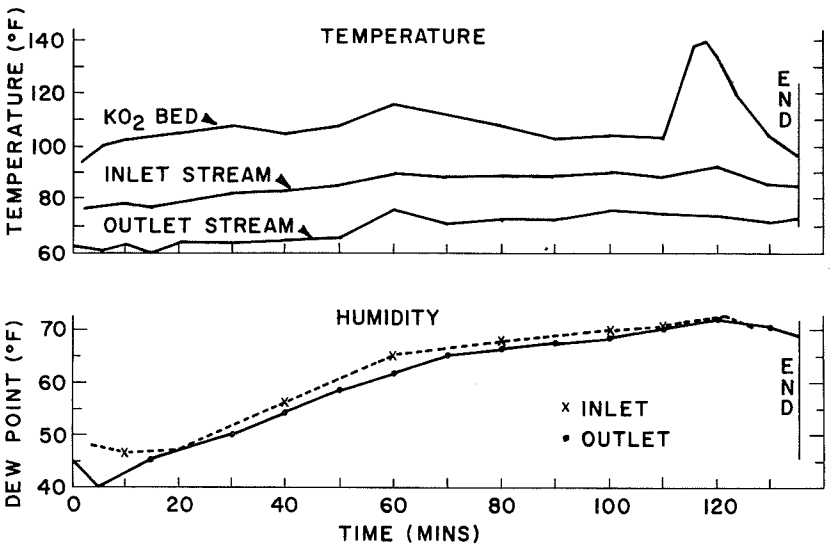

Figure 5.10 *Performance of chemical breathing canister.*

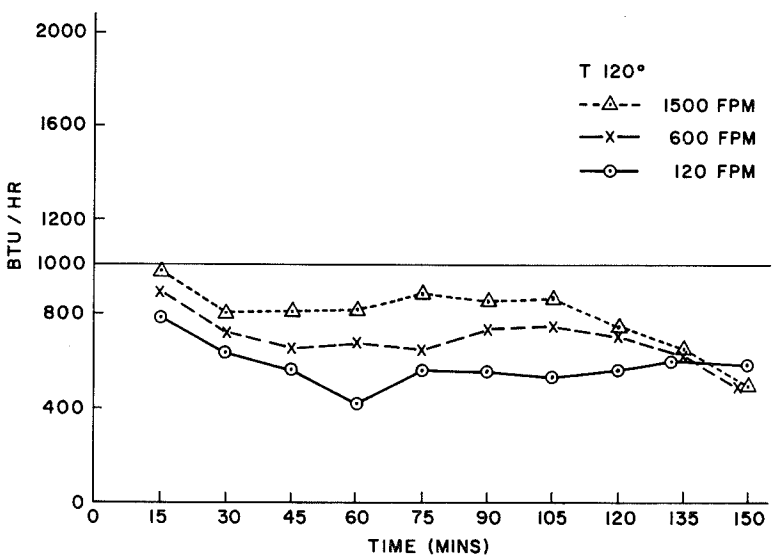

Figure 5.11 *Effect of wind velocity over damage control suit on heat absorbed with dummy in suit.*

ECU for different wind velocities. Figure 5.11 illustrates the effect of wind velocity on the rate at which heat was absorbed through the suit. This heat has to be extracted by the ECU in addition to the heat emanating from the wearer's body and from the chemical pack. Note that, at the test temperature of 120° F in a wind of approximately 1500 ft/min (about 17 mph), approximately 900 Btu/hr of heat absorption was required to balance the heat being conducted through the walls of the suit. The temperature of the air at the outlet of the ECU during this test was in the 70° to 75° F range.

In table 5.1 the effect of external temperature on the heat absorbed through the suit is presented. These tests were run with a dummy inside the suit; thus internal temperatures were much lower than would have been the case had the suit been manned by a live subject. As a result, the values of heat absorbed are presumably unrealistically high. Note that, at 72° F external temperature, 230 Btu/hr were absorbed. If the suit had been manned the net heat flow would probably have been in the opposite direction, resulting in a heat loss instead of in a heat gain. The internal temperature of the suit for this test averaged a little below 60° F.

Table 5.1 *Effect of temperature on heat absorption through DCS (with dummy in suit, wind velocity 120 fpm).*

External temperature, °F	*Heat absorbed by suit, Btu/hr (average for 120 min)*
140	800
120	550
72	230

Manned Tests

Physiological testing of the system is currently being done but data are available at this time from only one manned test of the complete system. This test was conducted in nearly calm air at about 130° F. The subject was seated and was largely inactive. Although this test ran for 105 min, the subject was uncomfortable during the last 15 min. Six thermocouples placed in the suit at various locations showed an average temperature of 88° F after the first 15 min, which gradually rose to just over 99° F at the end of the run. Oxygen, monitored continuously, remained close to the 21 percent level throughout the test period.

CONCLUSION

The objective of this work was to develop an environmental control unit capable of supporting a man in an impermeable suit at ambient temperatures up to 140° F for periods up to 2 hr. The results indicate that these objectives have been largely met, although at high temperature (130° F), cooling is sufficient for about 90 min only. Oxygen production and carbon dioxide scrubbing appear to be adequate. The oxygen level monitoring system works very well and adds a new safety dimension to the system.

Modifications contemplated for the ECU, when funding is available, should make the suit more comfortable to wear and much more practical for use in the confined spaces found aboard ship.

APPENDIX A NAVAL EXPLOSIVE ORDNANCE DISPOSAL FACILITY LIFE SUPPORT SYSTEM

Update on Paper Presented at 1969 Conference on Portable Life Support System.

At the last conference on Portable Life Support Systems, a paper was presented on the modular toxic environmental protective suit (MODTEPS) developed for the Naval Explosive Ordnance Disposal Facility (NAVEODFAC).

Briefly, MODTEPS is a self-contained clothing system designed to protect the wearer from the effects of toxic environments created by the presence of biological or chemical agents. The basic suit operation consists of the evaporation of liquid air contained in a backpack. This air serves to provide both a cooling and a breathing medium. The system is designed so that the internal suit pressure is about 1 in. of water above ambient pressure. This is accomplished by the venting of some of the air to the environment through an exhaust valve. The rest of the air is recirculated to the backpack and aspirated with freshly vaporized liquid air.

As part of the technical evaluation program, a series of tests were performed at the Deseret Test Center, Dugway Proving Ground, Utah. During these tests the suit was subjected to environments contaminated by chemical agents and biological simulant agents.

The chemical agents used were VX, GB, and PS (chloropicrin); VX and GB are nerve agents, while PS is a simulant for some riot control agents.

The test to determine the susceptibility of the suit to GB penetration was conducted in a chamber where the GB concentration could be controlled. Four unmanned suits were placed in the chamber on supports. One suit was placed in an upright position while the other three were bent at the waist, at 30°, 60°, and 90°, respectively. The backpack was placed at low flow rate and the suits were properly inflated. Then 12 g of liquid GB were vaporized on a hot plate. The concentration was 100 mg/m^3. The suits were in this environment for 2 hr. At no time was any presence of GB detected within the suit. The resistance of MODTEPS to VX was determined by placing two suits in a test chamber. One was erect, the other was bent in an arms-extended position. The VX was then showered on the suits to give a contamination of greater than 2 g/m^2. The agent did not enter the suit.

Finally, the suits were subjected to the presence of a biological simulant. This nonpathogenic simulant was BG (Bacillus Globigii) and was present in concentrations of 1.9×10^5 to 3.4×10^5 organisms/liter. Four suits were worn by test subjects and one was placed on a manikin. The subjects changed the backpack on the manikin and performed light exercises for 20 min. The currently used M3 protective suit was also employed in this test. It was found that the MODTEPS provided better protection than the currently used suit against the simulant agent.

From these test results, it was concluded that MODTEPS afforded the wearer adequate protection in areas contaminated by chemical and biological agents.

To provide liquid air for MODTEPS, it was necessary for NAVEODFAC to provide a convenient source of liquid air. It was decided to develop a field portable cryogenerator to manufacture liquid air for use with the suit. A 50-gallon trailer-mounted Dewar will provide a storage and transportation container. Some problem areas have been found in making this unit field-usable.

In the cryogenerator, ambient air is liquefied by being placed in contact with a condenser plate that has been cooled by helium. Moisture is removed from the ambient air by a water and ice separator.

It has been found that on humid days a rapid buildup of moisture subsequently freezes, blocks air flow, and causes the cryogenerator to shut down. Moisture also forms on the condenser, causing production to decrease and eventually cease.

It has also been found that high ambient temperatures inhibit proper heat rejection and cause the unit to overheat and eventually cease operation. A decrease in operating pressure will increase operating time in both these cases; however, the quantity of liquid air produced is lowered. An alternate solution will be investigated.

BIBLIOGRAPHY

1. D'Amico, S. *et al.*: Development of an Air Circulating Unit for Ventilation of Impermeable Suits. U.S. Naval Supply Activities, New York Clothing Supply Office, Brooklyn, New York, July 1955.
2. Lash, S.; and D'Amico, S.: Development and Evaluation of a Machinery Spaces Air-Supplied Suit. Naval Supply Research and Development Facility, Bayonne, New Jersey, C & T Report 41, November 1959.

3. McLoughlin, R.: Evaluation of a Thermoelectric Suit for Cooling Capacity. U.S. Naval Supply Research and Development Facility, Bayonne, New Jersey, Informal Technical Report 24-12/61, December 1965.
4. Weiss, R. A.: Physiological Evaluation of a Liquid Air Protective Suit. U.S. Naval Supply Research and Development Facility, Bayonne, New Jersey, No. RENS 80-02-002-00-01, November 1965.
5. George, E. J.; and Klein, A. H.: Modular Toxic Environment Protective Suit. NASA SP-234, 1969, pp. 29-39.
6. King, J. C.; and McGoff, M. J.: Development of Chemical Breathing Canisters for a Closed System Maskless-Suit Application. MSA Research Corporation Report MSAR 70-30, under NAVCLOTEXTRSCHU Contract No. N00289-69-CB 054, July 1970.
7. Orner, G. M.: Evaluation of Oxygen Sensing and Warning Device. NAVCLOTEXTRSCHU Report. In press.

6 A CHLORATE CANDLE/LITHIUM HYDROXIDE PERSONAL BREATHING APPARATUS

Frank E. Martin
Westinghouse Ocean Research and Engineering Center
Annapolis, Md.

INTRODUCTION

A major cause of death in coal mine disasters, particularly when underground fires or explosions occur, is the presence of toxic gases in the mine atmosphere. The Coal Mine Health and Safety Act of 1969 was enacted partially to encourage immediate application of current technology toward providing protection from such toxic atmospheres. The March 1970 National Academy of Engineering report, "Mine Rescue and Survival," recommended several alternative techniques for accomplishing such a task. Subsequently, a coal mine rescue and survival system (CMRSS) contract was awarded to Westinghouse to proceed through a process of requirement establishment, concept identification, detail design, procurement, fabrication, assembly, and test of all components necessary to produce survival, communications, and rescue subsystems within an 8-month schedule.

Figure 6.1 provides a brief scenario of the subsystems involved. The communications subsystem consisted of seismic and through-the-earth radio signals, both miner to surface and

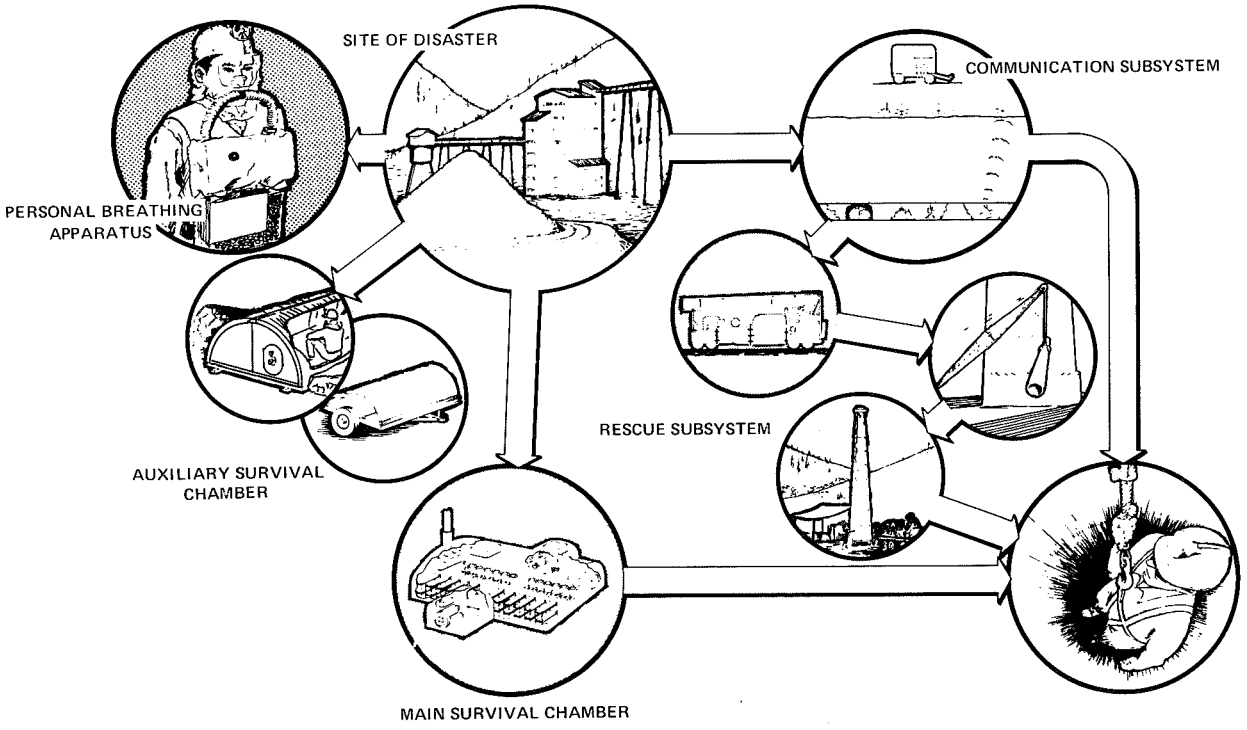

Figure 6.1 *Coal mine rescue and survival system.*

surface to miner. The rescue subsystem consisted basically of drilling technique development to provide a transportable, high-speed, high-precision drilling capability. Here we are concerned with the survival subsystem and, most particularly in this discussion, the personal breathing apparatus (PBA). The auxiliary survival chamber (ASC) is discussed in paper 9.

DESIGN REQUIREMENTS AND OBJECTIVES

The primary controlling document for breathing apparatus for coal mine use is Code of Federal Regulations, Title 30. To obtain Bureau certification, specific Title 30 requirements must be met dependent upon apparatus classification. With a view toward ultimate certification, Westinghouse design objectives sought to include satisfaction of most Title 30 stipulations. However, as a prototype unit, some Title 30 exceptions were taken while additional requirements outside of Title 30 were imposed.

Basic contract requirements for the PBA were to provide a respirable atmosphere regardless of environment for a 60-min duration at a very high metabolic rate while allowing intermittent voice communication. The NAE report also established a goal of $50 maximum sell price for the PBA when manufactured in lots of 50,000 to 75,000 units in a 2-year period. From these basic requirements and using Title 30 as a guideline, a complete set of requirements and objectives for the PBA was established.

The PBA offers the following features:

1. Nominal 1-hr endurance at a high work rate during which safe breathing mixtures are provided regardless of ambient atmosphere.
2. Nominal 3 SLPM oxygen generation throughout endurance.
3. Suppression of carbon dioxide level at mouthpiece inhalation side below 1 percent.
4. Breathing resistance maintained at less than 4 in. water total for inhalation and exhalation (generally less than 2 in. water for either).
5. Maximum gas inhalation temperature of 120° F at peak work rates and ambient 50°-60° F coal mine conditions (<120° F at reduced work levels) as per Title 30, table 4, work schedule.
6. Highly intelligible voice communication through man/apparatus interface.
7. Clear vision and environmental protection through man/apparatus interface.
8. Complete fill of 4-liter breathing bags with oxygen in 20-35 sec after actuation.
9. Complete apparatus don time of 60 sec.
10. Long storage life with no maintenance.
11. Minimum size and weight for present state of the art.
12. Estimated production cost of $50/unit for a volume of 50,000 to 75,000 units over a 2-year period.

SELECTION OF PBA CONCEPT

In this phase, emphasis was on the urgent requirement to meet an early program delivery commitment with a prototype apparatus that would represent current technology and would provide a means for subsequent design evaluation. Consequently, tradeoff analyses concentrated on those systems requiring minimal development and weighted this factor quite heavily. The goal was to give the Bureau of Mines the best possible results in the time available by achieving new applications of proven technology. This attitude is exemplified by the tradeoff most fundamental to design of the entire apparatus—oxygen source.

CRITERION	%	KO_2 W. Initiator		Chlorate/LiOH		Bottled O_2/LiOH	
		Rating	x%	Rating	x%	Rating	x%
I. Reliability	25	705	17,625	690	17,250	605	15,125
II. Portability	20	650	13,000	270	5,400	0	0
III. Cost	25	485	12,125	495	12,375	420	10,500
IV. Schedule	30	360	10,800	690	20,750	800	24,000
TOTALS (high score wins)			53,650		55,775		49,625

Figure 6.2(a) *PBA trade-off study on oxygen generators–systems.*

FACTOR 1 - 10	%	KO_2 W. Initiator		Chlorate/LiOH		Bottled O_2/LiOH	
		Rating	x%	Rating	x%	Rating	x%
A) No. of Seals, Moving Parts and Connections	15	8	120	6	90	4	60
B) Deterioration W. Use (Probable-possible-unlikely)	15	6	90	9	135	9	135
C) Maintenance (daily-monthly-none)	10	9	90	9	90	5	50
D) Durability	15	9	135	9	135	8	120
E) Inhalation Temp. (high - low)	15	4	60	4	60	4	60
F) Flexibility of use (Fixed rate-Demand rate)	10	9	90	1	10	1	10
G) Don Time	10	9	90	9	90	9	90
H) New Designs (complete-none)	10	3	30	8	80	8	80
TOTALS (high score wins)	100		705		690		605

Figure 6.2(b) *PBA trade-off study on oxygen generators–reliability.*

FACTOR 1-10	%	KO_2 W. Initiator		Chlorate/LiOH		Bottled O_2/LiOH	
		Rating	x%	Rating	x%	Rating	x%
A) Weight (10 lb - 5 lb)	70	5	350	3	210	0	0
B) Volume (200 in^3-100 in^3)	30	10	300	2	60	0	0
TOTALS (high score wins)	100		650		270		0

Figure 6.2(c) *PBA trade-off study on oxygen generators–portability.*

The tradeoff study for oxygen generator selection (fig. 6.2) considered three candidate systems: potassium superoxide with a chlorate candle initiator, chlorate candle with a lithium hydroxide carbon-dioxide absorbent, and compressed oxygen with lithium hydroxide absorbent. The chlorate candle lithium hydroxide system prevailed in the tradeoff primarily because of good scores in all areas related to schedule or development requirements while being at least equivalent with the potassium superoxide system in maintenance, durability, heat contribution, and fabrication cost. In addition, it eliminated at least two developmental requirements associated with potassium superoxide–the need for "quick start" capability and minimization of breathing resistance.

Inputs to the portability parameters were updated on the basis of current knowledge. The original inputs were somewhat more optimistic because of some naivete regarding chlorate candle modifications required to suit this application. However, the overall tradeoff result remained unaffected.

While schedule-related parameters were heavily weighted, it is also evident that good scores on these were not in themselves sufficient. This is shown by the fact that a bottled oxygen/lithium hydroxide system, despite its low development requirements, placed third in overall ratings primarily because of poor scores in material cost, portability parameters, and maintenance requirements.

FACTOR 1-10	%	KO_2 W. Initiator Rating	x%	Chlorate/LiOH Rating	x%	Bottled O_2/LiOH Rating	x%
A) Material ($25-$5)	20	8	160	7	140	0	0
B) Fabrication	25	2	50	5	125	8	200
D) Total Estimated Production Cost (>$50-$50-<$50)	55	5	275	6	330	4	220
TOTALS (high score wins)	100		485		495		420

Figure 6.2(d) *PBA trade-off study on oxygen generators–cost.*

FACTOR 1-10	%	KO_2 W. Initiator Rating	x%	Chlorate/LiOH Rating	x%	Bottled O_2/LiOH Rating	x%
A) No. Off-the-shelf components (10% - 100%)	30	4	120	8	240	8	240
B) Developmental Risk (High-Low)	30	4	120	7	210	8	240
C) Total Development Required	40	3	120	6	240	8	320
TOTALS (high score wins)	100		360		690		800

Figure 6.2(e) *PBA trade-off study on oxygen generators–contract schedule.*

THE CHLORATE CANDLE AS OXYGEN SOURCE

The PBA application requires what probably constitutes the most rigid set of specifications ever imposed on a chlorate candle system. The extremely close working relationship that had been developed with the chlorate candle subcontractor, Arrowhead Products Division of Federal-Mogul Corp., enabled us to participate in all major design decisions, material specifications, developmental testings, and concept selections. Charles Leffler, director of the Arrowhead PBA candle development, was particularly important to this effort.

Configuration

As shown in figure 6.3, the chlorate candle configuration chosen for the PBA is L shaped. This geometry facilitates volume minimization in packaging. Alternate configurations considered included two separate, parallel 30-min duration candle packages and two parallel sodium chlorate segments enclosed within the same envelope but connected by means of a "crossover" mixture. The former was rejected because of increased bulk requirements while the latter required undesirable chemical formulation compensation for complex thermal effects induced by the influence of first segment's decomposition on the burn rate of the second.

A similar situation was also encountered within the L-shaped envelope. The heat produced within the long leg of the L by decomposition would accelerate burn rate of the short leg if a uniform chemical formulation were employed. Consequently, a smaller amount of iron powder fuel was incorporated in the short leg to retain the 3 SLPM nominal rate and 60-min duration requirements. This situation was aggravated by the fact that the burn front area (and therefore burn rate) accelerates as it progresses through the elbow joint of the L shape.

Theory of Operation

The high temperature required to sustain the decomposition of sodium chlorate is obtained in part from the heat of decomposition of the chlorate itself and in part from the oxidation of the metallic fuel (1μ reduced iron powder), which is also an exothermic reaction. A combined catalyst and gas impurity getter (barium peroxide) is also included in the candle formulation. Its prime purpose in candle formulations is to react with free chlorine, thereby reducing its presence in the generated oxygen. All candles evaluated in this study were produced by the wet pressing technique.

As evidenced by analysis of the ash clinker constituents, many reactions are believed to take place in candle decomposition. The main reactions that illustrate oxygen evolution and chlorine elimination, however, include the following (refs. 1-4):

$$2NaClO_3 \longrightarrow 2NaCl + 3O_2$$

$$4NaClO_3 \longrightarrow 2Na_2O + 2Cl_2 + 5O_2 \text{(mechanism ill-defined)}$$

$$BaO_2 + Cl_2 \longrightarrow BaCl_2 + O_2$$

Free oxygen also combined with the iron fuel in varying degress of reaction completion to produce various oxides of iron. The main constituents of the ash clinker include sodium chlorate and oxides of iron.

Candle activation is a multiple stage requirement. The first stage includes a modified hand-grenade-type bouchon that uses a munitions primer. Mechanical activation of the primer immediately produces a flash of hot gases releasing about 800 cal of heat. This heat energy is sufficient to ignite a pyrotechnic first-fire composition. The heat energy released by the first-fire reaction (~5000 cal) then ignites a cone portion of the oxygen candle, which is a fuel-enriched composition of chlorate. Enough heat is then finally generated to initiate and sustain the main portion or core composition of the candle. The reaction then proceeds until the supply of chlorate is exhausted. The entire candle is wrapped in layers of a high-temperature-resistant, ceramic-type insulation material. The insulation serves to retain sufficient heat within the generator housing to sustain chemical decomposition, and also to help maintain generator wall temperatures within specification (350° F max).

Candle Reliability versus Burn Rate, Duration, and Temperature

This rather fine balance of heat containment (via insulative materials, radiative shields, and air gaps) versus heat dissipation (via skin material selection and surface emissivity) to maintain a 350° F maximum envelope skin temperature played the largest role in the magnitude of development required. Too much heat containment resulted in very rapid decomposition, while too much heat dissipation would result in too slow decomposition and at times premature extinguishment of the reaction. Moreover, the balance that was achieved had to be matched to a chemical formulation with heat content sufficient to guarantee reliability and yet meet the flow rate and duration requirements.

These requirements, as interpreted directly from Title 30, are: whenever oxygen is produced from a nondemand type source, flow rate must be a nominal 3.0 SLPM for a duration not less than the stated apparatus duration (in this case, 60 min). In-house calculations determined that either or both of these requirements could be relaxed (extent dependent on total system volume) and still possess an apparatus that would retain enough residual oxygen in 4-liter breathing bags to sustain comfortable respiration even under high work rate conditions for the 60-min duration. However, the Title 30 requirements were retained as contract objectives.

The maximum envelope skin temperature of 350° F was derived from a worst-case analysis of coal dust autoignition in which it was assumed that a coal dust layer composed exclusively of particles $<75\ \mu$ diam with 52 percent volatiles content has collected on the candle surface. Even though it is recognized that this constitutes a highly improbable situation, this specification also was retained as a design objective.

To satisfy these multiple requirements and yet retain reliability, a wide assortment of chemical formulations was evaluated. These included mixtures of low fuel with catalyst, mixtures with potassium perchlorate, and mixtures with silicon dioxide inert and several permutations thereof.

The addition of silicon dioxide inert (40-mesh granules) constitutes a unique method of stabilizing the decomposition front, thus controlling burn rate. Visual examination of spent clinkers and burns-in-progress confirmed that silicon dioxide maintained the front in an attitude transverse to the candle axis. Without silicon dioxide, the front often progressed in a random fashion, producing large variations in burn rate and consequent loss of duration. The formulation that ultimately displayed the greatest reliability under design constraints gave reproducible burn rate profiles with no chemical failures over 26 candle decompositions.

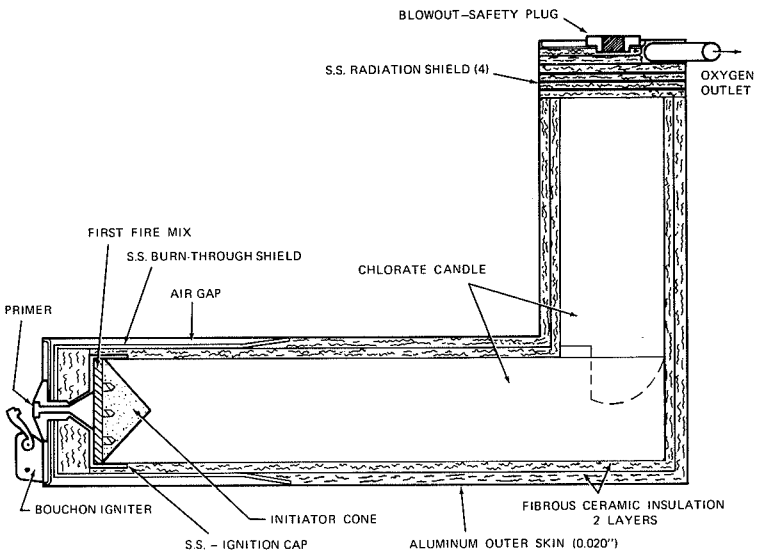

Figure 6.3 *PBA chlorate candle.*

Ambient Test Temperature: 51 - 77°F

Time for 4 liters (STP) Delivery: 22 - 35 seconds

Decomposition Duration: 56.75 - 64.0 min.

Maximum Tube Wall Temperatures:

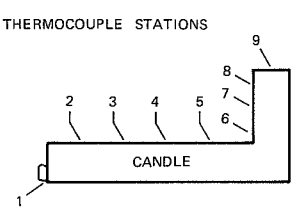

1) 275 - 330°F
2) 285 - 322°F
3) 289 - 327°F
4) 286 - 316°F
5) 273 - 294°F
6) 285 - 310°F
7) 303 - 346°F
8) 328 - 368°F
9) 315 - 360°F

Results were obtained while candle was subjected to multi-orientational movements.

Figure 6.4 *PBA chlorate candle final test data range.*

It had earlier been established that the preferable container material was black anodized aluminum due to its preferred heat dissipation qualities as contrasted with stainless steel, the more conventional candle container material. The combination of this container with the proper insulative materials and candle formulation produced the construction shown in figure 6.3 and the qual test results in figures 6.4 and 6.5.

These results show that all the design objectives have been successfully approximated; however, surface temperature of 350° F and duration of 60 min can not be reliably specified as minimum values without further development.

These two parameters can be met by a relatively simple redesign of the container with little or no additional development of the chlorate mix. In fact, solving the temperature problem, which calculations have shown can be accomplished by the addition of fins to the aluminum casing, may also solve the duration problem since the burn rate of the candle is partially a function of heat dissipation. The more efficient the dissipation, the slower the burn.

Should the duration not be achieved with the lower surface temperature, the case could be increased slightly to accommodate increased length of the candle.

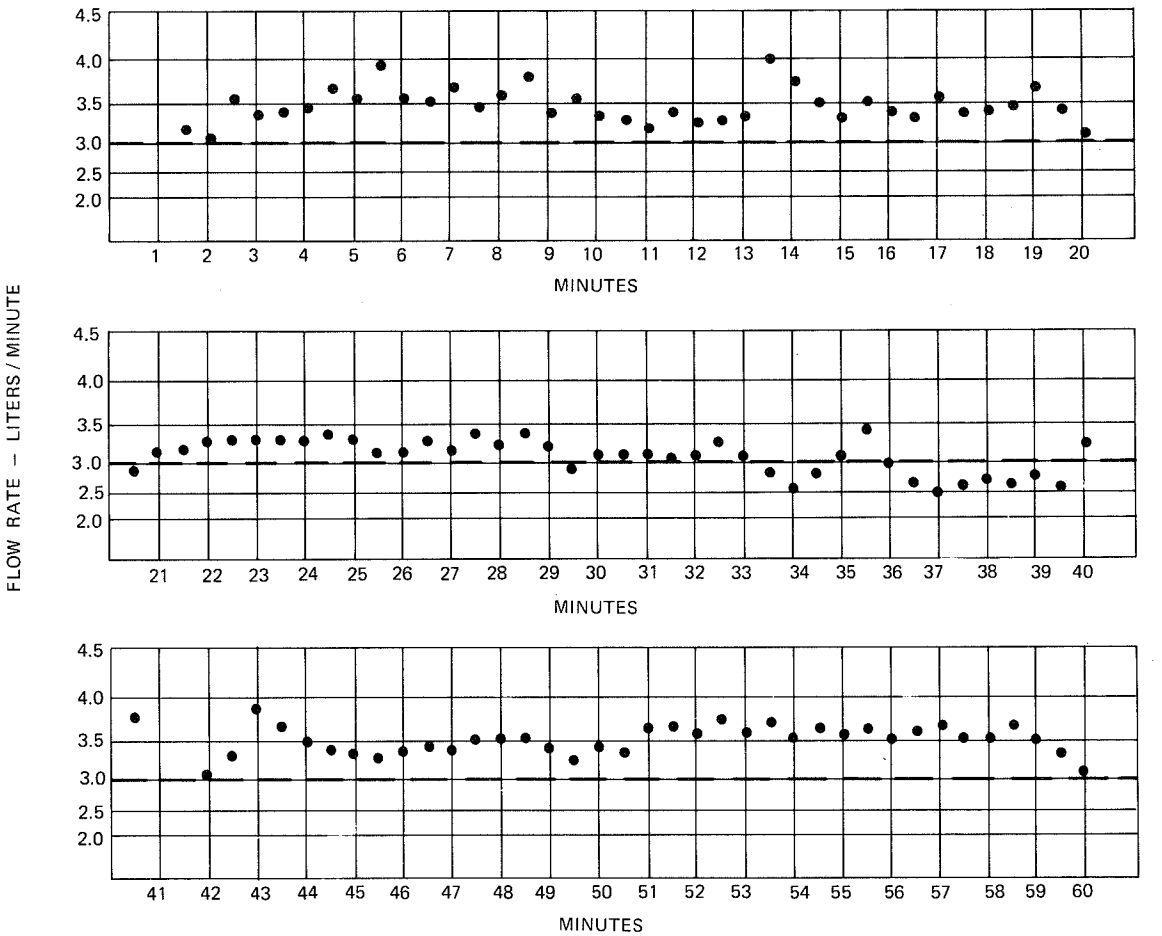

Figure 6.5 *Qualification test flow rate data.*

Candle Ignition Design

The multiple-stage sequence involved in candle ignition has previously been described; however, it was not then emphasized that critical requirements determined its design. These requirements are ignition reliability, production of 4 liters oxygen within the first 20 to 35 sec, prevention of burn-through to the aluminum casing, and maintenance of the 350° F surface temperature specification. The bulk of these requirements are satisfied by proper sizing and formulation of the cone material. The cone must both provide the initial 4 liters of oxygen and initiate sustained decomposition while itself decomposing in a minimally exothermic manner. As was revealed by the qual test data (figs. 6.4 and 6.5) and by the reliability shown over 26 qual and prequal runs, this balance of properties was successfully achieved.

Reliability was significantly enhanced by design of an intimate cone/first fire interface. The most successful such interface design involved drilling five 3/16"D holes to a depth of 5/8 in. into the cone and then packing these tightly with first fire. Additional first fire was then applied uniformly over the cone face before carefully inserting the candle into its stainless steel ignition cap (fig. 6.3).

This cap was designed to contain molten sodium chloride produced from the violent cone decomposition and prevent it from traveling to the package perimeter. This was further prevented by welding of the bouchon ignition channel and ignition cap into an integral part and by selection of high melting point refractory material as insulation. Finally, a stainless steel burn-through shield, lining the entire ignition end of the package, assures that molten material will not contact the aluminum exterior even if it does manage to travel to the perimeter.

Purity of Generated Oxygen

The normal exit path for oxygen generated by the chlorate candle is through flexible tubing attached at the far end of the short leg. Also located in this vicinity is a pressure-relief assembly provided for the event that gas pressure buildup occurs through any possible exit path blockage.

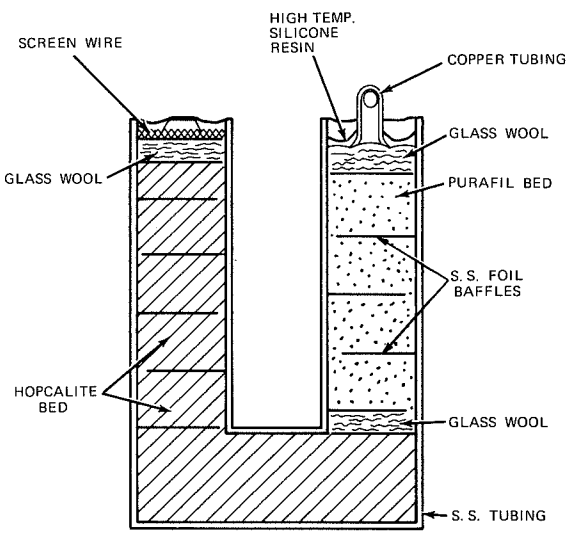

Figure 6.6 *Gas scrubbing unit for PBA chlorate candle.*

The flex tubing attaches to a separate U-shaped gas impurity scrubbing cartridge, designed for installation within the inlet plenum of the PBA carbon dioxide removal canister. This scrubbing unit (fig. 6.6) contains baffled beds of Purafil and hopcalite for removal of chlorine and carbon monoxide, respectively. Its performance has proven quite efficient as shown by gas analysis data in figure 6.7. The impurity levels of all gases are well within standards applicable to breathing mixtures with the exception of carbon dioxide. No provision was made within the gas scrubbing cartridge for carbon dioxide removal under the rationale that the lithium hydroxide bed downstream of the cartridge could readily accomplish this task.

LITHIUM HYDROXIDE CANISTER DESIGN

Carbon Dioxide Absorbent Selection

Three state-of-the-art chemical absorbents applicable for PBA use, lithium hydroxide, baralyme, and sodasorb, were evaluated on the criteria shown in figure 6.8. Lithium hydroxide is by far the most efficient absorbent of carbon dioxide by weight. Its theoretical absorption capacity is 0.92 lb CO_2/lb LiOH as opposed to a capacity of 0.50 lb CO_2/lb of baralyme (ref. 5). Its density, however, is quite low, giving it slightly less efficiency than baralyme in terms of volume.

It has slight defects also in its comparative cost effect on the PBA and in the amount of heat liberated; however, these are compensated by the assignment of less development risk. The lower development risk rating was achieved primarily because of preliminary testing by Foote Mineral Co. This testing produced an experimentally derived figure for the amount of lithium hydroxide required to meet PBA input conditions.

Sample Time (min)	O_2 (%)		CO_2 (%)		CO (ppm)		H_2O (ppm)		Hydrocarbons (ppm CH_4)		Cl_2 (ppm)
	A	B	A	B	A	B	A	B	A	B	A&B
5	99.90	99.93	0.10	0.07	0.60	0.55	0.0	15.0	2.5	6.4	<0.1
10	99.89	99.92	0.11	0.08	0.65	0.60	5.0	20.0	3.2	6.1	"
15	99.86	99.90	0.14	0.10	0.70	0.70	14.0	35.0	4.2	6.0	"
20	99.86	99.89	0.14	0.10	0.75	0.75	30.0	55.0	4.7	6.3	"
25	99.84	99.87	0.15	0.12	0.90	0.90	60.0	90.0	5.6	6.6	"
30	99.67	99.84	0.32	0.14	1.05	1.10	116	150	6.4	7.3	"
35	99.52	99.77	0.46	0.20	1.30	1.40	190	245	7.4	11.0	"
40	99.52	99.70	0.44	0.26	1.65	1.75	420	405	8.6	11.7	"
45	99.46	99.57	0.46	0.37	2.15	2.30	800	615	9.9	13.5	
50	99.32	99.40	0.62	0.52	2.95	3.15	630	820	12.2	15.7	"
55	99.12	99.15	0.86	0.75	4.85	4.75	200	915	15.0	18.6	"
60	Candle out		Candle out		Candle out		Candle out		Candle out		

Oxygen by Beckman O_2 Analyzer, Model E2.

Carbon Monoxide by Beckman Model GC-5 Gas Chromomatograph (helium ionization detector).

Water Vapor by Beckman Trace Moisture Analyzer P_2O_5 Electrolytic Cell.

Chlorine by General Electric Halogen Detector, Type H.

Hydrocarbons by Beckman Model 109 Flame Ionization Total Hydrocarbon Analyzer.

Carbon Dioxide by Beckman IR 20.

Figure 6.7 *PBA chlorate candle gas analyses.*

CRITERION 1-5-10	%	LiOH		Baralyme	
		Rating	%	Rating	%
1) Sensible heat BTU/ft^3 CO_2 absorbed	10	7	70	9	90
2) Cost Effect on PBA	20	4	80	6	120
3) Non Operational Reliability	15	9	135	9	135
4) Theoretical Weight req'd for 1 hour mission	20	9	180	5	100
5) Theoretical Bulk volume req'd for 1 hour mission	15	7	105	9	135
6) Development Risk (high low)	20	10	200	8	160
TOTALS	100%		770		740

NOTE: Sodasorb comparable to Baralyme in all parameters

Figure 6.8 *Carbon dioxide canister absorbent trade-off study.*

Even so, the tradeoff overall results were very close. As noted in figure 6.8, sodasorb is comparable in all parameters to baralyme. All other conventional carbon dioxide absorbent systems were considered either less efficient or not applicable to PBA use without entailing undue development risk. Accordingly, lithium hydroxide was selected as the absorption material, primarily because of higher probability of successful development.

Lithium Hydroxide Canister Design Requirements

In contrast to the chlorate candle, which must generate oxygen at a fixed rate based on highest expected workload, the carbon dioxide absorbent is sized to accommodate

fluctuations in workload and the total amount of carbon dioxide produced. Accordingly, the amount of carbon dioxide liberated during a 60-min high-work-rate program was estimated as shown in figure 6.7. This was accomplished by estimating from (ref. 6) the oxygen expenditure per activity, totaling the result, and applying an average respiratory quotient value of 0.85 to arrive at 82 liters carbon dioxide.

A safety factor of nearly 25 percent above this was included in our design considerations to cover the following:

1. The stated oxygen consumption rates are estimated for specific tasks and do not account for recovery time required in progressing from greater to lesser work rates.
2. Simulation of table 4 (Title 30) work tasks was accomplished on a bicycle-type ergometer (see fig. 6.9 for ergometer settings). Since the ergometer requires continual use of the same musculature, recovery times are yet more difficult to estimate.
3. Respiratory quotient (RQ) may reach values of 0.9 - 1.0 at high work rates.
4. Respiratory quotient may vary depending on the individual test subject. Therefore, in consultation with Westinghouse Physiology Department, a figure of 102 liters (0.41 lb) of carbon dioxide was estimated as the worst-case amount the canister would have to accommodate.

Activity	Time (min)	SLPM O_2	Total O_2 (ℓ)	Total CO_2	Ergometer Setting (Kiloponds)
1) Sampling & reading	2	0.7	1.4		0
2) Walk at 3 mph	2	1.2	2.4		1.5
3) Climb 75° treadmill	1	2.5	2.5		3.5
4) Walk at 3 mph	2	1.2	2.4		1.5
5) Pull 45 lb. wt. 5 ft. 60 times	5	2.1	10.5		3.0
6) Walk at 3 mph	3	1.2	3.6		1.5
7) Carry 50 lb. wt. over overcast 4 times	8	1.9	15.2		2.75
8) Sampling & reading	2	0.7	1.4		0
9) Walk at 3 mph	4	1.2	4.8		1.5
10) Runs at 6 mph	1	2.7	2.7		3.75
11) Carry 50 lb. wt. over overcast 6 times	9	1.9	17.1		2.75
12) Pull 45 lb. wt. 5 ft. 36 times	3	2.1	6.3		3.0
13) Sampling & reading	2	0.7	1.4		0
14) Walk at 3 mph	6	1.2	7.2		1.5
15) Pull 45 lb. wt. 5 ft. 60 times	5	2.1	10.5		3.0
16) Carry 45 lb. wt. walking at 3 mph	3	1.9	5.7		2.75
17) Sampling & reading	2	0.7	1.4		0
TOTAL	60		96.5	82 liters	

Figure 6.9 *Oxygen consumption*
CO_2 liberation estimate for Title 30, Test 4, Table 4 work schedule.

Pressure drop across the canister was another important design parameter. The theoretical plate area based on a 4 by 14 mesh size reactant material computed to be 15 $in.^2$ based on an flowrate of 85 SLPM air and a pressure drop not exceeding 2 in. water. The bed depth, given an experimentally derived figure for required lithium hydroxide volume, was computed to be 6 in. By adopting a canister geometry within these dimensions, we were confident of maintaining

pressure drop below 2 in. water at even the highest work rate called out by Title 30 (at which a velocity of 40 SLPM could occur).

Finally, a circle-flow breathing circuit was selected over pendulum flow, and axial flow through the canister was selected over radial flow. Since some problem was anticipated in dissipating the heat of reaction generated with the lithium hydroxide bed (sensible heat = 875 Btu/lb CO_2), circle flow appeared preferable because of greater opportunity for heat transfer as contrasted to the reduced circuitry of pendulum flow.

In addition, pendulum flow would have presented an opportunity for formation of depleted reactant dead spaces within the canister. Axial flow through the canister was chosen primarily because it afforded fewer fabrication difficulties, minimal bulk, and greater opportunity for internal canister modification. Some canister modification in the form of internal finning was comtemplated, once again, because of anticipated heat transfer difficulties.

Preliminary Unmanned Testing

Concurrent with the formation of our design decisions, Foote Mineral Co., agreed to conduct some preliminary performance evaluations on lithium hydroxide based on input conditions. We are especially indebted to Dr. Dan Boryta and Dr. Wm. Hart of Foote for their valuable cooperation in this test. The test was run by open-circuit flow of 100 percent RH air containing 4.3 percent carbon dioxide at 90° F through a quartz tube filled with 1 lb sm 4 by 14 LiOH and at a flow rate of 0.40 lb CO_2/hr. Breakthrough (rapid increase of carbon dioxide in effluent above 0.5 percent) did not occur until some 35 to 40 min into the test.

This result appeared quite encouraging in view of the fact that it was achieved in spite of low thermal conductivity of the quartz container. Thermocouple probes within the bed indicated that bed center temperature was in excess of the optimum operating range for our particular input conditions within 5 to 6 min. Thereafter, most of the bed was operating at greatly reduced efficiency because of steadily increasing thermal rise to a maximum of 284° F. According to a Foote Mineral Co., phase diagram (fig. 6.10), the optimum operating range for this application falls between 116° and 149° F.

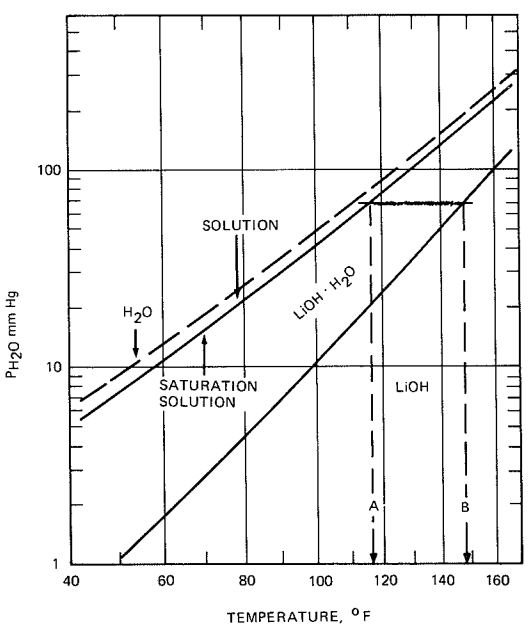

Figure 6.10 *Vapor pressure LiOH–H_2O (ref. 7)*

This diagram is based on experimental and literature evidence that the most efficient route for formation of lithium carbonate from lithium hydroxide proceeds through a lithium hydroxide monohydrate (LiOH • H_2O) intermediate (ref. 7):

$$2LiOH + 2H_2O \longrightarrow 2\ LiOH \bullet H_2O \qquad (1)$$

$$2LiOH \bullet H_2O + CO_2 \longrightarrow Li_2CO_3 + 3H_2O \qquad (2)$$

In figure 6.10, the lower curve represents the dissociation vapor pressure of lithium hydroxide monohydrate while the upper solid curve is LiOH • H_2O saturated solution vapor pressure. Poor absorption of carbon dioxide occurs when either dry

conditions (such as caused by excessive bed temperature) prevent formation of $LiOH \bullet H_2O$ or when excessive moisture causes formation of a saturated solution. Therefore, maximum utilization occurs when bed temperature is maintained between the two curves at the level determined by "effective" vapor pressure. Effective vapor pressure is defined as the sum of input water partial pressure and the partial pressure of input carbon dioxide converted to water. Under input PBA conditions, this works out to 68.2 mm Hg effective vapor pressure, thus establishing optimum range at 116° to 149° F.

Clearly, some measure of additional cooling capacity beyond that inherent to the packed quartz tube would be required for the PBA canister. It remained, however, to determine whether the use of more conductive canister material alone could accomplish this task because of the possibility that heat capacity of the bed itself was the limiting factor. Foote could offer no reliable estimate as to the actual thermal conductivity of the bed while in PBA use (consisting, as it would, of a complex mixture of H_2O, LiOH, $LiOH \bullet H_2O$, Li_2CO_3 and $LiHCO_3$). It was decided to defer a decision on the necessity for internal cooling fins until data were available from actual manned testing.

However, Foote was able to estimate the amount of lithium hydroxide required under the assumption that bed temperature could be controlled. Comparison of the unmanned testing data (which used a developmental grade of lithium hydroxide with background comparative runs and extrapolation of results under more suitable thermal conditions led Foote to conclude that a minimum of 1.36 lb standard Navy grade 4 by 14 mesh lithium hydroxide would be sufficient.

Developmental Lithium Hydroxide Canister

The canister designed to contain the lithium hydroxide is an axial flow type consisting of standard perforated brass screens at each end for retention of the lithium hydroxide charge (fig. 6.11). The body of the canister is made of red brass having a thermal conductivity of 92 Btu/hr-ft-°F. The amount of heat that will be generated by a man working to table 4 Title 30 work schedule computes to be approximately 357 Btu/hr. Considering the worst case of laminar flow convection cooling, which would be the case if the miner were not moving but standing in a stagnant air environment, the exposed surface area of the body of the canister is not enough to transfer this quantity of heat. Therefore, a corrugated heat exchanger surface affording additional surface area was built into the output end of the canister housing to help cool the effluent breathing gas.

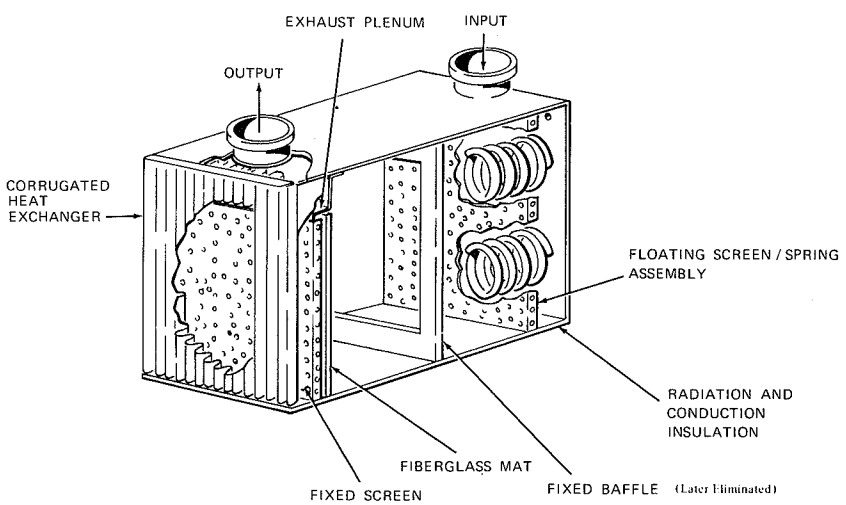

Figure 6.11 *Developmental LiOH canister.*

Two plies of Air-Mat No. 12 fiberglas mat were installed over the stationary output end screen. The canister was charged and closed up, thus compacting the input screen against the bed

by means of springs (2-3 psi pressure), and was then ready for pressure-drop and dust testing at 85 SLPM flow.

The canisters were first blown through with dry nitrogen at a flow rate of 85 SLPM and pressure drop measured across the inlet and outlet ports (~1.5 in. H_2O). The dust test was performed by placing a virgin piece of No. 12 Air-Mat filter material over the outlet port of the canister and purging the canister with 85 SLPM nitrogen introduced at the inlet port for 3 sec. The sample piece of filter material along with a nonexposed piece of same was subjected to titration pH analysis and the values compared. Both samples consistently registered the same pH. Therefore, the test was negative and the filter design acceptable.

Manned Testing and Heat Transfer Analysis of Developmental Canister

The next test was a manned test of the canister. The final breathing bags, man/apparatus interface, and chlorate candle, not yet delivered, were simulated with comparable in-house components. A candle simulator was built to the same configuration as the deliverable unit and was fitted with two electric-resistance heaters that would bring the surface temperature up to and beyond 350° F. The breathing bags consisted of two rubber anesthesiology bags, and man/apparatus interface was a standard scuba-type mouthpiece. Aside from these developmental modifications, the experimental setup was as shown in figure 6.12, with oxygen and carbon dioxide being monitored continuously and then returned to the system. Breathing resistance and gas inhalation temperature were also continuously monitored. Temperatures of the canister wall and lithium hydroxide bed were spot checked. The test subject was simulating the work schedule of figure 6.9 by riding a bicycle ergometer throughout the test at various kilopond settings.

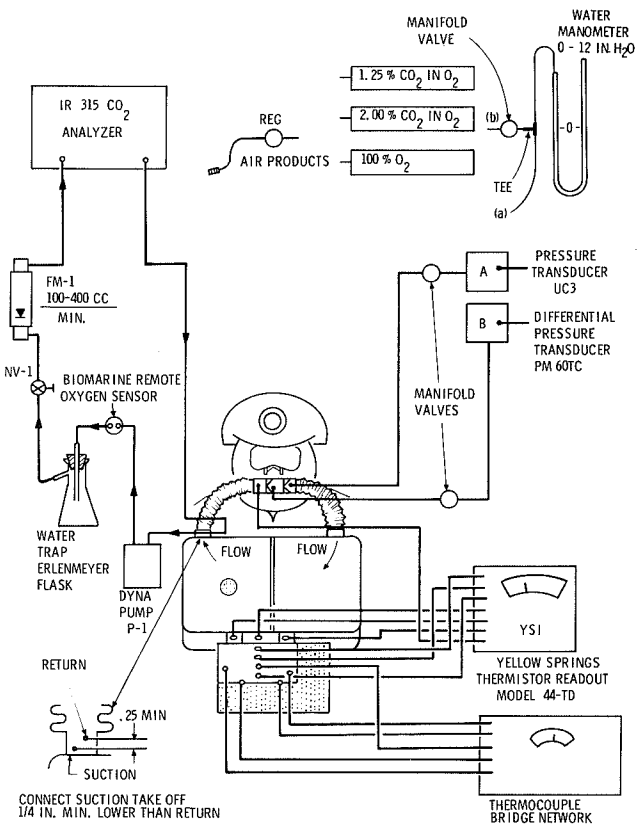

Figure 6.12 *Developmental test setup schematic.*

The data in figure 6.13 (runs 1, 2, and 3) on inspired gas temperature versus test duration show that the canister as then constructed possessed inadequate heat transfer characteristics.

The first man test, which ran for 33 min and 45 sec, was aborted because the inhalation temperature exceeded 115° F.

The second man test was run the same way as the first except that the candle simulator was not energized. This run lasted 34 min and was aborted, again because the inhalation temperature exceeded 115° F. Comparing the two sets of data showed that the heat generated by the candle simulator contributed little to the overall heat load of the canister and that the exothermic reaction and conductivity of the lithium hydroxide had to be determined.

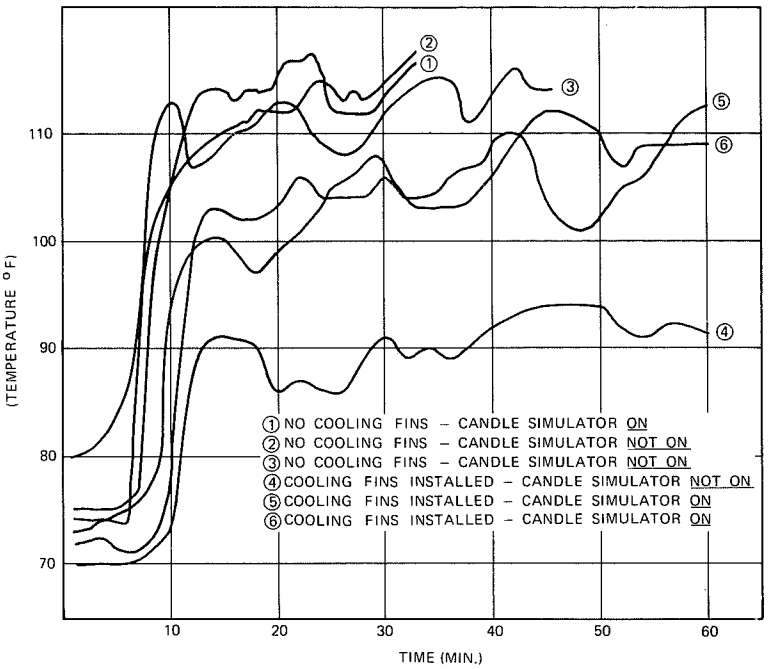

Figure 6.13 *Inspired gas temperature versus canister finning.*

The third test was conducted like the second, except that thermocouples were strategically imbedded into the lithium hydroxide charge. This test lasted 40 min. The data showed center bed temperatures as high as 270° F, while canister wall temperature remained typically 180° F.

From these data, heat transfer calculations were run that established thermal conductivity of the absorbent bed at 0.465 Btu/hr-ft-°F. Further calculations determined that, by internal addition of copper fins, a ΔT of 19° F could be established between the hottest spot in the lithium hydroxide bed and the canister wall. Additional calculations showed that the canister wall could be modified to dissipate heat efficiently enough so that overall rise of the center bed temperature would be only 85° F above a 60° F ambient air temperature for a total hot spot temperature of 145° F (just within optimum operating range). This value, however, was predicted on laminar-free convection and radiation cooling with the additional presence of external cooling fins, spaced along the canister front and back faces.

At the high work rates associated with maximum heat generation, it is a reasonable assumption that an individual using the PBA would be disturbing ambient air at an equivalent velocity of 1 to 3 mph and thereby inducing turbulent cooling air flow. On this premise, subject to additional testing, it was proposed that similar thermal control be achieved without requiring external fins, which would have had significant impact on already-frozen packaging considerations.

As can be seen in figure 6.13, further manned testing after internal fin modification verified the efficiency of this construction. Test 4 was performed without energizing the candle simulator. A lithium hydroxide bed temperature of 187° F was achieved and maximum inspired gas temperature was 94° F, as opposed to 270° F and 116° F, respectively, for an unfinned canister. For tests 5 and 6, the presence of an energized candle simulator had a pronounced effect; nevertheless, peak inspired gas temperatures below 115° F still were obtained.

Further evidence that the internal cooling fins did indeed maintain bed temperature much closer to the optimum operating range was produced from the carbon dioxide analyses. For tests 1 through 3 (no fins), carbon dioxide breakthrough occurrred at a 1.0 percent level within 30 to 40 min into the test. By contrast, tests 4 through 6 (with fins) maintained carbon dioxide below 1.0 percent for the entire 60 min.

Further evidence of design efficiency of the modified canister was obtained as follows. The canister was vibrated according to MIL-STD-810 method 514, procedure X, figure 514-6, curve AB modified. It was vibrated in all three X, Y, Z axes; Z was the vertical axis, X was sideways

along the short axis, Y was longitudinally along the long axis. The input acceleration in all three axes was from 2 to 5 G wherein the frequency ranged from 2 to 500 Hz. The fundamental resonant frequency at which the canister had the highest output acceleration was 115 Hz and 36 G; this frequency was noted to exist in the X axis. Following vibration testing, the canister was x-rayed, dust tested, and carbon dioxide tested. The x-rays showed no lithium hydroxide settling, and the dust test proved negative. Lastly, 2.25 percent carbon dioxide in oxygen was caused to flow through the canister at 300 cc/min for 6 min. The effluent gas was monitored with a Beckman 315 carbon dioxide analyzer. The effluent gas read zero carbon dioxide.

PBA COMPONENT INTEGRATION

Chlorate Candle Lithium Hydroxide Canister Interface

Figure 6.14 shows the internally finned canister just discussed and its interface with the chlorate candle. The candle is hung under the canister and is thermally insulated from the canister by the Teflon cradle and hanger strap assemblies (two each) and by urethane foam and Mystik reflective tape radiation and conduction insulation (located on the candle sides of the canister). The candle's exit gas filter cartridge is contained within the canister's exhalation plenum.

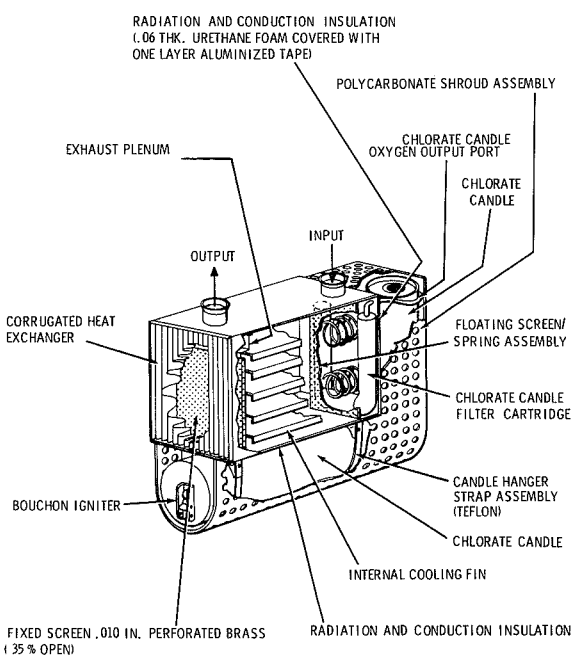

Figure 6.14 *PBA canister candle assembly.*

A perforated polycarbonate shroud covers the candle assembly, offering protection against possible contact burns while still providing convection cooling for the candle assembly. There is a polycarbonate standoff (not visible in the figure) on the back face of the canister to protect the wearer against canister surface temperatures.

Figure 6.15 shows the entire portable breathing apparatus.

Breathing Bags

The initial design decision for circle flow dictated the use of a split breathing bag with one compartment for exhalation and the other for inhalation. Title 30 specifies that the pressure relief valve must be located on the inhalation side. It is set to relieve at 1 in. water column overpressure. The inhalation compartment also contains a strip of open-cell foam along the gas exit path from the canister, which ensures gas flow even in the event of bag collapse under external force.

General requirements for the bags were that they be light weight, gas-tight, able to withstand long-term folding, and capable of folding into a compact storage configuration. The vendor selected for bag fabrication was the G. T. Schjeldahl Co. The material chosen for the prototype was nylon impregnated with polyurethane with cemented seams. The bags can be produced from a number of materials and by processes that are more cost-effective, such as blow molding and heat sealing.

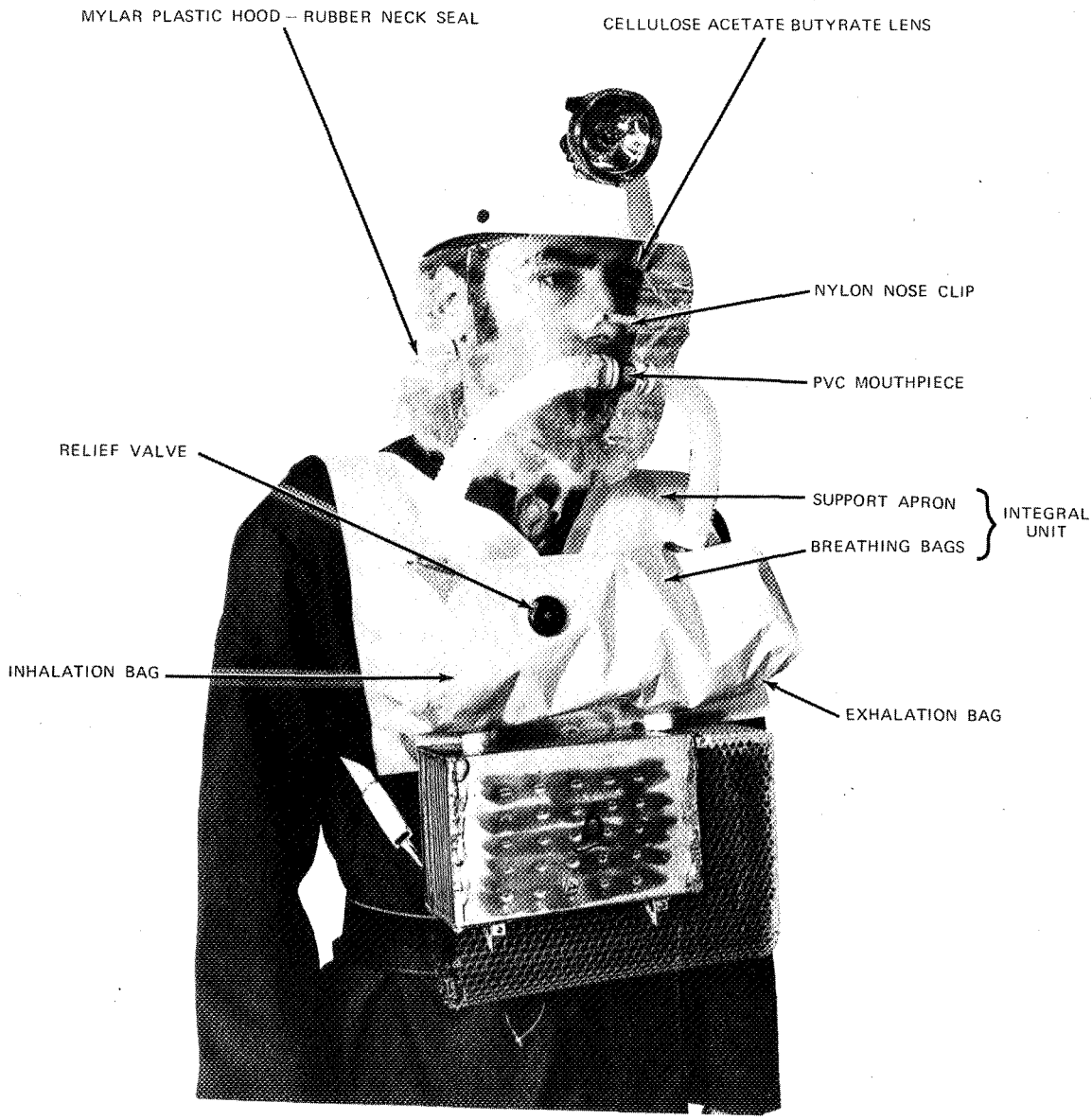

Figure 6.15 *PBA as worn.*

Man/Machine Interface

For the PBA application, interface requirements included not only the means to conduct breathing gas to and from the man but also to allow communication, provide eye protection, and prevent inhalation through the nose. The trade-off study considered six different interface means: mouthpiece, smoke hood, oral mask, oro-nasal mask, full face mask, and fright mask. The study showed that for the PBA application the smoke hood is the best choice.

The vendor selected to manufacture the PBA hood was, again, the Schjeldahl Co., which had previous experience in this type of product and had worked with the FAA on hood developments. The PBA hood differed from earlier ones in the requirements for incorporation of

a mouthpiece and means to prevent fogging. The original approach to the fogging problem was incorporation of an eyepiece of CR-39 allyldiglycolcarbonate into the hood and application of the antifogging compound DeMist manufactured by AID, Ltd. This combination was the result of an extensive literature search and contacts with NASA and the U.S. Army. However, difficulties were encountered in applying DeMist to the selected standard MSA lenses. To meet delivery commitments, an alternative compound, Hydrazorb (also from AID), was selected for application on cellulose acetate butyrate lenses; this coating ranks right behind DeMist in NASA ratings.

Other hood materials selected included a 1.5-mil laminated construction of Mylar® for the hood proper and a polyurethane elastometer for neck seal. The eyepiece was laminated to the inside surface of the hood so that all hood materials in direct contact with ambient atmosphere are self-extinguishing. The nosepiece is designed as an integral part of the lens and is constructed of nylon, while the mouthpiece is constructed of polyvinylchloride.

Acceptance testing performed on the hood included bond strength of lens, bond strength of mouthpiece, haze of lens, luminous transmittance of lens, pressure drop through mouthpiece, and leak integrity of neck seal. All specifications were met.

PROTOTYPE PBA MANNED TESTING

Manned testing on the completely fabricated PBA prototypes was conducted to the work schedule shown in figure 6.9 and in the manner shown in figure 6.12 except that no thermocouple taps were made into the canister. After running five such tests, the following observations were made.

1. The lithium hydroxide canister as coupled with the chlorate candle possesses heat transfer characteristics sufficient for a coal mine environment (50°-60° F) so long as high work rates in a stagnant air flow situation are not encountered. Under conditions of 50°-60° F ambient and average air velocities of 2 mph across the canister during high-work rate activities, the PBA can assure peak inspired gas temperatures no greater than 115°-120° F.
2. It was shown that the hood could be easily donned and doffed, provides an adequate seal without discomfort, does not interfere with the wearing of a hard hat, and allows good communication. However, light fogging of the lens was experienced after about 20 min into the tests. This light fog continued for about 5 min and then cleared somewhat by drainoff. Approximately a cupful of perspiration collected within the hood during this time. It is felt that use of DeMist antifog on CR-39 lenses as originally planned would alleviate this problem.
3. Although chlorate candle duration cannot be specified at 60 min minimum, the total PBA easily achieves this duration. Even at the end of 60 min of high-work-rate testing, the PBA breathing bags remained 60 to 70 percent filled with oxygen.
4. No additional qualifications need be taken to the design requirements and objectives previously listed.

PBA STORAGE AND DEPLOYMENT

It is obvious that, to supply the greatest degree of safety to the user, the PBA must be close to the user at the instant of the emergency. Ideally, the miner would have the PBA attached to his person. To be acceptable to the user and to be carried during his normal work day, the PBA must be of the minimum weight and size. As can be seen in the tradeoffs, these factors were heavily weighted. It was the design goal to make the PBA of such weight, bulk, and configuration that the miner would accept the hindrance. It was felt that the initial designs

would meet the criteria, and the carrying case was planned for wearing the PBA on the miner's belt. However, weight and bulk on several components had to be increased because of developmental problems in pushing current state-of-the-art. It became apparent that the prototype PBA would probably not be well suited to continuous carry by most miners without undergoing major redesign (see component and overall weights in fig. 6.16). Therefore, the carrying case configuration shown in figure 6.17 was adopted for at least intermittent carry by miners.

Item		Actual Weight	Estimated Weight
Canister Assembly:	(1)	6.200	--
Body	(1)		0.520
Cooling Fins	(5)		0.416
Exhaust Plenum	(1)		0.018
Exhaust Screen	(1)		0.051
Intake Screen	(1)		0.057
Heat Exchanger	(1)		0.210
Ports	(2)		0.054
End Closure	(1)		0.071
LiOH	-		1.480
Candle and Filter	(1 each)		3.100
Heat Shroud	(1)		0.102
Carrying Case	(1)	1.440	--
Carrying Case (Redesign)	(1)		1.437
Straps	(1)		0.060
Man-Apparatus Interface	(1)	0.120	0.120
Breathing Bags and Hoses	(1 set)	0.450	0.400
Barrier Bag	(1)	0.070	0.063
Solder and Shroud Assembly Clips			0.300
TOTALS:		8.280	8.459

Figure 6.16 *Overall PBA weight (lb).*

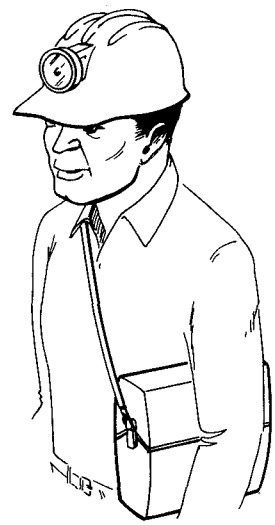

Figure 6.17 *PBA, stowed configuration.*

The next step was to select suitable materials for the case. This study considered not only material weight but manufacturing processes, strength (dent resistance), cost, process development, and number of fabrication steps. Both metals and plastics were considered. Plastics, although much better for dent resistance, are inherently porous. The study considered matalizing the inside of the case to eliminate the porosity, of the use of a very thin (0.005 in.) metal foil liner. It was learned that metalizing was not to be recommended, and the foil liner would complicate the manufacturing process and require much development. However, it was found that newly developed package material (using heavier foil) will provide the necessary seal.

The combination of a fiberglas case and heat-sealed packing bag (fig. 6.18) results in the best strength, weight, cost, and development combination.

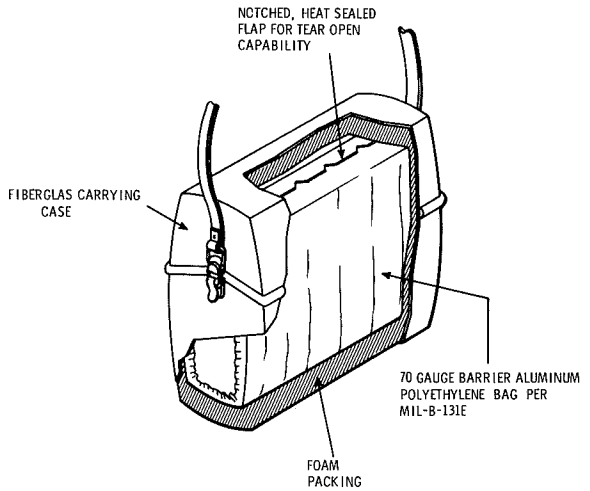

Figure 6.18 *PBA packaging.*

The PBA is contained within the hermetically sealed barrier bag. Notches along the top edges of the bag provide an easy tear-open unit. The sides of the case are slightly bowed to add deflection resistance; the two halves are joined together by a tongue-and-groove joint and secured by quick-action snaps. As shown, the PBA is supported within the case by foam rubber padding.

In addition to carrying case design and development, a system analysis study was conducted to determine criteria, recommendations, and guidelines for deployment of PBAs in strategically located caches proximal to major work areas.

CONCLUSIONS

This work has demonstrated that it is well within the reach of today's technology to produce a 1-hr closed-circuit, no-maintenance breathing apparatus that provides good voice communications and is inexpensive enough for widespread use in coal mines. Approach feasibility has been proven, and with improvements in technology, such as the chlorate candle improvements described by Dr. Malich in paper 25, the package weight and volume can be reduced. The only discomfort factor—high inhalation gas temperature—becomes prohibitive only during improbable operation at peak work rates in stagnant ambient air. Improvement of heat transfer characteristics to render the concept capable of broader application and use at higher ambient temperatures is readily achievable.

ACKNOWLEDGEMENT

In addition to those already mentioned within the text, acknowledgement is made to L. W. Fleischmann, A. R. Wilhelm, Dr. M. W. Goodman, J. E. Hudgens, W. S. Hamel, and Dr. D. Whirlow for their contributions to the program reported in this paper.

REFERENCES

1. Bovard, R. M.: Oxygen Sources for Space Flights. Aerospace Med, vol. 31, May 1960, pp. 407-412.
2. Schecter, W. S., *et al.*: Chlorate Candles as a Source of Oxygen. Industrial and Engineering Chemistry, vol. 42, November 1950, pp. 2348.
3. Hiroschinsky, V.: Solid State Oxygen Development Program. Scott Aviation (undated report).
4. Littman, Jack; and Prince, J. Norman: Research on Sodium Chlorate Candles for the Storage and Supply of Oxygen for Space Exploration. NASA SP-234, 1970, pp. 291-330.
5. Anon.: Experimental Evaluation of Environmental Control Systems for Closed Shelters. MRD Division of General American Transportation Corp., MRD 1242-2530, July 1964.
6. Webb, P.: Bioastronautics Data Book. NASA SP-3006, 1964.
7. Boryta, D. A.; and Maas, A. J.: Factors Influencing the Rate of Carbon Dioxide Absorption by Lithium Hydroxide. Foote Mineral Co., Eaton, Pa., (undated report).

7 ADVANCED EXTRAVEHICULAR PROTECTIVE SYSTEMS

James G. Sutton, Philip F. Heimlich, and Edward H. Tepper
Hamilton Standard Division, United Aircraft Corporation,
Windsor Locks, Conn.

INTRODUCTION

The U.S. manned space effort planned for the 1980s consists of long-duration missions with orbiting space stations, potential lunar bases, and possibly Mars landings. Extravehicular activity (EVA) is likely to take an increasingly important role in the completion of these future missions. With a potential need for two or three EVA missions per man per week, however, the use of expendables in the portable life support system may become prohibitively expensive and burdensome. For future EVAs to be effective in the total systems context, the portable life support system may need a regenerable capacity.

Hamilton Standard, with NASA funding, has been conducting an advanced extravehicular protective system (AEPS) study program. The objective of this AEPS study is to provide a meaningful appraisal of various regenerable and partially regenerable portable life support system concepts for EVA use in the 1980s and to identify the required new technology area.

STUDY METHOD

Study Evaluation Criteria

Selection of the most favorable EVA subsystem and system equipment has always posed a difficult problem. This is particularly true for the AEPS study, which deals with long-duration earth orbital, lunar surface, and martian surface missions in which the vehicle penalty for an AEPS configuration is more important than it was for the shorter term Gemini and Apollo programs. This factor reduces the validity of the traditional heavy emphasis on EVA equipment equivalent volume and weight within the evaluation criteria. Thus, to fulfill the objective of the AEPS study, it has been necessary to establish criteria reflecting an objective evaluation of not only the EVA crewman and his equipment, but also of the parent vehicle or shelter and the total mission.

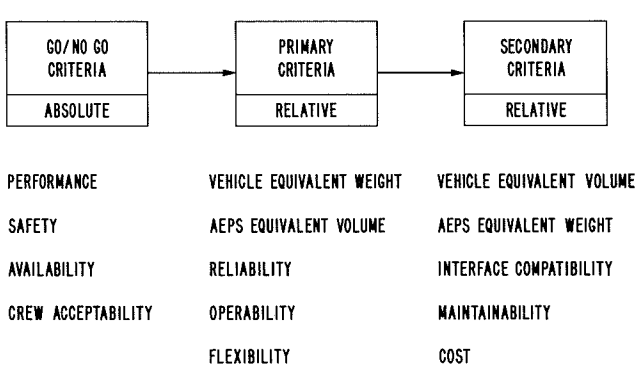

Figure 7.1 *Evaluation criteria.*

The determination of the AEPS study selection criteria is based on a recognition that some requirements are absolute, others are of primary importance, and still others represent second-order effects. The criteria used as a basis for the AEPS subsystem and system selection are shown in figure 7.1. The criteria are applied sequentially in the groups shown to eliminate concepts that fail on either an absolute (go/no go) or comparative basis, and to provide the basis for selection among surviving candidates.

The go/no go criteria define the minimum acceptable requirements for a concept. If a concept does not meet, or cannot be modified or augmented to meet, all the go/no go criteria, it receives no further consideration in the study and is listed as unacceptable and eliminated.

The primary criteria are the principal evaluation criteria for all concepts that pass the go/no go criteria requirements. The ratings applied to a candidate concept depend on its characteristics relative to the other candidates. Each candidate concept receives a rating of from 0 to 100 for each primary criterion. Each rating is then multiplied by the weighting factors defined in table 7.1 and these are added to obtain a total rating for each candidate concept. A candidate concept is selected if its overall rating is clearly the best of the competing concepts. If a clear-cut choice is not evident, the remaining competing concepts are reviewed against the secondary criteria.

Table 7.1 *Primary criteria weighting factors.*

Criteria	*Weighting Factors*		
	space station	*lunar base*	*Mars*
Vehicle equivalent weight	0.30	0.35	0.35
AEPS equivalent volume	0.30	0.25	0.25
Reliability	0.15	0.15	0.15
Operability	0.15	0.15	0.15
Flexibility	0.10	0.10	0.10

The secondary criteria represent a step in depth of competitive evaluation that is taken if no clear-cut selection is available from the primary criteria. Ratings of the candidate concepts against secondary characteristics are relative assessments within each area of consideration and, as in the implementation of the primary criteria, each candidate concept receives a rating from 0 to 100 for each criterion. Each rating is then multiplied by the weighting factors defined in table 7.2 and these are added to obtain a total rating for each candidate concept. A candidate concept is selected if its overall rating is clearly the best of all competing concepts.

In any event, the secondary criteria are applied against all recommended concepts to provide a systematic review of the overall acceptability of these selected concepts.

Study Flow

The AEPS study consisted of the following four basic tasks.

Study Plan and Specifications. The basic ingredients to a meaningful AEPS study are the study plan and the AEPS specifications. The diverse nature of earth orbital, lunar, and martian applications required that separate AEPS specifications be generated for each application.

The goal of these specifications are general guidelines representing the probable trends for earth orbital, lunar base, and martian landing missions in the 1980s. To support the specification generation effort, baseline EVA mission models were established to define work performance tasks and required crew skills; to determine representative time allocations for these tasks; to define

Table 7.2 *Secondary criteria weighting factors.*

Criteria	*Weighting Factors*		
	space station	*lunar base*	*Mars*
Vehicle equivalent volume	0.30	0.30	0.30
AEPS equivalent weight	0.15	0.20	0.20
Interface compatibility	0.25	0.20	0.20
Maintainability	0.20	0.20	0.20
Cost	0.10	0.10	0.10

operational procedures for donning/doffing, checkout, egress/ingress, recharge/regeneration, etc.; and to define applicable interface areas. In addition, vehicle environmental control/life support system models were established to serve as guides to determine the AEPS recharge/regeneration capabilities of the vehicle.

Subsystem Studies. The first step in the subsystem definition study was the preparation of subsystem requirements for each major functional area of each configuration. Based on these requirements candidate concepts were identified in each of the major subsystem areas (carbon dioxide control/oxygen supply, trace contaminant control, thermal control/humidity control, and power). In areas where in-house data were not complete, a literature survey was conducted and industry contacts made, as required. Once all data were assembled and candidate subsystem concepts identified, a preliminary evaluation was conducted to screen out and reject the obviously noncompetitive candidates. Performance characteristics (such as flow rates, temperature levels and pressure levels) of the selected candidate subsystems were roughly determined and preliminary schematics and component lists generated. The candidate subsystems were then sized to meet the subsystem requirements.

These subsystems were then compared against the go/no go evaluation criteria. If a concept was found unacceptable, sufficient auxiliary equipment was added to that subsystem, if possible, to meet the go/no go criteria. If a candidate concept could not be made acceptable, it was removed from further consideration at that point.

A parametric analysis of the remaining candidate subsystem concepts was then conducted. The following data were generated as required for comparison purposes among the candidate subsystems.

1. Vehicle launch weight (including expendables, spares, recharge or regeneration equipment, and checkout equipment, in addition to the basic subsystem) versus total mission duration.
2. EVA equipment volume versus EVA mission duration.
3. Vehicle launch volume versus total mission duration.
4. EVA equipment weight versus EVA mission duration.

The remaining candidate subsystems were then compared against the primary criteria. Further equipment was added or the arrangements modified, as required, to upgrade candidate subsystem concepts found unacceptable or inferior relative to the reliability and operability criteria. Of course, the associated weight, volume, and power penalties were also reflected in the parametric analyses. If

a candidate concept could not be made acceptable, or was still obviously grossly inferior to the other candidates, it was removed from further consideration at that point.

If a clear-cut choice still could not be made from the primary criteria evaluation, the remaining candidate subsystem concepts were compared against the secondary criteria. As in the primary criteria evaluation, equipment modifications were made to a candidate concept(s) to upgrade it relative to the qualitative criteria (interface compatibility and maintainability) if it appeared inferior to other competing concepts. Again, the associated penalities were reflected in the parametric analyses.

From the results of the subsystem evaluations, the best competing subsystems were selected for each AEPS configuration. Several subsystems that perform the same function were recommended for further study on the system levels.

System Studies. After completion of the subsystem studies, a systems integration effort was conducted wherein the selected candidate subsystem concepts were combined into several candidate baseline space station, lunar base, and martian base AEPS systems. The systems integration effort evaluated and defined the following elements, which could not be fully evaluated on the subsystem level:

1. Subsystem interfaces (both functional and physical).
2. Instrumentation and controls.
3. Thermal balance.
4. Equipment power requirements.
5. Humidity control.
6. Method of heat transport to heat rejection system and associated coolant flows.
7. Trace contaminant requirements.
8. Suit and vehicle interfaces.

The candidate baseline systems were then subjected to a competitive evaluation utilizing the established criteria and the parametric results of the subsystem studies. Results of the systems evaluation led to the selection of the candidate space station, lunar base and martian base AEPS baseline concepts.

Prior to a final review and interation of the AEPS baseline concepts, Hamilton Standard reviewed with NASA the general specifications and the evaluation criteria to assure that both are still consistent with the objectives of the study and the results to date. Upon satisfactory completion of this task, the AEPS baseline concepts were subjected to a detailed performance review and evaluation to optimize system performance. Components and subsystems were resized and system arrangements modified, as required.

The operational modes of each baseline concept were reviewed in detail to simplify operational procedures. Specific emphasis was placed on:

1. Startup, checkout, and shutdown procedures.
2. Recharge and regeneration procedures.
3. Maintenance procedures.

A safety/reliability evaluation of each baseline concept was conducted. Top level system FMEAs were conducted and single point and sequential failures were eliminated. This analysis also formed the basis for selection of the AEPS instrumentation.

The interface compatibility of each AEPS baseline concept was evaluated with respect to the crew, the space suit, the vehicle, and other EVA equipment. Specific emphasis was placed on location of AEPS control and displays, use of the time independent module/time dependent module

(TIM/TDM) concept, partial and full integration of the AEPS into the space suit, and compatibility of the AEPS subsystems with vehicle EC/LSS subsystems.

The final AEPS system recommendations resulted from this total effort.

New Technology. After establishment of the AEPS baseline concepts, a portion of the study effort was directed toward generation of a priority listing of new technology development activity required to permit the AEPS recommendations to be implemented.

The principal objectives of this effort were:

1. To provide confirmation of attractive concepts where, although feasibility may have been demonstrated, development status and confidence is marginal.
2. To define problems, recommend approaches, and estimate resources to solve these problems.

SUBSYSTEM STUDIES

To ensure that the results of this study were both meaningful and useful for future related efforts, Hamilton Standard adopted a broad-based approach to candidate subsystem concept identification. The whole gamut of concept approaches was investigated with a specific effort on our part to preclude any prejudgment of concept value prior to concept identification. Specific emphasis was placed in the areas of thermal control and CO_2 control/O_2 supply, as they represented the areas where the greatest benefits could be derived through reduction of vehicle penalties and AEPS volume and weight.

Initial effort results in the identification of 55 candidate thermal control concepts (table 7.3), 21 candidate CO_2 control concepts (table 7.4), 14 candidate O_2 supply concepts (table 7.5), and 3 candidate O_2 generation concepts (table 7.6). All these concepts were evaluated on a cursory basis, and those that were deemed to be "obviously noncompetitive" were eliminated. Of these original candidate concepts identified and analyzed on a preliminary basis, 25 thermal control concepts and 19 combined CO_2 control/O_2 supply concepts were carried into the evaluation. These candidate concepts were subjected to the go/no go, primary, and secondary evaluations in consecutive order and in accordance with the procedure described earlier.

Table 7.3 *Thermal control concepts.*

Expendables

- Water
  - Water boiler
  - Supercooled water boiler
  - Supercooled water boiler with vapor regenerative cooling
  - Water sublimator
  - Supercooled water sublimator
  - Supercooled water sublimator with vapor regenerative cooling
  - Plate fin flash evaporator
  - Nonesteady state pulse feed flash evaporator
  - Static vortex flash evaporator
  - Turbine-rotary vortex flash evaporator

Table 7.3 *Thermal control concepts. (Continued)*

Expendables (continued)

- Water (continued)
  - Motor-rotary vortex flash evaporator
  - Multistage flash evaporator
  - Vapor diffusion through suit pressure valves
  - Vapor diffusion through water permeable membrane
- Hydrogen Peroxide (H_2O_2)
  - H_2O_2 dissociation into H_2O and O_2
- Ammonia (NH_3)
  - NH_3 boiler
  - NH_3 sublimator
- Carbon Dioxide (CO_2)
  - CO_2 boiler
  - CO_2 sublimator
- Methane (CH_4)
  - CH_4 sublimator
- Cryogenics
  - Cryogenic O_2
  - Cryogenic H_2
- Feces/urine sludge
  - Evaporation of H_2O from feces/urine sludge

Conduction

- Conduction via the lunar or martian surface

Convection (Mars only)

- Free convection
- Forced convection
- Hilsch tube

Table 7.3 *Thermal control concepts. (Concluded)*

Radiation

- Direct cooling
  - LCG
  - Heat pipe
  - Water adsorption using:
    - $LiCl \cdot 3H_2O$
    - $CaCl \cdot 6H_2O$
    - Molecular sieve
    - Silica gel
    - $LiBr \cdot 3H_2O$
    - $Na_2Se \cdot 16H_2O$
- Indirect cooling
  - Vapor compression refrigeration cycle using Freon
  - Water adsorption cycle using NH_3
  - Water adsorption cycle using LiBr
  - Brayton cycle using Air

Thermal Storage

- Ice
- Subcooled ice
- Thermal wax—transit 86
- Eutectic salt—sodium sulphate ($Na_2SO_4 \cdot 10H_2O$)
- Phosphonium chloride (PH_4C1)
- Hydrogen (H_2)
- Lunar or martian rock

Energy Conversion

- Thermoelectric
- Thermionic
- Thermodielectric

Hybrids

- Expendable/radiation—direct cooling
- Expendable/radiation—indirect cooling
- Expendable/thermal storage
- Radiation/thermal storage
- Thermal storage/water adsorption

Table 7.4 *Carbon dioxide control concepts.*

- *Expendables*
  - Solid sorbents
    - Hydroxides
    - Superoxides
    - Peroxides
    - Ozonides
  - Liquid sorbent
    - Hydroxide solutions
  - Open loop
    - Purge flow
- *Regenerables*
  - Solid sorbents
    - Activated charcoal
    - Molecular sieve
    - Metallic oxides
    - Solid amines
  - Liquid sorbents
    - Carbonate solutions
    - Liquid amines
- *Electrochemical*
  - Hydrogen depolarized cell
  - Two-stage carbonation cell
  - One-stage carbonation cell
  - Electrodialysis
  - Fused salt
- *Mechanical*
  - Simple membrane diffusion
  - Immobilized liquid membrane diffusion
  - Mechanical freezeout
  - Cryogenic freezeout

Table 7.5 *Oxygen supply concepts.*

O_2 Storage

- Gaseous
- Supercritical utilizing thermal pressurization
- Subcritical utilizing thermal pressurization
- Subcritical utilizing positive expulsion
- Solid

Solid Decomposition

- Superoxides
- Peroxides
- Ozonides
- Sodium chlorate candles ($NaClO_3$)
- Lithium perchlorate candles ($LiClO_4$)

Liquid Decomposition

- Hydrogen peroxide (H_2O_2)
- Reactant storage (N_2H_4/N_2O_4)
- Reactant storage (N_2H_4/H_2O_2)

Electrolysis

- Water electrolysis

Table 7.6 *Oxygen generation concepts.*

- Solid electrolyte
- Bosch reactor/water electrolysis
- Sabatier reactor/water electrolysis

As a result of these evaluations, the following three general thermal control categories were selected for further study:

1. Expendable concepts utilizing water.
2. Radiation.
3. Thermal storage.

Five specific thermal control subsystem concepts were recommended to be carried into the systems integration phase of the AEPS study.

Water Boiler. The water boiler (fig. 7.2) is an expendable thermal control concept that utilizes the heat of vaporization of water to provide direct cooling of the liquid cooling garment (LCG) loop and vent loop. The wick-fed water boiler also acts as the storage vessel for the expendable water. The expendable water boiling temperature is controlled by a back pressure valve, which is either a temperature sensing or pressure sensing flow control valve. Crewman comfort is achieved automatically by the temperature control valve. Water removed by the water separator is fed into the water boiler, thus providing additional cooling capacity. A relief valve furnishes protection against overpressurization due to storage temperature fluctuations. Recharge is simply accomplished utilizing the fill valve. The water boiler is being recommended as a representative concept of all the expendable water concepts that utilize phase change to reject heat.

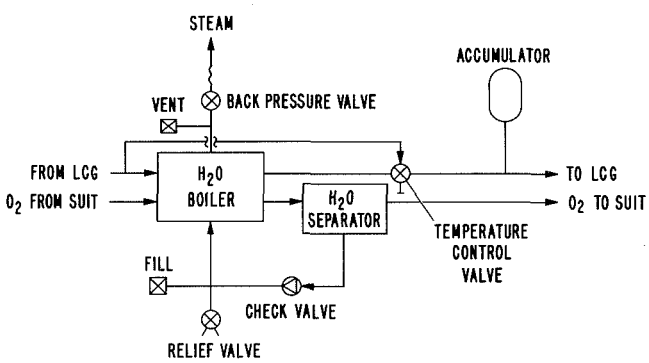

Figure 7.2 *Water boiler.*

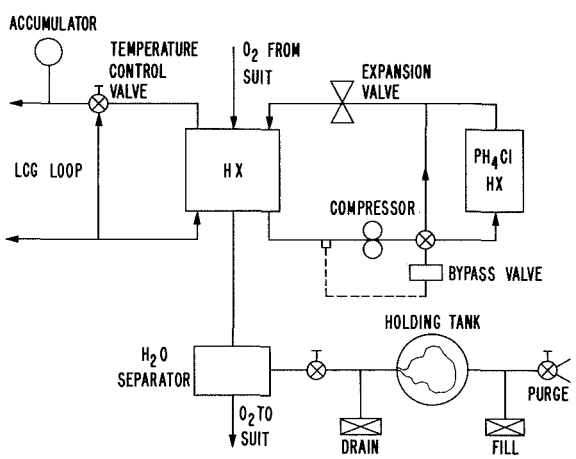

Figure 7.3 *Thermal storage using phosphonium chloride.*

Thermal Storage with Phosphonium Chloride (PH_4Cl). Thermal storage (fig. 7.3) utilizing phosphonium chloride is a self-regenerable thermal control concept. The heat of fusion of PH_4Cl is 324 Btu/lb at 82° F and above 48 atm pressure. A vapor compression intermediate loop is utilized to raise the desired coolant temperature of 50° F at the vent loop/liquid heat transport loop heat exchanger to 82° F at the thermal storage unit. Humidity control is furnished by a water separator and holding tank that remove and store vent loop condensate. Vehicle penalties associated with this concept are relatively low since PH_4Cl will resolidify of its own accord at normal cabin temperatures.

Solid PH_4Cl sublimates at pressures below 500 psia at room temperature. As pressure is decreased further, gaseous PH_4Cl dissociates into two gases: hydrogen chloride and phosphene

(PH_3); phosphene is highly toxic so the thermal storage unit has been concepted to minimize the probability of any failure resulting in external leakage.

Expendable/Direct Radiative Cooling. This concept (fig. 7.4) is a hybrid consisting of a water boiler and radiator connected in parallel through the LCG temperature control valve. The temperature control valve selects the percentage of the heat load from the LCG that is shared by each subsystem. The radiator is sized to handle the average heat load while the water boiler handles peak loads; thus radiator size and water expended in the boiler are minimized. Humidity control is provided by a condensing heat exchanger and a water separator that feeds the separated water to the water boiler to provide additional cooling capacity. For low or no-load conditions, a variable conductance, area, or emissivity device must be used to prevent overcooling of the LCG.

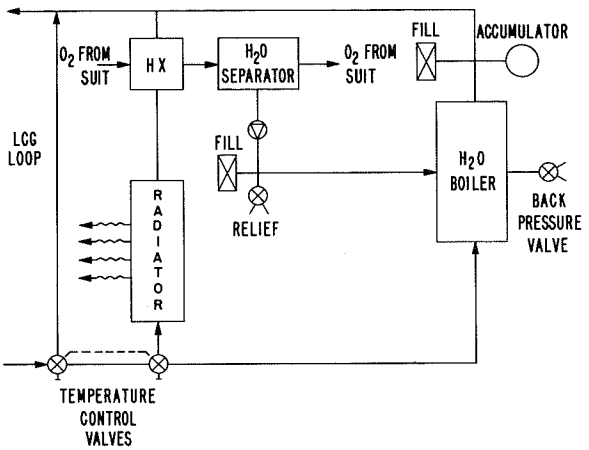

Figure 7.4 *Expendable/direct radiative cooling.*

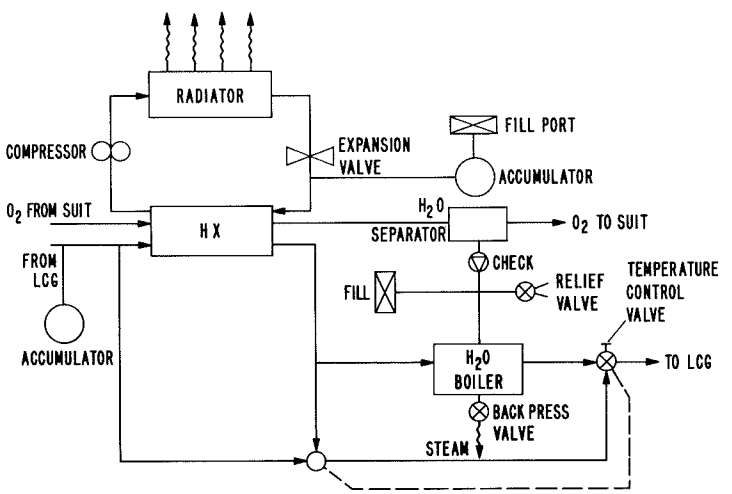

Figure 7.5 *Expendable/heat pump.*

Expendable/Heat Pump. This hybrid concept (fig. 7.5) consists of a radiator/vapor compression cycle and a water boiler connected in parallel through an automatic LCG temperature control valve. The temperature control valve selects the percentage of the heat load from the LCG that is shared by each subsystem. The radiator/vapor compression subsystem is sized to handle the average LCG heat load plus the heat load from the vent system while the water boiler handles peak heat loads. This minimizes radiator size, compressor size, and power consumption as well as water expended in the boiler. Humidity control is provided by the vapor compression cycle evaporator and the water separator that feeds the separated water to the water boiler to provide additional cooling capacity. For low or no-load conditions, a radiator bypass or compressor short circuit (not shown in schematic) or variable speed compressor is required to prevent overcooling at the evaporator.

Expendable/Thermal Storage (PH_4Cl). This hybrid concept (fig. 7.6) utilizes a water boiler in parallel with a PH_4Cl thermal storage unit via an LCG temperature control valve. The temperature control valve selects the percentage of the heat load from the LCG that is shared by each subsystem, the intention being that the PH_4Cl thermal storage unit will handle the average heat load and the

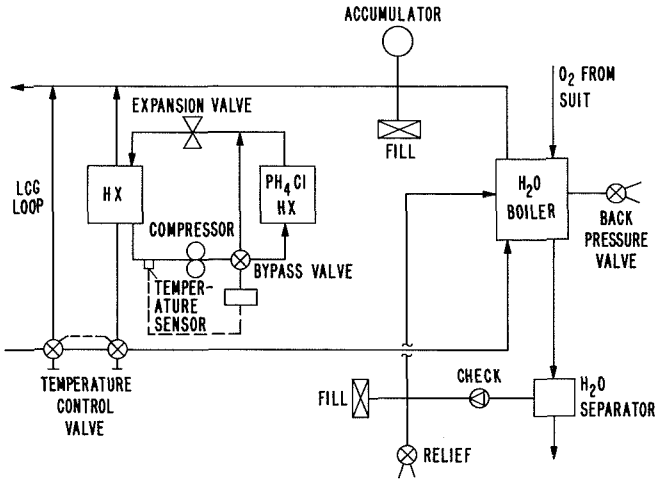

Figure 7.6 *Expendable/thermal storage using phosphonium chloride.*

water boiler will handle peak loads. Compressor power and expendable water thus are minimized. The water boiler provides humidity control by cooling the vent loop that feeds the separated water to the boiler via the water separator to provide additional cooling capacity. A bypass valve is utilized in the thermal storage subsystem to prevent overcooling under low or no-load conditions. This system is flexible in that it can be sized for a multitude of thermal load sharing combinations.

Carbon Dioxide Control/Oxygen Supply

One general CO_2 control/O_2 supply category was selected for further study–a solid regenerable sorbent combined with a high-pressure gaseous oxygen supply system. Two families of solid regenerable sorbents were identified as candidate materials: metallic oxides and solid amines.

The CO_2 control/O_2 supply subsystem concepts recommended to be carried into the systems integration phase of the AEPS study are described below. All of the concepts utilize a high-pressure gaseous O_2 supply system.

Metallic Oxides - Vehicle Regenerable. Metallic oxides (ZnO, MgO) react with CO_2 according to the reversible reaction

$$MO + CO_2 \rightleftharpoons MCO_3 + Q$$

The carbonate readily decomposes with increasing temperature and, in some cases, may be solely vacuum regenerable. However, excessive volume change during the adsorb/desorb cycle affects the chemical's physical stability and is a prime consideration in any future development effort. For this study, the adsorbent was contained between screens with gas flow over rather than through the packaging. CO_2 diffusion into the thin oxide bed will be sufficient as long as the solid volume transition during adsorb/desorb does not result in an impregnable surface or if any extremely fine screen is not required. An alternate concept would consider a carrier to stabilize the solid adsorbent–possibly a thin layer of the oxide flame sprayed on a screen matrix.

In the vehicle regenerable configuration (fig. 7.7), the adsorbent is packaged in a cartridge that is replaced after each mission. An oven/vacuum chamber is provided within the vehicle for cartridge regeneration. Reclamation of the oxygen is possible with this system by directing gas to the vehicle CO_2 reduction system.

Metallic Oxides - AEPS Regenerable. A variation of the metallic oxide concept considers a cyclic or AEPS regenerable configuration (fig. 7.8). This concept provides for regeneration of the metallic oxide subsystem during the actual EVA mission. Two beds, similar in design to that described for the vehicle regenerable system, are provided, each containing electrical elements for regeneration and a cooling loop to cool the regenerated bed and maintain temperature control during operation.

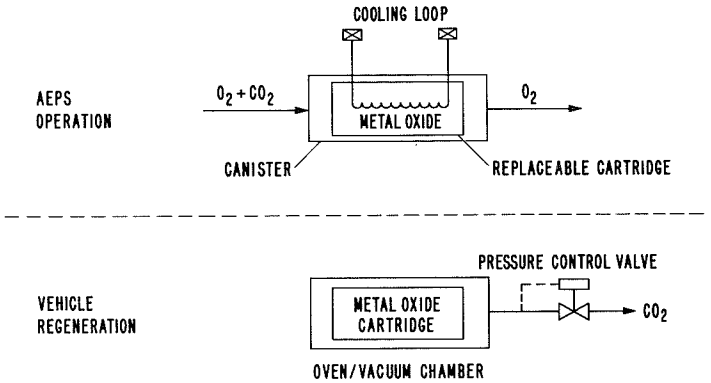

Figure 7.7 *Metallic oxide–vehicle regenerable.*

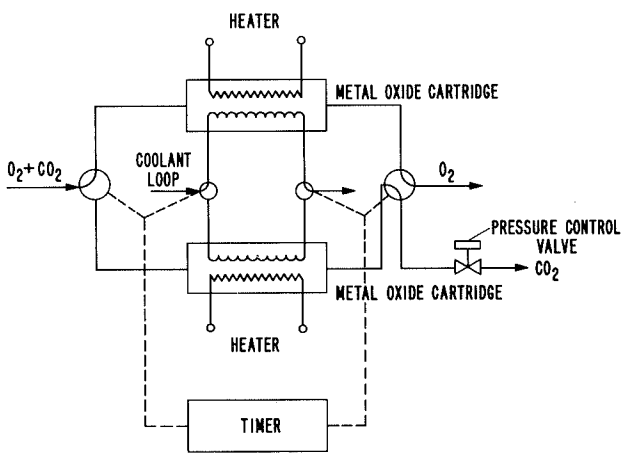

Figure 7.8 *Metallic oxide–AEPS regenerable.*

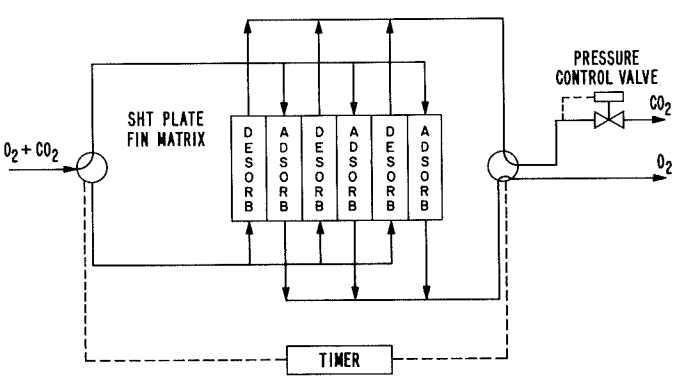

Figure 7.9 *Solid amine (SHT)–AEPS regenerable.*

A timer is provided to sequence the vent loop and coolant loop valves to allow the vent loop and coolant loop to flow to the onstream bed and to heat and expose to space vacuum the regenerating bed.

Solid Amine - AEPS Regenerable. An inert carrier is utilized to provide a stable amine adsorbent bed in this concept (fig. 7.9). The regenerable solid amine is packaged within the flow passages of a plate-fin matrix similar in design to an extended surface compact heat exchanger. Alternate flow passages contain adsorbing and desorbing material with the unique feature of an isothermal process. Energy released from the adsorbing passages is transferred by conduction through the metal matrix to the desorbing material to supply the requirements of the endothermic desorption. This concept neither imposes a thermal load on the AEPS nor requires energy for regeneration. A timer and valving is provided to cycle the packed beds from the online adsorb to the space vacuum desorb cycle.

The parametric analyses of the recommended subsystem concepts were then reviewed and updated to reflect the latest AEPS specification requirements for each of the three missions, space station, lunar base, and martian. Parametric data generated includes:

1. Vehicle equivalent weight versus total mission duration.
2. Vehicle equivalent volume versus total mission duration.
3. AEPS equivalent volume versus EVA mission duration.
4. AEPS equivalent weight versus EVA mission duration.
5. Accumulated resupply launch weight versus number of resupplies.

The results of these parametric analyses, which were utilized for selecting and sizing subsystems for the system studies, are presented in the following figures:

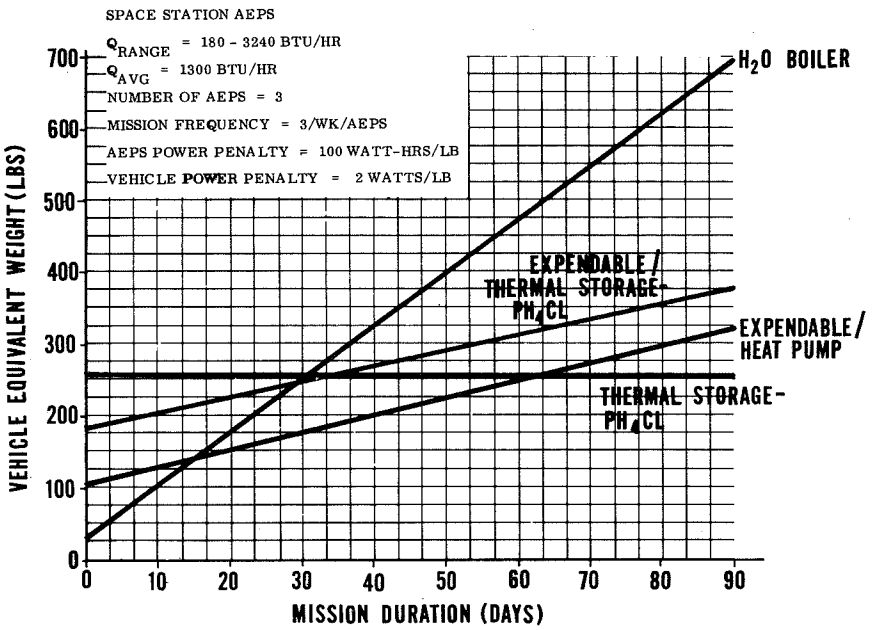

Figure 7.10 (a) *Thermal control for space station AEPS.*

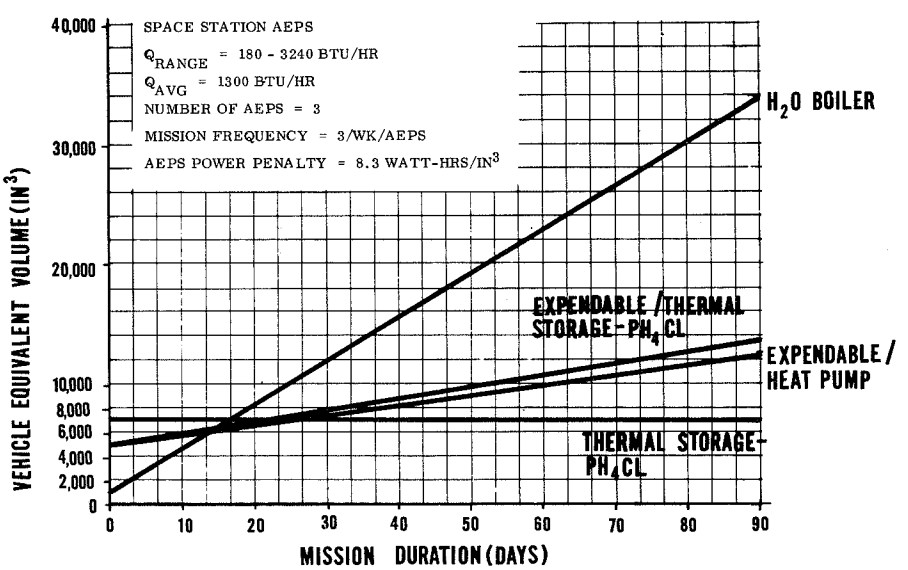

Figure 7.10 (b) *Thermal control for space station AEPS.*

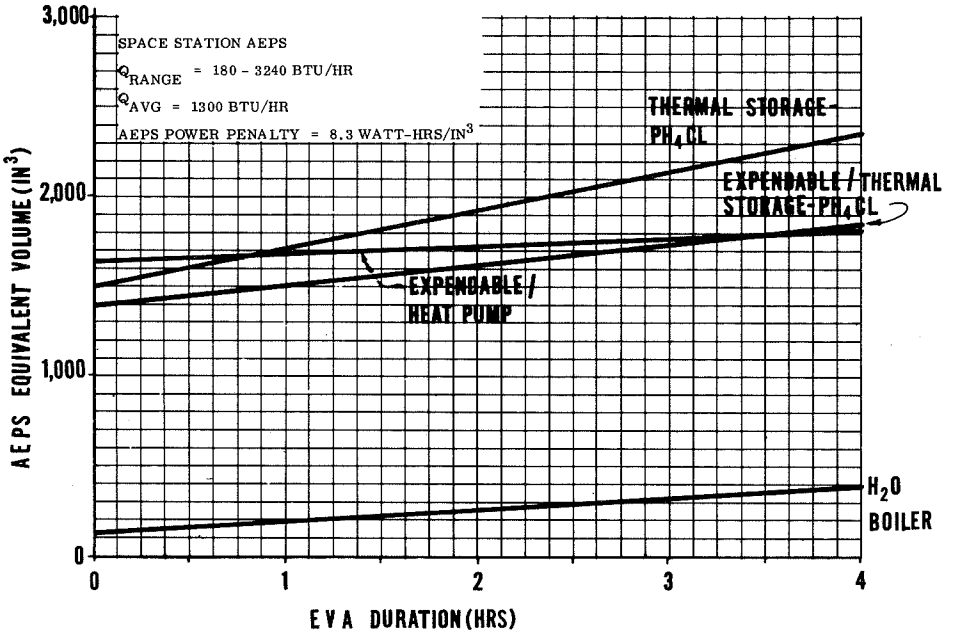

Figure 7.10 (c) *Thermal control for space station AEPS.*

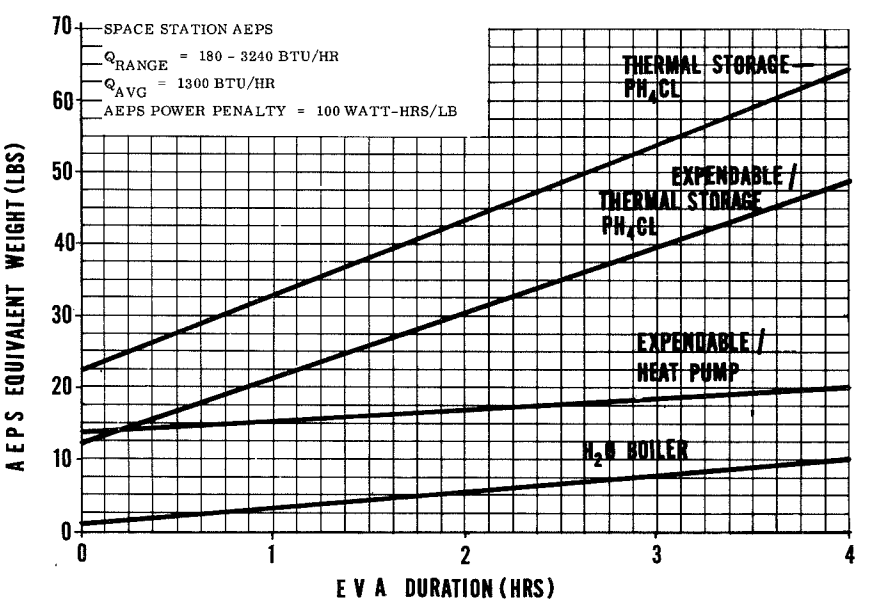

Figure 7.10 (d) *Thermal control for space station AEPS.*

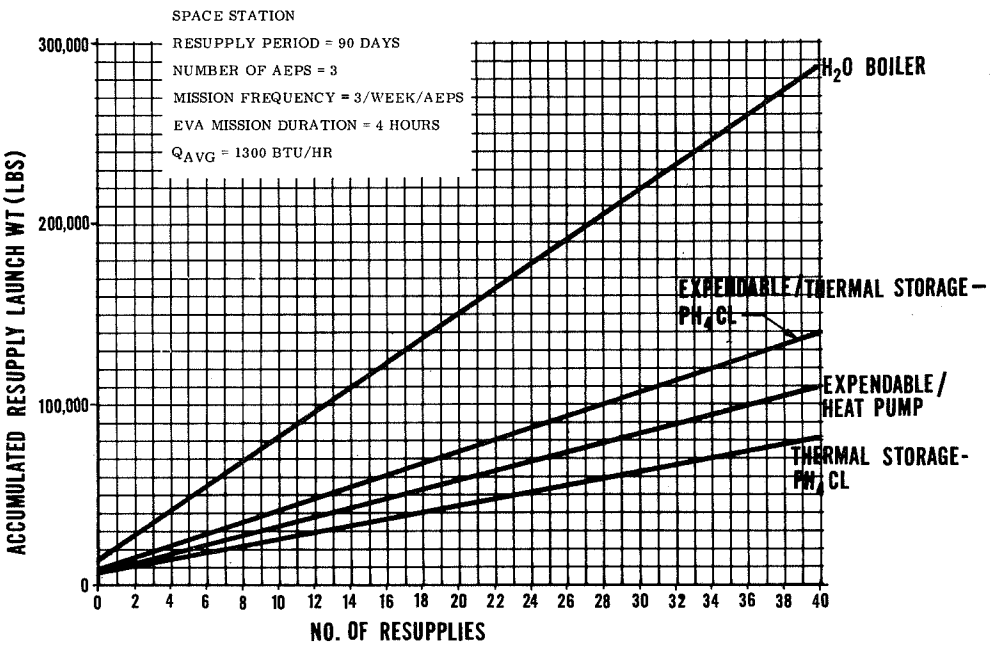

Figure 7.10 (e) *Thermal control for space station AEPS.*

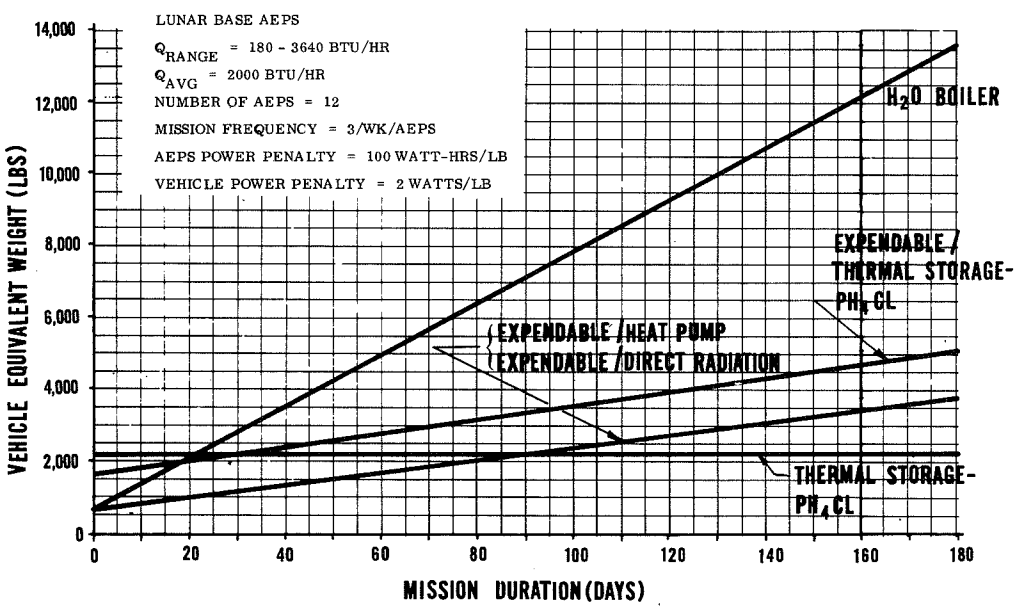

Figure 7.11 (a) *Thermal control for lunar base AEPS.*

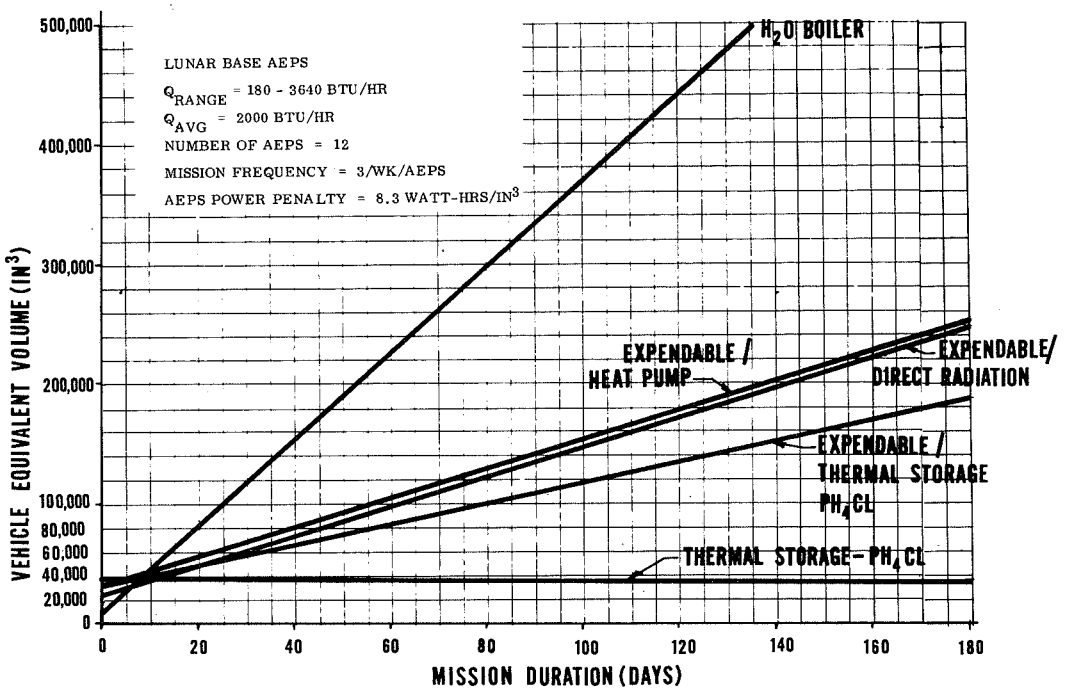

Figure 7.11 (b) *Thermal control for lunar base AEPS.*

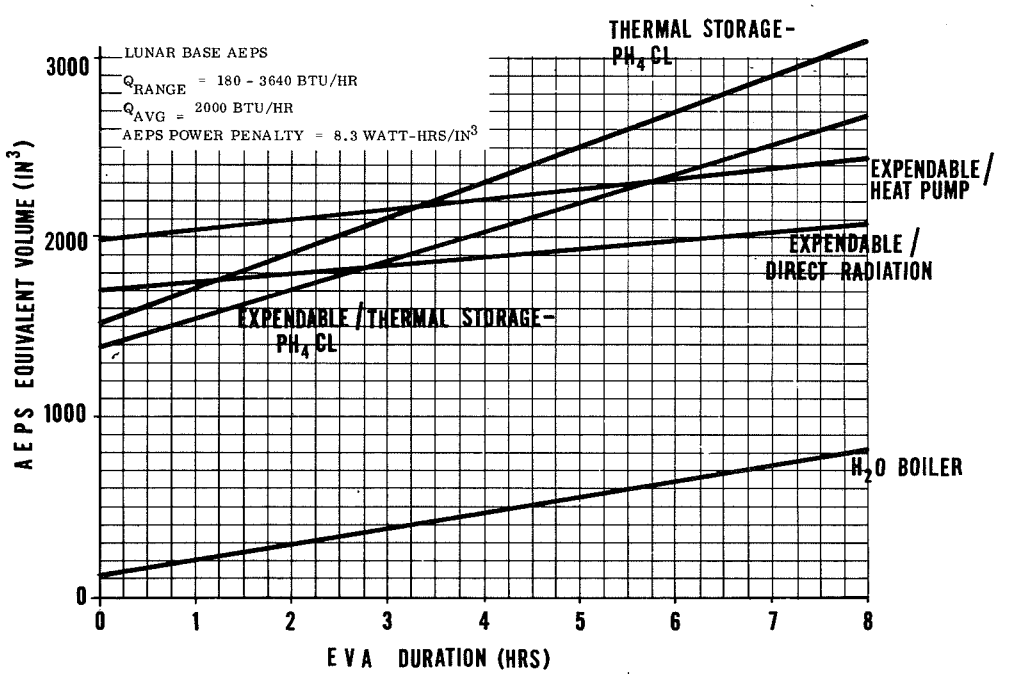

Figure 7.11 (c) *Thermal control for lunar base AEPS.*

3-6

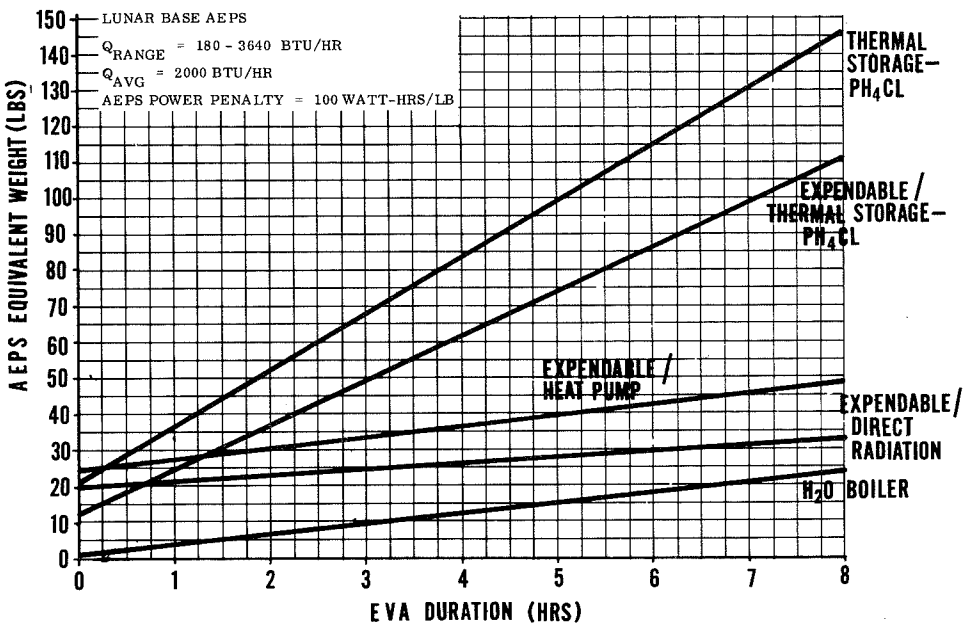

Figure 7.11 (d) *Thermal control for lunar base AEPS.*

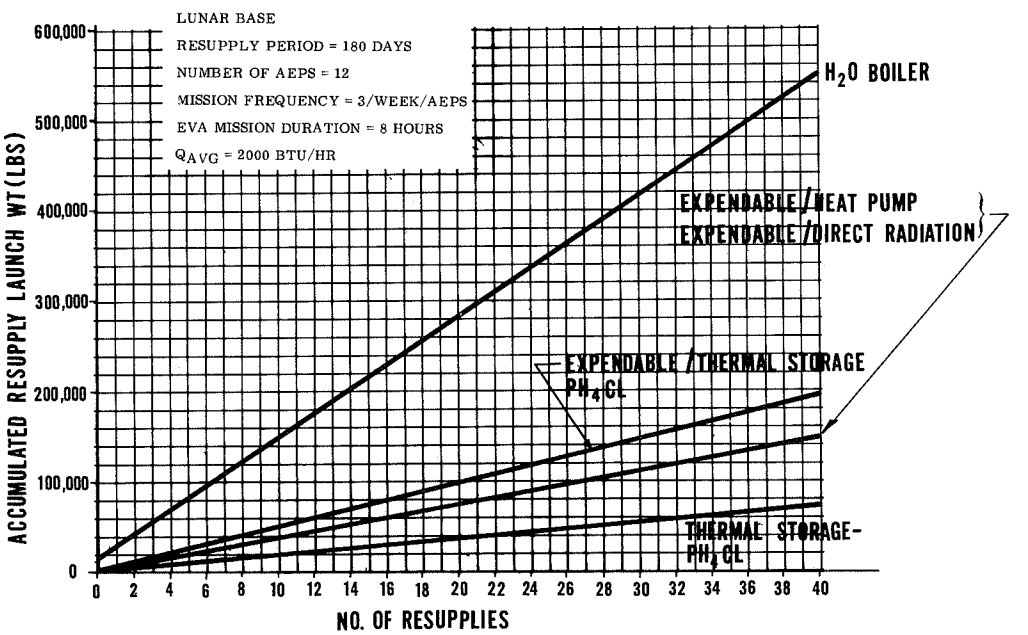

Figure 7.11 (e) *Thermal control for lunar base AEPS.*

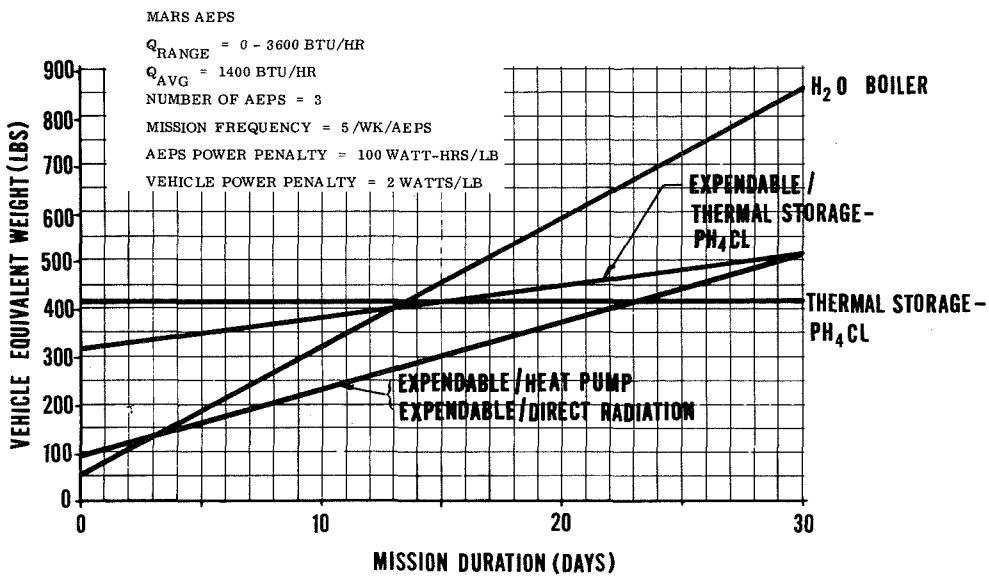

Figure 7.12 (a) *Thermal control for martian AEPS.*

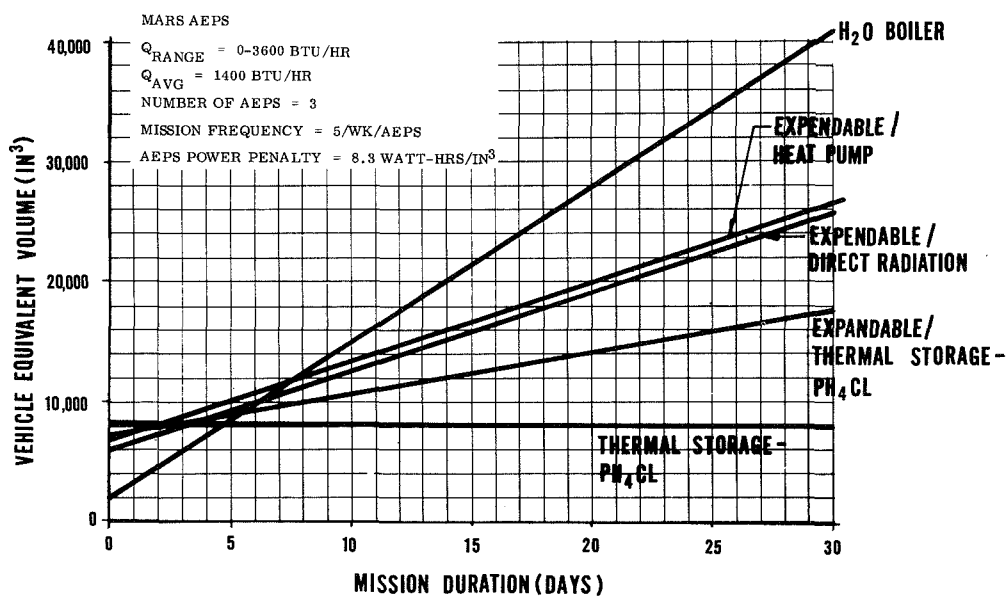

Figure 7.12 (b) *Thermal control for martian AEPS.*

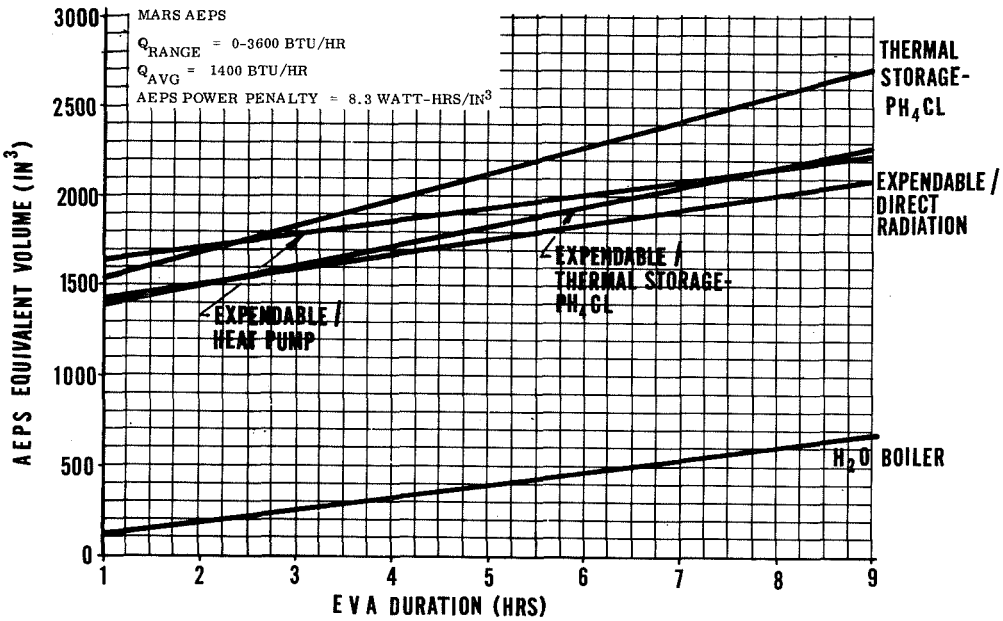

Figure 7.12 (c) *Thermal control for martian AEPS.*

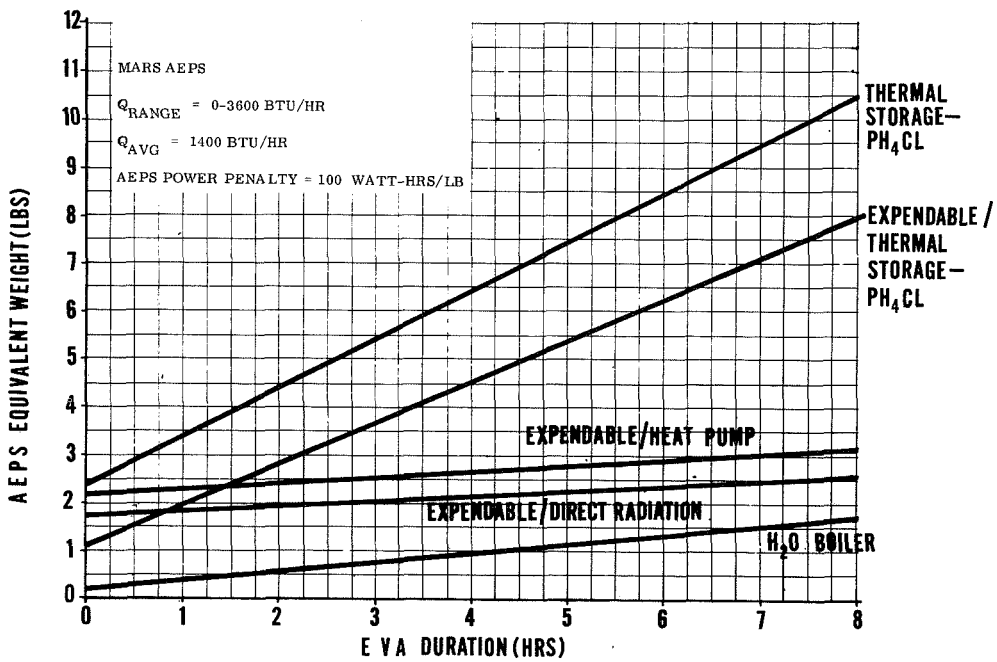

Figure 7.12 (d) *Thermal control for martian AEPS.*

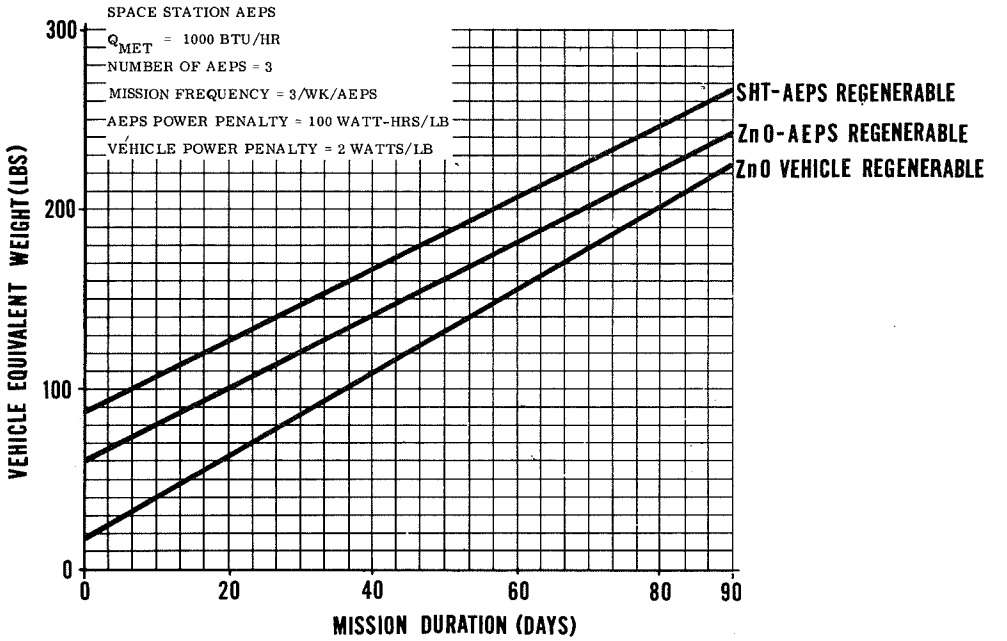

Figure 7.13 (a) *Carbon dioxide control/oxygen supply for space station AEPS.*

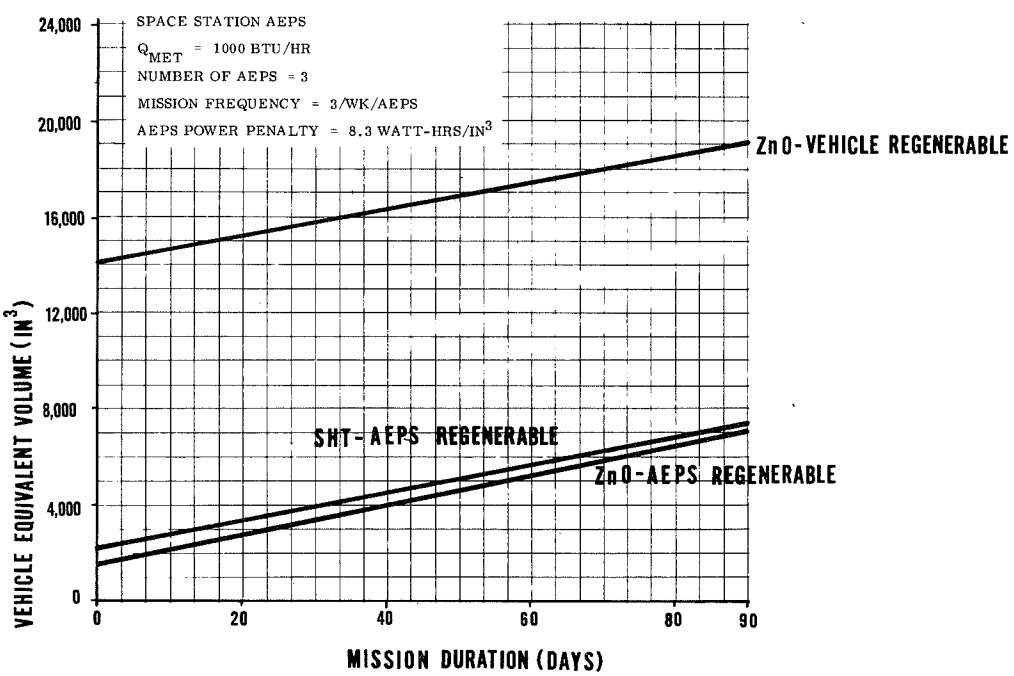

Figure 7.13 (b) *Carbon dioxide control/oxygen supply for space station AEPS.*

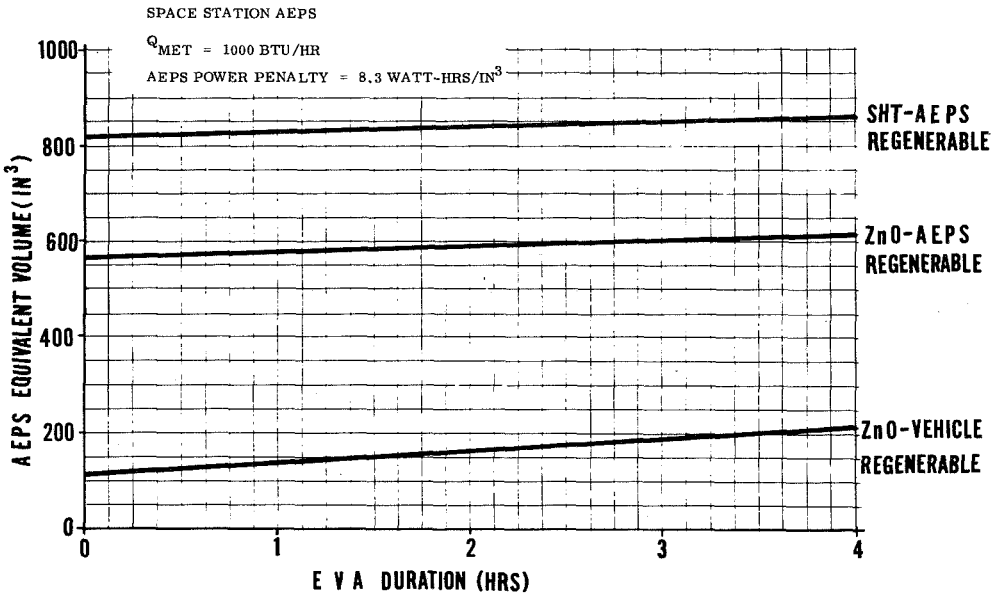

Figure 7.13 (c) *Carbon dioxide control/oxygen supply for space station AEPS.*

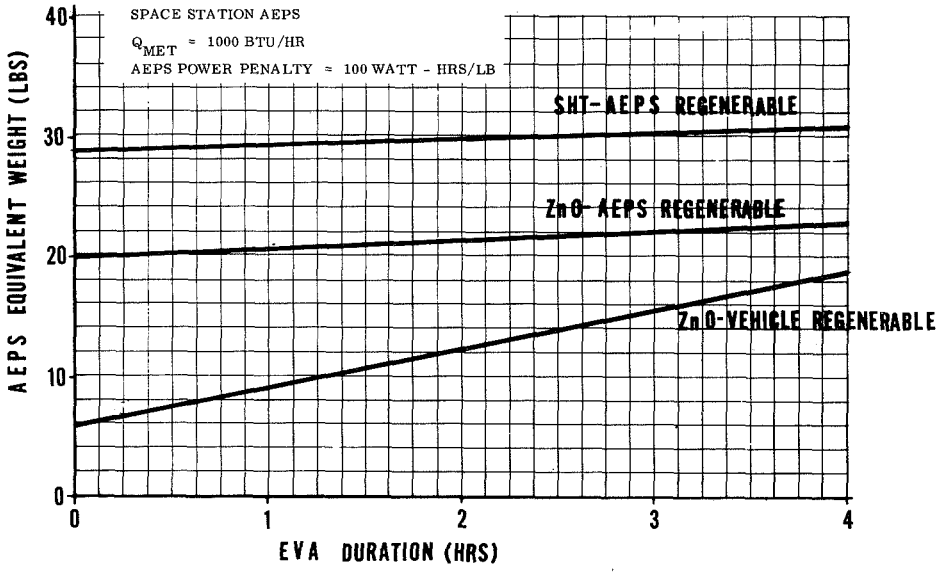

Figure 7.13 (d) *Carbon dioxide control/oxygen supply for space station AEPS.*

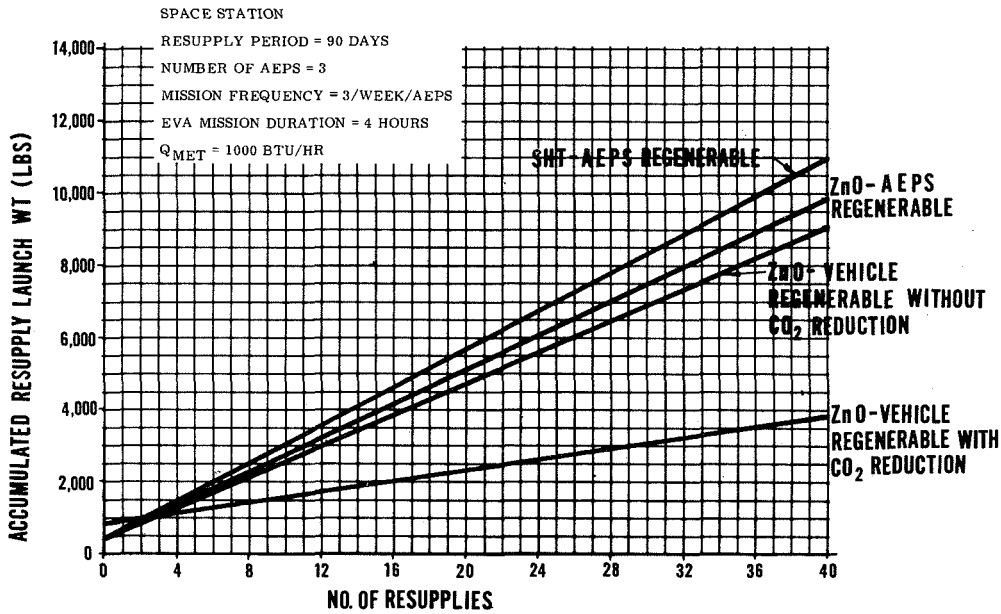

Figure 7.13 (e) *Carbon dioxide control/oxygen supply for space station AEPS.*

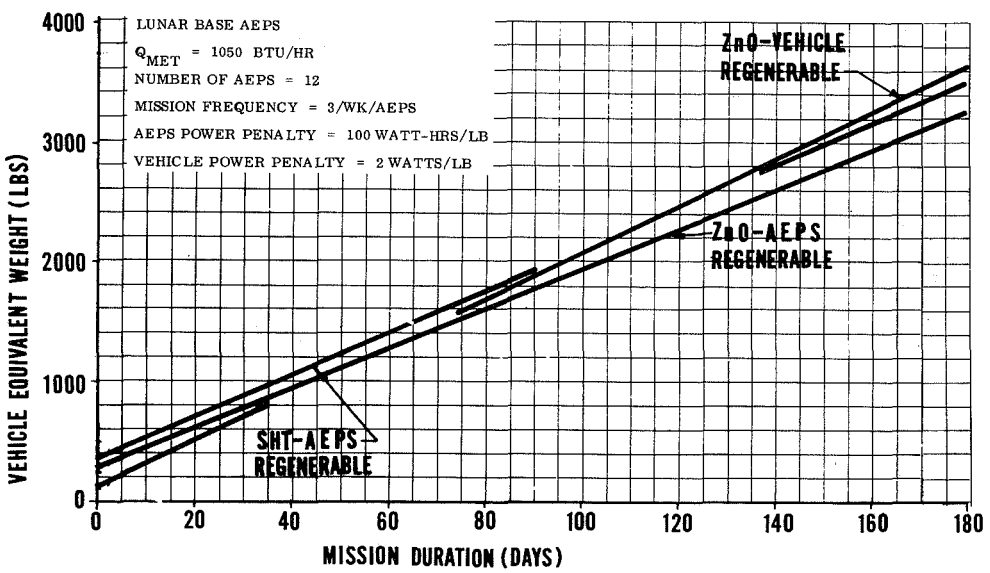

Figure 7.14 (a) *Carbon dioxide control/oxygen supply for lunar base AEPS.*

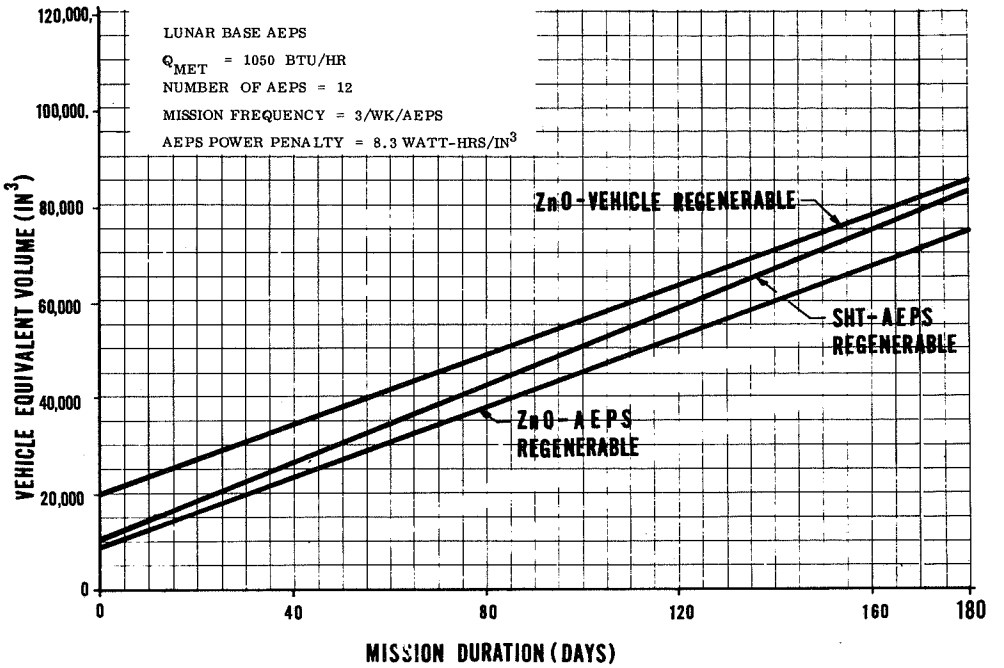

Figure 7.14 (b) *Carbon dioxide control/oxygen supply for lunar base AEPS.*

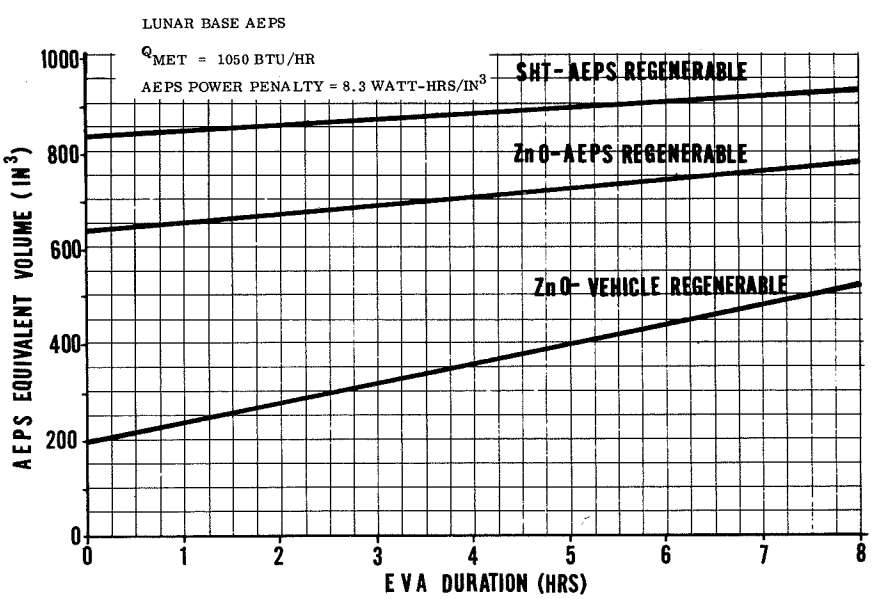

Figure 7.14 (c) *Carbon dioxide control/oxygen supply for lunar base AEPS.*

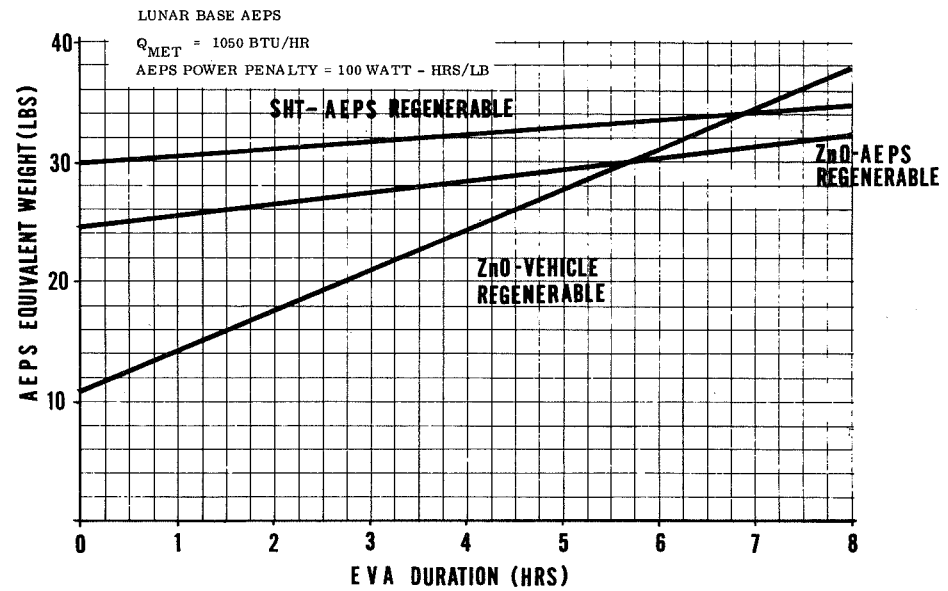

Figure 7.14 (d) *Carbon dioxide control/oxygen supply for lunar base AEPS.*

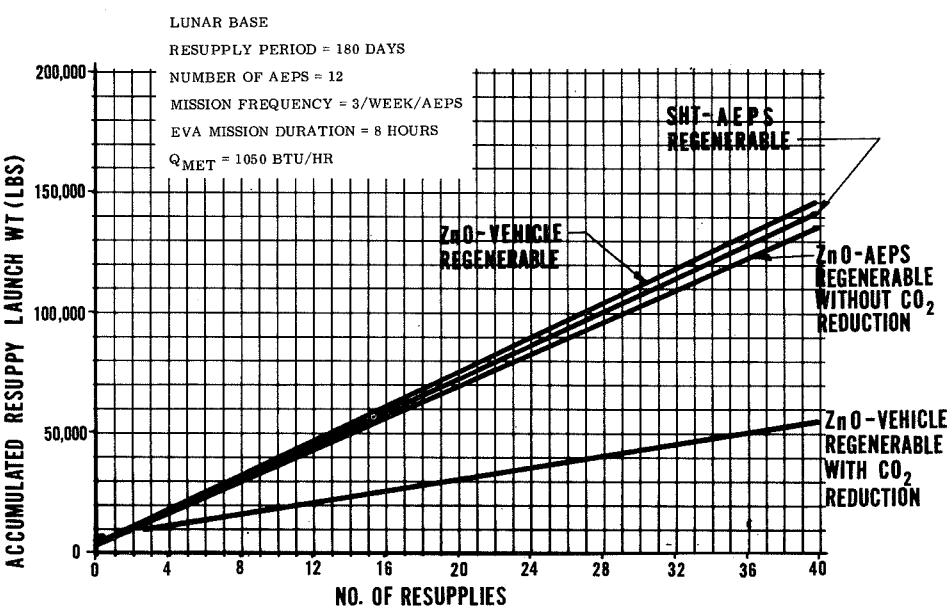

Figure 7.14 (e) *Carbon dioxide control/oxygen supply for lunar base AEPS.*

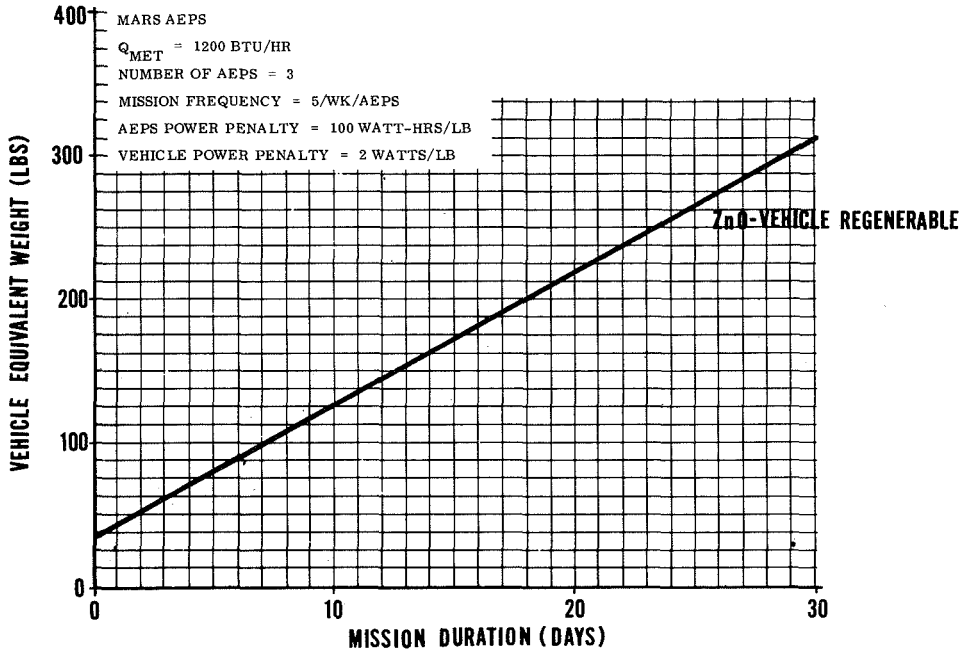

Figure 7.15 (a) *Carbon dioxide control/oxygen supply for martian AEPS.*

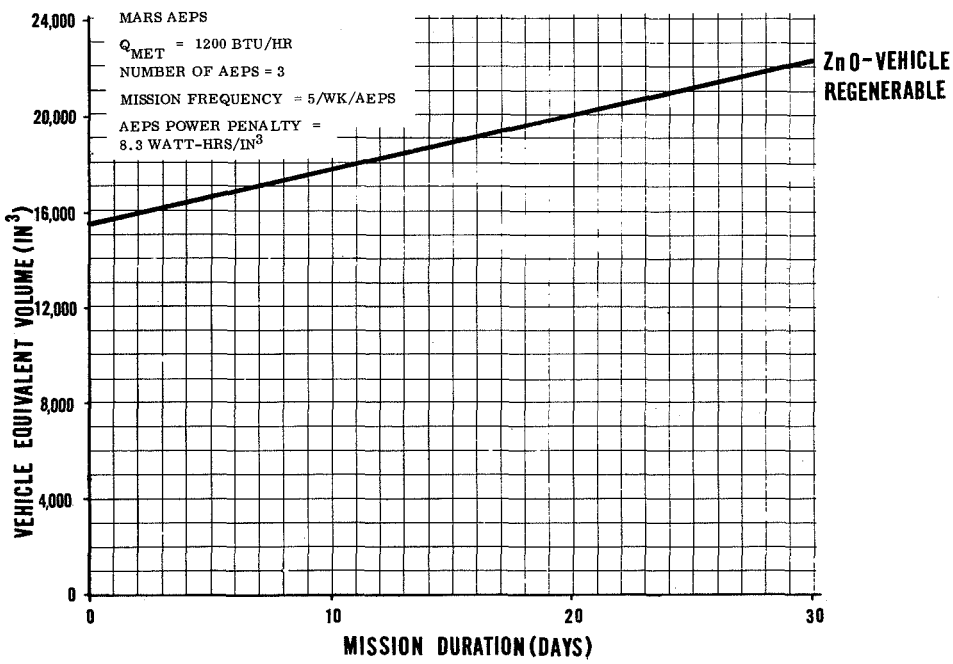

Figure 7.15 (b) *Carbon dioxide control/oxygen supply for martian AEPS.*

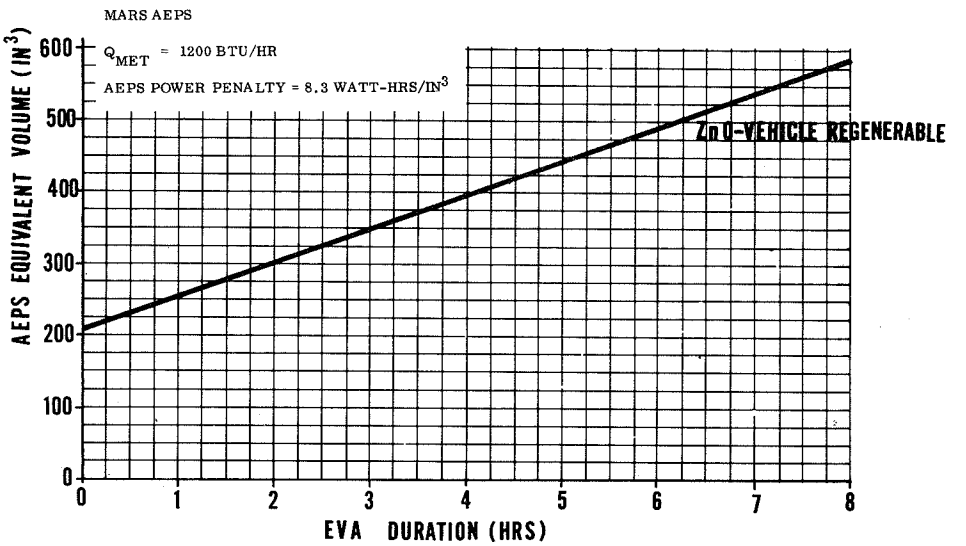

Figure 7.15 (c) *Carbon dioxide control/oxygen supply for martian AEPS.*

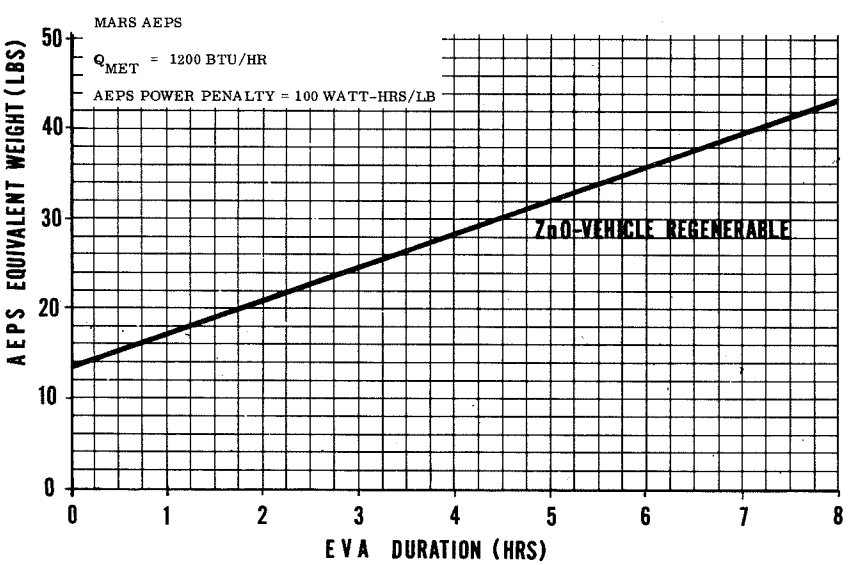

Figure 7.15 (d) *Carbon dioxide control/oxygen supply for martian AEPS.*

SYSTEM STUDIES

The system studies combined the selected candidate subsystem concepts into candidate baseline space station, lunar base, and martian AEPS schematics. The following schematics and flow charts are representative of potential AEPS configurations that might result if the technology recommendations emanating from the AEPS study are implemented.

AEPS Concepts

Space Station 1 (fig. 7.16). This AEPS concept contains all required life support equipment for extravehicular operation including an O_2 ventilation loop, a high-pressure O_2 subsystem, a water heat transport loop, a Freon 12 heat transport loop, a power supply, instrumentation, and operating controls and displays. The O_2 ventilation loop circulates a reconditioned and replenished O_2 supply through the suit. The O_2 from the suit enters the atmosphere regeneration subsystem and first passes through the debris trap where solid particles and droplets are removed; next CO_2 is removed by both physical adsorption and chemical absorption using a vehicle regenerable metallic oxide–zinc oxide; odors and trace contaminants are removed through physical adsorption by the activated charcoal in the contaminant control canister; and finally, an absolute filter provides dust and bacteria control. The O_2 then passes to a Freon evaporator heat exchanger that cools the circulated O_2 and condenses the entrained moisture. The cooled O_2 continues to the water separator where the condensed water vapor is removed and transferred to the water boiler to provide additional cooling capacity. The cool, dry O_2 then passes to the fan that circulates a ventilation flow of 6 acfm to the suit.

The high-pressure O_2 subsystem contains 0.75 lb of usable O_2 at 6000 psia and 65° F, and regulates the pressure in the O_2 ventilation loop to 7.0 ± 0.1 psia. This subsystem consists of an O_2 bottle, fill fitting, pressure sensor, shutoff valve, and pressure regulator.

The water heat transport loop cools the suited crewman by supplying and circulating cool water through a network of tubes built into his undergarment. The skin is cooled by direct conduction, and the mean skin temperature is lowered to a level where little, if any, perspiration occurs. A pump circulates the cooled water through the water heat transport loop at a flow rate of 4 lb/min. Flow through the thermal control subsystem is regulated by an automatic temperature control valve.

The thermal control subsystem is a hybrid expendable/thermal storage concept that consists of a water boiler and phosphonium chloride thermal storage unit. A Freon 12 heat transport loop consisting of a Freon evaporator, a variable speed compressor, and a variable orifice is utilized to transfer heat added at the evaporator to the phase change thermal storage unit. Average thermal loads are handled by the Freon evaporator. However, as the heat load increases above average levels, an increasing quantity of flow is precooled in the water boiler to prevent overloading of the evaporator and resultant loss of humidity control.

The estimated total volume and weight for this AEPS configuration are 2500 $in.^3$ and 77 lb based on average metabolic rate of 1000 Btu/hr for an EVA duration of 4 hr.

Space Station 2 (fig. 7.17). This AEPS concept is similar to concept 1 except:

1. The vehicle regenerable metallic oxide CO_2 control subsystem is replaced by an AEPS regenerable solid amine plate-fin matrix that removes both CO_2 and water vapor from the O_2 ventilation loop thus providing both CO_2 and humidity control. This is a cyclic concept using a 30-min full cycle. Energy released during the adsorb cycle is conducted to the regeneration portion of the subsystem thus supplying the endothermic heat of desorption.

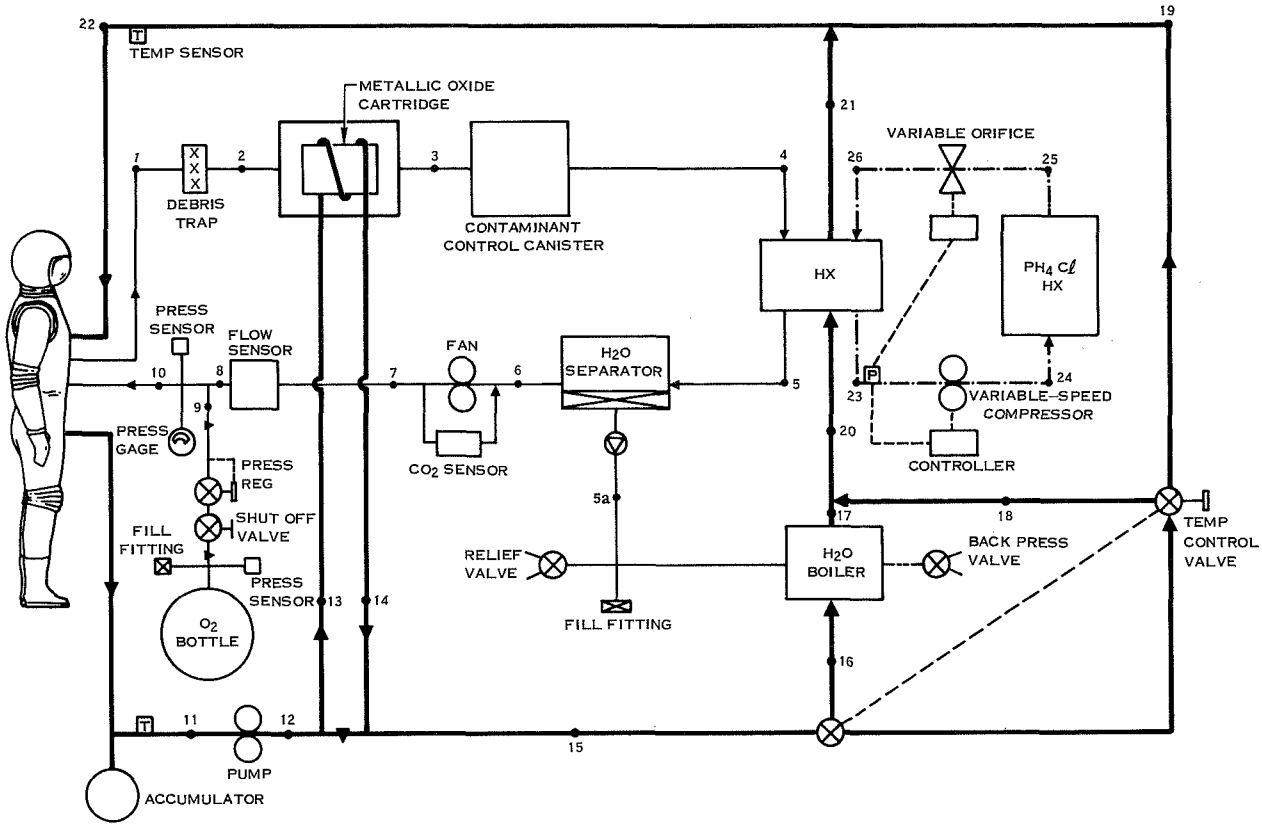

	Station										
Vent Loop	**1**	**2**	**3**	**4**	**5**	**5a**	**6**	**7**	**8**	**9**	**10**
Temperature, °F	79	79	79	79	50	---	50	72	72	72	72
Volume flow rate, FT^3/min	6.315	6.32	6.20	6.24	5.90	---	5.93	5.96	5.965	.072	6.037
Total pressure, psia	6.9	6.89	6.86	6.82	6.78	---	6.76	6.99	6.987	6.987	6.987
Total weight flow, lb/hr	14.225	13.225	14.030	14.030	13.898	---	13.898	13.898	13.898	.169	13.067
O_2 weight flow, lb/hr	13.531	13.531	13.531	13.531	13.531	---	13.531	13.531	13.531	.169	13.7
CO_2 weight flow, lb/hr	.357	.357	.162	.162	.162	---	.162	.162	.162	---	.162
H_2O weight flow, lb/hr	.337	.337	.337	.337	.205	.132	.205	.205	.205	---	.205
O_2 partial pressure, psia	6.49	6.48	6.51	6.48	6.55	---	6.52	6.75	6.75	6.987	6.75
CO_2 partial pressure, psia	.13	.13	.056	.056	.058	---	.059	.06	.06	---	.059
H_2O partial pressure, psia	.28	.28	.294	.285	.176	---	.175	.181	.181	---	.179
Dewpoint, °F	63	63	64	63	50	---	50	50	50	---	50

Figure 7.16 *AEPS concept 1, space station.*

	Station											
Liquid Loop	11	12	13	14	15	16	17	18	19	20	21	22
Weight flow lb/hr	240	240	40	40	240	18.2	18.2	221.8	0	240	240	240
Temperature, °F	64.7	64.8	64.8	68.2	65.5	65.5	45	65.5	--	63.7	60	60
Pressure, psia	18	22.3	22.3	22.3	22.1	22.0	21.7	21.7	20.4	21.7	20.4	20.4

	Station			
Freon Loop	23	24	25	26
Weight flow, lb/hr	18	18	18	18
Temperature, °F	50	150	82	45
Pressure, psia	61.4	103	102	61.8

Figure 7.16 *AEPS concept 1, space station. (Concluded)*

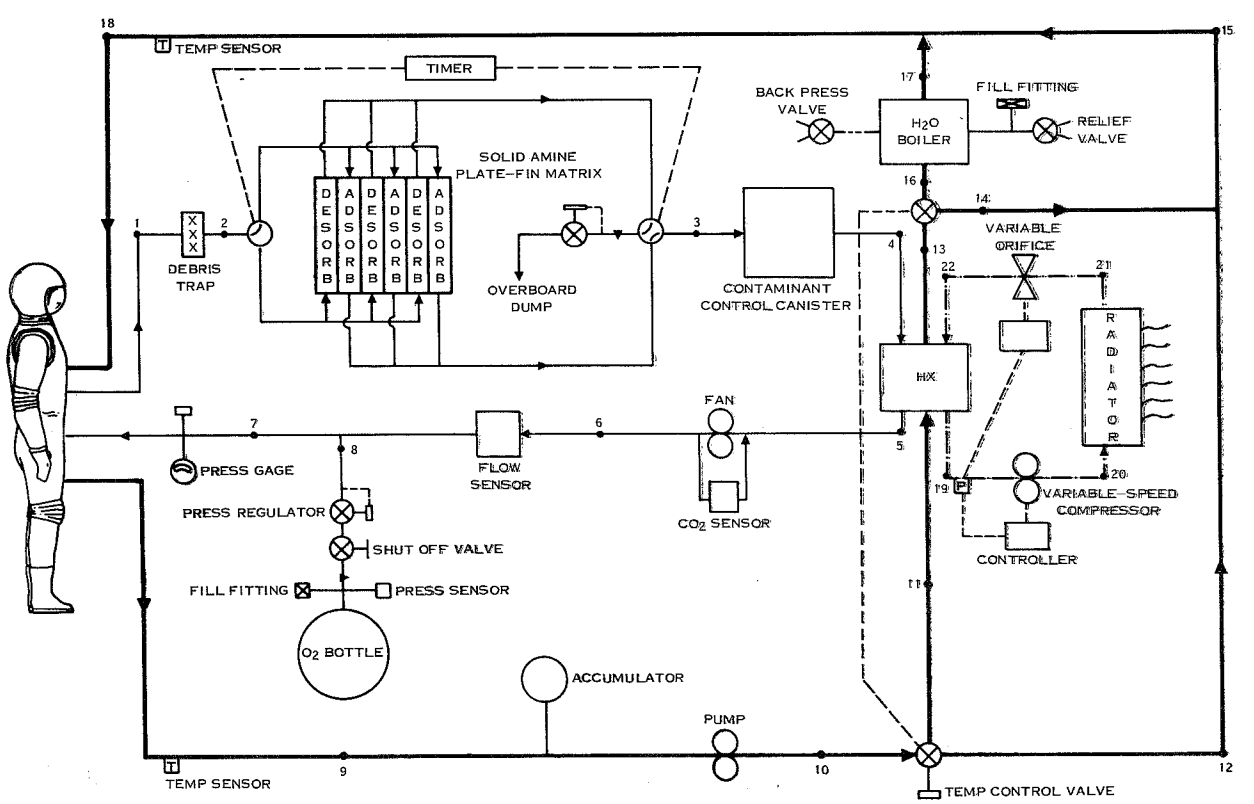

Figure 7.17 *AEPS concept 2, space station.*

	Station							
Vent Loop	1	2	3	4	5	6	7	8
Temperature, °F	79	79	79	79	50	72	72	72
Volume flow rate, FT^3/min	6.315	6.32	6.18	6.22	5.92	5.97	6.037	.072
Total pressure, psia	6.9	6.89	6.84	6.80	6.76	6.99	6.987	6.987
Total weight flow, lb/hr	14.225	14.225	13.898	13.898	13.898	13.898	14.067	.169
O_2 weight flow, lb/hr	13.531	13.531	13.531	13.531	13.531	13.531	13.7	.169
CO_2 weight flow, lb/hr	.357	.357	.162	.162	.162	.162	.162	---
H_2O weight flow, lb/hr	.337	.337	.205	.205	.205	.205	.205	---
O_2 partial pressure, psia	6.49	6.48	6.61	6.57	6.53	6.75	6.75	6.987
CO_2 partial pressure, psia	.13	.13	.055	.057	.057	.059	.059	---
H_2O partial pressure, psia	.28	.28	.178	.177	.175	.182	.179	---
Dew point, °F	63	63	50	50	50	51	50	---

	Station									
Liquid Loop	9	10	11	12	13	14	15	16	17	18
Weight flow, lb/hr	240	240	240	0	240	202	202	38	38	240
Temperature, °F	64.7	64.8	64.8	---	62.3	62.3	62.3	62.3	45	60
Pressure, psia	18	22.3	22.2	20.4	21.7	20.4	20.4	21.3	20.4	20.4

	Station			
Freon Loop	19	20	21	22
Weight flow, lb/hr	11	11	11	11
Temperature, °F	50	340	180	45
Pressure, psia	61.4	350	349	61.8

Figure 7.17 *AEPS concept 2, space station. (Concluded)*

2. The thermal control subsystem is a hybrid expendable/radiation heat pump subsystem and consists of a water boiler and a Freon 12 refrigeration system. The Freon 12 refrigeration system consists of a Freon evaporator, a variable speed compressor, a high temperature radiator, and a variable orifice. The Freon system is sized to reject average heat loads at nighttime conditions. Heat in excess of this amount is rejected by the water boiler. The automatic temperature control valve maintains the correct flow split between the two thermal control subsystems as well as conditioning the liquid transport loop. The estimated total volume and weight for this AEPS configuration are 3100 cu in. and 65 lb based on an average metabolic rate of 1000 Btu/hr for an EVA duration of 4 hr.

Lunar Base 3 (fig. 7.18). This AEPS concept is similar to concept 2 except the thermal control subsystem is composed of a PH_4Cl thermal storage unit and a Freon 12 refrigeration cycle consisting of a Freon evaporator, a variable speed compressor, and a variable orifice. Heat is added at the evaporator and stored at the thermal storage unit by the melting of PH_4Cl. The estimated total volume and weight for this AEPS configuration is 4500 cu in. and 193 lb based on an average metabolic rate of 1050 Btu/hr for an EVA duration of 8 hr.

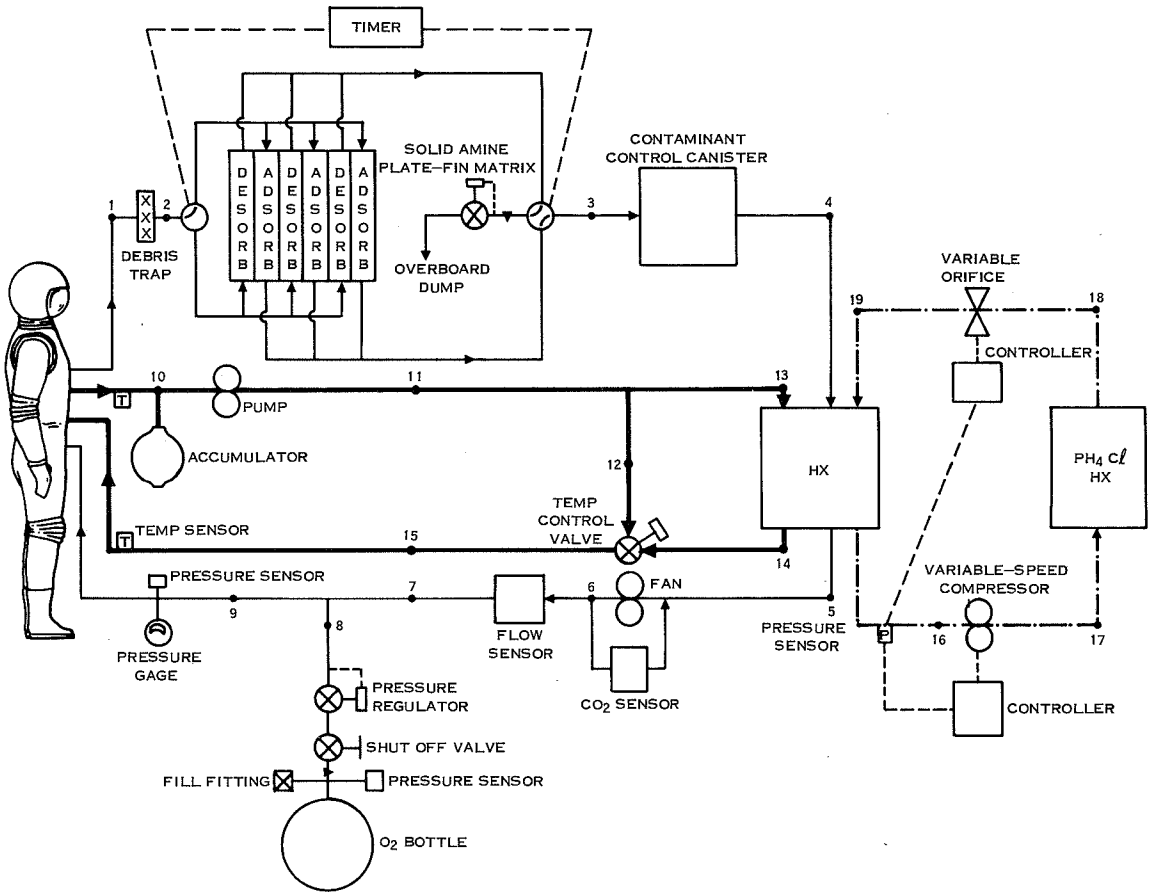

	Station								
Vent Loop	**1**	**2**	**3**	**4**	**5**	**6**	**7**	**8**	**9**
Temperature, °F	79	79	79	79	50	72	72	72	72
Volume flow rate, FT^3/min	6.31	6.31	6.21	6.25	5.94	6.00	6.00	.066	6.08
Total pressure, psia	6.9	6.89	6.84	6.80	6.76	6.99	6.987	6.987	6.987
Total weight flow, lb/hr	14.224	14.224	13.887	13.887	13.887	13.887	13.887	.178	14.067
O_2 weight flow, lb/hr	13.52	13.52	13.52	13.52	13.52	13.52	13.52	.178	13.7
CO_2 weight flow, lb/hr	.367	.367	.162	.162	.162	.162	.162	---	.162
H_2O weight flow, lb/hr	.337	.337	.205	.205	.205	.205	.205	---	.205
O_2 partial pressure, psia	6.46	6.46	6.60	6.56	6.52	6.75	6.75	6.987	6.75
CO_2 partial pressure, psia	.13	.13	.057	.057	.057	.058	.058	---	.058
H_2O partial pressure, psia	.29	.29	.18	.18	.18	.18	.18	---	.18
Dew point, °F	64	64	50	50	50	50	50	---	50

Figure 7.18 *AEPS concept 3, lunar base.*

	Station					
Liquid Loop	**10**	**11**	**12**	**13**	**14**	**15**
Weight flow, lb/hr	240	240	167	73	73	240
Temperature, °F	66.7	66.8	66.8	66.8	45	60
Pressure, psia	18	21.3	21.3	21.3	20.5	20.4

	Station			
Freon Loop	**16**	**17**	**18**	**19**
Weight, flow, lb/hr	27	27	27	27
Temperature, °F	50	150	82	45
Pressure, psia	61.4	103	102	61.8

Figure 7.18 *AEPS concept 3, lunar base. (Concluded)*

Lunar Base 4 (fig. 7.19). This AEPS concept is similar to concept 1 except the thermal control subsystem utilized is similar to that described in concept 2. The estimated total volume and weight for this AEPS configuration is 3500 cu in. and 100 lb based on an average metabolic rate of 1050 Btu/hr for an EVA duration of 8 hr.

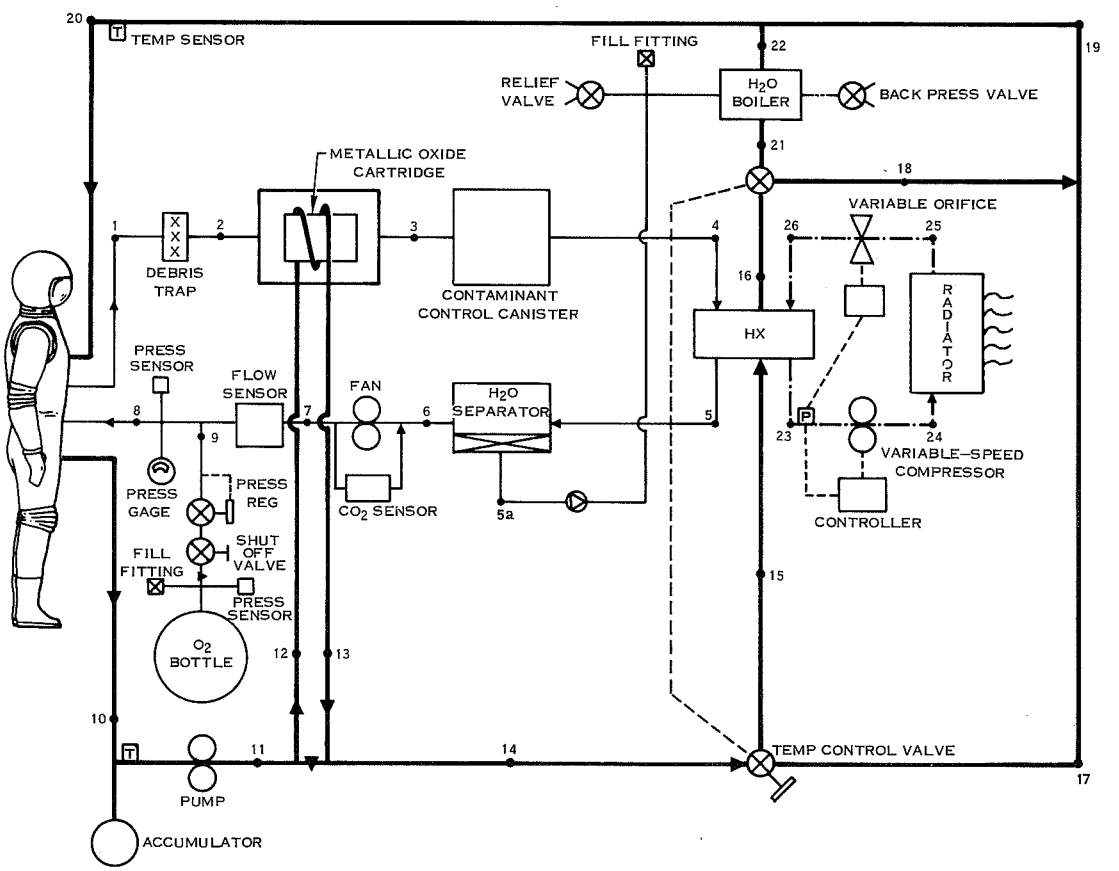

Figure 7.19 *AEPS concept 4, lunar base.*

Vent Loop	*Station* 1	2	3	4	5	5a	6	7	8	9
Temperature, °F	79	79	79	79	50	---	50	72	72	72
Volume flow rate, FT^3/min	6.3	6.3	6.25	6.29	5.91	---	5.93	5.99	6.09	.066
Total pressure, psia	6.9	6.89	6.86	6.82	6.78	---	6.76	6.99	6.987	6.987
Total weight flow, lb/hr	14.224	14.224	14.019	14.019	13.887	---	13.887	13.887	14.067	6.987
O_2 weight flow, lb/hr	13.52	13.52	13.52	13.52	13.52	---	13.52	13.52	13.7	.178
CO_2 wieght flow, lb/hr	.367	.367	.162	.162	.162	---	.162	.162	.162	---
H_2O weight flow, lb/hr	.337	.337	.337	.337	.205	.132	.205	.205	.205	---
O_2 partial pressure, psia	6.49	6.48	6.52	6.48	6.55	---	6.53	6.75	6.75	6.987
CO_2 partial pressure, psia	.13	.13	.056	.056	.056	---	.056	.059	.059	---
H_2O partial pressure, psia	.28	.28	.29	.29	.176	---	.175	.181	.179	---
Dew point, °F	63	63	64	64	50	---	50	50	50	---

Liquid Loop	*Station* 10	11	12	13	14	15	16	17	18	19	20	21	22
Weight flow, lb/hr	240	240	40	40	240	240	240	0	186	186	240	54	54
Temperature, °F	66.7	66.8	66.8	70.4	67.5	67.5	64.7	---	64.7	64.7	60	64.7	45
Pressure, psia	18	22.4	22.4	22.3	22.3	22.2	21.4	20.4	20.4	20.4	20.4	21.3	20.4

Freon Loop	*Station* 23	24	25	26
Weight flow, lb/hr	14.6	14.6	14.6	14.6
Temperature, °F	50	340	180	45
Pressure, psia	61.4	350	349	61.8

Figure 7.19 *AEPS concept 4, lunar base. (Concluded)*

Martian Base 5 (fig. 7.20). This AEPS concept is similar to concept 1 except the thermal control subsystem is a hybrid expendable/direct radiative cooling subsystem and consists of a water boiler and a direct radiator. Water in the heat transport loop exiting the radiator is the coolant in the humidity control condensing heat exchanger. As the radiator load increases and exceeds design values, a portion of the water heat transport loop flow bypasses to the water boiler, thus maintaining a constant radiator outlet temperature. The estimated total volume and weight for this AEPS configuration is 3100 cu in. and 84 lb based on an average metabolic rate of 1200 Btu/hr for an EVA duration of 8 hr.

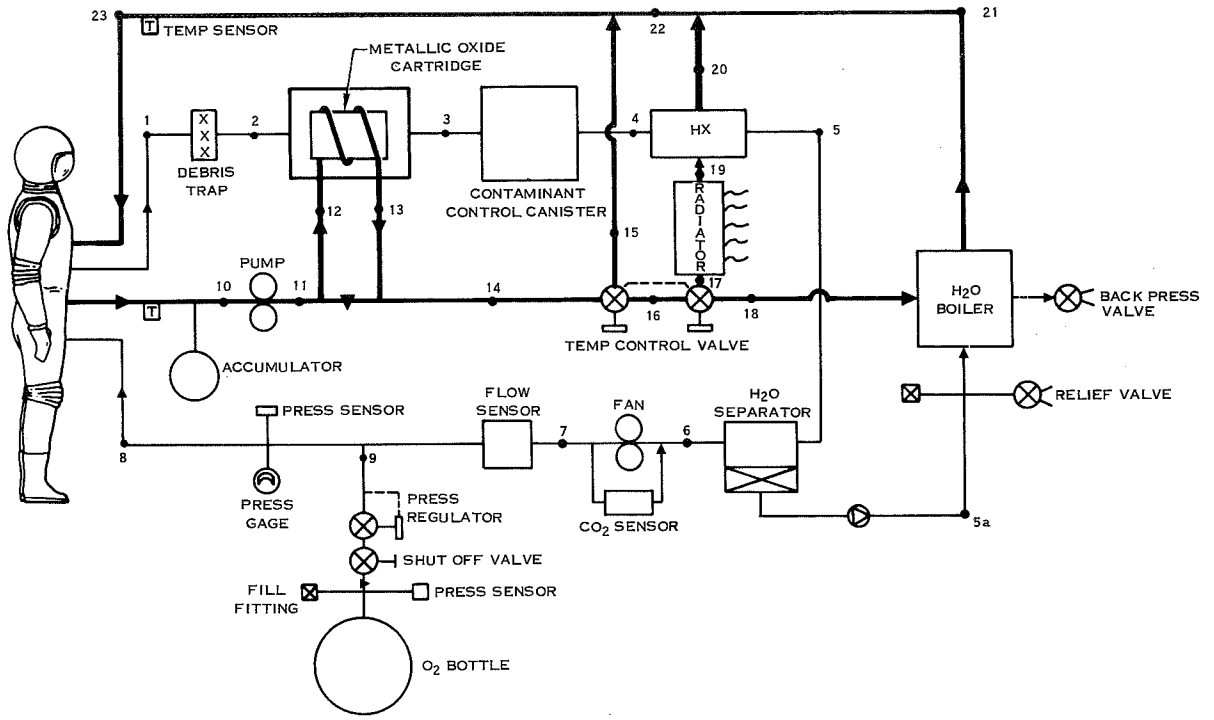

Station

Vent Loop	1	2	3	4	5	5a	6	7	8	9
Temperature, °F	79	79	79	79	50	---	50	72	72	72
Volume flow rate, FT^3/min	6.28	6.29	6.23	6.26	5.90	---	5.92	5.96	6.04	.086
Total pressure, psia	6.93	6.92	6.87	6.83	6.79	---	6.77	7.02	7.02	7.02
Total weight flow, lb/hr	14.24	14.24	14.01	13.01	13.87	---	13.87	13.87	14.07	.203
O_2 weight flow, lb/hr	13.5	13.5	13.5	13.5	13.5	---	13.5	13.5	13.7	.203
CO_2 weight flow, lb/hr	.396	.396	.162	.162	.162	---	.162	.162	.162	---
H_2O weight flow, lb/hr	.345	.345	.345	.345	.205	.141	.205	.205	.205	---
O_2 partial pressure, psia	6.50	6.49	6.52	6.48	6.55	---	6.53	6.76	6.75	7.02
CO_2 partial pressure, psia	.14	.14	.057	.057	.057	---	.057	.059	.058	---
H_2O partial pressure, psia	.29	.29	.29	.29	.18	---	.18	.17	.17	---
Dew point, °F	64	64	64	64	50	---	50	50	50	---

Station

Liquid Loop	10	11	12	13	14	15	16	17	18	19	20	21	22	23
Weight flow, lb/hr	240	230	40	40	240	167	240	45	28	45	45	28	240	240
Temperature, °F	64.3	64.4	64.4	68.5	65	65	65	65	65	45	49	45	60	60
Pressure, psia	18	21.5	21.5	21.4	21.4	20.4	21.3	21.2	20.8	20.8	20.4	20.4	20.4	20.4

Figure 7.20 *AEPS concept 5, martian base.*

NEW TECHNOLOGY RECOMMENDATIONS

As a result of the AEPS Study Program, the following areas of required new technology were identified and are recommended for future research and development.

Thermal Control

Thermal Storage. Investigate and develop a thermal storage material(s) whose heat of fusion exceeds 300 Btu/lb. One such candidate material, PH_4Cl, has already been identified and analytically evaluated during the AEPS study.

Radiation. Investigate and develop radiator surface coatings and treatments to optimize performance and minimize potential surface degradation. In addition, develop a lightweight, deployable radiator concept.

CO_2 Control

Develop a solid regenerable CO_2 sorbent that provides the performance, regeneration and life characteristics required for AEPS type applications. Two candidate families of solid regenerable sorbents—metallic oxides and solid amines—have already been identified and evaluated during the AEPS study.

O_2 Supply

Develop a high cyclic life/high static strength material for a 6000 psi oxygen bottle.

Power Supply

Operationally develop a high energy density, rechargeable electric storage battery. One candidate—a lithium-nickel halide battery—was identified during conduct of the AEPS study, and it (together with any other battery demonstrating a similar or greater energy capacity) is recommended for further research and development.

Contaminant Control

Confirm or modify the AEPS contaminant model selected and determine the effect of long term intermittent exposure upon the suited crewman; then design, develop and test the contaminant control subsystem to confirm performance characteristics.

Humidity Control

Results of the AEPS study indicate that a condensing heat exchanger in series with either an elbow wick separator or a hydrophobic/hydrophyllic screen separator are the optimum choices for an AEPS-type application. Research and development to determine the effect of contamination and bacterial/fungus growth upon the performance of both of these concepts is recommended to permit design and development of a long life humidity control subsystem.

Prime Movers

Design and develop longer life prime movers (i.e., fan, pump, and variable-spaced compressor) that have higher compressor efficiency and lower electronics and bearing losses than those presently being utilized in aerospace programs.

Automatic Temperature Control

Design and develop an automatic temperature controller. Further research and development is recommended to determine the signal parameters that provide accurate automatic temperature control, and to develop the required hardware.

Miscellaneous

a. Develop automated equipment to permit simple, rapid checkout of the AEPS. The present Apollo EMU PLSS requires approximately thirty (30) minutes for checkout prior to egress of the vehicle.

b. Investigate and evaluate potential integration (both functional and physical) of the crewman's personal maneuvering equipment with the AEPS for EVA missions in a zero gravity environment.

c. Improve the thermal isolation characteristics of the Thermal Meteoroid Garment (TMG), thus decreasing the peak thermal load on the AEPS thermal control subsystem.

d. Improve the Liquid Cooling Garment (LCG) heat transfer characteristics. This permits the liquid heat transport loop to operate at a higher temperature and thus decreases the power penalty associated with the thermal control subsystems which utilize a vapor compression (heat pump) cycle.

e. Conduct manned testing to evaluate the short-term and long-term physiological effects of various candidate pressure suit levels (3.5 to 14.7 psia) upon the crewman. Specific factors to be determined are:

- Required versus tolerable O_2 prebreathing time
- O_2 partial pressure exposure limitations including frequency and duration
- Safe decompression/recompression levels, rates and frequency

8 REGENERABLE THERMAL CONTROL AND CARBON DIOXIDE CONTROL TECHNIQUES FOR USE IN ADVANCED EXTRAVEHICULAR PROTECTIVE SYSTEMS

J. L. Williams, R. J. Copeland, and B. W. Webbon
Vought Missiles and Space Company
Dallas, Texas

INTRODUCTION

Realization of man's full potential for working in space during the ambitious programs of space exploration and research planned for the 1980s and beyond will require considerable extravehicular activity (EVA); longer EVA durations, and considerably more cumulative EVA hours per mission than on any mission to date. If the necessary EVA life support functions were performed using expendables, as is currently done in the Apollo portable life support system (PLSS), the materiel requirements at the vehicle/shelter would be prohibitive.

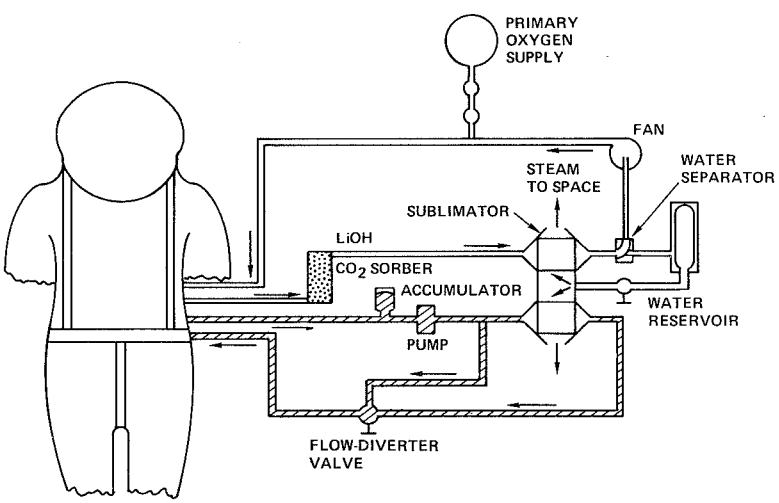

Figure 8.1 *Expendable PLSS-type system.*

Figure 8.1 shows an example of an expendable EVA life support system similar to the PLSS. The atmosphere makeup supply is oxygen stored as a gas in a relatively low pressure (1000 psia) bottle. Carbon dioxide (CO_2) is removed from the ventilation gas in a lithium hydroxide (LiOH) bed. Thermal control is achieved through use of a well-insulated suit, which limits the heat loss from the crewman and his support equipment to a value less than the crewman's metabolic load so that cooling is always required. This cooling is provided by vaporizing water, which is vented overboard, in a sublimator. The liquid-cooled garment (LCG) coolant and the ventilation gas are circulated past the crewman to pick up metabolic heat, through the sublimator for cooling, and then back to the suit.

The PLSS was originally designed for a 4-hr sortie; if the system were enlarged to provide an 8-hr sortie, then approximately 24 lb_m of expendables per man would be required for each EVA. Figure 8.2 shows the expendables breakdown for this case; note that the water expended in the sublimator to provide thermal control represents the bulk of the expendable weight. Carbon dioxide control in the form of LiOH requires approximately one fourth the weight of the water expended for thermal control. Oxygen, which is lost by leakage and in the form of CO_2, makes up about 10 percent of the total expendable weight. Figure 8.2 demonstrates that a closed thermal control system could reduce

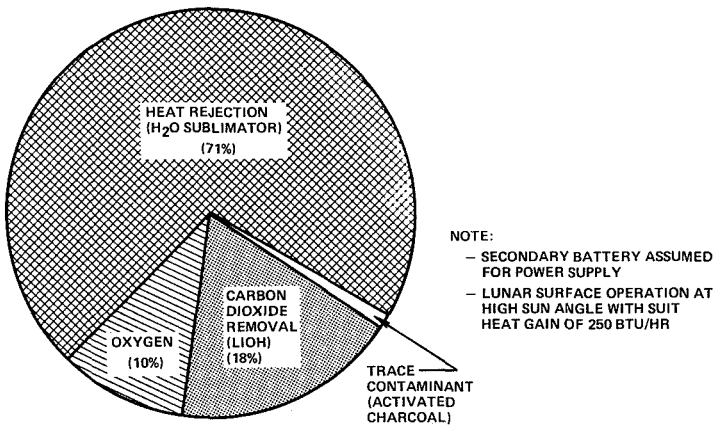

Figure 8.2 *Expendable breakdown for a PLSS-type system on an 8-hour mission.*

the expendables required per 8-hr sortie from 24 lb_m to about 30 percent of that, or 7 lb_m, and if it were coupled with a regenerable CO_2 control system from which oxygen can be recovered, then less than 1 lb_m of expendables would be required per 8-hr sortie.

An expendable EVA life support system such as PLSS is well suited for an Apollo-type mission, since only a few hours of EVA are planned for each mission, and the weight increase for the equipment required for regenerable life support would more than offset the savings in expendable weight. However, as the number of EVAs per mission is increased, the crossover point at which the weight of the expendables exceeds the weight of the regeneration equipment is quickly reached. Beyond this point, a regenerable system provides dramatic weight and volume savings for the vehicle/shelter.

This paper summarizes the work performed in a study of advanced extravehicular protective systems (AEPS) that might be used for extended EVA in earth orbit, on the lunar surface, or on Mars. The study was performed by Vought Missiles and Space Company (VMSC) of LTV Aerospace Corporation for the Biotechnology Division of NASA - Ames Research Center under contract NAS 2-6022.

OBJECTIVES

The primary objective of the AEPS study was to identify and define the most promising regenerable life support techniques and concepts that might be applied to a portable EVA life support system. Other objectives were to determine the tradeoff points between expendable, partially regenerable, and fully regenerable systems, and to generate the data necessary to define the weight and volume envelope required to support a given number of EVAs using the AEPS equipment.

Candidate life support subsystem concepts were separated into the following functional categories.

1. Expendable
2. Partially regenerable
   (a) Regenerated during the EVA
   (b) Regenerated at the base between EVAs
3. Fully regenerable
   (a) Regenerated during the EVA
   (b) Regenerated at the base between EVAs

The primary emphasis in this study was on fully regenerable systems. However, the most promising candidates in the other categories were also identified and characterized to determine the required tradeoff points.

AEPS SPECIFICATIONS, GUIDELINES, AND CONSTRAINTS

The specifications for the AEPS (ref. 1) are given in table 8.1. These specifications are generally intended to ensure the safety of the crewman and to maximize his mobility and work performance. The specifications most critical to the definition of the AEPS are the EVA duration and frequency (one 8-hr sortie per day), the allowable suit inlet CO_2 partial pressure (4 mm HgA nominal with 7.5 mm HgA maximum), and the metabolic rate (1600 Btu/hr average per sortie with a peak of 3500 Btu/hr and a mission average of 1200 Btu/EVA hour).

Table 8.1 *AEPS specifications.*

EVA DURATION (AT AVERAGE METABOLIC RATE)	8 + HOURS
FREQUENCY OF MISSIONS	1 PER DAY
MOBILITY	AEPS SHALL PROVIDE MINIMUM ENCUMBRANCE TO THE CREWMAN IN PERFORMANCE OF MISSION TASKS.
CENTER OF GRAVITY	CG OF THE EVA SUIT AND LIFE SUPPORT ELEMENTS ATTACHED TO OR INTEGRATED WITH THE SUIT SHALL NOT SHIFT MORE THAN ± 3 INCHES FROM THE CG OF THE NUDE CREWMAN.
SUIT GAS COMPOSITION	3.7 – 7.5 PSIA PURE OXYGEN
HUMIDITY CONTROL a. NOMINAL SUIT INLET DEW POINT b. MAXIMAL SUIT INLET DEW POINT	 45°F 60°F
VENTILATION (MINIMAL) a. INLET FLOW RATE b. INLET GAS TEMPERATURE c. SUIT LEAKAGE	 9 ACFM 50 – 70°F 180 SCCM
CONTAMINATION CONTROL a. NOMINAL INLET TO SUIT CO_2 LEVEL b. MAXIMUM INLET CO_2 LEVEL c. ODOR LEVEL	 4 MM Hg (NO MIXING IN FACE REGION) 7.5 MM Hg MUST NOT ADVERSELY AFFECT CREWMAN PERFORMANCE
METABOLIC PROFILE a. AVERAGE PER SORTIE b. PEAK (SUSTAINED) c. MINIMUM d. AVERAGE OVER ALL SORTIES	 1600 BTU/HR 3500 BTU/HR 250 BTU/HR 1200 BTU/HR
LIQUID TRANSPORT LOOP FLOW	4 LB/MIN.
LIQUID INLET TEMPERATURE TO SUIT	40°F
USE WITH VEHICLE OR SHELTER HAVING:	(a) 10 – 14.7 PSIA CABIN PRESSURE (b) 2.7 PSIA OXYGEN WITH DILUENT NITROGEN (c) RELATIVE HUMIDITY 55±5% (d) 65 – 75°F TEMPERATURE
SAFETY	THE SYSTEM SHALL PRECLUDE INJURY TO CREWMAN, SERVICE PERSONNEL, ETC., BECAUSE OF FIRE, EXPLOSION, TOXICITY, CONTAMINATION, AND BURNS OR SHOCK.
OPERATIONAL ENVIRONMENTS	ZERO g, 1/6 g, 0.37 g and 1 g
DONNING, DOFFING & CHECK-OUT TIME	MINIMIZE

The guidelines and constraints (ref. 1) shown in table 8.2 establish other criteria for defining and comparing different candidate AEPS and subsystems. The penalty factors for power and thermal energy are not conservative, but they should be well within the state-of-the-art in the AEPS operational time frame. These penalty factors were found to have a profound influence on the total weight of some regenerable systems, since large quantities of energy may be required for regeneration. Liberal EVA system weight and volume limits were deliberately selected to present as wide a range of candidate subsystem concepts for evaluation as possible.

Table 8.2 *Guidelines and constraints.*

BASE PENALTY FACTORS	
POWER	500 LB/KW_e
THERMAL ENERGY (HEATING OR COOLING)	100 LB/KW_t

ALLOWABLE AEPS WEIGHT AND VOLUME (DESIGN GOALS)

TRANSPORTER	WT. (LB)	VOL. (IN^3)
BACKPACK AND CHESTPACK	200	8,600
"MET" TYPE TRANSPORTER	200	8,600
POWERED VEHICLE	1000	40,000

DESIGN ENVIRONMENTS

As previously stated, the AEPS study was to consider EVA systems for missions in earth orbit, on the lunar surface, and on Mars. Table 8.3 summarizes the results of a brief investigation into the EVA environmental conditions that would be encountered on each of these missions.

Table 8.3 *AEPS design environments.*

	SOLAR FLUX (B/HR FT^2)	ALBEDO	EQUIV. SURFACE TEMP. RANGE ($^\circ$R)	MEAN GRAV. CONSTANT (g)	ROTATIONAL PERIOD (HRS)	ATMOS. PRESSURE (MB)
EARTH ORBIT	442	0.35	453	–	–	–
LUNAR SURFACE	442	0.07	170 – 760	0.17	655	–
MARS SURFACE	164 TO 240	0.17	POLE: 140 – 470 EQUATOR: 310 – 590	0.38	24.61	APPROX. 6 (0.088 PSIA)

The primary influence of the external environment on the AEPS is a heat leak either into or out of the AEPS control volume. The lunar surface is particularly severe in this respect since the long lunar day and the large solar flux cause the surface material to reach temperatures of more than 300° F (at the bottom of some craters). The lunar night is at the other extreme since the surface temperature may drop to -290° F. These extremes of thermal environment cause a heat leak through an Apollo suit ranging from about -300 to +350 Btu/hr and this can have a significant impact on the total AEPS heat load.

Another important factor is the lack of gravitational body force in earth orbit. This must be considered in determining the feasibility of actually constructing the hardware required to perform the life support functions.

The influence of all of the factors shown in table 8.3 was considered in the selection of life support concepts for the different missions. However, a different philosophy was assumed than was used for the selection of the Apollo PLSS. The PLSS was required to be operable both in earth orbit and on the lunar surface. As shown, the EVA conditions for these cases are significantly different, necessitating system compromises that would not be required if the system were optimized for a particular mission. This approach was necessary for the Apollo application, but for more advanced AEPS missions, requiring considerable EVA, there would be an advantage to tailoring the EVA systems for specific conditions.

LIFE SUPPORT SUBSYSTEM CANDIDATES

The generalized life support subsystems required in an AEPS are shown in figure 8.3. It was previously shown that the heat rejection and CO_2 control subsystems contribute about 90 percent of the expendable mass used in present-day systems. Therefore, these areas were given prime consideration. Other areas, such as atmosphere supply and power supply, were also investigated to determine if any significant improvements might be expected, and particularly to identify any subsystem concepts that might perform more than one life support function–for example, combined atmosphere supply and CO_2 control.

Atmosphere Supply Systems

The AEPS specifications (table 8.1) call for a pure oxygen atmosphere at 3.7 to 7.5 psia, and oxygen-nitrogen atmosphere at 10 to 14.7 psia for the primary vehicle/shelter. An evaluation of this difference in atmospheric pressure and composition indicated that it is not advisable for a crewman to transfer directly between these two atmospheres without some transition period. The primary problem is the possibility of aeroembolism (the bends) caused by a sudden reduction in

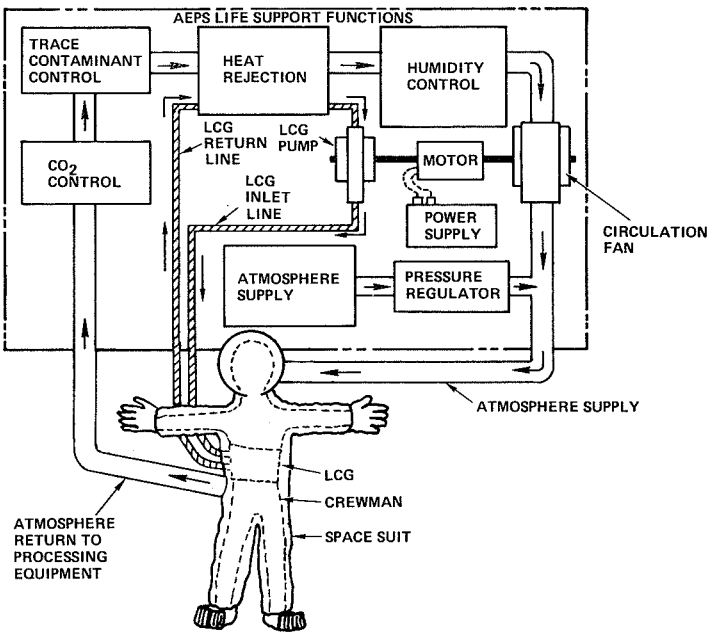

Figure 8.3 *AEPS life support system.*

the total pressure of the breathing gas. Avoidance of this problem requires either the adoption of a higher pressure, two-gas suit, or provision of equipment and time to reduce the nitrogen dissolved in the crewman's bloodstream to a safe level prior to the EVA. The first approach was found to be undesirable because of probable limitations in suit mobility associated with high suit pressure and the danger of crippling bends if the suit pressure was suddenly dropped—for example, as a result of suit puncture. Therefore, brief consideration was given to determining the techniques and types of equipment required to remove the nitrogen from the crewman's bloodstream prior to the EVA. For some missions the inclusion of the preconditioning equipment might be prohibitive, so a reliable, mobile, high-pressure two-gas suit might be required. A more detailed study of this problem [than was intended in the AEPS program] is required to determine the optimum suit gas composition and pressure and to more precisely identify the interfaces between the EVA and the base atmosphere systems.

Based on this preliminary investigation, a 5 psia, pure oxygen atmosphere was selected for the AEPS study in accord with the state of suit technology and the interests of system simplicity. The primary oxygen supply system is required to maintain this pressure by supplying gas at the proper pressure and flow rate to make up for normal suit leakage and the oxygen consumed by the man and removed by the CO_2 control system. It was assumed that an emergency system would be available to maintain suit pressure if required.

The candidate oxygen supply concepts that were considered are summarized in table 8.4, which shows that oxygen may be stored as a pure substance in various states or chemically combined in various ways. The chemical storage methods, such as chlorate candles and superoxides, and combined O_2 supply/CO_2 removal systems, were all found to have the problem of accurately controlling the rate of oxygen production to match the AEPS requirement of rapidly varying metabolic load in a small, closed volume. This problem may be overcome by using accumulators and other devices, but the addition of this equipment leads to excessive weight for an EVA system. There also is a problem in regenerating many of these chemicals to produce a closed system. Other systems, such as water electrolysis, and Bosch and Sabatier reactors, may be profitably applied at the primary base, but were found to be too large for EVA use.

It was concluded that high-pressure (approximately 5,000 psia) gaseous oxygen storage is the optimum method for AEPS. This system combines low weight and volume with maximum reliability and ease of integration with base systems. The only base regeneration requirement is a compressor to fill the EVA tank; the power required for this compressor is significantly less than that required for any other system. The construction of a 5,000-psia tank and pressure regulator

Table 8.4 *Candidate CO_2 supply systems.*

SUPPLY OR STORAGE TECHNIQUE	5000 PSI GAS	SUPER-CRITICAL	SUB-CRITICAL	WATER ELEC-TROLYSIS	HYDRO-GEN PEROXIDE	CHLO-RATES & PERCHLO-RATES	SUPER-OXIDES, OZANIDES	BOSCH REACTOR	SABA-TIER REACTOR	SOLID ELECTRO-LYTE	FUSED SALT
EVA WEIGHT $\frac{LB_m}{LB_m O_2}$	3	1.5	1.2	11	2.5	LARGE	2.5	LARGE	LARGE	LARGE	LARGE
EVA VOLUME	LOW	VERY LOW	VERY LOW	MEDIUM	MEDIUM	LOW	LOW	HIGH	HIGH	HIGH	HIGH
EVA RELIABILITY	HIGH	HIGH	HIGH	LOW	MEDIUM	MEDIUM	MEDIUM	LOW	LOW	LOW	LOW

is well within present technology. Further improvements to permit the use of higher pressures also may reduce the tank weight and volume. Therefore, it is recommended that a high-pressure oxygen supply be used for EVA systems for the foreseeable future.

Power Supply, Trace Contaminant Control, Humidity Control

It was found that the expendable weight and EVA equipment weight were so small that no significant total weight reduction would be realized by developing new concepts in the areas of power supply and control of trace contaminants and humidity. All AEPS were assumed to use rechargeable lithium halide batteries for power supply with expendable activated charcoal and biological filters for trace contaminant control. The humidity control system depends on the temperature level available from the heat rejection system. Simple condensation and separation were assumed for systems with low temperature heat rejection (below 45° F), and a silica-gel desiccant for systems with higher heat rejection temperatures (from 45° to 70° F). The weight and volume of all of these subsystems and the power supply recharge equipment were included in the AEPS total integrated system analysis.

Carbon Dioxide Control Systems

A comprehensive survey of the pertinent literature was made to identify previously investigated techniques for controlling the CO_2 level in a closed volume and to define new concepts that appear promising from a theoretical standpoint.

The most promising techniques identified are shown in table 8.5, and all are considered feasible for use in an AEPS. The concepts were screened in terms of system size, expendable requirements, power requirements, and similar factors; as shown in the table, many were discarded at this stage because of obvious problems with excess size, prohibitive regeneration penalties, or because they did not offer any potential improvement over existing systems. Detailed analysis was then performed and a conceptual system design produced for each remaining technique. A final screening process reduced the candidate systems to the following four: LiOH (expendable), solid amine (partially regenerable), $MgOH_2$ (regenerable at base), and KOH (regenerable at base).

Lithium hydroxide reacts readily with carbon dioxide, and the LiOH system, although fully expendable, is the lightest weight and most compact CO_2 control system available. Lithium hydroxide is thus very satisfactory for missions where a relatively small number of EVAs are required and for EVA sorties requiring maximum mobility. No other expendable CO_2 control method was found that would be competitive with LiOH from a weight and volume standpoint. It is possible to reverse the reaction and recover LiOH from the lithium carbonate (Li_2CO_3)

Table 8.5 *Candidate CO_2 control methods.*

METHOD	DETAILED ANALYSIS	PRELIMINARY ANALYSIS ONLY	COMMENTS
CHEMICAL EXPENDABLE			
• LiOH	X		GOOD FOR LIMITED NUMBER OF SORTIES
• KO_2, NaO_2		X	NO ADVANTAGE OVER LiOH
• Li_2O_2		X	NO ADVANTAGE OVER LiOH
CHEMICAL, REGENERABLE			
• LiOH	X		HIGH REGENERATION PENALTY
• KOH	X		MODERATE POWER FOR BASE REGENERATION
• KO_2, NaO_2, Li_2O_2		X	EXCESSIVE POWER FOR BASE REGENERATION
• KO_3		X	EXCESSIVE POWER FOR BASE REGENERATION
• $Mg(OH)_2$	X		MODERATE TEMPERATURE FOR REGENERATION
• $Ca(OH)_2$		X	EXCESSIVELY HIGH REGENERATION TEMPERATURE
ADSORPTION			
• DEAD END MOLE-SIEVES (ZEOLITE)		X	EXCESSIVE EVA MASS AND VOLUME
• VACUUM DESORBED MOLE SIEVES (ZEOLITE) CLASS B ONLY	X		GOOD FOR MODERATE NUMBER OF EVA'S, BUT HAS LARGE EVA MASS AND VOLUME
• VACUUM DESORBED ZEOLITE WITH LiOH "TOP-OFF" (CLASS A ONLY)	X		EXCESSIVELY LARGE EVA MASS WITHOUT ANY SIGNIFICANT REDUCTION IN EXPENDABLES
• NON-WATER SENSITIVE MOLE-SIEVES		X	NO ADVANTAGE OVER ZEOLITES
ABSORPTION			
• BATCH VACUUM DESORBED SOLID AMINES	X		LARGE EVA MASS SUITABLE FOR LIMITED NUMBER OF EVA'S
• LIQUID WATER SOLUTION OF AMINES VACUUM DESORBED		X	EXCESSIVE WATER LOSS DURING EVA
• LIQUID WATER SOLUTION OF CARBONATES WITH VACUUM DESORPTION		X	EXCESSIVE WATER LOSS
a. LIQUID LOOPS b. MEMBRANES			
• DEAD END WATER SOLUTION OF CARBONATES		X	EXCESSIVE EVA SIZE
VACUUM VENT			
• SIMPLE SYSTEM, NO UMBILICAL		X	EXCESSIVE EVA MASS AND EXPENDABLES
• 1.0 HR FREE FLIGHT WITH UMBILICAL TO PRIMARY BASE	X		SHOWS SOME PROMISE WHEN THE EVA MISSION DOES NOT REQUIRE LONG DURATIONS AT DISTANCES FROM THE SPACE BASE
OTHER			
• CONVERSION OF CO_2 TO WATER BY A BOSCH REACTOR FOR RECOVERY OF O_2 AT BASE		X	VERY HIGH EVA MASS
• H_2-DEPOLARIZED CARBONATION CELL, VACUUM VENT		X	LARGE SYSTEM SIZE, HIGH EXPENDABLES
• VACUUM VENTED SINGLE STAGE CARBONATION CELL		X	HIGH EVA SYSTEM MASS AND POWER, HIGH EXPENDABLES
• Cu/O_2 FUEL CELL CO_2 SORBER		X	LOW CONVERSION EFFICIENCY TO CARBONATE
• ANY SYSTEM CONCENTRATING CO_2 & THEN RECOVERING O_2 DURING THE EVA		X	EXTRAORDINARILY HIGH EVA MASS VOLUMES AND POWER PENALTIES

produced during the EVA. However, considerable amounts of power are required because Li_2CO_3 is relatively insoluble in water, making simple electrolysis impractical. Thermal regeneration is not feasible either. Therefore, LiOH was judged to be impractical for use in the nonexpendable mode.

Solid amine systems are being researched for use as CO_2 concentrators in a primary base system. The most promising solid amine system for AEPS incorporates a vacuum-vent mode of operation. This system uses two beds in a cyclic fashion: one bed absorbs CO_2 from the gas stream while the other bed is desorbed to space. The system is classed as partially expendable because the CO_2 sorbent is reused, but the CO_2, the water vapor, and oxygen contained in the bed free volume are vented to space. Solid amine CO_2 sorbents have a low capacity for CO_2 when compared to chemicals such as LiOH, and they have a lower reaction rate; thus the required bed size is much larger than a LiOH bed. The amine bed acts as a desiccant so that a separate humidity control system is not required. However, the CO_2 absorption capacity of the bed depends critically on the bed's moisture content so that precise control of the bed water content is required for efficient utilization. Operation in the vacuum desorbed mode has not been demonstrated, and it is anticipated that bed water management for this type of operation may be very difficult. The cyclic operation also requires relatively complex hardware with associated reliability problems. There is no base equipment required for this system since the CO_2 sorbent is regenerated by vacuum venting during the EVA. One significant advantage of this system is that it may be possible to adapt some of the technology already developed for space station systems and thereby reduce the development cost of the system.

The literature survey provided evidence of some preliminary investigations into the use of other alkaline-earth hydroxides other than LiOH as a CO_2 sorbent. All these materials are very basic and the reaction with the acid gas, CO_2, is an acid-base neutralization reaction, with the resulting formation of a carbonate salt and water. These hydroxides all have fairly high CO_2 capacity so that the bed size is comparatively small. Lithium hydroxide is preferred when the application requires an expendable sorbent because of its low molecular weight. However, as previously stated, the chemical properties of lithium carbonate formed during the EVA reaction are such that excessive energy is required to regenerate the hydroxide.

It was found that magnesium carbonate ($MgCO_3$) is relatively unstable so that thermal regeneration is possible and the relatively high solubility of potassium carbonate in water suggested the possibility of regeneration by electrolysis of a water solution.

Magnesium carbonate dissociates into magnesium oxide (MgO) and CO_2 at elevated temperatures. Thus if magnesium hydroxide ($Mg[OH]_2$) were used in solid form as a CO_2 sorbent during the EVA, in the same manner that LiOH is used, it should be possible to regenerate the resulting carbonate by simply heating the EVA canisters. The CO_2 will be driven off, leaving solid MgO, which can then by hydrated to $Mg(OH)_2$ by circulating wet steam through the bed.

A workable system concept is shown in figure 8.4. The $Mg(OH)_2$ canister is placed in a heated pressure vessel at the conclusion of the EVA. The system shown uses steam to heat the canister to the required dissociation temperature; however, any heat source could be used. A compressor is used to remove the evolved CO_2 for processing by the base CO_2 reduction system. After all the CO_2 has been driven off, wet steam is introduced into the chamber to hydrate the MgO. The canister can then be removed and reused.

The feasibility of this concept has been demonstrated (ref. 2). However, the lifetime of $Mg(OH)_2$ pellets after repeated cycling has not been investigated. Data are needed to determine whether the pellets need to be reformed after each regeneration cycle and to define the

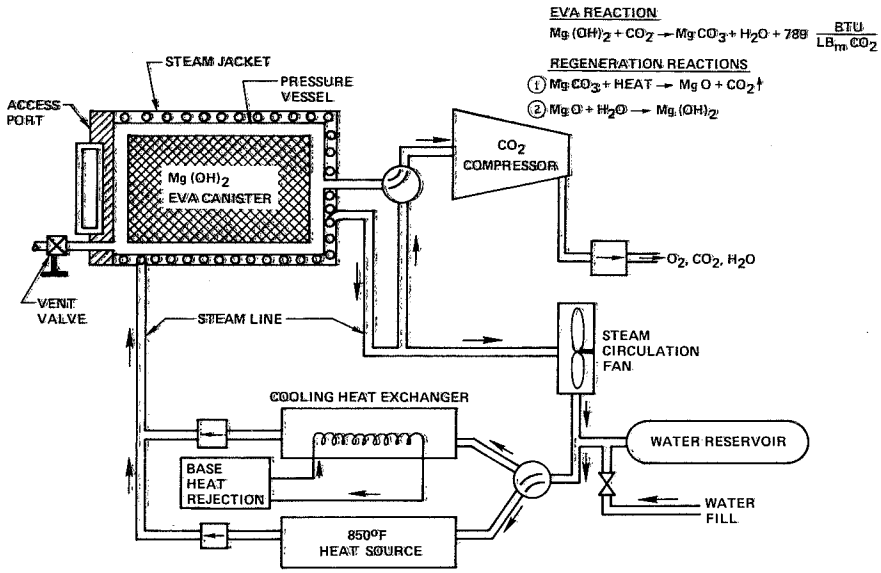

Figure 8.4 $Mg(OH)_2$ *regeneration facility.*

conversion efficiency of the $Mg(OH)_2$ that can be regenerated within a practical amount of time. The actual hardware weight required for regeneration of $Mg(OH)_2$ is projected to be about 230 lb_m for a two-man system. The total base penalty calculated for the system is 900 lb_m per two men with the additional weight attributed to energy penalties. Thus, the base weight of the system depends critically on the penalties assumed in table 8.2.

The EVA operation of the CO_2 sorber system is identical to that of the LiOH system, except that a larger canister is required. The system has considerable promise since the required technology has already been partially demonstrated.

A theoretical analysis of the energy requirements suggested the feasibility of using potassium hydroxide (KOH) as a regenerable CO_2 sorbent. Figure 8.5 shows a unique design, conceived by VMSC, that uses a circulating liquid solution of KOH rather than a solid particle bed. The advantage of this concept is that it overcomes one of the fundamental limitations on the efficient use of a solid sorbent bed—that is, the low solid diffusion rate of reacted carbonate and unreacted hydroxide in the pellet interior. The pellets are generally made as small as possible and somewhat porous to maximize the surface area exposed to the gas stream. These pellets tend to cake during the EVA due to trapping of the product water. This increases the pressure drop and further complicates regeneration since the pellets must be reformed.

Liquid loop systems eliminate these problems since the reacted carbonate is continuously removed from the reaction site by the flowing solvent water. The EVA is started with the liquid loop filled with a strong solution of KOH in water. The gas, containing CO_2, flows through the gas reactor where it is exposed to the liquid KOH. Part of the KOH is reacted to form potassium carbonate (K_2CO_3), which remains in liquid solution and is then pumped to the reactant storage container. There the solution is cooled, decreasing the solubility of the K_2CO_3, so that part of the carbonate is precipitated and filtered out of the solution. The remaining solution is then pumped back to the gas reactor. During the EVA, the solution strength of the KOH is reduced as K^+ ions are removed in the precipitation of K_2CO_3. The concentration of K_2CO_3 in the

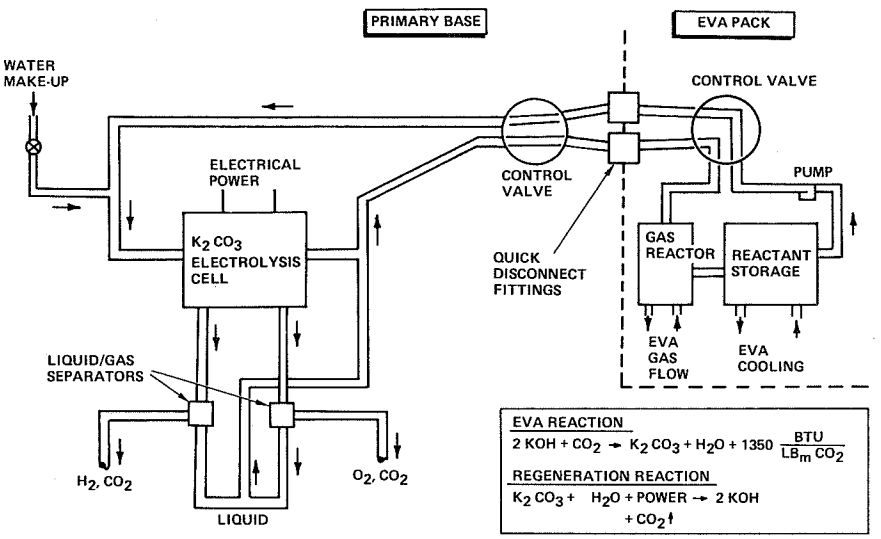

Figure 8.5 *Liquid* KOH/CO_2 *sorbent regeneration facility.*

solution is determined by the solution temperature at the outlet of the reactant storage container and by the efficiency of the filtration process.

Calculations have shown this process to be theoretically feasible and the required EVA weight, volume, and power may be significantly smaller than for any other regenerable system. However, considerable development is needed to provide an efficient and reliable EVA system.

Base regeneration (fig. 8.5) is accomplished by redissolving the precipitated carbonate and electrolysis of the resulting solution. The CO_2 is removed in the electrolysis cell, and the result is a concentrated solution of KOH ready for EVA use.

In a primitive experiment, VMSC demonstrated the feasibility of this system. With the simple apparatus used, it was not possible to evolve CO_2 at a significant rate without also electrolyzing water, even though it is theoretically possible to reduce the carbonate to CO_2 at a lower voltage than is required for water electrolysis. This is not a severe penalty since most base life support systems include a water electrolysis unit for the production of oxygen (ref. 3). Therefore, a partial credit can be taken for the oxygen produced by this method.

The projected total system size for the KOH system, including all penalties, is comparable to the $Mg(OH)_2$ system previously discussed, and for discussion at the total system level, these systems were considered to have the same weight and volume. The potential EVA system size advantage of the KOH system over other regenerable concepts is sufficient to warrant further investigation.

Figure 8.6 shows the total launch weight and volume as a function of EVA time for the most promising CO_2 control subsystems. The curves show that expendable LiOH is the smallest subsystem for less than about 50 hr EVA. Between 50 and 900 hr EVA the solid amine subsystem has the lowest total subsystem weight; it also has the largest EVA weight of all the systems considered in detail. Regenerable $Mg(OH)_2$ or KOH systems are the lightest total systems for more than 900 hr EVA, but at the penalty of increasing the EVA weight. This sacrifice is believed to be worthwhile since at 1600 hr EVA, the $Mg(OH)_2$ system saves more than 1000

lb_m over LiOH. The data presented in figure 8.6 were used in preparing similar curves for total AEPS.

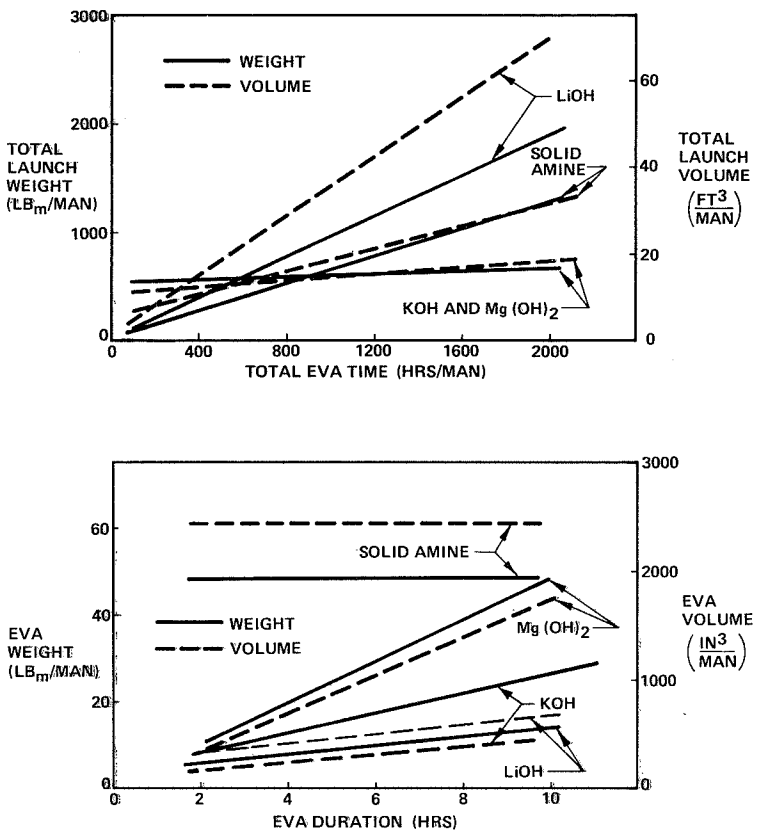

Figure 8.6 *AEPS CO_2 control system size comparison.*

Thermal Control Systems

Gemini experience has shown that gaseous convective cooling of a suited crewman is inadequate when the crewman is working at the high metabolic rates expected during orbital or surface EVA operations. Therefore, the AEPS study baselined a circulating water cooling system similar to the Apollo LCG. However, the low heat exchanger effectiveness of the current LCG requires an inlet temperature of about 40° F to remove the maximum metabolic load (3500 Btu/hr); the outlet temperature is only 55° F. This low temperature close to the skin can create physiological and comfort problems for the crewman. A brief investigation showed the feasibility of producing a more effective heat transfer between the heat sink and the LCG that could operate with inlet temperatures in the range of 60° to 70° F at the maximum metabolic load. This higher temperature level is beneficial to some heat rejection concepts so that an advanced LCG was assumed to be incorporated where appropriate.

Table 8.6 gives the methods of rejecting heat from an AEPS that were considered in this study. Several of the heat rejection mechanisms, such as conducting heat sinks, have specific applications, while others, such as evaporation, are more general.

Table 8.6 *Means for accomplishing heat removal from AEPS.*

MECHANISM	MASS & HEAT TRANSFER			PHASE CHANGE				
	CONDUCTION	CONVECTION	RADIATION	EVAPORATION	FUSION	CRYSTALLINE STRUCTURE CHANGE	WORK	CHEMICAL REACTION
GOVERNING EQUATION	$q_L = \frac{KA}{X}(T_L - T_S)$	$q_L = hA\,(T_L - T_S)$	$q_L = \sigma\epsilon A\,(T_L^4 - T_S^4)$	$q_L = \dot{m}\lambda$	$q_L = m\lambda$	$q_L = m\lambda$	$q_L = w\,(\frac{T_L}{T_S - T_L})$	$q_L = m\Delta h_o$
LIMITING FACTOR	RATE	RATE	RATE	CAPACITY	CAPACITY	CAPACITY	RATE	CAPACITY
TYPICAL CANDIDATE SYSTEMS	SUB-SURFACE HEAT SINK	MARS HEAT EXCHANGER	SPACE RADIATOR	SUBLIMATOR	ASTRONAUT HEAT SINK (AHS)	AHS	VAPOR COMPRESSION REFRIGERATOR	AHS
EXPENDABLE REQUIREMENTS	NONE	NONE	SMALL	LARGE	NONE	NONE	SMALL	NONE

NOTE: T_S = SINK TEMPERATURE

T_L = SYSTEM HEAT REJECTION TEMPERATURE 40°F

SYSTEMS SELECTED FOR FINAL SYSTEM INTEGRATION

- SPACE RADIATOR
- SUBLIMATOR
- AHS (WATER SELECTED AS FUSIBLE MATERIAL)
- REFRIGERATOR

AHS SYSTEM USES REPLACEABLE MODULES TO REDUCE PACK WEIGHT

REFRIGERATION SYSTEM USES PART-TIME (70%) UMBILICAL WITH AHS "TOP-OFF"

The limiting factors shown in the table are the fundamental physical factors that influence the system design. Systems such as a space radiator must be sized to reject the maximum expected rate of heat production. The capacity of the system (average rate multiplied by EVA duration) is a factor only in that the system battery must have the required capacity; thus, this type of system is said to be rate limited. The phase change concepts are said to be capacity limited because a fixed quantity of heat sink material is carried and all cooling capacity is lost when this material is expended. The rate at which the material is expended has little impact on system size and weight.

By means of a preliminary screening technique involving detailed analysis and preliminary sizing, the candidate concepts were reduced to four systems meriting consideration at the total system level: water evaporator (expendable), radiator (supplemented by expendables), refrigerator (supplemented by expendables), and astronaut heat sink (AHS) (fully regenerable).

No heat rejection subsystem having an 8-hr operating capacity without expendables was small enough to be integrated entirely into a backpack system. Thus, some type of separate support system is required, which could be mounted on a MET-type transporter or installed on a powered vehicle.

There are two functionally different methods of supporting the AEPS backpack from a separate system; the two systems can be connected by an umbilical, or the support system can hold cooling modules for manual installation into the AEPS pack as required. VMSC evaluated both approaches and found that it was not possible to prove one method superior to the other based on the general AEPS guidelines. It was assumed that any umbilical system must have the capability to operate without the umbilical for 30 percent of the EVA duration. Therefore, the radiator and refrigerator systems, which have the capability to operate as completely closed systems, nevertheless are considered to be supplemented by expendables, since expendables may be used during the nonumbilical portion of the EVA.

The water evaporation system is assumed to be a sublimator similar to that used in the Apollo PLSS with an enlarged water tank to increase the system capacity to 8 hr. This system would have a pack weight of about 40 lb_m and would expend approximately 17 lb_m of water during an 8-hr EVA. The sublimator is a compact and reliable heat rejection device, but its large expendable requirement makes it prohibitively heavy for missions requiring more than about five EVA per man.

The simple radiator and the refrigeration systems are rate limited, and they would be prohibitively large when designed to reject the maximum expected heat load. However, this maximum heat load is expected to occur infrequently and for short durations so that a more practical approach is to design the primary system to reject the average heat load with a secondary top-off system to accommodate the transient peaks. It was found that the total system heat load, including equipment cooling and a nominal environmental heat leak, is about 2000 Btu/hr for an average metabolic load of 1600 Btu/hr. Therefore, this value was taken as the baseline load for the design of the primary system.

A simple radiator system was found to be the lightest weight, closed heat rejection concept available. However, this system has several limitations. The radiating temperature is limited to the temperature available from the LCG and will therefore be less than about 70° F; heat rejection from the radiator is thereby limited to a maximum of 140 Btu/hr ft^2 so that the minimum possible radiator area is about 14 ft^2 for 2000 Btu/hr. The actual area will be considerably greater because of limitations imposed by radiator fin effectiveness, surface optical properties, and the influence of the thermal environment. Any thermal radiation incident on the radiator surface will decrease the radiator's net heat rejection per unit area. In some daytime thermal environments, such as inside a lunar crater or near mountains, the infrared radiation from topographical features can render a simple radiator completely useless. The radiator can be shielded or positioned by an orientation system to minimize the incident radiation, but these additions increase the weight and volume of the system so that it is not competitive with several other concepts. However, a radiator would be a very attractive system for a Martian EVA since the thermal environment is much less severe than on the moon.

The problems encountered with the simple radiator can be overcome by using a refrigeration cycle to increase the radiator temperature. A vapor compression refrigeration cycle was selected because of its high coefficient of performance (COP) and compact size. The energy required to drive the system is supplied by a lithium halide battery.

A conceptual design for an AEPS vapor compression refrigerator was created to allow weight, volume, power, and expendables estimates to be made. On the basis of conservative estimates for motor and compressor efficiency, it was found that a COP of 2.9 could be achieved with an evaporator temperature of 40° F and a condenser temperature of 130° F. The total EVA weight of the system, including power supply and radiator, was found to be about 70 lb_m for a 2000 Btu/hr system. This system employs a 25-ft umbilical with the evaporator built into the AEPS pack. Thus, any failure in the umbilical system would not cause a loss of LCG fluid, since the evaporator acts as a heat exchanger between the LCG loop and the refrigerant. A top-off system, to be discussed later, is also included in the backpack, bringing the total heat rejection system weight to about 95 lb_m. This system would provide cooling for nonumbilical operations, to accommodate transient peak heat loads, and in case of refrigeration system failure. The only base requirement for this system is recharge of the EVA battery.

The modular approach to a closed AEPS heat rejection system is illustrated in figure 8.7. This concept has been designated the astronaut heat sink (AHS). The basic concept is extremely simple. An aluminum pack containing 15 lb_m of ice is mechanically clamped between two heat

exchanger modules. Heat is rejected by melting the ice. Since the heat of fusion of ice is only about 15 percent of the heat of sublimation, approximately 75 lb_m of ice are required for a nominal EVA (1600 Btu/hr metabolic load). This is too large a subsystem mass to be included in a backpack so the ice is divided into modules with fresh modules carried in an insulated container. A spent (melted) module is replaced with a fresh one from the storage container as required. The AHS is carried in a chest pack to facilitate AHS module replacement.

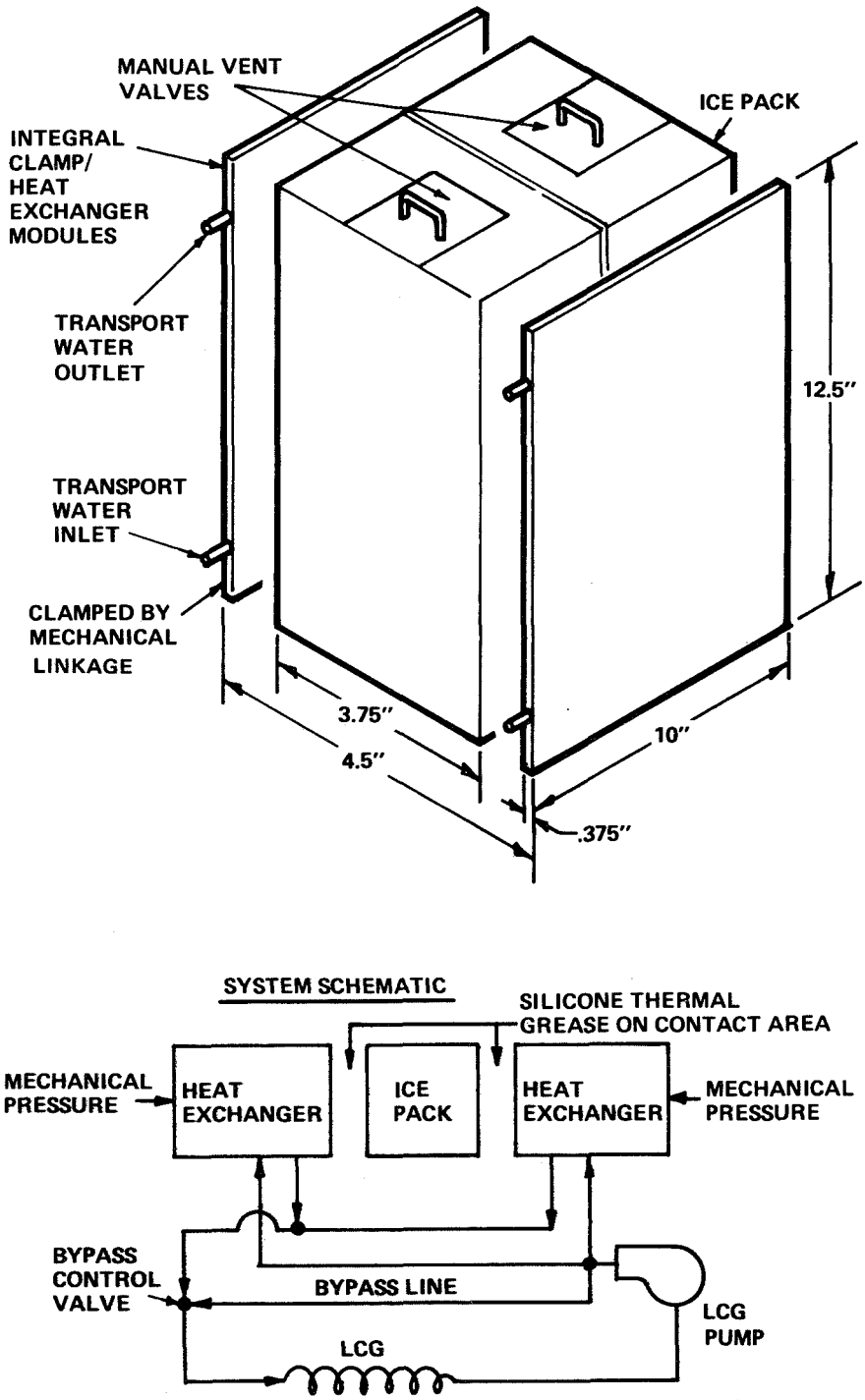

Figure 8.7 *Closed AEPS heat rejection system.*

The heat capacity of each AHS can be increased by subcooling the ice and heating the melted water above 32° F. A total heat sink of 175-200 Btu/lb_m ice can be achieved with only a moderate amount of subcooling. Moderate subcooling was assumed since cooling to very low temperatures increases the regeneration penalty and also complicates the subsystem design because freezing of the LCG water must be prevented.

An investigation of other phase change materials in addition to water was made as part of the study. It was concluded that water is superior to any other substance since it has a high heat capacity in a

temperature range that is suitable for the AEPS system, it is completely nontoxic in all forms, and it is readily available at the base without providing special equipment.

A unique feature of the AHS containing water is the contingency mode of operation. When it is not convenient to change AHS modules, the AHS in use can be converted to an evaporator simply by opening the manual vent valves. The 15 lb_m of water can then be expended by controlled evaporation. This extends the capability of the AHS system to allow a complete 8-hr EVA without the support modules but with a penalty in water expended. This contingency mode adds considerable flexibility to the AHS concept.

A fusible type heat sink is assumed to be integrated into the backpack for use as the top-off system required for the refrigeration system. This allows 1 to 2 hr of nonumbilical operation without expending any water; operation in the expendable mode affords an additional 5 to 6 hr.

The AHS packs are regenerated at the base simply by refreezing the ice. In some environments, such as the lunar night, the AHS packs can be regenerated without any special equipment by exposing them to the exterior environment. However, the total system weight calculated for the AHS system includes a base freezer system with all associated penalties.

The modular and umbilical approaches to AEPS thermal control are illustrated in figure 8.8. This figure shows an AHS chest pack with the insulated storage container integrated into a small MET-type equipment transporter. The umbilical refrigeration system is shown mounted on a small, powered transporter. This system could also be mounted on a man-powered equipment transporter or detached from the transporter for use at a work station. Both of these approaches have considerable promise for a wide range of AEPS missions.

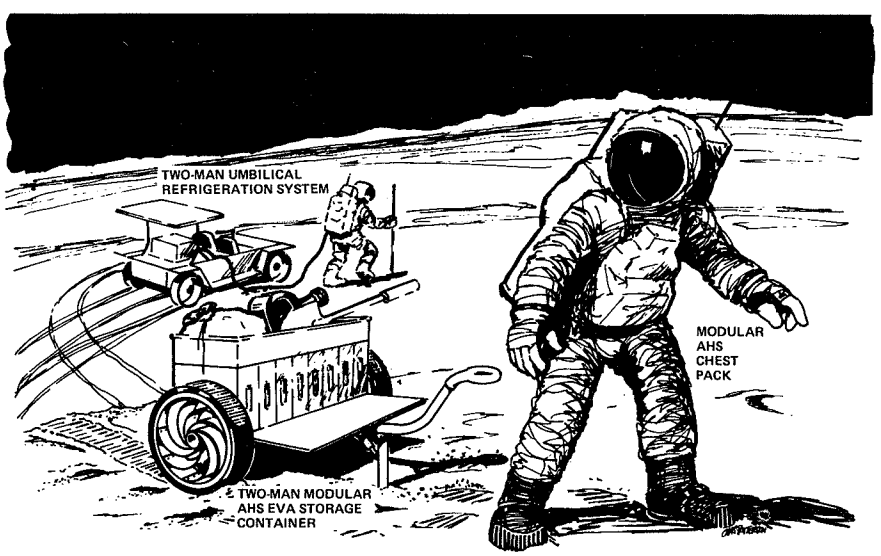

Figure 8.8 *Modular and umbilical approaches to AEPS thermal control.*

The weights and volumes of these promising systems are shown in figure 8.9. The figure shows that the expendable weight of the sublimator imposes an extremely large penalty for any mission requiring numerous EVAs. The weight and volume of the AHS/refrigerator system increases with the number of EVA hours, because of the assumption that 30 percent of the EVA duration is spent off the umbilical, thus requiring the system to expend some water on each EVA. If it were assumed that the umbilical could be used 80 percent of the time, no water would be expended on a nominal

EVA and the AHS/refrigerator would become the lightest weight thermal control system. For the simple AHS system, it was assumed that the expendable mode would be used only during emergencies, and therefore no expendable penalty was assigned to this system. Figure 8.9, which shows weight as a function of individual EVA duration, indicates that the rate-limited refrigeration system size does not change with increased EVA duration while the size of the capacity limited system does.

AEPS TOTAL SYSTEM CONCEPTS

The most promising total system concepts identified by the AEPS study are summarized in table 8.7. The first system, which uses LiOH and a sublimator for CO_2 control and thermal control, respectively, is similar to the PLSS except that it has been enlarged to accommodate an 8-hr EVA sortie and it is assumed to have long-term reuse capability. System 2 retains the LiOH for CO_2 control but uses an AHS heat rejection system; thus the expendables are reduced to about 7 lb_m per EVA. System 3 utilizes a solid amine CO_2 control subsystem with an AHS/refrigerator for thermal control. Systems 4 and 5 offer closed CO_2 control and closed heat rejection.

The total launch weight and volume of these systems as a function of cumulative EVA time are shown in figure 8.10. An expendable system is the lightest for less than about 50-hr of EVA because it does not require base regeneration equipment as the closed systems do. The LiOH/AHS

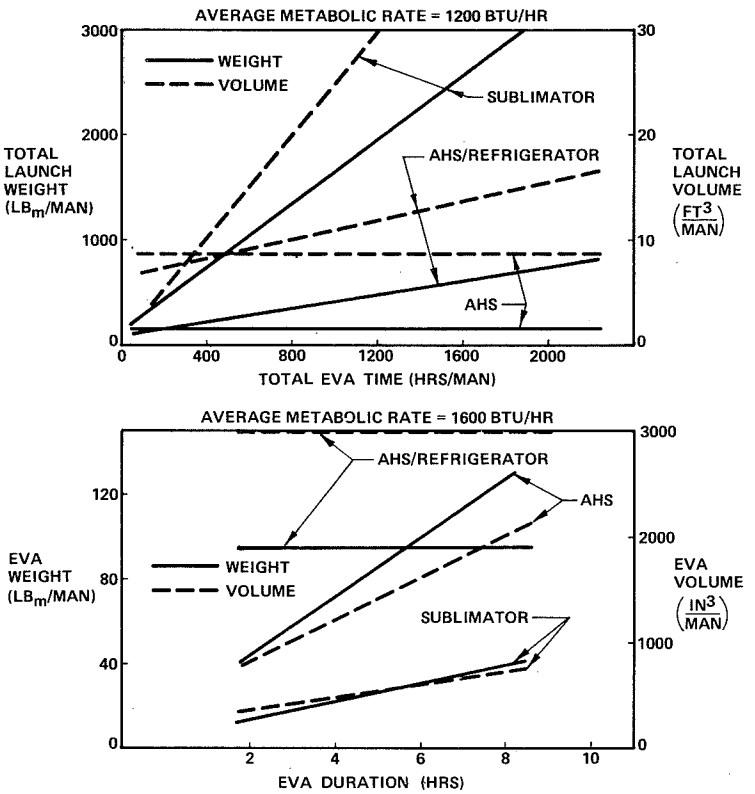

Figure 8.9 *AEPS thermal control system size comparison.*

Table 8.7 *Integrated AEPS systems.*

SYSTEM	CO_2 CONTROL	THERMAL CONTROL
1	LiOH	SUBLIMATOR
2	LiOH	AHS
3	SOLID AMINE	AHS/REFRIGERATOR
4	$Mg(OH)_2$	AHS
5	$Mg(OH)_2$	AHS/REFRIGERATOR

ALL SYSTEMS INCLUDE

- O_2 SUPPLY – HIGH PRESSURE GAS
- POWER SUPPLY – LITHIUM-HALIDE SECONDARY BATTERY
- TRACE CONTAMINANT – ACTIVATED CHARCOAL CONTROL

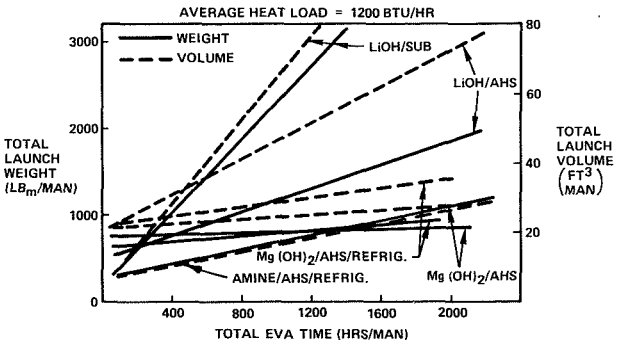

Figure 8.10 *Total launch weight and volume.*

system is shown to be noncompetitive with the closed systems on a total weight basis, regardless of the number of EVA hours. However, this system does offer a considerable weight saving when compared with a fully expendable system, and it would therefore seem to be a logical extension of present capabilities when a moderate number of EVAs are planned.

System 3 is shown to have the lowest total system weight from about 50 to 1300 hr EVA. The pack weight and volume of this system are extremely large and this, along with the inherent reliability problems associated with the cyclic solid amine system, makes this the least desirable of the AEPS total system concepts. The weight and volume savings possible by utilizing closed EVA life support systems for missions requiring more than about 1300 hr EVA is clearly indicated on figure 8.10. This figure can be used both to estimate the weight and volume required for a given number of EVA hours or conversely, to determine the number of EVA hours that can be accomplished within a given weight and volume envelope.

Figure 8.11 shows the influence of EVA duration on the size of the EVA system. Both pack weight and total EVA weight are shown. The pack weight is the actual weight carried per man while the total EVA weight includes the pack and the support system. Figure 8.11 shows that there is no significant weight reduction by reducing the EVA duration to less than 8 hr. The figure also illustrates that a savings in total system weight by reducing expendables can only be accomplished by increasing the EVA weight.

Conceptual system schematics and pack designs for Systems 4 and 5 are shown in figures 8.12 and 8.13, respectively. These designs were produced to demonstrate the feasibility of packaging the candidate regenerable subsystem concepts into a practical pack design. The weight breakdown of the packs is also included.

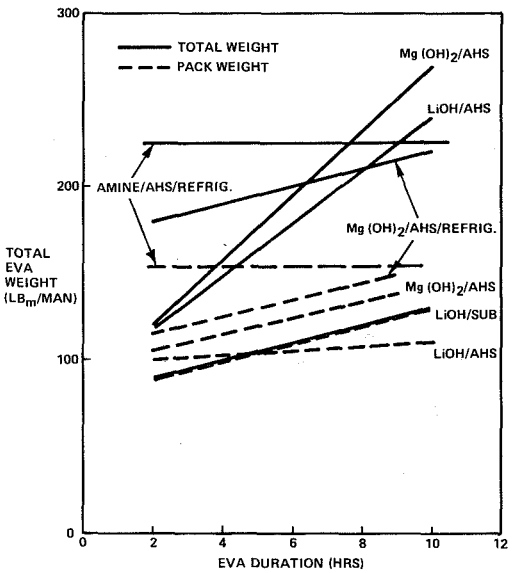

Figure 8.11 *Influence of duration on size of system.*

CONCLUSIONS AND RECOMMENDATIONS

The following conclusions were reached as a result of the AEPS study:

1. Regenerable EVA life support systems are feasible.
2. The most promising approach is to regenerate the EVA systems at the primary base.
3. Regenerable systems offer large total weight savings with an increase in EVA weight.

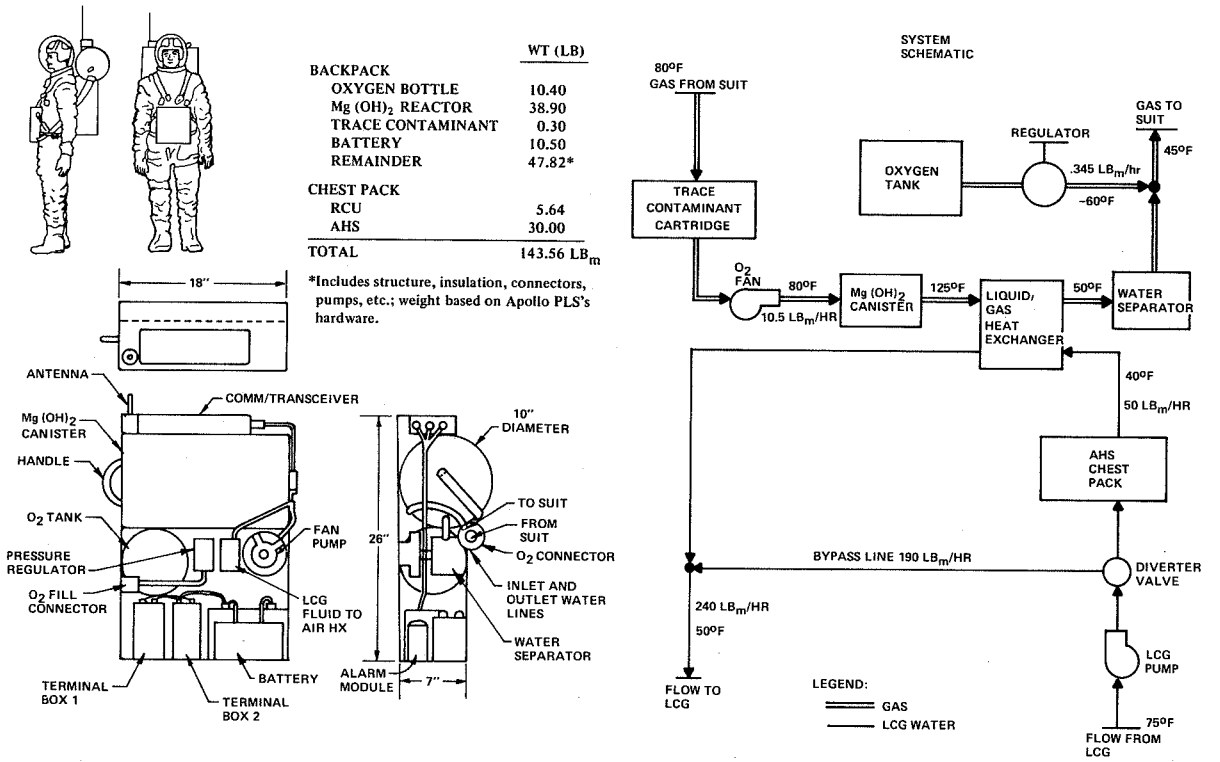

Figure 8.12 *Backpack with* $Mg(OH)_2/CO_2$ *control and chest pack AHS heat rejection system.*

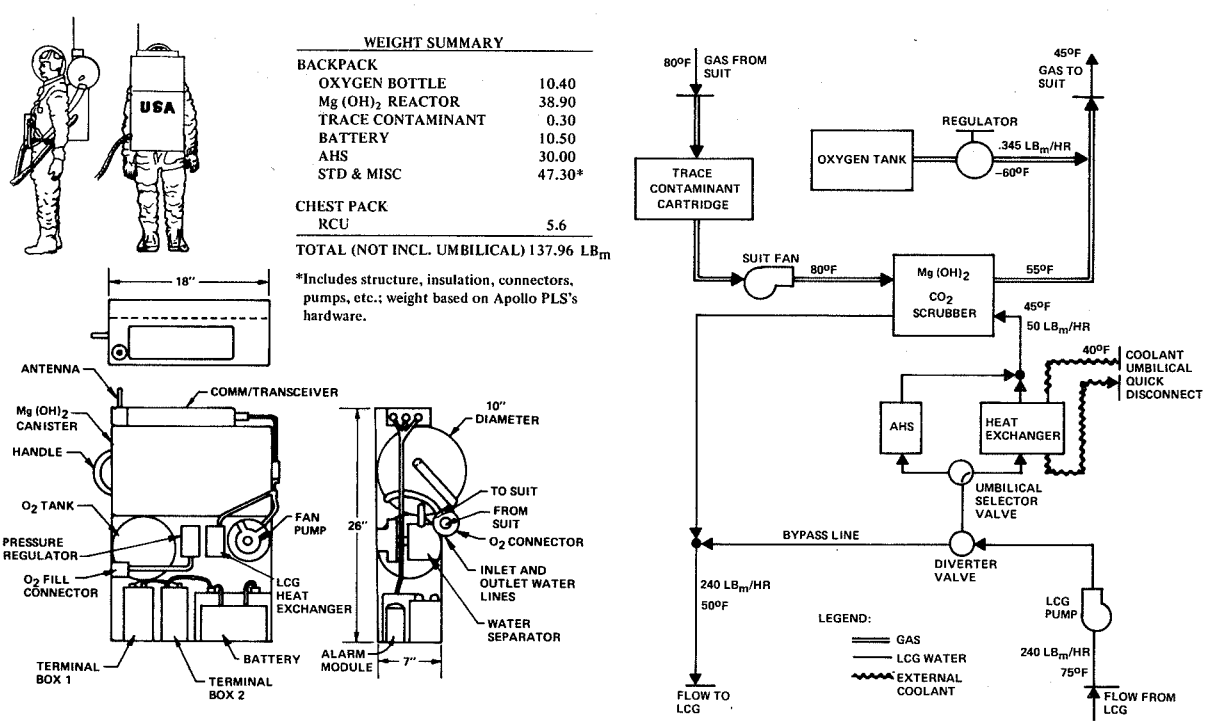

Figure 8.13 *Backpack with* $Mg(OH)_2/CO_2$ *control and AHS/refrigerator heat rejection system.*

Carbon Dioxide Control

The most promising closed CO_2 control concept identified by this study is the solid pellet, $Mg(OH)_2$ system. The liquid KOH system has the potential to have a smaller EVA mass and volume than that of the $Mg(OH)_2$ system, but its feasibility has not been demonstrated and should be investigated further.

Thermal Control

Two promising approaches to closed thermal control were identified. The AHS system uses modular fusible heat sinks, with a contingency evaporative mode, to allow maximum EVA mobility. The AHS/refrigerator top-off subsystem requires an umbilical to minimize expendables, but less EVA time is used to operate the system, since there is no requirement to change modules. Both of these subsystems are thought to be practical solutions to the problem of providing closed heat rejection for an EVA system. The selection of the optimum approach for a particular mission must be made at the detailed mission planning stage.

REFERENCES

1. Anon: Request for Proposal for Advanced Extravehicular Protective System (AEPS). Ames Research Center, RFP A-15999 (AC-30), Feb. 11, 1970.
2. Colombo, G. V.; and Mills, E. S.: Regenerative Separation of Carbon Dioxide via Metallic Oxides, Chemical Engineering Progress Symposium, vol. 62, no. 63, 1966, pp. 89-94.
3. Anon: Preliminary Results from an Operational 90-Day Manned Test of a Regenerative Life Support System. NASA SP-261, 1970.

9 A PORTABLE LIFE SUPPORT SYSTEM FOR USE IN MINES

Sanford S. Zeller
Westinghouse Ocean Research and Engineering Center
Annapolis, Md.

INTRODUCTION

This paper describes the life support system designed, developed, and tested by Westinghouse Electric Corporation for the Bureau of Mines as a part of contract H0101262. The prototype auxiliary survival chamber for use in mines consists of a mobile, collapsible, modular quonset hut-shaped shelter (fig. 9.1) containing atmosphere conditioning and monitoring equipment, communications and location equipment, battery-powered lights, food and water supplies, and a chemical toilet. The principal features of the system are simplicity, reliability, and shelter from toxic atmosphere and explosion.

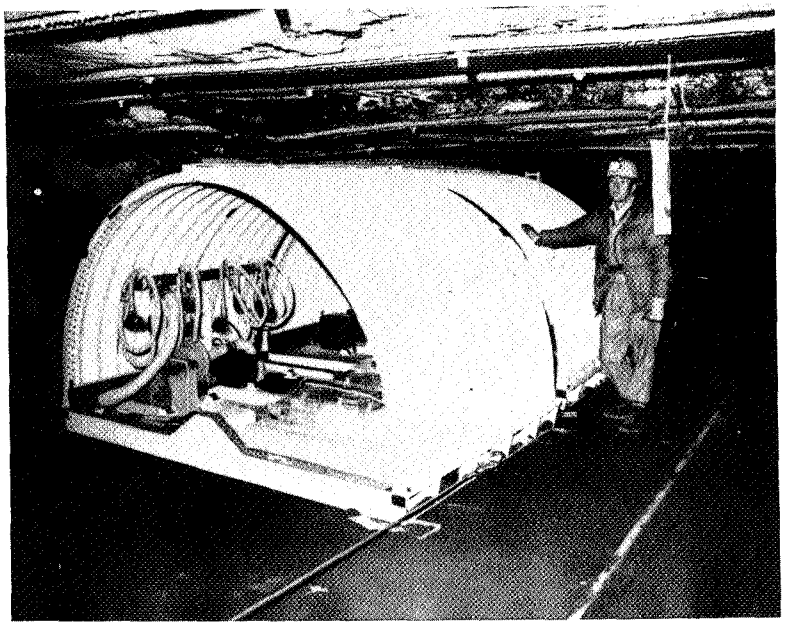

Figure 9.1 *Auxiliary survival chamber.*

The design and development of this system were undertaken to fill the need for protecting miners from blast, rockfall, flash fire and other conditions resulting from mine fires and explosions. This system is a potential improvement over barricading after a disaster.

The basic system requirement is life support for 15 miners for 14 days. Other requirements include mobility (to allow the system to follow the mine working faces), low production cost, long service life, short set-up and maintenance times, simplicity of operation, little training requirement, and tamper-proof supplies.

Chamber Structure

The chamber structure is made entirely of steel. The roof, divided in half at the midline with pinned connections, is made of corrugated steel 0.1 in. thick. Hinges connect the roof to the reinforced floor. The 9×6-ft floor of each module is a flat plate 1/4-in. thick, reinforced internally by 6×6-in. I-beams, 16 in. on centers. The chamber end walls are corrugated and reinforced externally by four vertical posts, four struts, and a reinforced platform bolted to the floor of the mine. Each of the

end walls has a ship's hatch, which can be opened or closed tightly from either side, with a 4-in. diameter view port.

Each module and end bulkhead has mounts for two wheels with stub axles and a towing fitting. For transport, the modules are unpinned at the roof centerline and folded to an overall height of 42 in. The end bulkheads also fold down to a height of 28 in. This prototype chamber has been tested for habitability, operability, and explosion resistance in a Bureau of Mines test mine.

ATMOSPHERIC CONDITIONING UNIT

Two atmospheric conditioning units (ACU) are provided for each survival chamber (fig. 9.2). These units chemically remove carbon monoxide and carbon dioxide from the chamber air, supply oxygen, provide a facemask breathing mode, and circulate the air within the chamber by means of a blower. The ACU was designed for the following performance parameters:

1. Inlet carbon monoxide concentration of 1000 ppm.
2. Inlet carbon dioxide concentration of 1.0 percent.
3. Inlet air flow of at least 15 SCFM.
4. Inlet humidity of 80 percent.
5. Inlet temperature of 50° to 80° F.
6. Outlet carbon monoxide concentration of less than 100 ppm.[1]
7. Outlet carbon dioxide concentration of less than 0.1 percent.
8. Outlet temperature of less than 100° F.
9. Control of the chamber seal leakage.

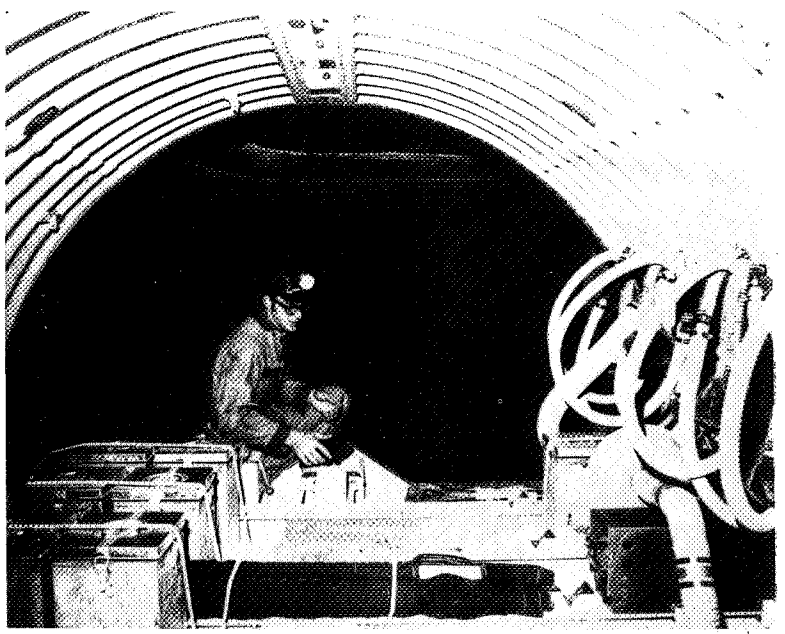

Figure 9.2 *Atmospheric conditioning unit.*

The design constraints included:

1. The blower must be manually powered.
2. An operational facemask breathing mode must be available.
3. The ACU must fit into the auxiliary survival chamber when the chamber is in the folded-down transportation position.
4. The oxygen supply will be connected to the unit, to increase the oxygen concentration of the air flow during the facemask breathing mode.
5. Only the correct assembly will be possible.
6. The assembly must be rapid even in low light levels.

[1]TLV is 50 ppm, but ACU design is based on 100 ppm.

7. One unit must be capable of removing all the carbon dioxide produced by 15 men, in case one of the two units should fail.
8. The unit will have sufficient flexibility to be used in other applications for various numbers of users.

The detailed design and selection of the ACU components is discussed below.

Oxygen Generation and Measurement

A tradeoff study was made to select a suitable oxygen supply. High-pressure storage of oxygen was eliminated by considerations of portability, reliability, and safety factors. Potassium superoxide was eliminated because the required development effort was precluded by program constraints. The final selection was a sodium chlorate oxygen-generating candle. The size of each candle was a compromise between the miners' oxygen requirement and constraints of storage space, handling, overpressure relief, and cylindrical shape. The result is a candle that generates 70 cu ft of oxygen in approximately 40 min.

The total quantity of candles was based on an oxygen consumption rate of 1.78 lb/man-day for 210 man-days plus 46 lb of oxygen for the oxidation of carbon monoxide. The concentration of oxygen in the surrounding mine air, which leaks into the chamber, affects the quantity of candles required; for the worst case of no oxygen in the mine, 14 additional oxygen candles are required. The candle is connected to the ACU so that the oxygen concentration of the airflow is increased by about 10 percent for facemask use. A candle holder, primarily a heat sink, is supplied to prevent the candle wall temperatures from reaching the ignition temperature of coal dust.

The oxygen-generating candles were bench-tested by the vendor and at two Westinghouse facilities. Analyses demonstrated that the effluent gases contained oxygen in sufficient purity and quantity, and were released at adequate rates and temperatures. Candle operation was found to require little training. The candle holder successfully kept the candle wall temperatures below the ignition temperature of coal dust during all bench and manned tests.

The effluent gas from the oxygen-generating candles was analyzed by spectrophotometers to assure that the composition was within the requirements of metabolic oxygen supplies. An internal flow restriction in the candle filter material will necessitate additional design effort before these candles can be put into general use.

The oxygen concentration meter was calibrated at 21 percent concentration and bench-tested with a gas of 98 percent oxygen. This meter was a small, portable fuel-cell type of oxygen analyzer. Manned tests indicated that the analyzer must be calibrated and used in the horizontal position to maintain the required 2 percent accuracy. This restriction on its operation was not considered too severe, so the analyzer was used in the shelter.

CARBON DIOXIDE ABSORPTION AND MEASUREMENT

The carbon-dioxide absorption method selected for use in the chamber atmospheric conditioning unit had to meet the following criteria: capacity for 210 man-days, short assembly and disassembly time, low cost, good portability in a mine, minimum development, and high safety and reliability.

There are three principal methods of carbon dioxide removal: chemical absorption, cryogenic condensation, and osmotic diffusion (refs. 1-6). A tradeoff study of available methods indicated that chemical absorption by means of baralyme in vertical, axial-flow, refillable canisters was the best means of absorbing the carbon dioxide produced by 15 men in 14 days in the survival chamber.

In the tradeoff analysis of available methods, cryogenic condensation and osmotic diffusion were summarily rejected for reasons of cost, portability, and safety. The method of chemical absorption

remained. Available chemical reactions utilized potassium superoxide, baralyme, sodasorb, and lithium hydroxide. Potassium superoxide was eliminated because of cost and required development. Baralyme was selected over sodasorb for final consideration because of lower dusting, higher efficiency, lower corrosion risk, and lower cost. Baralyme was selected over lithium hydroxide because of lower cost. To preclude the possibility of channelling in the canister, a vertical, axial-flow canister with laterial baffles was designed and developed.

The size of each canister is based on a design duration of 8 hr, manual handling considerations, and the available storage space in the chamber. The rate of carbon dioxide removal is based on generation of 1.26 lb of CO_2/hr from 15 men, 0.12 lb CO_2/hr from the carbon monoxide removal canister, and 0.10 lb CO_2/hr from the outside air drawn in through the leakage control hoses. The outside concentration of carbon dioxide is assumed to be a maximum of 10 percent. Forty-two baralyme canisters are required for the 14-day mission duration.

The carbon dioxide removal canister was bench-tested successfully, removing all but 0.06 percent carbon dioxide from an inlet air flow of 17 SCFM containing 1.0 percent calibrated carbon dioxide gas for 8 hr. The manned tests indicated that the canister required an initial temperature of at least 40° F to remove 90 percent of the incoming carbon dioxide. This requirement was not considered to be a problem for the expected mine storage conditions. Actual testing with 15 men for 2 days in a Bureau of Mines test mine demonstrated the operability and performance of the carbon dioxide removal canister.

The sampling pump and test tubes for measuring carbon monoxide and carbon dioxide concentrations were bench tested with certified calibration gases, giving accuracies of within ± 0.1 percent carbon dioxide and ± 25 ppm carbon monoxide. The manned tests revealed that simplification of operation was required for unskilled use of the instrument. This difficulty was overcome merely by changes in the packaging and operating instructions; after one reading of these instructions the test subjects had no trouble operating this instrument.

CARBON MONOXIDE REMOVAL CANISTER DEVELOPMENT

The available means of removing carbon monoxide from an air stream are absorption and catalytic oxidation. The method of carbon monoxide removal by absorption on solid molybdemum trioxide or tungsten is efficient at high carbon monoxide concentrations, but its performance is not known at the low concentrations expected in the chamber. This absorption method was rejected because of the requirement for basic research on its performance at the design conditions. The method of catalytic oxidation using hopcalite was acceptable in performance and operating requirements. Hopcalite is a coprecipitated mixture of manganese dioxide and cupric oxide with small percentages of cobalt and silver oxides added. It has the ability to catalyze the oxidation of carbon monoxide at mine temperatures. The hopcalite catalysis is used in portable respirators, high-pressure air filters, and submersible vehicle air conditioners.

Since hopcalite is poisoned by water vapor and by traces of antimony (ref. 1), these chemicals were eliminated from the materials, finishes, and assembly of the canister, and provisions were included for removal of water vapor during operation. Other design constraints of overall dimensions and manual operation were evaluated and incorporated into the canister design. Preliminary test results indicated a need for increased efficiency, so the original design was revised to include a hopcalite bed depth of 2.5 in. and a diffusing baffle, producing a canister of sufficient efficiency and duration.

In air conditioning systems for submersibles, carbon monoxide removal is combined with combustion of other contaminants. In high-pressure air filters, carbon monoxide removal is

combined with particle and oil mist filtration. Since no applicable standard design existed, the carbon monoxide removal canister for the shelter required a new filter bed design.

The canister performance requirements were (1) removal of all but 100 ppm of carbon monoxide from an inlet concentration of 0.1 percent (1000 ppm) carbon, and (2) a duration of approximately 4 hr. The design constraints were:

1. No antimony can be used in the materials, finishes, construction, or assembly of the canister.
2. The canister must be capable of being installed, removed, and handled entirely by hand.
3. The canister must not cause or become a fire hazard.
4. The canister must be refillable.
5. The design must be cost effective.
6. One overall dimension must be less than 7 in. and the other dimensions must be small enough to fit in the available shelter storage spaces.

The design conditions were:

1. An air flow rate of about 17 SCFM.
2. A relative humidity of the air flow of 80 percent.
3. An inlet carbon monoxide concentration of 1000 ppm.
4. Vibration and shock from transporation and blast.
5. Long-term storage at 60° F and 80 percent relative humidity.

Other desirable features were:

1. Hardware, finishes, and assembly methods should be similar or identical to the carbon dioxide removal canister to reduce costs.
2. The canister should have a size or shape different from the carbon dioxide removal canister to eliminate errors in operation in darkness.

The inlet carbon monoxide concentration is based on an assumed 10 cu ft of 10 percent carbon monoxide mine air entering the shelter with the miners, giving an initial concentration of 800 ppm.

The canister housing was designed to overall dimensions of approximately 6-3/4 by 9 by 13 in. The construction was of zinc-plated sheet steel, using spotwelded and soldered seams, reinforced points of wear, a latched, spring-loaded cover with gasket seal, "O" ring seals at both ports, and a spring-loaded filter bed retained by two metal screens. A wall baffle was included to prevent channeling of flow along the walls. All solder used contained no antimony.

The canister filter bed consisted of a metal top screen, a 1-1/2 in. thick layer of activated charcoal, a 5-1/2 in. thick layer of silica gel, a 1-1/2 in. thick layer of molecular sieve, a 1-in. thick layer of hopcalite, and a metal bottom screen. The flow direction was axially downward.

The charcoal layer was intended to absorb hydrocarbons and prevent their possible reaction with hydrogen, catalyzed by the hopcalite. Since neither hydrocarbons nor hydrogen will be present in the chamber in the high concentration required for a reaction, the charcoal layer was judged to be an unnecessary precaution in the revised canister design. The silica gel and molecular sieve layers are intended to absorb water vapor at high and low relative humidities, respectively. The quantities of these components determine the duration of the canister, since hopcalite is not used up in its catalysis of carbon monoxide. When the silica gel and molecular sieve layers are saturated with water vapor, the excess water vapor that passes through them poisons the hopcalite, resulting in a slow increase of carbon monoxide concentration at the outlet. The rate of this increase depends on the amount of time the airflow is in the hopcalite layer.

The hopcalite layer must be thick enough to complete the catalytic oxidation of carbon monoxide. The reaction requires close contact for a period of time between the gas stream and the hopcalite. To achieve this contact time existing hopcalite beds from 1/2 to 5 in. thick, maintain ambient temperatures to 650° F, and permit low flow speeds.

The results of the first bench test indicated low efficiency of carbon monoxide removal. In the revised design, the charcoal layer was removed and more hopcalite added to make a 2-1/2 in. thick bed. This revision also incorporated a baffle plate at the canister inlet to distribute the air flow. Test data showed that this design efficiently removed carbon monoxide at nearly the design conditions for exactly 6 hr. The data show that the breakthrough occurred slowly as humidity attacked the hopcalite bed.

Two atmospheric conditioning units operating simultaneously at 17 SCFM each would reduce an initial chamber concentration of carbon monoxide of 3 percent to 0.01 percent within 4 hr in the shelter volume of 1260 cu ft. Figure 9.3 shows the time required for removal of unsafe carbon monoxide and the formula used for the calculations, using 0.617 air change per hour.

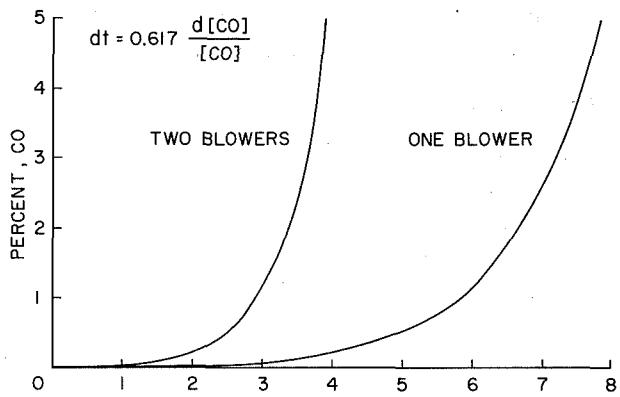

Figure 9.3 *Time required to remove unsafe carbon monoxide.*

The intermittent supply of oxygen gas from the chlorate candles reused shelter seal leakage, which was corrected by means of a 0.375-in. inner diameter leakage control hose leading through the chamber wall to a fitting at the inlet of the carbon monoxide removal canister in each atmospheric conditioning unit. When the chamber seals are properly installed the leakage control hoses provide lower resistance leakage paths than do the seals, so the inward flow of mine gas is immediately scrubbed. When the ACUs are in operation, the hoses will act as suction lines, maintaining a slight positive pressure and outward leakage through the seals.

Outward leakage through the hoses during candle firing results in the loss of about 12 cu ft of oxygen per firing. Check valves in the leakage control hoses (or no hoses) would result in the loss of about 10 cu ft of oxygen through the seals as the internal pressure rises. The 2 cu ft difference in oxygen loss is small compared to the 72 cu ft of oxygen produced by each of the candles. Also, it was decided that the risk of plugging, the added maintenance, and the difficulty of clearing any plug outweighed the possible oxygen savings from a check valve, so none was included in the hoses.

Under normal conditions of expected leak rates through both the seals and the leakage control hoses, activity levels, and gas contamination, the ACUs must operate about 51 min/hr to maintain the carbon dioxide and carbon monoxide concentrations below their design values of 1.0 percent and 100 ppm, respectively. Continuous operation is required when the gases exceed these levels. Because carbon monoxide concentration in a mine after a blast normally decreases with time, a design duration of 5 days of carbon monoxide removal was selected for the prototype shelter. Thus, the prototype survival chamber is equipped with 28 of the 4.5-hr carbon monoxide removal canisters.

VENTILATION COMPONENTS

The duct, hoses, manifold, and facemasks of each ACU are fireproof, easily attached and repaired, and spaced to avoid overcrowding. The blower outlet hose is disconnected from the distribution

manifold and is used as a ventilation duct in normal operation. The blower is a hand-cranked fallout shelter ventilator requiring about 0.10 hp. This gear-driven centrifugal blower is operated at 40 rpm by one man at a time for 30 min.

The other components of the ACU, such as the flexible hoses, facemask fittings, mountings, duct, and blower, performed well in bench tests and manned tests with the exception that the hand-cranked blower, which was developed for fallout shelter use, developed a seized bushing in its gear box after 4 hr of use. This bushing and its mounting were remanufactured by Westinghouse. After this modification, the blower was used in the chamber. Subjects had some difficulty in rapidly donning the facemasks, but this was corrected by preadjusting the straps on all facemasks.

TEMPERATURE AND HEAT BALANCE

The temperature and humidity inside the chamber are primary factors in determining whether the chamber is suitable for human habitation over long periods of time. A heat transfer analysis showed that, for a mine temperature range of 50° to 65° F, the interior temperature range of 60° to 81° F and the interior relative humidity range of 85 to 100 percent will be well within the limits of human tolerance. These calculations were verified in an 8-hr manned test and a 2-day field demonstration.

The nearly stagnant layers of air near the chamber walls act as insulation between the inhabitants and the surrounding mine walls, so the temperature inside the chamber is warmer than in the surrounding mine. The interrelating effects of temperature, humidity, and confined space on human beings were analyzed. By analyzing the heat sources and heat transmission methods, an estimate of 81° F dry bulb chamber temperature was made for 60° F dry bulb ambient. By estimating moisture evaporation and absorption rates, a relative humidity of 100 percent was calculated. By reference to experimental data including volume and area requirements, this environment was shown not to represent a stressful condition, so that no heat exchanger was required.

The chamber area of 21.6 sq ft per man is above the values proven acceptable for 15-day periods. The 84 cu ft volume per man in the chamber is above the Office of Civil Defense minimum recommendation of 80 cu ft (ref. 7).

CONSUMABLE SUPPLIES AND WASTE DISPOSAL

The food supply is a military food ration, MIL-F-43231, Food Packet, Survival, General Purpose. This ration was chosen primarily for its packaging density, packaging quality, and low desirability: It is not as much an object of pilferage as many other food supplies are. The supply provides two 12-oz cans per man-day, containing 1740 cal. These cans are packaged in boxes of 24, which fit into the floor of the survival chamber.

The water supply is 2 qt per man-day of chlorinated tapwater, in 5-1/4 gal plastic jerricans. These containers were chosen to fit into the floor of the chamber. The food ration cans serve as drinking cups.

The chemical toilet uses replaceable plastic bags as liners. All solid and liquid wastes are disposed of in this way, except for sharp metal and glass debris, which are packed in empty food boxes. The half-gallon of mouthwash provided is used as a bacteriostat and deodorant in the toilet after use. One plastic liner is used as a vapor seal across the top of the container when the toilet is not in use. The liners are changed at 8-hr intervals or when half full, whichever occurs first.

These supplies were all rated as acceptable for survival use by the manned test subjects after 8- and 48-hr tests. Two of the foods supplied were objectionable to some subjects because of their taste. This result agrees with data from the U.S. Army Natick Laboratories ration design specialist, Mrs. Mary V. Klicka, who helped greatly in the food ration selection.

CONCLUSIONS

1. The portable life support system described in this paper represents a potential increase in the probability of survival for miners who are trapped underground by a fire or explosion.
2. The habitability and life support capability of the prototype shelter have proved excellent.
3. Development of survival chamber life support systems for wide use in coal mines is definitely within the capabilities of current technology.

REFERENCES

1. Schaffer, A.: Analytical Methods for Space Vehicle Atmospheric Control Processes. SS-572, AiResearch Mfg. Co., ASD-TR-61-162 Los Angeles, Dec. 1961.
2. Anon: Trade-off Study and Conceptual Designs of Regenerative Advanced Integrated Life Support Systems. NASA CR-1458, 1970.
3. Anon: Mine Rescue and Survival. NAE Final Report, March, 1970.
4. Anon: Specifications and Costs of a Standardized Series of Fallout Shelters. USNRDL-TR-366, San Francisco, Oct. 1959.
5. Anon: Experimental Evaluation of Environmental Control Systems for Closed Shelters. MRD Division of General American Transportation Corporation, MRD 1242-2530, Washington, D.C., July, 1964.
6. Keating, D. A.: Baralyme and Molecular Seive Passive Air Regeneration Studies for Manned Sealed Environments. MRL-TDR-62-59, Wright-Patterson AFB, Ohio, May, 1962.
7. Anon: Family Shelters for Protection against Radioactive Fallout. FCDA Technical Bulletin S-3, Washington, D.C., May 1958.

10 SEMICLOSED-CIRCUIT ATMOSPHERE CONTROL IN A PORTABLE RECOMPRESSION CHAMBER*

Peter S. Riegel and Don W. Caudy
BATTELLE
Columbus Laboratories

INTRODUCTION

One of the better known hazards of diving is decompression sickness, or "the bends." As the diver goes deeper, his respiratory system and bloodstream are exposed to increased pressures of the gas he is breathing, commonly oxygen, helium, and nitrogen. In dives of extended duration, these gases become dissolved in his tissues. As the diver ascends gradually, the excess nitrogen or helium escapes through the lungs, while the oxygen is absorbed by the body. Rapid ascent may allow the inert gases to form bubbles in the tissues and bloodstream, blocking circulation and causing tissues to swell.

The probability of bubble formation increases with depth and duration of the dive and the speed of ascent. The severity of effect depends on the area of the body where the bubbles are formed. Pain, dizziness, respiratory difficulty, nervous disorders, or death may result.

Another serious hazard to the diver is air embolism. If a diver should unwittingly hold his breath during ascent, the expanding gas may overinflate his lungs, causing leakage of air bubbles into his chest cavity or bloodstream and possibly lead to blockage of blood vessels in the heart or brain. Convulsion, brain damage, or death may result.

Since these afflictions are consequences of gas bubbles in the diver's body, treatment is directed at removing the bubbles or reducing their size. This is commonly done by recompressing the diver in a chamber that reduces bubble size and promotes rediffusion of the gas into the tissues and bloodstream. Once relief of symptoms is reached, decompression may begin at a low rate to prevent recurrence of decompression sickness.

The main drawback to recompression treatment is that a pressure chamber is required, and generally it is not located at the site of the diving accident. Often a semiconscious, suffering man must be transported by the fastest means to reach the nearest recompression facility, with the probability of permanent damage increasing with every minute he remains untreated.

To provide means of protecting divers in remote worksites, some small, portable recompression chambers have been developed and marketed. These chambers are of various forms: some are cylindrical, some tapered, some telescoping. Entry may be head first or feet first. All chambers of this type are sized for one man and are intended to give immediate treatment to the sufferer, wherever he may be. Once the patient is under pressure, the chamber may be transported to the nearest recompression facility for subsequent treatment of the occupant. During transportation, the atmosphere in the chamber is kept pure by continuous ventilation with air, which supplies oxygen and removes unwanted carbon dioxide. During ventilation large flows of air are required to dilute and remove chamber carbon dioxide, but little of the oxygen content is used.

---

*Chamber development is being funded through Office of Naval Research Contract No. N00014-70-C-0072.

Because of the overlap among the fields of mechanical engineering, medicine, and air conditioning, units familiar to workers in those areas are used here. For example, pressure is expressed in feet of seawater, atmospheres absolute (ATA), lb/sq in., lb/sq ft, and in. of water, depending on the area of use. Man consumes and produces gasses at rates measured in standard liters per minute (SLPM) by medical people.

Gas flows, measured at standard conditions (essentially at atmospheric pressure, and at 0°, 68°, or 70° F, depending on the standard employed) are preceded by an "S"; if measured at flowing conditions, flows are preceded by an "A"—for example, at 6 ATA pressure, 1 ACFM = 6 SCFM.

A typical chamber occupant will consume about 0.24 SLPM oxygen and produce 0.20 SLPM carbon dioxide. Partial pressure of carbon dioxide could be maintained at less than 0.005 ATA, a safe level, by ventilation at a rate of 2 ACFM. However, to produce a flow of 2 ACFM at a typical treatment depth of 165 ft requires a flow of 12 SCFM of air. A typical commercial air flask contains about 240 cu ft, or enough for less than 20 min operation. Efficient treatment and transportation would require that enough of these heavy, cumbersome bottles accompany the chamber to provide air for the entire duration of the trip. In some cases, this is difficult or impossible, either through weight or size limitations of the carrier, or because not enough air is available.

The problem of efficient gas usage has been effectively solved in diving apparatus through use of recirculation systems, such as semiclosed-circuit and closed-circuit rebreathers. The same principles can be applied to operation of a recompression chamber.

In keeping with the need for a simple, foolproof system, the use of the oxygen sensors, batteries, and associated electronic circuits used in closed-circuit systems was rejected. To be effective, the system must be capable of surviving a long storage time and be quickly ready for use in remote locations with a readily obtained gas supply. Air was chosen as the ventilation gas because of its availability and suitable oxygen content. A semiclosed-circuit ventilation system offers the utmost in simplicity, reliability, and conservation of gas supply. Gas is admitted and circulated with little complexity, and maintenance and upkeep requirements are minimal.

DESIGN PHILOSOPHY

In creating a life support system, a consistent philosophy of design is necessary to keep unnecessary superfluities from creeping in as well as to assure that all necessary functions are present. The function of the chamber is to permit rapid insertion and recompression of an injured diver, and transportation to a suitable treatment facility where he can be removed to a larger chamber and treated by medical personnel.

Lightweight construction is important, as the system will sometimes have to be moved by hand. Compactness is desirable so that the system may be loaded into varied forms of transport. The equipment should require a minimum of operator training (instruction should be possible within a few minutes) and operation should be simple. Ability to perform well after long storage periods is desirable. Reliance on external power systems should be avoided for they may not be available in the field.

The system as designed carries no frills. It is simply a container for an injured man, and preservation of his life is the only consideration. Discomfort should certainly be avoided, but so should complexity. In our approach, we have tried to keep the system pared down to the minimum required to do the job effectively.

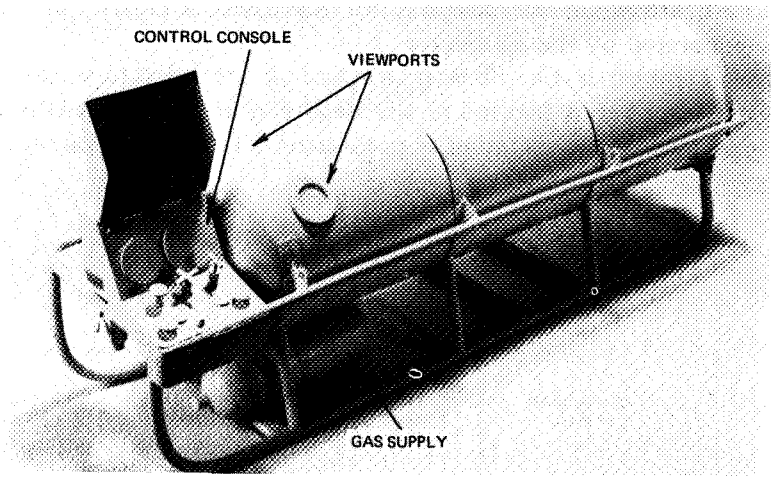

Figure 10.1 *Model of recompression chamber, front side.*

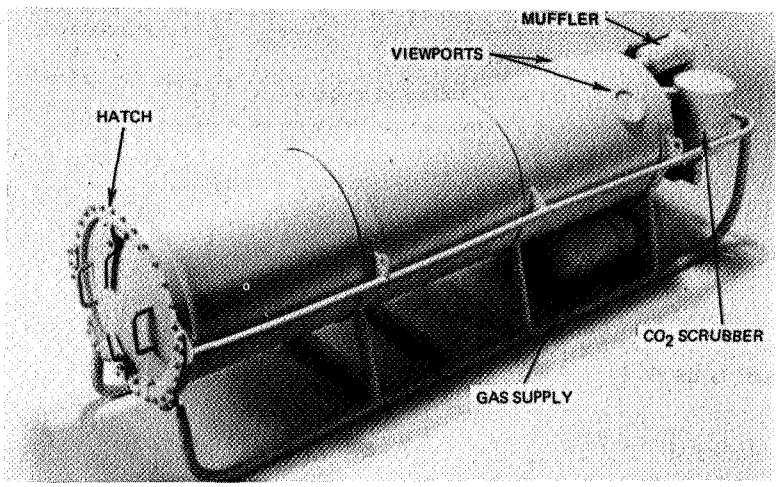

Figure 10.2 *Model of recompression chamber, back side.*

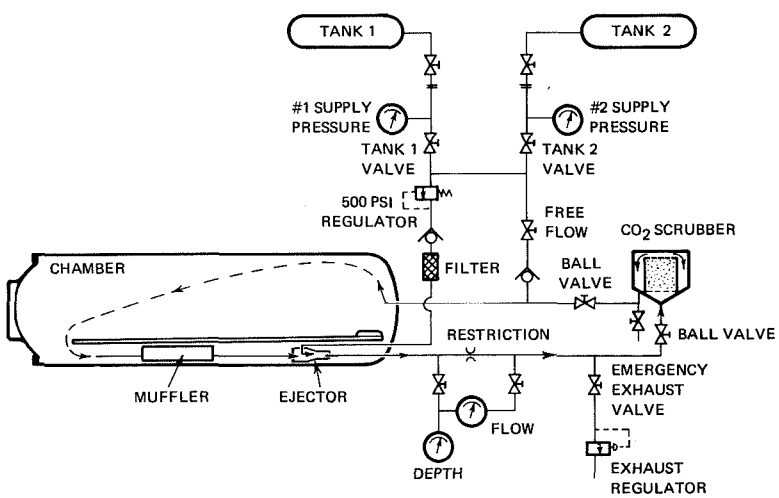

Figure 10.3 *System schematic.*

CHAMBER DESCRIPTION

The portable recompression chamber and its associated equipment is shown in model form in figures 10.1 and 10.2, and schematically in figure 10.3. The pressure shell is made of 5/32-in. rolled and welded 5083 aluminum with a semielliptical self-energizing hatch. The basic shape is a 22-in-diam cylinder with an inside length of about 84 in. Total system volume, including piping and canister, is about 18.3 cu ft. Pressure capability permits treatment to depths of 165 ft of seawater (6 ATA). Two 4-in. viewports permit observation of the patient.

To enter the chamber, the patient is placed on a stretcher, strapped down, and slid in head first. The hatch is closed and dogged, and the system is ready for pressurization. Water and food containers are placed within the patient's reach to keep him supplied for the duration of his stay. No medical lock is provided.

The chamber may be operated in two modes—open circuit or semiclosed circuit. In locations where either a large compressed air supply in tanks or a suitable compressor is available, open-circuit operation will be employed. During transportation and in places where limited compressed air in tanks is available, semiclosed-circuit operation will be used.

A chamber communications system permits two-way conversation between patient and attendant. The attendant must

push a button to talk; the patient can be heard when the button is not depressed. A muffler in the gas circulation system silences the noise generated by the air ejector.

A control console is located at the head end of the chamber. It contains all control valves, gages, and communications equipment. The gas scrubber is located at the head end also, with isolation valves provided to permit changing reagents while the chamber is pressurized. The entire system is mounted on skids to facilitate handling.

Total system weight is 330 lb.

SYSTEM ANALYSIS

Ventilation requirements were determined by means of a system analysis as follows (fig. 10.4). Note that the man is shown outside the system boundary. In fact, he is inside, of course, but in this analysis he serves only as a sink that removes oxygen from the system and adds carbon dioxide to the system. Similarly, the carbon dioxide absorber, although enclosed in the actual system, serves as a sink that removes carbon dioxide from the theoretical system.

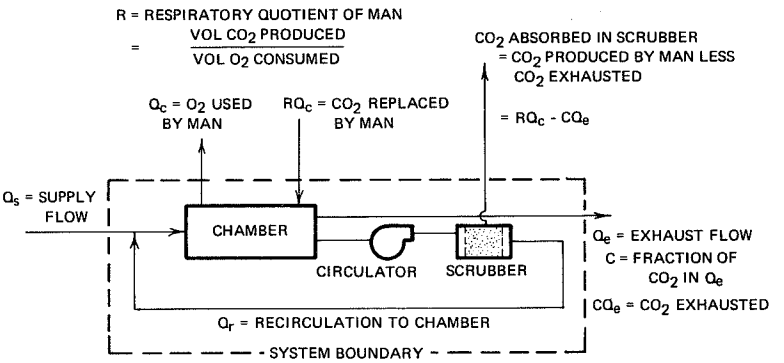

Figure 10.4 *Simplified system for analysis.*

In this discussion, the following notation is used.

- t = time, min.
- X = percent oxygen in chamber, decimal
- X_O = value of X at $t = 0$
- C = percent carbon dioxide in chamber, decimal
- Q_S = supply flow, SCFM
- Q_e = exhaust flow, SCFM
- Q_C = rate of oxygen consumption, SCFM, typically Q_3 = 0.24 SLPM = 0.0085 SCFM for man resting
- Q_r = recirculation flow, SCFM
- G = percent oxygen in supply gas (G = 0.21 for air)
- R = respiratory quotient, ratio carbon dioxide produced to oxygen consumed by occupant, typically R = 0.8 for man resting
- P = chamber pressure, ATA
- V = chamber volume, cu ft

An oxygen balance of the semiclosed-circuit recompression chamber comprises

System oxygen content, cu ft	$= PVX$
Oxygen flowing into system, SCFM	$= Q_S G$
Oxygen consumed by man, SCFM	$= Q_C$
Oxygen exhausted from systems, SCFM	$= Q_e X$

The rate of change of system oxygen content may be described by

$$\frac{d}{dt}(PVX) = Q_sG - Q_eX - Q_c \tag{1}$$

or, since P and V are constant at a given depth,

$$\frac{dX}{dt} + \left(\frac{Q_e}{PV}\right) X = \frac{Q_sG - Q_c}{PV} \tag{2}$$

Equation (2) may be solved by conventional methods, and after substitution of boundary conditions will yield

$$X = \underbrace{\left(X_O - \frac{B}{A}\right) e^{-At}}_{\text{transient}} + \underbrace{\frac{B}{A}}_{\text{steady state}} \tag{3}$$

where

$$A = \frac{Q_e}{PV} \tag{4}$$

$$B = \frac{Q_sG - Q_c}{PV} \tag{5}$$

Equation (3) will be useful, but not until the value of the exhaust flow Q_e, which is part of constant "A," is found.

To determine the value of Q_e, a total system flow balance must be taken. Since P is constant, the sum of all the flows entering and leaving the system will be zero, or

$$\begin{array}{ccccccccc} \text{Supply} & - & \text{O}_2 \text{ used} & + & \text{CO}_2 \text{ produced} & - & \text{Gas} & - & \text{CO}_2 \text{ absorbed} \\ \text{flow} & & \text{by man} & & \text{by man} & & \text{exhausted} & & \text{in scrubber} \end{array} = 0$$

or

$$Q_s - Q_c + RQ_c - Q_e - \left(RQ_c - CQ_e\right) = 0 \tag{6}$$

or

$$Q_e = \frac{Q_s - Q_c}{1 - C} \tag{7}$$

The value of C must now be found. The total flow of carbon dioxide through the chamber is that produced by the diver. The total flow of gas is equal to that entering the chamber, less the oxygen consumed, plus the carbon dioxide produced by the diver. The value of C will be the ratio of these two flows, or

$$C = \frac{RQ_c}{Q_s + Q_r - Q_c\ (1 - R)} \tag{8}$$

If we now substitute equation (8) into (7) and (7) into (4), we obtain equation (3):

$$X = \underbrace{\left(X_O - \frac{B}{A}\right) e^{-At}}_{\text{transient}} + \underbrace{\frac{B}{A}}_{\text{steady state}}$$

where

$$A = \frac{Q_s - Q_c}{PV\ (1 - C)} \tag{9}$$

$$B = \frac{Q_s G - Q_c}{PV} \tag{10}$$

$$C = \frac{RQ_c}{Q_s + Q_r - Q_c\ (1 - R)} \tag{11}$$

Equations (3) and (8) represent exact solutions to the problems of oxygen and carbon dioxide concentration variation within the system. They may be simplified considerably for engineering use as outlined below.

For proper chamber ventilation, $Q_s + Q_r$, the ventilation rate, is far in excess of Q_c, the rate of oxygen uptake. Therefore, equation (8) may be simplified to

$$C \cong \frac{RQ_c}{Q_s + Q_r} \tag{12}$$

This is not exact, but it is accurate enough for most purposes.

Since C is normally quite low, less than 1 percent in a properly operating chamber, then $(1 - C) \cong 1$ and from equation (9),

$$A = \frac{Q_s - Q_c}{PV} \tag{13}$$

Since our primary interest lies in the steady-state solution to equation (3) the above simplification leads to

$$X_{\text{steady state}} = \frac{B}{A} \cong \frac{Q_s G - Q_c}{Q_s - Q_c} \tag{14}$$

The above expression is familiar to users of semiclosed scuba as one long used to calculate levels of breathing-bag oxygen.

The foregoing expressions for carbon dioxide and oxygen concentrations were used to prepare figure 10.5 and 10.6, which show the steady-state variation of the levels of these gases.

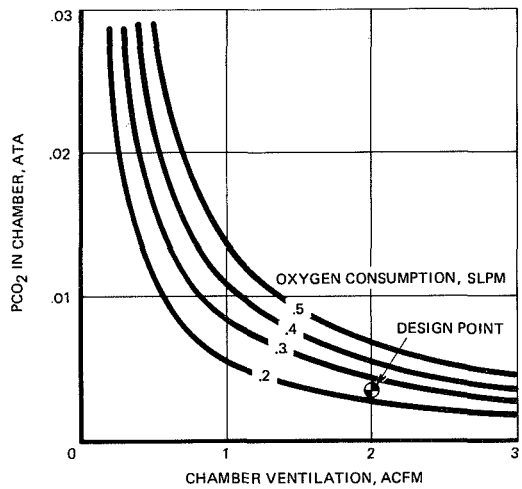

Figure 10.5 *Variation of pCO_2 with chamber ventilation.*

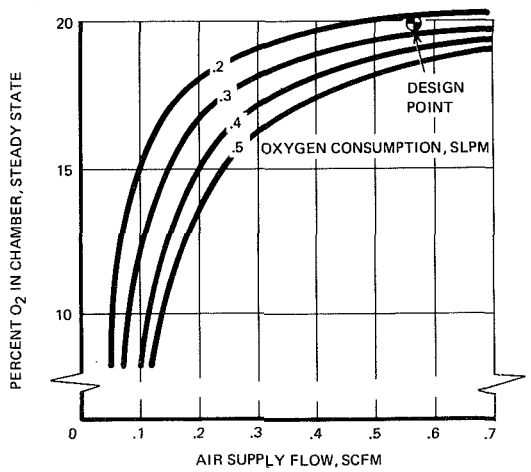

Figure 10.6 *Variation of percent O_2 with supply flow.*

DISCUSSION OF SYSTEM

Gas Circulation Methods

To remove the contaminants from the chamber atmosphere, it is necessary to circulate it through a scrubber and return it to the chamber. Some form of power is obviously required to operate the circulator. At the intended flow of 2 ACFM at depths to 165 ft, it was estimated that the pressure drop through the recirculation system would not be more than 4 in. of water. Three forms of power were considered—electric power, manpower, and gas power.

Because reliance on electrical power would require that batteries be charged and available at all times, and because this might not always be practical, it was considered that one of the other forms of power should be used, if possible.

Manpower, used to turn a crank or operate a treadmill, was not considered desirable because even at the low level of power required fatique could affect operation, and during transportation of the chamber it might not be possible to have the man accompany the chamber at all times unless the occupant was used as the source of power, which was quickly rejected. Besides, in the sort of emergency requiring the use of a recompression chamber, it would be a foolish waste of capability to use a man for such a simple task.

Gas power was considered an attractive alternative. Two approaches to gas power were apparent—an air motor to operate a circulating fan and an air ejector to circulate the atmosphere directly. The theoretical power required for circulating the gas was estimated to be on the order of 1/1000 hp. Even though dynamic shaft seals would have added to that, the power requirement was still far below the efficient capability of any commercial air motor. Although construction of such a motor was possible, its operating gas would have had to be wasted, since the necessary lubricants would contaminate the motor exhaust and make it unfit for breathing purposes.

Air Ejector

Use of an air ejector for circulation of the chamber atmosphere seemed very attractive, if feasible. The same air needed to replenish the chamber oxygen could be used to circulate the atmosphere. No batteries or moving parts were required. Ejectors have been used successfully for years on recirculating diving helmets, although not at the high flow ratios required on this chamber.

To determine the suitability of air ejectors, it was necessary to examine their characteristics and how they related to the gas supply requirements of the recompression system.

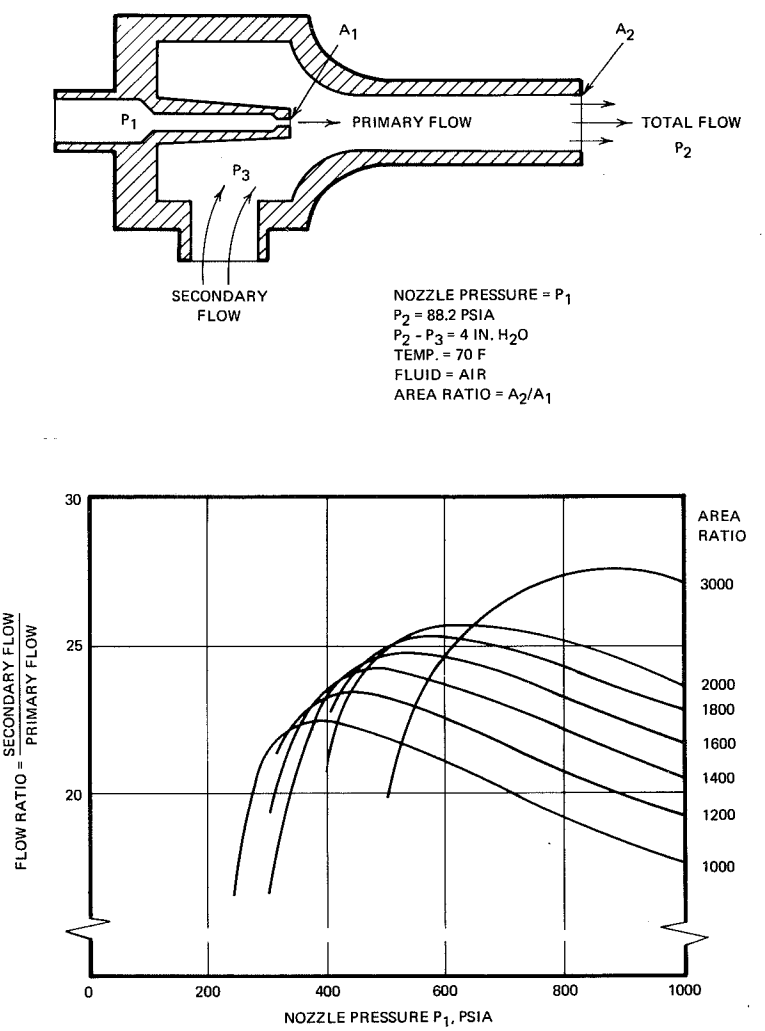

Figure 10.7 *Theoretical ejector characteristics.*

To estimate actual performance of an air ejector, the simultaneous solution of equations relating conservation of mass, energy, and momentum is required. Because there are many system variables, and because the solution is an iterative one, computer programs were written to aid in the computation. The results of the computation are shown in figure 10.7. In explanation of figure 10.7, the primary flow is that flow of gas which generates the circulation through the ejector. It is introduced through a high-pressure nozzle. The secondary flow is that flow induced in the chamber by the action of the ejector. Downstream pressure of 88.2 psia corresponds to the operating pressure of 165 ft of seawater. A pressure drop of 4 in water was estimated as the maximum that would be obtained through line friction in the system piping at the desired flow of 2 ACFM.

From figure 10.5, it has been seen that a flow of 2 ACFM per man is proper to maintain carbon dioxide in the 0.005 ATA range. Figure 10.7 shows that ejector flow ratios from 20 to 25 may

theoretically be obtained without requiring prohibitively large supply pressures. At 165 ft, 2 ACFM flow is 12 SCFM, and at a flow ratio of 20, a supply flow of 0.6 SCFM is required. Examination of figure 10.6 shows that 0.6 SCFM supply flow will keep the chamber oxygen level quite close to 20 percent. This is desirable, since effective recompression treatment by standard air tables is not possible if the breathed gas is markedly low in oxygen. Bends recurrence rate is already high using the air tables, and greatly lowering the oxygen level would tend to increase the recurrence rate.

An ejector was built and tested to be sure that the theoretical approach was valid. Results of flow tests may be seen in figure 10.8. Happily, the ejector performance was completely adequate and will be incorporated without change into the chamber prototype.

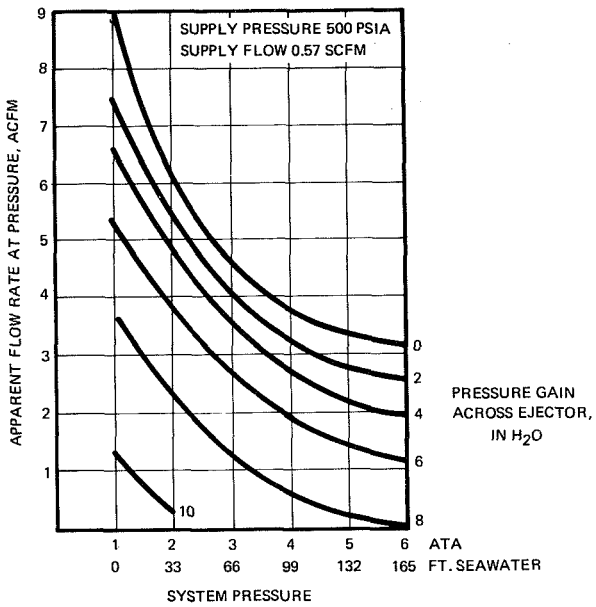

Figure 10.8 *Actual ejector performance.*

Actual System Flows

Because piping systems may not behave according to estimates of their characteristics, provision has been made for addition of a flow meter to the flow circuit. Without the meter orifice, it is estimated that system pressure drop will be in the 1 to 2 in. of water range, including canister losses at 6 ATA. Addition of the meter orifice will provide a pressure drop that will be used in conjunction with a differential pressure gage for flow measurement. An orifice of 0.45-in diam will theoretically produce about another 2 in. of water pressure drop at 2 ACFM and 6 ATA.

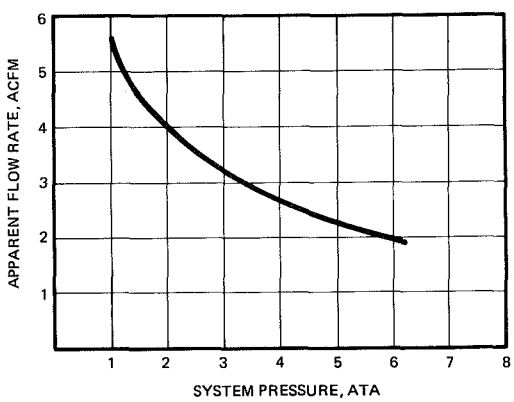

Figure 10.9 *Predicted system performance.*

When estimated system characteristics are correlated with the ejector characteristics shown in figure 10.8, the performance of the entire system can be estimated. It is shown in figure 10.9.

Supply and Exhaust Gas Flow Rates

Supply and exhaust gas flow during semiclosed-circuit operation has already been determined to be about 0.6 SCFM. For open-circuit operation, and for standard rates of ascent and descent, the flow rates may be calculated as follows.

Descent. At the standard descent rate of 25 ft/min, a chamber must gain pressure at the rate of 25/33 ATA/min; thus for an 18.3 cu ft chamber,

$$\text{Required supply flow} = \frac{25}{33} \times 18.3 = 14 \text{ SCFM during descent}$$

Normal Open-Circuit Ventilation. Normal open-circuit ventilation will be at least 2 ACFM as measured at the chamber depth and indicated by the built-in orifice meter. At 165 ft, or 6 ATA, this requires 12 SCFM.

Ascent. During ascent, the standard procedure is to ascend at the rate of 1 min per decompression stop. During each ascent, the chamber loses

$$\frac{18.3}{33} = 0.555 \frac{\text{ft}^3 \text{ gas}}{\text{ft of depth}}$$

Thus, for a 20-ft stop, flow = 20 × 0.555 = 11.1 SCFM; for a 15 ft-stop, flow = 15 × 0.555 = 8.3 SCFM; for a 10-ft stop, flow = 10 × 0.555 = 5.6 SCFM. The most severe flow requirement is from 10 feet to surface, since at this depth driving pressure across the exhaust valve is least. A 1/4-in. orifice will pass 16 SCFM to atmosphere with a 5 psi driving pressure, 12 SCFM with 3 psi, 7 SCFM with 1 psi. This flow capacity is adequate to provide for all treatment stages except for the 10-ft-to-surface stop. In that case, it will take 2 or 3 min to complete the ascent. However, this ascent is not made until treatment is complete, and the extra minutes are of little consequence. An exhaust valve having an equivalent orifice size of 1/4 in. was correspondingly employed.

Supply Piping and Valves. All supply piping is short, and deliberately kept larger than restricting valves to minimize pressure drop. Valves have been sized to be the smallest valves that can pass the required flow, as this generally gives fineness of control over the entire flow range.

CO_2 Absorption

It was originally planned that carbon dioxide absorption would be effected by use of a radial-flow canister containing concentric cylinders of lithium hydroxide (for carbon dioxide) and activated charcoal or alumina (for odor and dust removal). However, because of its general availability in Navy diving operations, granular baralyme has been selected as the system carbon dioxide absorbent. Its prime drawback is that it has low efficiency at low temperatures, requiring more frequent canister changes in cold conditions than would lithium hydroxide.

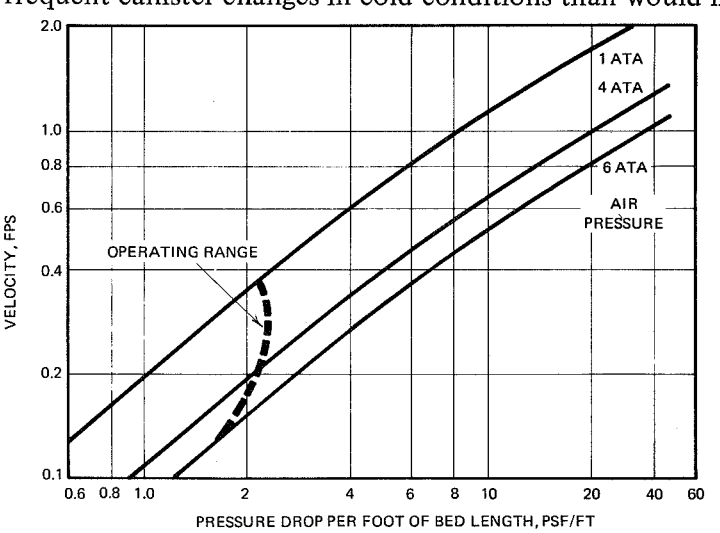

Figure 10.10 *Results of air flow tests conducted with granular baralyme.*

Present canister design is a cylinder 6-3/4-in. in diameter and 9-in. long. Flow is straight through vertically. Originally, the radial-flow approach was taken to minimize flow resistance, but flow tests showed such low resistance with straight-through flow that any reduction by design sophistication was unnecessary. Results of flow tests using baralyme in beds of different geometries are shown in figure 10.10.

Odors will be absorbed by a layer of activated charcoal located at one end of the baralyme bed. The carbon dioxide absorption capacity of the system is estimated to be at least 20 hr at 70° F

and 10 hr at 32° F, the reduction occurring because of the reduced efficiency of baralyme at low temperatures. A transparent lid on the canister permits visual evaluation of the baralyme, which turns bluishwhite when exhausted. Results of canister performance tests are shown in figure 10.11.

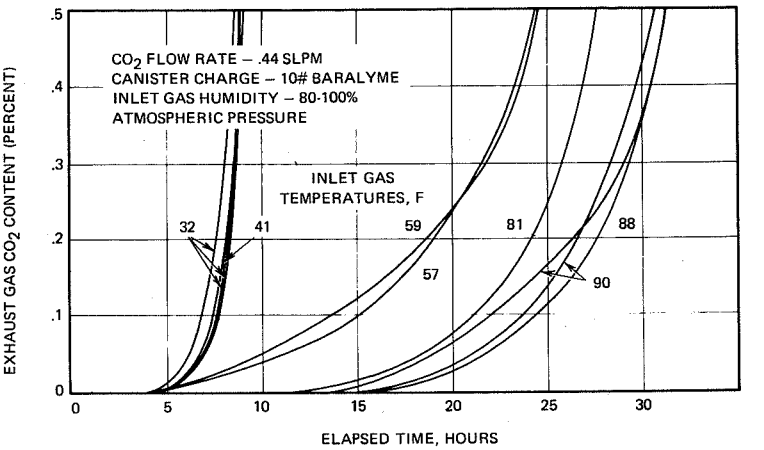

Figure 10.11 *Carbon dioxide scrubber test data.*

Humidity and Temperature

Because the human respiratory system effectively humidifies gas passed through it and because the chemical reaction in the canister produces moisture, after a time, the chamber will reach a high level of humidity; indeed it is probable that system humidity will be 90 to 100 percent. Some reduction of this will be caused by the addition of the ejector primary flow, but this flow is only 1/10 to 1/40 the total flow in the system. Therefore, the atmosphere will be very humid. This has been confirmed by experiments conducted using a similar chamber. Use of dessicants could reduce the humidity, but this could give the occupant an uncomfortably dry atmosphere to breathe, and would add somewhat to system complexity.

Temperature will be regulated by placing the chamber in a location where the surroundings are at a comfortable temperature, if possible. If not possible, the occupant must grit his teeth and be cheered by the thought that discomfort is preferable to decompression sickness. Experiments yet to be run will establish the true levels of temperature reached in the chamber. Present estimates indicate that interior temperatures will be 10° to 15° F higher than ambient, depending on chamber color, environment, and occupant dress.

Effect of Altitude on Operation

Because the chamber is controlled by ambient pressure-sensing regulators and pressure is read on an ambient-pressure-sensing gage, the chamber interior will drop in pressure during flight in an unpressurized aircraft. To keep ambient pressure change from affecting the chamber occupant, an instruction plate will be fixed to the control panel instructing the operator to add 1 ft of depth to the chamber for every 1000 ft of aircraft cabin altitude. This correction is valid to 15,000 ft altitude. Above that altitude, it is too cold to fly the chamber in ambient conditions.

APPLICATION OF THE SYSTEM

The recompression system discussed here may be used both to treat a diver for decompression sickness or to transport him to a larger chamber complex.

Stops		Bends–Pain only				Serious Symptoms	
Rate of descent–25 ft. per min. Rate of ascent–1 minute between stops.		Pain relieved at depths less than 66 ft. Use table 1–A if O_2 is not available.		Pain relieved at depths greater than 66 ft. Use table 2–A if O_2 is not available. If pain does not improve within 30 min. at 165 ft. the case is probably not bends. Decompress on table 2 or 2–A.		Serious symptoms include any one of the following: 1. Unconsciousness. 2. Convulsions. 3. Weakness or inability to use arms or legs. 4. Air embolism. 5. Any visual disturbances. 6. Dizziness. 7. Loss of speech or hearing. 8. Severe shortness of breath or chokes. 9. Bends occurring while still under pressure.	
						Symptoms relieved within 30 minutes at 165 ft. Use table 3	Symptoms not relieved within 30 minutes at 165 ft. Use table 4
Pounds	Feet	Table 1	Table 1-A	Table 2	Table 2-A	Table 3	Table 4
73.4	165	.....	.....	30 (air)	30 (air)	30 (air)	30 to 120 (air)
62.3	140	.....	.....	12 (air)	12 (air)	12 (air)	30 (air)
53.4	120	.....	.....	12 (air)	12 (air)	12 (air)	30 (air)
44.5	100	30 (air)	30 (air)	12 (air)	12 (air)	12 (air)	30 (air)
35.6	80	12 (air)	12 (air)	12 (air)	12 (air)	12 (air)	30 (air)
26.7	60	30 (O_2)	30 (air)	30 (O_2)	30 (air)	30 (O_2) or (air)	6 hrs. (air)
22.3	50	30 (O_2)	30 (air)	30 (O_2)	30 (air)	30 (O_2) or (air)	6 hrs. (air)
17.8	40	30 (O_2)	30 (air)	30 (O_2)	30 (air)	30 (O_2) or (air)	6 hrs. (air)
13.4	30	5 (O_2)	60 (air)	60 (O_2)	2 hrs. (air)	12 hrs. (air)	First 11 hrs. (air) Then 1 hr. (O_2) or (air)
8.9	20		60 (air)		2 hrs. (air)	2 hrs. (air)	First 1 hr. (air) Then 1 hr. (O_2) or (air)
4.5	10		2 hrs. (air)	5 (O_2)	4 hrs. (air)	2 hrs. (air)	First 1 hr. (air) Then 1 hr. (O_2) or (air)
Surface			1 min. (air)		1 min. (air)	1 min. (air)	1 min. (O_2)

Time at all stops in minutes unless otherwise indicated.

Figure 10.12 *Air treatment tables from U.S. Navy diving manual.*

If the chamber is used for treatment of the diver, pressurization and depressurization will follow the schedule prescribed in the U.S. Navy diving manual (fig. 10.12). Oxygen content of the chamber and gas usage will vary as shown in figure 10.13, a printout of a computer program that combines equation (3) with the diving manual's decompression schedules. The diving manual's table 4 is illustrated in figure 10.13 because it requires the longest treatment time–the other three tables effect similar results.

Of particular interest in figure 10.13 is the far right-hand column. Once the chamber has been pressurized to 165 ft, it may operate for 4 hr on 136 cu ft of gas, which can be supplied by a single pair of standard Navy 90 cu ft scuba bottles. Put in another way, the chamber can be pressurized and go on to operate for 3 hr using only a single 240 cu ft air flask. If open-circuit operation were used, the same air flask would last only 12 min. A clear improvement in gas economy is evident.

If the chamber is used only as a transportation capsule, the occupant will be pressurized until relief is reached. The chamber will be maintained at that pressure until the chamber can be mated to a larger treatment chamber and the patient removed. Figure 10.14 shows the variation in oxygen content in systems pressurized to different initial pressures and held at those pressures while circulation is maintained by the ejector air flow.

A variation of the same program is shown in figure 10.15, which illustrates the enormous oxygen capacity of the system. If the system is pressurized to 40 ft or more, operation can safely be maintained for more than 8 hr with the addition of no gas at all, providing circulation is maintained, say by a check-valved oral-nasal mask connected to the circulation piping. However, use of this mode of operation will result in depressed oxygen partial pressures, making the air tables unusable for this system.

FUTURE WORK

The chamber design is, at the time of this writing (May, 1971), being reviewed by the Certification Board, under the authority of the U.S. Navy Experimental Diving Unit. Upon approval of the design, construction will begin. We hope to have an operable chamber built by August 1971, and to begin fullscale experimental evaluation of it at that time.

4-6

Ejector air flow = 16.1 SLM = 0.57 SCFM
Weight of chamber occupant = 165 lb
Oxygen consumed by occupant = 0.25 SLM
Chamber volume = 18.3 ft^3

Depth, ft	*Time, hr*	*pO_2 ATA*	*Percent oxygen*	*Gas used cu/ft*
165	0	1.26	21.	78.2788
165	2	1.22179	20.3632	146.547
140	2	1.06753	20.3632	146.547
140	2.5	1.06161	20.2504	163.615
120	2.5	.938883	20.2504	163.615
120	3	.934127	20.1478	180.682
100	3	.812019	20.1478	180.682
100	3.5	.808307	20.0557	197.749
80	3.5	.686757	20.0557	197.749
80	4	.683977	19.9745	214.816
60	4	.562919	19.9745	214.816
60	10	.556766	19.7562	419.622
50	10	.496899	19.7562	419.622
50	16	.496842	19.754	624.427
40	16	.436981	19.754	624.427
40	22	.436981	19.7539	829.233
30	22	.377121	19.7539	829.233
30	34	.377121	19.7539	1238.84
20	34	.31726	19.7539	1238.84
20	36	.31726	19.7539	1307.11
10	36	.2574	19.7539	1307.11
10	38	.2574	19.7539	1375.38
0	38	.197539	19.7539	1375.38
0	38.0167	.197539	19.7539	1375.95

Figure 10.13 *Gas flows and usage for air decompression by Table 4.*

Weight of chamber occupant = 165 lb
Oxygen consumed by occupant = 0.25 SLM
Chamber volume = 18.3 ft^3

	Oxygen percentages at depths of			
Time, hr	*165 ft*	*100 ft*	*40 ft*	*0 ft*
0	21.	21.	21.	21.
.5	20.7959	20.7087	20.521	20.18
1	20.6253	20.4855	20.2262	19.8996
1.5	20.4825	20.3145	20.0446	19.8037
2	20.3632	20.1834	19.9329	19.771
2.5	20.2634	20.083	19.8641	19.7598
3	20.18	20.0061	19.8218	19.7559
3.5	20.1102	19.9471	19.7957	19.7546
4	20.0518	19.902	19.7796	19.7542
4.5	20.0031	19.8674	19.7698	19.754
5	19.9623	19.8409	19.7637	19.754
5.5	19.9281	19.8205	19.7599	19.754
6	19.8996	19.805	19.7576	19.7539
6.5	19.8757	19.793	19.7562	19.7539
7	19.8558	19.7839	19.7553	19.7539
7.5	19.8391	19.7769	19.7548	19.7539
8	19.8252	19.7715	19.7545	19.7539
8.5	19.8135	19.7674	19.7543	19.7539
9	19.8037	19.7643	19.7541	19.7539
9.5	19.7956	19.7619	19.7541	19.7539
10	19.7888	19.76	19.754	19.7539
10.5	19.7831	19.7586	19.754	19.7539
11	19.7783	19.7575	19.754	19.7539
11.5	19.7743	19.7567	19.754	19.7539
12	19.771	19.756	19.754	19.7539
12.5	19.7682	19.7555	19.754	19.7539
13	19.7659	19.7552	19.7539	19.7539
13.5	19.7639	19.7549	19.7539	19.7539
14	19.7623	19.7547	19.7539	19.7539
14.5	19.7609	19.7545	19.7539	19.7539
15	19.7598	19.7544	19.7539	19.7539
15.5	19.7588	19.7543	19.7539	19.7539
16	19.758	19.7542	19.7539	19.7539

Supply air flow = 0.57 SCFM

Figure 10.14 *Variation of percent O_2 with time in a recompression chamber at various depths.*

Weight of chamber occupant = 165 lb
Oxygen consumed by occupant = 0.24 SLM
Chamber volume = 18.3 ft^3

	Oxygen percentages at depths of			
Time, hr	*165 ft*	*100 ft*	*40 ft*	*0 ft*
0	21.	21.	21.	21.
.5	20.7857	20.6808	20.4175	19.7057
1	20.5709	20.3603	19.8307	18.3902
1.5	20.3555	20.0386	19.2396	17.0532
2	20.1395	19.7155	18.6442	15.6942
2.5	19.9229	19.3911	18.0443	14.313
3	19.7057	19.0655	17.44	12.9091
3.5	19.4879	18.7385	16.8313	11.4823
4	19.2696	18.4102	16.2181	10.0321
4.5	19.0506	18.0805	15.6003	8.55808
5	18.8311	17.7495	14.978	7.05995
5.5	18.6109	17.4172	14.3511	5.53727
6	18.3902	17.0836	13.7196	3.98964
6.5	18.1689	16.7486	13.0835	2.41666
7	17.9469	16.4122	12.4426	.817918
7.5	17.7244	16.0745	11.797	
8	17.5013	15.7354	11.1467	
8.5	17.2775	15.3949	10.4915	
9	17.0532	15.0531	9.83156	
9.5	16.8282	14.7099	9.16673	
10	16.6026	14.3653	8.49699	
10.5	16.3764	14.0193	7.82232	
11	16.1496	13.6719	7.14267	
11.5	15.9222	13.3232	6.45801	
12	15.6942	12.973	5.7683	
12.5	15.4656	12.6214	5.07351	
13	15.2363	12.2683	4.37359	
13.5	15.0064	11.9139	3.66851	
14	14.7759	11.558	2.95824	
14.5	14.5448	11.2006	2.24272	
15	14.313	10.8419	1.52193	
15.5	14.0806	10.4816	.795831	
16	13.8476	10.12		

Supply air flow = 0

Figure 10.15 *Variation of percent O_2 with time in a recompression chamber at various depths.*

BIBLIOGRAPHY

1. Anon: U.S. Navy Diving Manual. NAVSHIPS 0994-001-9010, March, 1970.
2. Anon: Compressed Air Data. Compressed Air Magazine, New York, 1960.
3. Anon: Flow of Fluids Through Valves, Fittings, and Pipe. Technical Paper 910, The Crane Co., Chicago, Illinois.
4. Comroe, J. H.; Forster, R. E.; Dubois, A. B.; Briscoe, W. A.; and Carlsen, E.: The Lung. Year Book Medical Publishers Inc., Chicago, 1962.
5. Riegel, P. S.: Liter Flow and Mix Selection in Semiclosed-Circuit Scuba. Marine Tech. Soc. J., March/April, 1970.
6. Caudy, D. W.; and Glasgow, J. S.: Final Report on Portable Recompression Chamber Environmental Control System Study to Supervisor of Diving, United States Navy, Battelle Memorial Institute, July 31, 1970.
7. Caudy, D. W.: Design Review Report for Portable Recompression System to U.S. Navy, Supervisor of Diving, Battelle Memorial Institute, April, 1971.
8. Alexander, J. M., assistant submarine medical officer: personal comm.
9. Milwee, W. I., supervisor of diving: personal comm.
10. Lower, B. R.: Removal of CO_2 from Closed-Circuit Breathing Apparatus, Equipment for the Working Diver. Symposium, Battelle Columbus Laboratories, Columbus, Ohio, 1970.
11. Keenan, J. H.; and Neumann, E. P.: A Simple Air Ejector. J. Appl. Mech., June, 1942.

11 SKYLAB ASTRONAUT LIFE SUPPORT ASSEMBLY

J. Travis Brown
NASA Manned Spacecraft Center

INTRODUCTION

In its early conceptual stages, the Skylab Program (originally the Apollo Applications Program) was concerned with maximum utilization of available flight-qualified equipment. A comparative study was performed to define an optimum portable life support system for suited operations inside and outside the Skylab cluster. Emphasis was placed on utilization of qualified equipment, modified versions of qualified equipment, and new systems made up to state-of-the-art components. This report outlines the mission constraints, operational modes, and evaluation ground rules by which the Skylab portable life support system was selected; this report also describes the resulting design now being developed.

MISSION MODES

The Skylab cluster is depicted in figures 11.1 and 11.2, and the mission profile is shown in figure 11.3. The associated extravehicular activity (EVA) is concerned primarily with retrieval of film from the Apollo telescope mount. The EVA is distributed among the missions as follows: Skylab 1 and 2 (SL 1/2), one EVA; SL 1/3, three EVAs; and SL 1/4, two EVAs. An EVA is initiated from and supported by the airlock module (AM), which is equipped with an EVA hatch and support panels providing oxygen, cooling water, communications, and electrical power. Hatches isolate the AM from the multiple docking adapter (MDA) and the orbital workshop so that only the AM volume of atmosphere is lost during EVA cabin decompression. During Skylab missions, there are two types of intravehicular activity (IVA) planned with the crewmen wearing a suit in a pressurized cabin: (1) suit vented, operations carried out by a crewman with the suit pressure equal to local ambient, and (2) suit pressurized, operations carried out by a crewman with the suit pressurized to approximately 3.9 psi above local ambient pressure.

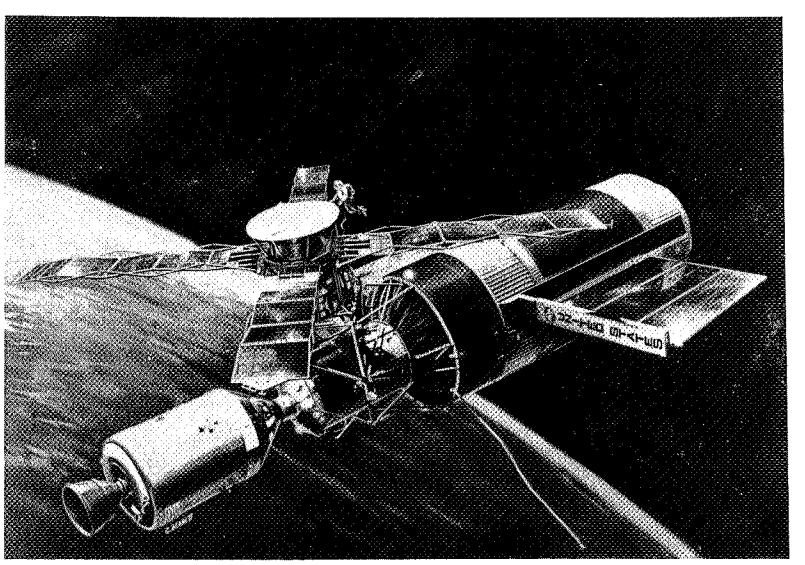

Figure 11.1 *Skylab I.*

In addition to the nominal EVA and IVA mission modes, certain contingency modes must be accommodated inside the Skylab cluster, in a vacuum (or near vacuum) environment. The

contingency modes involve (1) suited entrance through the command module tunnel into the MDA in the event the MDA remote pressurization system malfunctions and (2) suited transfer across the AM-MDA hatch, isolation of the AM, and subsequent repressurization of the MDA due to inability of AM repressurization following EVA. A portable life support system must be capable of properly cooling and ventilating a suited crewman for the EVA, IVA, and contingency modes of operation. The system must also have the capability of automatic compensation for a change from either of the IVA modes of operation to the EVA mode (i.e., protection against loss of cabin pressure).

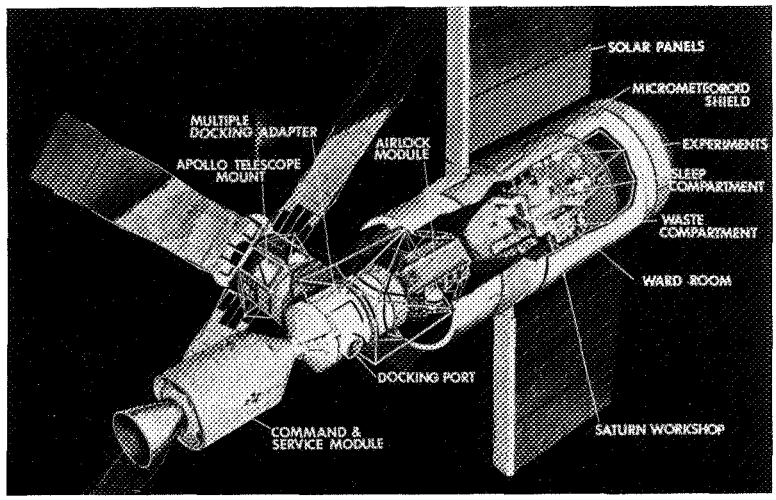

Figure 11.2 *Orbital workshop.*

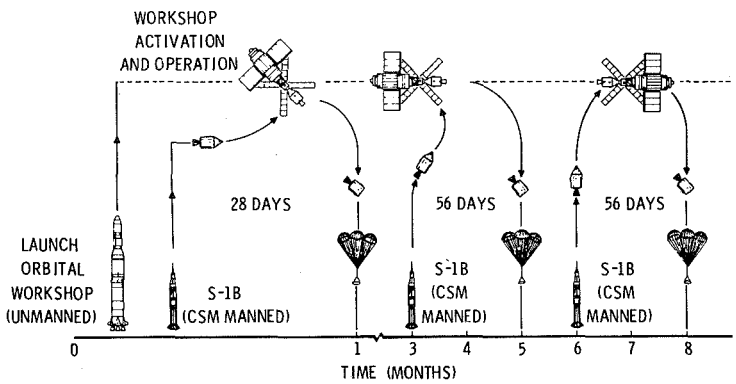

Figure 11.3 *Skylab mission profile.*

CONSTRAINTS

The following technical constraints were adhered to in the comparative study effort:

1. Two men in EVA simultaneously or 1-man IVA
2. An EVA duration of 3 hr nominal
3. Prebreathing time (45 min)
4. No low-pressure umbilical (i.e., suit hose) connections or disconnections in a vacuum environment
5. Provision of hardline communications and biomedical data to spacecraft
6. Provision for the following contingencies with allowable degradation as shown:
   a. Loss of primary cooling mode
      (1) 30 min
      (2) 300 Btu maximum body heat storage
      (3) 2000 Btu/hr metabolic rate
   b. Loss of primary ventilation mode
      (1) 30 min
      (2) 15 torr maximum inspired carbon dioxide partial pressure
   c. Loss of primary oxygen supply
      (1) 30 min
      (2) Audible and visible warnings if secondary oxygen supply is automatically activated

d. Fail open of any ventilation loop relief valve
   (1) 30 min
   (2) Suit pressure maintained
   (3) Relief valve override or sufficient makeup oxygen

7. Must have minimum volume, high reliability, and uncomplicated checkout and service requirements

Evaluation Ground Rules

The comparative study results were dependent on the evaluation ground rules and their order of preference. The following ground rules, listed in order of priority, were used for the optimization study.

1. Probability of accomplishing all tasks
2. Cost
3. Spacecraft system impact
4. Total launch weight

CANDIDATE SYSTEMS

From approximately 40 combinations of portable life support systems investigated, the following were candidates for the final, complete tradeoff analysis.

1. Astronaut life support assembly (ALSA). Nonexisting system with design based on the use of state-of-the-art components. The system will be composed of the following:
   a. Pressure control unit (PCU)
   b. Life support umbilical (LSU)
   c. Secondary oxygen pack (SOP)
2. Apollo portable life support system (PLSS). Developed by Hamilton Standard Division of United Aircraft Corporation; now used for lunar exploration.
3. Modified PLSS. Apollo PLSS modified to utilize oxygen/electrical/spacecraft umbilical. Augmented by a suit ventilation unit (SVU) – (simplified open-loop oxygen system) to satisfy the IVA mission modes.
4. Portable environmental control system (PECS). Advanced backpack being developed by AiResearch Manufacturing Company, Garrett Corporation, at the time of the study (was later canceled).
5. New system (hybrid backpack, oxygen/electrical/spacecraft umbilical). Designed specifically for Skylab mission requirements.
6. New system (hybrid backpack, oxygen/electrical/cooling-water umbilical). Designed specifically for Skylab mission requirements.

Descriptions of Systems

The ALSA. (See "System Advantages and Disadvantages.")

Apollo PLSS (fig. 11.4). This system contains closed-loop ventilation, a cooling-water circulation loop, a sublimator heat-rejection source, a primary oxygen supply, a battery power supply, and a space suit communications system. There is no umbilical associated with employment of this system. An oxygen purge system (OPS) and separate high-pressure oxygen bottles and regulator are employed as a backup oxygen supply and backup to the primary cooling subsystem.

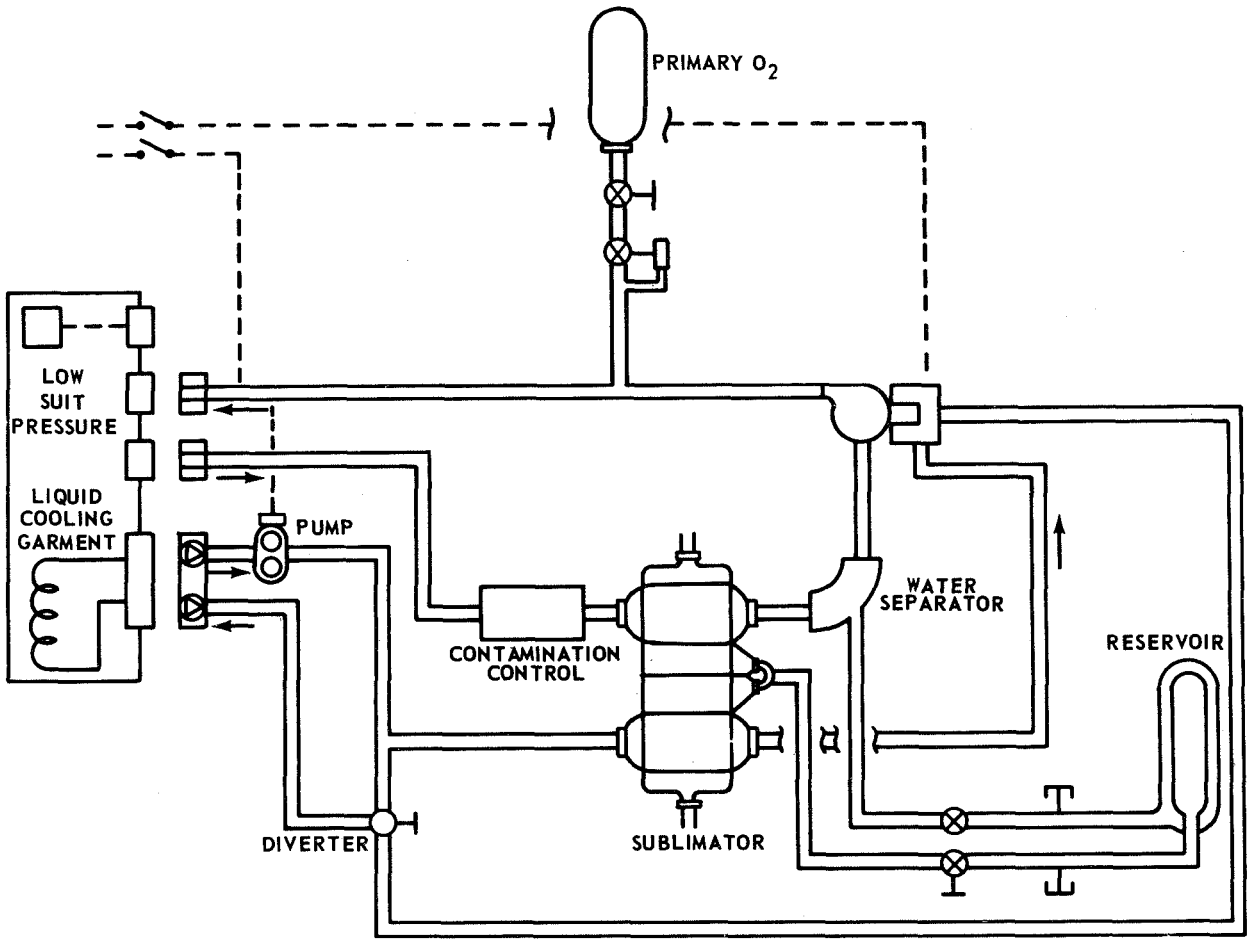

Figure 11.4 *Apollo portable life support system.*

The ventilation loop provides carbon dioxide removal, humidity control, and oxygen makeup from the primary oxygen supply. Suit pressure is controlled to approximately 3.9 psia. The cooling-water circulation loop provides heat transport from the liquid cooling garment (LCG) to the sublimator, which rejects heat by sublimation of stored water to a vacuum environment. The space suit communications system provides two-way voice communications between the crewman inside the spacecraft and the EVA crewmen; processing of physiological, environmental, and expendable status outputs for telemetry transmission to the spacecraft; and generation of signals for audible alarm to indicate critical environmental conditions. Two Apollo PLSS versions are available, providing up to 8 hr of use. To provide pressurized-suit operations capability inside the spacecraft (i.e., IVA pressurized), an SVU and umbilical are required. The SVU is a suit pressure regulator that plugs into the suit-outlet port and maintains suit pressure above local ambient pressure. Oxygen must be supplied to the suit inlet by a spacecraft umbilical. The associated umbilical uses supply and return cooling-water lines for metabolic cooling via an LCG.

Modified PLSS (oxygen/electrical spacecraft umbilical). The battery and primary oxygen bottle are used as backup, with electrical/communications and oxygen being supplied through an umbilical for normal operation. Figure 11.5 is a schematic of the modified PLSS and shows how the

umbilical/PLSS interface is configured. In the event the umbilical or spacecraft oxygen supply is lost, the emergency oxygen supply automatically actuates because of the oxygen regulator configuration, and visible and audible warnings will be triggered. An oxygen valve allows a high oxygen flow to bypass the 3.9-psi regulator, thus providing a means of backup cooling from the umbilical supply. The higher flow rate vents at the suit relief valve, which is an added component to the PLSS. This unit can be used with or without an umbilical; but without an umbilical, it will not provide backup electrical power, instrumentation, and communications. The IVA suit-pressurized operations must be accommodated by use of an SVU and oxygen/electrical/water umbilical.

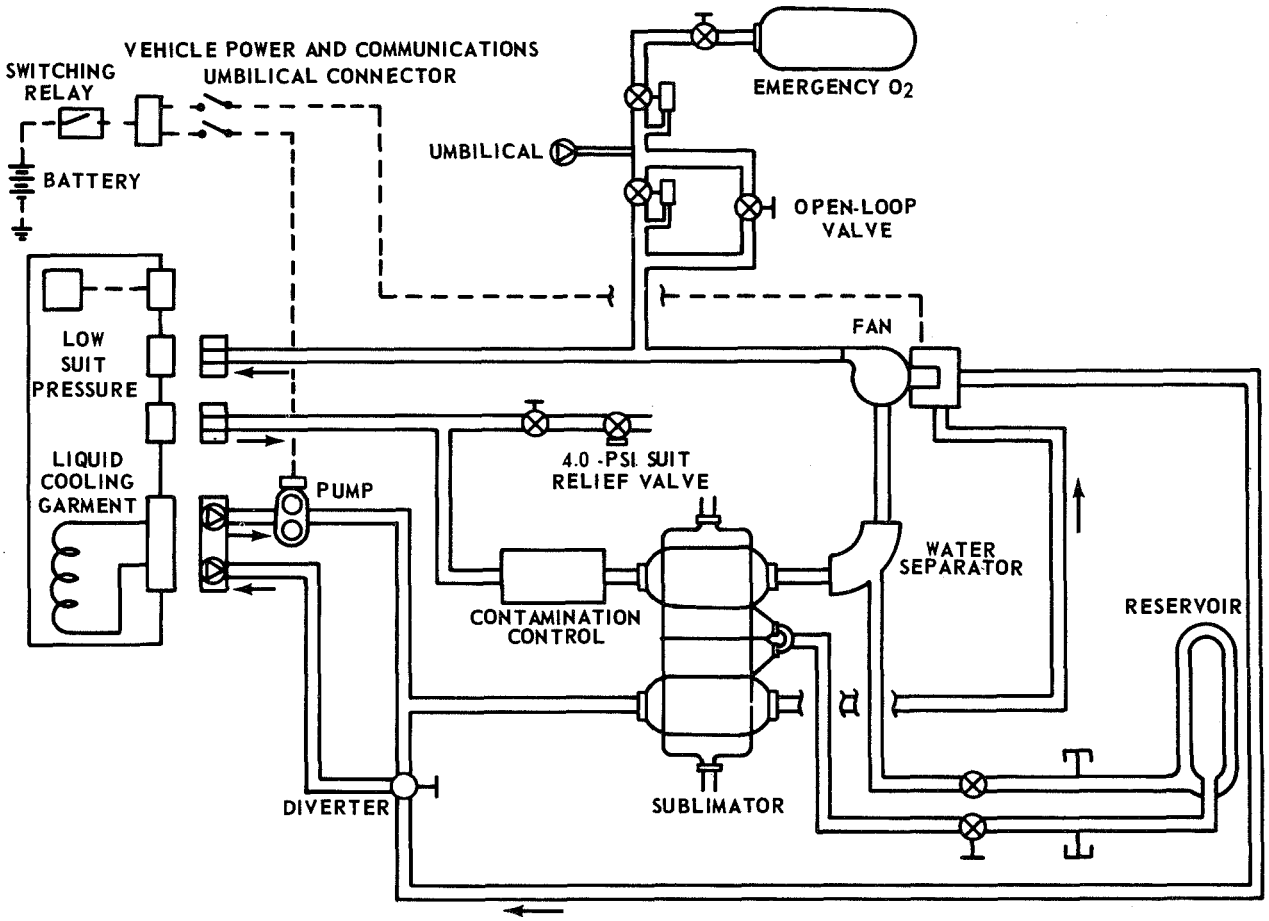

Figure 11.5 *Modified Apollo portable life support system.*

The PECS. Figure 11.6 schematically illustrates the PECS, which contains closed-loop oxygen ventilation, a cooling-water circulation loop, an evaporator heat-rejection source, an oxygen supply, a battery, and a liquid-to-liquid heat exchanger. The system expendables are sized such that EVA may be performed with or without an umbilical, and IVA can be accomplished by using a special umbilical that provides circulating cooling water to the liquid-to-liquid heat exchanger. When operating EVA on an oxygen/electrical umbilical, the evaporator serves as the prime heat-rejection source with umbilical high-flow gas as a backup. If an oxygen/electrical/water umbilical is used, the PECS liquid-to-liquid heat exchanger serves as the prime cooling mode, with the evaporator utilized

as a backup. Electrical power and communications can be provided by the umbilical; electrical power can be obtained from the PECS battery; and a transceiver unit can be installed for biomedical/communications.

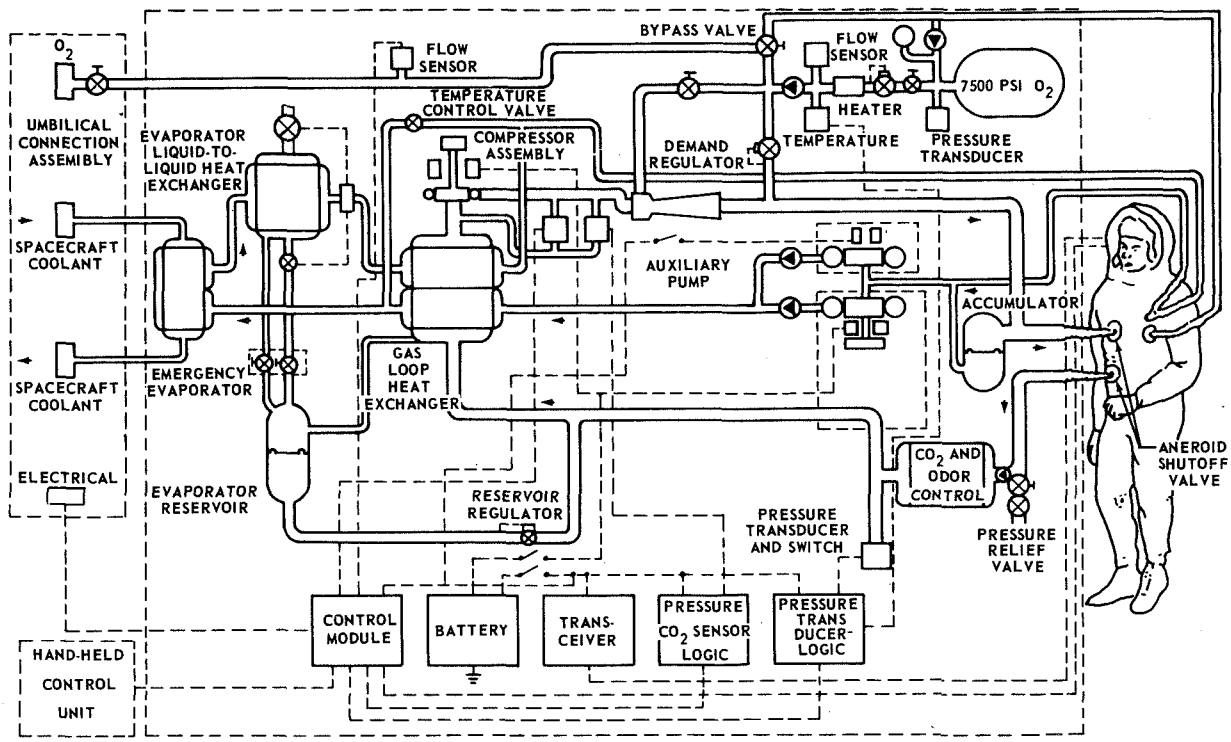

Figure 11.6 *Portable environmental control system.*

New System (hybrid backpack, oxygen/electrical/spacecraft umbilical). Figure 11.7 is a schematic of the new system that is designed specifically for Skylab mission requirements. The system contains closed-loop oxygen ventilation, a cooling-water circulation loop, an evaporator heat-rejection source, an emergency oxygen supply, an emergency power supply, and an evaporative water reservoir. The system is dependent on an umbilical for primary oxygen supply, high-flow oxygen backup cooling, electrical power, and biomedical/communications. The evaporator is the prime mode of cooling, while both the battery and the oxygen bottle serve as backups. This system has self-contained capability for emergency cases where umbilical independence is necessary, but, in this event, would be time limited (i.e., the oxygen bottle and battery sized for 30 min).

New System (hybrid backpack, oxygen/electrical/cooling-water umbilical). This system, figure 11.8, is designed specifically for Skylab mission requirements. This system is similar to the new system explained in the previous paragraph except that it employs a liquid-to-liquid heat exchanger for water umbilical use. The evaporator serves as a backup but unlike the PECS, the evaporator water supply, oxygen supply, and battery are sized for a 30-min emergency situation. The system can be used for IVA with a water umbilical since it employs a liquid-to-liquid heat exchanger. It has self-contained capability for EVA, but only for the 30-min emergency time.

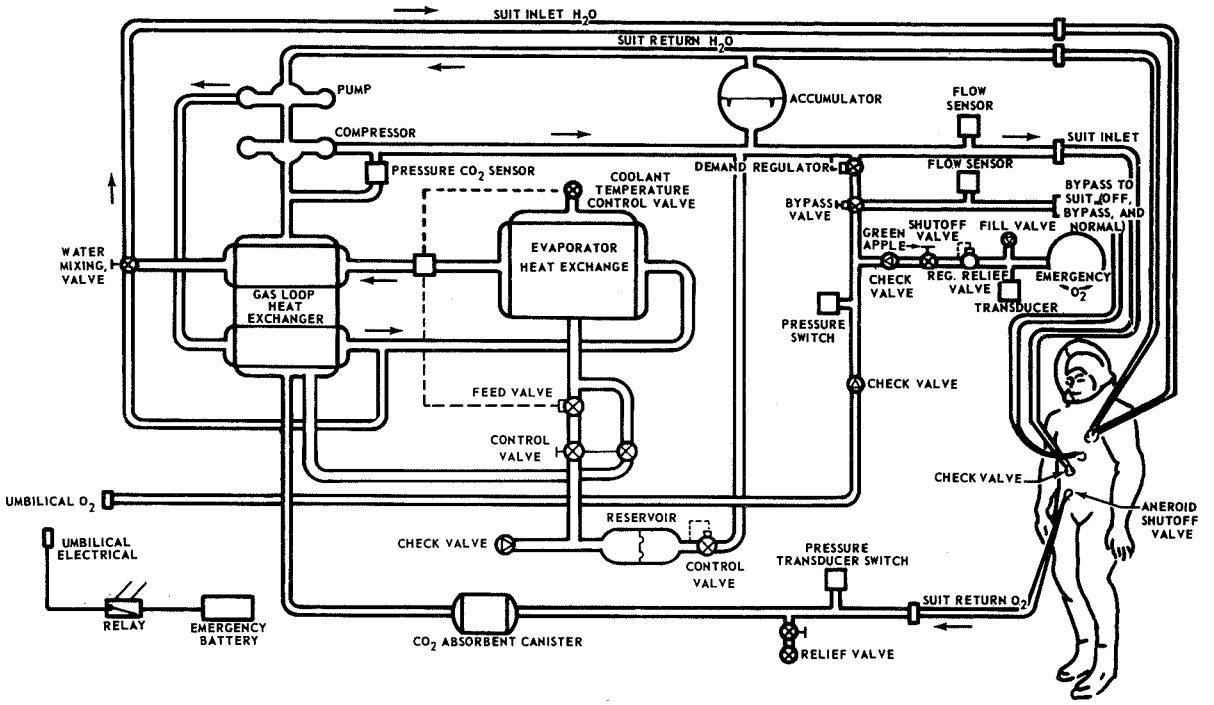

Figure 11.7 *Electrical/oxygen umbilical, new system (hybrid backpack).*

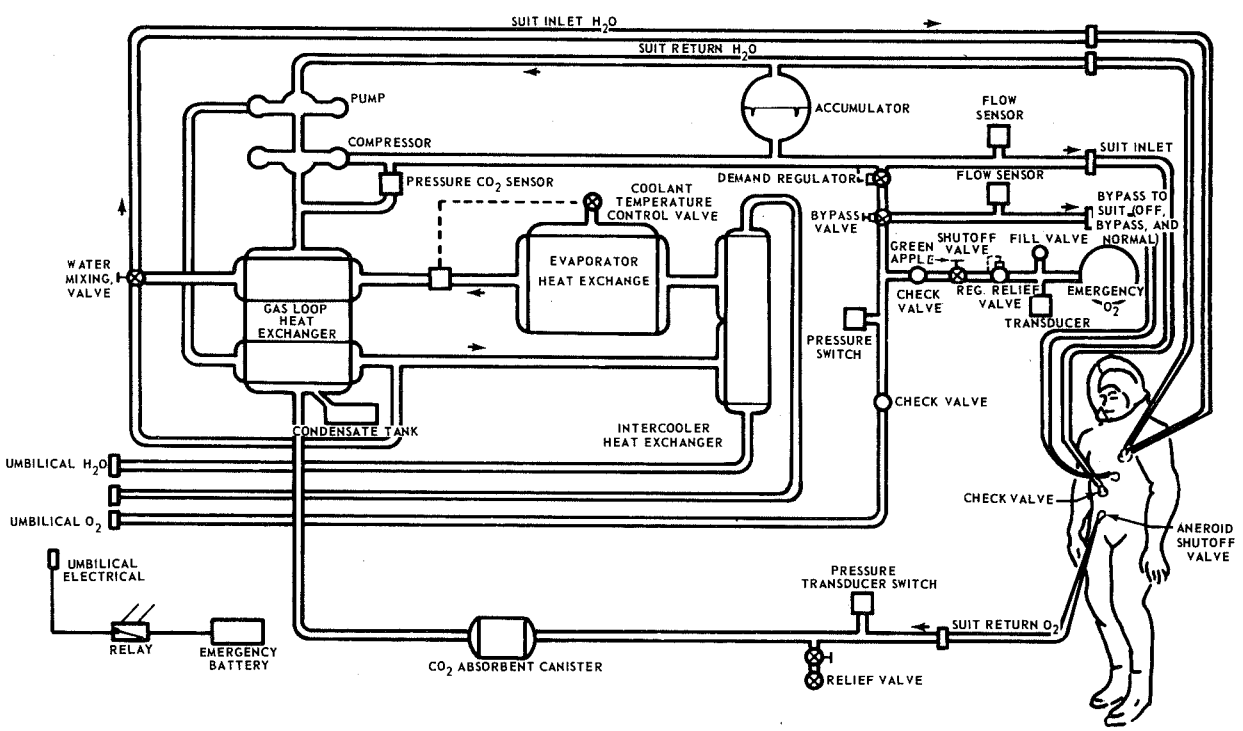

Figure 11.8 *Electrical/oxygen/water umbilical, new system (hybrid backpack).*

SYSTEM ADVANTAGES AND DISADVANTAGES

All of the portable life support systems chosen as candidates for the trade-off are capable of meeting the Skylab mission requirements, but each has definite advantages and disadvantages. Each candidate system is listed with its relative basic advantages and disadvantages (excluding cost and weight, which are discussed later).

1. The ALSA
   a. Advantages
      (1) Small volume
      (2) No recharge requirements
      (3) Minimum checkout requirements
      (4) The EVA and IVA accommodated with the same equipment
      (5) No time-dependent PCU expendables except for emergency
   b. Disadvantages
      (1) The ALSA is not self-contained (i.e., insufficient emergency oxygen for gas cooling for nonumbilical operation).
      (2) The continuous oxygen flow requirement from spacecraft makes the system time-weight critical.

2. The Apollo PLSS
   a. Advantages
      (1) Qualified, available with EVA usage history
      (2) Self-contained
   b. Disadvantages
      (1) Large volume (i.e., has been demonstrated that it is difficult to maneuver in truss area)
      (2) Less backup cooling than other systems (OPS used for backup cooling)
      (3) Complex recharge requirements (water and oxygen recharge systems must be added to either the command module or the AM)
      (4) No cooling capability in pressurized cabin (requires a cooling-water umbilical and SVU for IVA)
      (5) No provision for hardline communications or bioinstrumentation

3. The modified PLSS
   a. Advantages
      (1) Adequate backup modes
      (2) No oxygen recharge or battery replacement requirements
      (3) No OPS required
   b. Disadvantages
      (1) Large volume (has been demonstrated that it is difficult to maneuver in truss area)
      (2) No cooling capability in pressurized cabin (requires a cooling-water umbilical and SVU for IVA)
      (3) Complex recharge requirements (same as for Apollo PLSS)
      (4) Oversized backup expendables for Skylab EVA

4. The PECS
   a. Advantages
      (1) Good backup modes
      (2) Minimum recharge
      (3) Cooling capability in pressurized cabin
      (4) Smaller than PLSS
      (5) Only system with 4-hr self-contained capability that can also be used with an umbilical
      (6) Not as stringent on AM heat-rejection system design as other water umbilicals (i.e., has water boiler topoff capability or capability of using oxygen/electrical umbilical with water boiler as prime heat rejection)
   b. Disadvantages
      (1) More new development involved than PLSS or ALSA
      (2) Larger than ALSA
      (3) For nonumbilical operation, a water recharge system and an oxygen recharge system required in the spacecraft
5. The new system (hybrid backpack, oxygen/electrical umbilical)
   a. Advantages
      (1) Good backup mode designs
      (2) Optimum-sized backup expandables
      (3) Minimum size for closed-loop portable system
      (4) Smaller than PLSS and PECS
      (5) The AM heat-rejection system design not impacted as with water umbilical systems
      (6) Very little service and deservice required
      (7) Self-contained capability (for 30-min period)
   b. Disadvantages
      (1) More new development involved than with PLSS or ALSA
      (2) A water recharge system required in the spacecraft
      (3) No cooling capability in pressurized cabin (requires a cooling-water umbilical and SVU for IVA)
      (4) Larger than ALSA
6. The new system (hybrid backpack, oxygen/electrical/cooling-water umbilical):
   a. Advantages
      (1) Good backup mode designs
      (2) Optimum-sized backup expendables
      (3) Minimum size for closed-loop portable system
      (4) Smaller than PLSS and PECS
      (5) Minimum service and deservice required
      (6) Provides cooling capability in pressurized cabin
      (7) Self-contained capability (for 30-min period)
   b. Disadvantages
      (1) More new development involved than PLSS or ALSA
      (2) Cannot be used for a great length of time as a self-contained system
      (3) Larger than ALSA

OPTIMIZATION STUDY RESULTS

The study included a weight and volume analysis, mission accomplishment assessment, spacecraft impact investigation, and cost analysis. In considering each system with respect to the rating factors, it was found that no set of candidate equipment qualifies as optimum for all rating factors. "Probability of accomplishing all tasks" is best supported by the ALSA, because of its small volume and minimum checkout, service, and deservice requirements. Outstanding advantages are the relative ease of suit-pressurized transfer through the command module tunnel as compared to other candidate systems, accommodation of EVA and IVA requirements with one system (thus minimizing extra hardware for IVA as compared to other systems), and minimum volume carried on the suited astronaut (eases crowded AM interior problem and truss area EVA operations).

The trade off analysis indicates that the ALSA is optimum from a cost standpoint, because of its simplicity and its ability to accommodate both EVA and IVA with the same system, thus minimizing hardware. The other candidate systems are either very complex and undeveloped or developed but more complex than required for Skylab requirements, either of which involves added costs. Several of the other candidate systems also require different sets of hardware for EVA and IVA.

All combinations of PLSS are similar with respect to "spacecraft system impact" because each requires either umbilical spacecraft support or water and oxygen recharge capability.

The weight tradeoff shows that the ALSA has the greatest total launch weight and that the two closed-loop systems with pressurized cabin cooling capability (PECS and new system—oxygen/electrical/water umbilical) offer the lowest weight penalties. It is concluded, however, that the degree of weight difference between the ALSA and other systems is outweighed by the operational and cost advantages of the ALSA. Therefore, based on the guidelines of the study, the ALSA is the optimum PLSS for supporting the Skylab missions.

ALSA CONTRACT

After review of the study and assessment of Skylab requirements by various Manned Spacecraft Center organizations, it was decided to develop the ALSA for Skylab mission EVA and IVA life support.

A request for proposal was distributed, and a Source Evaluation Board was used in selecting the contractor for PCU and SOP development. Contractual effort was initiated with the AiResearch Manufacturing Company, Garrett Corporation, in January 1970. A separate request for proposal was released for the LSU, and effort was initiated in June 1970 with AiResearch. The three subassemblies (PCU, SOP, and LSU) were combined into one contract and renamed the ALSA. The Critical Design Review was held in December 1970, and the First Article Configuration Inspection is scheduled for July 1971. Unmanned qualification testing will begin in July 1971, and manned qualification testing is scheduled for January 1972.

ALSA DESCRIPTION

General Description of the ALSA

The ALSA consists of three major subassemblies: the PCU, LSU, and SOP. Figure 11.9 depicts the ALSA as worn by a suited astronaut, while figure 11.10 illustrates the ALSA schematically.

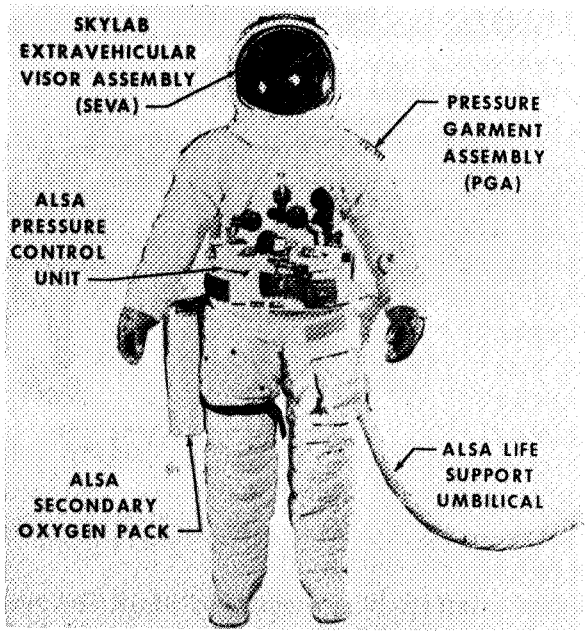

Figure 11.9 *Skylab extravehicular mobility unit.*

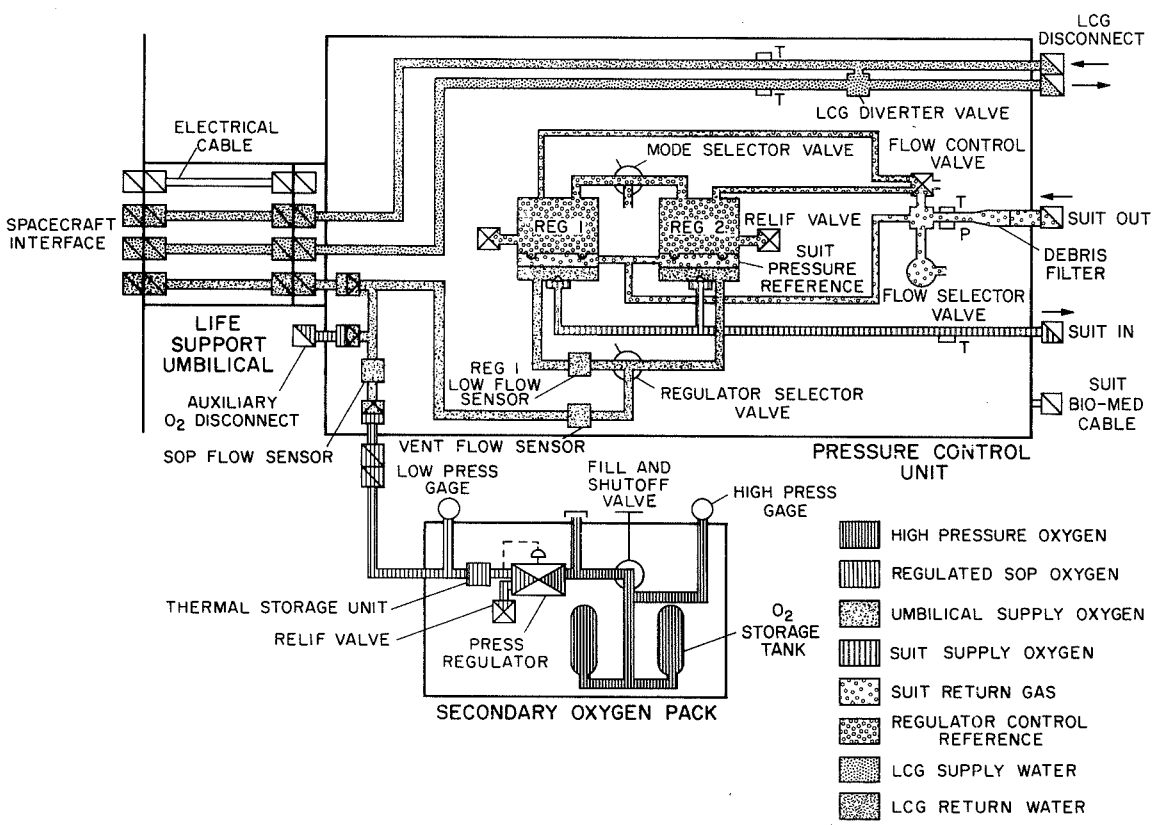

Figure 11.10 *Astronaut life support assembly schematic.*

The PCU. The PCU (fig. 11.11) provides oxygen ventilation, pressure control, cooling-water flow control, communications, instrumentation biomedical transmission, and an audiovisual warning system for a suited astronaut. The PCU provides the capability for maintaining a proper ventilation/pressurization balance for suited modes (see "Mission Modes") by receiving oxygen via a spacecraft-supplied umbilical or the SOP. Cooling water is provided to the LCG and returned to the spacecraft via the LSU; then it is routed into or around the LCG for astronaut comfort by a manually controlled water-diverter valve contained within the PCU.

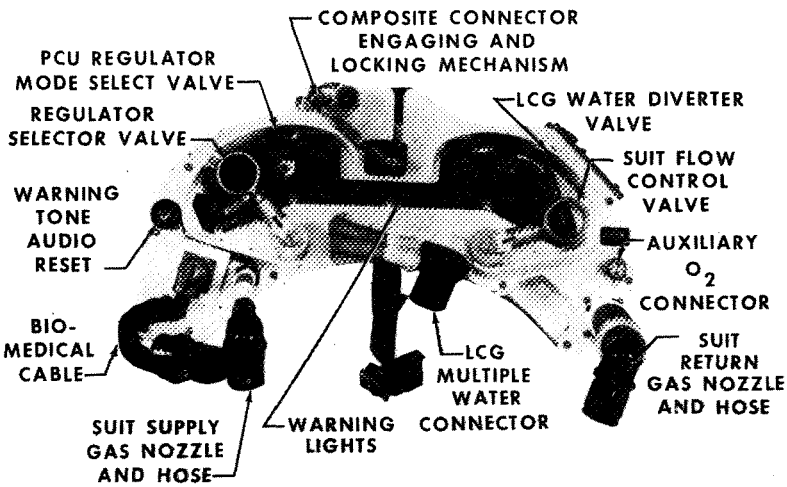

Figure 11.11 *Pressure control unit.*

The LSU. The LSU contains one oxygen hose, two water hoses, a structural restraint tether, thermal insulation and cover, and an electrical cable for providing power from the spacecraft to the PCU, voice communications, and biomedical and suit-loop instrumentation readouts to the spacecraft from the PCU. Figure 11.12 shows a coiled LSU. At the astronaut end of the LSU, each hose terminates at a disconnect, and the electrical cable terminates at the connector. The three disconnects and the electrical connector are contained in a single, composite housing, thus allowing one operation for LSU/PCU mating. The LSU spacecraft end contains quick disconnects for the oxygen and water hoses, an electrical connector for the electrical cable, and a tether hook to structurally link the astronaut to the spacecraft.

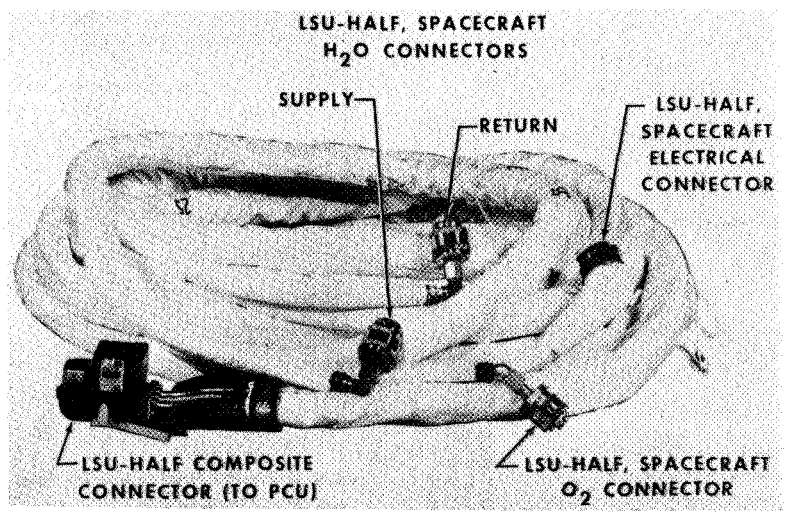

Figure 11.12 *Life support umbilical.*

The SOP. The SOP, (fig. 11.13) serves as a backup oxygen supply to the PCU in case of an insufficient supply from the LSU or an increased flow demand (beyond the capacity of the spacecraft supply) created at the pressure garment assembly (PGA) because of a tear or other off-nominal condition. The SOP provides 4.0 lb of usable gaseous oxygen, regulated to interface with the PCU pressure and temperature requirements. The SOP assembly, less gages and manual controls, is encased within a protective cover that limits the temperature extremes to which the gas

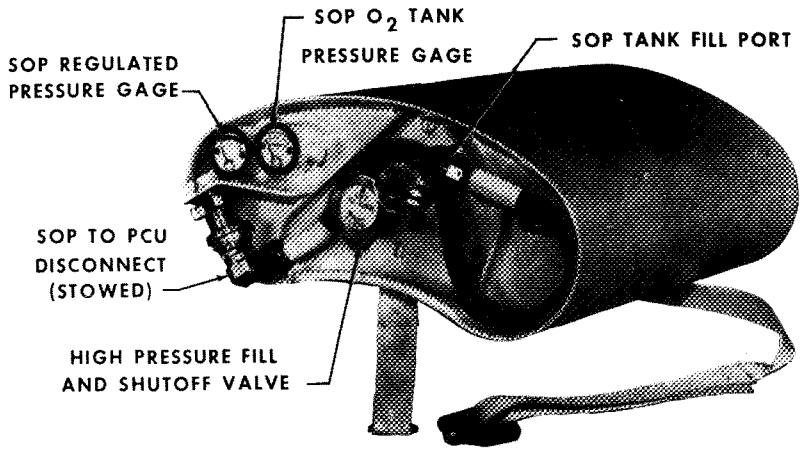

Figure 11.13 *Secondary oxygen pack.*

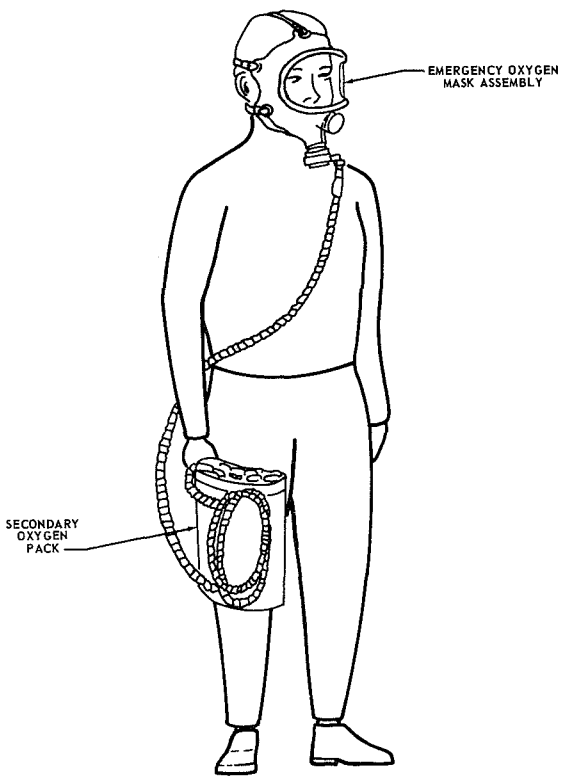

Figure 11.14 *Skylab walkaround emergency oxygen system.*

temperatures may vary during a 4-hr EVA mission. The thermal cover also serves as protection against impact or scratching of the tank outer shell and as a meteoroid protective cover for the SOP assembly.

The SOP has acquired two mission functions in addition to its basic function with the PCU. The SOP will be used in combination with an Apollo emergency oxygen mask assembly (fig. 11.14) to provide a "walkaround" emergency oxygen system for crewman protection during any atmosphere contamination occurrence. Also, the SOP will serve as the breathing oxygen supply for a suited, untethered portion of the M-509 experiment (astronaut maneuvering equipment experiment).

PCU Detailed Description

The PCU (fig. 11.10) contains the following functional subsystems:

- Oxygen circuit
  - Oxygen supply
  - Pressure regulation
  - Suit pressure circuit
  - Flow control
- Electrical circuit
  - Pressure control unit power
  - Communications
  - Biomedical
  - Suit loop instrumentation
  - Warning logic and display

Oxygen Circuit. The characteristics of the oxygen circuit follow:

Oxygen supply. Oxygen may be supplied to the PCU from any one of three sources, (1) normal LSU supply which connects to the PCU at the composite disconnect, (2) SOP supply which is connected to the PCU by a flex hose and disconnect on the bottom right side of the PCU, and (3) an auxiliary disconnect on the top right side of the PCU. This disconnect may be used to connect a second SOP to the PCU; however, it is normally not employed. The three separate connections are manifolded together, internal to the PCU. Separate filters and check valve assemblies for each

oxygen supply are provided. The check valves permit isolation of the supplies in case one of the supply lines fails. Pressure at the manifold assembly interface determines which supply will furnish oxygen to the crewman. If the supply pressure from the umbilical should decrease below SOP regulation pressure (30 to 45 psig) because of high demand flow requirements or loss of supply pressure, SOP flow will automatically commence and make up the required demand flow until supply pressure again increases to above 30 to 45 psig. The nominal maximum flow to the suit, if demanded (e.g., for a suit tear), is 27 lb/hr with an approximately 30-psia supply pressure at the pressure-flow control valve. The two flow sensors that provide a caution and warning signal, visible and audible, to the crewman are located within the oxygen supply system, upstream of the pressure-flow control valve. The SOP flow sensor, located in the SOP supply line, provides a caution and warning signal when SOP flow commences at 0.05 to 0.20 lb/hr. The low-vent flow sensor, located downstream of where the three supplies are manifolded together, provides warning to the crewman when flow decreases to approximately 5.0 lb/hr, which is insufficient for proper carbon dioxide washout.

Pressure regulation and control. Flow from the oxygen manifold proceeds directly into the pressure-flow control valve inlet selector where either (or both) of two pressure regulators may be selected for automatic control of suit pressure. An OFF position is also provided. The regulators are identical in construction and may be individually selected by the regulator selector valve for checkout or for isolation to correct a regulator failure. Suit pressure control points within each regulator are set at different levels so that when the regulator selector valve is in the BOTH position, regulator 1 is normally used to control suit pressure. Regulator 2 is used as a backup in case regulator 1 fails. A flow sensor in the regulator 1 triggers a warning REG. 1 LOW FLOW when flow decreases to approximately 3.0 lb/hr, indicating a regulator 1 failure. Each regulator can flow up to 13.0 lb/hr, with an inlet pressure of 30 psia and 0° F at the inlet. The suit-pressure reference, common for both regulators, is downstream of the suit within the debris filter housing.

Low-pressure circuit. Flow from the pressure-flow regulator proceeds to the suit via the suit-inlet hose and nozzle assembly. From the suit, exhaust gas enters a 1-in.-inside-diam hose and disconnect assembly and proceeds through the debris filter. A bypass relief valve is provided in the debris filter so that if clogging occurs, full flow will bypass the filter through the relief valve. Downstream of the debris filter, suit exhaust gas temperature and pressure are measured. A warning indicator is provided at this point for either low or high suit pressure. Audio and visual indication is given when the suit-to-ambient pressure differential has decreased to 3.2 ± 0.1 psid or increased to 4.35 ± 0.15 psid.

Flow control. Suit exhaust gas proceeds to one of four orifices within the flow control valve, which provides the capability necessary to control flow at the various cabin and suit pressures. Three of the four orifices within the flow control valve are selectable by manual control, (1) the EVA NORM position, (2) the EVA HI FLO position, and (3) the IVA position. The fourth orifice is controlled by a shuttle valve that references ambient pressure on one side of a diaphragm within the valve and suit-pressure-regulator reference pressure on the other side of the diaphragm. The valve begins to shuttle closed when suit-to-ambient differential is approximately 1 psid, thus providing the proper oxygen flow rate when the suit is pressurized from a soft suit mode. Downstream of the flow control valve orifices, an annular exhaust section is provided that vents exhaust gas overboard through vent holes within the PCU. These vent hoses are placed such that venting is thrust canceling.

Water Circuit. The ALSA/spacecraft cooling-water circuit is a closed-loop system. Water cooled by the AM cooling system enters the PCU via the LSU, at the composite disconnect with a maximum pressure of 37.2 psig and a maximum flow rate of 250 lb/hr. The water system within the PCU has two functions, (1) to transport water from the umbilical to the LCG and (2) to provide supply-water diversion from the LCG via the water diverter valve. The diverter valve provides from 0 to 100 percent flow bypass capability of the LCG. The valve is manually controlled and is accessible to the suited crewman. The flow schematic for the water circuit is shown in figure 11.10. As shown, water supply and return to the LCG are accomplished through two hoses and a single disconnect assembly. Temperature sensors, located in the PCU, monitor LCG inlet temperature and diverter valve mixed-return-water temperature.

Electrical System. The characteristics of the electrical system follow:

PCU power. Spacecraft electrical power (25 to 30 V dc and maximum current of 2.0 A) is provided to the PCU via the LSU. A single electrical connector for all LSU electrical conductors is provided at the composite disconnect. The PCU will withstand over and under voltage variations of 3.0 V from the steady-state upper and lower limits, without damage, for a maximum period of 1 sec.

Communications. Voice communications between the spacecraft and the suited crewman are transmitted and received via the biomedical cable (PGA electrical interface to the PCU), PCU internal wiring, and the LSU electrical cable.

Biomedical. Biomedical data are transmitted to the spacecraft via the biomedical cable, PCU internal wiring, and the LSU electrical cable.

Suit loop instrumentation. The control module within the PCU continuously receives and conditions the signals from the following suit loop sensors:

The PGA inlet gas temperature
The PGA outlet gas temperature
The PGA pressure
The LCG water inlet temperature
The LCG water outlet temperature

Each suit loop parameter voltage analog is provided by the control module to the PCU internal wiring and is then transmitted to the spacecraft via the LSU electrical cable.

Warning logic and display. The control module continuously monitors and evaluates the ALSA performance, based upon signals from the following sensors:

Suit pressure
Regulator 1 flow
Secondary oxygen pack flow
Vent flow

The suit pressure transducer is in the debris-filter-assembly duct, downstream of the suit. The regulator 1 flow sensor is between the regulator selector and the regulator 1 inlet. The SOP sensor is in the oxygen manifold, downstream of the SOP check valve. The vent flow sensor is between the oxygen manifold and the regulator selector valve.

The control module signal conditioning and logic will provide a 1.7 kHz modulating warning tone to the suited crewman if any of the following events occur:

Low or high suit pressure
Regulator 1 low flow
Secondary oxygen pack flow
Low vent flow

Coincident to the warning tone, the appropriate event warning message on the display panel (mounted on top of the PCU and visible to the suited crewman) will illuminate (fig. 11.11). The warning messages displayed from left to right are suit pressure, regulator 1 low flow, SOP flow, and low vent flow. The suited crewman may turn off the warning tone by depressing the RESET switch on the top left of the PCU. The illuminated warning message, however, will stay illuminated as long as the off-nominal conditions exist. All warning message lamps and their respective lamp drivers, the warning logic, and the warning tone generator may be tested by depressing the TEST switch on the bottom right of the PCU.

LSU Detailed Description

The LSU provides the following functions: (1) transports gaseous oxygen from the spacecraft to the PCU for ventilation and pressurization of the PGA, (2) serves as a cooling-water supply and return between the spacecraft and the PCU, (3) couples voice communications, biomedical, and other instrumentation readouts from the suited astronaut to the spacecraft, (4) provides structural linkage between the spacecraft and the astronaut, and (5) supplies spacecraft power to the PCU.

Figure 11.15 illustrates schematically how these functions are provided, while figure 11.12 is a photograph of the coiled LSU. The LSU is 60 ft long, with a diameter of approximately 1.75 in.

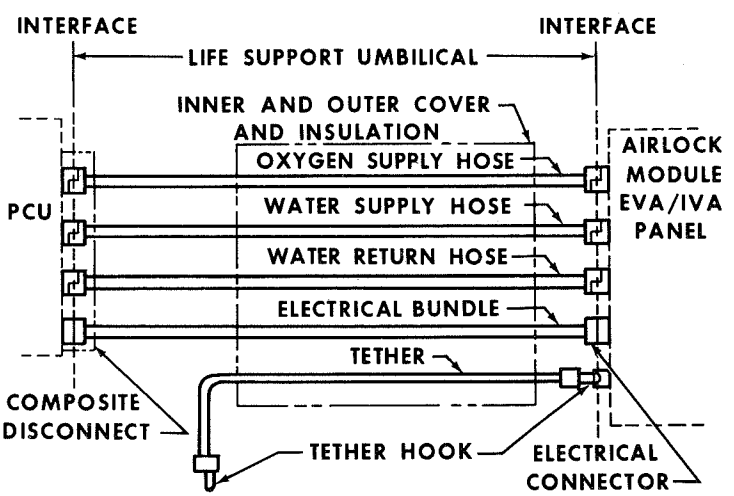

Figure 11.15 *Life support umbilical schematic.*

Oxygen Supply Hose. The oxygen supply hose is flexible, silicone rubber, and metal reinforced with an outer covering of Viton-coated Beta glass. The hose has a 0.25-in. internal diam and a 0.11-in. wall thickness. The B-nut fittings are molded into the hose ends for quick-disconnect attachment.

Water Supply and Return Hoses. The water supply and return hoses are identical to the oxygen supply hose described previously except that the internal diameter is 0.375 in. rather than 0.25 in. Quick disconnects are attached to the B-nut fittings molded into the hose ends in the same manner as on the oxygen supply hose.

Electrical Cable Assembly. The electrical cable assembly provides the interface between the PCU and the spacecraft for electrical power, communications, and instrumentation. The electrical cable consists of two connectors, wires, and two layers of Beta glass covering to isolate the cable from the other parts of the LSU.

Tether Assembly. The tether assembly serves as a structural connection between the suited crewman and the spacecraft. This assembly is shorter than the LSU assembly to prevent undue loads from being applied to the hoses or electrical wires. The tether is made from Nomex webbing. Quick-release hook assemblies are fastened to each end, allowing attachment of the tether to the PCU/PGA and to the spacecraft.

Cover Assembly. The cover assembly provides thermal and micrometeoroid protection to the enclosed hoses, electrical cable, and tether. The cover is loosely fitted around the assembly to allow relative action between hoses, electrical bundle, and tether to prevent wear at local stress points during use and to provide flexibility. The protective cover (from inner to outer) consists of an inner cover, two layers of gold-coated Kapton separated by one layer of Beta marquisette, six layers of aluminized Kapton separated by layers of Beta marquisette, two more layers of gold-coated Kapton separated by Beta marquisette, and an outer cover. The inner and outer covers are fabricated with Teflon-coated Beta glass. This assembly is fabricated in a flat pattern and then hand stitched around the umbilical assembly.

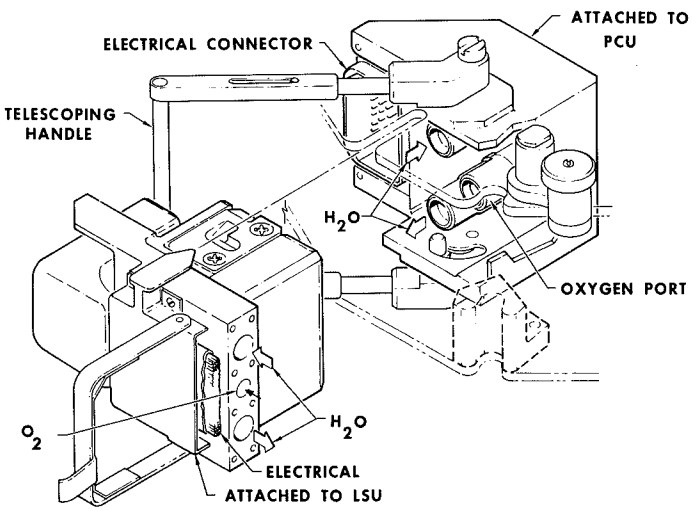

Figure 11.16 *Composite disconnect.*

Composite Disconnect. The LSU half of the composite disconnect provides a single operation for PCU attachment and detachment. This single operation connects the water lines, oxygen line, and electrical cable to the PCU corresponding subassemblies. An isometric drawing of the composite disconnect is shown in figure 11.16. Connection to the PCU is made by inserting the LSU half of the composite disconnect into the PCU half and operating the handle extension on the PCU. This single manual operation cams the two halves together and locks them in place, completing the connection.

SOP Detailed Description

The SOP is used as a backup oxygen supply for the PCU in case of an insufficient supply from the spacecraft/LSU or in the event of an increased flow demand beyond the capacity of the LSU due to a PGA tear or other off-nominal occurrence. The SOP provides 4.0 lb of usable gaseous oxygen, regulated to interface with the PCU pressure and temperature requirements. Figure 11.17 is a schematic illustration of the SOP, and figure 11.13 shows the external design of the SOP.

High-Pressure Circuit. The SOP high-pressure circuit consists of two oxygen tanks, a 0- to 10,000-psig pressure gage, a fill and shutoff valve, a pressure regulator, and interconnecting plumbing.

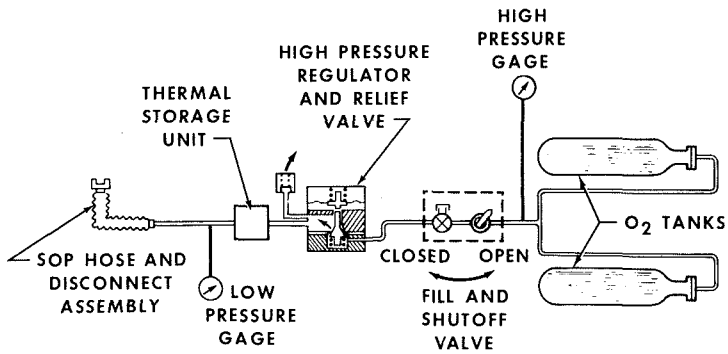

Figure 11.17 *Secondary oxygen pack schematic.*

Oxygen tanks. Each tank is fabricated of Inconel 718 and incorporates internal copper fins that are brazed to the internal wall of the tanks. The copper fins are required to provide sufficient heat transfer from the tank wall to the fluid during tank blowdown from 6000 to 200 psig such that gas discharge temperature is maintained above -20° F throughout this period. The tank is designed to fracture mechanics criteria; that is, a leakage failure mode will occur rather than a rupture or fragmentation failure at maximum operating pressure.

High-pressure gage. The high-pressure gage is used to monitor the oxygen pressure in the high-pressure oxygen tanks before and during use.

Fill and shutoff valve. The fill and shutoff valve is used to fill the high-pressure oxygen tanks with 6000 psig of gaseous oxygen and also provides a means of isolating the tanks after filling and during storage.

High-pressure regulator. The high-pressure regulator controls downstream pressure to 30 to 45 psig during flow (up to 13 lb/hr), while inlet pressure to the regulator may vary from 200 to 6850 psig. The unit contains a metal diaphragm-operated poppet metering valve. Regulated pressure is a result of force balance or unbalance on the metal diaphragm.

Low-Pressure Circuit. The low-pressure circuit of the SOP consists of the regulating and relief section of the high-pressure regulator, the thermal storage unit, the low-pressure gage, and the SOP hose and disconnect assembly. Normal operating pressure of the circuit is 30 to 45 psig maximum.

Pressure regulation. The high-pressure regulator (see previous section "High-pressure regulator") is capable of supplying from 0 to 13 lb/hr to the PCU at a regulated pressure of 30 to 45 psig; the inlet pressure to the regulator is 200 to 6850 psig. Within the regulator assembly, on the low-pressure side, is a relief valve that limits the regulated pressure with a failed-open regulator condition.

Thermal storage unit. The thermal storage unit is a 3-lb aluminum block with manifolds at each end and 21 flow-through passages each 0.25-in. diam. The oxygen from the high-pressure regulator valve enters the unit, makes one pass through the unit, and flows out the other side. The gas is warmed approximately 15° F during blowdown, and the aluminum block is cooled down to the exit gas temperature. The unit is also utilized as part of the support structure for the SOP assembly. It is centrally located between the two oxygen tanks.

Low-pressure gage. The low-pressure gage is used to monitor the regulated oxygen pressure or lockup pressure from the high-pressure regulator before and during use of the SOP. It is a 0- to 150-psig bourdon-tube-type gage.

Hose and disconnect. The SOP hose and disconnect assembly mates to the PCU disconnect and enables easy disengagement of the SOP from the PCU. The disconnect is self-sealing to prevent loss of oxygen and to prevent contamination of the SOP when disconnected from the PCU. When mated, the disconnects form a zero-leakage minimal-inclusion flow-through fitting assembly. The SOP hose is 18 in. long and similar to the LSU oxygen supply hose. It is covered with a fire protection cover consisting of two layers of Beta glass.

CONCLUSIONS

Based on evaluation thus far, it appears that the astronaut life support assembly accommodates all Skylab mission requirements and that the optimization study conclusions are valid. For example, evaluation of high-fidelity mockups indicates the astronaut life support assembly is favorable from a crewman's usefulness standpoint and that minimizing the expendables carried by the crewman for near-spacecraft-type extravehicular activity is the most desirable approach.

Also, it is concluded that the comparative study approach as described herein is a reasonable method for choosing an optimum portable life support system for any particular space program.

12

ADVANCED DEEP SEA DIVING EQUIPMENT

William A. Danesi
General Electric Company
Ocean Systems Programs
Philadelphia, Penn.

INTRODUCTION

As a result of recommendations of several committees convened by the U.S. Navy supervisor of diving for the purpose of reviewing conventional Navy diving equipments, General Electric Company proposed a deep sea diving system development program to the Navy. This program, a proposal for the survey and engineering evaulation of deep sea heavy duty diving equipment, was approved by the Navy on February 2, 1970, and the program was initiated.

The overall goal of this program is to equip the Navy salvage diver with equipment and tools that will enable him to perform work of the same quality and in times approaching that done on the surface.

MARK V DIVING SYSTEM

Mark V denotes two distinct deep sea diving systems. The air outfit (fig. 12.1) is for heavy duty diving and is issued to vessels and shore activities whose function is to undertake extensive salvage operations. The helium oxygen outfit is a special system issued only to submarine rescue units. The

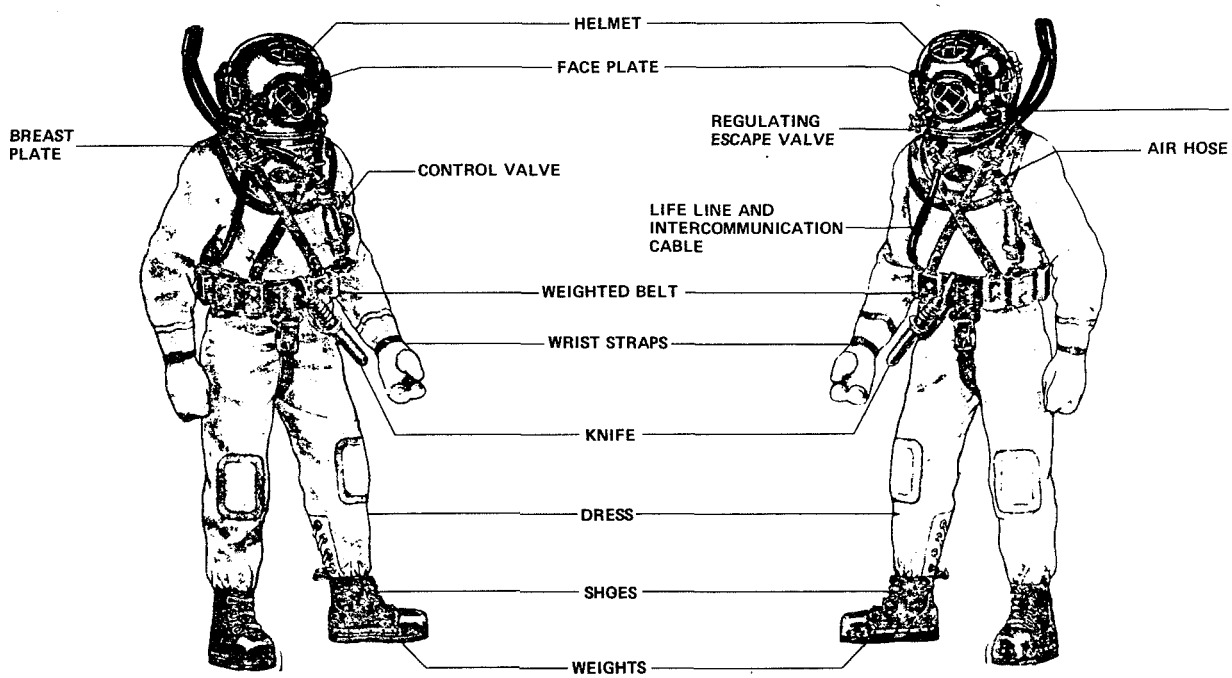

Figure 12.1 *Deep-sea diving outfit.*

deep sea diving outfit consists of the helmet and the dress, which provide water tightness; weights for overcoming positive buoyancy gained by the volume of the helmet and the inflated dress; hoses and control valves for furnishing air; and a nonreturn valve used to prevent seawater from entering and air from escaping from the dress in the event of accidental rupture of the air hose. This Mark V system has been used for many years with remarkable success. In addition to all submarine rescue and salvage work undertaken in peacetime, practically all salvage work of any extent undertaken during World War II was accomplished with this equipment. The system is designed for extensive, rugged diving work and provides the diver with maximum physical protection. It is now used in general types of work such as submarine salvage, initial inspection, placing moorings, attaching hose for blowing and venting, ship salvage underwater inspection, internal repairs, installation of patches on ship hulls, construction of dams, harbor work, and other standard industrial and commercial forms of diving. There are also many diving operations undertaken with this equipment in shallow depths in which the rugged equipment provides protection for the diver. It is a fact that today, more than 100 years after its basic development, the "hard hat" diving system is essentially unchanged in form; yet it is still the standard for salvage diving throughout the world.

The Navy standard diving helmet consists of a spun copper helmet with its fittings and a breast plate (fig. 12.2). The interface between the helmet and the breast plate is an interrupted thread breech joint. There are four viewports on the helmet. The one directly in front of the divers face is the faceplate. The faceplate is hinged and held in the closed position by a swing bolt and wing nut. All four ports are protected from breakage by metal guards. Inlet air is controlled by a regulating valve attached to the air supply hose and fixed to the breast plate. A regulating exhaust valve controls the internal pressure of the helmet and the flow of gas from the helmet.

The helmet has many good features that account for the high degree of acceptance throughout the world diving community. However, apart from some modifications in response to advances in technology, until now no overall system study had been undertaken to update the equipment in light of new materials and advances in fabrication technologies, and little attention had been given to new requirements for the function of diving.

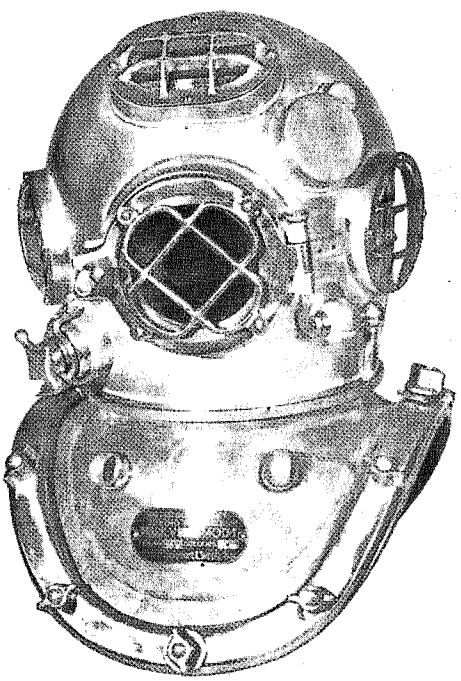

Figure 12.2 *Diving helmet and breast plate.*

PROGRAM TASKS

The overall program was divided into four tasks (fig. 12.3). Initially, a survey was performed to determine the extent of equipment development and the areas where there had been significant improvements in existing equipment. A preliminary system design was evolved with the objective of correcting the deficiencies noted in existing equipment and improving the design to meet the new requirements. In the third task, now in process, sufficient component testing was identified to demonstrate that the system deficiencies could be overcome. This task also includes the final

TASK 1 – SURVEY AND RECOMMENDATIONS

TASK 2 – PRELIMINARY DESIGN

TASK 3 – CRITICAL COMPONENT TEST

TASK 4 – PROTOTYPE SYSTEM FABRICATION AND TEST

Figure 12.3 *Program plan.*

WRITTEN QUESTIONNAIRE – 88 OF 150 REPLIED

VISITS: 8 U.S. DIVING COMPANIES

8 U.S. EQUIPMENT MFGRS

10 FRENCH DIVING & MFG

4 GERMAN DIVING & MFG

5 ITALIAN DIVING & MFG

8 BRITISH DIVING & MFG

Figure 12.4 *Equipment survey.*

definition of the recommended system, by drawings and specifications. Finally, a prototype system is to be fabricated and delivered to the Navy for evaluation in the field.

EQUIPMENT SURVEY

Two basic objectives were established for the survey: to achieve sufficient depth to obtain significant information, and to obtain a proper interpretation of the results. An extensive list of diving companies and equipment manufacturers was generated, which included as wide a range of types of diving as possible. This was quite difficult in the United States, since more than 90 percent of the major diving companies are engaged almost exclusively in oil and offshore support diving. To ensure that the information would be meaningful, the survey was divided into phases and activities. Initially, selected diving firms were visited to obtain the information required. The remaining diving firms were sent a questionnaire. Of 150 companies queries, 88 responded to the questionnaire (fig. 12.4). Of the total number of commercial divers in the United States, the survey records pertinent diver equipment information from more than 1000 active commercial divers. The second part of the survey entailed questioning the equipment manufacturers. Their design rationales were referenced to divers requirements to determine the appropriateness of the design features. The survey also included a survey of the European diving community. Because of timing and geographical limitations, the overseas survey was less detailed than the domestic portion, but the data were essentially complete.

The survey concluded that the most significant and varied developments in heavy duty diving breathing equipment have occurred in the United States. The advances have been achieved by a small group of low volume equipment manufacturers at their own initiative and expense. Little testing of these devices has been done and it is difficult to compare their performance since all have resulted from different interpretations of the requirements for the designs.

Significant improvements have been made in diver dress in the European diving community particularly in the area of heating and in general diver comfort.

The present Mark V diving system, or a modification of it, is the standard equipment for heavy duty salvage operations throughout the world. There is considerable area for improvement of the many features of this equipment, however, this improvement must be based on the operational parameters of the Mark V system.

SURVEY RESULTS

The results of the survey are published in reference 1. Since the survey was conducted on a subjective basis, and since divers, justifiably, have very strong opinions regarding the attributes of their equipment, the survey sometimes resulted in widely divergent opinions on some features. However, a number of inadequacies in present equipment were identified and efforts were initiated to correct these situations (fig. 12.5).

- NOISE REDUCTION
- IMPROVE RECIRCULATION
- SELF DONNING
- POSITIVE RESERVE GAS
- BETTER MATERIALS
- LINEAR CONTROL VALVES
- AIR OR MIXED GAS
- IMPROVED WEIGHT MATRICES

Figure 12.5 *Areas of improvement.*

Nearly all divers complained about excessive noise within their helmet and gas system. This did not imply that they desired all noise eliminated. The psychological and safety aspects of hearing gas flowing are quite important. However, a number of divers found it necessary, when using certain equipment, to turn the gas supply off to permit communication—a very dangerous practice.

The process of gas circulation and recirculation varied widely in all of the systems studied. The flow of gas within the helmet performs two functions. One is the removal of carbon dioxide and replenishment of oxygen, and the second is clearing the window ports of moisture to permit visibility. In the recircular mode of operation described later, the ratio of recirculated gas to inlet gas must be maintained as high as possible, over a range of inlet flows.

The Mark V and many commercial systems are of such weight and complexity that they require the assistance of a tender to dress the diver. As diving from habitats increases, the diver must be able to dress in cramped, confined spaces.

The divers prefer the large volume common to the Mark V helmet because it provides a reserve should the gas supply be cut off. Almost all divers tell of ration-breathing gas from the helmet in emergency conditions—a capability unavailable in a mask. However, it takes an exceptionally trained person to take maximum advantage of this reserve gas.

New materials and material fabrication techniques have generally been ignored in most designs of the diving equipment surveyed. New materials are being used, but they rarely are tailored specifically to the total application.

The control valves were mainly selected from those available at standard valve suppliers. However, very few commercially available valves are required to control precisely over both a wide range of flows and a fairly wide range of inlet pressures.

The Mark V system for air is considerably different, lighter, and much less cumbersome, than the system for mixed gas operation. Most commercially available mixed gas helmets can be used for air operation but not the converse. No single helmet was found that was designed to operate efficiently with both gas combinations.

Significant areas of improvement were identified for the allocation and positioning of weights to control buoyancy and mass properties of the diver in the water and yet allow him mobility on the surface.

From the results of this survey and an assessment of the areas of required improvement a system design requirement was generated (fig. 12.6). The first four parameters delineate the conventional diving environment. The last seven are goals to be achieved in a single diving system design. It was

found that many of the diving systems were designed by divers with a particular mission in mind or a particular improvement desired. Necessary functions of the helmet, such as provisions for communication, were all too often ignored until after the helmet was designed, and then added as an afterthought.

- SINGLE SYSTEM – AIR OR MIXED GAS
- DEPTH – SURFACE TO 1500 FEET
- TEMPERATURE – SURFACE –20°F TO +110°F
  – WATER 28° F TO 96°F
- WATER – PURE
  – SALT
  – POLLUTED
- SIMPLE
- SAFE
- COMFORTABLE
- MOBILE
- MAINTAINABLE
- VERSATILE
- DURABLE

Figure 12.6 *System design requirements.*

THE DIVING SYSTEM

The system (fig. 12.7) consists of a helmet, a recirculator for removing carbon dioxide and economizing on gas, and the diver's dress. The dress includes a comfortor for distributing the weight of the helmet over the divers shoulders. Over the comfortor is a standard diver's dry suit, which interfaces with the neck ring. Over the dry suit is a nylon coverall with straps and belts to accommodate the weights, which are distributed low on the diver's waist and on his thighs. He also wears molded rubber boots with integral weights.

The combination of the coverall and the comfortor is designed to distribute the weight uniformly over the diver's body for comfort and mobility on the surface, and to minimize weight shift in the water. Each diver can adjust the straps on the coverall to his own stature and minimize the time and adjustments required to dress. The color of the coverall can be changed to permit covert operations, high visibility, etc. The coverall also serves the function formerly performed by chafing gear. The coverall will also contain a pocket for a smaller version of the bailout bottle when the rig is

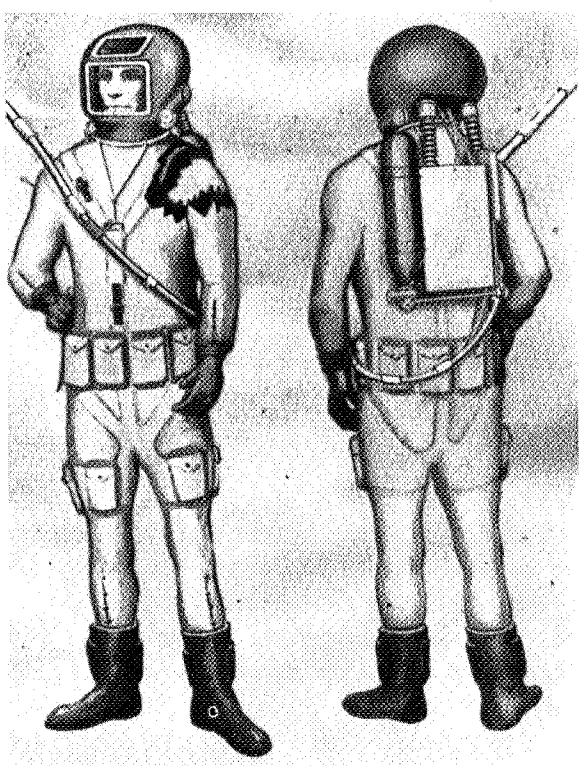

Figure 12.7 *Diving system.*

used for air diving. Weights are placed in the pocket and can be varied according to the dress and support equipment.

The recirculator is covered by a shroud to minimize hydrodynamic drag if the diver is in strong currents or moving about. It is, however, not a swimmable system as such. The shoes are rubber with steel foot and toe protection. The foot pad is corrugated rubber and has a definite breakpoint to permit foot movement while walking on rough or slippery surfaces.

The diver dons his insulated undergarment and places the comfort ring on his shoulders. He then enters his dry suit with the neck ring already attached. The dry suit has a back entry with a waterproof zipper. The diver then puts on his coveralls and attaches the cinch cables on the neck ring. Finally, he adjusts his cable and belt tensions to the required fit. At this point, he may have his weights in place or not, depending on his desire for mobility. Just before the dive he places his helmet in position, rotates it, and locks. He is ready now to dive.

The system is designed to be compatible with all types of swim dress (fig. 12.8). The interface in all instances is the neck ring. If the user dives without a suit, a conventional neck seal is attached to the neck ring at the same interface.

- DRY SUIT
- CONSTANT VOLUME SUIT
- WET SUIT
- NO SUIT
- ADVANCED SUITS
  - HEATED
  - SUPER INSULATIVE

Figure 12.8 *Diver dress compatibility.*

WEIGHT	26.83 LBS
VOLUME (TOTAL)	0.67 FT^3
VOLUME (FREE)	0.57 FT^3
BUOYANCY	16 LBS POSITIVE
FLOW – AIR	0–140 ℓ/MIN (5 FT^3/MIN)
– MIXED GAS	0–140 ℓ/MIN (5 FT^3/MIN)
CONTROL VALVE	3 TURN-NEEDLE
SOUND LEVEL	< 90 db
WINDOWS	3/16" LEXAN
MATERIALS:	
SHELL	GLASS EPOXY
BREECH	316 SS
VALVES	PLATED BRASS

Figure 12.9 *Helmet.*

The design of the helmet (fig. 12.9) and recirculator will be covered in some detail because they are the major factors affecting the ability to provide a system that meets the goals of the program.

The helmet weight selection is based on several factors, particularly the tradeoff of handling and inertia against buoyancy considerations. The center of gravity and center of buoyancy must be maintained at the same point so that when the diver moves his head underwater the helmet will follow his movement, not resist. The volume of the helmet is sufficient to permit head movement, both to reduce fatigue and to take advantage of the window position, particularly that of the top window. Airflows are compatible with the acceptable values for minimizing the collection of carbon dioxide in dead areas. The inlet valve will allow linear control of the flow evenly across the three turns. Sound levels are set by acoustic standards to permit 8 hr of work without fatigue or irritation.

SYSTEM OPERATION

Taking a front view of the helmet (fig. 12.10), the inlet air control is on the left (diver's right) and the exhaust control on the right. The diver has easy access to the valves even when the suit is inflated. The valves are snagproof yet have positive grip profiles. The window is easily removable when scratched or damaged. The communications interface is just below the window in a recess especially provided to keep the pickup out of the air stream.

When operating open cycle (fig. 12.11) the gas flows from the inlet fitting to the control valve in a tube along the inner wall of the helmet. Expansion chambers are provided for muffling and acoustic deadening. A distributor with a sintered metal filter reduces inlet air noise and flows the gas uniformly across the window for moisture removal. All plumbing for the open-cycle operation is easily removable for maintenance and cleaning and is fabricated from standard parts where possible. The sintered filter is removable for easy cleaning and replacement.

When the recirculator is in operation (fig. 12.12), gas is gradually expanded after it enters the helmet. The gas progresses across the window and enters the circulator inlet tube. As this gas leaves the helmet it passes through a venturi, which aspirates gas from the perforated tube in the bottom of the helmet. Thus, any carbon dioxide accumulating near the neck ring is swept out into the scrubber.

The comfortor supports the neck ring but is not directly attached (fig. 12.13). When the diver enters the water the helmet is likely to float a fraction of an inch above the comfort ring (fig. 12.14).

The recirculator consists of a scrubber to remove carbon dioxide, an inlet to receive the mix gas supply and trap the excess water, a venturi to recirculate and mix the gas from the scrubber with the inlet gas, and connection fittings to the helmet hoses (fig. 12.15). An expansion chamber above the venturi is designed to minimize noise

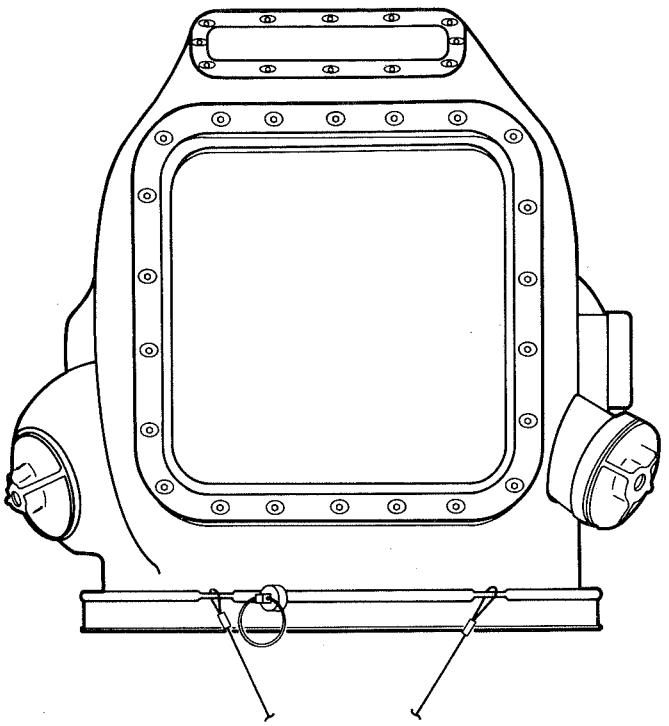

Figure 12.10 *Front view of helmet.*

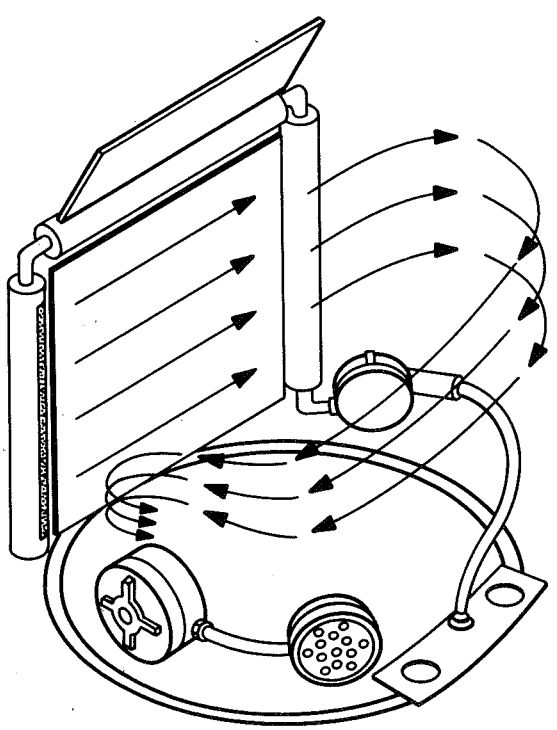

Figure 12.11 *Flow pattern open cycle.*

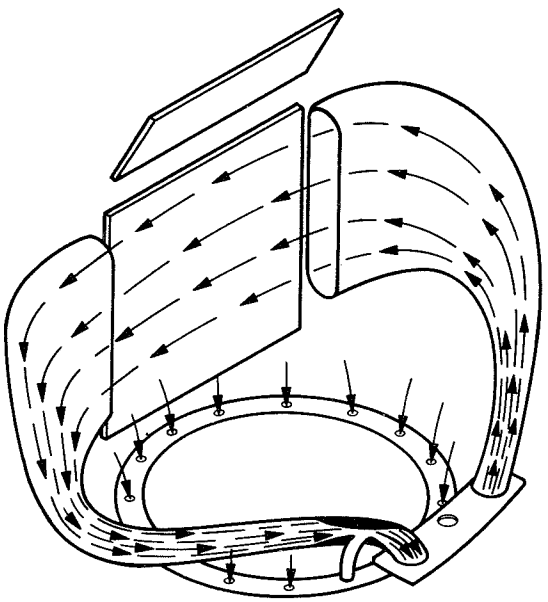

Figure 12.12 *Flow pattern recirculator.*

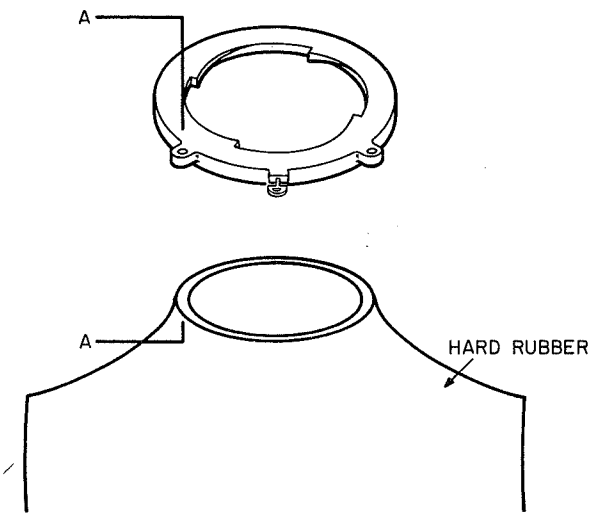

Figure 12.13 *Comfort ring.*

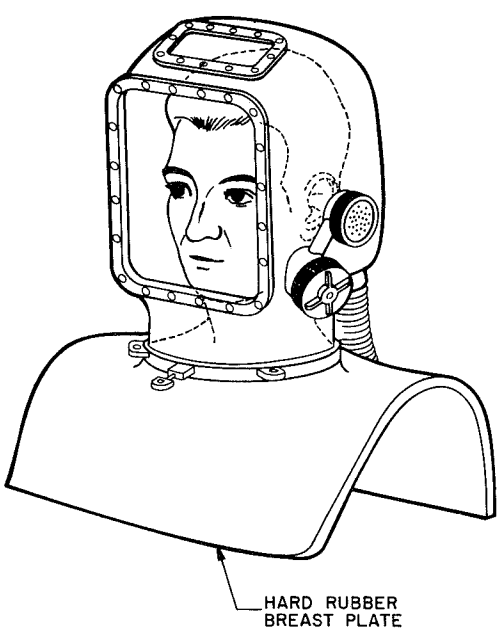

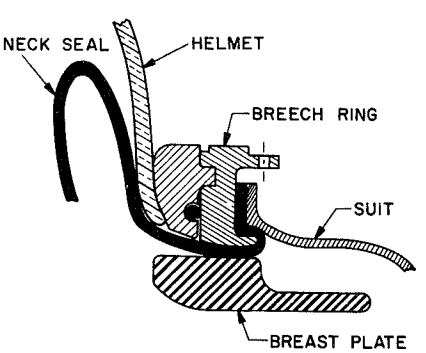

Figure 12.14 *Comfort ring attached.*

VALVES	
RECIRC.	OPEN
GAS INLET	CLOSED
EXHAUST	CRACKED
"K" VALVE	CLOSED

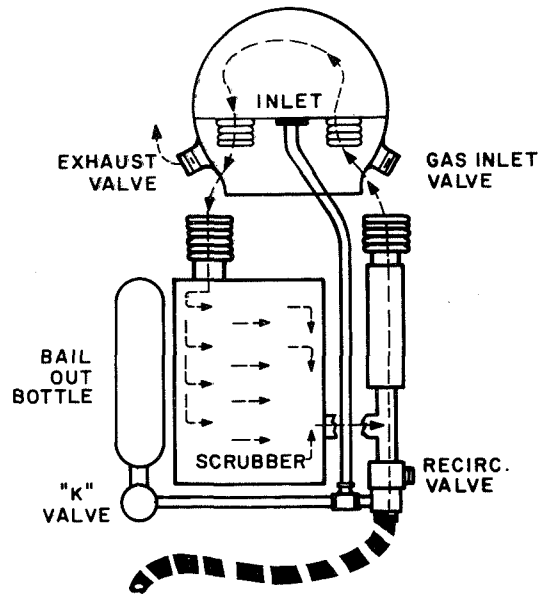

Figure 12.15 *Normal recirculator mode.*

generation by the aspirator. A bailout bottle is provided to supply emergency breathing gas. A check valve is provided at the air inlet to shut off flow if the pressure drops below ambient. In normal operation, the supply gas enters the venturi and is augumented by a factor of about 10 times by the aspiration action. The gas then enters the helmet, crosses the front of the divers face and across the window, and exits to the recirculator return line. The gas is then drawn into the scrubber by the pressure drop of the venturi and the cycle is continued.

The diver controls his inlet flow by the recirculator control valve. The exhaust valve pressure is then adjusted to vent the excess gas.

Should a malfunction occur in the venturi or in the scrubber, the diver can change to open-cycle operation by opening his air control and exhaust valves, and closing his recirculator valve (fig. 12.16). The gas will then follow the normal air flow for open-cycle operation.

If the air supply is interrupted, the diver can open his bailout bottle valve and continue operation in the normal recirculator mode (fig. 12.17). Should the diver lose his gas supply to both the recirculator and the scrubber, he can change to open-cycle emergency mode and return to the surface or to his habitat (fig. 12.18). In this case, he opens his bailout bottle valve, the gas inlet control, and his exhaust valve.

Recirculator performance is summarized in figure 12.19. Flow rates are compatible with the interface flows in the helmet. The absorbent selected for the design is baralyme. The specification duration is the minimum at - 28° F and over 10 hr at normal or higher temperatures. The reserve gas capacity depends on depth: It will allow only two breaths at 1000 ft on open cycle, but should be sufficient to permit the diver to return to his bell or habitat.

The key to recirculator operation is the proper function of the scrubber (fig. 12.20). The scrubber is designed to maximize the dwell time in contact in the absorbent and to minimize temperature and humidity effects. Return gas enters the scrubber inlet and is distributed across the bed by a porous screen. The gas then passes through the bed and traverses the front of the scrubber where it is drawn into the venturi. The low gas velocity in the front and back areas minimize heat transfer from the sea into the absorbent bed and allow the bed to come to, and maintain, an

VALVES	
RECIRC.	CLOSED
GAS INLET	OPEN
EXHAUST	OPEN
"K" VALVE	CLOSED

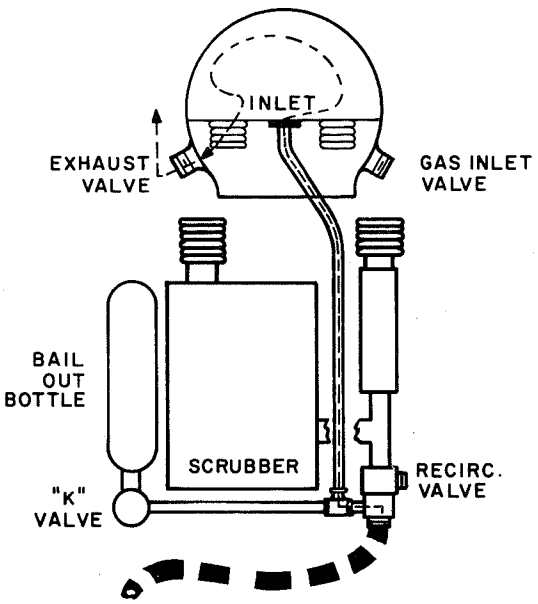

Figure 12.16 *Open cycle (surface).*

VALVES	
RECIRC.	OPEN
GAS INLET	CLOSED
EXHAUST	CRACKED
"K" VALVE	OPEN

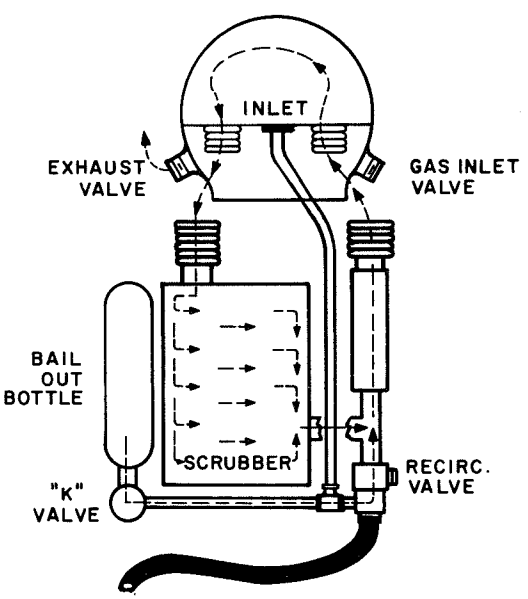

Figure 12.17 *Emergency recirculator.*

VALVES

RECIRC.	CLOSED
GAS INLET	OPEN
EXHAUST	CRACKED
" K" VALVE	OPEN

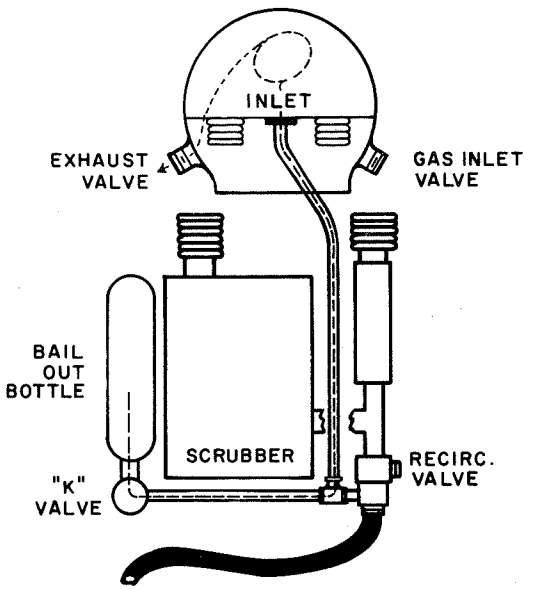

Figure 12.18 *Emergency open cycle.*

WEIGHT		45 LBS.	RECIRCULATION RATIO		>10:1
BUOYANCY		NEUTRAL	ABSORBANT		BARALYME
FLOW	– INLET	0–14 ℓ/MIN	DURATION		4–6 HOURS
	– RECIRCULATION	0–140ℓ/MIN	RESERVE GAS		18 S. CU. FT.

Figure 12.19 *Recirculator.*

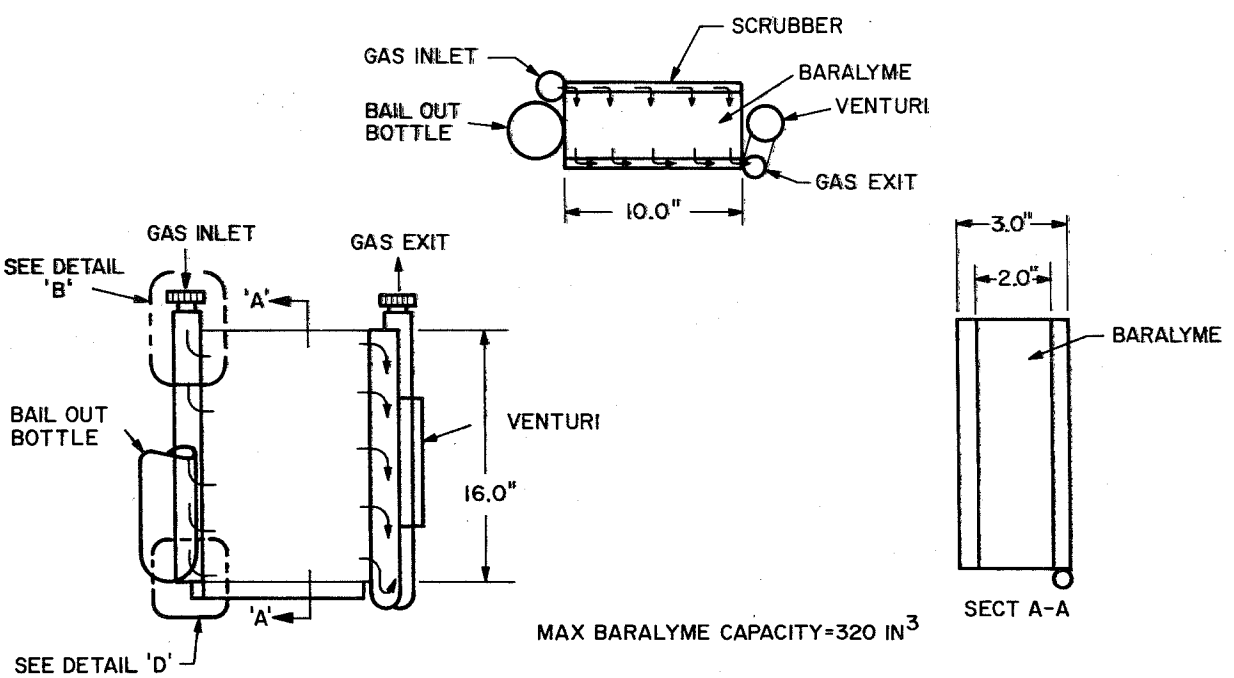

Figure 12.20 *Scrubber.*

optimum operating temperature. The scrubber inlet has a trap to remove moisture from either the helmet or the breathing gas (fig. 12.21). The trap prevents this moisture from entering the plenum occupied by the porous filter, and prevents clogging of the filter by moisture.

Water is collected in the lower collection tube and kept in place by a simple labyrinth design (fig. 12.22). The accumulated water may be drawn off on the surface by removal of the end cap.

The scrubber is designed to be constructed simply and economically (fig. 12.23). A single multichannel extrusion forms four of the sides providing flanges, holders for the porous plates, and guards to prevent bypass of gases through the bed.

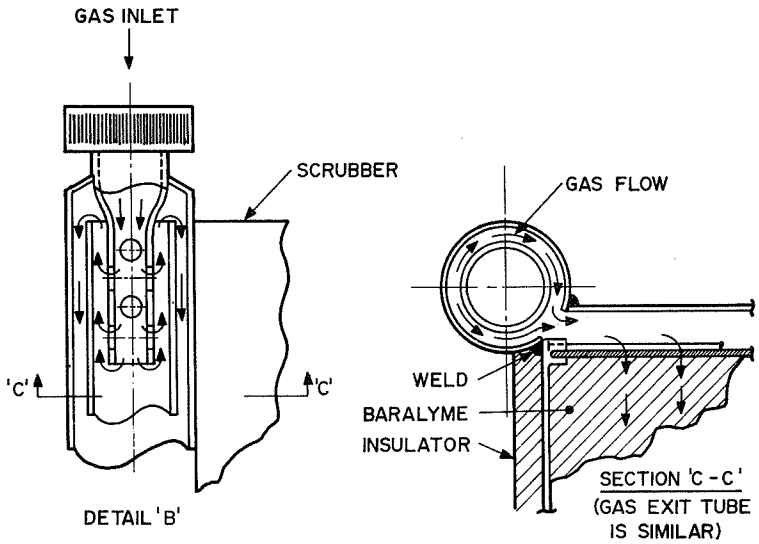

Figure 12.21 *Scrubber inlet details.*

The scrubber shown is a test scrubber to permit sizing of the bed and optimizing operational parameters. Exact dimension and design of this and other parts will be completed when the component test is completed.

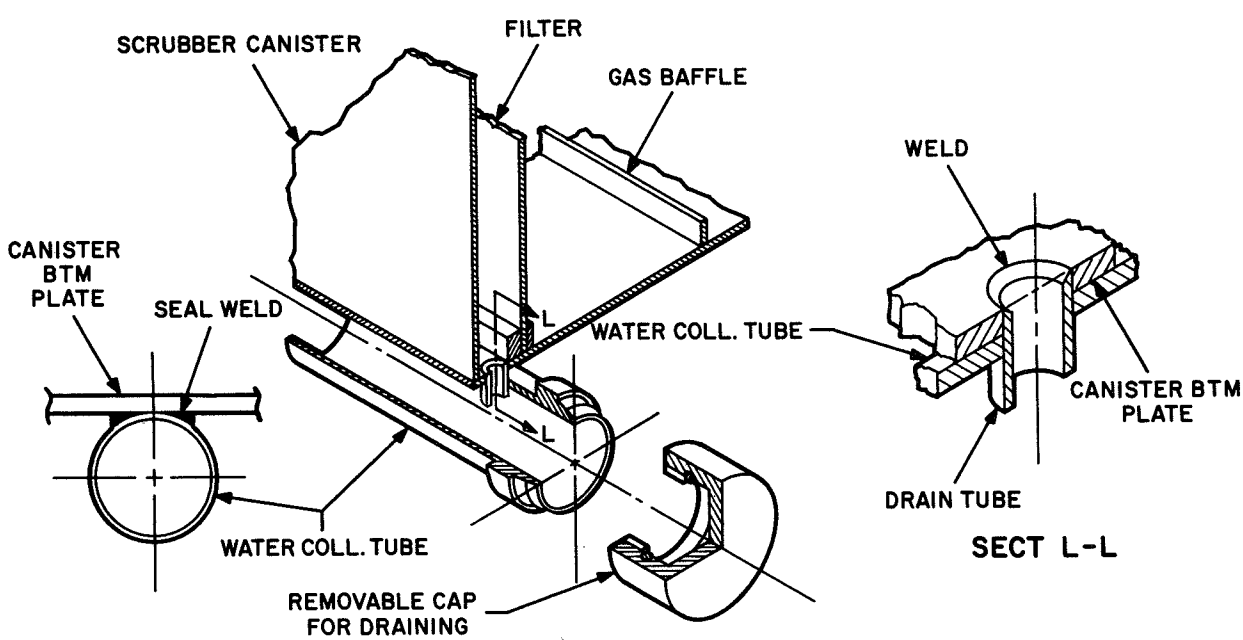

Figure 12.22 *Method for water collection.*

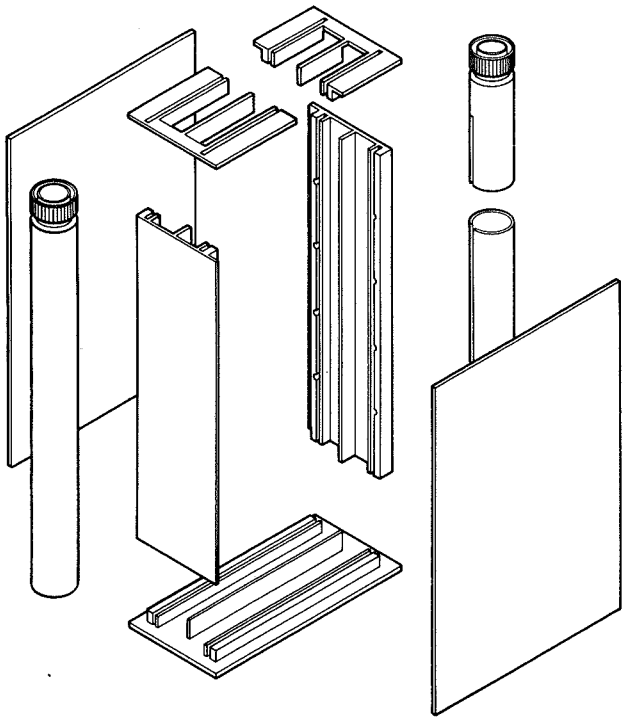

Figure 12.23 *Parts of the scrubber.*

PROGRAM STATUS

The status of the program is shown in figure 12.24. It is expected that the prototype system will be available for swimming in early 1972.

- COMPLETED WORLD-WIDE SURVEY AND REPORT
- STARTING CRITICAL COMPONENT TEST PHASE TO INCLUDE
  - ACOUSTIC TESTING
  - RECIRCULATOR CO_2 SCRUBBING TESTS
  - GAS INLET AND EXHAUST VALVE EVALUATION TESTS
- NEXT PHASE TO BUILD TEST AND DELIVER THREE (3) ENGINEERING PROTOTYPES

Figure 12.24 *Program status.*

REFERENCE

1. Anon: Research Report 12-70. U.S. Navy Supervisor of Diving, Nov. 15, 1970.

13 OPERATION AND TESTING OF MARK 10 MOD 3 UNDERWATER BREATHING APPARATUS

William I. Milwee, Jr.
U.S. Navy Experimental Diving Unit
Washington Navy Yard

INTRODUCTION

The deep ocean is the most difficult environment in which man has chosen to work. Life support equipment used in the deep ocean must be of the finest design because the ocean and the physical laws governing diving are unforgiving.

Closed-circuit apparatus for deep diving are highly desirable because of the breathing gas economics that can be effected. Helium gas, used in deep diving to eliminate the inert gas narcosis problem, is expensive and is a logistic problem because of the great amounts required if open-circuit or semiclosed circuit breathing apparatus are used. Gas consumption in open- and semiclosed-circuit apparatus increases with depth so that the gas consumption of a diver at 1000 ft is about 30 times as great as on the surface.

The Mark 10 Mod 3 is a closed-circuit, mixed gas underwater breathing apparatus designed for use from the surface to 1500 ft and to provide a minimum duration of 4 hours under any sea conditions. The Mark 10 Mod 3 (fig. 13.1) is a completely self-contained unit weighing about 62 lb in air. The apparatus senses oxygen partial pressure in the breathing gas mix and controls oxygen content of the breathing gas within narrow limits about a preset value.

It is this ability to sense and control oxygen partial pressure in an atmosphere that may contain less than 1 percent oxygen in a total pressure of 30 atm that is difficult to obtain but absolutely mandatory in closed-circuit, mixed gas underwater breathing apparatus.

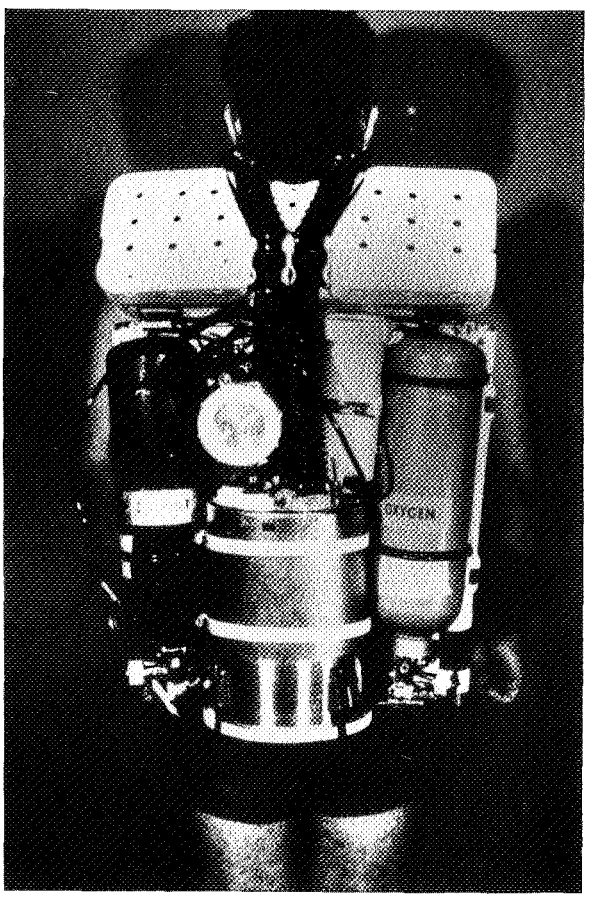

Figure 13.1 *Mark 10 Mod 3 breathing apparatus.*

SUBSYSTEMS OPERATION

Figure 13.2 is an overall schematic of the Mark 10 Mod 3. While the Mark 10 is and operates as a total system, it is composed of three subsystems:

1. The gas supply subsystem
2. The oxygen partial pressure control subsystem
3. The breathing circuit subsystem

Each of the subsystems will be discussed separately.

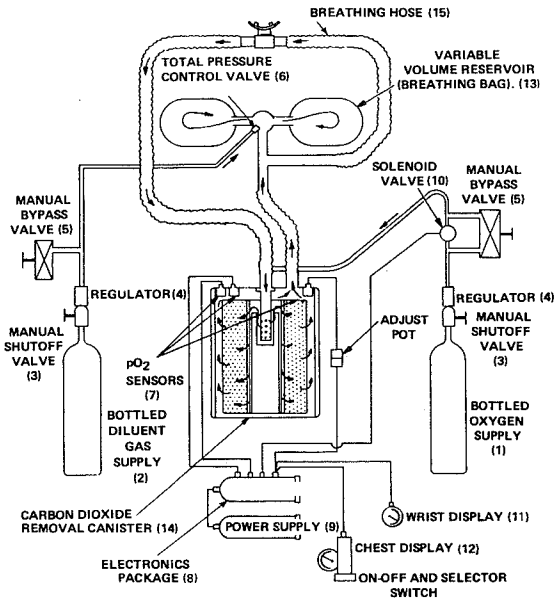

Figure 13.2 *Overall schematic of system.*

Gas Supply

The purpose of the gas supply subsystem is to store oxygen and diluent gases and introduce them, when required, into the breathing circuit in a controlled manner.

Oxygen and diluent gases are stored in individual 150 cu in. steel cylinders with a working pressure of 3000 psi (1) and (2). A manually operated shutoff valve (3) is attached to the cylinder. A constant differential pressure regulator (4) referenced to ambient pressure is attached to the shutoff valve by a yoke. This regulator is nothing more than a first stage regulator found in ordinary scuba equipment. Manually operated, spring-loaded bypass valves (5) downstream of the regulator provide an auxiliary method of adding diluent gas and oxygen.

Pressure Control

The total pressure control system (6) contains diluent add and gas vent valves that act to maintain breathing gas present in the breathing circuit in equilibrium with environmental water pressure. Threshold limits of 4 in. of water or gas pressure below ambient and 6 in. of water or gas pressure above ambient are established for diluent addition and venting.

The purpose of the oxygen partial pressure control subsystem is to ensure that the breathing gas delivered to the diver contains a constant predetermined partial pressure of oxygen regardless of depth.

Three oxygen partial pressure sensors (7) are located in the plenum on the outlet (inhalation) side of the carbon dioxide removal canister. The sensors are galvanic cells that generate a voltage proportional to the oxygen partial pressure in the gas at the sensor face. Each sensor is completely independent of the others so that there is redundant measurement of the oxygen partial pressure. The output of two of the three sensors is fed to the electronics package (8), where it is used to control oxygen partial pressure in the gas supplied to the diver. The output from the third sensor bypasses the electronics package and goes directly to the wrist and chest displays (11) and (12).

The signals from the sensors, which are fed to the electronics module, are amplified and compared to a preset reference voltage corresponding to the desired oxygen partial pressure. If the highest sensor output is less than the reference, voltage power is applied to the solenoid valve (10).

The valve opens and admits oxygen to the breathing circuit for 0.5 sec. If the highest amplified input is higher or equivalent to the reference voltage, the solenoid valve does not open and oxygen partial pressure is decreased through metabolic consumption. The sensors sample the breathing gas every 5 sec.

The reference voltage is set prior to each dive. The system can accept two reference voltages. This enables the apparatus to provide a low oxygen partial pressure for normal diving operations and to provide a high oxygen partial pressure when accelerated decompression is desired. The low oxygen partial pressure set point can be varied between 0.20 and 1.0 atm. The range of the high oxygen set point is from 0.95 to 1.25 atm. Adjustment of the set points is accomplished by adjustment of two potentiometers in the electronics module.

Power to operate the electronic components comes from 20 rechargeable nickel cadium batteries housed in a separate module (9). They are charged with a special battery charger provided with the apparatus. The battery module may be removed for charging or charging may be accomplished with the module attached to the structural frame. Provision is made for normal charge, trickle charge, and automatic switchdown from normal to trickle charge so the charger may be connected for an indefinite period without danger of overcharging.

The wrist display (11) is connected to the third oxygen partial pressure sensor through a calibration trim pot. The wrist meter provides an independent indication of the oxygen partial pressure in the inhalation side of the breathing circuit, thus providing a basis for manual control of the apparatus should the automatic control system fail. The meter face is marked to indicate the two ranges of oxygen partial pressure control. Two lamps in the wrist display are responsive to the alarm circuitry contained in the electronics module. The alarm circuitry monitors three functions:

1. Sensor 1 output compared to the reference voltage
2. Sensor 2 output compared to the reference voltage
3. Battery voltage level

When all functions are within normal tolerances the amber lamp is lit. If the output of either control sensor is ±25 percent from the reference voltage or the battery voltage is below 22.5 V, the amber lamp is extinguished and the red lamp lit. The red lamp serves as a warning to the diver that an out-of-tolerance condition exists and corrective action must be taken.

The chest display (12) has two meters: one calibrated to read in atmospheres and one calibrated to read in volts dc. The tolerance band for normal operation is marked with luminous material as on the wrist display. A multiposition selector switch on the chest display provides for:

1. Turning power to the apparatus off (OFF).
2. Reading high and low oxygen partial pressure settings (low oxygen set, high oxygen set).
3. Reading battery voltage (low bat/high bat).
4. Selecting high or low oxygen partial pressure operation (low sen 1, low sen 2, high sen 1, high sen 2).
5. Reading the output of sensors 1 and 2 (low sen 1, low sen 2, high sen 1, high sen 2).

When the selector switch is in either the low sen 1 or low sen 2, the apparatus will control about the low oxygen partial pressure set point and the output of either sensor 1 or 2, whichever is set, will be displayed on the chest display. Similarly, when the selector switch is in the high sen 1 or high sen 2 positions the apparatus controls about the high set point and displays the output of the appropriate sensor on the chest display. Detents are provided so that the apparatus cannot be accidentally turned off or switched from one control range to another. Positions are provided so that battery voltage may be monitored while the apparatus is operating in either the high or low range.

The device on the left in figure 13.3 is the chest display. Note the two scales, luminous materials, and detents on the switching device. The switch is so constructed that a diver wearing bulky gloves or mittens can easily operate it. The wrist display is on the right. Notice the simplified scale and warning lights. The diver normally wears the wrist display on his left wrist and clips the chest display to a D ring provided for it on the right shoulder strap. The wrist display is out of the way but readily accessible to the diver.

Breathing Circuit

The breathing circuit subsystem provides respirable gas to the diver in sufficient quantity and removes carbon dioxide and moisture from the expired gas.

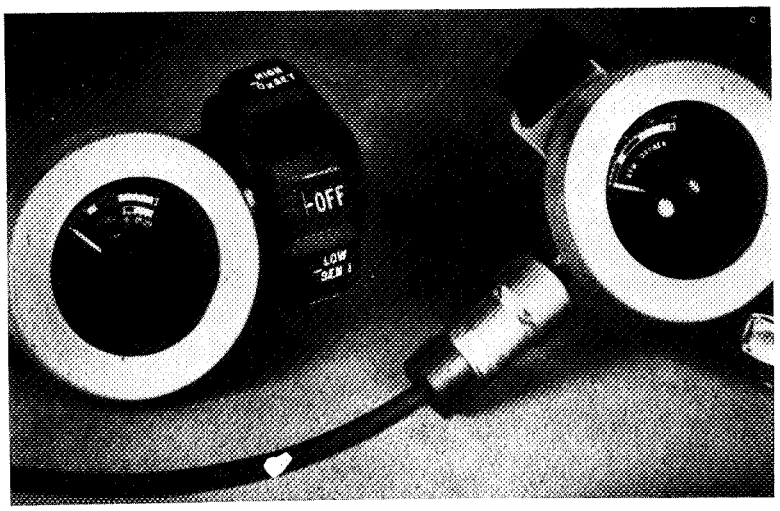

Figure 13.3 *Wrist displays.*

The variable volume reservoir (fig. 13.2 (13)) is composed of two neoprene bags and acts as an accumulator for the gas while it is outside the diver's lungs. The reservoir, which has a total volume of 6.25 liters, is located on the inhalation side of the circuit.

The carbon dioxide removal canister is located in the center of the backpack. The canister is of unique design for diving equipment in that it is radial flow and is provided in prepackaged units. Figure 13.4 shows the principal components. Expired gas enters the center of the canister, passes through a moisture absorber and into the outlet plenum. The three oxygen sensors and oxygen addition line are located in the plenum at the top of the chamber. The carbon dioxide absorbent cartridge forms an integral part of the canister assembly in that the bottom of the cartridge forms the bottom of the canister so with this arrangement it is not possible to dive with an empty canister. To reduce the possibility of diving with a used cartridge, a piece of soluable paper dissolves on water entry to reveal the word "used." All portions of the breathing circuit are connected by flexible neoprene hoses. Note that the breathing hose (15) fits down the center of the breathing bag box and lies very close to the diver's head. This is a comfort feature and reduces the possibility of the hose snagging.

Although the apparatus is shown with a mouthbit, it may be used with a variety of full facemasks (fig. 13.5). The normal use is a face-sealed full facemask with an oral-nasal insert, communications, and respiratory gas temperature monitoring.

Figure 13.6 shows integration of the three subsystems to form the complete breathing apparatus. Note that the subsystems are all interdependent.

While component testing and extensive unmanned systems testing are carried out in the development of deep diving life support systems, it is imperative that manned testing be done in a simulated deep ocean dive. Simulated environment testing allows careful monitoring of the divers and equipment that is not yet possible in the deep ocean and allows immediate assistance should trouble develop. Such equipment testing

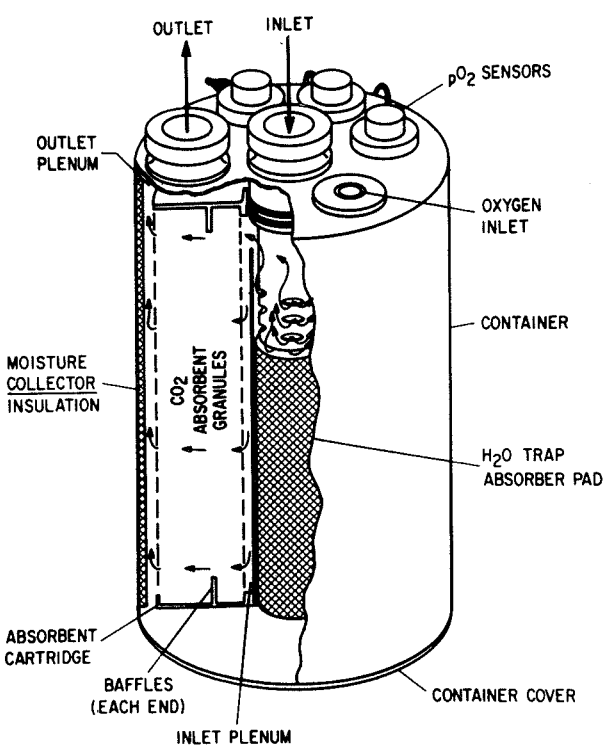

Figure 13.4 *Carbon dioxide removal canister.*

Figure 13.5 *Full-face mask.*

is generally done in two phases. The first is in warm (70° to 80° F) water and the second in cold (29° F) water, both at the simulated depth at which the expected use will occur. The warm water test verifies the basic function of the apparatus and establishes its ability to effectively serve as life support equipment. In the cold water testing, a condition simulating the extreme conditions that can be reached in the ocean is reached. The cold water imposes a stressful condition on the apparatus such as is likely to occur in actual service. While 29° F may not seem to be an extreme condition in conjunction with dense helium it imposes severe stresses on mechanical and electrical functions, and the carbon dioxide absorption process.

HYPERBARIC TESTING

Facilities for conducting such hyperbaric tests are rare and highly specialized. Figure 13.7 does not represent any particular facility or an ideal facility, but is a composite of features generally found. The hyperbaric facility is a complex of pressure chambers designed for living and testing at elevated pressures. At least one of the chambers can be filled with water. A dry chamber, generally known as an igloo, is provided directly above the wet chamber as a diver tender station and as additional living

space. A living chamber and separate entrance lock are usually provided. Supply locks are provided so that equipment, medical supplies, food and the like may be passed into and out of the chamber.

Ancillary systems include:

1. An environmental control system to control temperature humidity and odor in the chambers as well as to remove carbon dioxide
2. A master control console and chamber atmospheric monitoring equipment
3. Closed circuit television with videotape capability
4. A water filtration system to provide clarity and biological purity
5. A water temperature control system
6. Appropriate test instrumentation
7. Gas storage and mixing facilities
8. A helium reclamation facility

Phase I Tests

The first test dive with the Mark 10 Mod 3 was in June 1970 at the Navy Experimental Diving Unit (EDU) in Washington. The dive profile was essentially as shown in figure 13.8. Compression was in 200-ft increments with three-day stops at each depth. Two days at each depth were spent in testing the apparatus while the third day was used for experiments in breathing cold gas at depth. The results of the cold gas studies had a significant effect on subsequent testing.

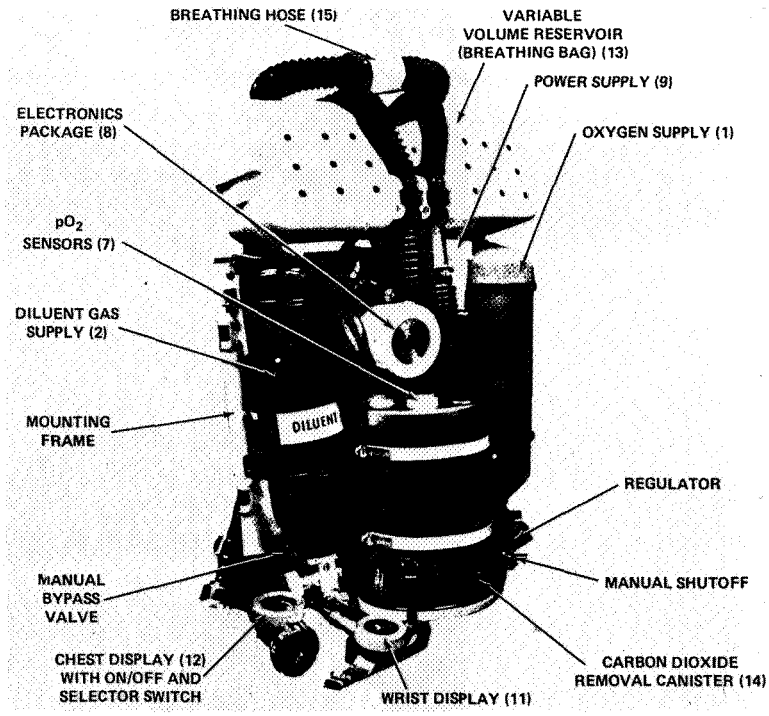

Figure 13.6 *Complete breathing apparatus.*

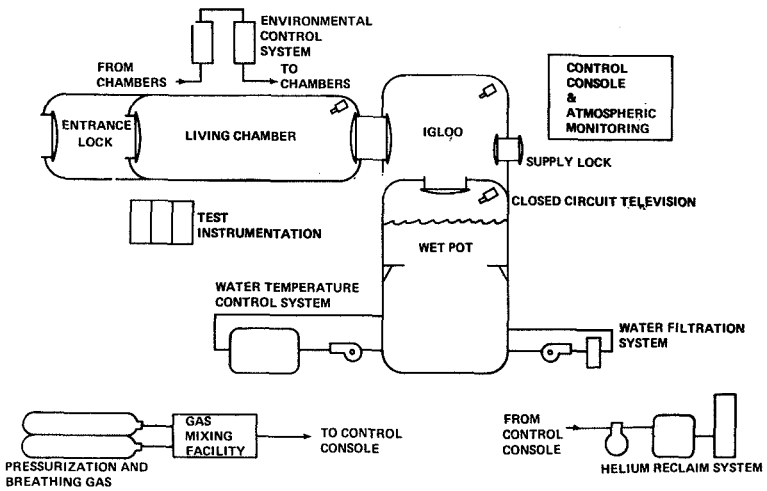

Figure 13.7 *Typical hyperbaric test facility.*

The primary areas of interest in this test were:

1. The ability of the apparatus to effectively control oxygen partial pressure and to provide the diver with an adequate amount of breathing gas while working at a known work rate under controlled conditions
2. The duration of self-contained gas supply at various depths between 200 and 1000 ft
3. The duration of the carbon dioxide absorbent canister at various depths.
4. Reliability and maintainability of the apparatus

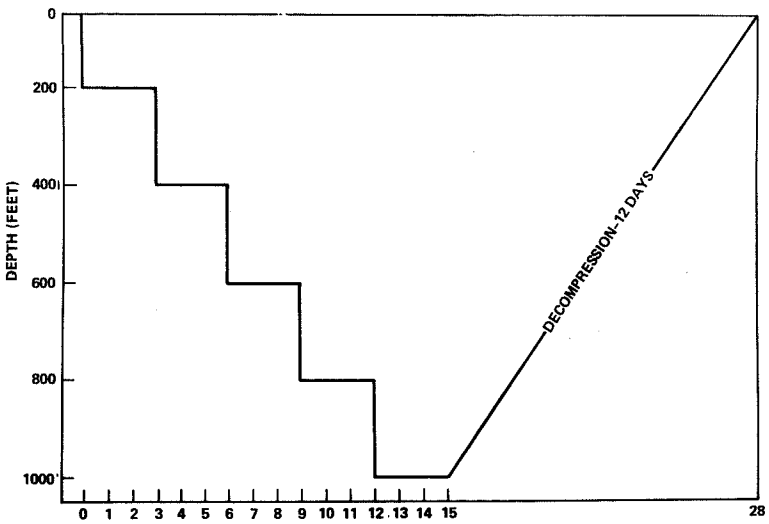

Figure 13.8 *Approximate dive profile of test at NEDU.*

In conducting these experiments the primary parameters to be measured are oxygen and carbon dioxide content in the inspired gas. To measure these a sample is drawn from the inhalation side of the breathing circuit and analyzed by instrumentation outside the chamber. In the chamber one diver swims against a counterbalanced trapeze weighted to represent a current of 0.8 knots, the other lifts a 70-lb weight to a height of 30 in. 10 times/min (10-min work periods alternate with 5-min rest periods).

The dive is terminated when the gas supply is exhausted or when the partial pressure or carbon dioxide level in the inspired gas reaches 3.8 mmHg or 0.5 percent, surface equivalent.

The dive at EDU was a success. Canister durations greatly exceeded expectations showing little or no effect from increased gas density at greater depths. Gas supply durations became longer as divers became used to the apparatus and stopped wasting diluent gas by unnecessary clearing of the face mask. In all cases where gas consumption was limiting, the limitation was exhaustion of diluent gas rather than oxygen. In some cases the divers were terminated prior to exhaustion of the gas supply or carbon dioxide absorbent because of diver fatigue or because the judgement of the diving officer indicated early termination was desirable. One anamoly that was discovered was that as depth increased the oxygen partial pressure variation that occurred when oxygen was added increased. This is understandable because the regulator outlet pressure was a constant amount above ambient, and oxygen addition was for a fixed period. As an example, at 1,000 ft with a nominal oxygen partial pressure of 0.40 atm the partial pressure would rise on addition of oxygen to between 0.60 and 0.70 atm. The variation was not physiologically dangerous but was greater than was desirable. As a result of the success of this dive the second phase of the testing was begun without major modification of the apparatus.

Phase II Tests

The second phase of the testing was carried out in the hyperbaric complex of Taylor Diving and Salvage Company in Belle Chase, Louisiana. Taylor was chosen because it has a large modern hyperbaric facility and a staff with unusual experience in experimental diving. The dive was to be in

200-ft increments to a depth of 1000 ft. During the period at 1000 ft an excursion was made to 1100 ft where the divers worked for 40 min and returned directly to the saturation depth. This was the deepest wet dive yet made in the United States.

Water temperature was maintained at 29° F throughout the dive. While the equipment parameters remained the same (i.e., gas consumption, carbon dioxide removal system performance, and oxygen partial pressure control system performance) much more extensive monitoring of the divers was required and considerable equipment was provided for thermal protection.

Thermal protection to the divers was provided by a hot water system integral to the hyperbaric facility. Hot water was supplied to each diver's open circuit suit at 110° F and a flow rate of 3 to 4 gal/min. A 0.125 in. thick closed-cell neoprene suit was worn under the free flooding suit as protection against burning should the hot water temperature momentarily become excessive.

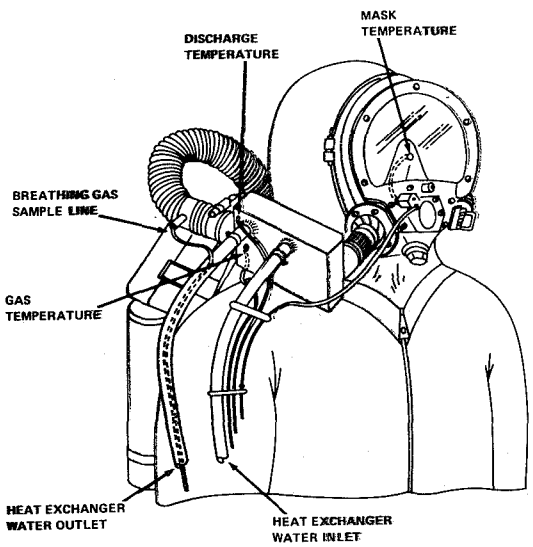

Figure 13.9 *Breathing gas sampling line and thermistor placements.*

The cold gas testing, mentioned previously as having been carried out at the EDU in conjunction with the first phase testing, showed that the diver's breathing gas must be heated in deep diving. If it is not heated, the heat loss through the diver's respiratory tract will be intolerable. To provide respiratory heating a heat exchanger was attached to the diver's mask (fig. 13.9). The heat exchanger was a hot water to gas heat exchanger supplied with hot water from the diver's breathing gas supply. The exchanger was intended as an engineering model only and not as an operational piece of equipment. It was successful in that it provided satisfactorily warm gas thereby making it possible to conduct the dive.

Continuous samples of diver breathing gas were drawn from the inhalation side of the circuit and for analysis outside the chamber for carbon dioxide and oxygen content. Both quantities were recorded on strip charts. Notice that the breathing gas sampling line passed through the gas heat exchanger outlet line. This was necessary to prevent condensation and freezing of the moisture in the sample line. Freezing could cause blockage of the line and make it necessary to abort the dive.

A temperature harness was provided for monitoring of significant temperatures (fig. 13.10). Six skin probes located as shown were provided in addition to a rectal probe and gas heater and mask temperature monitoring. The mask temperature was the only one that changed rapidly so it was the only one connected to a continuous recording device, the variation in mask temperature provided the diver's respiration rate.

The dive profile (figure 13.11) shows that essentially one day was spent at each depth with the time varied as necessary to accomplish the purposes of the dive. Problem areas that are worthy of discussion because they influenced the conduct of the evaluation showed up at various times.

The gas regulators provided with the apparatus were specially made of 90-10 copper-nickel. These regulators proved to have such an extremely high failure rate that their use was discontinued at the 200-ft dives and all regulators were replaced by conventional brass regulators. Upon replacement no more failures ocurred.

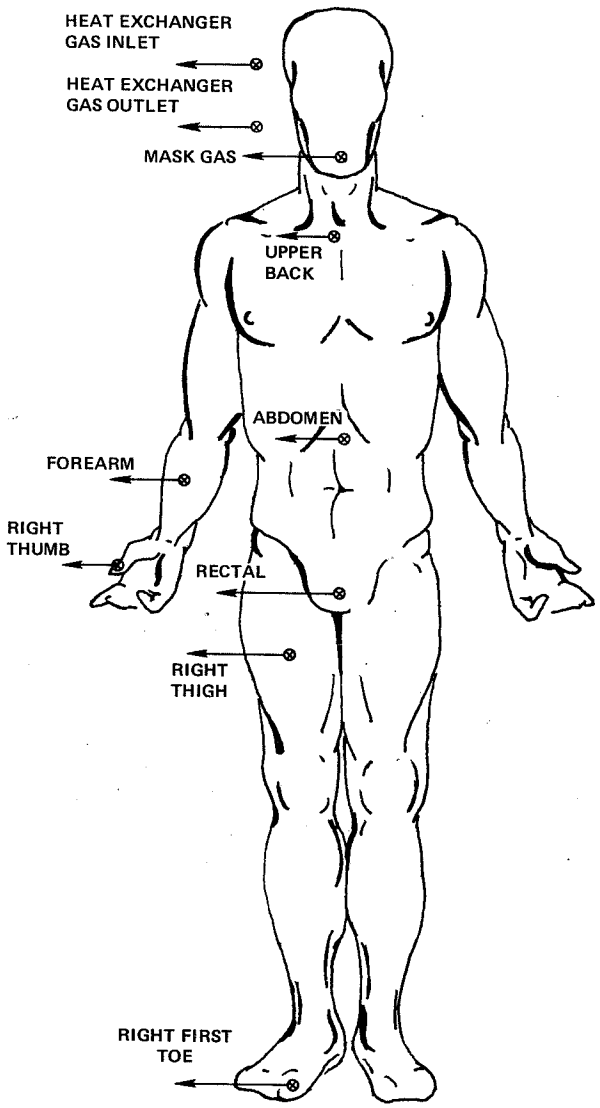

Figure 13.10 *Temperature monitoring of diver.*

The annoying and frustrating ability of helium to be absorbed by almost everything requires that equipment be decompressed in the same matter as people. Even though the equipment was decompressed slowly in accordance with a schedule that should have been extremely safe, the sensors and cables proved to be as unpredictable as the divers in reactions to decompression. Several sensors and cable assemblies suffered from the bends and had to be replaced. A number of electronics packages failed and had to be replaced.

Leakage into the mask was a problem during all dives. The original mask seals of open-cell neoprene foam were replaced by individually-fitted mask seals with a covering of closed-cell neoprene foam that were fabricated by General Electric. Face seals were slightly more effective after the replacement, but leakage into the mask continued to be a problem. Divers said that the torque of the heat exchanger attached to the mask tended to break the mask seal when turning the head. The adverse effect on evaluation of the apparatus from mask leaks derives from canister flooding resulting in decreased function time and increased diluent gas usage rate to purge the mask of brine. Gas cylinders were thus exhausted prematurely and had to be replaced.

Internal blockage of the heat exchanger core occurred as a result of the reaction of the calcium chloride brine with the aluminum core. The heat exchangers were clogged to the extent that only a trickle of water could be forced through them. Flushing with inhibited sulfamic acid solution cleared corrosion and reestablished water flow; however, one exchanger then leaked water into the gas breathing side and had to be replaced.

It was necessary to use calcium chloride brine to lower the freezing point of the wet pot liquid to 20° F, so that freeze-up of the heat exchanger would be avoided in cooling the wet pot liquid to 29° F. Although calcium chloride solution was less corrosive than sodium chloride solution, it caused severe irritation of the skin of the divers and extended small scratches and abrasions to weeping purulent ulcerations of the skin. Eye and ear canal irritation was a problem. These factors progressively affected more divers and prevented their further immersion in the wet pot in an effort to avoid worsening of their conditions. This problem adversely affected evaluation of the Ex 10-Mod 3, especially during the ascent phase when more of the scheduled time on the apparatus

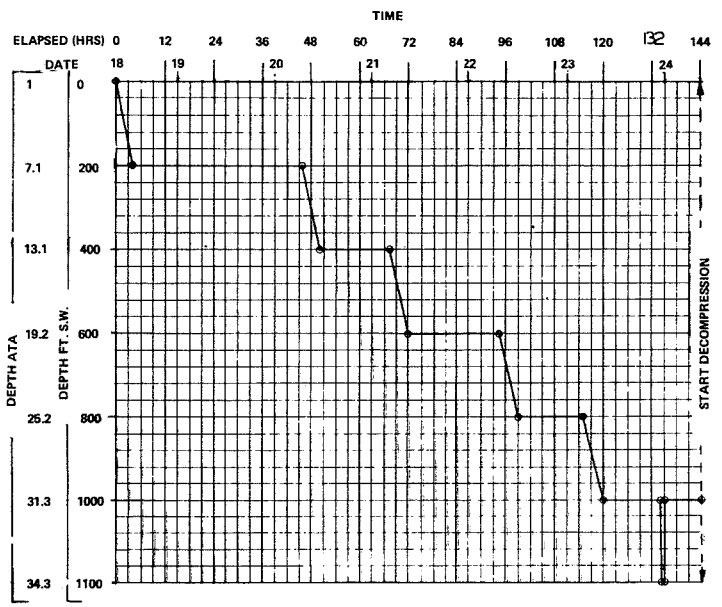

Figure 13.11 *Compression profile.*

would have been accumulated. Warm fresh water showers, skin lotion, and ear canal hygiene with acid-alcohol drops were all to little avail in preventing the irritating effects of the brine on the diver's ears, eyes, and skin.

In spite of the problems encountered during the dive, sufficient data were gathered to make reliable statements about the performance of the apparatus and enough information was gathered to positively identify problem areas.

The oxygen partial pressure control was reliable and always within safe limits using the low oxygen partial pressure range. In the high range, oxygen partial pressures soon became higher than would be tolerable for long exposures.

Excursions of oxygen partial pressure about the set point had a total value that averaged between 0.15 and 0.20 atm as shown in figure 13.12, a typical strip chart. While this variation is within physiologically safe limits it is greater than desired. The apparatus is now being modified to reduce these excursions. Two basic changes are being made: sensor sampling will occur at 2-sec intervals with a 200-msec oxygen addition to reduce the mass of gas added at any one time, and oxygen

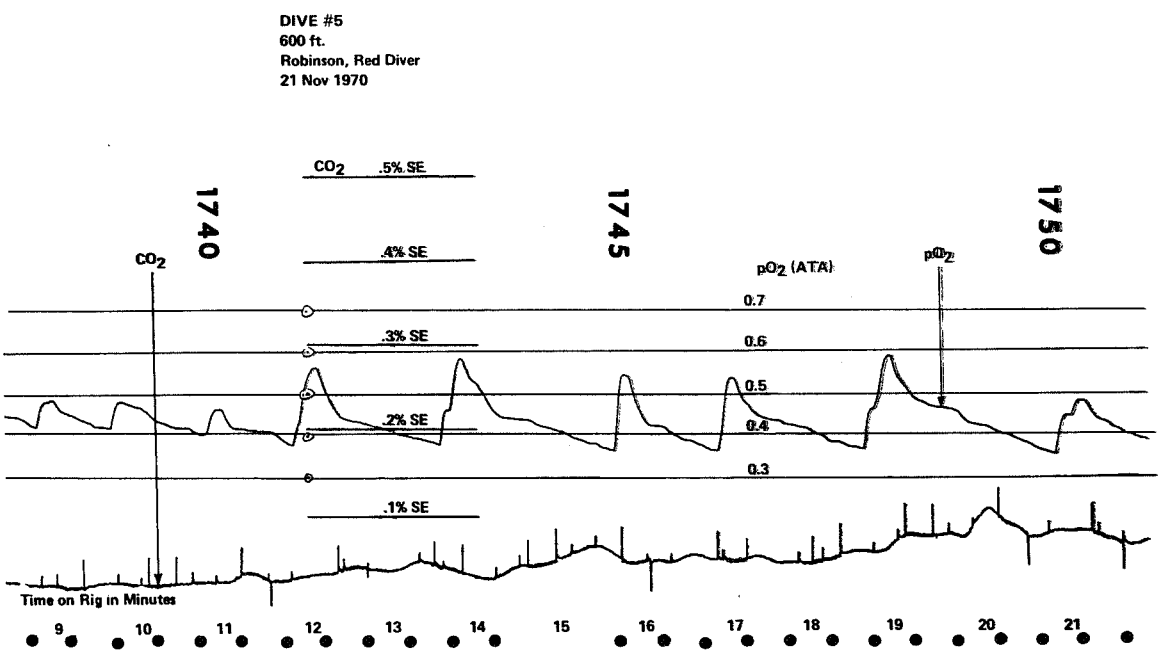

Figure 13.12 *Typical strip chart.*

addition will be divided between canister inlet and outlet to permit more thorough mixing before sampling.

The phenomena of set point drift remains unexplained but is believed to be related to the establishment of thermal equilibrium in the apparatus as it occurred within the first 15 min of the dive.

Carbon dioxide absorption performance was very disappointing. The predicted minimum durations are in all cases well below the desired 4-hr durations and well below the values obtained from the warm water dive at the EDU. The reduced canister performance can be attributed directly to the cold water and the cold dense gas that was being scrubbed. The heat capacity of a helium oxygen mixture at 30 atm is huge and the gas entering the canister was at ambient temperature. The carbon dioxide absorption reaction could not function effectively. Careful thought indicated that because of the radical flow through the canister, heating it with a water jacket as is usually done would not be satisfactory. A heat exchanger (fig. 13.13) was installed in the breathing gas circuit ahead of the canister with the exhaust water led down through a sheath covering the remaining hose and over the canister. This system was used on some swims during decompression. The results indicated an improvement in performance, but as swims during decompression were limited to 2 hr, the useful canister life was not determined. The installation of a complete heating system for the apparatus and for breathing gas systems is planned that will enclose the entire apparatus in a hot water filled bag with water flowing out through the double walled breathing hoses.

On the positive side, the self-contained gas supply proved adequate for working dives at all depths with predicted gas durations far in excess of expected diving times. Results are summarized in figure 13.14.

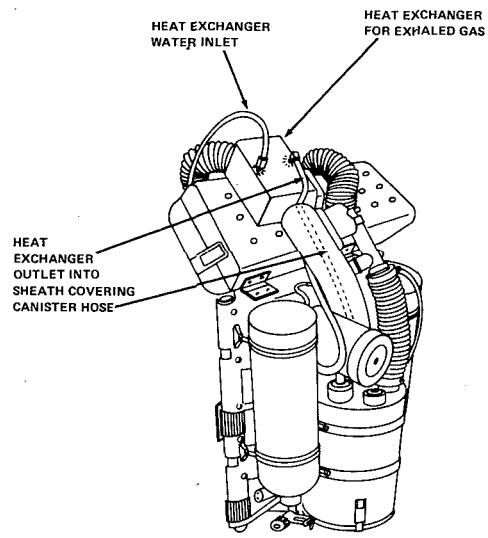

Figure 13.13 *Special canister heating system.*

CONCLUSIONS AND PROSPECTS

The total test results indicate that the Mark 10 Mod 3 apparatus has certain inadequacies but with modifications that are well within the engineering state-of-the-art can be used to support divers at low temperatures and great depths. A program is currently underway to make the necessary modifications. In the immediate future, another cold water test is planned for 1971 after the modifications have been made. A technical evaluation in the open sea will be conducted off Hawaii at 520 ft. If the results of these evaluations are satisfactory, an operational evaluation using the Mark 1 deep dive system will be conducted in the spring of 1972. This evaluation will be a series of open sea dives to 1000 ft. In addition to its use as a deep diving apparatus the Mark 10 has obvious application in clandestine operations. Its use in this area will be the subject of thorough investigations.

RESULTS OF COLD WATER TESTING
OXYGEN PARTIAL PRESSURE CONTROL

1. PHYSIOLOGICALLY ACCEPTABLE CONTROL OF OXYGEN PARTIAL PRESSURE
2. UNDESIRABLY GREAT VARIATIONS IN OXYGEN PARTIAL PRESSURE WITH OXYGEN ADDITION
3. UNDETERMINED BUT PHYSIOLOGICALLY SAFE VARIATION OF OXYGEN SET POINT

CARBON DIOXIDE ABSORPTION
EFFECTIVENESS INSUFFICIENT

1. CANISTER DURATION

PREDICTED MINIMUM DURATIONS:

200–400 FSW	90 MINUTES
600 FSW	70 MINUTES
800–1000 FSW	45 MINUTES

GAS CONSUMPTION

1. ADEQUATE FOR WORKING DIVES AT ALL DEPTHS

	OXYGEN	HELIUM
GAS CONSUMPTION:	0.93 slpm	0.68 slpm
PREDICTED DURATION:	9.575 HRS	10.920 HRS

Figure 13.14 *Test results.*

14

THERMAL PROTECTION OF DIVERS

Patrick F. Dowland
Royal Navy

INTRODUCTION

The U.S. Navy is directing development efforts toward achieving a capability to dive and work at depths to 1000 ft in water temperatures down to 29° F. Whatever the depth or duration of dive, in all but the warmest sea temperatures the diver must have thermal protection to prevent impairment of his mental and physical performance by cold. The aim is to achieve a "steady state" where:

1. Deep body temperature is constant around 99° F.
2. Mean weighted skin temperature is constant around 94° F.
3. The power input to achieve steady skin and deep body temperatures is constant within narrow limits.
4. The diver is subjectively comfortable.

This condition can be expressed by:

$$\begin{pmatrix}\text{Metabolic}\\ \text{heat}\end{pmatrix}+\begin{pmatrix}\text{Suit heat}\\ \text{replacement}\end{pmatrix}=\begin{pmatrix}\text{Respiratory heat}\\ \text{loss}\end{pmatrix}+\begin{pmatrix}\text{Suit heat}\\ \text{loss}\end{pmatrix}$$

It has been shown that metabolic heat production exceeds respiratory heat loss at depths shallower than 600 ft and in seawater temperatures above 40° F. The diver therefore can be kept in thermal balance by the use of insulation alone. But at very deep depths, the situation is reversed and some method of heating the inspired gas is necessary. The amount of heat required to compensate for heat loss is a function of the water temperature, the depth, the gas mixture breathed, and the effectiveness of the insulation.

SUIT HEAT LOSS

The Wet Suit

The wet suit, probably the most widely used suit today, is usually made of foamed neoprene. The suit is normally made to the user's measurements, and only a small quantity of water is allowed to enter, which is quickly warmed by the body. Heat loss thus depends on the insulating properties of the material.

Foamed neoprene is subject to compression under pressure and becomes less and less effective with depth (fig. 14-1, 1-11), In addition, when this material is placed in a helium-rich environment under pressure, the nitrogen and oxygen diffuse out of the neoprene and are replaced with helium at a pressure equal to that of the chamber; the neoprene re-expands to about 65 percent of its original thickness.

When the diver enters the water, the helium outgasses; when he returns to his personal transfer capsule (PTC) or habitat, however, there is no re-expansion, since the pressure in the suit cell equals that of the habitat.

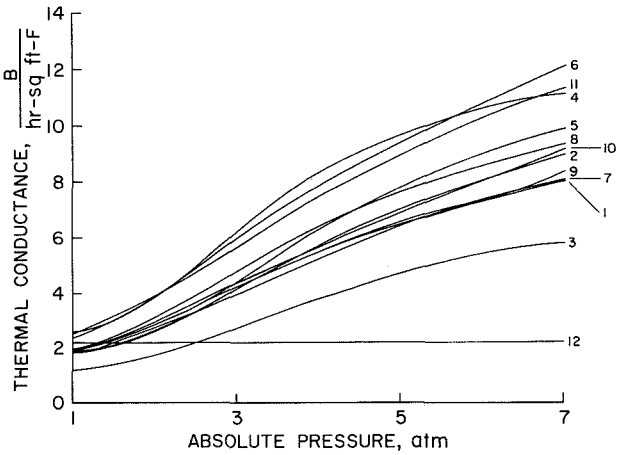

Figure 14.1 *Conductance of wet suit materials in comparison with noncompressible material (1-11 foamed neoprene, 12 incompressible material).*

Since this process is repeated with each excursion, the diver ends up with a suit of very poor insulating quality. In fact, at 600 ft, the insulation is about one quarter of that at the surface. For this reason, the conventional wet suit is unsuitable for deep diving.

The Dry Suit

A dry suit usually keeps the diver dry, and minimizes heat loss by providing an insulating air gap and an undersuit between the diver and the water. A constant volume regulation system has to be provided to maintain the air gap and reduce the possibility of squeeze.

During a dive from a habitat or PTC in a helium environment, the air trapped in the suit is replaced by helium, which greatly reduces the thermal insulating properties. It would be logical, therefore, to replace the gas layer with a nitrogen/oxygen mixture or carbon dioxide. However, nitrogen will contaminate the atmosphere, and carbon dioxide is unsatisfactory at deep depths and cold temperatures.

The dry suit then has certain advantages over the wet suit:

1. The diver is kept dry, a big advantage in deep diving on return to the PTC.
2. The insulation tends to remain constant with depth.
3. The diver can alter his insulation by increasing or decreasing his undergarments.

Incompressible Suits

Suits made of incompressible materials are under development. The material is made of glass microspheres held together by polymerized mineral oil and coated with a rubber type material on either side. Some manufacturing difficulties still exist, and suits constructed of this material tend to be slightly heavy on the surface, but development has been encouraging and recent swimming trials have been favorable.

Such suits will improve the thermal protection of divers operating below about 100 ft (fig. 14.1, 12), but this material alone is inadequate in deep depths where supplementary heat is required. It is as an insulative covering over some form of heating undergarment that this material will come into use in the field of deep diving. However, before it is acceptable for such a purpose, tests of flammability and toxic off-gassing are needed.

SUIT HEAT REPLACEMENT

Hot water has been the primary means of heat replacement. By this approach, the suit and power source must be considered together and the following requirements taken into account:

1. The diver must not be burned; water temperature in the suit must not rise above 110° F.
2. The diver must be kept warm; 1.2 kWh is required with present insulation but as much as 3.4 kWh may be required.
3. The diver must have freedom of movement with no bulky equipment or heavy umbilical.

4. There must be no off-gassing to contaminate the environment or disclose the diver's position on clandestine operations.
5. The diver must be protected in case of system failure. He must have time to return to his base of operation before he freezes.
6. The diver must not be electrocuted; electrical hazards must be known.
7. The diver must not be subjected to radiation hazards.

No system that fulfills all these requirements has yet been accepted into service.

The most widely used system is the open-circuit hot water suit supplied through an umbilical with water heated by an oil-fired boiler on the surface (fig. 14.2). The suit is made of open-cell neoprene and contains perforated tubes that distribute the water over the diver's body. Controls on the suit allow the wearer to control the flow to the upper and lower parts of the body or to dump to the sea at the suit inlet. When the system is fully open, the diver is kept in a bath of hot water. Temperature controls and fail-safe arrangements are fitted to the boiler (fig. 14.3) to prevent excessively hot water from getting to the diver.

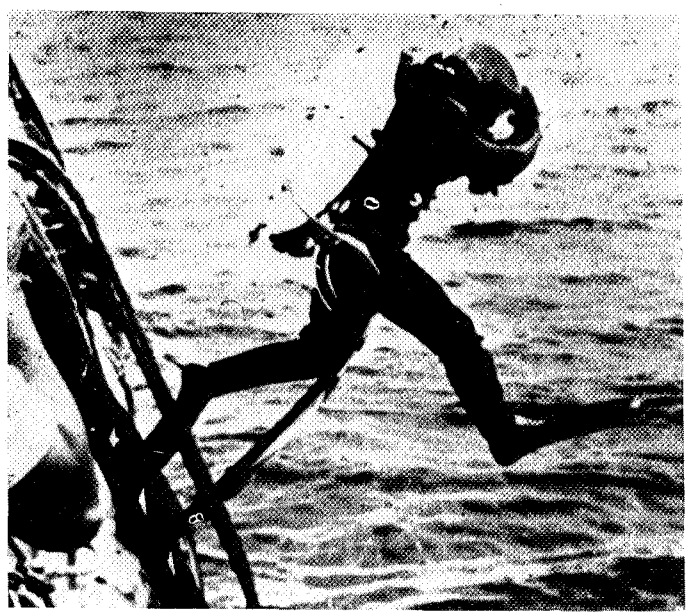

Figure 14.2 *Open circuit hot water suit in wide use at present.*

This suit is extremely comfortable to work in and has been used effectively in the open sea at depths to 850 ft in 40° F water and at depths of 1100 ft in 29° F water in hyperbaric chambers. The system is extremely wasteful of energy, however, and suffers from the serious shortcoming that should the hot water supply be interrupted, the diver is immediately exposed to ambient water temperatures, which in extreme conditions can incapacitate him within 1 min. Although now used in deep diving, this system is considered more effective in depths above 300 ft.

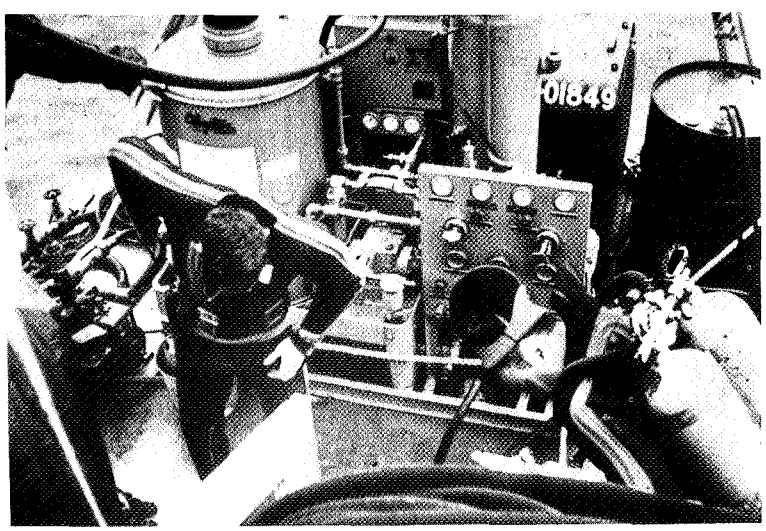

Figure 14.3 *Surface installed boiler for use with open circuit hot water suits.*

It is believed that a closed-circuit hot water system will give a more efficient solution to the problem of operating at greater depths. If such a system can be provided with a heat source carried by the diver, the excessive heat losses in the umbilical between the boiler and the suit can be minimized. As far as is known, only three closed-circuit suit designs exist.

In the Apollo suit, water is passed through small diameter tubes covering the diver's body. This undergarment was tried under both wet and dry suits, but the distribution of the tubes and their comparative inflexibility caused diver discomfort. Another suit is being tested in which the heated water passages are built into the entire suit surface, leaving virtually no areas unheated and permitting circulation of the heating fluid over a maximum body area (fig. 14. 4) at a very low pressure. This suit is being used under a dry suit at the present time; however, it is hoped to weld an incompressible covering to it to provide ease of donning and maximum insulation.

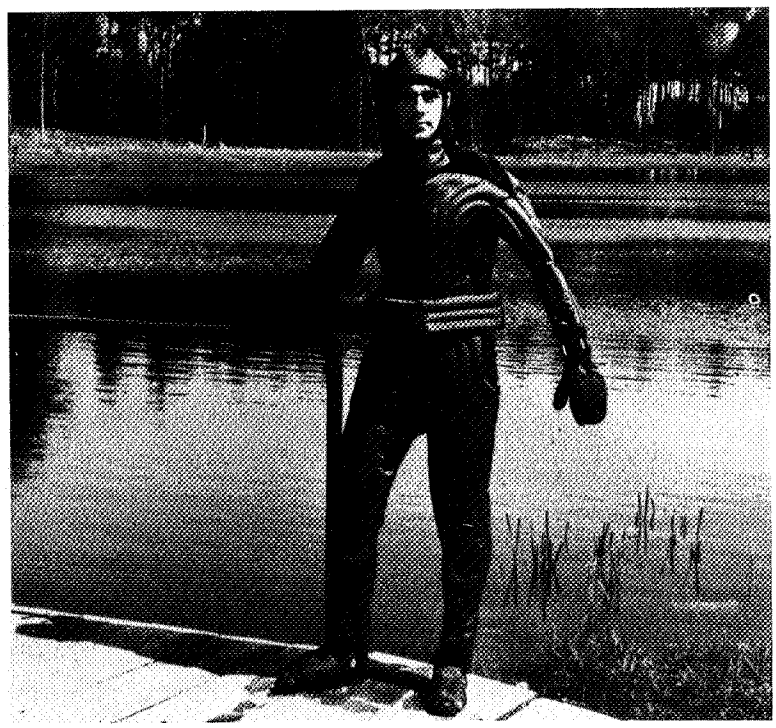

Figure 14.4 *Closed circuit hot water undersuit at present under trial.*

The third suit being tested is an adaptation of the open-circuit suit described in which the water enters and exits at the waist area.

Closed-circuit suits can be supplied with hot water from boilers at the surface, mounted on the PTC or habitat, or carried by the diver. The surface boiler is widely used, and many ideas for PTC/habitat and diver-carried heat have been examined but most do not yet meet the requirements previously outlined.

The systems most worthy of consideration to provide a long-term solution to the problem of diving in very low temperatures are those using isotopes, electrical power, the latent heat of crystallization or salts, or heat pumps. However, none of these systems are sufficiently developed to permit conclusive evaluation of their potential.

The two heaters selected for trial are in the laboratory test stage. (It is hoped to evaluate these at depth in 29° F water in the fall of 1971.) The first of these heaters (figs. 14.5 and 14.6) works on the principle of the controlled oxidization of magnesium chip fuel charges and the transfer of the accompanying heat to a water loop connected to a closed-circuit suit. The oxygen flow to the combustion zone is controlled so that the desired heat output is achieved. The heat generated by the oxidization process is transferred to the water loop by a heat exchanger jacketed around the

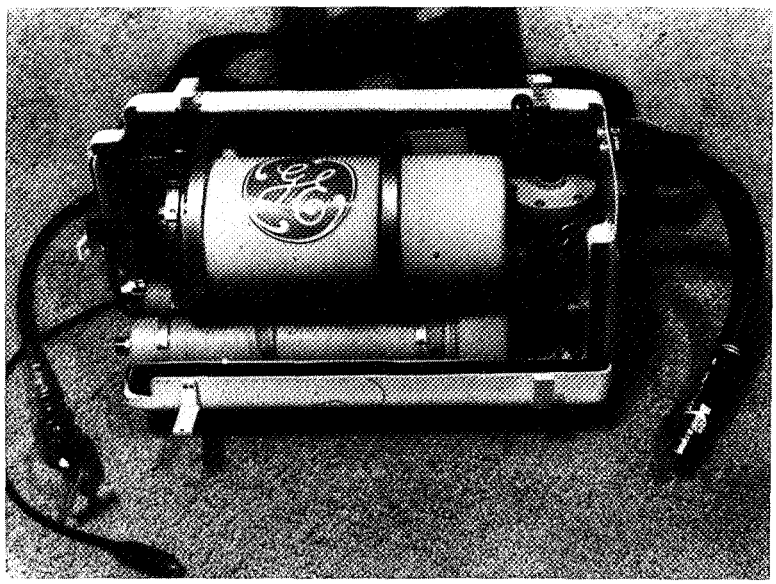

Figure 14.5 *General Electric CONOX diver carried boiler.*

combustion chamber. The heated water is circulated by an efficient pump powered by rechargeable nickel-cadmium batteries. The pump employs a magnetic coupling between the pump and motor to eliminate problems associated with sealing shaft penetrations.

The system is designed to automatically maintain a diving suit outlet temperature of between 95° and 100° F. A total of 6 kWh of thermal energy is provided to the diver swimming at 850 ft. The heater case weighs 35 lb in air and fits under the breathing apparatus on the lower part of the diver's back. The oxygen bottle fits in the harness assembly on the abdomen of the diver.

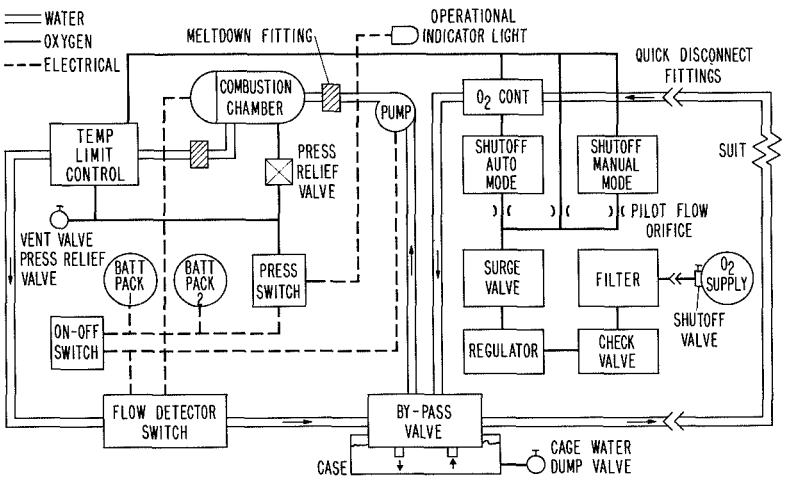

Figure 14.6 *Schematic of CONOX heater.*

The other heater under trial (fig. 14.7) uses the chemical energy stored in discrete sealed packages of solid fuel and solid oxidizers known as heat sticks. Initiated by an electrical impulse, these stable chemicals break down and recombine exothermally. The resulting reaction produces only heat as a by-product. Up to 8000 Btu are stored in a thermal surge, metallic salt reservoir at a constant temperature. A pump circulates water around the molten salt and through the loop suit. The

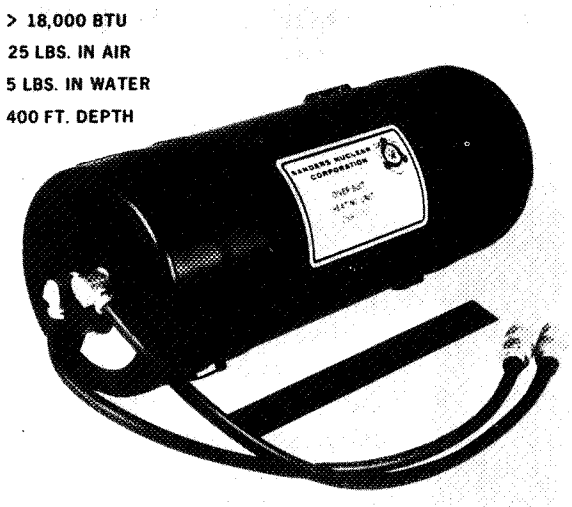

Figure 14.7 *Sanders nuclear chemical heater.*

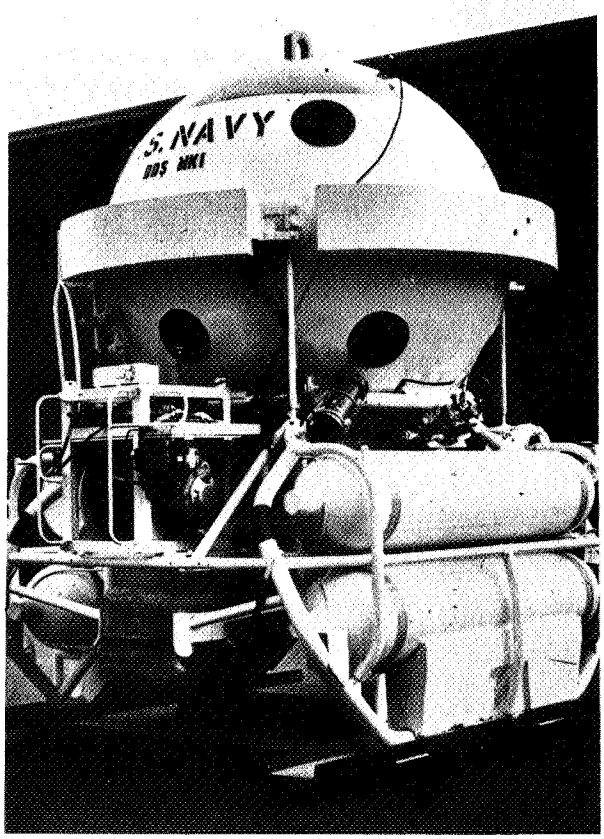

Figure 14.8 *Mark I Mod 10 deep dive system personnel transfer capsule.*

heating operation can be interrupted and restarted at any time and is designed to provide heat for 6 hr in 30° F water temperature. The heater weighs 25 lb in air and may be fitted to the breathing rig as required.

RESPIRATORY GAS HEATING

Work carried out last year at the Navy Experimental Diving Unit in Washington, D.C., has confirmed the need to heat the gas breathed by the diver at depths below 600 ft and temperatures below 40° F. Dives conducted in 1000 ft at 29° F water have confirmed that the carbon dioxide absorbent carried on existing breathing apparatus must be heated to maintain the endurance of the equipment. These problems are being overcome by using the hot water provided to the diver's suit to also heat the breathing equipment. The methods used for doing this are crude and hastily fabricated, but pressure chamber tests in 32° F water at 850 ft have been successful and it now remains to clean up the design.

Whether the diver-carried power sources now under trial can accept this additional loading has yet to be determined and depends on the final design of the equipment insulation package and the suit to be used.

PTC HEATING

Whatever suit and boiler combination is finally chosen for a safe dive, the divers in the PTC (fig. 14.8) must be kept adequately warm on their way to and from the work site and when waiting to enter the water.

Tests of the Mark I Deep Dive System PTC showed that a heat input of 1620 Btu is required for each degree of temperature differential to be maintained over and above ambient. Insulation of the Mark I DDS PTC was achieved by cementing electrical heating elements to the outside of the PTC using a cement with a high heat conductance (fig. 14.9). The hull is then insulated with just over 1 in. of syntactic foam. The electrical heating elements are contained in copper tubing. In the event of a short circuit,

each element is protected so that no shock hazard to the divers is possible.

This method of providing heat to the PTC has several advantages. No extra space is required inside the PTC. If power should fail, the hull takes several hours to cool down so that divers will have heat for a considerable time. If it is required that the power to the heating elements be used for other services, it can be diverted for considerable periods of time without great degradation to the heating system. This system has been completely successful in tests at sea.

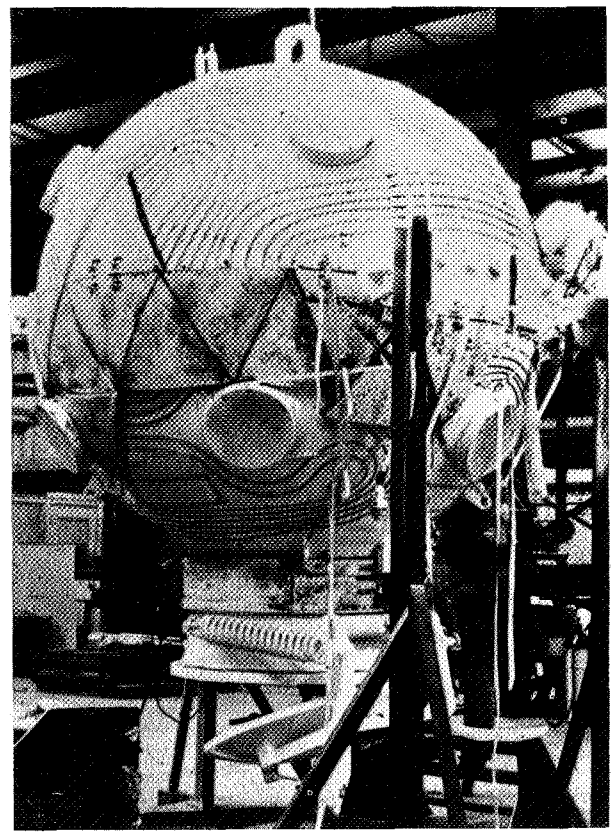

Figure 14.9 *Heating elements cemented to Mark I PTC before receiving the insulative shell.*

BIBLIOGRAPHY

1. The Supervisor of Diving. Report No. 10 – 70, 11 Sept. 1970.
2. Rawlin, J. S. P.; and Tauber, J.: Thermal Balance at Depth. Naval Med. Res. Inst. Internal Report, 1969.
3. Hoke, B.; Jackson, D. L.; Alexander, J.; and Flynn, E.: Respiratory Heat Loss From Breathing Cold Gas at High Pressures. Bu. Med. Surg. Report, Feb. 1971.
4. Beckman, E. L.: Thermal Protective Suits for Underwater Swimmers. MF 011.99-1001 Naval Med. Res. Inst. Report 8, 1966.
5. Rawlins, J. S. P.; and Tauber, J.: Heater Suit Design and Evaluation Problems. Symp. on Diving Safety, Naval Sub. Res. Dev. Lab., Panama City, Fla., Oct. 1969.
6. Bondi, K. R.; and Tauber, U. F.: Physiological Evaluation of a Free Flooding Diver Heat Replacement Garment. Naval Med. Res. Inst. Report 17, 1969.
7. Majendie, J. L. A.: Diver Heating, Equipment for the Working Diver. Battelle Memorial Inst., 1970.

15 A FLIGHT-RATED LIQUID-COOLED GARMENT FOR USE WITHIN A FULL-PRESSURE SUIT

Richard Carpenter and William R. Winter
NASA Flight Research Center
and John D. Wilde Computing and Software, Inc.,
Edwards, Calif.

INTRODUCTION

Many of the flights conducted at the NASA Flight Research Center (FRC) require the use of pressure suits for high-altitude operation. In the summer on the Mojave desert, temperatures inside these suits can become extremely hot because of insufficient cooling air during preflight, standby, and taxiing. To reduce temperatures to comfortable levels, a liquid-cooled garment (LCG) was considered desirable for use by pilots when wearing full-pressure suits.

Most of the development of self-contained liquid-cooled garment systems (ref. 1) has been directed toward the particular problems of spacecraft extravehicular activities. The approach taken by the FRC has been to attempt to cool a pilot seated in a closed cockpit of a research aircraft by using a limited supply of cooling air. For aircraft use, the desired system had to be lightweight and self-contained on the pilot because of weight and space limitations on aircraft such as the lifting bodies. Actual requirements precluded placing electrical components inside the pressure suit and required a system proportioned to fit comfortably inside the suit and not interface with pilot tasks.

This paper presents the results of tests conducted at the FRC to define the heat removal requirements of a pressure-suited pilot wearing an LCG when seated in the cockpit of a research vehicle. The system that was developed and fabricated to meet these requirements is described, and results of actual tests conducted to evaluate the performance of the system are discussed.

DESIGN CRITERIA

The thermodynamic design criteria for the cooling system were established by experiments at the FRC with subjects wearing pressure suits and the Apollo type of liquid-cooled garment (ref. 2 - 4), which is cooled by external refrigeration and completely covers a subject except for his face. These experiments were conducted in a cockpit simulator exposed to the sun at zenith with the subjects performing typical pilot tasks. Measurements included garment coolant inlet and outlet temperatures and flow rates. For all experiments, cockpit temperatures were maintained at 66° C (150° F). These tests were performed using different canopy configurations, and significant changes in heat loading values were noted; for example, the heat loading was one-third less with an X-15 type of canopy having a 0.3-m^2 (3.2 sq ft) window surface than on the subject with an HL-10 type of canopy with a window surface area of 1.6 m^2 (17.5 sq ft). Thus, the change in solar radiant energy significantly affected the heat loading on a subject wearing a full-pressure suit. These tests also indicated that when the suit was ventilated, lower cooling rates were required to prevent the subject from sweating. Therefore, a 57-liter (2-cfm) air supply, which is typically available in research vehicles, was used for suit venting. These findings led to adopting a reflective outer garment and a 57-liter/min (2-cfm) air ventilation rate for the pressure suit to minimize the heat absorbing requirements for the cooling system heat sink.

Maximum temperature tests were again conducted with subjects wearing a reflective garment over a ventilated pressure suit. The measurements indicated that a garment heat absorption rate in the range of 250 kg-cal/hr (1000 Btu/hr) to 175 kg-cal/hr (700 Btu/hr) would generally prevent sweating and maintain comfort for a 70 percentile pilot seated in a cockpit with 1.6 m^2 (17.5 sq ft) of canopy glass.

SYSTEM DESCRIPTION

Figure 15.1 is a block diagram of the cooling system components. The pulse pump converts pneumatic pressure to hydraulic pressure that circulates the coolant through the garment and the heat sink. The temperature controller regulates the amount of flow through the heat sink, depending on the garment inlet temperatures. For aircraft operations during hot weather, the controller does not allow coolant flow through the heat sink below 24° C (75° F), and as the temperature inside the pressure suit rises, the controller gradually allows an increasing coolant flow through the heat sink until full flow is established at a garment inlet temperature of 30° C (86° F). At altitude, because of external pressure changes, the volume of the coolant tubing changes, which reduces the coolant pressure. To compensate for this volume change, an accumulator is included in the system to ensure that a slug of coolant is always fed into the pump, thus assuring continuous operation during rapid altitude changes.

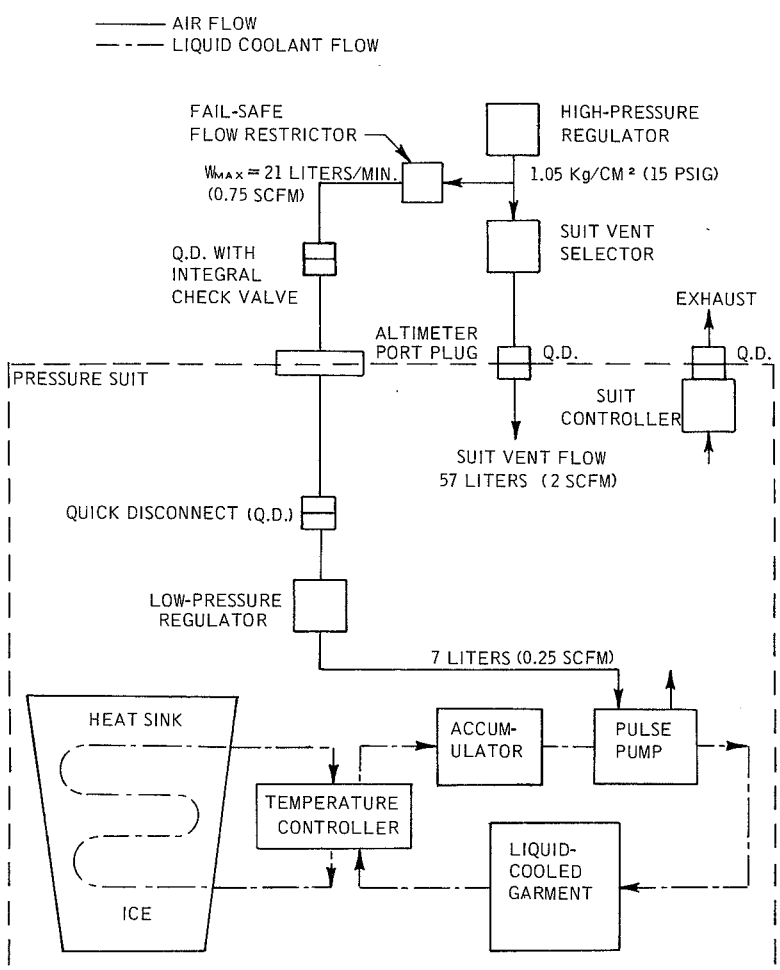

Figure 15.1 *Liquid-cooled garment with pressure suit interface.*

The heat sink is composed of spirally wound tubing (fig. 15.2), with a smaller tygon tube placed inside a larger tube. The inner tube carries the coolant and the larger outer tube contains 2 kg (4.4 lb) of ice. The outer tubing is constructed of neoprene-covered nylon and is further insulated from the wearer by 1.3 cm (0.5 in.) of urethane foam (fig. 15.3). The 3.3-cm (1.3-in.) thick heat sink is designed to fit comfortably on any particular individual by freezing the water while the pliable heat sink is resting on a mold of the pilot's back. The result is a thin, formfitting, backpack heat sink suitable for wear under a pressure suit.

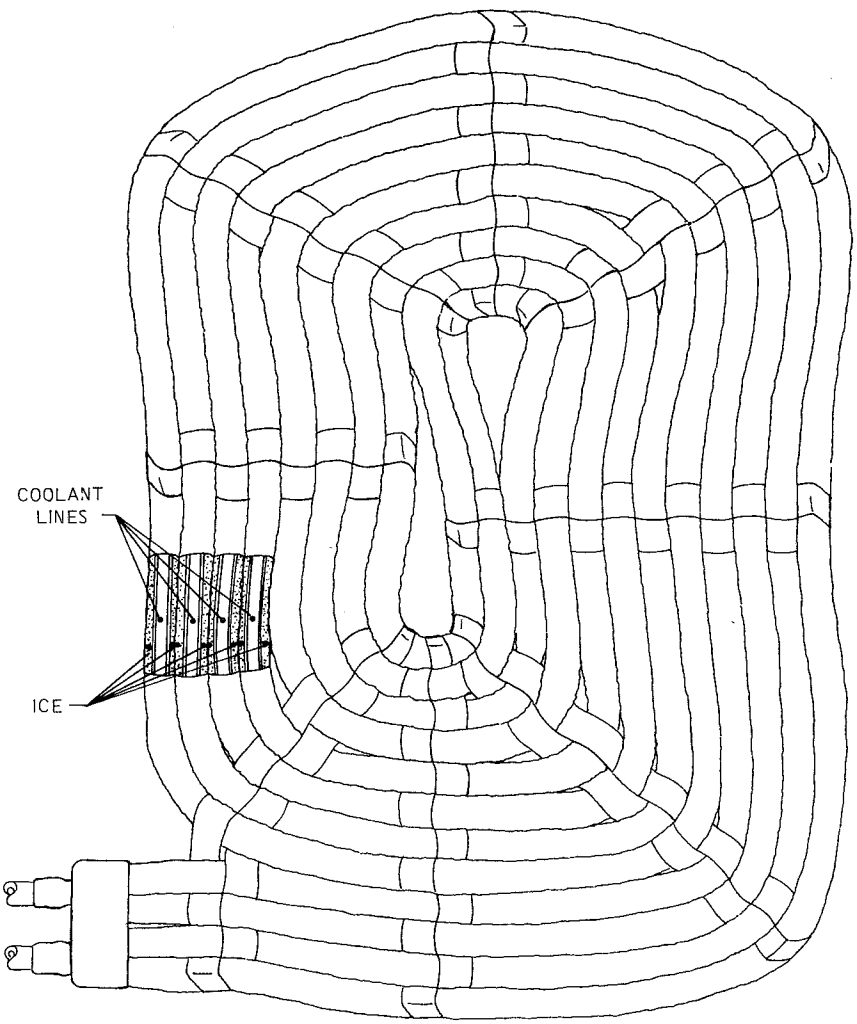

Figure 15.2 *Backpack heat sink.*

Figure 15.3 illustrates the location of the components on a pilot. The garment, containing 89 m (292 ft) of tubing, distributes the coolant over all surfaces of the pilot except for his ears, face, fingers, and the bottoms of his feet. The control hardware and pump are mounted on the left side, which least hinders pilot movement in an airplane. The heat sink is formfitted to the back with the coolant manifolds placed near the lower right abdomen.

The fully assembled system weighing 7.2 kg (16.0 lb), is charged for operation by placing the entire garment system in a freezer at -8° C (+18° F) for 20 hr. To prevent the coolant from freezing, a mixture of 20-percent glycol and 80-percent water is used. The heat sink is positioned on

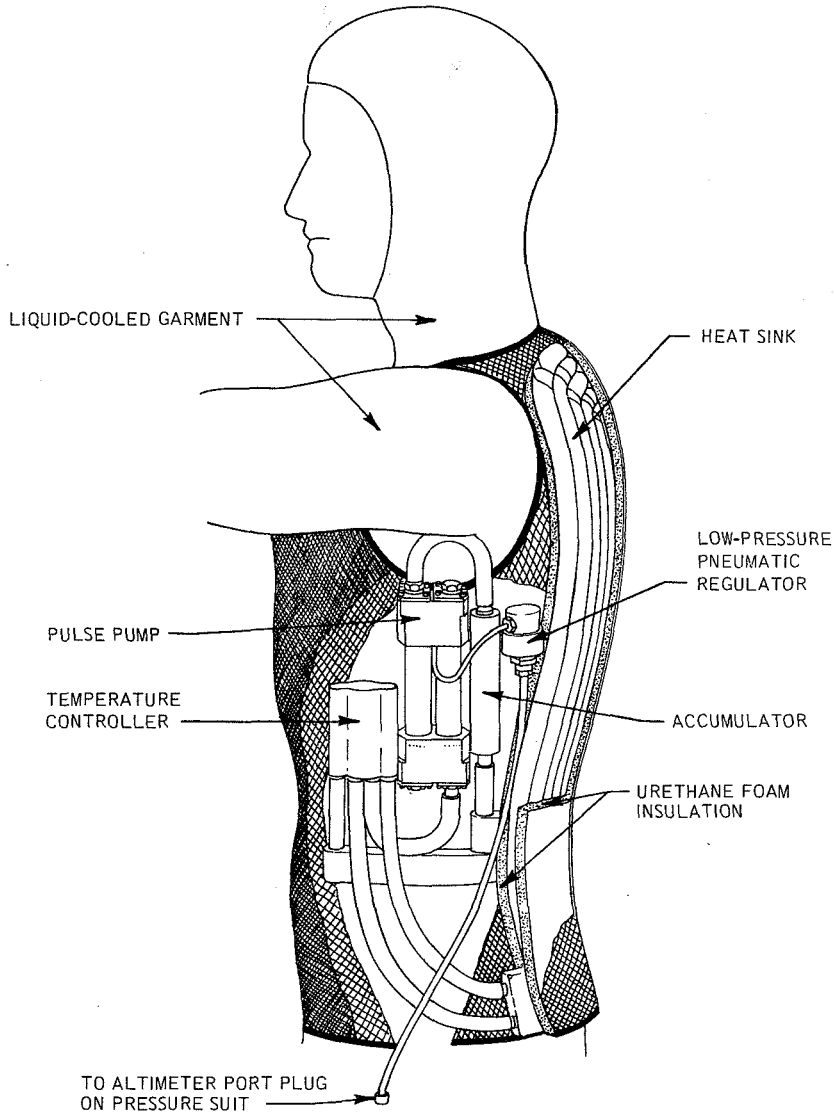

Figure 15.3 *Cooling system components positioned on a pilot.*

a mold of the back of the pilot who intends to use the system and formfitted during the freezing process to fit the pilot. After 20 hr the fully assembled and charged system is ready for use and may be donned immediately by the pilot.

With an assistant, the time required for a pilot to dress in this cooling garment system is approximately 90 sec (fig. 15.4); about 2-1/2 min are required if the pilot dresses himself. The cooling system does not add any appreciable time to that required to put on a pressure suit; however, if a pressure suit is nearly skintight, a suit of the next larger size may be required to accommodate the extra thickness of the heat sink backpack. Experiments have shown that physical movement is normal when the cooling garment is worn with the pressure suit fully inflated to 0.245 kg/cm^2 (3.5 psig).

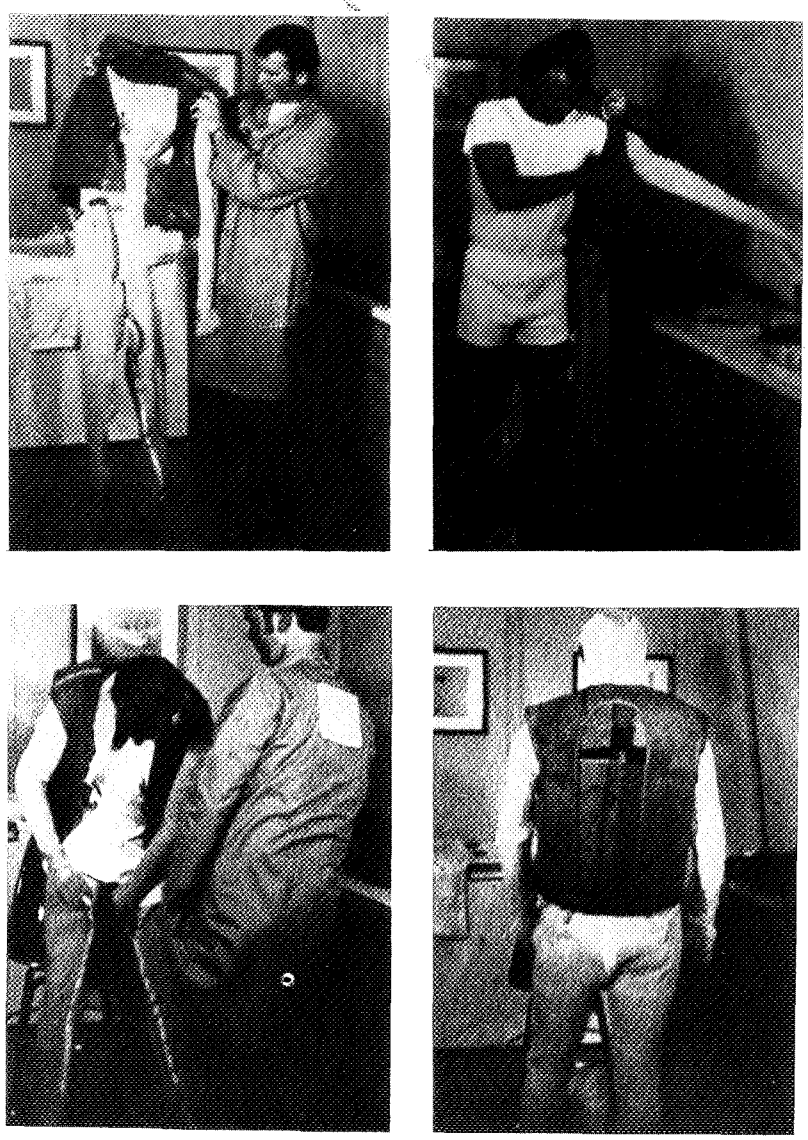

Figure 15.4 *Dressing sequence.*

TESTS AND TEST RESULTS

The cooling garment system was tested for heat absorption capability in a typical cockpit configuration (fig. 15.5) with subjects wearing full-pressure suits and reflective garments. Figure 15.6 illustrates where measurements of coolant flow rate and temperatures were taken during these tests. The heat-absorbing rates of the system were determined from flow rates and inlet and outlet temperatures of the garment.

Figure 15.7 shows the cockpit temperatures and the differential temperatures measured across the garment. The cockpit temperatures generally stay at 66° C (150° F), and the difference in temperature between the inlet and outlet valves of the garment decreases from 3.2° C (5.8° F) to 2.4° C (4.3° F) during a 40-min period.

4-6

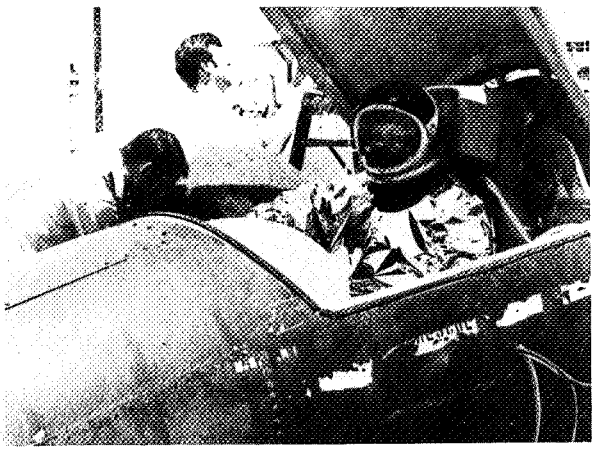

Figure 15.5 *Pressure-suited subject in cockpit simulator during high-temperature tests.*

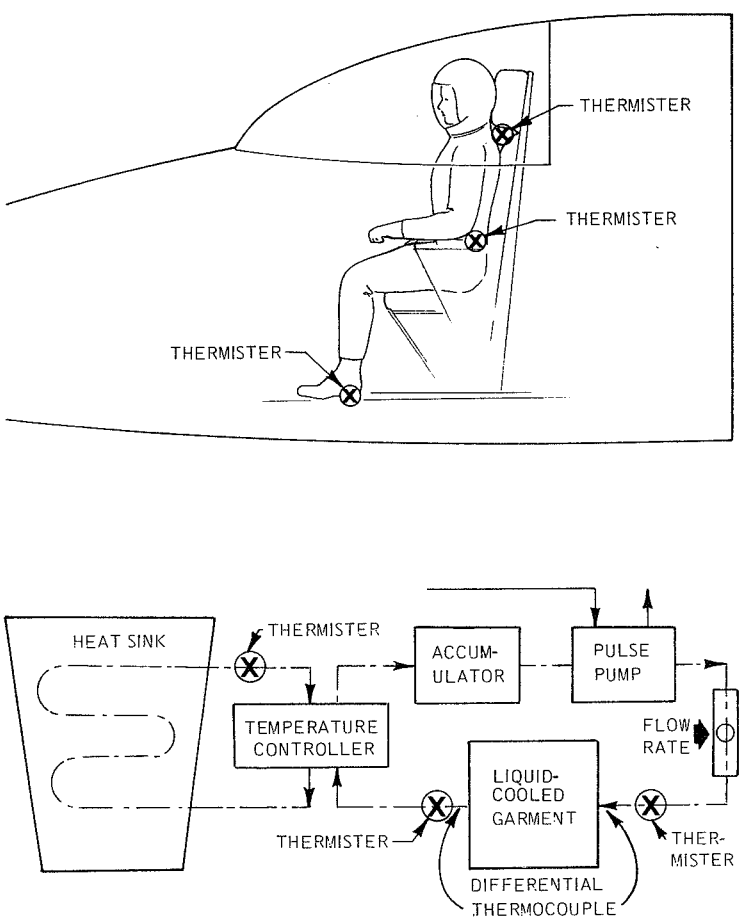

Figure 15.6 *Location and types of measurements made during tests.*

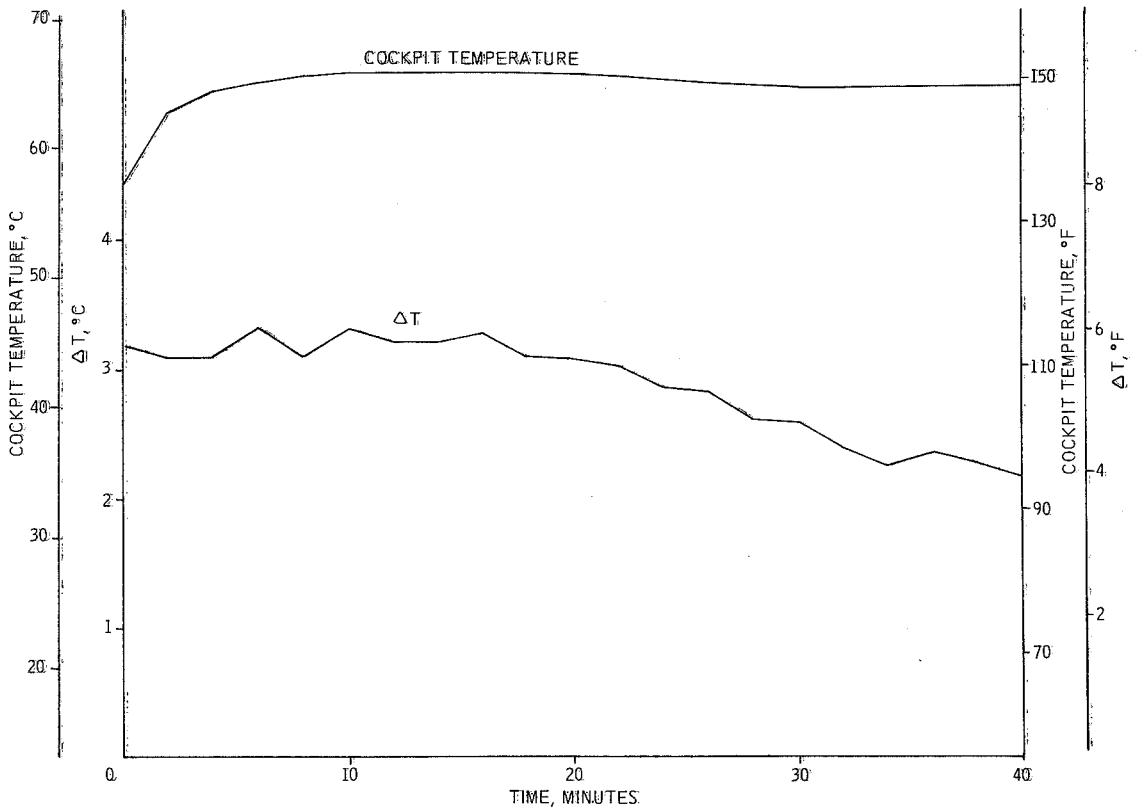

Figure 15.7 *Typical time history of cockpit temperature and the differential temperature of the liquid-cooled garment.*

Figure 15.8 illustrates the effect of the temperature controller on the heat sink outlet temperature and the inlet and outlet temperatures across the suit. As the garment inlet temperature increases, the valve opens allowing an increased flow through the heat sink. The temperature controller acts only to prevent too much cooling to the pilot. When the heat sink temperature equals the garment inlet temperature, the valve is fully open and no further reduction in temperature is possible.

Figure 15.9 is a typical graph of the system heat removal rate, Q, based on the equation $Q = Wc_p\Delta T$, where the coolant flow rate, W, ranges from 1.2 liters/min (2.7 lb/min) to 1.0 liter/min (2.3 lb/min) and the differential temperatures, ΔT, across the garment range as previously stated from 3.2° C (5.8° F) to 2.4° C (4.3° F). The specific heat, c_p, is unity for the coolant. The flow rate gradually decreases with time as the temperature controller diverts more flow through the heat sink, which increases the system pressure drop. Heat absorption rates decrease from approximately 224 kg-cal/hr (890 Btu/hr) to 143 kg-cal/hr (570 Btu/hr) in 40 min. The first 30 min are generally very comfortable for the subject; during the remaining minutes, a gradual heat load builds up which results in mild sweating during the last few minutes of the test.

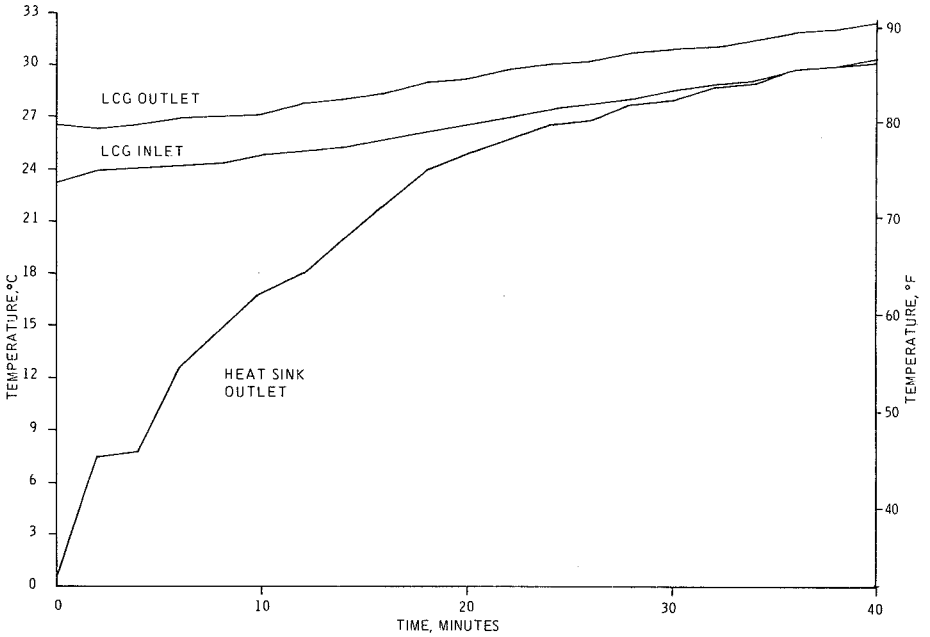

Figure 15.8 *Typical time history of liquid-cooled garment inlet and outlet temperatures and heat sink outlet temperature.*

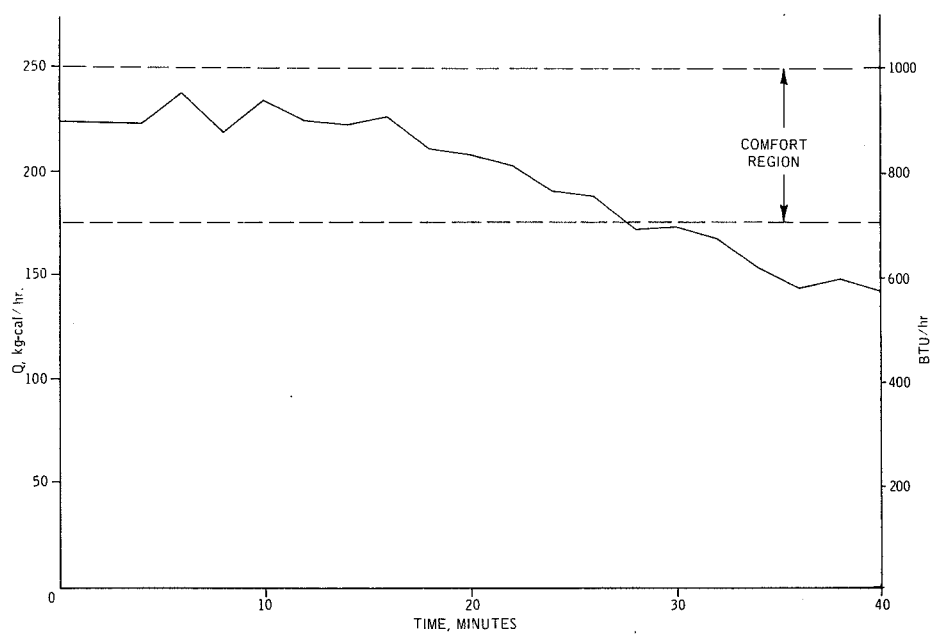

Figure 15.9 *Typical time history of liquid-cooled garment heat absorption rate.*

DISCUSSION

Under actual flight conditions, after a maximum of 40 min, the pilot will be airborne and a generous supply of cold air will be available in the cockpit for cooling. In the event the pilot is quickly airborne and rapidly cooled, the temperature controller reduces the flow to the heat sink to prevent too much cooling. During cold or long operations without the heat sink in the loop, the pump continues to circulate liquid through the garment, which evenly distributes the body heat.

A prototype cooling system garment (fig. 15.10) has been flown in high-performance aircraft (F-104B) with the test pilot wearing a regulation summer flight suit over the cooling system. Figure 15.11 illustrates the lack of bulkiness of the system and the pilot's freedom when the cooling system is being worn. These first flight tests will be followed by full-pressure suit flights. During the first test flights, the pilot reported that the garment was comfortable and provided adequate cooling in the hot cockpit during standby and taxiing. The FRC is buying four of these cooling garment systems for use with pressure suits. The garments will be evaluated by NASA test pilots during high-altitude flight missions.

Figure 15.10 *Flight-rated liquid-cooled garment.*

Figure 15.11 *Pilot wearing liquid-cooled garment.*

SUMMARY

Aircraft operations in the desert have shown a need for additional crew cooling during the ground phases of a mission when pressure suits are being worn. Tests at the FRC with pressure-suited subjects exposed to high temperatures inside a cockpit simulator have indicated that comfortable

conditions may be achieved with the combination of a reflective outer garment, a suit vent of 57 liters/min (2 cfm), and a liquid-cooled inner garment capable of absorbing heat in the range of 250 kg-cal/hr (1000 Btu/hr) to 175 kg-cal/hr (700 Btu/hr).

A flight-rated liquid-cooled-garment system for use inside a full-pressure suit has been designed, fabricated, and tested. High-temperature tests with this system have indicated that heat is absorbed at a rate decreasing from 224 kg-cal/hr (890 Btu/hr) to 143 kg-cal/hr (570 Btu/hr) over a 40-min period. The first 30 min are very comfortable; thereafter a gradual heat load builds that results in mild sweating at the end of the 40-min period.

In flight tests during hot weather when this cooling system was worn under a regulation flight suit, the pilot reported that temperatures were comfortable and that the garment prevented sweating.

REFERENCES

1. Nunneley, Sarah A.: Water Cooled Garments: A Review. Space Life Sciences, vol. 2, 1970, pp. 335-360.
2. Chambers, A. B.: Controlling Thermal Comfort in the EVA Space Suit. ASHRAE, March 1970, pp. 33-38.
3. Jurgens, F.: Aircrew Cooling Study. TG-945, Applied Physics Laboratory, Johns Hopkins University, 1968.
4. Waligora, J. S.; and Michel, E. L.: Application of Conductive Cooling for Working Men in a Thermally Isolated Environment. Aerospace Med. vol. 39, 1968, pp. 485-487.

16 POTENTIAL TECHNIQUES AND DEVELOPMENT ACTIVITIES IN DIVER SUIT HEATING

A. P. Shlosinger
Systems Group of TRW, Inc.
Redondo Beach, Calif.

INTRODUCTION

Thermal insulating materials, suitable for application in diving suits, so far are unable to provide sufficient protection against excessive heat loss. Low water temperatures, the high thermal conductivity of water (relative to air), and heat loss resulting from breathing of cold gas result in body heat losses far exceeding metabolic heat production.

Insulating materials are normally made of low thermal conductivity solids arranged such that heat paths in the solid are long and devious. The bulk of the insulating material consists of small gas-filled pores. External pressures of deep submergence tend to collapse these pores; hence, insulating capability degrades with increased submergence pressure.

Attempts have been made to provide pores structurally capable of withstanding the external pressures. Microspheres were embedded in elastomeric materials in the expectation that the small diameter and spherical shape would provide sufficient resistance against collapse under deep submergence pressures. The resulting materials, while providing an improvement relative to the elastomeric foam materials used in standard wet suits, still do not provide, at acceptable thickness, sufficient thermal protection. The special-purpose vacuum insulating techniques, used for cryogenic and space applications, are obviously not applicable where flexibility is required and external pressures are high. Thermal insulation, as applied in standard wet suits, provides only limited protection, suitable for shallow dives, so long as water temperatures are mild.

Satisfactory thermal protection of a diver can be defined as the capability to maintain a sufficient temperature gradient between skin surface and surrounding ambient water. For the extreme case of a water temperature of 28° F (freezing point of seawater), a skin temperature of 90° F, and an assumed metabolic rate of 400 Btu/hr (essentially a resting diver), maintenance of the 62° F temperature gradient would require a thermal conductance as low as 0.02 Btu/hr-ft-° F for a 0.75 in. thick thermal insulating material. Only a drastic breakthrough in thermal insulating techniques could achieve a thermal conductance as low as this under deep submergence pressures in a suitably flexible material; thus, a heat supply is necessary to keep the diver's body temperature at an acceptable level.

Supplying heat from a heat source to the proximity of the diver's body surface does not mean that heat is actually added to the diver's body. Rather, metabolic heat generated by his body and lost through thermal insulation is supplemented by additional heat from an auxiliary source to maintain a sufficient temperature gradient. Using Ohm's law as an analogy, "current flow" is increased to maintain a sufficient "potential difference," because "resistance" cannot be increased beyond a certain value.

Heat transfer analysis based on available thermal insulating materials and reports from experimental investigations indicate that approximately 1500 thermal watts are required to keep a

diver sufficiently warm for efficient performance and reasonable comfort. A large fraction of this amount of heat must be supplied to the proximity of the diver's body surfaces. Some of it will be applied to preheating the breathing gas and to other parts of the diver support system.

DIVER SUIT HEATER SYSTEM

The complete diver suit heater system has three elements:

1. A source of thermal energy.
2. A means of transmitting energy to the proximity of the diver's body surfaces.
3. A means of controlling heat supply and temperature in accordance with requirements, and adapting system operation to the variations of pressure from sea level to the maximum submergence level anticipated.

Sources of thermal energy considered include electrical energy from batteries, nuclear energy from an isotope heat source, heat stored by a suitable method (such as a liquid/solid phase change), and exothermic chemical reactions.

Techniques for transmission of energy to the proximity of the diver's body require only a wiring system for electric heating. Forced circulation of a heat transfer fluid in a fashion similar to that of the Apollo suit undergarment will apply to systems generating heat in a portable pack carried by the diver.

Techniques for control of heat supply vary. Electric energy can easily be controlled by switching arrangements, turning heat supply on or off, or reducing or increasing the number of heating circuits. For an electric blanket-type garment no adaption to pressure variation is required. Heat from isotope heat sources, with their fixed-energy output, would be controlled by valves in the forced flow circulating loop, providing control of heat supplied and rejection of excess heat to the surrounding water. Similar techniques will apply to the application of stored heat, except that excess heat rejection is neither required nor desirable.

Exothermic chemical reactions have the advantage that reaction rates can be made variable over a relatively wide range and reactant (fuel) consumption can be adjusted to heat requirements.

Pressure equalization with the submergence ambient is normally accomplished for submerged hydraulic systems by use of a flexible diaphragm or bellows that transmits submergence pressure to the closed hydraulic system's loop. Similar techniques will satisfy the requirements of a diving suit fluid loop.

The availability of enough thermal energy for the full duration of a mission appears to be the key for a practical and satisfactory diving suit heater system.

THE HEAT SOURCE

As transmission of thermal energy to the body surfaces and control of fluid flow or electric current do not represent fundamental problems, this paper is concerned mainly with the source of thermal energy.

Assuming missions in the order of 2- to 6-hr duration, requiring 1500 W or over 5000 Btu/hr, requires a high energy-density source of heat. Electric resistance heating in an arrangement similar to an electric blanket was tested during the Sea Lab II mission. Results were not too satisfactory. Difficulties included distribution of heat over the body surfaces, and resistance wires getting too hot. While better design could overcome these difficulties, the total amount of available energy was limited by battery size to 3 hr at only 350 W (ref. 1).

After Sea Lab II, heating with circulating warm water by a water tube-type undergarment, similar to the one used on the Apollo extravehicular space suit, was suggested. A radioisotope was suggested as a convenient, compact source of heat. References 2 and 3 discuss a system, applying a Plutonium 238 heat source of 420 thermal W. Reference 2 describes the difficulties of shielding of even this inadequate heat source in an experimental diving suit heater system, built under a joint effort by the Navy and the AEC. The same reference mentions that during the development time span of this system the initial requirement of 300 W was upgraded, first to 800 W, then to 1100-1500 W. Only 270 thermal W (about 64 percent) were eventually useful to the diver from the 420 W isotope heat source used. It became apparent that isotopes would not provide a practical solution when energy levels in the range of 1500 W are required.

Interest was then directed to exothermic chemical reactions. Since diver suit heater systems application differs significantly from space suit applications in regard to probable number of units required, first cost and fuel costs would have to be moderate. The objective was a suit heater system that would serve both military applications and commercial divers. Desirable objectives were formulated as a set of design criteria (table 16.1), which provided a basis for the evaluation of several selected exothermic processes (table 16.2). Engineering problems connected with the design, development, and fabrication of a suitable reactor were considered, along with operational aspects such as refueling, storage, cost, and availability of the reactants.

Table 16.1 *Diving suit heater criteria.*

The self-contained heater system will permit free-swimming for 4 hr or longer
The free-swimming diver will have minimum encumbrance
Complete system including heat generator for heating of circulating water, circulating pump, and controls for temperature and submergence level will require only a minimum of battery-supplied electric energy
Construction materials will be conventional (such as stainless steel, copper alloys, and plastics) so no exotic alloys, refractories, or other expensive materials can be used
Fuel and oxidizer will be readily available, of low cost, and permit simple refueling
Fuel will be of high energy-density, and exothermic chemical reactions should be essentially stoichiometric to avoid the need for excess fuel or oxidizer
Fuel and oxidizer will be used in their undiluted form to avoid excess storage bulk
Reaction products discharged into the ocean should not cause "telltale" of diver operation

Table 16.2 *Exothermic processes evaluated.*

Catalytic decomposition of hydrogen peroxide
Rocket fuels
Oxidation of shredded or powdered metals with oxygen
Hydration of alkali metals
Combustion of hydrocarbon fuels with oxygen

Hydrogen Peroxide

Hydrogen peroxide decomposes exothermally in contact with a catalyst, forming gaseous oxygen, steam, and heat by the reaction

$$H_2O_2 \rightarrow H_2O + 1/2\ O_2 + 21980 \text{ Btu/lb mole}$$

Hydrogen peroxide is attractive because it is a single fluid that will generate heat when brought in contact with a catalyst. The water vapor (steam) formed could be used to heat the diver if condensed and circulated through the suit or routed through a heat exchanger. One pound of peroxide (approximately 25 cu in. at 70 percent concentration) will provide approximately 1150 Btu after the steam is condensed. There are two obstacles to application:

1. Hydrogen peroxide in concentrations sufficiently high to undergo exothermic decomposition is dangerous to handle. Almost any metal and a number of other substances will act as catalysts and induce the above reaction. The reaction could occur in storage tanks during shipment, in transfer hoses or any container used, unless extreme cleanliness precautions are applied. The reaction generates heat and tends to become spontaneous above 350° F. The oxygen generated is in a highly reactive state and presence of organic contaminations would aggravate the danger of explosions.
2. Decomposition products of the peroxide dissociation must be expelled into the ambient ocean environment. This requires the reactor to operate above the submergence ambient pressure. The hydrogen peroxide decomposition process is accompanied by an increase in volume; hence, increased pressure may adversely affect decomposition.

Rocket Fuels

As in the case of hydrogen peroxide, rocket fuels, such as hydrazine or hydrazine hydrate, require special precautions in storage and handling. Extreme cleanliness, protection against toxic effects of vapors or contact with the human skin, and the difficulties in shipping, storing, and handling of fluids with inherently dangerous characteristics preclude the application of these fuels, for logistic reasons, to diving suit heaters.

Metal Combustion with Oxygen

Several metals in a form providing a large surface area and small bulk density, as when powdered or shredded like steel wool, can be burned with oxygen, yielding significant amounts of heat. Flammability of magnesium, even in air, is well known. Aluminum and steel will sustain combustion processes at sufficiently high temperatures and in the presence of sufficient oxygen concentrations. Combustion of aluminum is used in flashbulbs and in the aluminothermic (thermit) welding process. Combustion of iron takes place in oxygen torch-cutting of iron or steel, which when heated to approximately 1500° F is cut by a stream of oxygen. Potentially, a number of other metals could be used for this purpose. Iron, copper, and aluminum are readily available in shredded form, and they are perfectly safe to handle.

Combustion of a metal with oxygen for generation of heat becomes attractive when the combustion product is a solid, which because of its high density can be retained in the combustor for the duration of a mission. This eliminates the need of expelling of combustion products against submergence pressure.

For iron/oxygen, for example, each of the following possible reactions will result in a solid reaction product:

1. $2Fe + O_2 \rightarrow 2FeO + 1608$ Btu/lb reactants
2. $4Fe + 3O_2 \rightarrow 2Fe_2O_3 + 2243$ Btu/lb reactants
3. $3Fe + 2O_2 \rightarrow Fe_3O_4 + 2071$ Btu/lb reactants

Apparent difficulties in application of these reactions include the requirement that the metals be maintained at their combustion temperature, which in the case of iron is ~ 1500° F.

The technique normally applied to obtain useful heat output from combustion processes is to first complete the combustion process at the temperature required to sustain the reaction, and then route the gaseous products of combustion through a heat exchanger. This technique is obviously not applicable when the combustion product is a solid. It will probably be necessary to maintain a sufficiently high temperature gradient between the burning metal and the water to be heated such that the temperature of the burning metal is not reduced below the temperature at which efficient combustion can be sustained. If water is to be heated to 110° F and a combustion temperature of 1500° F is required, a temperature gradient between combustion zone and circulating water in the order of 1390° F must be maintained.

A metal fuel such as iron in the form of steel wool must have a relatively low bulk density to sustain combustion. With the assumption that the steel wool could be compressed to one-half its normal commercially available bulk volume, it was found that for a mission at 1500 W heat requirement, 0.22 cu ft of steel wool would be required for each hour of operation.

It is difficult to visualize that a volume of steel wool sufficient for 4- or 6-hr mission (0.88 or 1.3 cu ft) could be directly incorporated into the combustor. Steel wool cannot be fed from a storage tank through tubes like a gaseous or liquid fuel to the combustion zone, but it could be applied in the form of a cartridge–like package. Recharging would be accomplished by removal of the old cartridge containing iron oxide and insertion of a new cartridge. To start combustion after recharging–that is, initiate the reaction with oxygen–the temperature must be raised by some means to about 1500° to 1800° F. Such a temperature increase will require the use of an auxiliary fuel or a relatively large amount of electric power. In spite of these problems, it is understood that a diving suit heater of this type has been developed.

Hydration Reactions of Alkali Metals

Alkali metals react violently when brought into contact with water, forming hydroxides of the metals, gaseous hydrogen, and heat. These reactions appear attractive because the diver is surrounded by one of the two reactants–that is, water. Both metallic calcium (Ca) and metallic sodium (Na) have been considered. The reaction of metallic sodium with water is possibly more difficult to control than that of calcium, but the former, used extensively as a heat transfer medium in nuclear reactors, is more readily available and lower priced. The thermal energy yield is high, as shown here for calcium:

$$1 \text{ lb } Ca + 0.899 \text{ lb } H_2O \rightarrow 1.849 \text{ lb } Ca(OH)_2 + 0.050 \text{ lb } H_2 + 7692 \text{ Btu}$$

However, the volumetric yield (heat per cu ft fuel) depends on the form in which the fuel is applied. For application of this approach to be practical, the metal must be packaged in such a way that the reaction can be slowed and controlled.

One approach would be to diffuse the metal in powder form into a water-soluble inert material. As the inert material is slowly dissolved, water will contact the small metal particles, which will react one at a time. The otherwise explosion–like reaction between metal and water may be controllable by this method, but fuel volume will be increased by the inert material. Whether, in practice, seawater can be used as one of the reactants is uncertain. Its composition is not always predictable, and certain areas show high turbidity (solid content) while in other areas where a diver must operate oil or other contaminations could be present.

The metal/water reaction results in the production of gaseous hydrogen, which must be expelled. Hydrogen is only slightly soluble in water and would possibly indicate the presence of a diver. Hydrogen would further present a danger if permitted to enter habitats or collect in the cavity of a shipwreck or sunken airplane, which may be the objective of a diver's activity.

Although the use of alkali metal/water reactions is an interesting possibility, the safety aspects, control of the reaction, and logistics, including manufacturing methods for inerted fuel cartridges, would entail extensive and probably quite costly development work.

Hydrocarbon Fuels and Oxygen

Combustion of hydrocarbon fuel with oxygen is attractive from the viewpoint of logistics as well as thermal yield. Oxygen, usually in the form of compressed gas, is used for breathing atmosphere replenishment in many diving operations. Its handling, shipment, and storage, therefore, is well known to diver support personnel. Hydrocarbon fuels such as kerosine, gasoline, propane, and butane are readily available, inexpensive, and can be applied in the commercially available form without special packaging in fuel cartridges or dispersions. A further advantage is that these reactants are liquids or gases, which can be easily transmitted through tubing, controlled by valves, pumped, and stored in containers. Safety precautions in handling are those normally observed in refueling automobile gas tanks or recharging cigarette lighters. Heat values are high, in the order of 20,000 Btu/lb of fuel at a liquid fuel density between 30 and 50 lb/ft^3.

From the criteria shown in table 16.1, the advantages of logistics and practicability were believed to warrant selection of this system for further development. As with any other system, certain engineering problems remained, but essentially all of these have now been resolved.

The objective was the development of a compact reactor, suitable for combustion of a selected hydrocarbon fuel with oxygen under shallow as well as deep submergence diving conditions. This development work was undertaken by the TRW Systems Group in Redondo Beach, Calif., as an in-house funded effort. For this reason, the information presented here is limited to results of these development activities.

Table 16.3 summarizes the engineering problems to be solved before the selected reaction could be used in heating water circulated through a water tube-type diving suit.

Table 16.3 *Engineering problems of water tube-type diver heating systems.*

Reaction must be confined in a fully enclosed reaction chamber
Reactor and heat exchange provisions for heating fo circulating water must be included in a compact, portable package
Stoichiometric reaction without significant fuel, oxidizer excess, or any dilutent is required to minimize storage tank size for fuel and oxidizer
Means are required to obtain efficient combustion without the need for temperatures of 3000° to 4000° F, as normally required, to avoid costly materials and construction

Table 16.3 *Engineering problems of water tube-type diver heating systems. (Concluded)*

	Reaction chamber must operate at a pressure in excess of submergence ambient to permit expelling of combustion product against submergence ambient pressure
	Combustion products expelled from the combustor must not result in "telltale" bubbles rising to the surface

The fuel selected was propane, which is readily available and, even in the commercially available form, is predominantly a single compound rather than a mixture (like gasoline). The use of a single compound simplified calculations of theoretical performance for comparison with measured heat output (thus establishing overall efficiency). Propane is sold in pressurized containers as a saturated liquid, and container pressure depends on temperature. For experimental work, tank pressure could be controlled by controlling tank temperature.

A basic closed-reactor design was developed and then upgraded as development work progressed. The third prototype is being tested. Each prototype included a reactor chamber, heat exchange surfaces, and channels for flow of the water to be heated.

The first prototype was a rather clumsy device made partially of leftover parts from another experiment, but sufficient for demonstration of basic feasibility of the concept. The second-generation prototype is shown in figure 16.1.

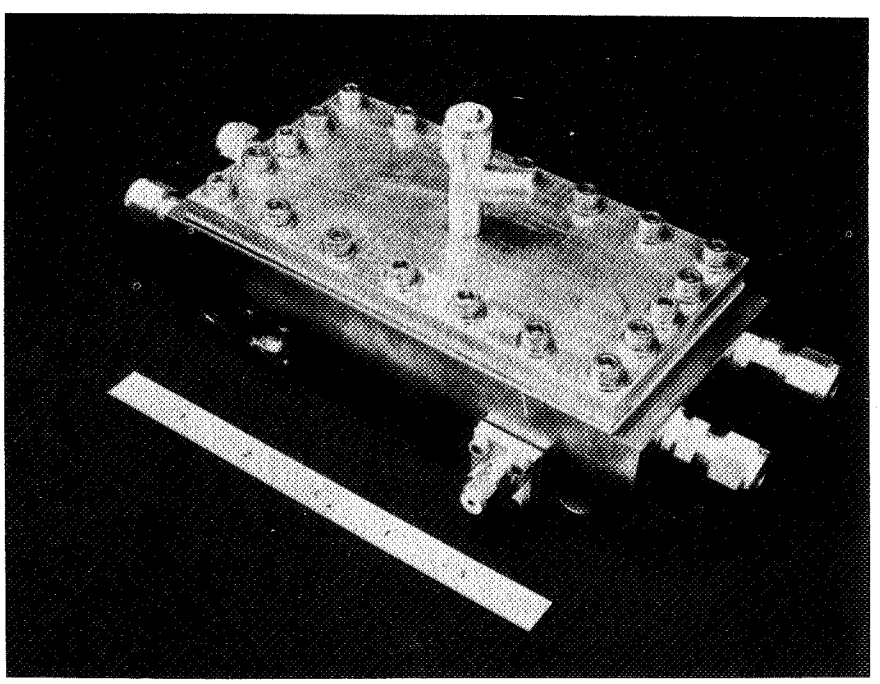

Figure 16.1 *Second generation prototype reactor.*

The efficient combustion of hydrocarbon fuel-oxygen mixtures usually requires temperatures of 3000° to 4000° F. In the presence of a catalyst, however, high combustion efficiency can be achieved at less than 1000° F, and high temperature resistant and costly materials are not needed.

In fact, the second prototype was machined from a solid block of copper with a flanged-on lid (fig. 16.1). After more than 200 hr of operation for data taking, there was no indication of melting or excessive oxidation of the copper. Dimensions of the prototype were 6 by 4 by 2 in.

Figure 16.2 shows a third-generation prototype, which is smaller than the second (6 by 3.75 by 1 in.) and is made of stainless steel.

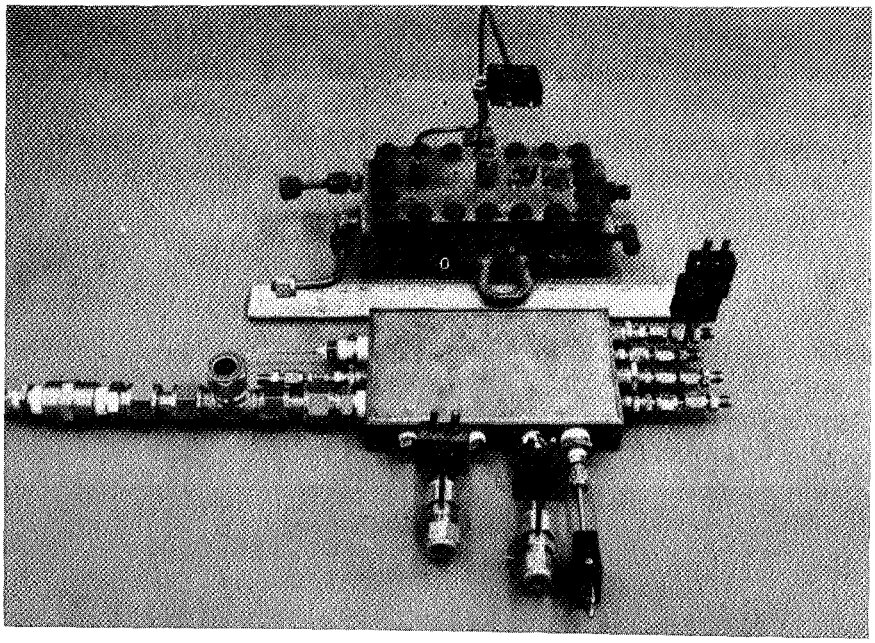

Figure 16.2 *Third generation prototype reactor.*

The prototypes were tested for performance, combustion efficiency, start-up characteristics, and flexibility of heat output. Figure 16.3 is a view of the test setup now in use. Water is circulated in a closed loop through the reactor and a water chiller, which serves as heat sink. The flow of fuel, oxidizer, and circulating water are measured. Temperatures are measured at several points including water "in" and "out," exhaust gas, casing, and combustion chamber.

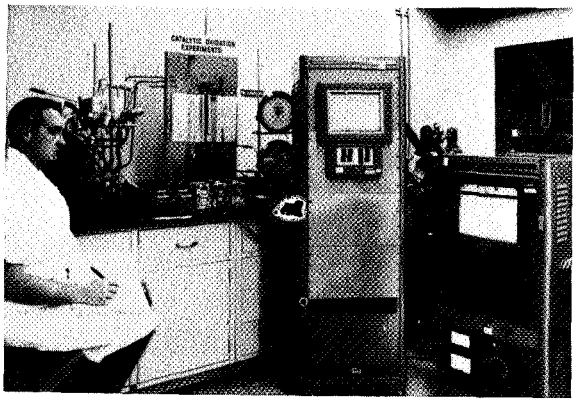

Figure 16.3 *Test setup.*

Figure 16.4 shows an example of data on heat output performance obtained on one test run; for comparison the calculated heat output for a stoichiometric fuel-oxidizer mixture is shown. The performance data points are based on measured water flow and temperature rise of the water. The difference between the calculated and actual measured performance includes, therefore, the effects of combustion and heat exchange efficiency. Efficiency at various heat output rates varies, but is, in general, better than 80 percent.

Other results of these test runs include:

1. Good overall efficiency.
2. Good combustion efficiency verified by gas chromatography.
3. Low casing temperature, generally well below 200° F. This is important because of the difficulties of providing thermal insulation under deep submergence pressure; little insulation is needed for personnel protection or reduction of heat loss to ambient.
4. Combustion process flexibility, which allows control of heat output by throttling of fuel and oxidizer flow over a wide range.
5. Measured heat output of these small and compact "water heaters" better than 2000 W, providing the potential for an abundant supply of heat to the diving system.

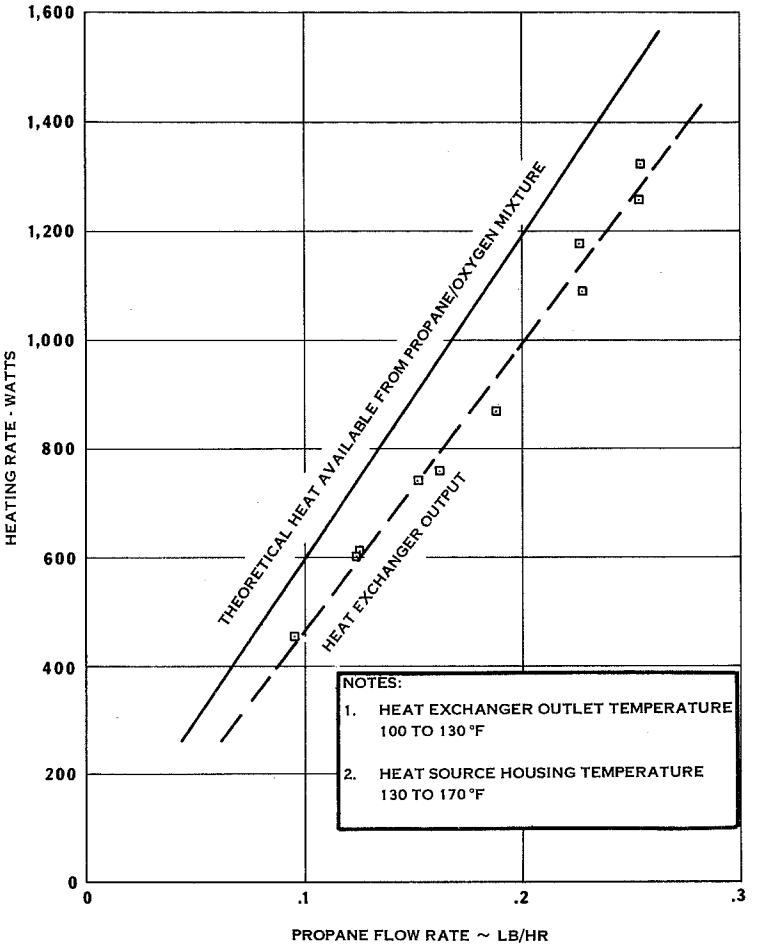

Figure 16.4 *Test results of catalytic heat source operated at stoichiometric mixture ratio.*

With this type of system, combustion products are expelled into the ambient. Therefore, combustion chamber pressure greater than that of the submergence ambient must be maintained. Supply pressure will therefore be regulated just as it is done on the surface, in relation to ambient pressure. This is the type of downstream pressure control normally used on standard compressed gas bottles.

In theory, the combustion process will be enhanced by increased pressure. Preliminary tests up to 30 psig have shown that operation of the reactor is unaffected. Test runs at higher pressures are in preparation.

In accordance with the criteria of table 16.2, there will be no indication of diver presence as a result of diving suit heater operation. The combustion products expelled into the ocean are carbon dioxide and water vapor. When expelled into the ocean ambient, the water vapor will, of course, immediately condense and disappear. Carbon dioxide is highly soluble in water, and preliminary experiments verify that it will disappear by going into solution. When carbon dioxide was injected, by nozzle, into the bottom of an approximately 8 ft tall glass tube filled with seawater, bubbles about 0.25-in. in size were released from the nozzle at the bottom. When they had risen approximately 4 ft, their size was noticeably reduced, and by the time they reached the top of the glass tube, some of them completely disappeared while others had shrunk in size to roughly the

dimensions of the bubbles in soda pop. The exhaust port can be designed such that the emitted carbon dioxide gas will disappear by solution in water within a few feet from the diver.

The successful testing of a heat source capable of providing an abundant amount of heat from a small portable package opens the way to development of a complete system for the free-swimming diver. Work has begun on a heat-operated pump for the circulation of water through the diver's suit and conceptual design has been completed of the system controls that will provide automatic adaption to variations of submergence level and control of temperatures and heat produced.

REFERENCES

1. Cannon, Berry L.: Unusual Engineering Problems in Undersea Living. Trans. Joint Symposium on Man's Extension into the Sea, Washington, D.C., Jan 1966.
2. Zimmer, Glenn W.: Radioisotope Heated Swimsuit. NASA SP-234, 1970, pp. 115-126.
3. Anon.: AEC's Radioisotope-Powered Heater for Diving Suits to Get U.S. Navy Test. AEC, miscellaneous release K-234, Washington, D.C., Oct. 1967.

17 PORTABLE LIFE SUPPORT FOR INSTRUMENTATION OF AN OFFSHORE PLATFORM

Michael M. Mull and Clarkson L. Coffin
Mechanics Research, Inc.
Los Angeles, Calif.

INTRODUCTION

Not all portable life support system design takes place in the laboratory. Occasionally a situation arises in an industrial or military operation that requires a unique or unavailable system. The people involved must rely on their own ingenuity to develop a new system or to modify an existing one to meet their needs. This paper discusses just such a situation.

Mechanics Research, Inc. (MRI) received a contract from Continental Oil Company to instrument an offshore drilling platform for measurement of structural response of the platform to severe storms and hurricanes. A typical platform is shown in figure 17.1. Specifically, this instrumentation consisted of the following measurements:

Structural response of a piling driven into the ocean floor
Structural response of the jacket members, including typical welded joints

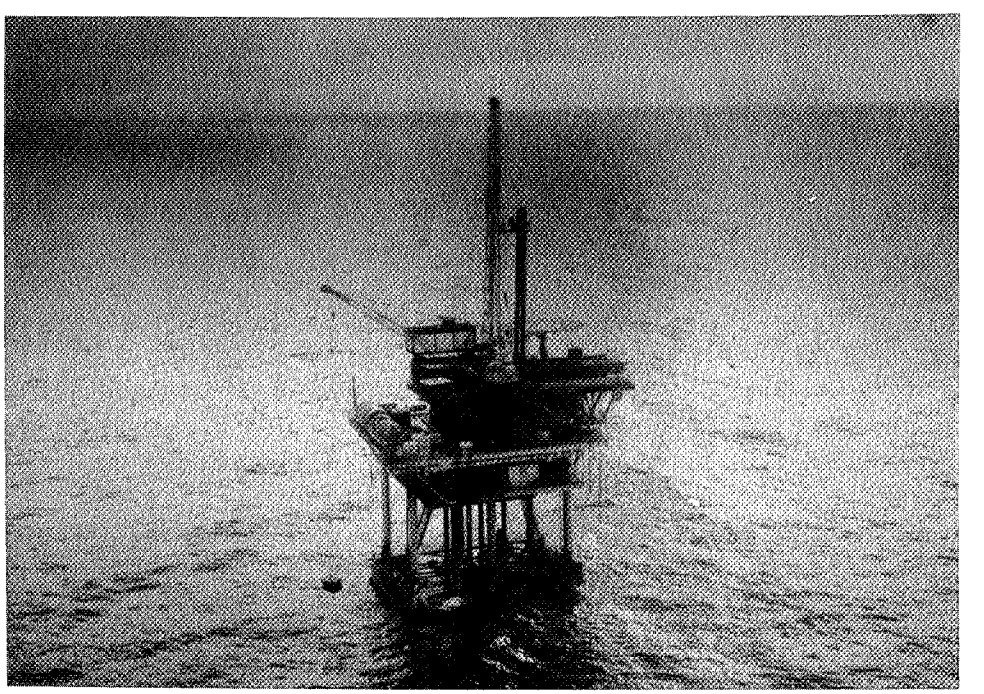

Figure 17.1 *Typical Gulf offshore drilling platform.*

The hydrodynamic parameters of wave height, direction, velocity, and force on a typical structural member

The aerodynamic parameters of wind velocity and direction

This paper discusses the life support considerations for the field engineer installing the instrumentation for the first item listed above. Strain gages were installed in the piling after it had been driven through the leg of the jacket into the ocean floor. The life support requirements are unique in that instrumenting inside a piling below the mud line is a new activity. In this regard, the MRI program constituted a totally new application for portable life support systems.

Life support requirements for this application included the following elements:

Sustaining air supply

Emergency air supply

Provision for monitoring concentrations of CO_2, CO, H_2S and combustible gases such as methane.

For this program, all system requirements were satisfied by commercially available hardware.

PLATFORM DESCRIPTION

As shown in figure 17.2, a typical offshore platform of the type used in the Gulf of Mexico consists of three basic structural components: jacket, deck, and pilings.

The ocean depth at the site involved in this installation was 176 ft, and the resulting jacket was approximately 186 ft high. The pilings are long tubular members that are driven through the legs of the jacket into the ocean floor to anchor the platform. They are then welded to the top of the jacket leg. The deck section legs are then stabbed into the pilings and welded.

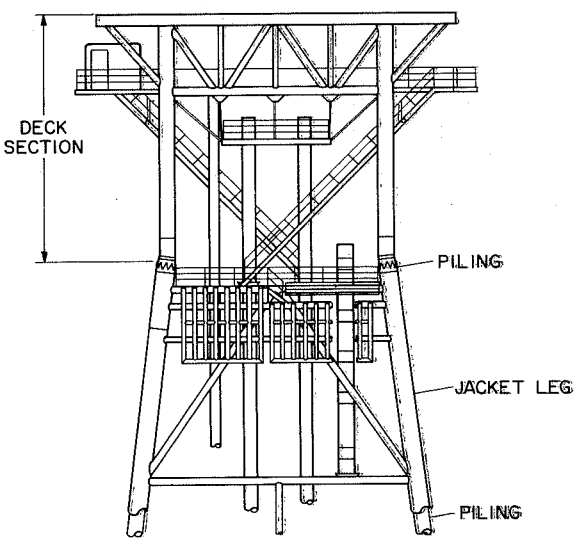

Figure 17.2 *Assembled platform structure.*

ENVIRONMENT

The working area for this program was in one of the cylindrical pilings. The pilings, which are approximately 550 ft long, taper from an inside diameter of 31 in. at the top to 29-1/2 in. at about the mud line. As these pilings are driven into the ocean floor, they fill with mud and water. Prior to installation of the deck structure, the piling to be instrumented is cleaned out to a depth of approximately 70 ft below the mud line. A concrete plug is then poured into the bottom to seal the end. The top of the plug is approximately 60 ft below the mud line.

As shown in figure 17.3, a door cut in the leg at the cellar deck level provided access to the piling work area. Figure 17.4 shows the elevator (powered cage) for transporting the instrumentation engineer and his equipment up and down within the piling. Figure 17.5 shows the elevator equipment compartment with the electrical equipment and welder in place. Figure 17.6 is a top view of the elevator moving within the piling. A view of strain gages in place looking up from the elevator is shown in figure 17.7. There were six vertical strain gage locations starting at the mud line (ocean floor) and terminating 54 ft below the mud line. Work duty cycles within the piling ranged from 3 to 5 hr.

Figure 17.3 *Access door in deck leg.*

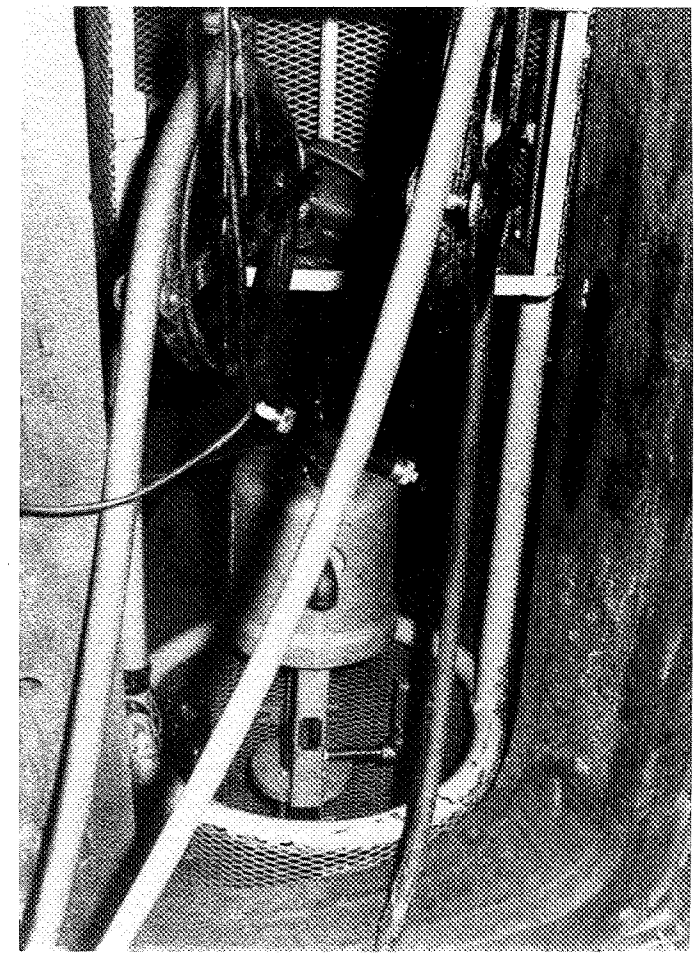

Figure 17.4 *Piling elevator.*

The gaseous environment within the piling was comprised of the following constituents:

Air supplied continuously from the surface
Carbon dioxide from normal respiration
Carbon monoxide from internal combustion engines located at the surface
Acetylene from metal cutting operations
Gases such as methane and sulphur dioxide from the soil into which the piling is imbedded

Air composed the major volume of gas present in the piling during the time that people were working. However, at the outset, it was not known how the concentrations of the other gases would vary during the work period. In this regard, ground gases, such as methane, were of primary concern, because the ground structure had been disturbed by the entrance of the piling.

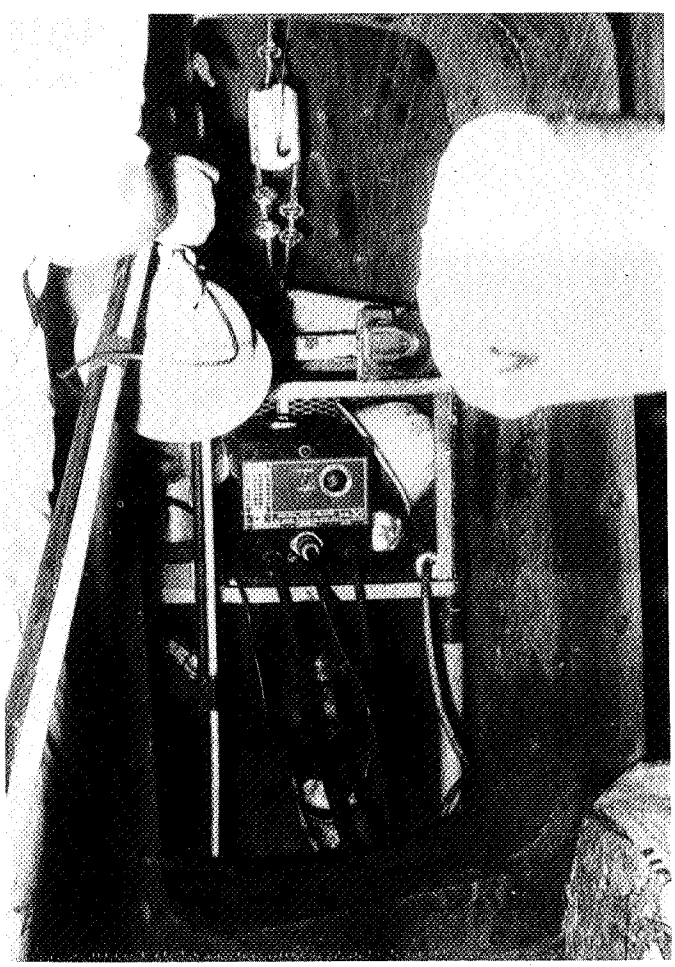

Figure 17.5 *Elevator equipment compartment.*

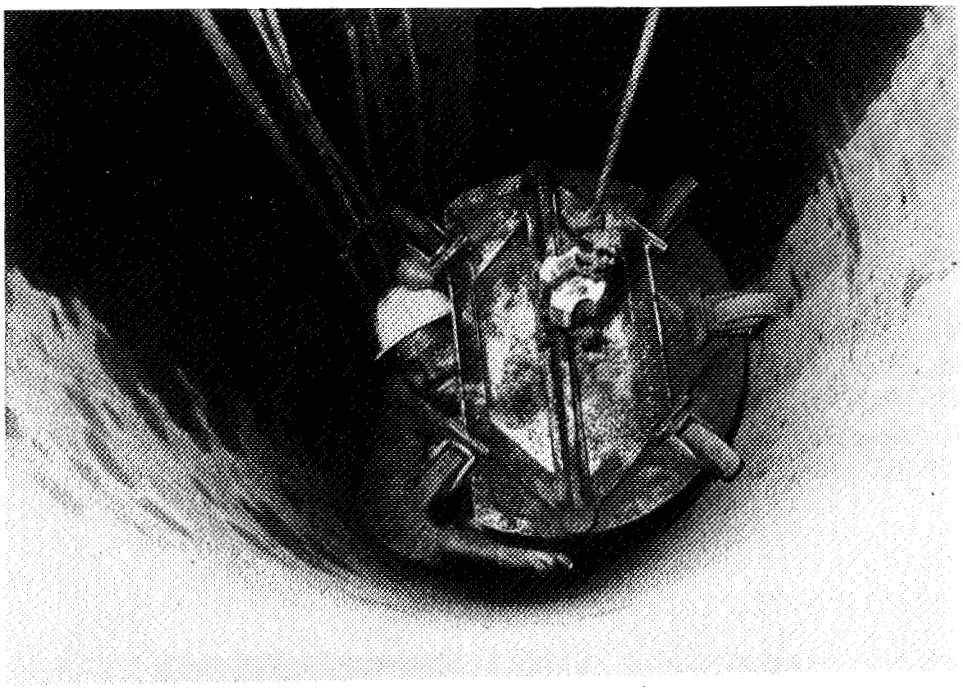

Figure 17.6 *Elevator moving down in the piling.*

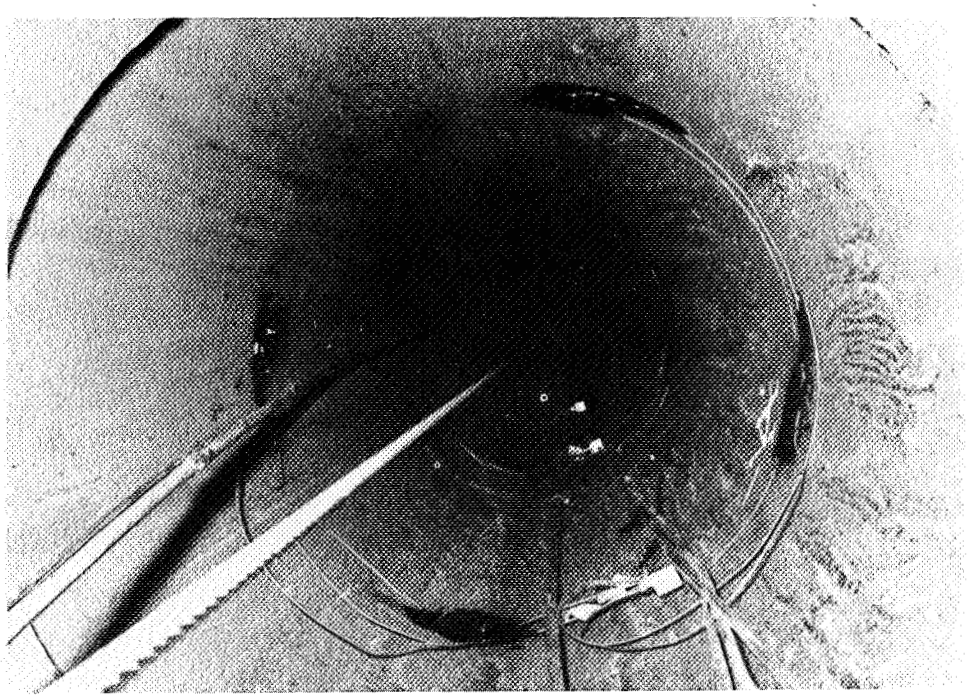

Figure 17.7 *Piling with strain gages in place.*

LIFE SUPPORT SYSTEM

Main Air Supply

The major consideration for life support was supplying clean air to the man working at the bottom of the piling. This clean air was necessary both to satisfy his oxygen needs and to continuously purge the piling of hazardous gases. This was accomplished by a compressor supplying air to the bottom of the piling through a reinforced nylon hose. The compressor used was a two-cylinder two-stage vee-type driven by a three-cylinder air-cooled diesel engine. The compressor was rated at 80 scfm, at a maximum operating pressure of 200 psig. This compressor had a power rating of 35 horsepower.

This type of compressor engine combination (fig. 17.8) is commonly used in the gulf by commercial divers and is considered to be a diving compressor. However, the actual compressor used was a standard commercial unit, not rated as a diving compressor, because of oil lubrication in the cylinder area. Rated diving compressors are either soap lubricated or use nonmetallic carbon or Teflon-coated piston rings to preclude air contamination. Also, the compression cylinders are isolated from the crankcase by a crosshead piston and piston rod seal. However, experience has shown that if the piston rings are in good condition, oil fouling of the air supply is not a serious problem.

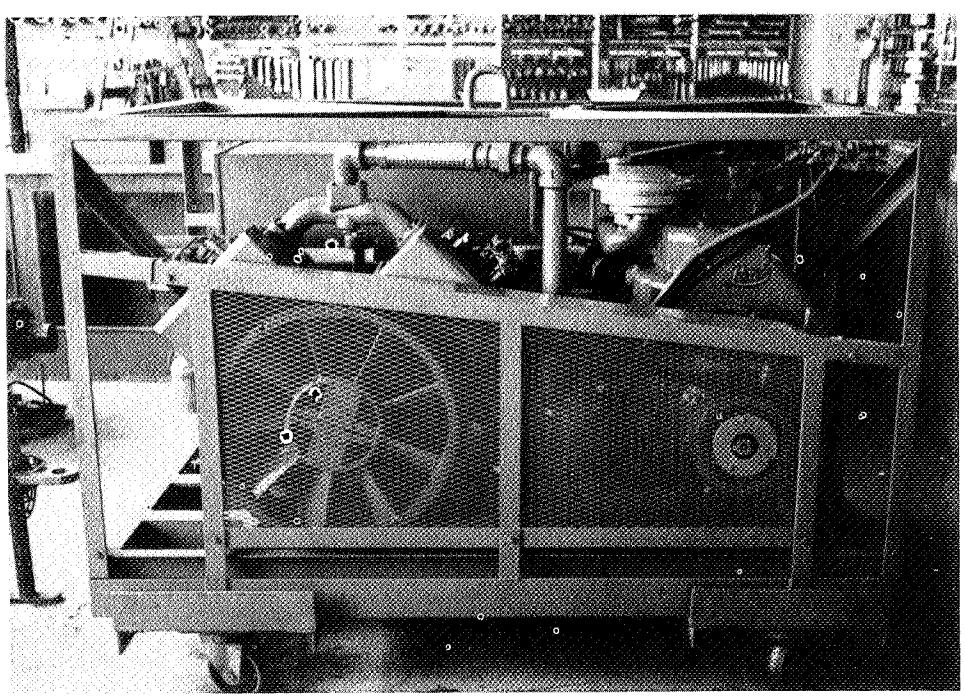

Figure 17.8 *Sustaining air supply compressor-engine combination.*

The air from the compressor was routed to a 50 gallon storage tank where the pressure was regulated between 80 and 120 psig. Discharge air was piped from the reservoir through two centrifugal separators mounted in series to remove water and condensed oil vapors. From the centrifugal separators, the air was routed through an absorption type oil scrubber to remove oil vapor. This system was modified after the first day of operation by the removing the oil scrubber, because the scrubbing material was becoming saturated with water. The water caused the material to pack tightly and thus restrict air flow through the scrubber. The removal of the oil scrubber was not a serious omission because the scrubber was fitted with a visual oil-indicating dye. Results of the first day of operation indicated that no detectable amount of oil was getting into the air.

After leaving the separators, the air was transported 300 ft down the pile where it discharged through a muffler. The air line, shown in figure 17.9 was a lightweight nylon double braid reinforced hose with an inside diameter of 0.5 in., rated for a working pressure of 250 psig. The air line size provided sufficient air flow within the pile to carry debris up the pipe and out the door. This debris resulted from the grinding that had to be done to remove rust prior to strain gage installation. This debris sweeping feature was efficient so when pile grinding was in progress the rust and metal powder was processed out through the top.

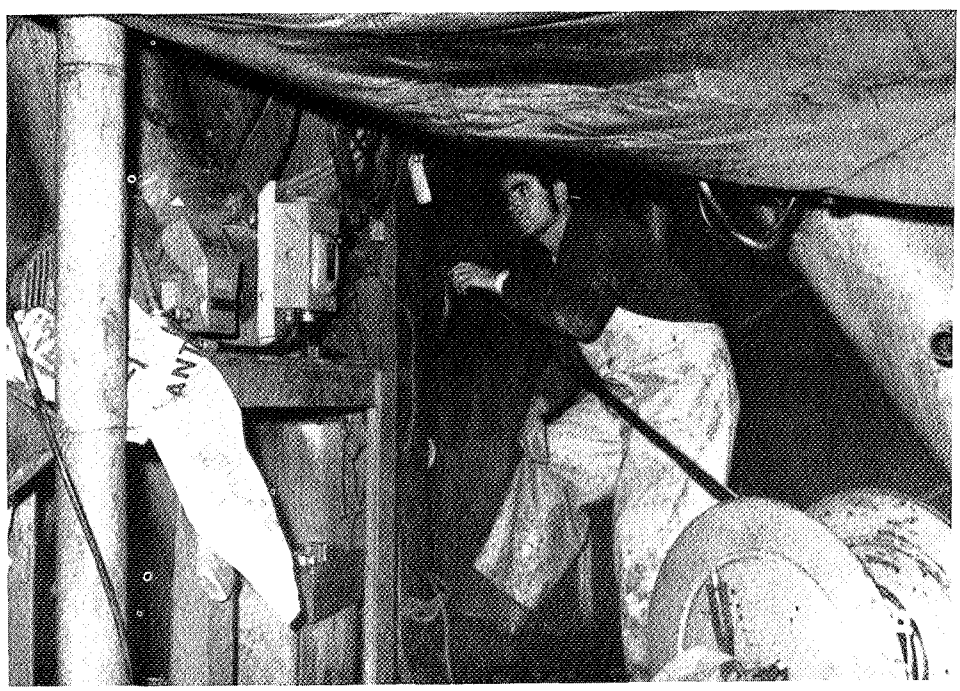

Figure 17.9 *Main air hose being fed into piling.*

Air Monitoring

Air quality in the pile was sampled periodically by two devices manufactured by the Mine Safety Appliance Company, a universal tester and an explosion meter.

The universal tester draws a controlled volume of air across a reagent bed contained in a glass indicating tube. A separate glass indicating tube is used for each gas to be detected. The concentration of gas present in the air is indicated by either a color change or the length of stain mark in the reagent bed. If a gas is present in the air sample, the quantity in parts per million or by volume, is determined by comparing the stain color or length to a calibration sheet. The glass indicating tubes used are for the detection of carbon dioxide, carbon monoxide and hydrogen sulfide. This tester required about 5 min for each series tests. On the first round trip to the bottom of the pile, the air was sampled about every 50 ft down to the 300-ft mark.

The explosion meter detects explosive mixtures of gas and air. The explosive mixture can consist of one specific gas and air or many gases in a mixture of air. However, this unit only determines the percent of explosive mixture, and does not identify the constituent gases. The explosion meter operates on the principle of a particular gas or air sample changing the resistance of a heated element, which is part of a Wheatstone bridge. If an air sample contains a combustible gas, the gas will be oxidized by the heated element, and additional heating of the sensitive element will occur, thus changing its resistance even though there is insufficient gas to support combustion. The device is enclosed within a screen to prevent ignition of the test area in the event that enough gas is present to cause an explosion. Readout on the indicator is in percent of an explosive mixture. This device was used to detect the presence of methane and acetylene, and other explosive gases that may have been present in the piling. This device proved to be much simpler and faster to use than the universal tester, and could be used while the elevator was in motion.

Emergency Air Supply

The personnel working in the piling requested that an emergency breathing supply system be used during the initial trips to the bottom, until confidence could be gained in the life support system. Several alternative schemes were investigated and the one selected was a scuba diving unit. This unit consisted of a U.S. Divers single hose two-stage unit attached to a 72 cu ft compressed air tank.

This unit was selected because it is extremely quick donning, simple to use, and can be left on and ready to use without consuming any of the air supply in the standby mode. Storage space was at a premium in the elevator so the compressed air tank was set on the floor of the basket between the workers legs. The mouthpiece was placed in a hanger at waist height, where it would be readily accessible in an emergency.

CONCLUSIONS

The life support system described in this paper proved to be a key item in satisfying the program goals. The commercial elements that made up the system operated satisfactorily during all work modes, and provided a high level of confidence for the men working in the piling.

The assemblage of components that made up this system was tailored to the vertical piling environment. In this regard, the long umbilical (air hose) approach proved satisfactory. On the other hand, it may be worthwhile to consider the development of a compact portable life support system that would have universal application for future offshore platform work activities.

18 REMOVAL OF METABOLIC HEAT FROM MAN WORKING IN A PROTECTIVE SUIT*

Avraham Shitzer, John C. Chato and Bruce A. Hertig
Department of Mechanical and Industrial Engineering
University of Illinois at Urbana – Champaign

INTRODUCTION

Although water-cooled Apollo EVA space suits with a single, controlled inlet temperature proved to be relatively simple and quite effective in maintaining acceptable thermal conditions, they did have certain short-comings (refs. 1, 2, 3). Among these was the limitation of the minimum inlet temperature by the most sensitive part of the body. This present work was undertaken primarily to explore the feasibility of independently cooling separate regions of the body. Specific purposes included (1) determination of preferred coolant inlet temperatures and the amounts of heat removed at each region, and (2) the order of cooling or warming preferences at different metabolic rates. The subject's own sense of comfort was the criterion used in each case.

EXPERIMENTAL SETUP

A water-cooled suit was constructed for the purpose of testing the characteristics of the proposed differential scheme of cooling the body. The suit consisted of 16 individual pads made of 3/32-in. i.d. by 5/32-in. o.d. Tygon tubes running parallel, 5/8-in. apart. The cooling pads covered the head (2)[1], front and back, upper and lower torso (4), upper and lower, right and left arms (4), right and left thighs (4), and right and left lower legs (2). The face, neck, hands, and feet were not covered with cooling tubes. Table 18.1 gives pertinent dimensions of the cooling pads and the whole suit. All the pads, excluding the ones for the head, were stitched on the inside of a man's thermal union underwear garment. The cooling hood was made of a snow suit hood with the cooling tubes stitched onto the inside,

The body was divided into six regions for cooling purposes:

Head
Upper torso
Lower torso
Arms
Thighs
Lower legs

These regions were supplied with water mixed from cold and hot headers. Before entering the suit, the two streams were mixed separately for each region, thus allowing for continuous regulation of water inlet temperatures. These temperatures were measured by interchangeable, multipurpose No. 401 Yellow Springs Co. thermistors and a Tele-Thermometer. The difference between outlet

*Supported in part by NASA Grant NGR 14-005-103.

[1]Numbers in parentheses represent number of pads.

Table 18.1 *Data on the cooling garment.*

Pad	*Number of pads*	*Number of tube rows in pad*	*Area covered by pad*		*Total area covered by pads*		*Percent area covered*
			in²	*cm²*	*in²*	*cm²*	
Head	2	12	65	419	130	838	9.6
Front and back, upper and lower torso	4	14	111	716	444	2864	33.0
Upper arms	2	11	62	400	124	800	9.2
Lower arms	2	12	60	387	120	774	8.9
Upper thighs	2	7	83	535	166	1070	12.3
Lower thighs	2	10	96	619	192	1238	14.2
Lower legs	2	16	86	555	172	1110	12.8
Total	16	–	–	–	1348	8694	100

	Cooling garment		*Insulating suit*		*Cooling hood*		*Insulating hood*		*Total*	
	kg	*lb*	*kg*	*lb*	*kg*	*lb*	*kg*	*lb*	*kg*	*lb*
Weight, dry	4.41	9.72	0.80	1.61	0.25	0.55	0.31	0.68	5.77	12.56
Weight, wet	4.88	10.77	–	–	0.30	0.66	–	–	6.29	19.33

and inlet temperatures of each pad was measured by thermopiles consisting of five 30-gage copper-constantan thermocouples. The temperatures were continuously recorded on a recording potentiometer. Water flow rates through each of the regions were measured by a rotameter. Figure 18.1 shows a schematic diagram of the cooling pads and the control, supply, and measuring systems.

Over the underwear garment, the subjects wore an insulating suit that thermally isolated them from the environment. A heavily furred hood was used for the same purpose on the head. All test subjects wore tennis shoes.

An A.R. Young treadmill was used for the walking sessions. The speed of the belt was controlled to correspond to the desired level of activity and was timed with a stop watch.

For metabolic measurements, expired air samples were taken with metalized Douglass bags (ref. 4). The bags were placed inside a tightly sealed Plexiglas chamber that was under a vacuum of about 5 mmHg (ref. 5). One-minute sampling was used. Air volumetric flow rates were measured by means of a Parkinson–Cowan dry gas meter. Inlet and outlet air temperatures were measured by two

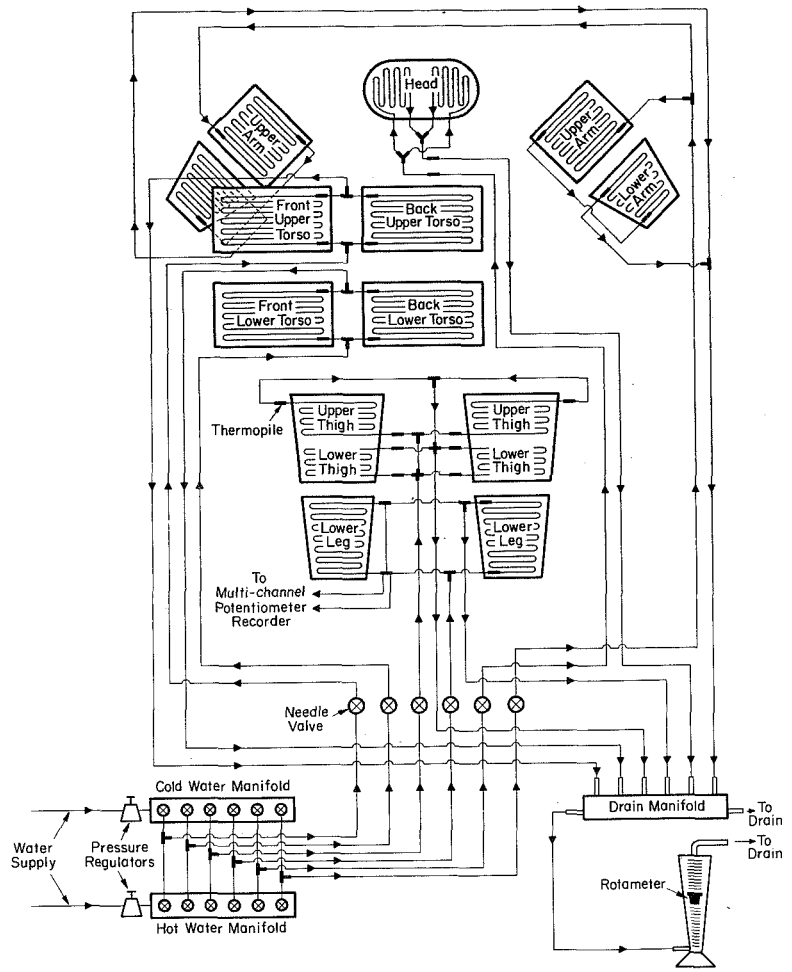

Figure 18.1 *The cooling garment and the control, supply, and measuring systems.*

interchangeable, multipurpose No. 401 Yellow Springs Co. thermistors and a Tele-Thermometer. Air samples were analyzed for carbon dioxide and oxygen content. A Godard-Mijnhardt carbon dioxide thermal conductivity meter, Pulmo Analysor Type 44-A-2 and a Beckmann Paramagnetic oxygen analyzer, Model C2, were used. These data were used to evaluate energy expenditure (refs. 6,7).

The temperature of the ear canal was taken as a measure of deep body temperature. For this purpose a No. 510 Yellow Springs Co. ear thermistor was inserted approximately 1/2 in. into the ear canal and was held in place by a specially prepared ear plug made of medical grade silicone rubber. The outside ear was covered by a piece of polyurethane foam to exclude possible effects of the cooling tubes. Measurement of the temperature of the ear canal rather than the more commonly used rectal temperature was more convenient for walking, and it gave a closer indication of the hypothalamic temperature regulated by the body. Figure 18.2 shows a general view of the setup with a test subject dressed in the cooling and insulating suits, but without shoes, walking on the treadmill.

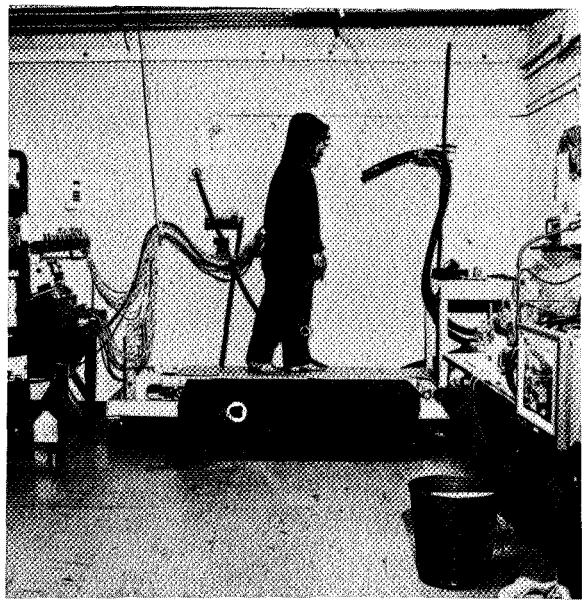

Figure 18.2 *The experimental setup. A test subject is shown dressed in the complete cooling suit walking on the treadmill. He wears no tennis shoes here and the ear canal thermistor is not connected.*

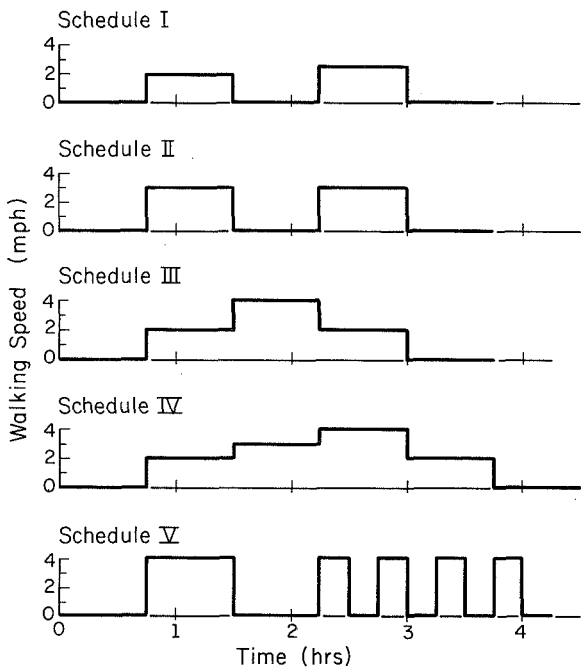

Figure 18.3 *Activity schedule used for the experiments with the cooling suit.*

A Buffalo special physiological beam scale was used to determine weight losses during the experiments. The sensitivity of this scale was estimated at ±0.25g.

EXPERIMENTS WITH THE COOLING SUIT

Activity Schedules

Five different activity schedules were used for all test subjects. The schedules consisted of alternate periods of standing and level walking on the treadmill with or without the cooling suit. The various levels of activity were chosen to cover a variety of different activity loads. The steady state and, to some extent, transient characteristics of the cooling suit were studied under those conditions. Each of the schedules started with the subject standing still for at least 45 min. During this period water inlet temperatures were adjusted to correspond to the subject's own sense of comfort. The duration of each of the standing and walking sessions (except the second part of Schedule V) was 45 min. It was assumed that after 45 min from the onset of a new activity level the subjects reached a thermal quasisteady state.[2] Figure 18.3 illustrates the details of the five activity schedules.

Schedule I, with the lowest activity levels, consisted of four step changes: standing, walking at 2 mph, standing, walking at 2.5 mph, and standing. Once the subject's comfort was achieved while standing, no deliberate changes were made in water inlet temperatures; although small changes did occur because of the instability of the water supply system. The purpose was to test the cooling capacity of the suit at higher metabolic rates while operating at the temperature levels that were considered comfortable at the lower metabolic rate.

Schedule II was designed to compare the effect of changing the water inlet temperature at the same activity level. It consisted of two identical, periodic step changes: standing,

[2]Quasisteady state was defined as the state when no significant changes in the difference between outlet and inlet water temperatures were noticeable.

walking at 3 mph, standing, again walking at 3 mph, and standing. During the first walking session no adjustments in water inlet temperatures were permitted. During the second cycle, however, the water temperatures were adjusted to correspond to the subject's comfort.

Schedule III consisted of four step changes: standing, walking at 2 mph, walking at 4 mph, walking at 2 mph, and standing. The purpose of this schedule of activities was to study the characteristics of the suit at moderately high activity levels (approximately 1650 Btu/hr, 480 W). The intermediate 2 mph walking sessions were used to allow a gradual change to the high activity level and condition the subjects for the relatively high speed that was also included in the last two schedules. Adjustments of water inlet temperatures were permitted throughout the entire duration of the experiment.

Schedule IV was almost identical to Schedule III, but it included an additional walking session at 3 mph immediately preceding the 4 mph walking period. This was done to study the effect of a more gradual change in activity levels.

Schedule V was used to examine the performance of the suit with a direct step change from standing to the moderately high activity level and determine the characteristics of the suit with thermal transients produced by identically repeated activity levels. This schedule consisted of standing, walking at 4 mph, and standing followed by four short, identical, periodic sessions of walking at 4 mph and standing. The duration of each of the short walking and standing sessions was 15 min. Readjustments in water inlet temperatures were permitted throughout this entire schedule.

Test Subjects

Five male students, aged 18 to 29 years, served as test subjects. They represented a variety of physical fitnesses from poor to athletic. The physical characteristics of the test subjects are summarized in table 18.2. Surface areas were determined from the Dubois height/weight formula. All but one subject completed all five experiments. One did not complete Schedule V because of a cramped thigh muscle.

Table 18.2 *Characteristics of the test subjects.*

Subject	*Age*	*Height*		*Weight*		*Surface area*		*Percent area covered by cooling pads*
		cm	*in*	*kg*	*lb*	m^2	ft^2	
A. SGP	20	173	68	65.7	144.8	1.78	19.2	48.8
B. SKB	22	170	67	61.1	134.7	1.71	18.4	50.8
C. HNT	27	170	67	64.2	141.5	1.74	18.7	50.0
D. RET	18	169	66.5	64.2	141.5	1.74	18.7	50.0
E. PF	29	161	63.5	55.8	123.0	1.58	17.0	55.0
Means	23.2	169	66.4	62.2	137.1	1.71	18.4	50.9

Experimental Procedure

All experiments were performed at the Laboratory for Ergonomics Research, University of Illinois at Urbana–Champaign. This laboratory is air conditioned at about 73° F (23° C) and 60 percent relative humidity. A total of 29 experiments were run of which 24 were performed with the cooling suit. Five comparison runs were performed by subject SKB repeating the regular activity schedules without the suit. During these comparison runs the subject wore tennis shoes, shorts, and a light T-shirt. All subjects started with Schedule I and, in order, completed the other schedules. They were permitted to listen to the radio and read while standing; but no eating, drinking, or smoking was allowed during the experiments.

At the beginning and end of each experiment the subjects were weighed, and their oral temperature and blood pressure was taken. The last two measurements were taken only as precautionary measures against any acute effects of the experiment on the subject. During the experiments the following data were collected: ear canal temperature, water inlet temperatures, differences between water outlet and inlet temperatures at each of the six regions of the body, water flow rates, respiratory volumetric rates, and temperature of the expired air. During Schedule V and the runs without the suit, pulse rates were also taken. All measurements were taken at the end of each activity in the schedule and were assumed to represent the quasisteady state.

After the preliminary measurements the subject donned the cooling garment. Then the thermally insulating suit was put over the cooling garment. Next the ear thermistor was inserted into the ear and was covered by thermal insulation. Finally the water flow and all measuring systems were started. Figures 18.4 and 18.2 show one of the subjects in various stages of dressing.

During the first standing period the water inlet temperatures were adjusted to conform to the subject's sense of comfort. After 45 min, when a thermal quasisteady state was reached, the subject started to walk on the treadmill. Subsequent activities were as described before.

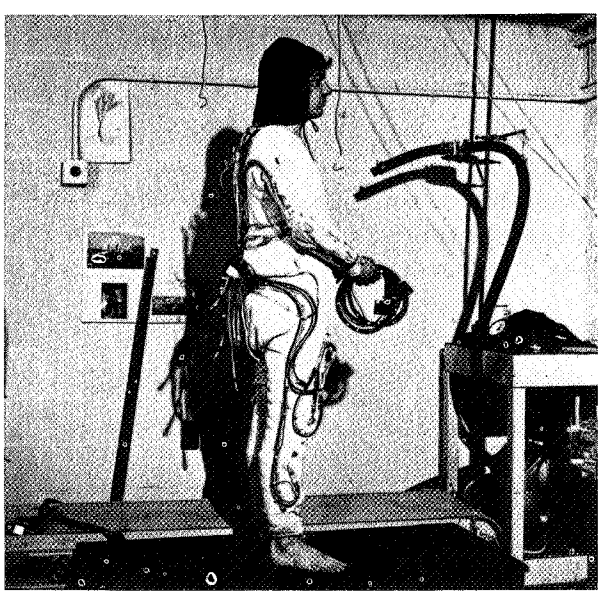

Figure 18.4 *The cooling garment.*

Measured, Recorded, and Calculated Quantities

The following quantities were measured, recorded, or calculated from measured data.

1. Total metabolic rate was calculated from volumetric flow rate of the expired air and the carbon dioxide content obtained from the gas analysis. The caloric value of oxygen was assumed at 5.0 kcal/liter (ref. 6). Although slightly high, this value conformed well with the respiratory quotients found in most of the runs. Maximum deviation from the actual caloric value was estimated to be about 4 percent.
2. Rate of heat removed by the suit in each region was taken as the product of the difference between water outlet and inlet temperatures, specific heat and mass flow rate of the cooling water.

3. Rate of heat lost by respiration was calculated from the flow rate, temperature, and enthalpy of the expired air, assuming it to be saturated.
4. Weight loss during the experiment was the difference between the initial and final weights of the subject.
5. Ear canal temperature was measured with an ear thermistor, as discussed before.
6. Water inlet temperatures to each region were measured with thermistors in the water streams.
7. Order of preferred changes in water inlet temperatures to the different regions was recorded for the purposes of identifying those zones of the body that require such changes and establishing this order as a function of activity level.
8. Comfort vote was based on the subject's own evaluation of three choices: slightly cold, comfortable, slightly warm.
9. Pulse rate was measured only during Schedule V and the comparison runs without the suit. The pulse rate was assumed to be an index of the metabolic and cardiac costs of physical work. Pulse rate was not taken during the other schedules because they were considered to represent quasisteady states.

DISCUSSION

Most of the results were averaged for all subjects and are presented in this form. Wherever feasible, entire ranges of individual variations are also shown.

Figure 18.5 shows mean values of metabolic rates and of the heat removed by the suit and by respiration during Schedule II. These results are typical for all schedules. Also shown are the ranges of metabolic rates included in the mean values. It is seen that during the standing sessions most of the heat produced in the body was removed by the cooling suit. In many cases the heat removed by the suit even exceeded slightly the total metabolic rate. This phenomenon is believed to be due to possible thermal transients indicated by a decrease of "deep body" temperature following a change in activity from walking to standing (fig. 18.6) and also to cumulative measurement errors.

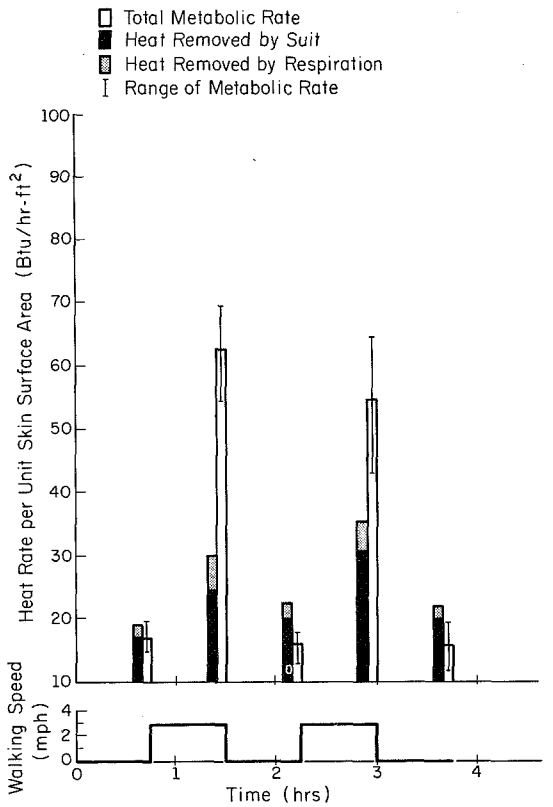

Figure 18.5 *Mean values of metabolic rates and of the amounts of heat removed by the cooling suit and by respiration for Schedule II.*

During all of the walking sessions the relative amount of heat removed by the suit dropped significantly. At best it was only about 70 percent of the total metabolic rate; but it was usually closer to 50 percent. Possible reasons to account for the portion of the total metabolic rate that was not removed by the cooling suit follow.

1. Thermal transients with heat still being stored inside the body were indicated by an increase in "deep body" temperature (fig. 18.6)
2. Heat dissipated to the environment from the uncovered surfaces (e.g., face, forehead, and hands)
3. Heat removed by respiration

4. Heat removed by perspiration evaporated by the air that was pumped under the somewhat loose insulating suit by movement of the subject
5. Work done by the muscles
6. Heat lost to the environment through the clothing
7. Measurement errors and inaccuracies

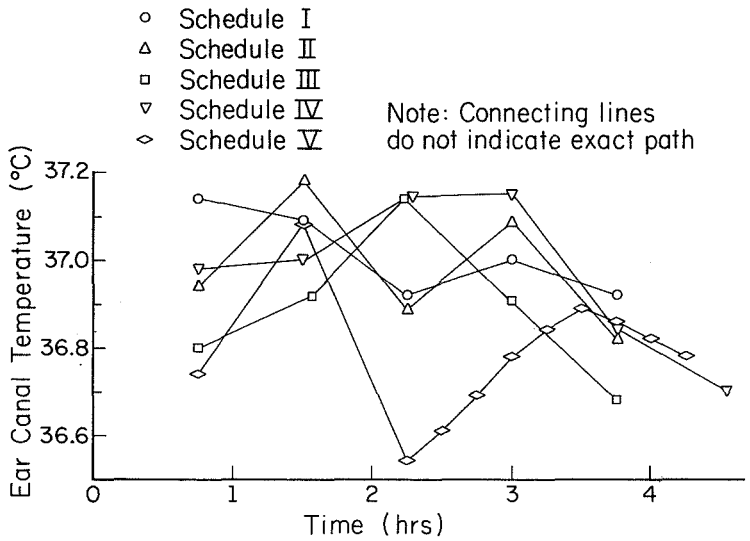

Figure 18.6 *Average ear canal temperatures for the various schedules.*

Among these, only the contribution of item 3 (i.e., respiration) was estimated. This alone amounted from 7.3 to 14.8 percent of the total metabolic rate. These values are consistent with those reported by Bazett (ref. 8). With the increase in metabolic rate the amount of heat carried away by respiration also increased. However, the relative amount of heat removed by the exhaled air decreased. The remaining, unaccounted for portion of the metabolic rate was assumed to have been removed by the other means mentioned above.

From the comfort standpoint, the cooling system was found to be insufficient to accommodate metabolic rates in excess of about 1200 Btu/hr (350 W). The subjects felt consistently too warm at the moderately high activity levels. This insufficiency was due primarily to two reasons: too small a contact area between the skin and the cooling tubes, and too high water inlet temperatures. The actual contact area was estimated to be about 10 percent of the total skin surface area. The lowest water inlet temperature obtained in most of the experiments was about 61° F (16° C). Increasing the contact area between the skin and the cooling tubes or lowering the water inlet temperatures or both would improve the cooling capacity of the suit. This conclusion is supported by the results obtained by Webb and Annis (ref. 9). They estimated that 22 percent of the total skin surface area was in contact with the cooling tubes in their experiments. All of their subjects were reported to have been comfortable with the lowest water inlet temperature of 61° F (16° C) and high metabolic rates of 2400 Btu/hr (700 W) for 2 hours.

During the second part of the experiments in Schedule V, no quasisteady state was ever reached. This finding was true for the metabolic rates and amounts of heat removed by the cooling suit as well as for the heart rates and ear canal temperatures (fig. 18.7). These quantities show a clear trend of increase with time, at least during the 2 hours of the short 15-min alternate changes in levels of activity. The amount of heat removed by respiration, however, seems to have reached a quasisteady state within 15 min from the onset of a change in exercise level. This result indicates that the transient time of the respiratory system is much shorter than that of the thermal system of the human body within the investigated range.

During the second part of Schedule V, heart rates not only showed a trend to increase with time, but also exceeded the values found in the first part (fig. 18.6). This observation indicates possibly a fatigue effect that was supported by the feelings of all subjects. It is also indicative of a lack of steady state.

During the experiments of Schedules III, IV, and V, the effects of gradual and abrupt step changes from standing to walking at 4 mph were considered. No significant differences were found in total metabolic rates and amounts of heat removed by the cooling suit. Of these two quantities, only the cooling effectiveness, the fraction of the total metabolic heat removed by the suit, seemed to have changed during Schedule IV. This result may mean that during Schedule IV the thermal steady state of the moderately high activity level was more nearly attained because of the two intermediate step changes preceding it. However, there were differences in the temperature of the ear canal. It was lower by about 0.5° C when a step change from standing to walking at 4 mph was introduced without any intermediate changes (fig. 18.6). There were no major differences between the temperatures of the ear canal measured during Schedules III and IV that involved gradual changes. This observation may indicate that the transient time until a complete thermal steady state is reached in the human body is longer than 45 min and is more likely to be of the order of 2 hours.

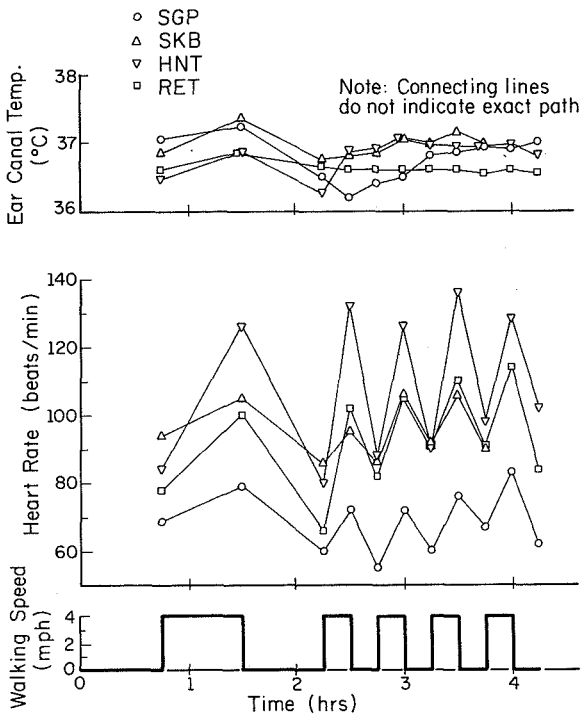

Figure 18.7 *Individual variations in ear canal temperatures and heart rates for Schedule V.*

Figures 18.8 through 18.12 show the relative amounts of heat removed by the suit at the various regions of the body during the different schedules of activity. Based on these data, the following observations were made.

1. The relative amount of heat removed from the arms was the lowest in most cases. It ranged from 1.7 to 7.2 percent of the total heat removed by the suit and was usually around 3 to 4 percent. This occurred despite the fact that the arm pads covered about 18 percent of the total skin surface area covered by the suit. This finding can be attributed, in part, to the nature of the activities used in

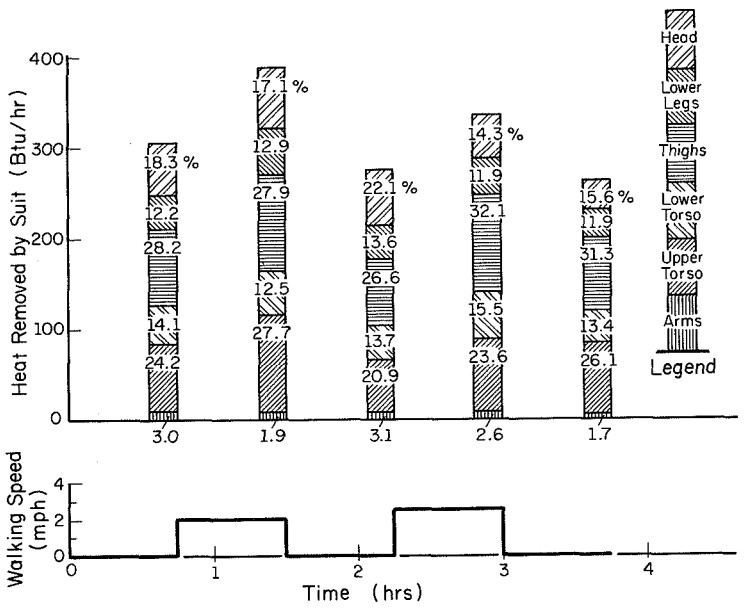

Figure 18.8 *Mean values of the amounts of heat removed by the cooling pads for Schedule I.*

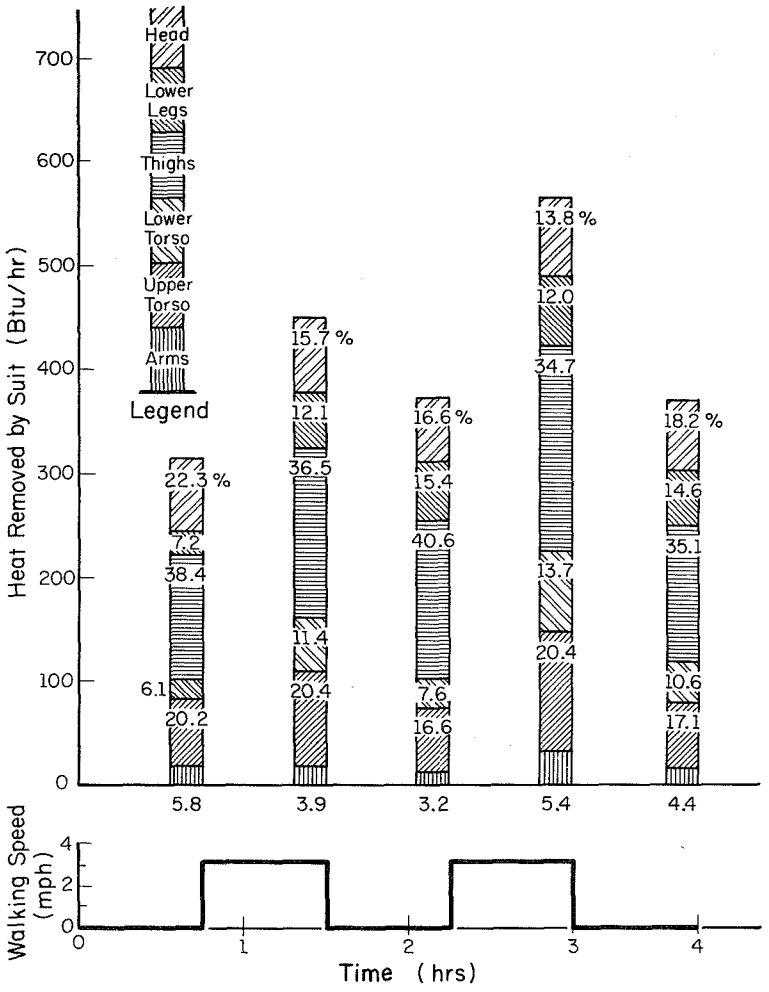

Figure 18.9 *Mean values of the amounts of heat removed by the cooling pads for Schedule II.*

this study; these were composed primarily of work of the leg muscles and did not involve much arm work. This assumption is supported by the fact that the relative value of the heat removed at the arms increased during the walking sessions when the subjects were swinging their arms.

2. The largest amount of heat removed by the suit from a single region came from the thighs. It ranged from a low of 25.8 percent, while standing, to a high of 41.7 percent, while walking at 3 mph, of the total heat removed by the suit. As the metabolic rate exceeded the upper limit that could be accommodated by the suit, the relative amount of heat removed from the thighs decreased. Because of the limits imposed by the minimum water inlet temperature and the contact area between the skin of the thighs and the cooling tubes, heat was probably carried away from the thighs by the blood stream to be dissipated elsewhere. Also the "deep body" temperature increased and sweating was enhanced, as indicated by higher weight losses.
3. A relatively high percentage of the total heat removed by the suit came from the head, which constituted only about 7 percent of the total surface area. It ranged from 10.3 to 36.9 percent. The highest values were obtained during the second part of Schedule V (fig. 18.12). Thus

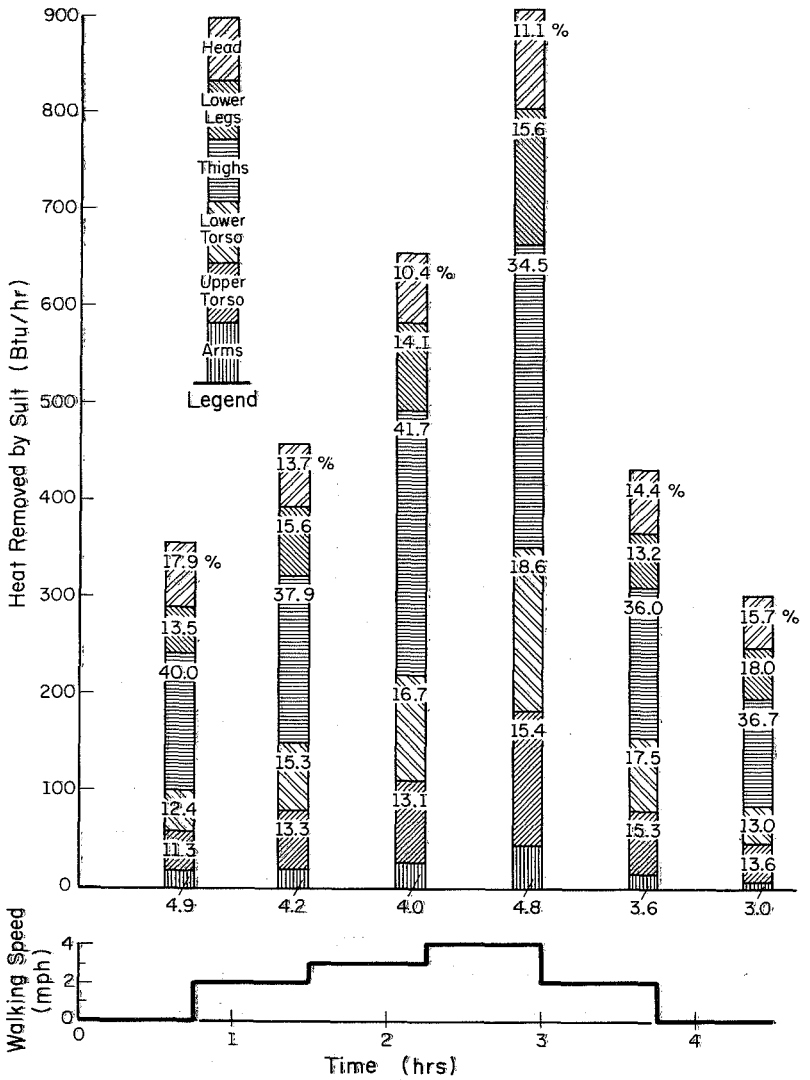

Figure 18.10 *Mean values of the amounts of heat removed by the cooling pads for Schedule III.*

thermal transients seem to enhance heat removal from the head. According to Nunneley (ref. 10), up to 40 percent of the total metabolic rate was removed from the head during resting and steady states by a cap with cooling tubes. Nunneley however, did not use a cooling suit along with the cap. Shvartz (ref. 11), in a study with a cooling suit that included a cooling hood, found that during steady states the hood removed about 40 percent of the total removed by the cooling suit assembly. However, 12 percent of the total surface area was covered by the hood in his studies as compared to only about 5 percent in the present study.

4. During Schedule I more heat was removed by the cooling suit during the first walking session at 2 mph than during the second at 2.5 mph (fig. 16.8). The reason was the unexpected drop in "deep body" temperature as indicated in figure 18.6 by the temperature of the ear canal. Since no readjustments in water inlet temperatures were permitted during these experiments,

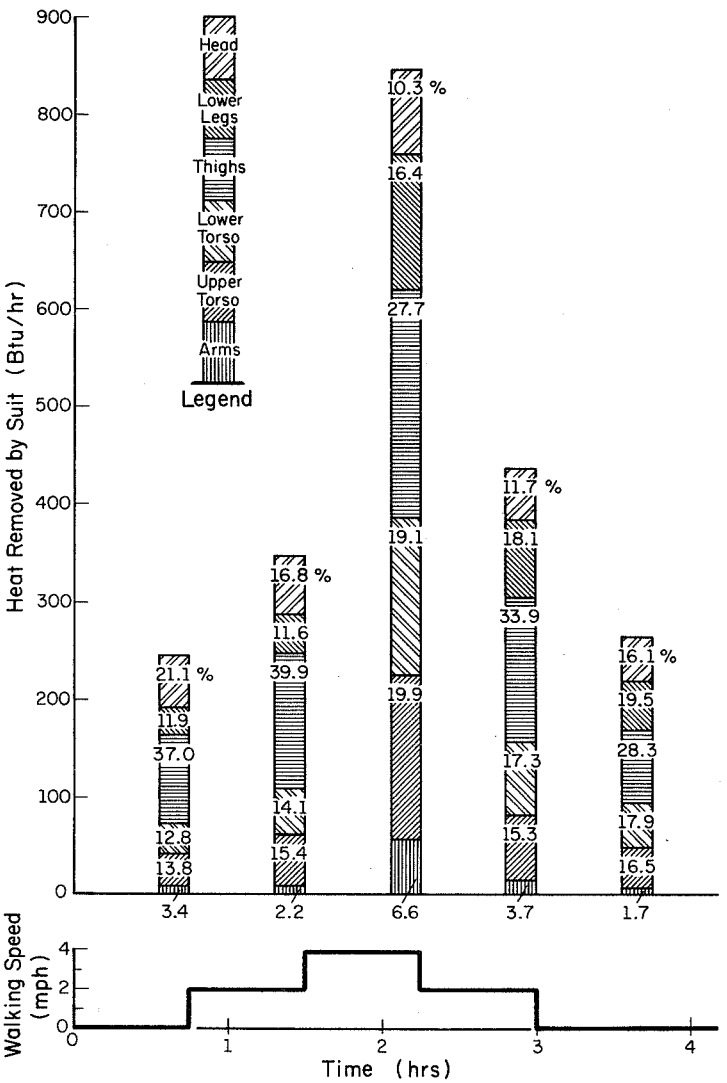

Figure 18.11 *Mean values of the amounts of heat removed by the cooling pads for Schedule IV.*

this phenomenon of less heat removed by the suit at a higher metabolic rate is not considered to have any physiological meaning.

5. During Schedule II, readjustments of the water inlet temperatures at the same level of activity caused the following changes.
   The total metabolic rate decreased (fig. 18.5)
   The amount of heat removed by the cooling suit increased (fig. 18.9)
   The temperature of the ear canal dropped (fig. 18.6)
   Consequently, the cooling effectiveness of the suit increased from 0.39 to 0.56. Also, adjustments of the water inlet temperatures actually diminished the subject's heat strain.[3] This

[3] Heat strain is often referred to as the physiological response in consequence of a heat load (ref. 12). It should be distinguished from the heat stress used to denote the heat load imposed on man (ref. 12). A commonly used index to assess physiological strain was developed by Craig (ref. 13) and modified by others (ref. 14). It is a linear combination of heart rate, rise in rectal temperature, and sweat production rate.

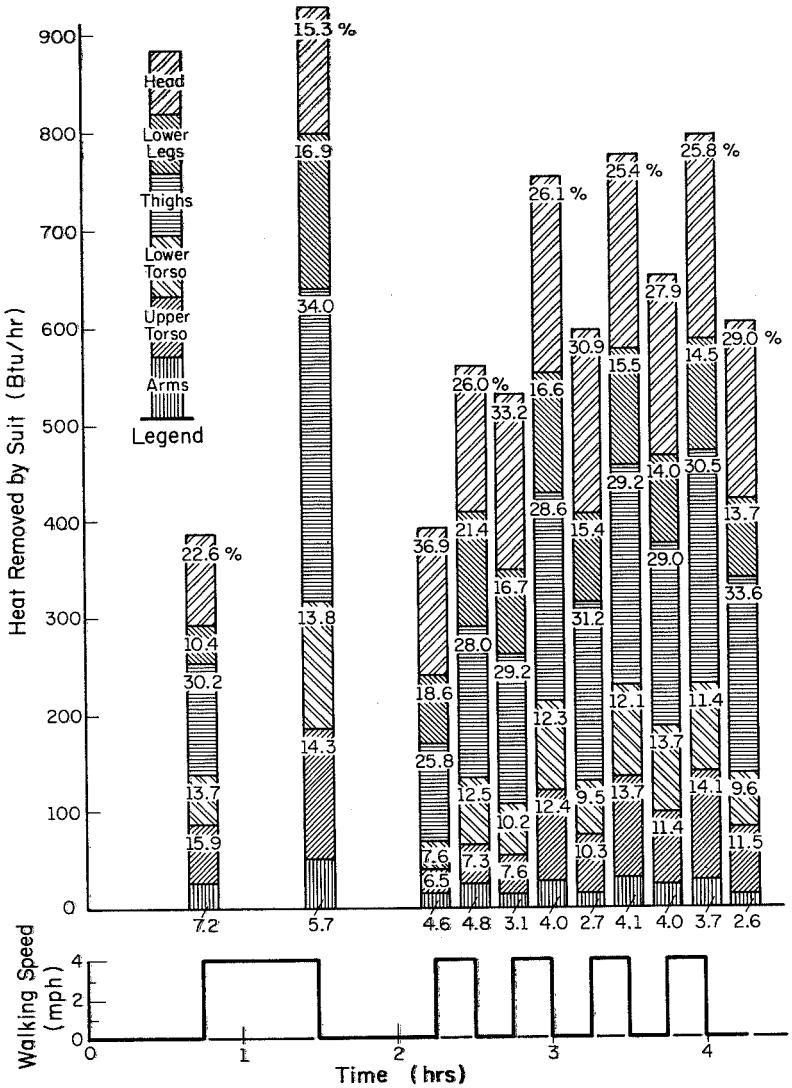

Figure 18.12 *Mean values of the amounts of heat removed by the cooling pads for Schedule V.*

reduction of heat strain occurred even though a consistent comfort vote of "comfortable" was obtained through the entire Schedule II. These findings indicate that additional cooling provided by some artificial means, such as a cooling suit, may reduce the heat strain beyond that considered comfortable by human subjects. A similar conclusion was also reached by Gold and Zornitzer (ref. 15).

Figure 18.13 shows the average water inlet temperatures at the various regions of the body for Schedule II. This schedule was selected for comparative presentation because (1) the effect of additional cooling at the same level of activity was studied during these experiments, and (2) the metabolic rates encountered during this schedule never exceeded the cooling capacity of the suit.

During the initial standing session most of the subjects preferred an almost uniform temperature over the entire body (fig. 18.13(a)). This situation did not change during the first walking session where no additional cooling was permitted (fig. 18.13(b)). Immediately following the first walking session, the restriction on additional cooling was removed. A decrease in most water inlet temperatures was requested by all subjects (fig. 18.13(c)). The average changes requested were 1.2 to 1.3° C for the arms and thighs and 0.2 to 0.6° C for the head and upper and lower torso. The highest decrease in water inlet temperature, 2.3° C, was requested for the lower legs. During the second walking session at 3 mph (fig. 18.13(d)) the requests for decreases in water inlet temperatures were arms, upper torso, and thighs 3.4 to 3.8° C, head 1.4° C, and lower torso 2.5° C. The highest decrease, 4.7° C, was for the lower legs. During the last standing period the requested changes in water inlet temperatures were such that they essentially reproduced the situation that prevailed during the second standing session with only minor differences (fig. 18.13(e)).

As a consequence of the results presented in the preceding section, the following observations were made.

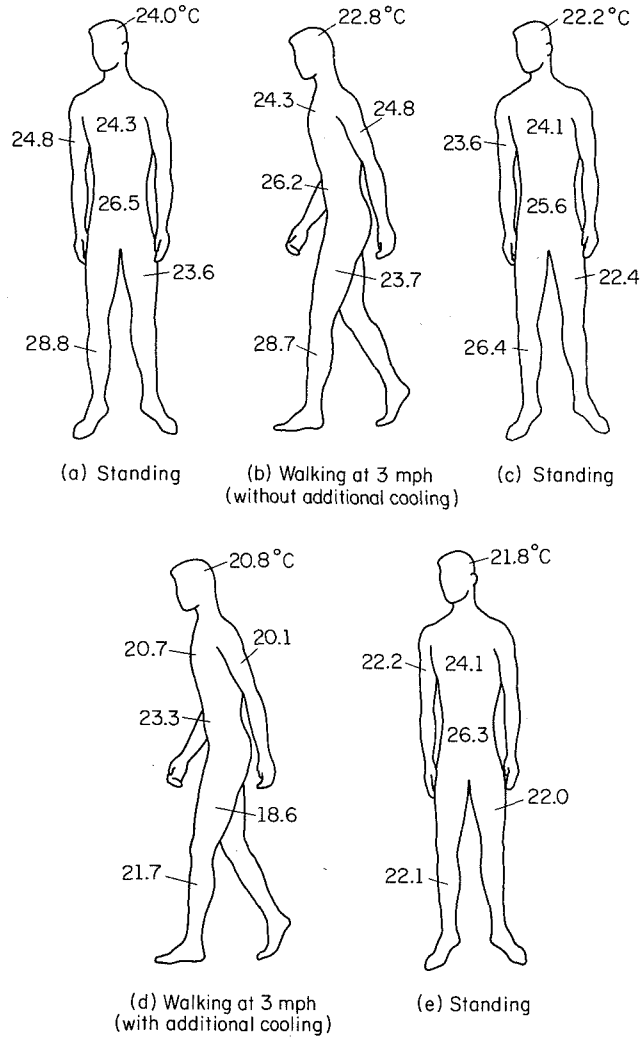

Figure 18.13 *Mean water inlet temperatures at the various regions of the body for Schedule II.*

1. The working muscle (i.e., thighs and lower legs) exhibited the highest variability in water inlet temperatures, as expected.
2. While the changes in water inlet temperatures to the head were the smallest, they were also, on the average, starting from the lowest temperature level among all the water inlet temperatures. Thus, cooling the head seems to have a profound effect on the sensation of comfort, as noted also by Nunneley (ref. 10) and Shvartz (ref. 11).

There did not seem to be any consistency in the order of changes requested in water inlet temperatures by different subjects. Many more experiments with more subjects are needed to identify those regions in the body that require faster cooling or warming as a result of a change in the level of activity (ref. 7).

The mean values of weight losses ranged from 65 gm/hr in Schedule I to 118 gm/hr in Schedules III and IV. These values, although slightly higher, are consistent with those reported by Webb and Annis (ref. 9). In four out of five cases the heat rates were higher during the runs without the suit as

compared to the runs with the suit. No fundamental explanation was found for the exception, Schedule III; it may have been due to a measurement error.

Examining the results of the comparative experiments with and without the cooling suit reveals that the total metabolic rate was generally higher during the experiments with the suit. This finding is probably due to the fact that there was a certain energy cost in wearing the suit. At the same time, the temperature of the ear canal seemed to have been only slightly lower during the experiments without the suit. Also (fig. 18.14) the heart rate was usually lower during at least the comparative experiments of Schedule V with the suit. The lower heart rates with only slightly higher "deep body" temperatures seem to indicate reduced heat strain during the experiments with the cooling suit.

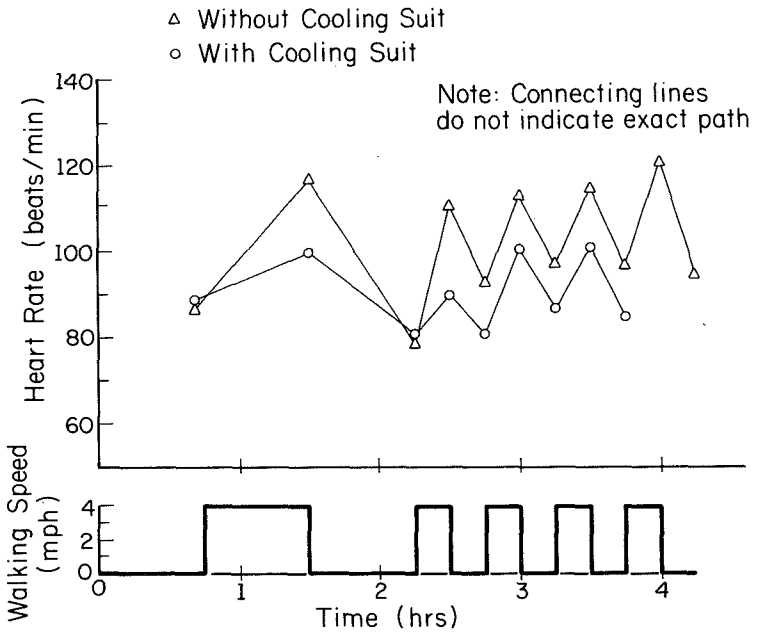

Figure 18.14 *Heart rates of the test subject during the comparative experiments with and without the cooling suit for Schedule V.*

The large amount of data gathered was reported in detail in reference 7, and was not repeated here except as needed.

SUMMARY AND CONCLUSIONS

A water cooled garment was constructed and used to study the characteristics of independent regional cooling of the body in contrast to the current practice of uniform cooling. The cooling pads in the garment were grouped to provide independent control of water inlet temperatures and flow rates to six regions: head, upper torso, lower torso, arms, thighs, and lower legs. Experiments with and without the cooling suit were conducted with five test subjects standing and walking on a treadmill on selected schedules. Steady state and, to a lesser extent, transient characteristics were obtained.

Based on the experiments with the cooling suit, the following conclusions were reached.

1. Some regions of the body require more cooling during walking than others (e.g., thighs, head, and lower legs).
2. During standing an almost uniform water inlet temperature was requested for all regions of the body by the subjects but the situation changed significantly during exercise. Conclusions 1 and 2 indicate that independent regional cooling may be more effective than the present scheme of uniform cooling.
3. Cooling of the head during exercise affects comfort profoundly.
4. Transient times for reaching a thermal steady state from the onset of a new exercise level are of the order of two hours. This transient time, however, includes a relatively slow, active response of the human thermoregulatory system to changes in exercise rate (i.e., the shifting of the deep body temperature).
5. During exercise the thermal effectiveness of the cooling suit decreased as compared to the values obtained for standing.
6. Intermediate changes in the level of activity between an initial and final level do not have a noticeable effect on the thermal state so long as sufficient time is allowed for reaching a steady state corresponding to the final level of activity.
7. The cooling suit seemed to actually diminish the heat strain of the test subjects beyond what was considered comfortable by them.
8. No regional order of preferred changes in water inlet temperatures could be determined. More experiments are required to determine if there are regions of the body that require faster cooling or warming than others.

Based on the comparative experiments with and without the cooling suit, the following observations were made.

1. Metabolic rates were, in most cases, higher during the experiments with the cooling suit, indicating that additional energy cost was associated with wearing the suit.
2. Ear canal temperatures were usually slightly lower during the experiments without the cooling suit.
3. Heart rates were lower during the experiments with the cooling suit.
4. Weight losses were usually lower during the experiments with the suit.

Thus, the cooling suit seems to have reduced the heat strain even though the heat stress was increased slightly.

REFERENCES

1. Chambers, A. B.: Controlling Thermal Comfort in the EVA Space Suit. ASHARA Journal, vol. 12, 1970, pp. 33-38.
2. Portable Life Support Systems, NASA SP-234, 1970.

3. Nunneley, S. A.: Water Cooled Garments: A Review. Space Life Sciences, vol. 2, 1970, pp. 335-360.
4. Johnson, R. E.; Robbins, F.; Schilke, R.; Mole, P.; Harris, J.; and Wakat, D.: A Versatile System for Measuring Oxygen Consumption in Man. J. Appl. Physiol., vol. 22, 1967, pp. 377-379.
5. Molnar, S.: The Relationship between Cardiac Time Components, Maximal Oxygen Consumption, and Endurance Performance. Ph. D. Thesis, Univ. Illinois at Urbana-Champaign, 1970.
6. Consolazio, F. C.; Johnson, R. E.; and Pecora, L. J.: Physiological Measurements of Metabolic Functions in Man, McGraw-Hill Book Co., New York, 1963.
7. Shitzer, A.; Chato, J. C.; and Hertig, B. A.: A Study of the Thermal Behavior of Living Biological Tissue with Application to Thermal Control of Protective Suits. Technical Report ME-TR-207, Dept. of Mechanical and Industrial Engineering, Univ. Illinois at Urbana-Champaign, 1971.
8. Bazett, H. C.: The Regulation of Body Temperatures. Physiology of Heat Regulation and the Science of Clothing, L. H. Newburgh, ed., Hafner Pub. Co., New York, 1968, pp. 109-192.
9. Webb, P.; and Annis, J. F.: Bio-Thermal Responses to Varied Work Programs in Men Kept Thermally Neutral by Water Cooled Clothing. NASA CR-739, 1967.
10. Nunneley, S. A.: Head Cooling in Work and Heat Stress. M.S. Thesis, Ohio State Univ., 1970.
11. Shvartz, E.: Effect of Cooling Hood on Physiological Responses to Work in a Hot Environment. J. Appl. Physiol., vol. 29, 1970, pp. 36-39.
12. Hatch, T.: Assessment of Heat Stress. Temperature, Its Measurement and Control in Science and Industry, J. D. Hardy, ed., vol. 3, P. 3, Reinhold Pub. Co., New York, 1963, pp. 307-318.
13. Craig, F. N.: Med. Div. Res. Report No. 5, Chem. Corps Army Med. Center, 1950.
14. Hall, J. F.; and Polte, J. W.: Physiological Index of Strain and Body Heat Storage in Hyperthermia. J. Appl. Physiol., vol. 15, 1960, pp. 1027-1030.
15. Gold, A. J.; and Zornitzer, A.: Effect of Partial Body Cooling on Man Exercising in a Hot, Dry Environment. Aerospace Med., vol. 39, 1968, pp. 944-946.

19 A LIQUID COOLED GARMENT TEMPERATURE CONTROLLER BASED ON SWEAT RATE

Alan Chambers and James Blackaby
Ames Research Center

INTRODUCTION

When a man is isolated from his environment—as is an astronaut in a pressure suit—auxiliary cooling is required to remove excess metabolic heat to maintain thermal balance (ref. 1). The major portion of this cooling is often accomplished by a liquid cooled garment (LCG), and, in current operations with the Apollo LCG, the astronauts maintain comfort by manually adjusting the inlet temperature of the coolant. This method of control has been adequate, but it would be preferable to have automatic temperature control. In an emergency, an astronaut should be free to concentrate entirely on his immediate situation; furthermore, man may be a poor judge of his own thermal state, especially when his attention is distracted so that his reactions to sensations of warmth and cold are delayed. The development of automatic LCG temperature controllers, responding to an astronaut's heat production rate, has been the subject of several studies. Three of these efforts are reviewed, and the design and operation of an Ames-developed controller based on sweat rate is presented in detail.

REVIEW

Three LCG temperature controllers that have been reported are a "metabolic rate" controller (ref. 2 and fig. 19.1), a "constant skin temperature" controller (ref. 3 and fig. 19.2), and a "differential temperature" controller (ref. 4 and fig. 19.3). In the "metabolic rate" controller, the subject's oxygen consumption is monitored and the controller automatically adjusts the LCG inlet temperature to remove the appropriate amount of heat. A linear relation between the metabolic heat produced and oxygen consumption is assumed. Difficulties develop with this approach during periods of rest when slight overcooling sometimes brings about lowering of skin temperature and results in shivering; oxygen consumption then increases, and the controller lowers the temperature still further. Another feedback element would have to be added to the controller to correct this difficulty. In addition, this controller requires a satisfactory method for continuous monitoring of the oxygen consumption of the astronaut in his pressure suit.

The second proposed controller attempts to maintain a constant skin temperature. This system has proved to be stable, but the basic philosophy of a

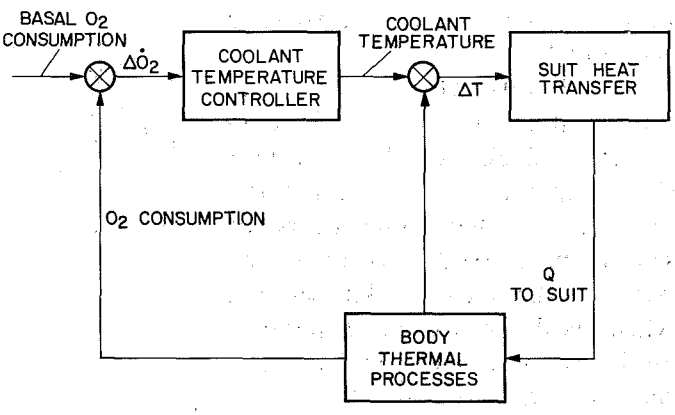

Figure 19.1 *"Metabolic rate" temperature controller (ref. 2).*

constant skin temperature is at odds with the findings of an Ames study (ref. 5) illustrated in figure 19.4, which shows that for optimum comfort, skin temperature should decrease with an increase in heat production. The "constant skin temperature" controller should be adequate for low metabolic rates; however, it may allow an excessive amount of sweating at high metabolic rates when a decrease in skin temperature is desirable.

The "differential temperature" controller attempts to regulate cooling as a function of skin temperature and heat removal. A linear relationship between the heat removal rate and comfortable skin temperature is assumed. Skin temperature is determined by averaging the temperatures at four selected points (right calf, over the right kidney, right lower abdomen, and lift bicep). The heat removal rate is determined by measuring the difference between the LCG inlet and exit water temperatures. For any given heat removal rate the optimum skin temperature is compared with the actual skin temperature, and the LCG inlet temperature is adjusted accordingly.

A disadvantage of the "differential temperature" controller (and also of the "constant skin temperature" controller) is the requirement that transducers or sensors be affixed directly on the body of the subject. Skin sensors, when used for extended periods, are likely to cause discomfort; thus, the acceptability of these controllers is likely to be limited. The

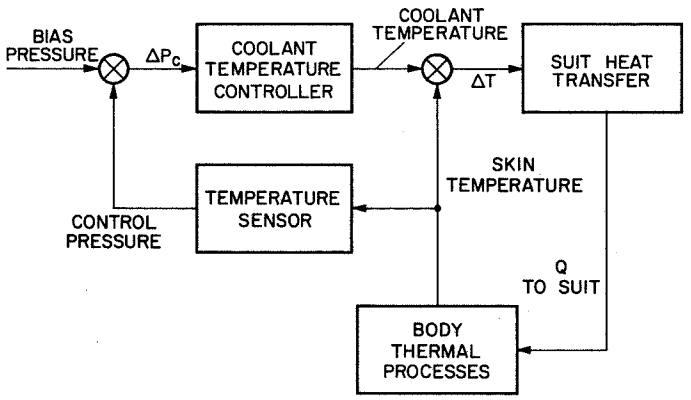

Figure 19.2 *"Constant skin temperature" thermal controller (ref. 3).*

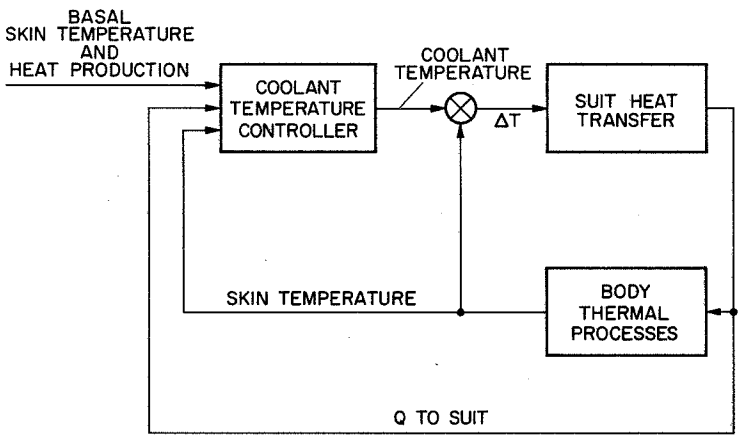

Figure 19.3 *"Differential temperature" thermal controller (ref. 4).*

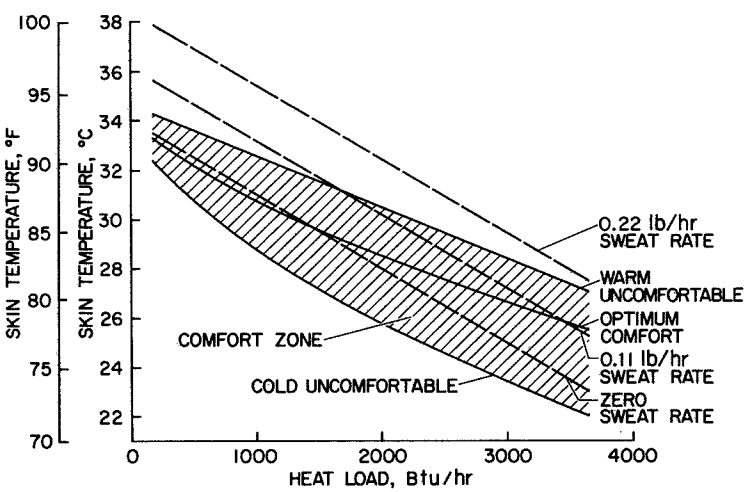

Figure 19.4 *Conduction cooling comfort zone (ref. 5).*

Environmental Control Research Branch at Ames Research Center has, therefore, undertaken the development of an LCG automatic controller that does not require skin sensors.

AMES CONTROLLER DESIGN

The comfort and sweat rate data in figure 19.4 illustrate three interrelated concepts applicable to subjects wearing a cooling garment such as the Apollo LCG.

1. Skin temperature should decrease with increasing heat load
2. Zero sweat rate is not necessary and may not be preferable at the higher heat loads
3. Sensible cooling of the skin can be directly related to the increase of sweat rate with increasing heat load

With these concepts defined, the Ames controller development has been based on the utilization of sweat rate as a primary input signal.

Three approaches were considered in formulating the logic for a sweat rate controller.

1. The controller could be designed to adjust coolant inlet temperature T_{IN} to the LCG such that the subject's sensible heat loss is kept proportional to his latent heat loss, thereby maintaining an acceptable balance between the normal modes of heat transfer. The heat losses would be determined from measurements of the inlet and outlet LCG and ventilating air temperatures and the subject's sweat rate. The T_{IN} to the LCG would be increased or decreased depending on whether sensible heat loss was too large or too small with respect to the latent heat loss.
2. Sweat rate could be kept constant at a set level (i.e., 100 g/hr). The controller would vary T_{IN} inversely with respect to any change in sweat rate. To perform correctly, the controller set point would have to be above the subject's normal insensible water loss rate; therefore, a slight amount of sweating would occur at all times.
3. The controller could be designed such that T_{IN} would be inversely proportional to the subject's latent heat loss as evidenced by evaporative water loss. This logic is similar to that of approach 2, but sweat rate would be permitted to increase with increasing work rate.

In the study described here, the third controller logic approach was used because the instrumentation and computation requirements for its implementation were considered to be the simplest. A block diagram of the logic is shown in figure 19.5. The controller in this system regulates LCG coolant inlet temperature T_{IN} as a function of two parameters: (a) a basal inlet water temperature T'_{IN} and, (b) the increment $\Delta\dot{S}$ in evaporative water loss rate with respect to a basal rate $\dot{S}'$. The T'_{IN} is the coolant temperature that provides comfort for the subject in a sedentary mode, and $\dot{S}'$ is the corresponding rate of evaporative water loss (which includes insensible water loss as well as loss due to active sweating). The controller algorithm is

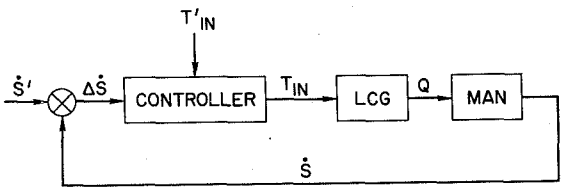

Figure 19.5 *Temperature controller logic.*

$$T_{IN} = T'_{IN} - K_1(\Delta\dot{S})$$

Evaporative water loss (which is representative of latent heat loss) can be determined from measurements of specific humidity (dewpoint) in the outlet and inlet air lines of the subject's pressure suit or similar ventilating garment. If inlet air dewpoint is maintained at a constant low

value, then $\Delta\dot{S}$ can be expressed simply as a function of air flow rate $\dot{w}$, the outlet air dewpoint T_{dp} during exercise, and the outlet air dewpoint T'_{dp} measured with the subject in the sedentary mode described above

$$\Delta\dot{S} = K_2(\dot{w})(T_{dp} - T'_{dp})$$

ECRB CONTROLLER OPERATION

Experiments with the controller were conducted with subjects wearing a whole-body air-ventilated suit over an Apollo LCG. The dewpoint of the suit inlet air was kept approximately constant at -2° C. The inlet air temperature was maintained at 20° C with an air circulation rate of 29 m^3/hr. The dewpoint of the suit outlet air thus became the only variable used in controlling T_{IN}. The subjects exercised on a treadmill at various metabolic rates; the metabolic rates were calculated based on oxygen consumption measurements during the tests. During initial tests, subjective evaluations of thermal comfort were recorded while several values of the proportionality constants K_1 and K_2 were set in the analog computer, which served as the controller for the tests. Based on these evaluations proportionality constants selected for the controller equations were K_1= 0.09[(°C · hr)/gm] and K_2 = 0.40[gm/(m^3 · °C)].

The coolant supply system (fig. 19.6) introduced considerable mechanical delay (of the order of 3 min) into the overall controller response time because of backlash in the hot and cold metering valves, slow reaction in the heat exchanger, and a long coolant supply line to the LCG. Nonlinearity of the hot and cold metering valves also affected the response of the controller. The problems of nonlinearity and delay were overcome, for these tests, by operation of the controller in a sample data system mode. The sampling rate was made proportional to the difference between LCG inlet temperature $T_{IN|actual}$ and the desired inlet temperature $T_{IN|control}$ as computed by the controller. At each sample time the hot and cold metering valve motors were energized for a short, fixed length of time (approximately 50 msec) so that $T_{IN|actual}$ was, in effect, caused to approach $T_{IN|control}$ in steps. This mode of operation reduced the effects of the inadequacies of the coolant supply components and resulted in relatively quick and stable response of the system.

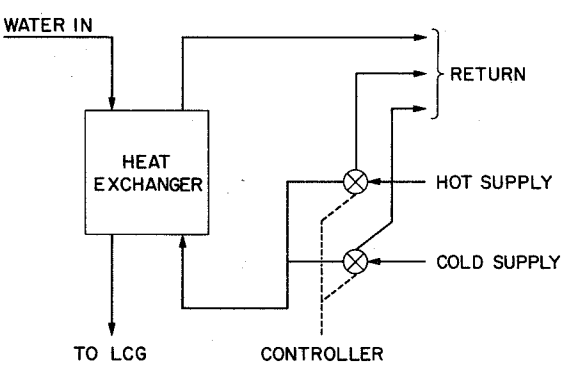

Figure 19.6 *Coolant supply system.*

Figures 19.7 and 19.8 show recorder tracings of treadmill speed, $T_{IN|control}$, and $T_{IN|actual}$ for two levels of exercise. The subjects were kept thermally comfortable during the tests illustrated, and for all tests with work rates up to about 3000 kJ/hr. The only major difficulty with the controller occurred for a subject exercising at a high work rate (4200 kJ/hr) for 1/2 hr. In this test, the subject could not be adequately cooled, especially around the head and neck (the Apollo LCG provides no head or neck cooling). A

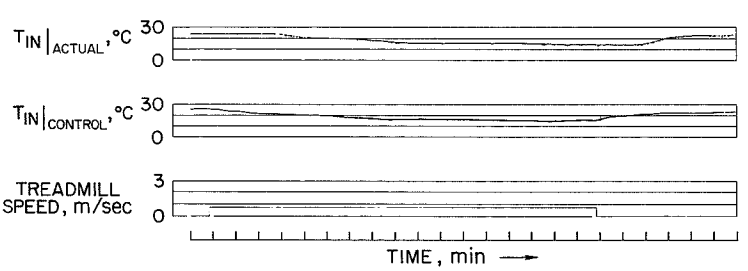

Figure 19.7 *Test results–work rate 1250 kJ/hr.*

portion of the subject's sweat was not evaporated by the ventilating air, but was absorbed by the fabric of the LCG. When the subject stopped exercising, the absorbed sweat began to evaporate; the controller sensed this as continued sweating and maintained an LCG temperature lower than was comfortable for the subject. In other respects, the performance of the sweat rate automatic controller was promising. Continuing tests are scheduled with the hardware modified to eliminate the causes of most of the nonlinearities and transport delays of the original system.

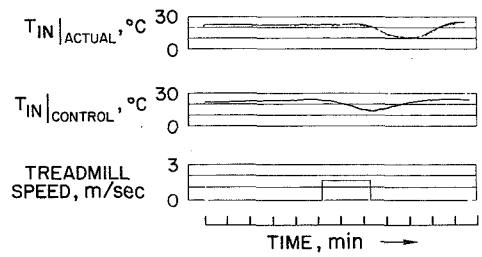

Figure 19.8 *Test results–work rate 2900 kJ/hr.*

REFERENCES

1. Nunneley, S. A.: Space Life Sciences, vol. 2, 1970, pp. 335-360.
2. Webb, P.; Annis, J. F.; and Troutman, S. J.: Automatic Control of Water Cooling in Space Suits, NASA CR-1085, 1968.
3. Merrill, G. L.; and Starr, J. B.: Automatic Temperature Control for Liquid Cooled Flight Suits, NADC-AC-6702, August 3, 1967.
4. Troutman, S. J.; and Webb, P.: Automatic Control of Water Cooled Suits from Differential Temperature Measurements, Report for NASA Contract NAS12-682, 1969.
5. Unpublished study in Environmental Control Research Branch, Ames Research Center, NASA.

20

EFFECT OF NECK WARMING AND COOLING ON THERMAL COMFORT

Bill A. Williams and Alan B. Chambers
Ames Research Center

INTRODUCTION

Efforts to remove metabolic heat by partial or differential body cooling have been undertaken for many body regions (refs. 1-5). Recent studies have shown the potential use of head cooling as a means of removing significant amounts of heat from the body (as much as 30 percent) in attempts to alleviate thermal stress (refs. 6-8).

Studies conducted in this laboratory have taken a different approach by using only local neck cooling in an area superficial to the cerebral (carotid) arteries. The purpose of these experiments was to determine the effects of a small local heat flux applied to this neck area on subjective feelings of thermal comfort and other physiological parameters during exposure to heat or cold stress.

METHODS

Six men aged 21 to 40 were used in this study. The subjects were seated and inactive in a controlled environment room dressed only in shorts. Each experimental run consisted of two sequential test periods with identical air temperature profiles. At the beginning of each test the subject was allowed to come to equilibrium in the room at 25° C (30-40 min). The first test period was then begun. The room temperature was raised to 33° C (or lowered to 19° C) for 20 min. This was followed by a recovery period at 25° C for 20 min. The second test period was then begun and the air temperature changes were repeated.

Experimental data collected during the first test period were used as baseline control information. During the second period the temperature of the neck superficial to the carotid arteries was lowered to 16° C (or raised to 43° C) by circulating cold or hot water through two copper discs (7 cm^2 each) held firmly against the neck (fig. 20.1). The skin surface area covered by these discs represented less than 0.0006 of the total skin surface area.

Three subjective indices of thermal comfort were recorded: (1) thermal zone, graded from hot to cold; (2) Comfort index, graded comfortable to very uncomfortable; and (3) air temperature estimate, an estimation of ambient temperature by the subject (fig. 20.2). The subjects orally reported the subjective responses every 5 min via a closed circuit TV system.

The following physiological data were measured: heart rate, ambient air temperature, skin temperature (six locations), rectal temperature, and ear canal temperature. Thermocouples located directly inside the circulating water measured the inlet and outlet temperatures used to determine the approximate heat load added to or removed from the neck by the collar.

The physiological data were automatically recorded and stored on magnetic tape at 30-sec intervals. The data were later processed and plotted by a digital computer.

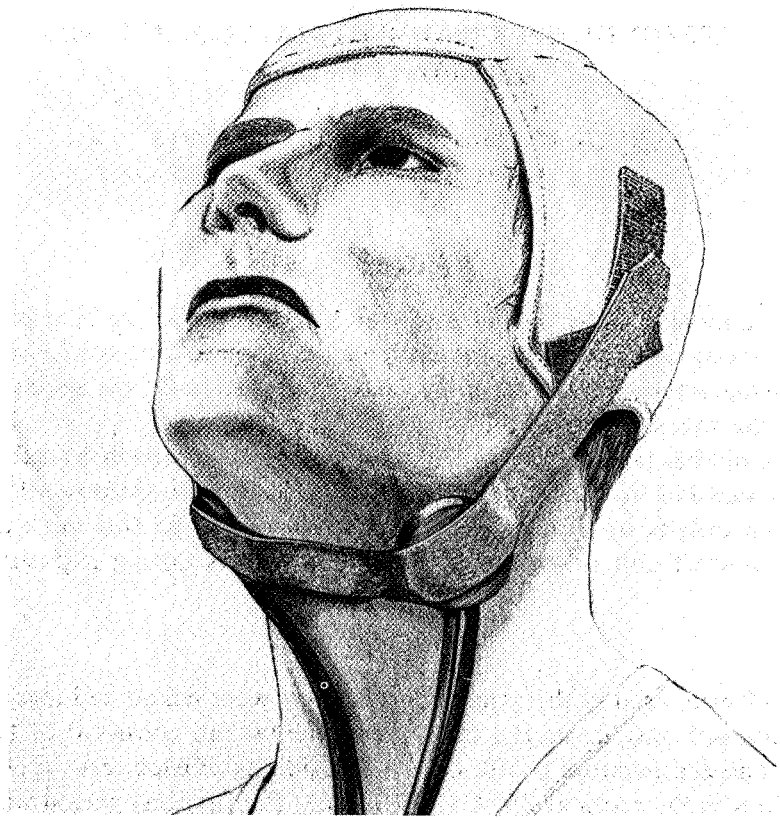

Figure 20.1 *Collar placement on the neck of the subject. Velcro straps on collar and on hat allow the discs to be adjusted for each subject.*

RESULTS

The subjects, after training sessions, were able to consistently estimate thermal zone, comfort level, and room air temperature in response to air temperature changes. Since each subject served as his own control, emphasis was placed on the *relative* rather than the absolute subjective responses. When a subject became consistent in his estimations of the comfort indices he was exposed to the experimental protocol.

Warming the collar to 43° C produced no significant changes in subjective responses or physiological parameters during exposure to either high or low air temperature. On the other hand, a dramatic alteration of subjective comfort occurred while the collar was being cooled. This alteration was most apparent during collar cooling in the hot (33° C) environment. In all cases the subjects at an air temperature of 33° C responded to collar cooling by indicating improvement of thermal comfort (fig. 20.3). The "thermal zone" estimations were markedly improved during collar cooling. All subjects indicated more "neutral" thermal comfort levels (fig. 20.4) and felt more

"comfortable" during collar cooling in the high air temperature. Since each subject served as his own control for the "room air temperature" estimations, the results are best represented as the estimation of *change* in air temperature indicated by each subject (fig. 20.5(a), (b)).

It is apparent from all of these subjective indices that a relative improvement in comfort could be produced using neck cooling in a warm environment.

Control experiments conducted with the collar inoperative during the second temperature profile did not show any alteration in subjective comfort levels. Responses in this case were identical in both profiles indicating that the alterations in comfort were not merely the result of the second exposure.

The physiological parameters measured remained mostly unaffected by the neck cooling. No differences were observed in the rectal and skin temperature responses to the ambient temperature changes with or without collar warming or cooling. However, the ear canal temperature showed a significant alteration during neck cooling. In this case the ear canal temperature did not rise as high during neck cooling as it did during the control period. The cooling effect of the collar appears to have spread to this area to produce the slight lowering in ear canal temperature in response to the rise in ambient air temperature (fig. 20.6).

Another physiological change that occurred was the initiation of shivering during exposure to 19° C, while cooling the collar. The subjects did not, in any instance, shiver during exposure to 19° C without neck cooling.

Alteration of subjective thermal comfort also occurred with neck cooling during cold (19° C) exposure. In this case, however, the alterations were all detrimental to the overall well-being and comfort of the subject.

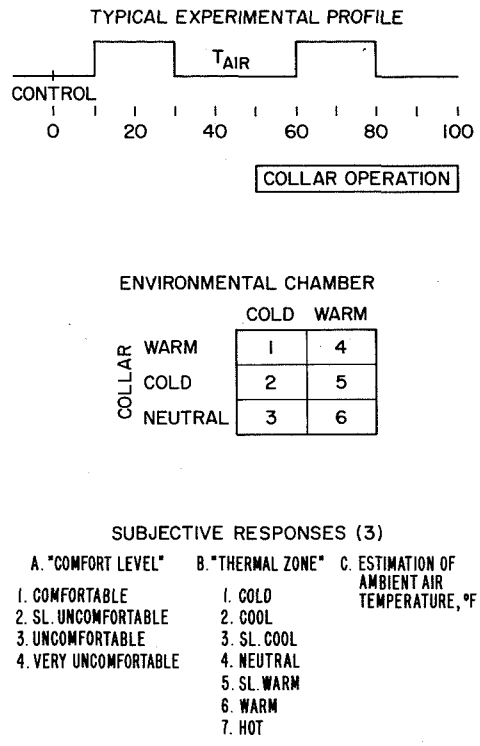

Figure 20.2 *Experimental Protocol. (Top) Air temperature during experiment profile and collar operation. Air temperature was raised to 33° C (or lowered to 19° C) from the equilibrium temperature of 25° C. (Center) Combinations of temperature exposures and collar operation. (Bottom) Three subjective indices used for determination of comfort. Rating scales and air temperature estimates were recorded every 5 min.*

Adverse subjective reaction to the cold was magnified during neck cooling (fig. 20.7).

DISCUSSION

We have demonstrated that it may be possible to improve the subjective assessment of a hot thermal environment by direct neck cooling.

Whether or not we are actually affecting the brain thermostat to produce these alterations is unresolved. During the sessions when the collar was being cooled there was a substantially greater difference ($\Delta T = 18°$ C) between the neck skin temperature (34° C) and the disc temperature (16° C) than in sessions when the discs were being warmed ($\Delta T = 9°$ C). Since we could not directly measure the changes in brain or blood temperature in our subjects, a computer-simulated model of the

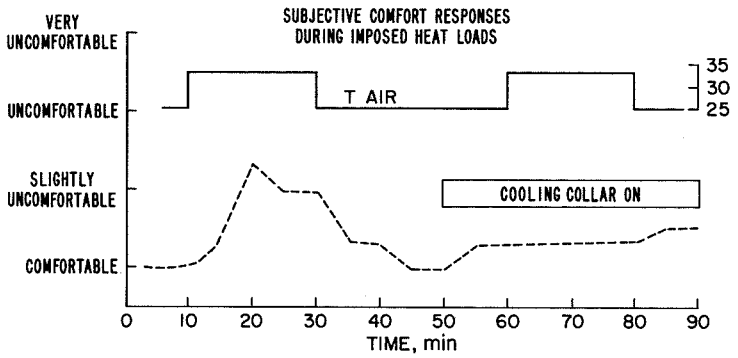

Figure 20.3 *Mean change in comfort rating with collar cooling in hot room. The second half of the graph (collar cooling) illustrates the improvement in thermal comfort.*

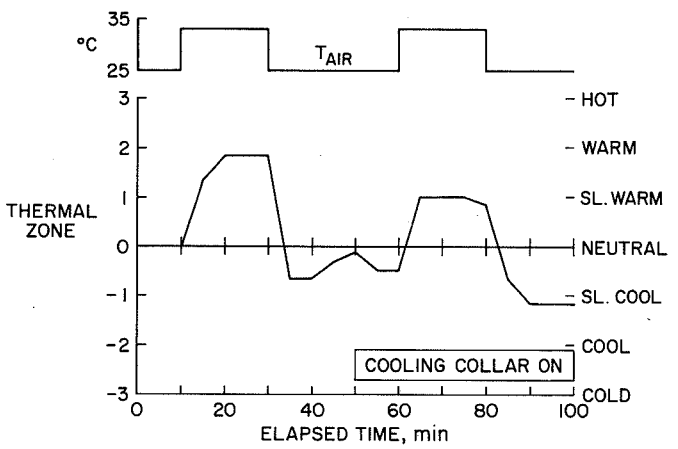

Figure 20.4 *Mean response to the "thermal zone" index illustrating improvement in comfort rating (more neutral) during collar cooling in hot room.*

interaction of our cooling patches with the carotid arteries was created to determine theoretically whether the cerebral blood could have been cooled enough to produce changes in brain temperature. Our data and parameters were used to plot the potential interactions of the cooling patches with the carotid blood (fig. 20.8). The lines of isothermy indicate predicted thermal gradients below the patches.

The computer simulation predicts that a carotid blood temperature change in the order of only 0.1° to 0.2° C is possible using this technique. Such a gradient *directly* below the patches would surely be insufficient to change the temperature of the brain thermostat.

The only indication that the collar altered cerebral blood temperature was the lower increase of ear canal temperature in response to an air temperature rise indicating that the ear area was slightly cooled, possibly by the blood perfusing it. Further, *exact* placement of the discs over the carotid area was necessary for the subjective thermal improvement.

It is also possible that the noticeable effect on subjective thermal comfort may be due to a "local" sensor effect or a change in the integration of total skin temperature input to the brain.

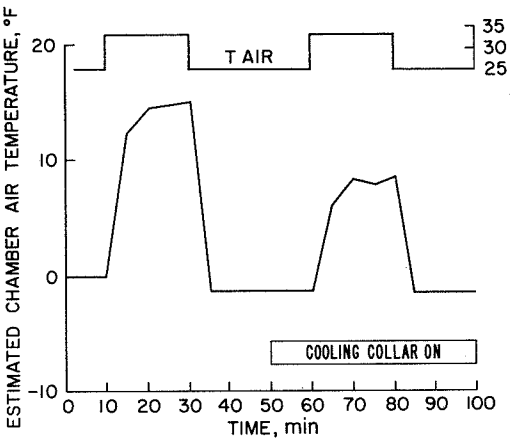

Figure 20.5(a) *Mean normalized responses of subjects in hot room with collar cooling. Estimations of air temperature were dramatically lowered with collar cooling. Responses of each subject were normalized for comparison.*

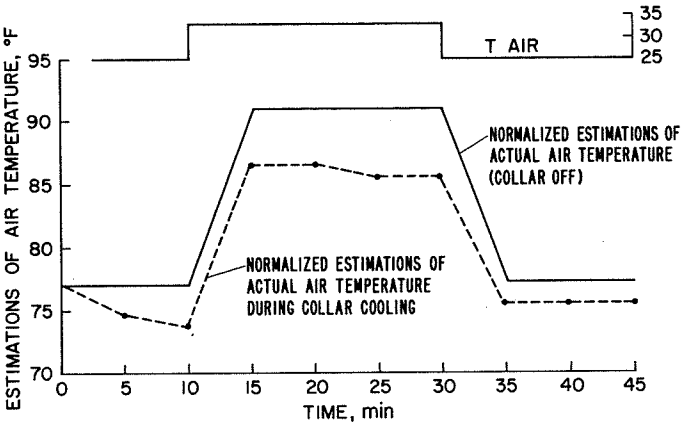

Figure 20.5(b) *Illustration of the effect of collar cooling on estimation of air temperature by the subjects.*

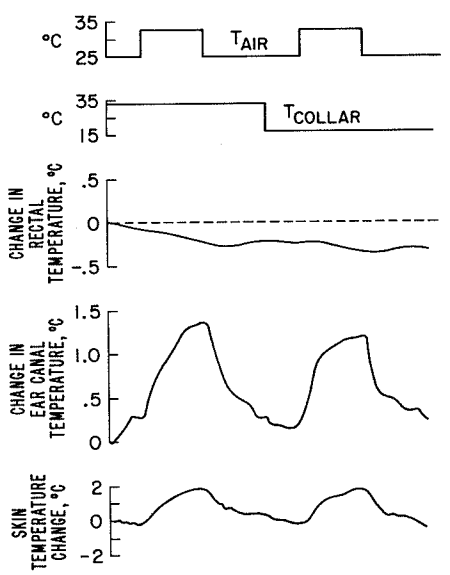

Figure 20.6 *Some physiological responses occurring during collar cooling in hot room. There was no significant change in any observed physiological parameters except the slight depression of ear canal temperature (see text).*

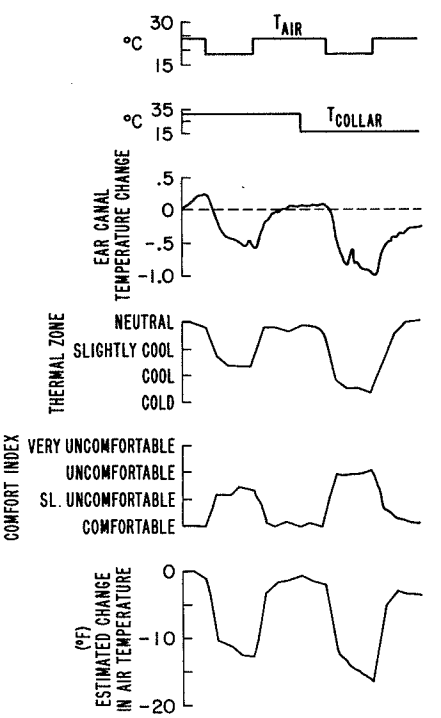

Figure 20.7 *Some changes during collar cooling in cold room. Note increased depression of ear canal temperature and detrimental effect on subjective comfort responses.*

It is evident from these data that thermal comfort may be improved in a hot environment by cooling the neck in the area of the carotid arteries. The means of achieving this subjective thermal improvement are not clearly delineated, but indicate that important consideration must be given to neck and head cooling in any attempts to use artificial cooling for thermal comfort and heat balance. In our laboratory we are attempting to integrate this concept into potential means of improving total thermal comfort using head-neck cooling in heat stressed aircrews. Further, consideration should be given to head cooling integration into any LCG system.

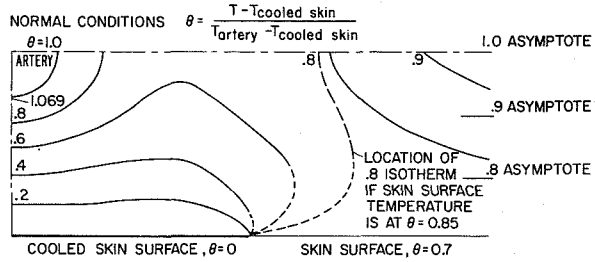

Figure 20.8 *Representation of the interaction of the collar with surface and deep tissues of the neck as determined by computer simulation. Lines of isothermy relate theoretical heat flow under the collar using data and parameters of the experiment.*

REFERENCES

1. Billingham, J.: Heat Exchange between Man and His Environment on the Surface of The Moon. J. British Interplanatary Society, vol. 17. 17, 1959, pp. 297-300.
2. Burton, D. R.: Performance of Water Conditioned Suits. Aerospace Med. vol. 37, 1966, pp. 500-504.
3. Gold, A. J.; and Zornitzer, A.: Effect of Partial Body Cooling on Man Exercising in a Hot, Dry Environment. Aerospace Med. vol. 39, 1968, pp. 944-946.
4. Nunneley, S. A.: Water Cooled Garments: A Review Space Life Sciences, vol. 2, 1970, pp. 335-360.
5. Webb, P.; and Annis, J. F.: Biothermal Responses to Varied Work Programs in Men Kept Thermally Neutral by Water Cooled Clothing. NASA CR-739, 1967.
6. Konz, S.; and Duncan J.: Cooling with a Water-Cooled Hood. Proc. Symposium on Individual Cooling. Kansas State University, 1969, pp. 138-169.
7. Nunneley, S. A.; Troutmen, S. J.; and Webb, P.: Head Cooling in Work and Heat Stress. Aerospace Med. vol. 42, No. 1 1971, pp. 64-68.
8. Shvartz, E.: Effect of a Cooling Hood on Physiological Responses to Work in a Hot Environment. J. Applied Physiol. vol. 29, 1970, pp. 36-39.

21 TOLERANCE TO EXTERNAL BREATHING RESISTANCE WITH PARTICULAR REFERENCE TO HIGH INSPIRATORY RESISTANCE

R. A. Bentley, O. G. Griffin, R. G. Love,
D.C.F. Muir, and K. F. Sweetland
Safety in Mines Research Establishment,
Department of Trade and Industry, Sheffield, England, and
Institute of Occupational Medicine, Edinburgh, Scotland

INTRODUCTION

Many previous investigations have been made into the effects of external respiratory workloads in men to define acceptable standards for men wearing respiratory apparatus. A comprehensive study of the problem was made by Silverman et al. (refs. 1, 2) who investigated the effects on young men of breathing against resistance while working at various rates on a bicycle ergometer.

Cooper (ref. 3) and Senneck (ref. 4) reviewed the work of Silverman *et al.* and from it derived standards for the maximum permitted total rate of respiratory work done on a breathing apparatus. Cooper stressed that Silverman's subjects were not accustomed to breathing through resistances and only exercised for 15 min, whereas most of the men likely to wear respiratory apparatus would be trained in their use and would probably be required to wear them for a much longer period.

Underground workers in the British coal industry have recently been issued emergency "self-rescuer" filter-type apparatus to protect them from carbon monoxide. These respirators are designed to last for about an hour and should enable men to reach safety following an underground fire or explosion. The potential use of the equipment by a large population of men has prompted us to re-examine the ability of men to exercise while breathing through graded inspiratory resistances. The information obtained should be relevant to the design and use of most types of breathing equipment. We were not concerned with the effects of the added resistances on such factors as the rate or depth of breathing or on gas exchange but simply on the subjects' ability to tolerate the added respiratory workload.

Particular care was taken to ensure that the apparatus and exercise were appropriate to that encountered in practice. In most industrial breathing equipment the relation between airflow and work rate is far from linear over an extended range of airflows, so experimental resistances were constructed having similar nonlinear characteristics. The duration and severity of exercise were intended to match and exceed those anticipated in men escaping in an emergency, and be similar to those encountered in routine use. The exhalation valve was of a standard low resistance type and extra resistances were added only to the inhalation side.

METHODS

The relationship between the pressure p required to maintain a rate of airflow dV/dt through a respiratory apparatus may be expressed to a close approximation, as $p = k\,(dV/dt)^n$ where n and k are constants characteristic of the resistance to flow of the apparatus. Single values of n and k may hold throughout a wide range of flow rates in some types of respiratory apparatus, while two or even three values may be required to define the pressure-flow relationship of the patterns of flow in other apparatus.

Several designs of experimental resistance were examined, but the design found to give the most appropriate values for n and k was constructed as follows. Several stainless steel plates (3.8 by 1.9 by 0.01 cm) that had a radius of curvature about their major axis of approximately 8 cm, were mounted in pairs, with their concave surfaces facing each other, into a perspex holder (fig. 21.1). Increasing the number of plates inserted into a holder increased the resistance to flow and vice-versa. This method of construction yielded the desired resistance to airflow. The resistances were calibrated during their construction, and when a particular resistance was judged to have an acceptable value, the plates were fixed in position by epoxy resin along their edges. Ten such resistances were produced (fig. 21.2).

The experimental mouthpiece assembly (fig. 21.3) consisted of the head and headstrap of a self-rescuer into which had been inserted a pressure measuring port. The experimental resistance and respirometer were connected by a short piece of rubber tubing to the mouthpiece. The complete apparatus weighed about 415 g and was easily dismantled for cleaning and sterilizing.

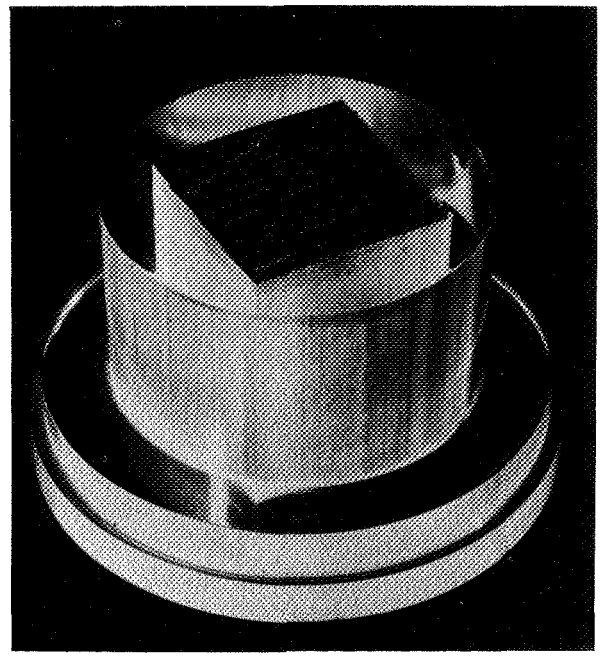

Figure 21.1 *Experimental inspiratory resistance.*

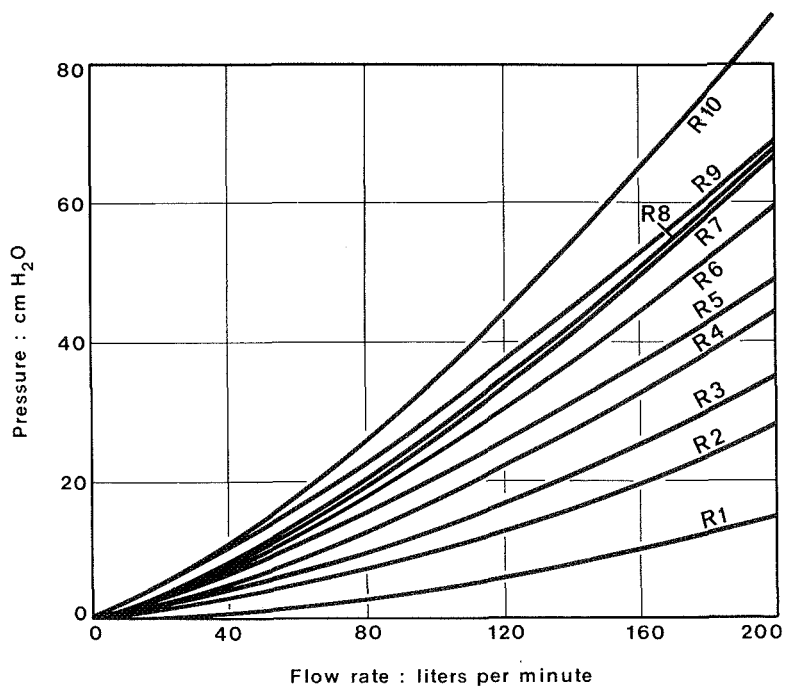

Figure 21.2 *Pressure-flow curves of resistances R_1 to R_{10}.*

The ventilation of each subject was measured with a respirometer (ref. 5), a small instrument that allows the subject to exercise freely. Each respirometer was calibrated by means of a breathing simulator.

The experimental subjects were all members of the Mines Rescue Service of the British National Coal Board. Seven were full-time members and the remainder were part-time men who were also employed in various underground trades. Their ages ranged from 21 to 45 years. A total of 158 men participated in the study; each man took part in only one experiment.

The exercise consisted of a 30-min walk on a treadmill whose speed and inclination could be varied. The work rate was altered between subjects so that a wide range of minute ventilations was obtained. Each man wore shorts, boots, and stockings as well as a safety helmet, battery, and cap lamp similar to those used when working underground. He was given a brief description of the experiment and of its aim, and was then allowed to take a short practice walk on the treadmill. The ten resistances were allocated at random among the subjects, who wore them throughout the exercise.

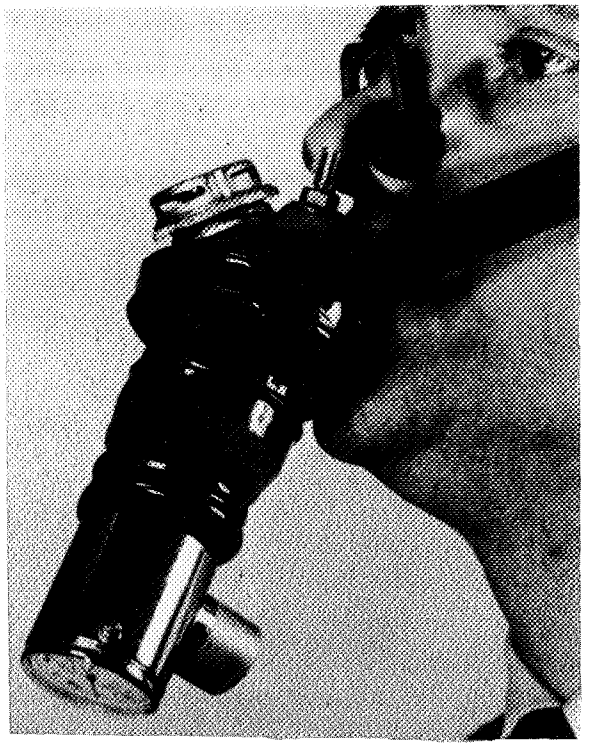

Figure 21.3 *Experimental mouthpiece assembly.*

Each man was questioned after completing the exercise. He was asked to select from a printed card the condition that most closely described the effect of the apparatus on his breathing. The wording of the questionnaire was based on phrases used by the men in conversation. The choices are shown in table 21.1. Several subjects expressed a need for intermediate answers, and these were recorded as one/two or two/three, etc.

Table 21.1 *Questionnaire shown to each subject after completing the exercise.*

Did you find breathing:-

1. Not noticeable
2. Noticeable but not difficult
3. Difficult
4. Very difficult

CALCULATION OF THE EXTERNAL WORK OF BREATHING

Inspiratory Work Rate

The resistances were designed to have characteristics similar to those of breathing equipment in current use. However, the nonlinear pressure-flow relationships necessitate some complexity in the calculation of the respiratory work rate. The mathematical approach used allowed the work rate to be calculated from the minute volume, peak pressure measurement, and the proportion of each respiratory cycle spent on inhaling or exhaling. The range of flow rates encountered in the experiments permitted single values of n and k for each resistance to be used for all the calculations.

It can be shown that when the flow pattern is sinusoidal and the pressure-flow curve of the external resistance can be represented by one value for n and k, then the inspiratory work done per minute (W_i) is given by

$$W_i = \frac{k}{100} \frac{\dot{V}_E^{n+1}}{I^n} \left(\frac{\pi}{2}\right)^n \int_0^{\pi/2} \sin^{n+1} x \, dx \quad \text{kg-m/min} \qquad (1)$$

where $\dot{V}_E$ is the minute volume and I is defined by

$$I = \frac{\text{time occupied by one inhalation}}{\text{time occupied by one complete respiratory cycle}}$$

In practice, the value of n is not an integer; therefore, the integral in equation (1) is not easily solved. A graphical solution was obtained for noninteger values of n, after solving equation (1) using values of $n = 1, 2, 3$.

It can also be shown that when the flow pattern is rectangular or triangular the inspiratory work done per minute is given by

$$W_i = \frac{k}{100} \frac{\dot{V}_E^{n+1}}{I^n} \text{ kg-m/min} \tag{2}$$

for rectangular flow and

$$W_i = \frac{k}{100} \frac{\dot{V}_E^{n+1}}{I^n} \frac{2^{n+1}}{n+2} \text{ kg-m/min} \tag{3}$$

for triangular flow. It follows, therefore, that for each resistance used in the experiments the equations for external inspiratory work rate, albeit a sine, rectangular or triangular waveform, simplify to

$$W_i = A \frac{\dot{V}_E^{n+1}}{I^n} \text{ kg-m/min} \tag{4}$$

where A is a constant for a particular resistance and waveform.

By introducing the concept of a shape factor (Q), it is possible to quantify the shape of the waveform and thereby take account of its shape when calculating external respiratory work. This shape factor is defined as the ratio peak flow rate/minute volume; that is, the larger the peak flow rate (for a particular minute volume) the larger the shape factor. It can be shown that

1. The peak flow rate in sinusoidal flow = $\pi \times$ minute volume.
2. The peak flow rate in rectangular flow = 2.0 × minute volume.
3. The peak flow rate in triangular flow = 4.0 × minute volume.

From calculated values of the constant A, for sinusoidal ($Q = 3.14$), rectangular ($Q = 2.0$) and triangular ($Q = 4.0$) flow, graphs of shape factor against A were drawn for each resistance.

The shape factor Q was determined for each experiment and the value of the constant A deduced from the appropriate graph. The ratio I was also determined for each experiment from the continuous recording of the pressure in the mouthpiece. The external inspiratory work rate was then calculated from equation (4).

Validity of the Calculation

Calculation results were compared with those obtained by a conventional method. The inspiratory work rate in ten subjects was calculated from the continuous record of the pressure drop across the resistances. Each measurement of pressure was associated with its appropriate work rate as derived from a knowledge of the pressure-flow relationship of the resistance in use. The total expenditure of work during each inspiration was then obtained by integration of the area under the curve. Ten respiratory cycles were examined in each subject, and the work rates obtained were compared with

those obtained by indirect calculation using equations (1) through (4). The correlation coefficient between the two methods was 0.99.

Expiratory Work Rate

Although the method of determining the external expiratory work rate was identical to that used for the inspiratory work rate, the calculations were more difficult because the pressure-flow characteristics of the expiratory valve could not be defined by single values of n and k. It was therefore necessary to evaluate the general equations for respiratory work rate; the results of these calculations were obtained by means of a FORTRAN program on an ICL 1907 computer. The external expiratory work rate for each exercise was then obtained by interpolating, using the appropriate shape factor, between the work rate calculated for sinusoidal, rectangular, or triangular waveforms.

RESULTS

The replies to the questionnaire were divided into two groups. Those men who indicated that their breathing was not difficult (response 2 or less) were deemed to have an acceptable respiratory workload. Those who assessed their sensation of breathing as more difficult than "noticeable but not difficult" were considered to have an excessive respiratory load. The relation between the responses and the rate of respiratory work is illustrated in figure 21.4 with the associated minute ventilation. The curves shown in figure 21.4 will be referred to later in the text.

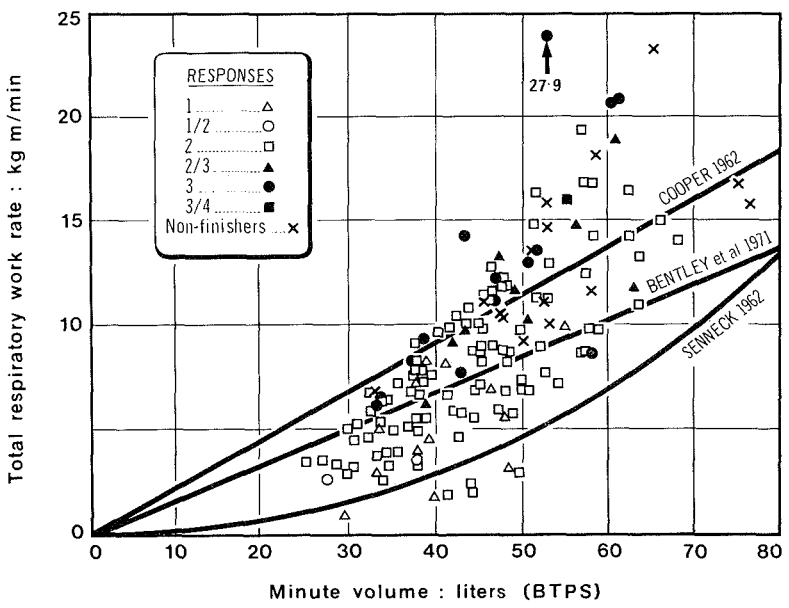

Figure 21.4 *Subjective response to breathing resistance related to total respiratory work rate and minute volume.*

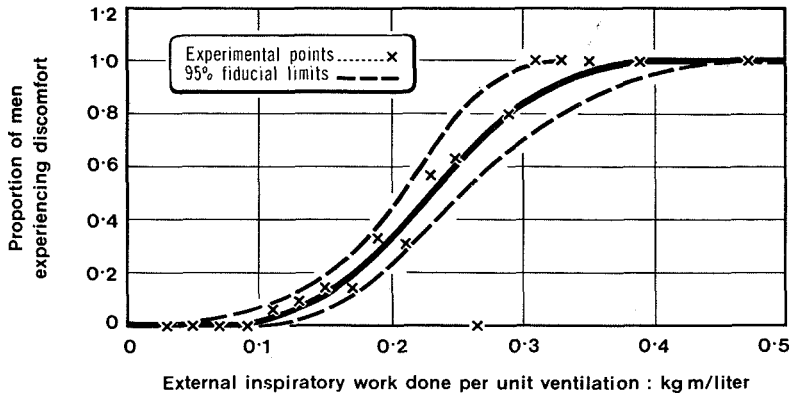

Figure 21.5 *Proportion of men experiencing discomfort related to inspiratory work rate.*

The distribution of the points in the figures is determined by the design of the experiment. Since a fixed number of resistances was used by men exercising at various rates on the treadmill, the overall pattern of the points reflects the pressure-flow characteristics of these particular resistances. There is thus no general physiological relationship implied by the correlation between minute ventilation and respiratory work rate apparent in figure 21.4. However, the figures do give information about the factors determining the sensation of discomfort when breathing through an inspiratory resistance. Although there is a good deal of overlap between the two groups it can be seen that both the rate of respiratory work and the minute ventilation play a part. A workload apparently judged acceptable at a high minute ventilation may be unpleasant at a lower minute ventilation. The relationship may be simplified by calculating the inspiratory work done per liter of air breathed. The subjective responses to this single parameter are shown in figure 21.5. The data are seen to fit closely to a sigmoid dose-response type of curve that expressed the probability that a given value on the abscissa will be judged unacceptable by the population of men tested. The fitted curve and 95 percent fiducial limits were obtained by the method of probit analysis (ref. 6). Similar data for the total respiratory work did not give such a close fit to a single line (fig. 21.6). This is not unexpected since the men, when commenting on their assessment of the apparatus, tended to concentrate on the characteristics of the inspiratory resistance.

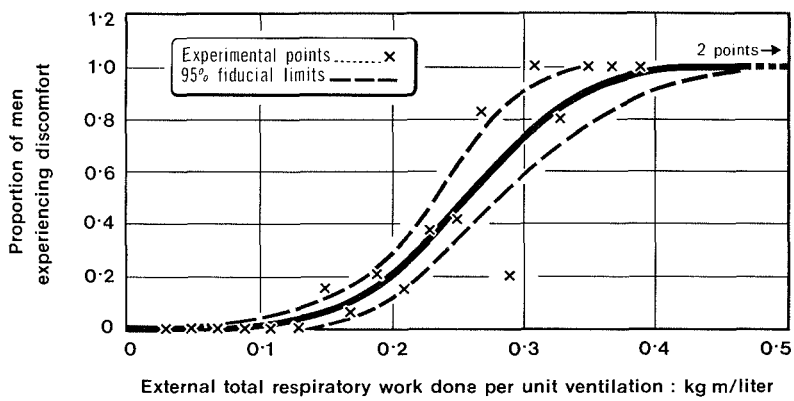

Figure 21.6 *Proportion of men experiencing discomfort related to total respiratory work rate.*

The relation between the subjective response and the measurements of the peak inspiratory pressure swing was also examined. Again there is a good deal of overlap between the two groups of points but no suggestion of association with minute ventilation. The level of the peak pressure swing alone appears to distinguish those men who felt discomfort on breathing from those who did not. The results are expressed in probability form in figure 21.7.

A highly significant correlation ($P < 0.001$) was found by Students t test between the proportion of subjects noting discomfort on breathing and each of the parameters shown in figures 21.5, 21.6, and 21.7.

It was found that, in practice, the waveform was neither rectangular nor truly sinusoidal, but rather a flattened sine wave. The degree of flattening did not depend on the magnitude of the resistance. Similarly, the proportion of each respiratory cycle spent on inspiration varied little throughout the entire range of the experiments. The shape factor was also nearly constant (Q = 2.67 ± 0.23). These studies thus gave no evidence that the pattern of breathing changed significantly in response to varying inspiratory workloads within the range tested.

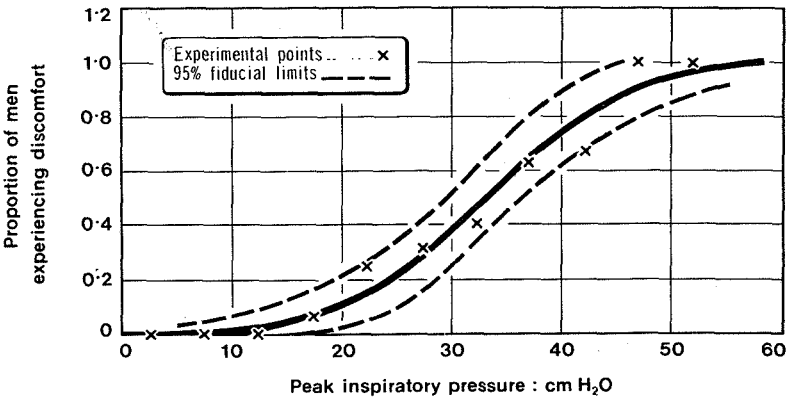

Figure 21.7 *Proportion of men experiencing discomfort related to peak inspiratory pressure.*

The results were examined to see whether men who found the inspiratory workload acceptable (group 1; response 2 or less) had a higher ventilatory capacity than those who were distressed (group 2; response two/three or greater) when breathing under the same conditions (table 21.2). Eighteen subjects were selected from each group, so that each man in group 1 was matched with a man in group 2 based on the following criteria: treadmill speed and inclination, resistance to breathing, and body weight and height. It can be seen that there was a slight but insignificant difference in the ventilatory capacities of the two groups, although the average age was slightly higher for group 2. However, group 2 had, on average, a significantly higher peak inspiratory pressure, and inspiratory and total respiratory work done per minute and per liter of air breathed (table 21.2).

Table 21.2 *Ventilatory characteristics (mean + S.D.) of 18 subjects (Group 1) who found the work of breathing acceptable compared with 18 subjects (Group 2) who found the work of breathing difficult.*

Group	Response†	Age yr	Weight kg	Height cm	FEV_1‡ liters	FVC‡ (BTPS)	Pp cm H_2O	V_E liters min^{-1} BTPS	f min^{-1}	W_i kg m min^{-1}	W_t kg m min^{-1}	W_i/V_E kg m $liter^{-1}$	W_t/V_E kg m $liter^{-1}$
1	<2	31·5	73·7	172·7	3·56	4·45	31·8	46·2	24·4	9·6	10·8	0·208	0·228
		±5	±7·5	±7·8	±0·66	±0·74	±6·3	±10·7	±4·5	±2·8	±3·9	±0·040	±0·047
2	>2/3	34·1	73·7	173·0	3·85	4·84	35·7	49·2	24·5	13·9	15·1	0·282	0·312
		±7	±7·5	±6·1	±0·61	±0·56	±7·7	±10·9	±5·8	±5·5	±7·4	±0·068	±0·084
Differences (P values*)			-	-	N.S.	N.S.	<0:05	N.S.	N.S.	<0·01	<0·01	<0·01	<0·001

Pp = Peak inspiratory pressure; W_i, W_t = Inspiratory and total respiratory work done per minute; V_E = minute volume; f = breathing frequency; W_i/V_E, W_t/V_E = inspiratory and total respiratory work done per liter.
†See Table 21.1 ‡For 10 subjects only in each group; *single sample t test: significance levels

DISCUSSION

The sensation of discomfort during breathing in these experiments was related closely to the additional work done per liter of air inhaled and to the peak pressure swing. However, the former was calculated by dividing the inspiratory work rate (kg-m/min) by the minute ventilation (liters/min). As noted by Cooper (ref. 7) the derived term has the dimensions of pressure. The results therefore indicate that the degree of dysponoea (shortness of breath) was a function of the negative intrathoracic pressure. These conclusions support those of Silverman (ref. 2) and Cooper (ref. 3) but not the findings of McIlroy (ref. 8) who considered that the absolute respiratory workload was a major factor in the causation of dyspnoea.

The levels of resistance investigated by us and also by Silverman (ref. 2) fall between those that are detectable but not uncomfortable (refs. 9, 10) and those that are the maximum tolerable (refs. 11, 12, 13). The dividing line in our experiments (fig. 21.4) is drawn at the point where subjective discomfort is first noticed.

Two factors must be considered in using the results to formulate standards that may be used for acceptance testing of respiratory apparatus. In the first place, the standard must not be set so low that it is ignored. It also is necessary to ensure that the most men can and will use the apparatus. A compromise is suggested by taking a value from figure 21.5 such that 90 percent of the population tested will not experience respiratory discomfort. The appropriate level is 0.14 kg-m/liter (1.4J/liter) of air inhaled.

This unit has the dimensions of pressure and it can be shown that 0.14 kg-m/liter is equivalent to a pressure drop across the inspiratory valve of 14 cm H_2O (1.4 kN/m^2) during conditions of steady flow. By applying the criteria used to obtain a limit on inspiratory work rate it can be deduced from figure 21.6 that the total external respiratory work permissible when using low resistance expiratory valves amounts to 0.17 kg-m/liter (1.7J/liter) of air breathed.

These levels are below those suggested by Cooper (ref. 3) but above those suggested by Silverman (ref. 2) and Senneck (ref. 4) (fig. 21.4). Their results refer to the situation in which there is a combination of inspiratory and expiratory resistances.

The type of airflow used in the laboratory testing procedure must be considered in defining an acceptable resistance for the assessment of respiratory apparatus. We have found that the normal waveform of subjects breathing through inspiratory resistances is flattened with a mean shape factor (peak inspiratory flow/minute volume) of 2.7. We have also shown that some discomfort in breathing was experienced by 10 percent of the population of the peak inspiratory pressure exceeded 19.5 cm H_2O (1.95 kN/m^2) (fig. 21.7). If apparatus is tested with a sine wave pump, the peak inspiratory flow approximates to $\pi\times$ minute volume. Under these conditions, therefore, it is suggested that the peak pressure drop across the equipment under test should not exceed $\pi/2.7 \times 19.5 = 22.3$ cm H_2O (2.2 kN/m^2). When using the steady flow method the rate of airflow must be 2.7 times the minute volume.

With either method of testing, the airflow must be appropriate to the upper limit of minute ventilation likely to be encountered in the men wearing the apparatus.

ACKNOWLEDGMENTS

Our thanks are due to M. D. Attfield of Statistics Branch, Institute of Occupational Medicine for his help in the statistical analysis of the results.

REFERENCES

1. Silverman, L.; Lee, R. C.; Lee, G.; Drinker, K. R.; and Carpenter, T. M.: Fundamental Factors in the Design of Respiratory Equipment. Inspiratory Airflow Measurements on Human Subjects with and without Resistance. Office of Scientific Research and Development, 1943, p. 1222.
2. Silverman, L.; Lee, G.; Yancey, A. R.; Amory, L.; Barney, L. J.; and Lee, R. C.: Fundamental Factors in the Design of Respiratory Equipment. A study and an evaluation of inspiratory and expiratory resistances for protective respiratory equipment. Office of Scientific Research and Development. 1945, p. 5339.
3. Cooper, E. A.: Suggested Methods of Testing and Standards of Resistance for Respiratory Protective Devices. J. Appl. Physiol. vol. 15 1960, pp. 1053-1061.
4. Senneck, C. R.: Breathing Apparatus for Use in Mines. In: Design and Use of Respirators, ed. C. N. Davies, Oxford, Pergamon, 1962, pp. 143-159.
5. Wright, B. M.: A Respiratory Anemometer. J. Physiol. vol. 127 1955, 25p.
6. Finney, D. J.: Statistical Method in Biological Assay. London, Charles Griffin, 1964.
7. Cooper, E. A.: Physiological Effects and Suggested Standards of External Respiratory Resistance. National Coal Board, Medical Service Research Report No. 29, 1957.
8. McIlroy, M. B.: Dyspnoea and the Work of Breathing in Diseases of the Heart and Lungs. Progr. Cardiovasc. Dis. vol. 1 1959, pp. 284-297.
9. Bennett, E. D.; Jayson, M. I. V.; Rubenstein, D.; and Campbell, E. J. M.: The Ability of Man to Detect Added Nonelastic Loads to Breathing. Clin. Sci. vol. 23 1962, pp. 155-162.
10. Campbell, E. J. M.; Freedman, S.; Smith, P. S.; and Taylor, M. E.: The Ability of Man to Detect Added Elastic Loads to Breathing. Clin. Sci. vol. 20 1961, pp. 223-231.
11. Cerretelli, P.; Sikand, R. S.; and Farhi, L. E.: Effect of Increased Airway Resistance on Ventilation and Gas Exchange during Exercise. J. Appl. Physiol. vol. 27 1969, pp. 597-600.
12. Freedman, S.; and Campbell, E. J. M.: The Ability of Normal Subjects to Tolerate Added Inspiratory Loads. Resp. Physiol. vol. 10 1970, pp. 213-235.
13. Marshall, R.; Stone, R. W.; and Christie, R. V.: The Relationship of Dyspnoea to Respiratory Effort in Normal Subjects, Mitral Stenosis and Emphysema. Clin. Sci. vol. 13 1954, pp. 625-631.

22 RESPIRATORY PROTECTIVE DEVICE DESIGN USING CONTROL SYSTEM TECHNIQUES

William A. Burgess, Harvard School of Public Health,
and Donald Yankovich, Charles Stark Draper Laboratory
Massachusetts Institute of Technology

INTRODUCTION

In reviewing the history of respiratory protection, one finds that developments up to 1950 resulted in a variety of air-purifying, supplied-atmosphere, and self-contained respiratory protective devices (RPDs). Since 1950, the RPD designs have been relatively static mainly because neither the military nor the commercial designer has had a rational design base available for use. We have explored the feasibility of a control system analysis approach to provide such a design base that will benefit all sectors interested in vigorous RPD design evolution.

A system design approach requires that all functions and components of the system be mathematically identified in a model of the RPD. The mathematical notations must describe the operation of the components as closely as possible. The individual component mathematical descriptions are then combined to describe the complete RPD. Finally, analysis of the mathematical notation by control system theory is used to derive compensating component values that force the system to operate in a stable and predictable manner. As a further step, optimal control theory may be applied to obtain an optimally designed system. This system design procedure permits the designer to work with quantitative values for the system parameters prior to building the system. He can consider simplification, improvement of the system, and cost reduction before prototypes are constructed.

A mathematical description of the RPD is the basis of its system design. From such a system model the designer can calculate those parameters or characteristics for which the model has been developed as a function of the mechanical characteristics of the RPD.

SUBSYSTEMS AND NOMENCLATURE

The first step in the modeling process was to break the RPD into subsystems and then into individual components. RPD system models will be generated by properly combining models of these small subsystems. A nomenclature for systems and subsystems is given in table 22.1.

There are four major subsystems in a RPD system: the mask, the air delivery system, the environmental maintenance system, and the communications system. The mask is a respiratory enclosure that covers at least the nose and mouth or is held in the mouth. It is a mechanical barrier to a hostile environment and includes all parts of the "facepiece" except valves and external air passages. (Internal air passages are considered resistances and are lumped together with port resistance.)

The air delivery system (ADS) is made up of valves, external air passages, and valve control systems. Valve control can be either pneumatic or electronic.

Table 22.1 *Respiratory protective device (RPD).*

Mask	*Air delivery system (ADS)*	*Environmental maintenance system (EMS)*	*Communications*
Seals	Electronic control subsystem (ECS^2)	Environment supply subsystem (ESS^2)	Diaphragm
		Tank	
		Heat exchanger	
Suspension system	Air passage subsystem (APS^2)	Pressure and venting subsystem (PVS^2)	Electronic
		Regulator	
		Pressure supplementary source	
Envelope	Valve control subsystem (VCS^2)	Air reconditioning subsystem (ARS^2)	
	Valves	H_2O removal	
	Control system	CO_2 scrubber	
		Heat exchanger	
Eyepiece		Filters	
Ports			

The environmental maintenance system (EMS) consists of the components that supply air, filter air, or process air. It has four major subsystems: environmental supply, pressure regulating and venting, filtering, and air reconditioning. With the summation of these subsystems as generalized models, any RPD system can be mathematically constructed.

Models of present RPD systems were constructed by drawing mathematical analogies with electrical systems. This required that RPD systems be made up of effects such as resistance, compliance (capacitance), and inertance (inductance). The state variables of these models therefore were gas pressure and flow.

Resistance is a restriction to gas flow and is primarily due to ports, filters, and air passages. Compliance encompasses those characteristics of the RPD system that allow for gas "storage" including RPD component expansion and gas compression. Inertance is directly related to the same characteristics that cause compliance coupled with the effect of mass. As the system expands or the gas compresses there is an increase in internal pressure that tends to maintain gas flow should a change in flow direction be attempted, hence the analogy to electrical inductance.

Diodes, pressure sources, and flow sources are added to complete the list of component analogies used to model the RPD. Diodes allow flow in only one direction and are primarily used to model the nonlinear behavior of valves, regulators, and seals. Pressure sources are direct analogies to voltage sources and have the property of supplying a constant pressure across any impedance to current flow. Flow sources supply a constant flow through any impedance.

RESISTANCE (R)

The apparatus described in figure 22.1 was used to measure resistance with a unidirectional blower for the flow source and Q_{out} removed. Tests for R were conducted for both inhalation and exhalation. For inhalation tests the exhalation ports were sealed and visa versa. Pressure in the mask was measured with a static probe mounted on the middle of the mannequin forehead for flows of up to 3 liters/sec. Resistance is defined as

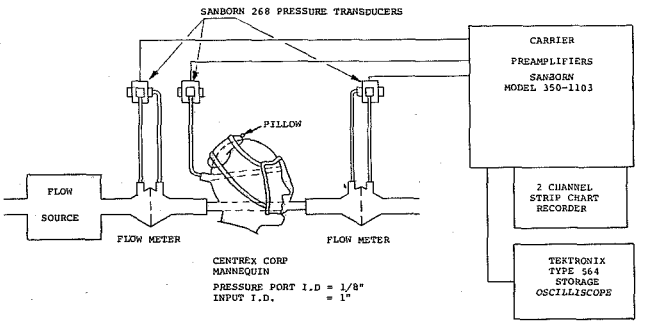

Figure 22.1 *Test apparatus used to obtain RPD parameters.*

$$R = \frac{dP}{dQ_{in}} \qquad [\text{cm } H_2O/(\text{liters/sec})]$$

CAPACITANCE (C)

For the capacitance measurements both flow meters in figure 22.1 were removed and all valves and ports were sealed except for two ports. One port was used to monitor pressure in the mask and the other was connected to a 5 cc syringe. The syringe was used to provide both negative and positive changes in volume by 1 cc increments (dV), and the pressure change (dP) was monitored. The capacitance can be found from

$$C = \frac{dV}{dP} \qquad [\text{cm}^3/\text{cmH}_2O]$$

If the mask were rigid, the pressure change would be equal to

$$dP = \left(\frac{dV}{\text{volume of mask}}\right) \qquad (\text{Pressure absolute}) = \frac{1\text{cm}^3 \times 1033.6\ \text{cmH}_2O}{\text{volume of mask}}$$

If the mask was not rigid, then the pressure change would not be as great and the value of capacity would be greater. Actual measurements on masks gave values six times greater than that calculated for a rigid mask.

INERTANCE (I)

A method for obtaining I is to use an oscilloscope to observe the pattern formed by driving the X axis with the pressure transducer connected to the static pressure tap at the input to the mannequin and the Y axis with the pressure transducer connected to the static pressure tap at the forehead of the mannequin. The resonating frequency (the frequency at which the mask was vibrating with its maximum excursion) occurs when the pressure at the input of the mannequin is 90° out of phase with the pressure inside the mask.

Knowing the lowest resonant frequency allows one to calculate the value of I from the relationship

$$\omega = 2\pi f = \frac{1}{\sqrt{IC/1000}} \quad \text{or} \quad I = \frac{1}{4\pi^2 f^2 C/1000}$$

if damping is ignored.

When the first attempt was made to measure the resonant frequency in this manner, several extraneous resonant frequencies were found near the resonant frequency of the mask. To isolate the undesirable resonances, the mask was damped with weights. Now the low resonances were located and by shortening up various pieces of connecting tubing, they were eliminated or shifted to higher frequencies away from the mask resonance.

Resonant frequencies were found with the valves removed and ports open. In all cases they were at relatively high frequencies that indicated extremely low values of I. Then the ports were sealed and much lower resonant frequencies resulted. The ports were then unsealed and with the valves in place the same low resonant frequency occurred as with the ports sealed. The actual frequency depended somewhat on the level of pressure in the mask. The frequency increased at lower pressure levels towards the slightly higher values found with the mask sealed up, as might be expected. All testing was done with dry exhalation valves. The value of I used for the model was that determined with the valves in place.

MASK MODEL

Since there are pressure gradients throughout the mask void, the mask can be modeled by a distributed parameter system. Since in most applications the various pressure gradients throughout a mask are small, mask pressure can be assumed uniform throughout the mask void and the mask model reduces to the lumped parameter system of figure 22.2

Also, if the inhalation and exhalation ports are not sealed the port resistance is shorted to the return and the resulting system is governed by a second order equation.

Two first order equations thus describe the mask pressure-flow relationships

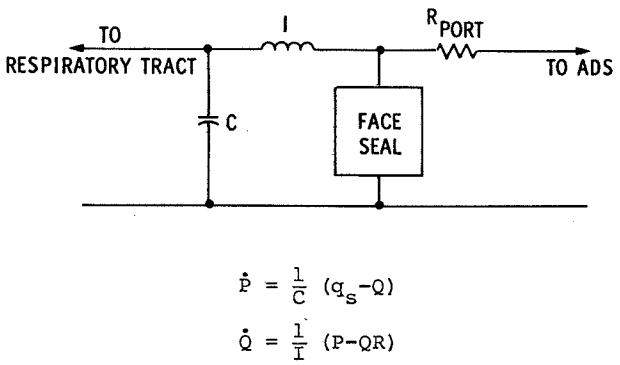

Figure 22.2 *Mask model showing facial seal model location.*

$$\dot{P} = \frac{1}{C}(q_s - Q)$$

$$\dot{Q} = \frac{1}{I}(P - QR)$$

CONTAMINANT LEAKAGE

Modeling of the mask must include the seal, which is the interface between the user's face and the respirator system. Inevitably, seals are subject to leakage between the controlled atmosphere within the respirator and the outside contaminated environment. The magnitude of this leakage is acceptably small at normal mask operating conditions; however, if mask pressure relative to ambient becomes sufficiently large, the mask seal will separate from the user's face, allowing much greater leakage to occur. Similarly, at sufficiently low mask pressure relative to ambient, the face seal will tend to buckle, also resulting in large amounts of leakage.

An electrical system exhibiting these properties is shown in figure 22.3. The linear resistors R_{ℓ_1} and R_{ℓ_2} represent seal leakage under normal mask operating conditions; for positive mask pressures (exhalation), diode D_2 is open, allowing a flow out of the mask whose magnitude is dependent on the value of R_{ℓ_2}, while for negative mask pressures (inhalation) diode D_1 is open, and the amount of leakage into the mask depends on the value of R_{ℓ_2}. The pressure source P_{ℓ_e} represents the positive mask pressure at which the seal will break away from the user's face; if this pressure is exceeded, diode D_4 opens, and there is additional flow out of the mask through R_{ℓ_4}. In a similar manner, if the mask pressure drops below $-P_{\ell_i}$, representing the pressure level at which the mask seal will buckle, diode D_3 opens, and flow is allowed into the mask through R_{ℓ_3}.

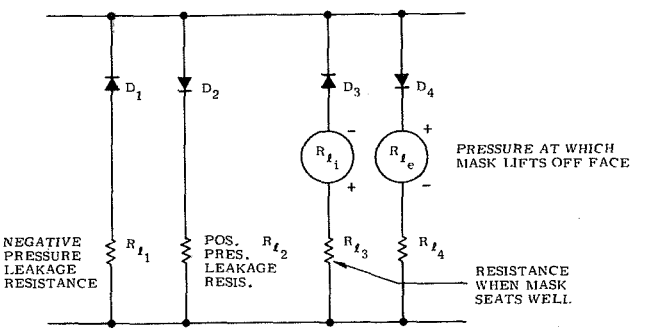

Figure 22.3 *Facial seal model.*

The block labeled "PORTS" in figure 22.3 contains linear resistors to represent the openings in the mask that house inhalation and exhalation valves. For simplicity, resistance to flow due to any air passages within the mask is lumped together with the port resistance.

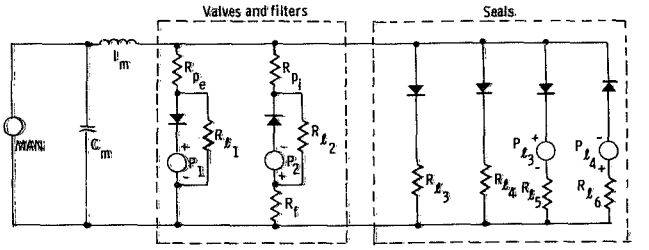

Figure 22.4 *Model of filter-type RPD.*

SYSTEMS

Air Delivery System (ADS)

Electronic Control Subsystem (ECS²). Any electronic control can be modeled mathematically, where the output equals f (input, t). If the ECS² is linear, a transfer function can be used.

Air Passage Subsystem (APS²). Air passages have their analogy in transmission lines, with distributed parameters of the resistance, inertance and compliance. In most cases, inertance and compliance will be negligible.

Valve Control Subsystem (VCS²). Valves are modeled as resistances. Simple valves such as flap-type valves are modeled as in figure 22.4 where R_L is leakage resistance, R_P is port resistance, and P is pressure at which valve opens. Valve control is described with transfer functions, as is the ECS².

Environmental Maintenance System

Environment Supply Subsystem (ES^3). The model of a supply cylinder used here is a pressure source. A breathing bag is normally at 1 atm when partially full and is modeled as a 1 atm pressure source in that state. When empty it has no effect and when full it has the characteristics of a charged parallel compliance and inertance. A heat exchanger is modeled as a resistance.

Pressure and Venting Subsystem (PVS^2). A demand regulator is modeled as a biased diode, where the value of bias is equal to the opening pressure of the demand valve. It is returned to ground, but is understood to be a supply of "good" air. A constant pressure regulator is modeled as a zener diode. Blower systems are referred to as supplementary pressure sources and are modeled as such.

Air Reconditioning Subsystem (ARS^2). Water removal, carbon dioxide scrubber, filters, and heat exchanger are modeled as resistances unless they are active components. If these are flexible components or very large, compliance or inertance or both must be included.

As an example of the modeling process, an air-purifying RPD is shown in figure 22.4. For this system the ADS consisted only of valves and the EMS consisted only of a filter (R_1). Since the capacitance of the filter was very small it was not included in the model, nor was the operating time of the valves.

Using electrical circuit analysis simplifications, the model diagram reduces to a simple three-component system with a single compliance, inertance, and resistance. In addition there are a number of valve activating pressures specified that merely change the value of resistance, R_{eq}, when valves open and close or seal resistance changes. The two state variables for a filter type system are Q_I and P. System state equations are

$$\dot{P} = \frac{q_s - Q_I}{C}$$

$$\dot{Q}_I = \frac{P - R_{eq} Q_I}{I}$$

Diode states are determined by the pressure (P_R) across the valves calculated from the equation $\dot{P}_R = \dot{Q}_I R_{eq}$. This equation was written in differential rather than algebraic form to acknowledge the physical fact that the opening or closing of valves, which are modeled as step changes in R, can cause instantaneous changes in the rate of change of P_R, but not in P_R itself. These differential equations were integrated in a digital computer using a fourth-order Runge-Kutta integration algorithm. Parameters for several different types of mask models were measured as previously discussed and are given in table 22.2.

To check the validity of the modeling, the physical system and the computer model must be driven with similar input functions and their outputs compared.

Table 22.2 *Values of model components as determined for four RPDs.*

Mask \ Units	Resistance Q = 1 liter/sec Inhalation [cm H_2O/(liters/sec)]	Resistance Q = 1 liter/sec Exhalation [cm H_2O/(liters/sec)]	Capacitance cm^3/cmH_2O	Inertance cm H_2O sec^2/liter
A	3	1.2	4	0.039
B	4.4	1.85	0.76	–
C	1.5	1.50	2.1	0.00984
D	2.9	0.85	3.3	–

The test function used was generated by a human subject breathing into the test mannequin through a flowmeter. The breathing flow and the pressure in the mask were recorded on a strip chart recorder. These curves were modeled mathematically as piecewise-linear functions with enough data points to insure that the important characteristics of the functions were preserved. The flow curve was then used as the driving function for the computer model.

The important quantity in the evaluation of the dynamic performance of a respiratory protective device is the mask pressure, which is represented here by P_R, the pressure drop across the valves and filters. Therefore, the model performance criterion chosen was (P_{EXP}-P_R,) where P_{EXP} is mask pressure measured while the subject was breathing.

The graphs in figures 22.5, 22.6, 22.7, and 22.8 depict the driving function, the experimentally determined pressure, the pressure of the simulated model, and the relative error, respectively. As can be seen, the general shape of the two pressure curves is quite similar. The error curve shows roughly 10 percent disagreement. The large peaks in the error curve are associated with errors in

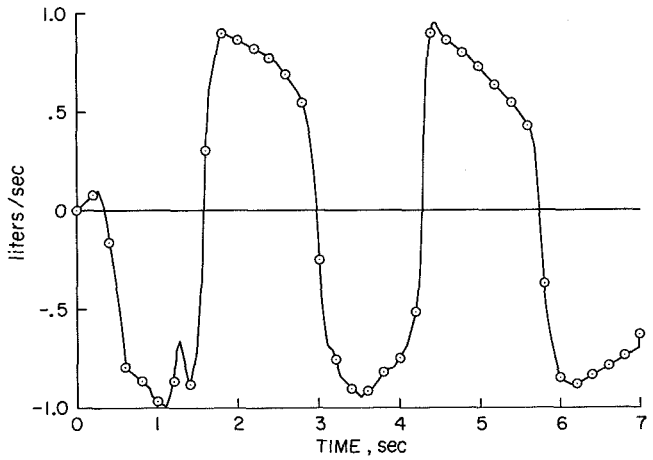

Figure 22.5 *Breathing flow pattern driving both test RPD and computer simulation.*

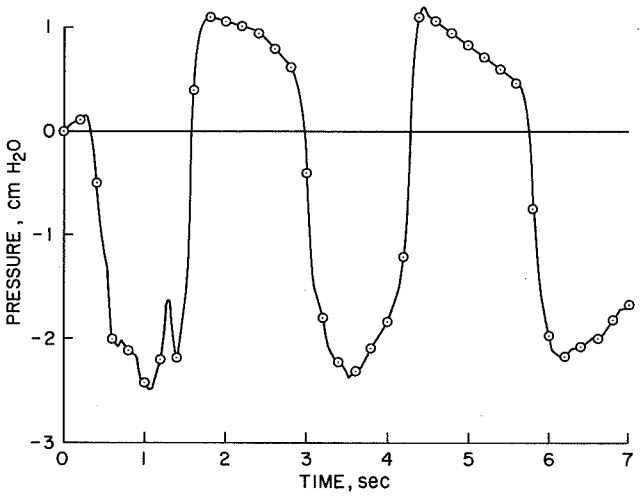

Figure 22.6 *Mask pressure as measured for Army M-17 system with driving function of figure 22.5.*

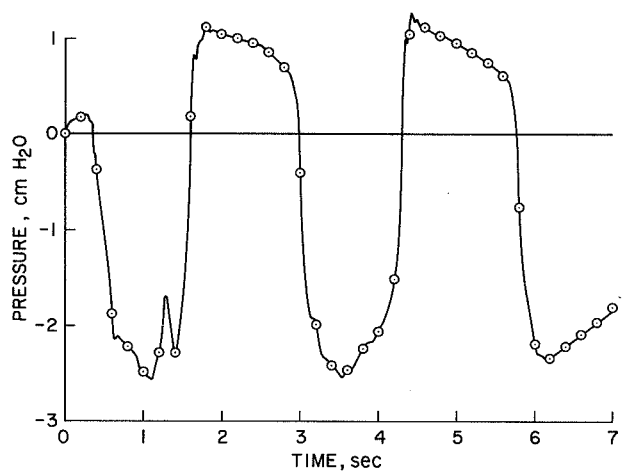

Figure 22.7 *Mask pressure as calculated from computer simulation of Army M-17 with driving function of figure 22.5.*

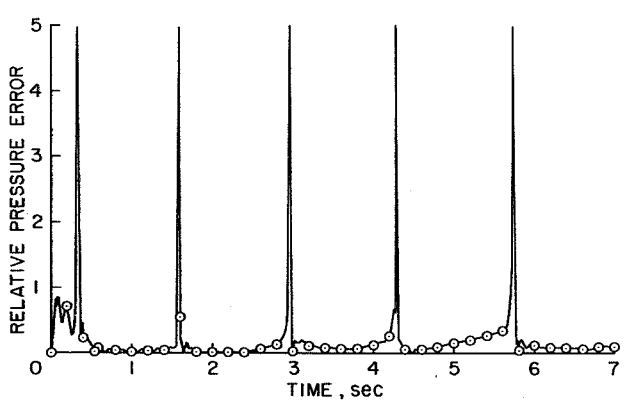

Figure 22.8 *Relative error ($P_{MEAS} - P_{CAL}$) of computer simulation of Army M-17 RPD.*

reading time visually from the strip chart in regions of large slope. The fact that there are no regions of higher disagreement seems to indicate that the error in the physical measurements of I, C, and R are a substantial part of the error, as is the error due to transferring data from the strip chart recording.

Values of sensitivity to errors in parameter measurements for R, C, and I during both inhalation and exhalation are shown in figures 22.9 through 22.14. The quantities graphed are the magnitude of the expressions $Y(s)$ of the form

$$\frac{\partial P(s)}{\partial x} = Y(s)P(s)$$

where $P(s)$ is the transform of pressure and x is the pertinent parameter. Percentage changes in pressure due to given percentage changes in x are

$$\left|\frac{\Delta P(s)}{P(s)}\right| = x\left|Y(s)\right|\left|\frac{\Delta x}{x}\right|$$

Peak sensitivities are given on each graph.

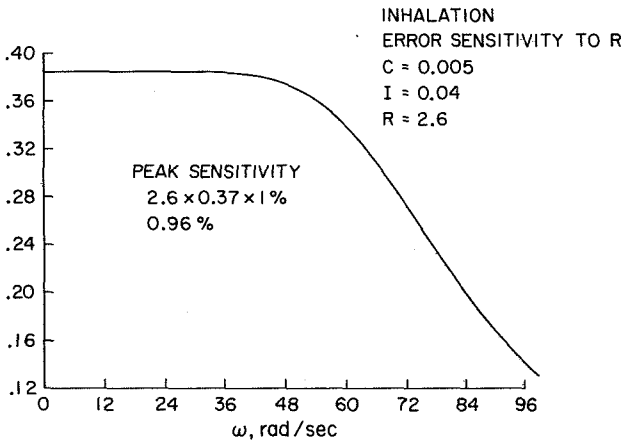

Figure 22.9 *Sensitivity of Army M-17 simulation to R during inhalation.*

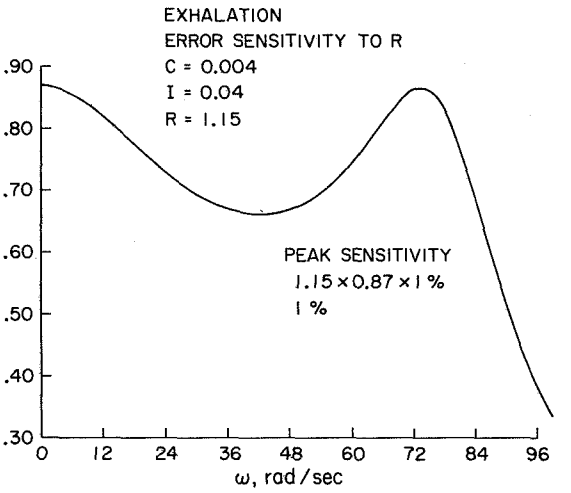

Figure 22.10 *Sensitivity of Army M-17 simulation to R during exhalation.*

Much has been learned about the problems of physical measurements of RPDs and refinements will certainly reduce present errors. Also, much improvement in data handling, such as the use of an A to D converter directly to tape for computer use, will be a much more accurate way of evaluating the model. Furthermore, more data will indicate statistically the range over which the models are valid. Completion of this work should provide the RPD Engineer with a valuable analytical engineering tool.

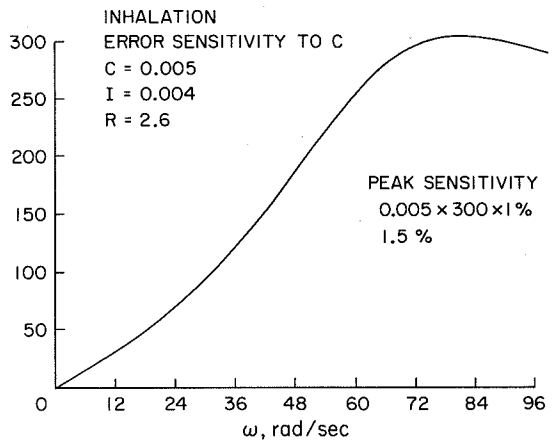

Figure 22.11 *Sensitivity of Army M-17 simulation to C during inhalation.*

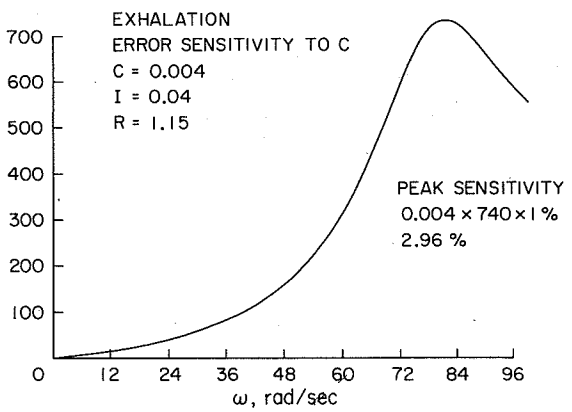

Figure 22.12 *Sensitivity of Army M-17 simulation to C during exhalation.*

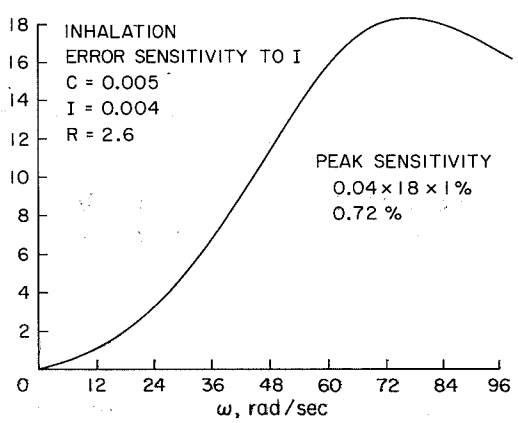

Figure 22.13 *Sensitivity of Army M-17 simulation to I during inhalation.*

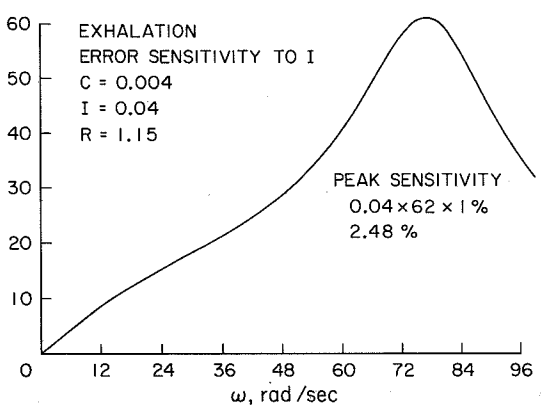

Figure 22.14 *Sensitivity of Army M-17 simulation to I during exhalation.*

23

BREATHING METABOLIC SIMULATOR

R. G. Bartlett, C. M. Hendricks, and W. B. Morison
Federal Systems Division
International Business Machines Corporation
Gaithersburg, Md.

INTRODUCTION

The NASA Office of Advanced Research and Technology and the Bureau of Mines have jointly funded the development of a breathing metabolic simulator (BMS) under contract NASW-2032. This BMS simulates all of the breathing and metabolic parameters required for complete evaluation and test of life support and resuscitation equipment. It is also useful for calibrating and validating mechanical and gaseous pulmonary function test procedures. Breathing rate, breathing depth, breath velocity contour, oxygen uptake, and carbon dioxide release are all variable over wide ranges simulating conditions from sleep to hard work with respiratory exchange ratios (R) covering the range from hypoventiliation to hyperventilation. In addition, all of these parameters are remotely controllable to facilitate use of the device in hostile or remote environments. The exhaled breath is also maintained at body temperature and a high humidity. The simulation is accurate to the extent of having a variable functional residual capacity (FRC) independent of other parameters.

SIMULATION DESIGN CONSIDERATIONS

The following breathing characteristics were considered in implementing the BMS design.

Breathing Rate

The breathing rate adjustment provided by the BMS covers the rates that occur in the human, ranging from rest to hard work conditions, Although this wide range is available, most subjects would fall into a much narrower range.

Breathing Depth

The breathing depth adjustment provided by the BMS covers a wide range up to 3 liters/breath. Although an individual breath may exceed 3 liters under some conditions, the depth under continuous hard exercise should not exceed simulator capacity. Individual breath (tidal volume) is normally on the order of 0.5-0.6 liter under rest conditions, and it increases with activity. The minimum simulator capacity includes this normal rest capacity. Selection of the appropriate combination of breathing rate and depth will allow the simulation of a wide range of breathing activity.

For special applications the breathing depth can be made greater than 3 liters. It can be made to simulate a full vital capacity (e.g., 6 liters).

Velocity-Time Waveform

The breath velocity pattern in the human is not generally represented by a true sinewave. It may vary from a slightly blunted sinewave under some conditions to a drastic variation under conditions

encountered during forced exhalation. To provide a faithful simulation, a waveform control is provided, allowing a wide range of variations from a basic sinewave.

Functional Residual Capacity

The FRC is the volume of air remaining in the lungs at the end of normal exhalation. To obtain faithful simulation, the FRC must remain constant for breathing rate or depth changes or both. It is also necessary to have the FRC variable so that individuals with different FRCs can be simulated. Both of the conditions are provided by the BMS.

Exhaled Breath Temperature and Humidity

In the human the exhaled breath is at body temperature and, except for conditions of extremely hard breathing, is at 100 percent relative humidity. Both of these conditions are provided by the BMS.

Oxygen Consumption

The simulation of the metabolic range between sleep and medium hard work requires a variable oxygen consumption rate. The range of the adjustable consumption rate of the BMS includes these conditions. For special applications the BMS can be made to simulate maximum oxygen consumption rates for the human undergoing maximum physical work.

Carbon Dioxide Production

The amount of carbon dioxide produced in the human is related to the amount of oxygen consumed. This ratio os 0.707 if the fuel is fat and is 1.0 if the fuel is carbohydrates. This ratio, when referenced to tissue metabolic activity, is referred to as the respiratory quotient (RQ). When referenced to the ratio of gases in the exhaled breath (as in the BMS), it is referred to as the respiratory exchange ratio (R). (This differentiation is made because an individual may be underbreathing or overbreathing, markedly affecting the amount of carbon dioxide removed from the body and thus the value of R.) To simulate these conditions, the BMS provides a range of carbon dioxide/oxygen (R) wider than the normal range of 0.7 to 1.0.

HARDWARE FUNCTIONAL DESCRIPTION

The BMS has been implemented in a configuration that may be described as consisting of three subsystems: temperature/humidity, breathing, and metabolism. These subsystems are shown in the simplified system schematic (fig. 23.1) and are then described individually. Performance specifications are shown in table 23.1.

Temperature/Humidity Subsystem (fig. 23.2)

Functions. Incoming air from the artificial trachea is fed into an exchange box, where it is blocked from entering the humidity chamber by a check valve. The air then passes through another check valve and enters the main connection to the top of the bellows during bellows expansion.

Outgoing (exhaled) air comes from the main connection to the top of the bellows during bellows contraction. The air passes through a check valve and enters the input end of the humidity chamber. The air entering the chamber displaces air from the output end of the chamber through a check valve, where it enters the exchange box and exits to the artificial trachea.

Features. The check valves and exchange box are used to control air flow direction and to permit a single connection to the artificial trachea.

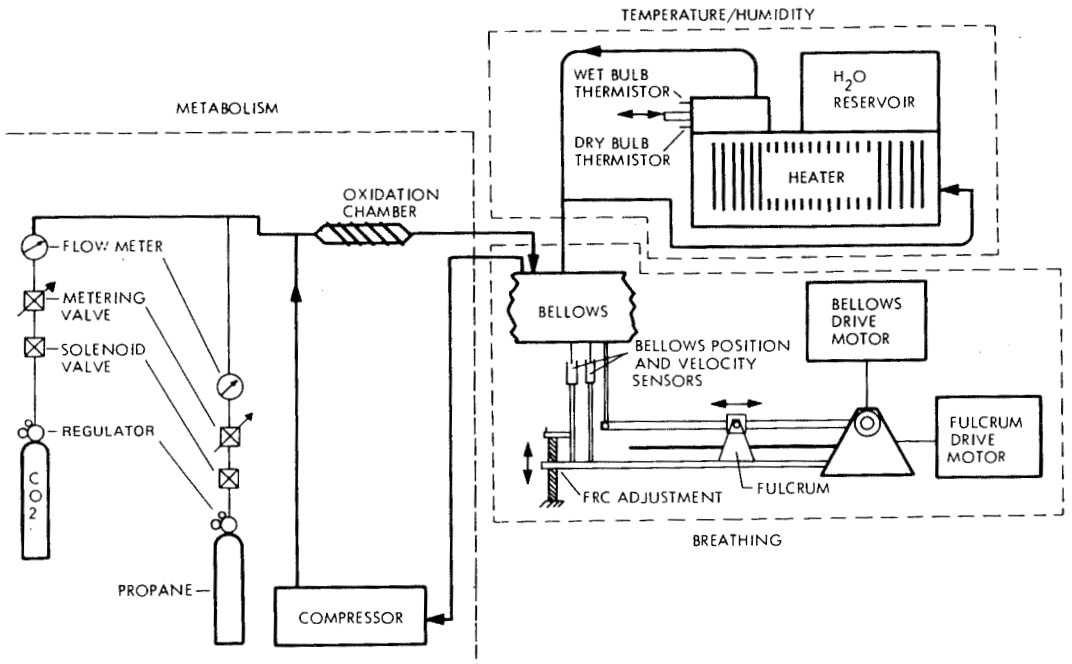

Figure 23.1 *Simplified system schematic.*

Table 23.1 *Performance specifications.*

Breathing Simulation Subsystem	
Rate adjustment	5-60 breaths/minute
Depth adjustment	400-3000 ml/breath (up to 6000 ml for special applications
FRC adjustment	1.7 - 4.0 liters, constant with rate, depth and waveform changes
Velocity-time waveform	Variable, from sinewave to other shapes as obtained via 12 separately controllable velocity regions within a breath cycle
Humidity/Temperature Subsystem	
Humidity	Gas exhaled with a humidity between 96 percent and 100 percent through medium high volumes, to 90 percent for extreme high volumes
Temperature	Gas exhaled with a temperature controlled to 98.6° F within ± 2° F for all volumes
Metabolic Simulation Subsystem	
O_2 consumption rate	Adjustable within the range of 250 to 2000 ml/min (up to 3000 ml/min for special applications)
CO_2 production rate	Adjustable within a range to produce a respiratory exchange ratio of 0.6 to 1.5.

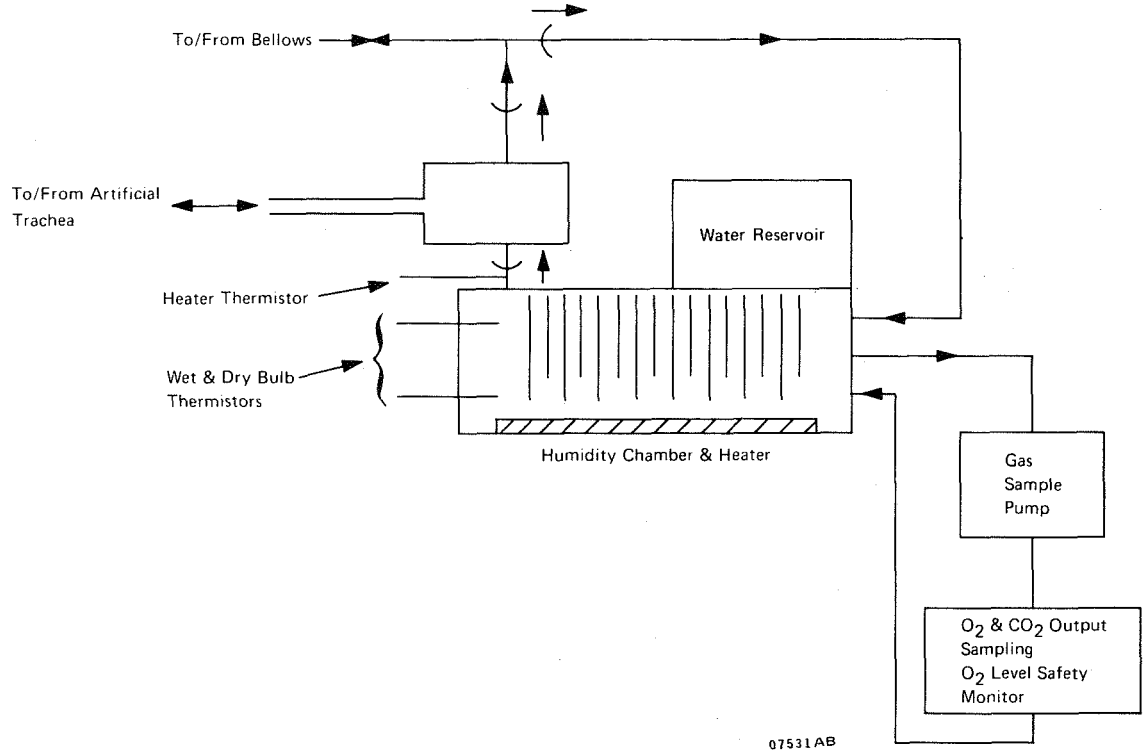

Figure 23.2 *Temperature/humidity subsystem.*

The humidity chamber is used to add moisture to the exhaled air and to maintain temperature within specified limits. The moisture transfer media (surgical sponges) remain saturated with water from a separate reservoir. (Actual humidity is also affected by the dwell time of a breath inside the chamber.) Temperature maintenance, accomplished by a heater blanket in the bottom of the chamber, is controlled by a thermistor placed in the path of the chamber output. Heater power is remotely controlled by the appropriately labeled switch on the control unit.

This subsystem also contains sensors for monitoring the characteristics of the air to be exhaled. Wet- and dry-bulb thermistors placed in the output end of the chamber can be monitored by positions 5 and 4, respectively, of the control unit digital voltmeter. A gas sample line connected to the chamber input end allows a sample pump, operating when the carbon dioxide analyzer is on, to extract gas samples, that are fed to the sensors of an oxygen analyzer and a carbon dioxide analyzer and returned to the chamber. The readout of these analyzers is accomplished on the control unit. (These analyzers can be calibrated from separate gas inputs, as described in detail in the operations manual.)

Breathing Subsystem (Fig. 23.3)

Functions. This subsystem controls expansion and contraction of a bellows to draw air from and expel air to the temperature/humidity subsystem. The bellows motion is independently variable in rate, magnitude of periodic motion and volume remaining at point of minimum periodic volume change. The periodic motion of the bellows is accomplished by a bellows drive motor operating a crankshaft/connecting rod combination through a 30:1 gear reduction. The drive motor speed is

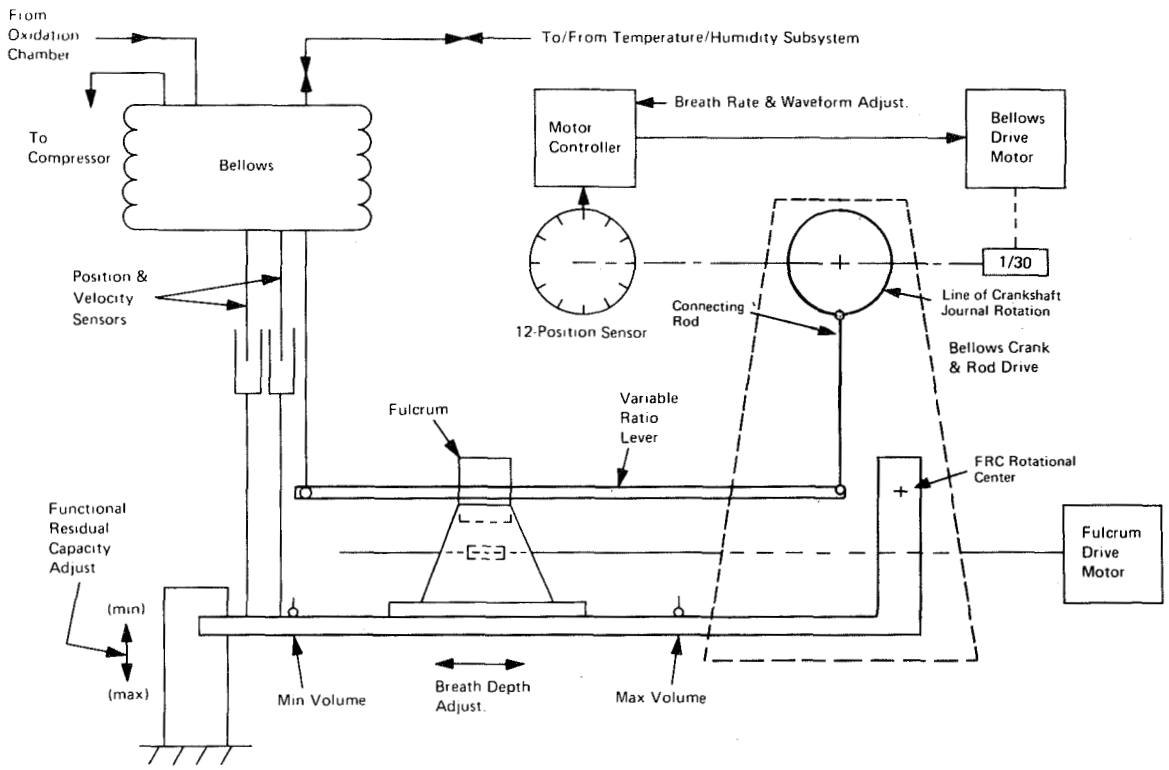

Figure 23.3 *Breathing system.*

varied by means of a motor controller. Long-term variations, greater than one crankshaft revolution, correspond to changes in breathing rate and are varied from the control unit by means of the labeled control. Short-term variations, within one crankshaft revolution, correspond to changes in breath waveform and are varied by the individual settings of 12 waveform controls on the control unit. Each control is effective during one-twelfth of a crankshaft revolution as determined by a 12-position read switch.

Connecting rod motion is transmitted to the bellows by means of a lever arm operating on a movable fulcrum. Fulcrum motion along the lever arm varies the level arm ratio corresponding to changes in breath depth. This motion is accomplished by means of a lead screw from the fulcrum drive motor, which is in turn controlled by the bidirectional fulcrum switch on the control unit. Fulcrum driving toward minimum and maximum volume per breath is indicated on the control unit by the right and left limit lights illuminating, respectively. (The lights will extinguish if a limit is encountered while driving.) Fulcrum motion normal to the lever arm (i.e., moving the position of the bottom of the bellows for a fixed crank position and lever arm ratio) will change the minimum bellows volume obtainable through periodic motion. This corresponds to a functional residual capacity adjustment and is controlled by a manual screw adjustment on the support for the fulcrum base. This adjustment has a scale calibrated in FRC volume in liters adjacent to the screw.

Features. The top of the bellows contains two separate gas lines to provide an output to the compressor of the metabolism subsystem and to receive the output of this subsystem.

Two separate magnetic flux type sensors are mounted between the bottom of the bellows and the adjustable support for the fulcrum base. These sensors measure position and velocity between

mountings (thus sensing breath characteristics independent of FRC adjustment) and are input to the oscilloscope in the control unit, where either may be selected for waveform display.

Metabolism Subsystem (fig. 23.4)

Functions. This subsystem is used to control R. Since R is a carbon dioxide to oxygen ratio, metabolism is simulated by consuming oxygen and producing carbon dioxide. This is accomplished by oxidizing propane and adding varying amounts of carbon dioxide in the following manner.

Air is drawn from the top of the bellows by a compressor. The compressed air output is then fed to an accumulator used to eliminate surging caused by bellows motion. The accumulator output is connected to an adjustable orifice used to preset the flow rate for more than sufficient air for all oxidation conditions; the accumulator is then connected to a gas line input to the oxidation chamber. A size D tank of CP grade propane is fitted with a manual regulator (set to 15 psi). The regulator output is connected to a solenoid shutoff valve controlled by the manual switch on the control unit (and the series safety circuitry, discussed later). The solenoid valve output is connected to a remotely adjustable metering valve (controlled by valve enable and carbon dioxide adjustment on the control unit). The metering valve output is connected to a flow meter sensor (the flow meter is located on the control unit panel) and finally to the oxidation chamber input line. A size D carbon dioxide tank is fitted with a duplicate of the propane controls (except safety circuit not required) and also connected to the oxidation chamber input line.

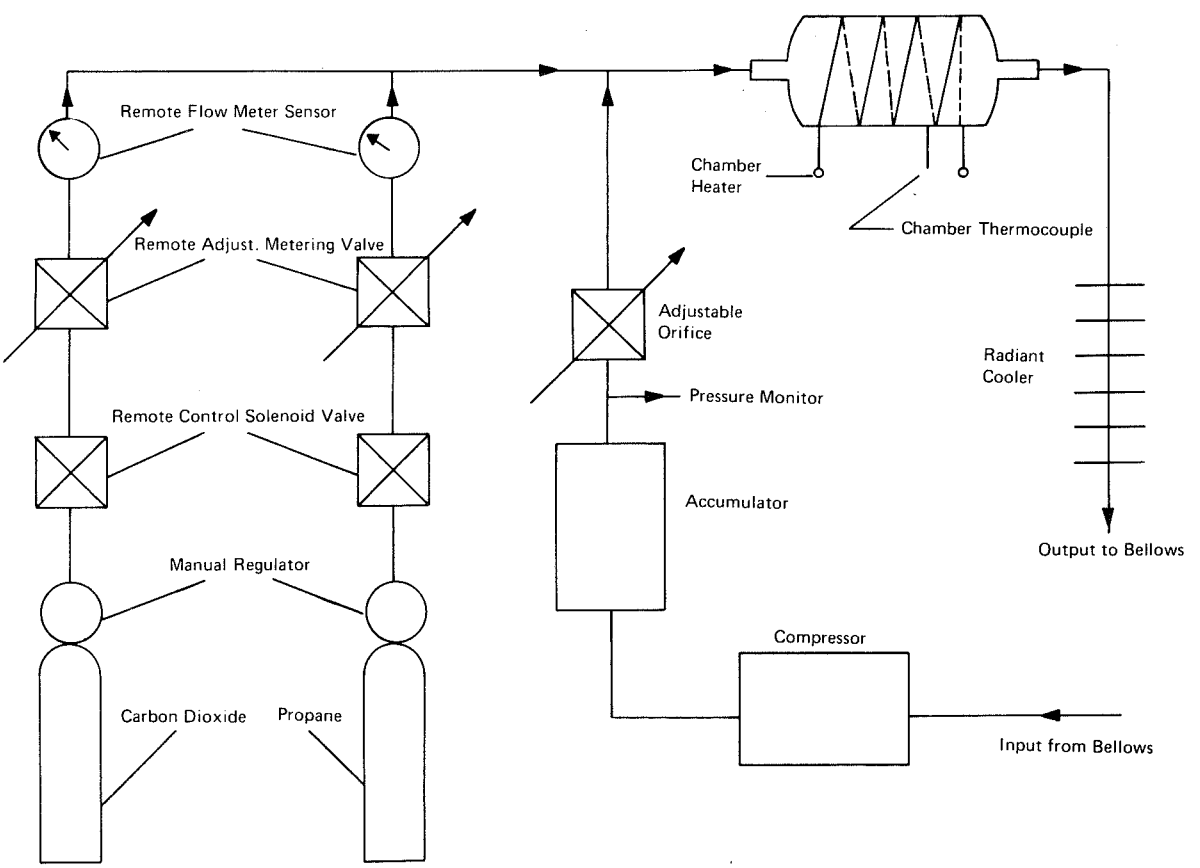

Figure 23.4 *Metabolism subsystem.*

The oxidation chamber is an expanded line area (made of quartz) containing a probe input for a chamber thermocouple and surrounded by an encased insulated heating element. Power to the heater is manually controlled (ON/OFF only) from the control panel combustion heater switch and maintains the chambers temperature above that required for oxidation of propane. In operation, complete oxidation occurs with the chamber output having a carbon dioxide/oxygen ratio that is variable, dependent upon the carbon dioxide and propane flow rates into the chamber (air input is a constant). The chamber output is fed to a radiant series cooler to reduce temperature to a safe level and then is returned to the top of the bellows.

Features. A safety circuit (fig. 23.5) used to control propane flow will not allow the solenoid valve to be opened unless the proper oxidation conditions exist. The conditions monitored are the oxygen output level in the temperature/humidity subsystem, the compressor output pressure at the accumulator, and the chamber temperature at the output end.

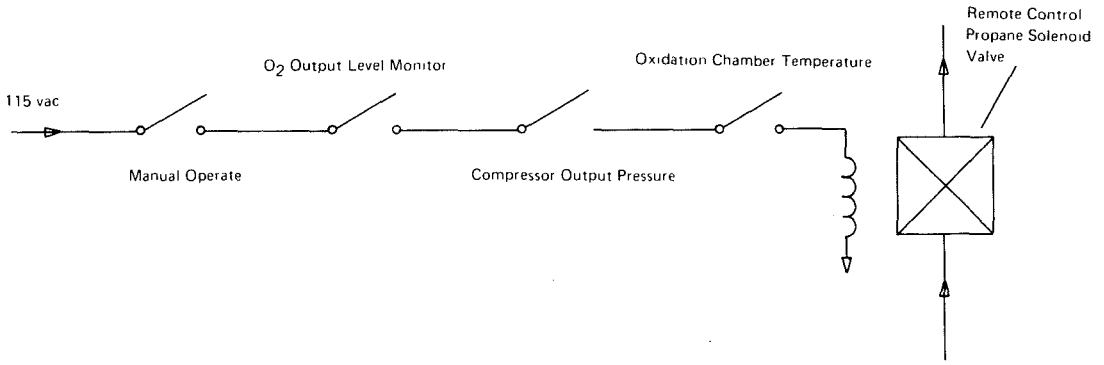

Figure 23.5 *Propane safety control circuit.*

The chamber thermocouple output can be monitored (position 3 of the digital voltmeter) to determine temperature during preheating or other conditions as desired. Installation considerations are shown in table 23.2. Figures 23.6 and 23.7 are photographs of the device delivered under contract funded by NASA.

Table 23.2 *Installation considerations.*

Physical Characteristics		
Control unit	Size	60 in. H X 20 3/8 in. W X 19-7/8 in. D (including castered support cart)
	Weight approximately 200 lb	
Simulator unit	Size	59 in. H X 18 in. W X 25-1/2 in. D
	Weight approximately 250 lb	
Interconnection		
Electrical cables	4, with disconnects	
No other interconnections required.	Length - 8 ft	

Table 23.2 *Installation considerations. (Concluded)*

Electrical Input Characteristics

Voltage	115 vac (60 cy) single phase, with ground
Current	Control unit input cable - less than 20 A Simulator unit input cable - less than 20 A

Safety Consideration

Contains combustible gas and, for safety, should be used only in a well ventilated area.

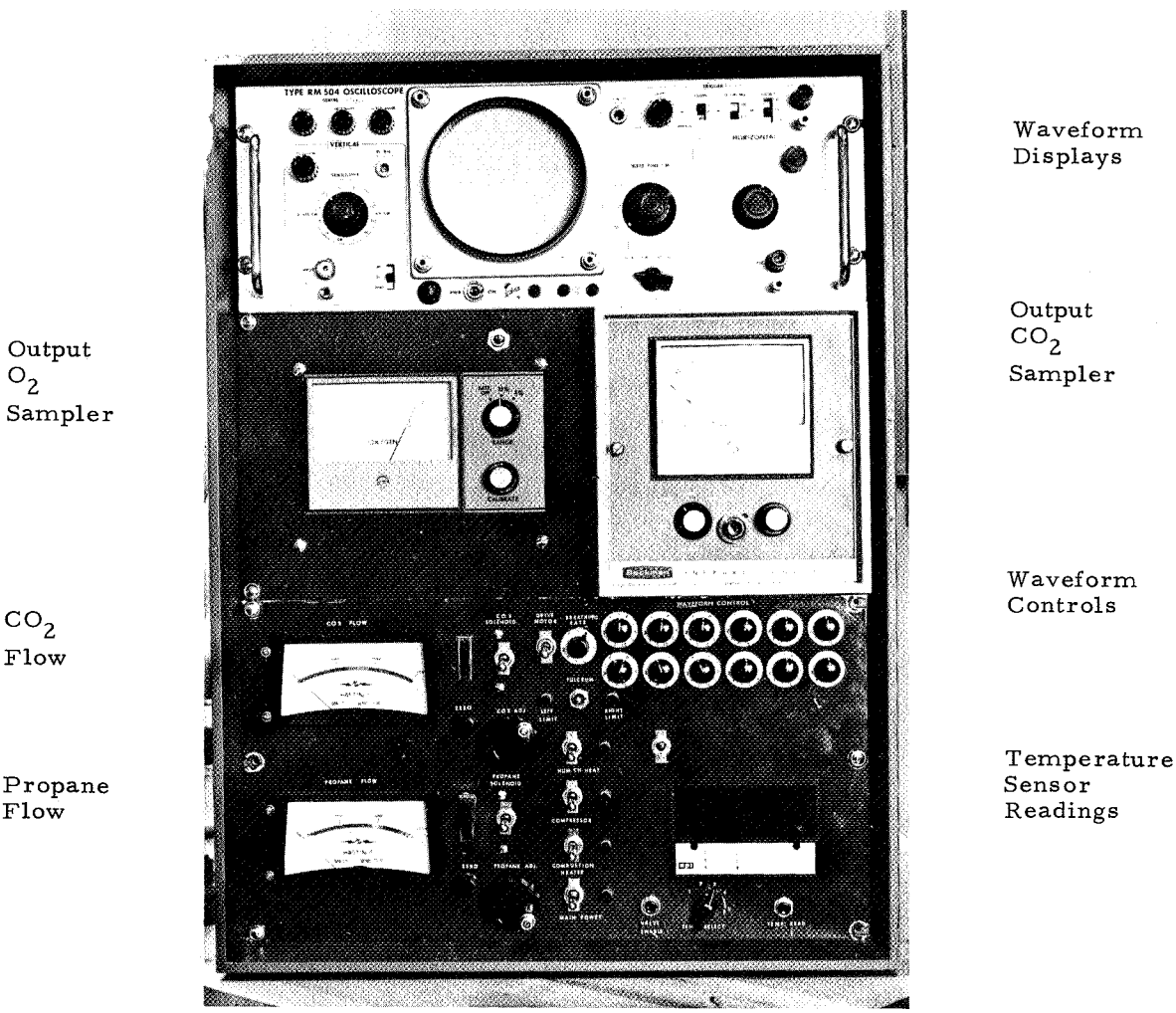

Figure 23.6 *Control unit functions.*

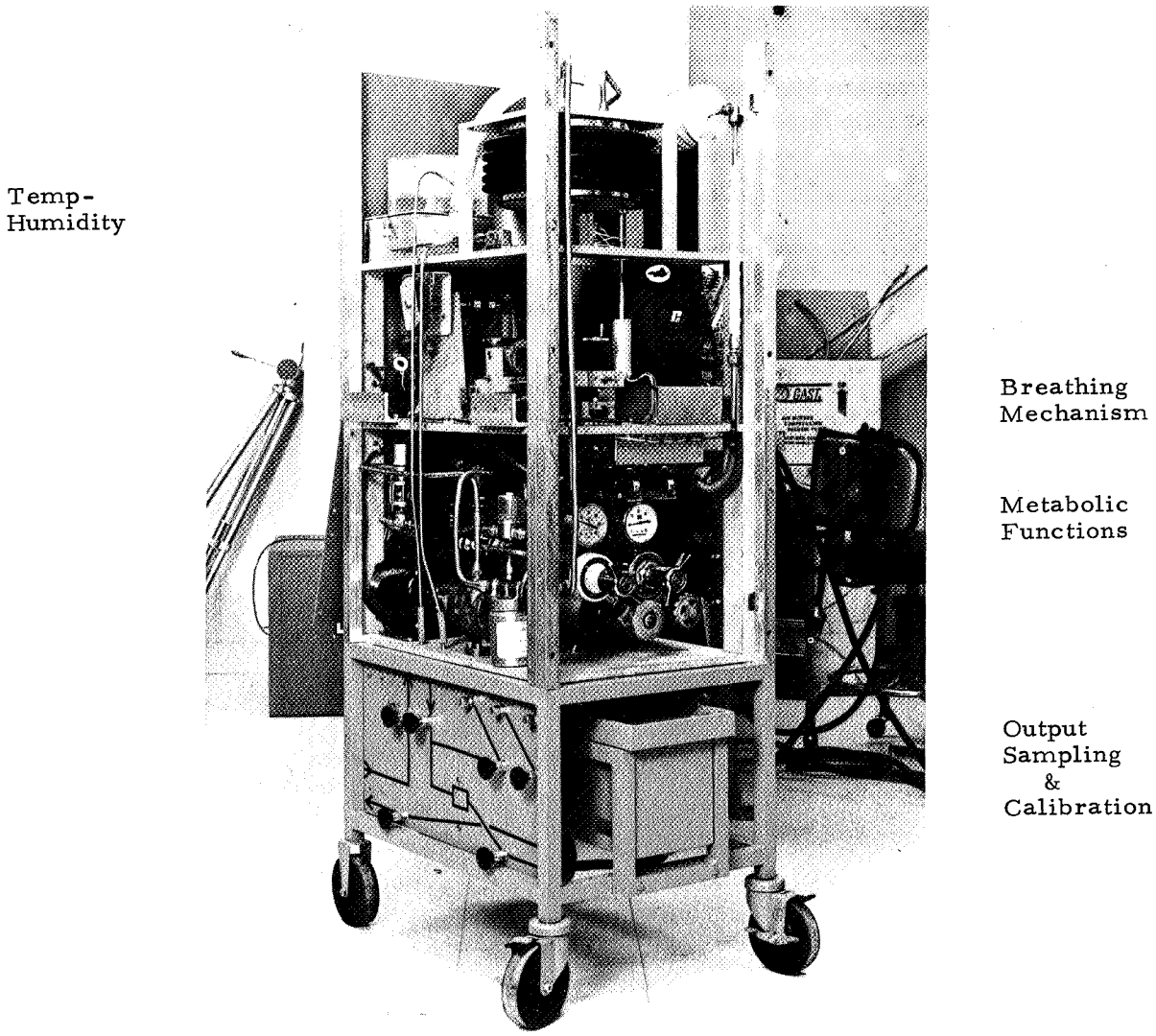

Figure 23.7 *Simulator unit functions.*

The following expendables are required for operation:

Carbon dioxide	Air products size D tank (4 by 17 in.)
Propane (CP)	Air products size D tank (4 by 18 in.)
Distilled water	Reservoir capacity approximately 2.33 quarts
Surgical sponge	Parke-Davis gauze 4 by 8 in. approximately (one package of 100 required for replacement)

BIBLIOGRAPHY

1. Anon.: First Quarterly Progress Report BMS, April 27, 1970 to July 27, 1970 (IBM No. 70-A95-0001)

2. Anon.: Second Quarterly Progress Report BMS, July 27, 1970 to October 27, 1970 (IBM No. 70-A95-0001)
3. Anon.: BMS Operations Manual, April 1971
4. Anon.: BMS Test Data Report, June 1971

24 INFLUENCE OF FACEMASK DESIGN ON OPERATIONAL PERFORMANCE

O. G. Griffin and D. J. Longson
Safety in Mines Research Establishment,
Department of Trade and Industry, Sheffield, England

FACEMASK LEAKAGE

The increasing use of full facemasks with respiratory apparatus emphasizes the need for accurate methods of evaluating facemask efficiency. All facemasks leak to some extent; the leakage is past the peripheral seal and is governed by the fit of the mask, which can be adversely affected by facial hair and movement of the head and facial muscles.

Inward Leakage

Recent methods of evaluating facemask efficiency employ either an aerosol or a halogenated hydrocarbon gas in the atmosphere surrounding the mask. The aerosol methods, which include the use of sodium chloride (refs. 1 and 2), uranine (ref. 3), and bacterial spores (refs. 4 and 5), are not, in general, considered suitable for the rapid determination of inward leakage of gas into a full facemask. The sodium chloride aerosol method in particular suffers from the disadvantage that particles are absorbed in the respiratory tract and that the subject must breathe regularly, and there might therefore be difficulties in applying the method while the subject is exercising. Halogenated hydrocarbons such as dichlorodifluoromethane (freon 12) (ref. 6) have the disadvantage of being mildly toxic so that the concentration in the test gas atmosphere must be kept relatively low; the sensitivity of the method might therefore be limited.

A dynamic method developed at the Safety in Mines Research Establishment determines accurately the leakage of the external atmosphere into the mask while the subject is performing various exercises. In this method the subject, wearing the facemask complete with breathing tubes, is enclosed in a transparent plastic hood large enough for him to move his head while wearing the mask (fig. 24.1). Pure argon is fed into the top of the hood from a regulated cylinder supply. Argon is used as the atmosphere in the hood because it is physiologically inert, inexpensive, and available in a pure form.

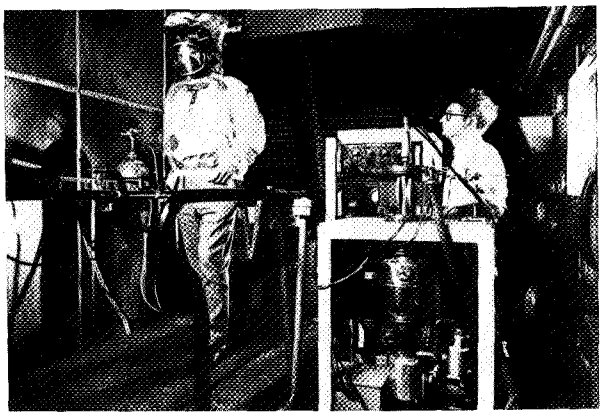

Figure 24.1 *Test equipment.*

The subject inhales medical quality oxygen supplied from a cylinder fitted with a pressure reducer and a lung-governed demand valve, so that the wearer can draw as much oxygen as he needs. The oxygen breathing tube is fitted with a sampling port. A spirometer measures the volume of oxygen used.

The facemask is fitted with two nonreturn valves, controlling the direction of flow of oxygen in the two breathing tubes. The exhaled gas passes through the second breathing tube into a sampling bladder fitted with a sampling port, and then passes to atmosphere.

The amount of argon in the exhaled gas is determined by means of an MS10 mass spectrometer. This instrument is capable of detecting at least 10 ppm of argon in the exhaled breath. A multiway tap is connected to the spectrometer and the various sampling ports. Sampling is by means of a small suction pump. With the mass spectrometer tuned to mass number 40, the principal number of argon, and the multiway tap positioned to sample the wearer's oxygen supply, a trace is obtained on the mass spectrometer recorder that corresponds to the concentration of argon in the oxygen supply; this is usually less than 50 ppm. The tap is then repositioned to enable the exhaled breath in the sampling bladder to be sampled. A second trace is obtained on the recorder corresponding to the concentration of argon in the exhaled breath. The difference between the two gives a measure of the rate of flow of argon leaking into the mask.

In each test the subject walks at 6.4 km/h (4 mph) on a treadmill inclined at 2.5° (fig. 24.1), and carries out slowly, at his own pace, a prearranged series of head movements.

This method has been used to determine the inward leakage rate into various facemasks in two series of experiments. The first series was with 29 clean-shaven subjects wearing two types of facemask. The second series was with 12 unshaven subjects wearing three types of facemask.

Experimental Results with Clean-Shaven Subjects Wearing Two Types of Facemask. The two masks tested were of the plain-seal and pneumatic-seal types. The inward leakage rate of each type of mask was determined for 29 clean-shaven subjects. The subjects (SMRE staff) fitted the facemasks themselves and checked for gross leakage by gripping the breathing tubes and trying to inhale. When leakage was apparent the mask was readjusted. No attempt was made to refit a mask during a test even when leakage became apparent. Tables 24.1 and 24.2 show the results obtained with the plain-seal mask and the pneumatic-seal mask. One subject, whose results are marked with an asterisk in table 24.1, had a visible gap between the mask and face that could not be improved. The leakage is expressed in the conventional way—that is, concentration of argon appearing in the exhaled breath.

The subject whose results are marked with an asterisk in table 24.2 could not be fitted satisfactorily with a facemask; although no gap was

Table 24.1 *Leakage with plain-seal mask.*

Subject number	Minute volume l min BTPS	Leakage : ppm				
		Head steady	Head side to side	Head up and down	Head steady talking	Mean of the exercises
1	46·0	411	316	282	300	327
2	30·7	414	376	387	379	389
3	32·0	2090	1855	1722	836	1626
4†	-	-	-	-	-	-
5	40·1	128	107	92	86	103
6	48·2	3859	1760	11863	4512	5499
7	33·9	461	442	366	392	415
8	37·7	88	67	67	67	72
9	38·4	251	196	8467	-	2971
10	38·7	4734	6545	137	185	2900
11	36·6	980	1684	1113	602	1095
12	39·0	220	191	196	198	201
13	34·6	104	83	410	99	174
14	35·8	109	88	92	76	91
15	40·7	81	72	9458	129	2435
16	41·0	110	81	84	96	93
17	36·2	108	87	77	102	94
18	45·5	102	76	4397	1368	1468
19	40·8	429	433	481	533	469
20	47·8	834	482	182	99	399
21	44·2	131	94	95	113	108
22	38·1	111	192	1040	112	364
23	36·6	136	99	9637	460	2583
24	45·9	95	73	67	74	77
25	45·1	21364	16009	46253	61600	36307
26	38·6	168	522	772	245	427
27	43·8	725	651	630	648	664
28	39·0	149	130	28341	219	7210
29	39·0	792	963	1418	982	1039

†Visible gap between mask and face

Table 24.2 *Leakage with pneumatic-seal mask.*

Subject number	Minute volume l/min BTPS	Leakage : ppm				
		Head steady	Head side to side	Head up and down	Head steady talking	Mean of the exercises
1	43·6	155	125	127	151	140
2	23·6	82	35	42	50	52
3	35·4	50	50	50	30	45
4	30·7	90	39	35	25	47
5	25·1	194	146	125	117	146
6	46·2	57	40	46	56	50
7	38·7	241	100	85	222	162
8	40·2	82	77	74	100	83
9	40·0	96	40	33	59	57
10	35·3	84	52	50	43	57
11	49·2	155	125	125	125	140
12	39·8	105	94	85	100	96
13†	-	-	-	-	-	-
14	38·3	534	359	82	52	257
15	46·2	154	138	150	150	148
16	44·7	180	105	110	176	143
17	46·4	188	136	119	150	148
18	43·3	65	35	42	50	48
19	41·1	146	125	119	237	157
20	43·6	132	45	80	90	87
21	49·2	47	42	40	60	47
22	43·4	69	75	71	52	67
23	50·4	35	42	50	50	44
24	44·2	75	75	75	75	75
25	32·4	49	90	172	271	146
26	40·6	32	25	25	25	27
27	38·4	140	130	67	255	148
28	34·5	62	217	142	250	168
29	34·7	86	64	64	86	75

†Badly fitting mask

visible between the mask and the face, leakage could be felt in the suction test and repeat fittings made no improvement.

The method described above allows facemask leakages of the order of 0.001 percent to be detected. Also, the leakage may be measured while the subject is carrying out various exercises.

The results obtained using this method confirm the superiority of the pneumatic-seal type of mask compared to the plain-seal type. It is likely that the fit of the plain-seal mask can be improved by very careful adjustment by the subject or fitter. In exceptional cases, however, there may be subjects who, because of facial characteristics, cannot be satisfactorily fitted with either type of facemask.

Experimental Results with Unshaven Subjects Wearing Three Types of Facemask. These tests were conducted on 12 volunteers from the City of Manchester Fire Brigade. Two of the subjects normally wore a substantial beard (fig. 24.2(a)). The other 10 men had beard growths ranging from 15 days to one month. Three facemask leakage tests were carried out on each man: unshaven, beard shaved but sideburns left to below the ear lobe, and clean-shaven. The results of these tests are shown in tables 24.3, 24.4 and 24.5.

Some of the men retained moustaches, but these were always small enough to be completely contained within the masks. The two men who were normally bearded chose not to be completely clean-shaven but retained much smaller beards (fig. 24.2(b)), supposedly small enough to lie within the sealing rim of the mask.

The three facemasks used in the tests were of the plain-seal, revert-seal, and pneumatic-seal types. Each man wore the same mask for each of the three tests. Additional tests, in which the pneumatic-seal mask was worn by the subjects in the clean-shaven condition, were made with the subjects who wore the plain and revert-seal masks.

As before the subjects fitted the facemasks themselves and checked for gross leakage by gripping the breathing tubes and trying to inhale. When leakage was apparent the mask was readjusted. No attempt was made to refit a mask during a test even when leakage became apparent.

From this series of experiments, it is concluded that when the subject has

A full beard: Beard growth substantially increases the inward leakage rate of all the facemasks used in the tests.

Sideburns only: Results show considerable variation. Modest sideburns (fig. 24.2(d)) that lie outside the facemask seal cause leakage rates similar to those obtained in the clean-shaven condition. Large bushy sideburns (fig. 24.2(c)), sufficiently large and bushy to lie between the facemask seal and the face, are likely to cause a substantial increase in leakage rate.

In all cases, when the subject was clean-shaven the pneumatic-seal mask gave a low leakage figure while the revert-seal and plain-seal masks showed considerable variation in the leakage rate. In the case of the two men who retained small beards, the beards were trimmed under the chin so that no hair was across the mask seal before a fairly good fit could be obtained (fig. 24.2(b)). The leakage rate, however, was still noticeably higher than with the clean-shaven subjects.

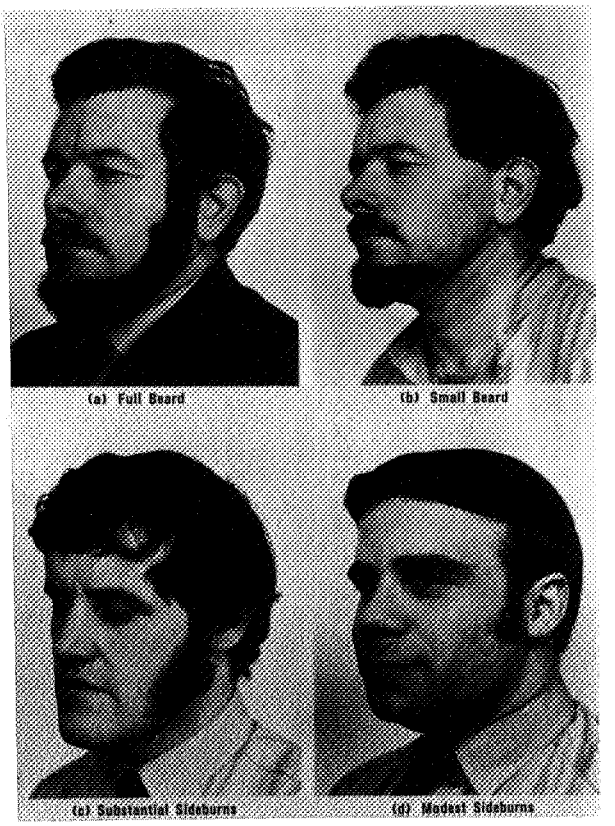

Figure 24.2 *Types of beard growth investigated.*

Discussion. When facemasks are worn in some toxic atmospheres a certain amount of leakage may be tolerable. It is important to remember, however, that this tolerable leakage will be less when the facemask is used with closed-circuit breathing apparatus than when it is worn with any other type of respiratory apparatus because the toxic gas leaking in with each breath may accumulate in the air in the closed circuit. In practice, the concentration of gas breathed in by the wearer will rapidly increase to an equilibrium value, which in the case of carbon monoxide would increase the concentration in the facemask by approximately 2.5 times the concentration that otherwise would have been breathed.

Table 24.3 *Summary of facemask leakage results in ppm, obtained with the plain- and revert-seal facemasks, and when cleanshaven, the pneumatic-seal facemask.*

Subject	Minute volume l/min BTPS	Type of mask	Leakage : ppm			
			Full beard	Sideburns only	Clean-shaven	Pneumatic type. Clean-shaven
R.S.	49·7	Revert	6,710	1,900	2,580	25
G.H.	56·7	Revert	13,220	10,140	20	25
B.P.	48·6	Plain	190*	25	25	25
L.J.	48·0	Plain	390	30	255	15
Average	50·7		5,130	3,020	720	22

*Beard growth not substantial

These results clearly demonstrate the superiority of the pneumatic-seal facemask. The manufacture of the plain-seal type has recently been discontinued in the United Kingdon; however, many plain-seal facemasks are still in regular use in industry. Since it appears that all facemasks leak, care must be taken in the choice of facemask and particular care must be exercised before facemasks are used in highly toxic atmospheres. Also it is important to remember that facial hair, when present between the face and the facemask seal, will substantially increase the facemask leakage.

Outward Leakage

Since inward leakage occurs in all the masks examined, outward leakage is also likely to occur when there is a positive pressure in the facemask. When facemasks are used with closed-circuit breathing apparatus, which normally supply oxygen to breathe, the outward leakage of oxygen may be sufficient to create a flammability hazard (ref. 7).

The outward oxygen leakage from full facemasks has been measured in a series of tests. Four types of mask were investigated, each considered suitable for use with closed-circuit breathing apparatus: plain-seal, revert-seal, pneumatic-seal, and water-filled pneumatic seal.

The leakage rate of each of the above facemasks was determined while the masks were being worn by four subjects of differing facial shapes and sizes. All the facemasks examined were supplied with two short breathing tubes fitted to a connecting piece at the front of the mask, and opening into the mask. Inside the facemask, each subject wore a noseclip and mouthpiece. The mouthpiece was joined to one of the breathing tubes by tubing that passed out through the connecting piece. Such an arrangement allowed inspiration and expiration independent of the air in the facemask. The second breathing tube was connected to an air line and maintained the pressure in the mask at a selected value, measured with a water manometer. The flow of air through this line at the selected pressure was measured by a flowmeter and was equal to the leakage rate out of the mask. The average values of the four subjects with each type of mask are shown in figure 24.3.

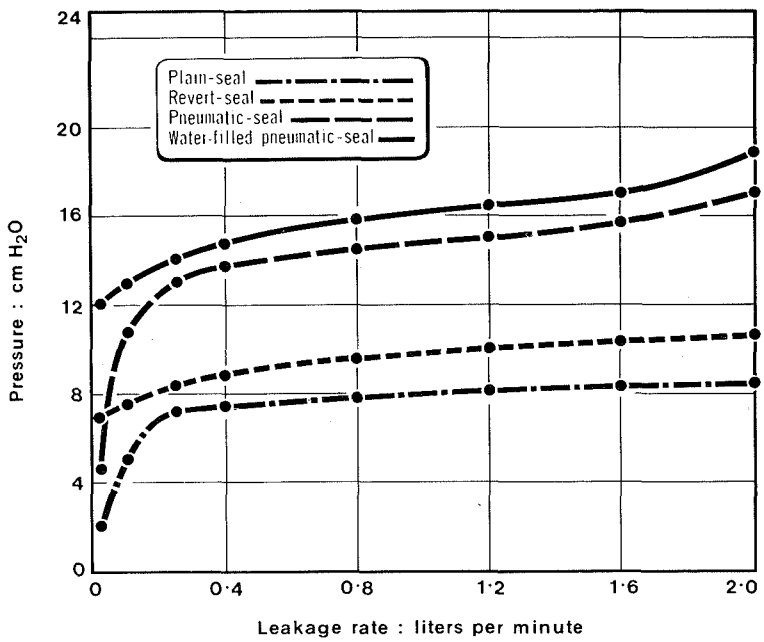

Figure 24.3 *Outward leakage rate from full facemask.*

In general, the pressures in a mask are determined by the breathing apparatus, and in particular by the relief valve. With an automatic relief valve the pressure in the mask depends largely on the opening pressure of the valve. With a manually operated relief valve the position is rather more complicated, since the wearer's use of the relief valve depends on his subjective response to breathing resistance.

When the pressure in the facemask approaches about 12 cm H_2O (1.2 kN/m^2) it is to be expected that the wearer will have difficulty in breathing out and he will become aware of the need to operate his relief valve. However, figure 24.3 indicates that when plain- or revert-seal facemasks are worn in conjunction with the apparatus, there may be a substantial outward leakage at the mask that prevents such a build-up of pressure. In practice, it has been confirmed that some wearers of these masks, when preoccupied with work, do not feel the need to operate the relief valve; large outward leakage occurs, and the pressure in the mask on exhalation remains fairly constant at about 9 cm H_2O (0.9 kN/m^2). Less leakage occurs with wearers who use their relief valves, but the amount is still considerable. Pressure is reduced to about 4 cm H_2O (0.4 kN/m^2); this then increases

to nearly 9 cm H_2O (0.9 kN/m^2) before the relief valves are used again. Outward mask leakage from either type of pneumatic-seal facemask is substantially less than plain- or revert-seal types.

Another series of experiments was carried out to examine the ignition hazard associated with mask leakage. A full plain-seal facemask was fitted to a dummy head, and hair cuttings were placed around the edges of the mask. A controlled flow of oxygen was allowed to escape around the edges of the mask and attempts were made to ignite the hair cuttings; a glowing splint held near to the rim of the mask was used as the source of ignition. When the leakage rate exceeded 0.25 liters/min the hair cuttings were ignited rapidly and the rim of the mask was also ignited. Figure 24.3 shows that the leakage is probably harmless when the pressure in pneumatic-seal masks is less than 12 cm H_2O (1.2 kN/m^2).

Table 24.4 *Summary of facemask leakage results in ppm, obtained with the pneumatic-seal facemask when worn by the two subjects with substantial beard growth.*

Subject	Minute volume l/min BTPS	Leakage : ppm		
		Full beard	Reduced beard with sideburns	Smaller beard within mask. No sideburns
L.R.	41·5	30,670	27,570	320
E.R.	51·1	11,730	55	225
Average	46·3	21,200	13,810	270

This work confirms the need for care in the choice of facemasks, the importance of correctly fitting the facemask to the wearer and the advisability of using breathing apparatus supplied with a well-designed automatic relief valve.

Table 24.5 *Summary of facemask leakage results in ppm, obtained with six subjects wearing the pneumatic-seal facemask.*

Subject	Minute volume l/min BTPS	Leakage : ppm		
		Full beard	Sideburns only	Clean-shaven
M.B.	51·0	3,790	310	70
H.L.	57·0	470	25	20
F.M.	47·9	–†	790	25
L.R.	44·5	600	195	35
G.P.	42·8	5,130	35	30
B.B.	51·2	4,880	35	95
Average	49·1	2,970	235	45

†Substantial sideburns but no beard

FACEMASK DEAD SPACE

The term "dead space" when applied to a facemask may mean either the "geometric" dead space, which is the volume between the mask and the wearer's face, or the "effective" dead space, which is a measure of the exhaled breath rebreathed by the wearer. A measure of the geometric dead space can be determined by measuring the volume of water required to fill the space between a mask and a dummy head. Determination of the effective dead space, which is a more realistic measurement, requires a more complicated technique. The facepiece, complete with valves and breathing tubes, is fitted onto a dummy head in a leak-tight manner. The expiratory and inspiratory ports of a (two-cylinder) breathing simulator are connected via a T-piece to the dummy head's throat. On

expiration, the breathing simulator delivers a known mixture of carbon dioxide and air (usually 5 percent carbon dioxide) into the facepiece and out through the expiration breathing tube to the atmosphere. On inspiration, laboratory air is drawn through the inspiration breathing tube and facepiece into the breathing simulator; part of the inhaled air will thus be supplied from previously exhaled air in the dead space. The inhaled, exhaled, and laboratory air are analyzed for their carbon dioxide contents. The effective dead space of the facepiece is then given by $V(x - a)/(y - a)$, where V is the volume per stroke of the breathing simulator and x, y, and a, are the percentage of carbon dioxide in the inhaled, the exhaled, and the laboratory air, respectively. By this means, the effective dead space of the facepieces may be measured at different tidal volumes and respiration rates.

This method has been applied to six commercially available facemasks. The effective dead spaces were measured at tidal volumes of 1, 2, and 3 liters and at respiration rates of 10, 20, and 30 rpm for each tidal volume. The facemasks used were:

A. A British pneumatic-seal mask of recent design, fitted with an inner nose cup and a self-demisting arrangement. This arrangement is such that on inhalation air is drawn through a duct, which directs the air over the surface of the visor before entering the nose cup through nonreturn valves. The exhaled breath passes direct from the nose cup and out of the exhalation breathing tube.

B. A mask similar in design to mask (A) but made by a different British manufacturer.

C. A British pneumatic-seal facemask molded to the shape of a face and having separate eye lenses, an inner nose cup, and self-demisting arrangement.

D. An earlier wide-vision facemask of British manufacture, of the plain-seal type, not fitted with a nose cup or demisting arrangement.

E. A Finnish revert-seal facemask with combined inhalation and exhalation valve, fitted with an inner nose cup and self-demisting arrangement.

F. A German revert-seal facemask fitted with an inner nose cup, but without self-demisting arrangement. The visor is fitted internally with a mechanical wiper blade operated externally by hand for demisting.

Figure 24.4 shows the effective dead space of all the masks fitted with inhalation and exhalation valves in the "as worn" condition.

Figure 24.5 shows the effective dead space of two of the pneumatic-seal types of facemasks (masks A and B) (a) as normally worn, i.e., demisting, (b) fitted with nose cup but with the demisting arrangement closed, and (c) without nose cup.

It was found that the respiration rate at each tidal volume had little effect on the effective dead space (usually less than 5 percent of the mean); the graphs are therefore a plot of the mean of the respirations at each tidal volume.

The recent British Standard (ref. 8) states that the carbon dioxide concentration breathed by the wearer must not exceed an average of 1 percent. It follows that to satisfy this requirement the facemask dead space should not be greater than 400 cm^3 at 2 liter tidal volume. Since this concentration in closed-circuit breathing apparatus may include a contribution from the slip of the purifier in addition to the dead space in the complete apparatus, it is recommended that the effective facemask dead space should be less than 300 cm^3.

The pneumatic-seal type of facemask was shown superior to other types as far as face-seal leakage is concerned. This work on dead space has shown that the pneumatic-seal type has a low dead space, particularly when an inner nose cup is fitted. The value of the nose cup is clearly apparent in figure 24.5.

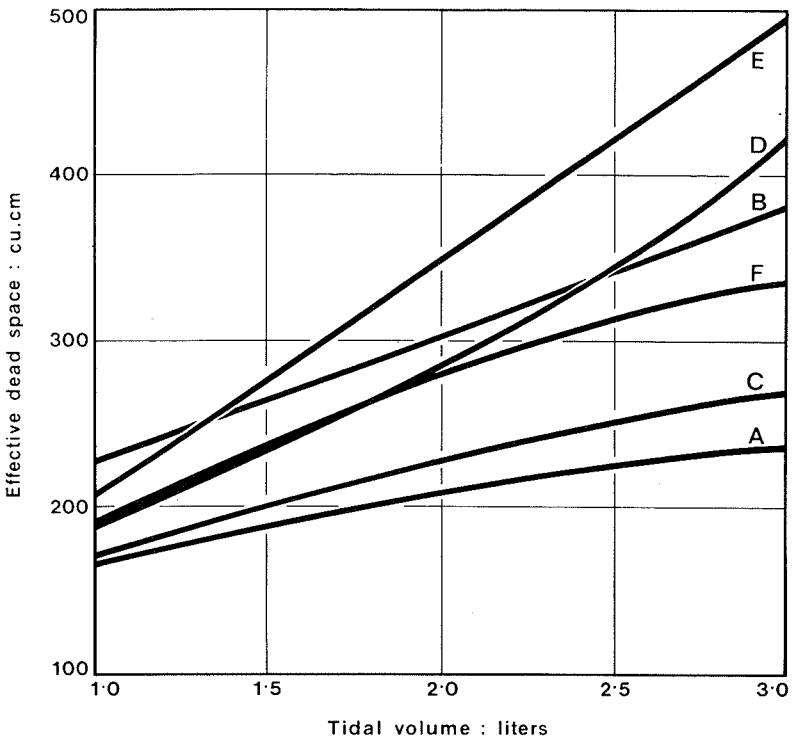

Figure 24.4 *Effective dead space of six facemasks.*

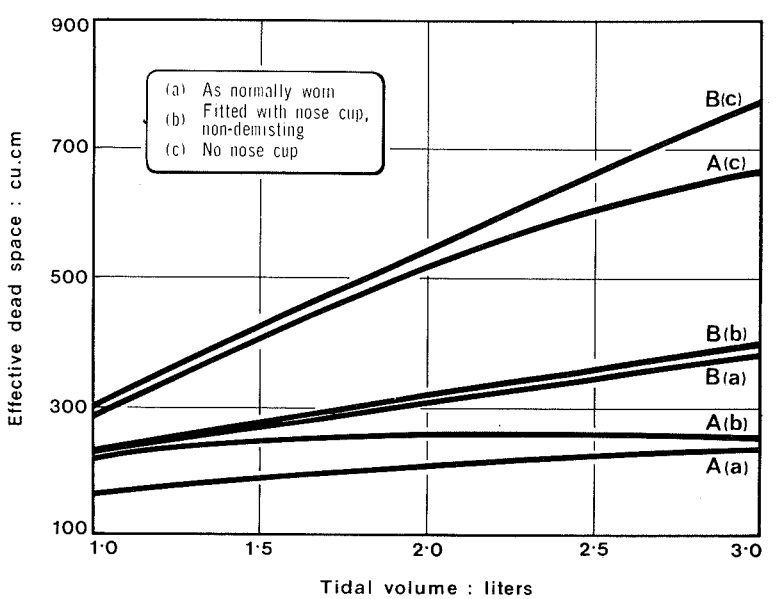

Figure 24.5 *Effective dead space of facemasks A and B.*

REFERENCES

1. Hounam, R. F.: A Method for Evaluating the Protection Afforded when Wearing a Respirator, United Kingdom Atomic Energy Authority Research Group Report No. AERE – R4125, 1962.
2. Hounam. R. F.; Morgan, D. J.; O'Conner, D. T. and Sherwood, R. K.: Ann. Occup. Hyg., vol 7, p. 353, 1964.
3. Burgess, W. A.; Silverman, L.; and Stein, F.: Am. Ind. Hyg. Assoc. J., vol. 22, 1967, p. 422.
4. Guyton, H. G.; Mick, C. E.; Decker, H. M.; and Burgess, W. A.: Am. Ind. Hyg. Assoc.J., vol. 28, 1967, p. 462.
5. Letts, H. J. R.: Design and Use of Respirators (edited by C. N. Davies,) p. 119, Pergamon Press, Oxford, 1961.
6. Morgan, D. J.: A Method of Testing the Efficiency of a Respirator Using a Haolgenated Hydrocarbon Test Gas. United Kingdom Atomic Energy Authority Research Group Report No. AERE – R4485, 1964.
7. Denison, D. M. and Tonkins, W. J.: Further Studies Upon the Human Aspects of Fire in Artificial Gas Environments. Ministry of Defence, London, Flying Personnel Research Committee Report No. FPRC/1270, 1967.
8. British Standards 1971, Specification for Breathing Apparatus BS 4667:1971.

25

CATALYZED SODIUM CHLORATE CANDLES

C. W. Malich and T. Wydeven
Ames Research Center

INTRODUCTION

State-of-the-art chlorate candles have been used for decades as emergency oxygen sources in submarines (ref. 1). Reliability in present units is achieved mainly by overdesign (ref. 2), which imposes undesirable weight and volume penalties on portable systems. Recent work at Ames Research Center on basic advances in oxygen storage and regeneration has emphasized catalytic decomposition of sodium chlorate to achieve increased gas purity, lower operating temperatures, and improved reliability.

A typical chlorate candle unit (ref. 1) is illustrated in figure 25.1. A firing device in the ignition assembly starts the ignition cone burning. This in turn initiates the decomposition of the sodium chlorate in the solid composite of the body so that oxygen is released as a hot gas. A clinker of sodium chloride (with the binders used in the composite) remains. The simplified chemistry is represented by (ref. 3):

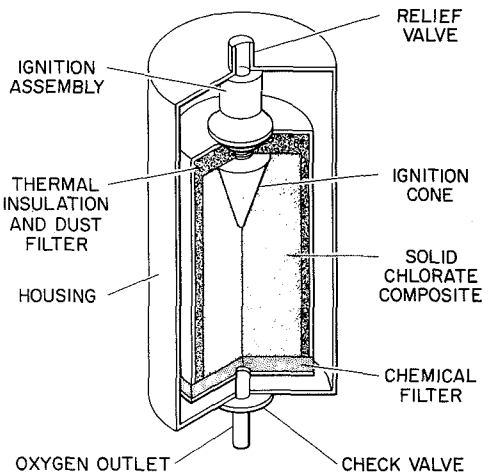

Figure 25.1 *Chlorate candle assembly.*

$$NaClO_3 \rightarrow NaCl + 1.5O_2 \quad (1)$$

$$4NaClO_3 \rightarrow 3NaClO_4 + NaCl \quad (2)$$

$$NaClO_4 \rightarrow NaCl + 2O_2 \quad (3)$$

The sodium chlorate can decompose directly at high temperatures to give sodium chloride and oxygen gas, or to sodium perchlorate, which at a still higher temperature produces the same end products. Side reactions can lead to traces of chlorine that are usually minimized by a suppressor such as barium peroxide. Conventional candles are mixed with a fuel (typically iron powder) and some type of binder. Asbestos fiber, glass fiber, and steel wool have been used as binders. Usually some chemical filtering is used to assure adequate purity of the gas. For example, hopcalite catalyst can be inserted in the effluent line to oxidize traces of carbon monoxide.

EXPERIMENTAL ARRANGEMENTS

Cylindrical segments, 1 in. diam by 1 in. length, were used for most of the survey work on optimizing composition using a catalyst. These short candles are the subject here. Sodium chlorate was purified by recrystallization, followed by drying and grinding. Chemical analysis showed 0.017-percent carbon, with water <0.05 percent and chlorite <0.003 percent. All candle segments were mixed using 6 wt percent silicon dioxide fibers as a binder, which is a standard procedure reported to have a mildly catalytic effect on chlorate decomposition (ref. 4). Cobalt metal powder

was used as a fuel. The supplier's (African Metals Corporation) analysis listed impurities as 0.035-percent carbon, 0.020-percent calcium, 0.010-percent sulfur, 0.005-percent silicon, 0.025-percent iron, 0.026-percent nickel, and traces of calcium, magnesium, and manganese. Catalysts often were used in addition to or in place of the fuel. The ingredients were mixed by hand in a dry inert gas atmosphere and pressed to 40,000 lb in a single ram press. The findings of Gustafson et al. (ref. 5) that only trapped water leads to chlorine evolution and that glass fiber increases production of chlorine have not been tested. Chemical filters and chlorine suppressors were not used in this work because one object was to learn whether purity and dryness would be adequate to keep free chlorine within acceptable limits.

Uniform mixing of candle ingredients varying in particle size and density is difficult. Early candles contained small white lumps presumed to be almost pure sodium chlorate. Chemical analyses of fractional gram portions excluding these visible anomalies showed that the catalyst also was distributed nonuniformly. Better blending of materials greatly improved homogeneity (table 25.1). The later candles (represented by the 6.7 percent fuel, no catalyst formulation in this table) did not have the white lumps and showed much more uniformity. This better mixing markedly improved the reproducibility of candle segment performance and the smoothness of burning.

Table 25.1 *Test of candle uniformity.*

EARLY CANDLE % CATALYST	LATER CANDLE % COBALT
5.76	6.78
5.91	6.75
3.75	6.59
3.75	6.67
3.71	6.46
3.76	6.76
3.88	6.63
4.50±0.91	6.66±0.09

CHEMICAL ANALYSIS OF APPROXIMATELY 0.2 gm PORTIONS OF CANDLES, SELECTED AT RANDOM (EXCLUDING LUMPS OF PURE SODIUM CHLORATE)

Many catalysts have been proposed (refs. 5-8) for thermal decomposition of chlorates. The effects of cobalt chloride and cobalt oxide are shown in figure 25.2. The percentage of available oxygen W in the material is plotted against the temperature to show the extent of the decomposition. Sodium chlorate decomposes rapidly near 500° C and sodium perchlorate at a higher temperature. The catalysts lower the decomposition temperatures appreciably. Cobalt oxide was used for most of the studies because cobalt chloride is difficult to dry. Only the results of the cobalt oxide catalysts are reported. In addition to the thermogravimetric analyses, differential thermogravimetric studies and differential scanning calorimetry of candle chips weighing a few milligrams were performed.

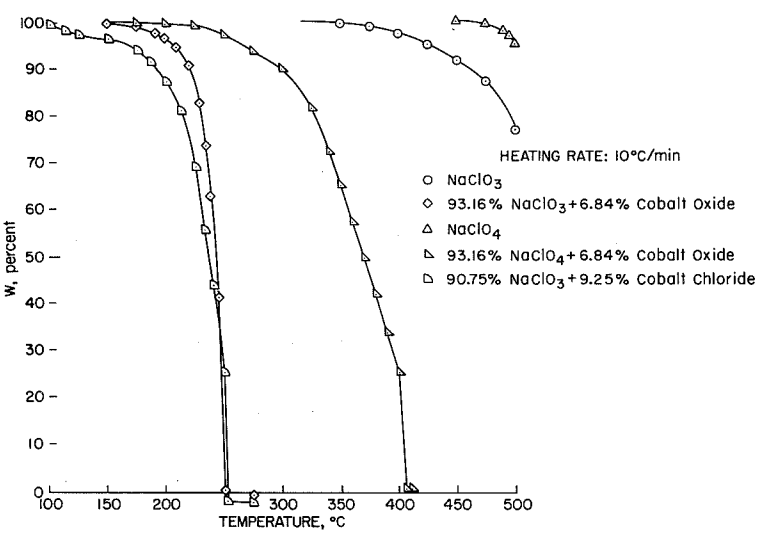

Figure 25.2 *Catalytic decomposition of sodium chlorate and perchlorate.*

The 1-in. candle segments were generally capped by a 35 percent cobalt-fuel-rich ignition section. Ignition was accomplished by electrical heating of a platinum wire incorporated in the ignition

section. Burning was usually done with no thermal insulation, with the segment completely insulated by firebrick or with a standardized partial insulation. Internal temperatures were measured by chromel-alumel thermocouples inserted 0.25 in. into the candle. Linear burn rates have been calculated from the burn time for complete segments or portions of segments. The decomposition rate depends critically on heat transfer characteristics. More elaborate studies are planned to design containers for practical candle units.

DIFFERENTIAL SCANNING CALORIMETRY

One of the major analytical tools of this study has been differential scanning calorimetry (DSC). The net rate of heat release from the exothermic decomposition of chlorate as a function of temperature is a measure of the rate of production of oxygen. Figure 25.3 shows DSC results for a chip from a candle made with 5 percent cobalt fuel. The baseline is indicated by a dashed line. The endothermic melting of the sodium chlorate occurs near 260° C, followed by exothermic decomposition with peaks around 340° C and 440° C. The studies indicate that the second peak is connected with the decomposition of sodium perchlorate as an intermediate, but this has not yet been shown quantitatively. In addition to the DSC, there is a simultaneous differential thermogravimetric trace (DTG) of the rate of change of weight versus temperature of a similar sample. As expected, there is no weight change during the melting, but the two curves match well during decomposition where the weight loss measures the oxygen evolution.

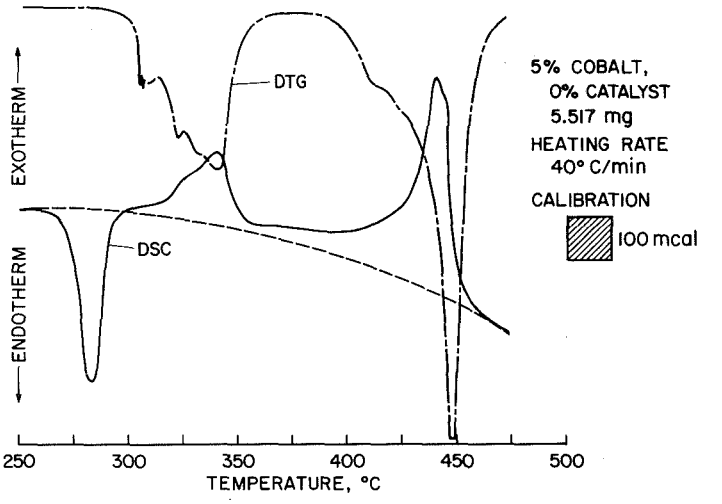

Figure 25.3 *Differential scanning calorimetry of chlorate candle with no catalyst.*

The effect of catalysts on the cobalt-fueled candles is illustrated in figures 25.4 and 25.5. A trace of catalyst lowers the reaction temperature so that the two DSC peaks now appear near 320° C and 370° C. Three percent catalyst shows a single decomposition region around 300° C. Decomposition is essentially complete by 310° C or 315° C.

Some results obtained with candles containing no fuel are presented in figures 25.6 and 25.7. The shape of the curve for 3-percent catalyst with no fuel is similar to that shown in figure 25.5 for a candle containing 3 percent catalyst and 5-percent fuel. The decomposition without fuel is complete below 300° C

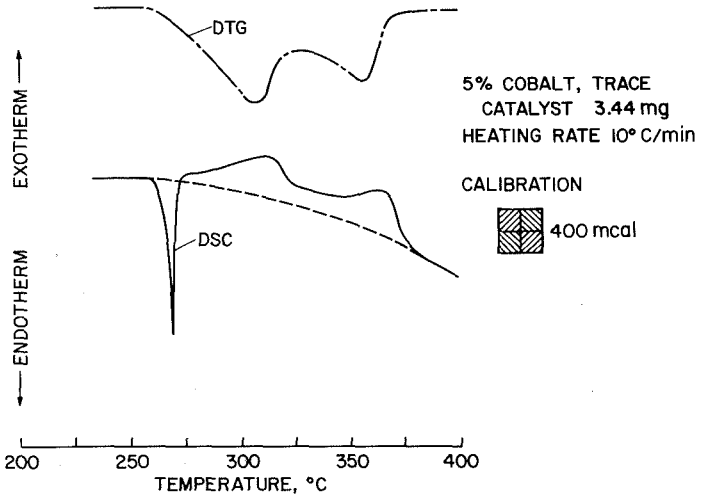

Figure 25.4 *Differential scanning calorimetry of chlorate candle with a trace of catalyst.*

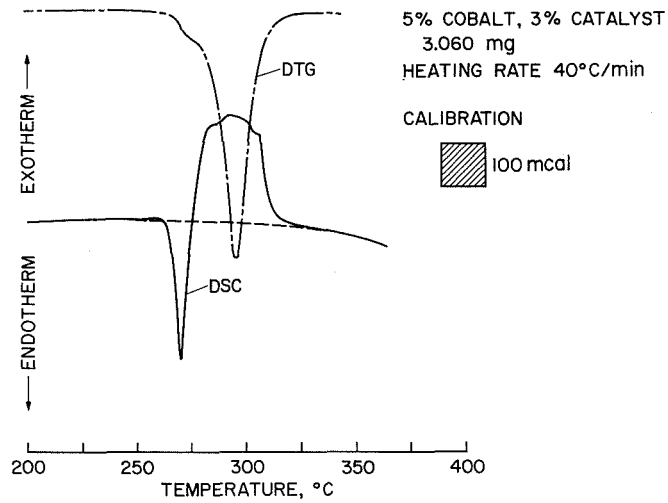

Figure 25.5 *Differential scanning calorimetry of chlorate candle with 3 percent catalyst.*

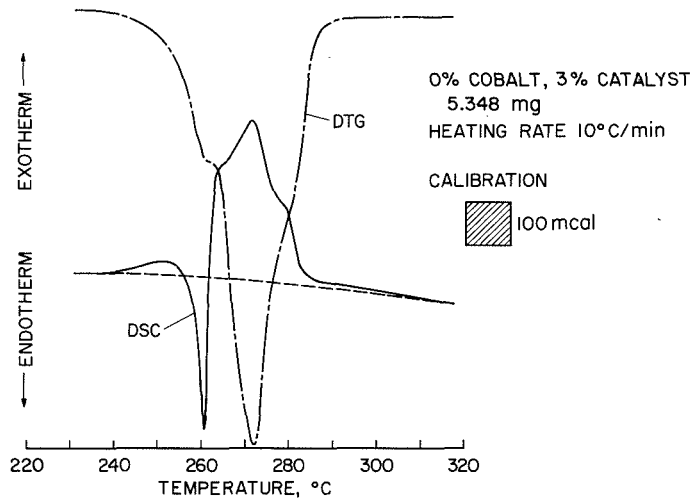

Figure 25.6 *Differential scanning calorimetry of chlorate candle (without fuel) containing 3 percent catalyst.*

at this slower heating rate of 10° C/min. Not all candle segments burn to completion, however, when only 3 percent catalyst is used. Complete burn is achieved with 9-percent catalyst. The DSC in figure 25.7 shows that nearly half the decomposition occurs below the melting point and that the melting endotherm is masked by the exothermic decomposition.

The DSC results depend on the heating rate, sometimes quite strongly, as illustrated in figures 25.8, 25.9, and 25.10, for a 5 percent cobalt, 6 percent catalyst candle. The change in weight versus temperature of similar samples, rather than rate of change or DTG, is shown in addition to the DSC trace. The mass dial numbers are related to the upper limit of the recorded mass in micrograms, and

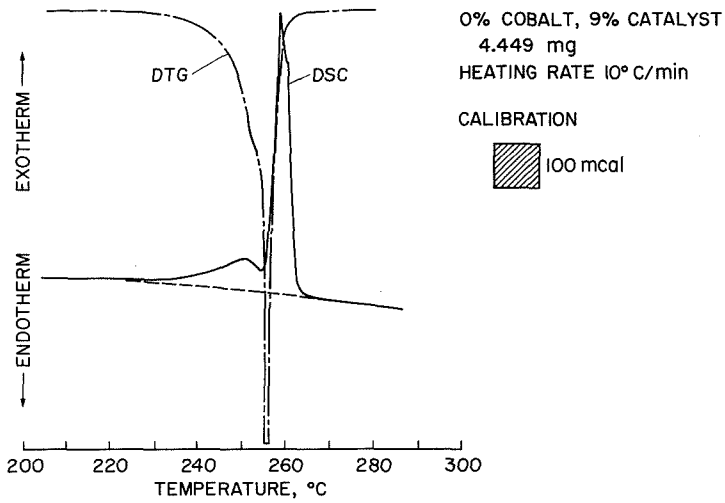

Figure 25.7 *Differential scanning calorimetry of chlorate candle (without fuel) containing 9 percent catalyst.*

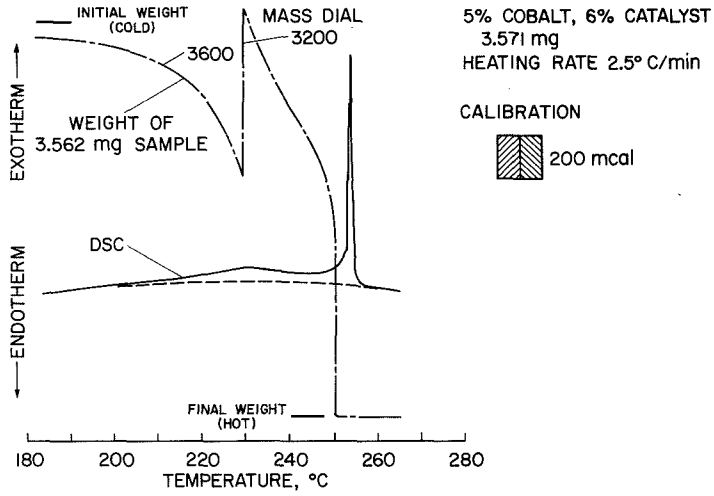

Figure 25.8 *Differential scanning calorimetry of chlorate candle using slow heating rate.*

were shifted by the operator to keep the trace on scale. At a slow heating rate of 2.5° C/min there is extensive decomposition in the solid phase, and less at a rate of 10° C/min. A reduced melting endotherm appears again at the faster rate of 40° C/min. The general appearance of this latter curve is quite similar to the 5 percent cobalt, 3 percent catalyst candle shown in figure 25.5. Even 40° C/min is lower than the heating rate in a burning candle, as discussed in the next section, so further tests at higher heating rates are planned.

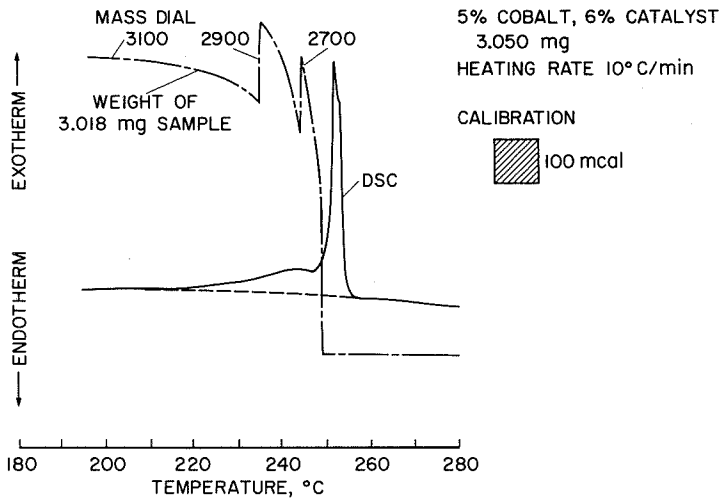

Figure 25.9 *Differential scanning calorimetry of chlorate candle using moderate heating rate.*

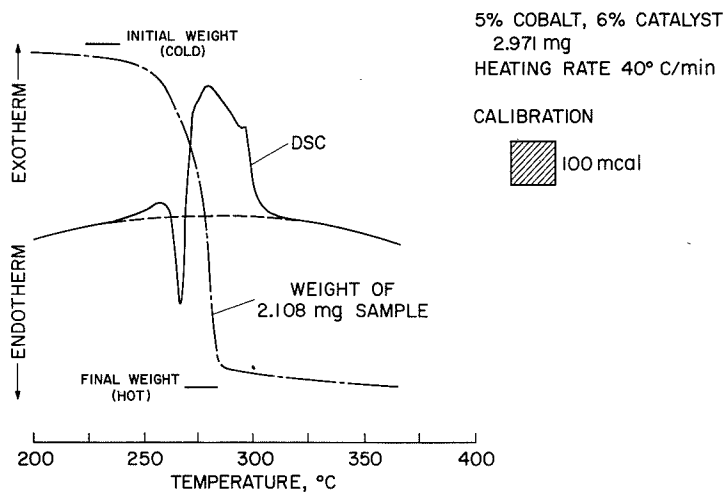

Figure 25.10 *Differential scanning calorimetry of chlorate candle using faster heating rate.*

INTERNAL TEMPERATURES DURING DECOMPOSITION OF CANDLE SEGMENTS

Temperatures recorded by thermocouples inserted 0.25 in. into the burning 1-in. segments are shown in figure 25.11 for uncatalyzed compositions and in figure 25.12 for the 5 percent cobalt, 3 percent catalyst short candles. Two temperatures from two thermocouples at different locations are measured simultaneously with a dual pen recorder. Heating of roughly 100° C/min arises from conduction in advance of the burn front. This rate is much accelerated just as the decomposition zone reaches the thermocouple. The temperature does not increase rapidly above the melting point of sodium chlorate for a while, especially in the uncatalyzed segment. The endothermic melting absorbs much of the heat released during early decomposition and stabilizes the temperature. The maximum temperature is recorded considerably later than the beginning of decomposition at the

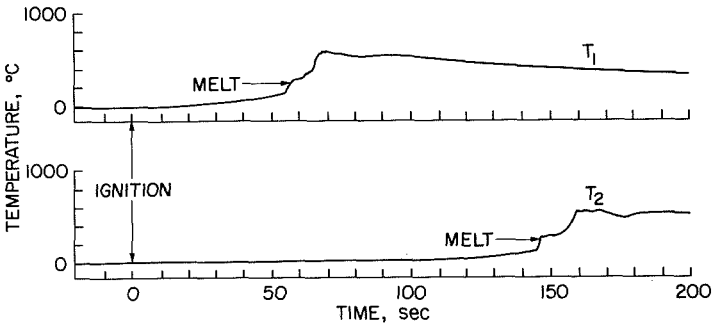

Figure 25.11 *Internal temperatures during decomposition of chlorate candle without catalyst.*

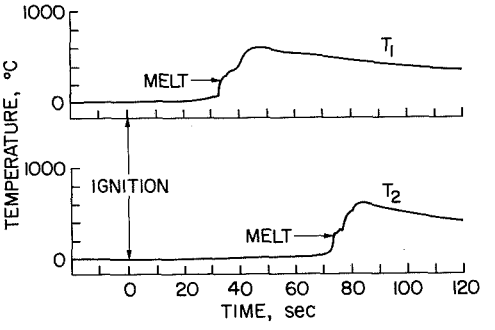

Figure 25.12 *Internal temperatures during decomposition of chlorate candle with 3 percent catalyst.*

thermocouple (the DSC results show appreciable reaction near the melting point). Frequently expansion of the clinker causes erratic cooling after this maximum. It is important to realize that the maximum temperature is reached after decomposition is complete, by conduction of heat from adjacent portions of the candle. Heat losses cause considerable variation in the maximum temperatures recorded. These losses are greater in slowly burning segments than in rapidly burning segments. Very large voids are occasionally seen in clinkers of incompletely burned candles, which seems to indicate that temporary excessive cooling may have extinguished the segment. Maximum temperatures in catalyzed candles are reached rather quickly after melting, and burning is generally smoother than with uncatalyzed candles. Some average maximum temperatures of candle segments insulated in firebrick are tabulated in table 25.2. The lowest temperature of 560° C (for candle formulations burning completely) was obtained with no fuel in a 9 percent catalyst segment. The other formulations listed here contained no catalyst. The rather limited variation in average maximum temperature from 630° C to 700° C as the fuel content is increased from 3 to 7 percent is due partly to heat losses and probably also to incomplete combustion of the fuel (ref. 1). The highest fuel concentration studied, 35 percent cobalt, gave an average maximum temperature of 1110° C while oxidizing the fuel nearly completely to cobalt oxide based on measurements of weight change and oxygen yield. The carbon monoxide production was greater for segments burning at higher temperatures, probably because of the greater stability of carbon monoxide relative to carbon dioxide at higher temperatures. Further observations on gaseous contaminants and candle temperatures are given in a subsequent section.

Table 25.2 *Maximum internal temperatures during burning of chlorate candles without catalyst, insulated with firebrick.*

COBALT, %	T_{max}, °C
0	560
3	630
5	670
7	700
35	1110

Additional internal temperature measurements are presented in table 25.3, which shows the effect of insulation on burn rate and maximum temperature for both catalyzed and uncatalyzed compositions. Results are enclosed in parentheses when only a portion of the samples burned completely. Burn rates for these less complete tests, although consistent, are considered less reliable. Also, maximum temperatures are abnormally low when a candle goes out near the thermocouple, even if burning has progressed beyond this point. No obviously abnormal data have been included,

but the results should be used with caution. The variation in average maximum temperature with insulation is quite limited, indicating that 0.25-in. inside the clinker generally shielded the thermocouple adequately from outside influences. The burn rate depends markedly on insulation, while internal temperatures do not. The uninsulated burning in this study was not as successful as that reported in reference 7, perhaps because this work was done in a hood where the airflow may have produced appreciable cooling or because of some unexplained variation in components.

Table 25.3 *Effect of insulation on chlorate candle burning.*

COBALT, %	CATALYST, %	INSULATION	BURN RATE, mm/sec	MAXIMUM INTERNAL TEMPERATURE, °C
5	0	NONE	(0.08)	(640)
5	0	PARTIAL	(0.11)	(640)
5	0	COMPLETE	0.21	670
5	3	NONE	(0.17)	(540)
5	3	PARTIAL	0.20	600
5	3	COMPLETE	0.34	640

The trend of maximum temperature with fuel concentration is tabulated in table 25.4 for candles containing 3 percent catalyst. Temperatures are slightly lower than the uncatalyzed candles of table 25.2. As before, the low temperatures below 500° C are probably not reliable because of incomplete burning. The internal temperatures with higher fuel concentrations indicate heat losses and possibly incomplete combustion, as before. Burning proceeds steadily with less fuel when catalyst is used. Since the heat of combustion of the fuel in typical commercial candles is about equal to that generated by the chlorate decomposition, savings of up to a factor of 2 are anticipated with catalyzed candles containing minimal fuel. Quantitative calorimetric measurements are needed in addition to the internal temperatures to accurately determine the savings. Calorimetric data also contribute significantly in the design of an insulated container.

Table 25.4 *Effect of fuel concentration on chlorate candle burning.*

COBALT, %	CATALYST, %	BURN RATE, mm/sec	MAXIMUM INTERNAL TEMPERATURE, °C
0	3	(0.19)	(480)
1	3	(0.25)	(490)
3	3	0.36	560
5	3	0.34	640

PURITY OF GENERATED GAS

There is a definite correlation between burn temperature and the amount of impurities produced. All segments had a slight aerosol of sodium chloride particles in the effluent oxygen (based on visual observations). Few quantitative measurements have been made of these solids, but their volume clearly is far less than that of the smoky gas from the few iron-fueled commercial candles tested, which burned at higher temperatures. All experimental compositions produced detectable amounts of chlorine, and the chlorine odor increased with temperature. Additional heating of candle clinkers with a torch increased the amount of chlorine, also indicating the effect of high temperature on contaminant production. The chlorine contamination will not be reported until an absolute calibration is performed for the mass spectrometer used for the most precise purity measurements. The reactivity of chlorine is apparently so great that low measured values are suspected.

Results of mass spectrographic analyses of three formulations—a high temperature starter with 35 percent cobalt and no catalyst; a 5 percent cobalt, 3 percent catalyst composition with a starter section; and a no-fuel, 9 percent catalyst segment made without a starter—are given in table 25.5. The 1110° C starter produces 95 ppm of carbon monoxide and the no-fuel, no-starter segment only

1 ppm of carbon monoxide. The other segment showed 13 ppm of carbon monoxide, most of which probably came from the starter material. The carbon dioxide measurements indicate probable complete combustion of the carbon impurities in the candles. Total carbon calculated from chemical assays of the ingredients ranges from 0.018 to 0.025 percent. The greater variation of 100 to 2500 ppm carbon dioxide in the mass spectrographic analyses is largely due to the low yield of total gas from the fuel rich starter; most of the oxygen produced is consumed in combustion of the fuel, increasing the concentration of a given quantity of impurities. Thus it is important to keep total carbon content low to limit carbon dioxide contamination, and to have a candle formulation burning at a low temperature to minimize the more toxic carbon monoxide contamination. Minimizing fuel also increases the total yield of oxygen and decreases the concentration of contaminants.

Table 25.5 *Mass spectrographic measurements of gaseous contaminants in oxygen generated by chlorate candles.*

COMPOUND	STARTER (35% Co) ppm	(A) 5% Co 3% CATALYST ppm	(B) 0% Co 9% CATALYST ppm
CARBON MONOXIDE	95	13	1
CARBON DIOXIDE	2500	100	170
METHANE	< 7	< 7	< 1
ETHANE	< 0.5	0.4	0.02
ACETYLENE	< 0.05	< 0.02	< 0.01
ETHYLENE	< 0.02	< 0.02	< 0.01
C_3 AND HIGHER HYDROCARBONS	17	< 0.2	< 0.1
NITROUS OXIDES	< 0.05	< 0.05	< 0.1
HALOGENATED COMPOUNDS	< 0.05	< 0.1	< 0.1
SULFUR DIOXIDE	< 0.02	< 0.01	< 0.01
HYDROGEN CHLORIDE	< 0.02	< 0.09	< 0.01
CARBONYL SULFIDE	< 0.01	< 0.01	< 0.01
CARBON DISULFIDE	< 0.01	< 0.01	< 0.01
HYDROGEN	< 20	< 20	< 20
METHYL CHLORIDE	—	—	0.04
CHLORINE	PRESENT*	PRESENT*	PRESENT*

*MEASUREMENTS OF REACTIVE GASES CONSIDERED UNRELIABLE
(A) 6 gm STARTER AND 30 gm BODY
(B) 36 gm BODY - NO STARTER

The only other considerable contaminant is 17 ppm of higher hydrocarbons from the high temperature starter. This observation underscores the efficacy of high purity ingredients and low decomposition temperatures in keeping dangerous gases to tolerable limits. Dryness of the chemicals has not completely eliminated the annoyance of chlorine odor, and use of a suppressor is probably better than further efforts at purifying candle segment ingredients.

Much confusion has arisen in the past over acceptable levels of contaminants in breathing oxygen. Toxicity is an important criterion in setting limits, but other factors such as explosive mixtures and objectionable odors also need consideration. Physiological tolerances in short duration emergency oxygen supplies can be less stringent than those applied to continuous long-term supplies, while physical safety factors may be greater if the emergency supplies are to be used in extreme environments such as firefighting. Purity specifications derived for one intended use often cannot satisfactorily be applied to other situations without modification.

The specifications listed in table 25.6 illustrate some of the foregoing points. The portable environmental control system (PECS) requirements taken from reference 7 are quite stringent and seem to be based on out-gassing limitations for closed systems. The carbon dioxide and carbon monoxide values of 5 ppm for PECS are easily obtainable in compressed gas from liquid air plants, so it is perhaps reasonable (and economically feasible) to specify this purity for tank oxygen. The carbon dioxide limit can be increased by a factor of 100 without physiological harm, so it is not reasonable to apply the same standards to chemical oxygen sources for use in open-loop systems, for example, without some consideration of the economics and the complexity of design. Other partial specifications are also listed in table 25.6 for guidance in potential applications of chlorate candle oxygen generators. Reference 11 gives a more extensive list with some discussion of the relative importance of various potential contaminants. It does not seem appropriate to select arbitrary purity standards at this stage of development of this candle. Some filtering is necessary with present formulations, and gas scrubbing or the equivalent is needed in closed-loop systems to maintain carbon dioxide and water vapor within physiologically acceptable limits. A good design

will balance the various factors to optimize the intended use, rather than work to arbitrary limits.

CONCLUSIONS

Appropriate catalysts can lower the effective decomposition temperature of sodium chlorate to near its melting point, permitting major improvements in the design of conventional chlorate candles. This has been verified by the complete burning of units made without fuel, using two different batches of cobalt oxide catalyst. Even more dramatic has been the initiation of the decomposition with a hot wire igniter without using high fuel starter material. Each of a set of five candles was successfully ignited with about 10 W of low voltage power. Combustion was too slow in the laboratory model for practical use as an emergency supply. However, it is a straightforward matter to substitute catalyst for most if not all the fuel in a conventional starter cone and greatly reduce the contaminant levels while obtaining a fast start.

Table 25.6 *Some breathing oxygen specifications giving limits for certain contaminants.*

CONSTITUENTS	ALLOWABLE LEVEL IN ppm BY VOLUME		
	PECS (A)	SAE (B)	NAS/NRC (C)
ACETYLENE, C_2H_2	0.02		6000
CARBON DIOXIDE, CO_2	5.0	1000	5000
CARBON MONOXIDE, CO	5.0	25	15
HYDROCARBONS (C_3H_3 AND HIGHER)	1.0§		*
ETHANE, C_2H_6	2.0		*
ETHYLENE, C_2H_4	0.2		*
HALOGENATED COMPOUNDS	0.1		VARIED
METHANE, CH_4	25.0		13,000
NITROUS OXIDE, N_2O	1.0		

§HEXANE EQUIVALENT
*ALIPHATIC HYDROCARBONS 60 mg/m³, AROMATIC HYDROCARBONS 10 mg/m³ (BENZENE 3 mg/m³)
(A) REFS 7 AND 9 (B) REFS 9 AND 10 (C) REF. 11, 90-DAY EXPOSURE LIMIT FOR SPACE CABINS OR SUBMARINES

The catalytic effect of cobalt powder on chlorate decomposition has been confirmed. Catalysis is enhanced by oxidation of the metal during burning. Catalysts other than cobalt compounds should also be effective; the complete elimination of fuel has shown that the oxidation of cobalt during decomposition is not a vital factor in the improved performance of catalyzed candles.

Additional work is being done on control of the oxygen production rate. This is a complex function depending on the heat consumed in melting the chlorate, the rate of heat loss to the container and from it to the surroundings, the contact between the catalyst and chlorate, candle composition, and other factors. The design of the container has a considerable influence on the burn rate and is an important factor in the design and production of a practical candle unit.

Gas purity has been improved considerably with the catalyzed compositions having lower decomposition temperatures. No further efforts are planned at present to improve oxygen purity, as burn rate could be affected adversely if only gas purity were stressed.

Other applications of the catalyzed chlorate composition are apparent. The increased reaction rate should be quite useful in units with cold start requirements. The amount of catalyst can be varied if nonuniform burn profiles are desired. Effective modulation of the burn rate is much closer to realization, and unconventional designs using a catalyst in chlorate oxygen generators now appear practical.

REFERENCES

1. Schecter, W. H. and Miller, R. R.: Chlorate Candles as a Source of Oxygen. Ind. and Eng. Chem., vol. 42, 1950, p. 2348.
2. Thompson, Edward B., Jr.: Test of State-of-the-Technology Solid Chemical Oxygen Generators for Aircraft Application. AFFDL-TM-70-7-FEE, Oct. 1970.
3. Markowitz, M. W.; Boryta, D. A.; and Stewart, H., Jr.: J. Phys. Chem., vol. 68, 1964, p. 2282.

4. Mellor, J. W.: Comprehensive Treatise on Inorganic and Theoretical Chemistry, vol. II. Longmans, Green and Co., New York, 1922.
5. Gustafson, P. R.; Smith, S. H., Jr.; and Miller, R. R.: Chlorate-Candle Fabrication by Hot Pressing. NRL Report 5732, Jan. 23, 1962.
6. Musik, J. K.; and Gustafson, P. R.: Chlorate Candles. NRL Report 5814, Aug. 29, 1962, p. 35.
7. Littman, Jack; and Prince, R. Norman: Research on Sodium Chlorate Candles for the Storage and Supply of Oxygen for Space Exploration. NASA SP-234, 1970, pp. 291-330.
8. Wydeven, T.: J. Catalysis, vol. 19, 1970, p. 162.
9. Anon.: Development of Sodium Chlorate Candles for the Storage and Supply of Oxygen for Space Exploration Applications. Rept. 69-4695, AiResearch Manufacturing Co., July 18, 1962.
10. Anon.: Proposed AIR on Chemical Oxygen (Solid State) Systems. Project A-10-13, Soc. Automotive Engr., 1968.
11. Anon.: Atmospheric Contaminants in Spacecraft. Report of the Panel on Air Standards for Manual Space Flight, Space Sciences Board, Natl. Acad. Sci., Washington D.C., Oct. 1968.

26

AN EMERGENCY SURVIVAL SUIT

Daniel L. Curtis
Mechanics Research, Inc.

INTRODUCTION

This paper describes a thermally insulative garment designed specifically as a lightweight, low stowage volume emergency suit for subzero weather survival. The insulating principal employed can be applied to many other thermal applications.

The primary design objective was to construct a minimum weight, insulative garment capable of providing thermal protection for sedentary metabolic rates of 450 Btu/hr, with an environmental temperature of -40° F. It was intended that the garment be stored as a part of a survival kit, or as a piece of emergency cold weather gear for motorists in the northern portions of the country.

DESIGN CONFIGURATION

Testing confirmed that the inflating suit design satisfies the objectives for a subject standing at rest with environmental temperatures down to -45° F. The garment weighs 11 oz excluding the weight of the inflating-gas source. Initially, the use of lung power or a small hand pump was planned for filling the suit walls. This would have resulted in an 11 ounce system with a stored voluem of approximately 30 cu in. However, a small, compressed-gas source was introduced to provide for rapid inflation. This addition increased the total system weight to about 2-1/2 lb.

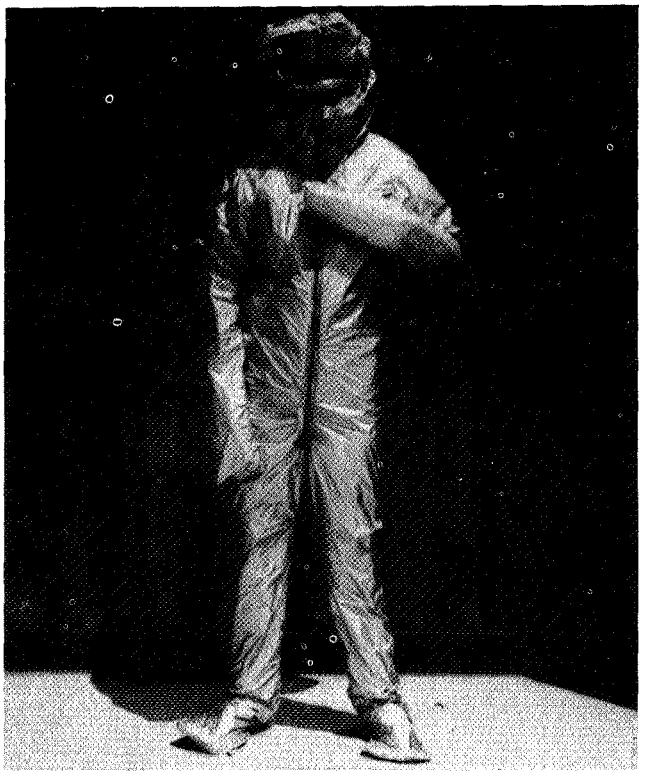

Figure 26.1 *Emergency survival suit.*

Figure 26.1 shows a photograph of the suit being worn for the cold room test. As shown, the garment is a form of superinsulator composed of multilayer, aluminized plastic. Specifically, the suit is constructed of three layers of aluminized polyethelyne with the edges sealed for suit-wall inflation. It is donned in the same manner as coveralls with a zipper down the front. The zipper serves both as the suit closure device and as the means of adjusting suit heat loss. The wearer simply opens the zipper if he becomes too warm.

The suit completely covers the body, including the hands and the head. For simplicity, an extension of the sleeves

surrounds the hands. A head covering and viewing visor are also included. However, for future models, the visor will probably be replaced with an open slit in the covering to prevent internal fogging.

DESIGN CALCULATIONS

Figure 26.2 shows the suit wall model used for radiation and conduction calculations. Boundary condition temperatures were -40° F for the exterior surface and 80° F for the interior surface.

Radiation heat transfer was computed using an emittance value of 0.2, characteristic of polyethylene aluminized on only one surface. The surface area of the garment was estimated to be 20 ft^2. For these conditions, the heat loss by radiation is approximately 210 Btu/hr. A lower value could be obtained by introducing double surface aluminization of the polyethylene. A single surface was used for the prototype suit, because this was the only material available at that time.

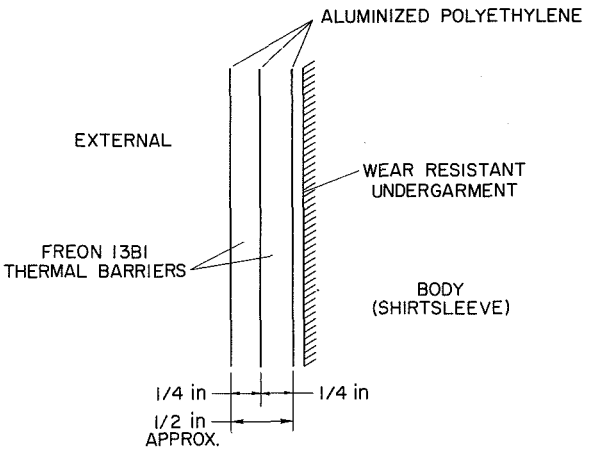

Figure 26.2 *Garment cross section.*

Heat loss also occurs by conduction through the garment wall. In space, this term is quite small for a superinsulator because of the vacuum-inner-space between the aluminized surfaces. For the 1 atm condition, however, it is necessary to fill the suit inner space with a gas, which increases wall conduction. Convection is considered negligible because the close spacing of the suit walls prevents appreciable gas circulation within.

Designing for air as the insulating gas with a suit conduction heat loss equal to one half the total allowable (100 Btu/hr for the -40° F condition), requires an inflated suit thickness of about 1.1 in. Inflating the suit to this thickness is considered practical. However, a better alternative is the use of another gas with better thermal insulative properties. This permits a thinner suit wall.

The gases that were considered are shown in figure 26.3, with thermal conductivities plotted as a function of molecular weight. As a general rule, the greater the molecular weight, the lower the conductivity value. Hydrogen and helium are also shown for comparison. The most favorable gas was found to be Freon 13B1, which is relatively inexpensive and is used for fire fighting because of its inertness and comparatively high density.

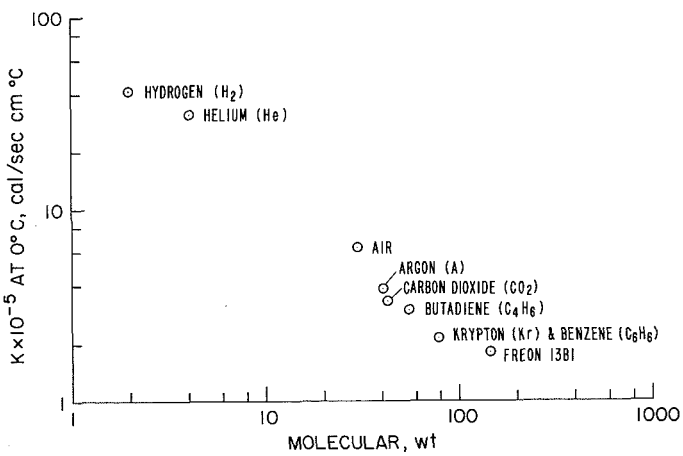

Figure 26.3 *Thermal conductivity of various gases as a function of molecular weight.*

Compared to air, Freon 13B1 is more than twice as good an insulator. In addition, it has a liquification temperature of -70° F, which provides an ample safety margin for a system designed for a minimum environmental temperature of -40° F. With Freon 13B1, the required inflated suit wall thickness is 0.5 in. This provides for a conduction heat loss of 240 Btu/hr. The total calculated heat loss is

then 450 Btu/hr for the conditions given. Respiratory heat loss is also included for a total heat balance. The sensible heat loss resulting from breathing 40° F air is about 40 Btu/hr for the sedentary condition. An additional 30 Btu/hr is lost through the latent heat for vaporizing lung moisture. Carbon dioxide was also considered because it is a better insulator than air, and it is readily available in small, high pressure vessels.

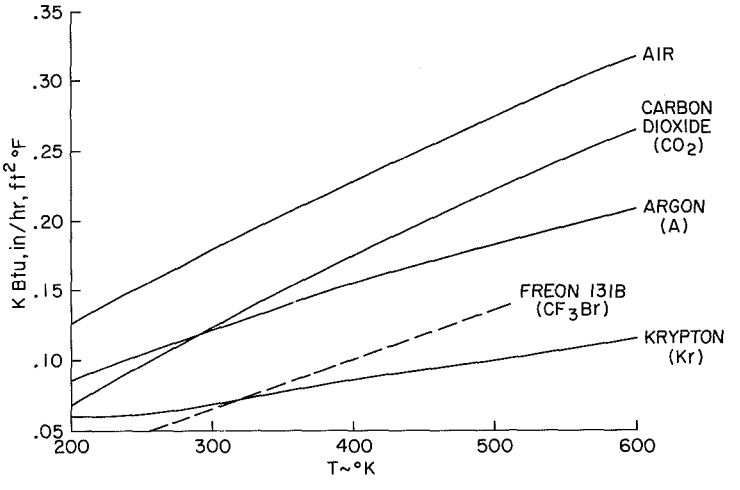

Figure 26.4 *Thermal conductivity of various heavy gases and air.*

Figure 26.4 shows a plot of thermal conductivities for various gases as a function of temperature. In the temperature range from -40° F to normal body temperatures, the conductivity of the Freon is approximately 0.05 Btu-in/hr-ft^2-°F.

TESTING

A cold room with a liquid nitrogen cooling source was used for testing. The test subject wore a short-sleeved shirt, slacks, and socks without shoes. He stood in a small insulated enclosure approximately 3 X 3 X 6 ft with a thick piece of foam plastic on the floor. The foam simulated insulating shoes that would be incorporated into the final design. The enclosure was cooled by a liquid nitrogen baffle and a large air circulating fan mounted directly in front of the subject. During the test, it was necessary to exhaust the cold, vaporized nitrogen directly into the cabinet to attain the coldest air temperatures. The cabinet was inclosed to minimize heat loss to the lab environment, with a fresh air duct used during the latter portion of the test to facilitate breathing. Air temperature was measured with an iron-constantan thermocouple and a Leeds and Northrup potentiometer. The thermocouple was placed in front of the fan next to the test subject.

The garment without Freon was found to be a satisfactory insulator down to about 10° F. At approximately this air temperature, the test subject began to feel cold, and the Freon was introduced. The coldness soon disappeared and test subject again began to feel comfortable. The temperature was then lowered to - 20° F. The test subject was comfortable except for his hand that was holding the air duct. Also, the elbow became somewhat cold because in the bent position it created a thermal short through the radiation shields in the area of the bend. By alternately using the other hand to hold the breathing duct, the previously cold region became warm as soon as the insulation was restored.

The temperature was then lowered to -40° F and held for 15 min. Temperature was then reduced to -45° F for an additional 15 min. At this temperature the test subject's hands and elbows became quite cold where thermal shorts occurred. The subject noted that his toes were also cold, and with shirt sleeves, that his bare arms were cool. He mentioned that a sweater would have made him more comfortable. However, he reiterated that the rest of his body was comfortable. He felt the test could have continued much longer, and perhaps indefinitely, had he been wearing shoes, and had he not had to grip the breathing duct with his hands.

CONCLUSION

The test subject had been in an environment corresponding to a moderate wind at a temperature of -20° F, or lower, for more than an hour with 0.5 hour of this time at or below -40° F. The test was considered a success with the results showing the technical feasibility of the design approach.

27

AN ALTITUDE CHAMBER RESCUE ENSEMBLE

Russell P. Lloyd, Engineering Division
Support Operations Directorate, KSC, NASA

INTRODUCTION

The John F. Kennedy Space Center of the National Aeronautics and Space Administration is responsible for the launching of the Apollo space vehicles. One phase of the preflight checkout of these vehicles is the altitude chamber testing of the command/service modules (CSM) and the lunar module (LM). A portion of the altitude chamber tests are accomplished with the astronaut crews in the spacecraft. The fact that the astronauts are in the spacecraft at a simulated altitude of above 200,000 ft requires that a rescue team be provided in the event of an accident in the spacecraft. The rescue crew is stationed in an airlock maintained at an altitude of 18,000 ft. A protective ensemble therefore is needed that will provide the rescue crew with life support capabilities, communications, and protection in the event of an emergency. In the event of an emergency, repressurization of the chamber is initiated; as the chamber descends, the airlock ascends and the two meet at 25,000 ft. This phase of the emergency repressurization takes less than 30 sec. Each rescue team is allowed to remain at the 18,000 ft altitude for only 4 hr; therefore, 2 or 3 rescue teams may be utilized during the usual 10 to 12 hr spacecraft test.

HISTORY

At the initiation of the Apollo program the only equipment KSC had for the rescue ensemble consisted of some gear from the Mercury program; all Gemini program altitude testing had been done at the manufacturer's plant. The first manned altitude testing of Apollo hardware was CSM-012, which was to have flown on Apollo 1—the flight that was prevented by the disastrous fire on Launch Complex 34 in January 1967. When the chamber testing was accomplished on this spacecraft, a final ensemble configuration had not been selected; however, the following equipment was to be used (fig. 27.1):

1. Helmet, mask, regulator assembly.
2. Liquid oxygen backpack, ELSA.
3. Dacron coverall with conventional underwear.
4. Safety boots.
5. FM Handi Talki.

THE ELSA

The backpack shown in figure 27.1 is an early ELSA (environmental life support assembly), not yet fully qualified, which was used only as backup to a hose-line breathing system. This early ELSA, which uses a 3.5 liter dewar and provides 80 psig to a mask, was developed at KSC as an alternate to a similar backpack, which was too bulky and heavy owing to the use of a larger liquid oxygen dewar. This unit is essentially the same as that now used at KSC with some changes to reduce flammability and to increase reliability.

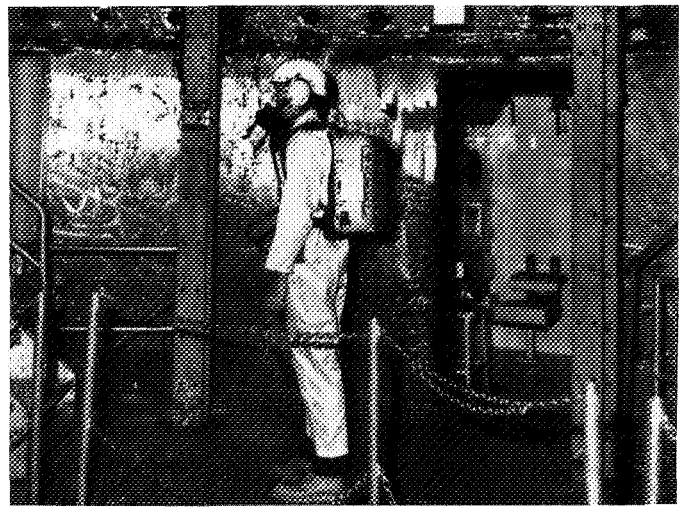

Figure 27.1 *The original rescue ensemble.*

The performance specifications for the ELSA are:

1. Liquid oxygen service.
2. Full weight not to exceed 25 lb.
3. Liquid oxygen capacity of 3.5 liters.
4. Ambient operating temperature of 50° to 90° F.
5. Gaseous oxygen temperature at the mask of 70° F ±20° F.
6. Normal operating pressure of 100 ±5 psig.
7. The unit must be operational through an operating pressure range of 50 to 155 psig.
8. Relief valve setting at 150 ±5 psig.
9. Standby time of 16 hr.
10. Operating altitude from sea level to 30,000 ft.
11. Oxygen flow rate to meet the following conditions:

Liters/ min	*Mask inlet temperature (° F)*	*Minimum time*	*System psig*	*Altitude ft*
15	70 ± 5	2.5 hr	80 ± 10	Sea level
25	60 ±5	30 min	80 ± 10	Sea level
45	50 (minimum)	5 min	70 ± 20	Sea level
15	70 ± 5	5 hr	80 ± 10	18,000
25	60 ± 5	1 hr	80 ± 10	18,000
45	50 (minimum)	15 min	70 ± 20	18,000

ELSA performance specifications today are the same as those originally given except that standby time has been reduced from 16 hr to 8 hr. The spacecraft tests at altitude are not as long as they were originally, thereby reducing the standby time required; furthermore, only new or newly overhauled dewars are suitable for the longer standby time—normal degradation of the dewar causes too great a loss of heat to maintain pressure below the relief valve setting.

The normal operating profile of the ELSA is 10 min at sea level, an ascent to 18,000 ft, and a normal stay time of just under 4 hr at that altitude, and a descent to sea level at 5,000 fpm. The activity of the personnel during this profile would be light. The heaviest demand on the ELSA would be during a rescue operation, which could take place at any time during the 4-hr stay at

18,000 ft. Under rescue conditions, the airlock is ascended to 25,000 ft in approximately 5 sec, after which there would be a high demand on the ELSA through the rescue, which takes 1-1/2 to 2 min, followed by, or in parallel with, a descent to sea level possibly as fast as 17,000 fpm.

The ELSA was qualified for operational use in early 1968 through a qualification program designed to demonstrate the units capabilities under both normal and extreme operating conditions. The qualification program included tests at altitudes up to 43,000 ft, tests at attitudes from 0 to 180° from vertical, and tests at flow rates of 15, 25, and 45 liters/min. Numerous tests combined the above variables under various planned and unplanned situations. These unmanned qualification tests were followed by a man-rating test in the altitude chamber, including a test to determine the actual useful capacity under normal operating conditions. The units lasted the required 5 hr with liquid to spare. It was extrapolated that the ELSA would last over 7 hr at 18,000 ft. Note that these tests were made with dewars capable of passing the 16-hr standby test; the overall operating time is reduced somewhat by a dewar having less efficient insulation.

Simplicity is a major factor in the reliability of the ELSA, which consists of a 3-1/2 liter dewar, heat exchanger coils, pressure control valves, and valves for filling and venting (fig. 27.2). The unit is filled by introducing liquid through the fill valve and out the vent valve; a minimum of 8.5 lb of liquid is put in the dewar. To put the ELSA into service, one simply opens the build-up valve, allowing the high pressure PCV (pressure closing valve) to maintain 100 psig on the liquid in the dewar. This pressure in turn forces liquid into the primary coil, and the low pressure PCV then controls the pressure in the secondary coil at 80 psig, which is the pressure supplied to the pressure-demand regulator in the helmet assembly. Figures 27.3, 27.4, and 27.5 show the ELSA construction.

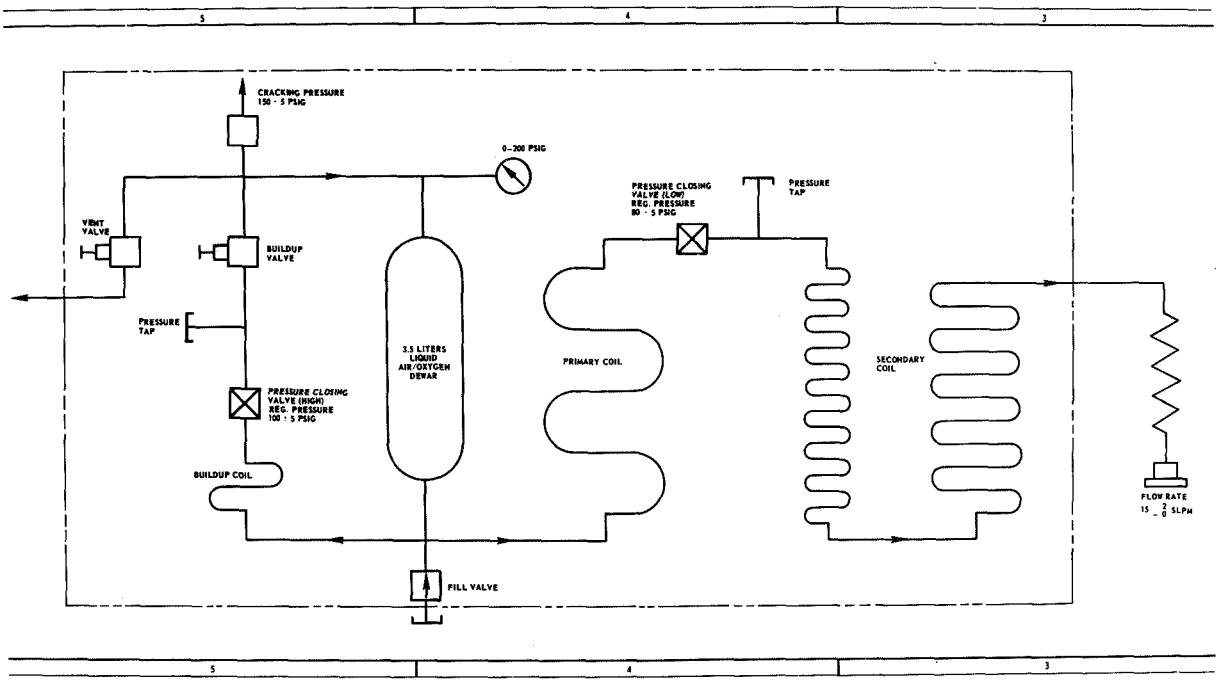

Figure 27.2 *ELSA schematic.*

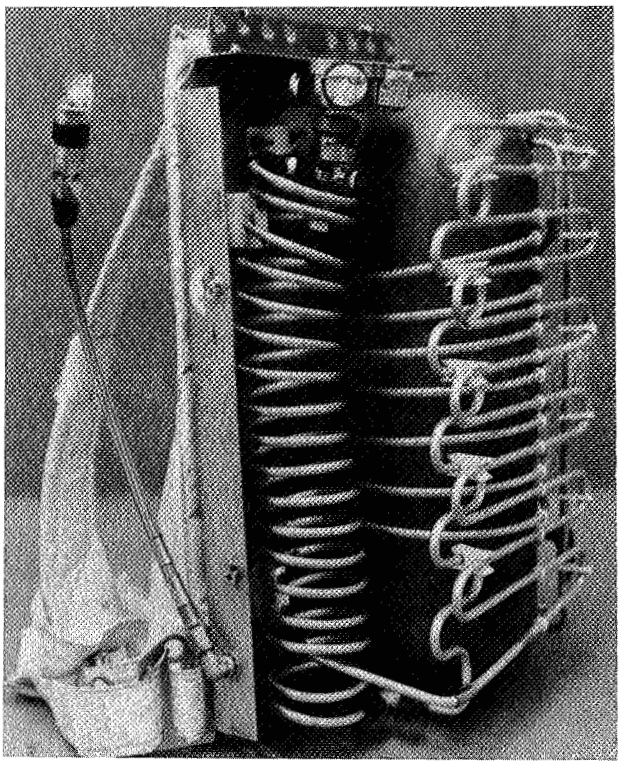

Figure 27.3 *Left side view of ELSA with cover removed.*

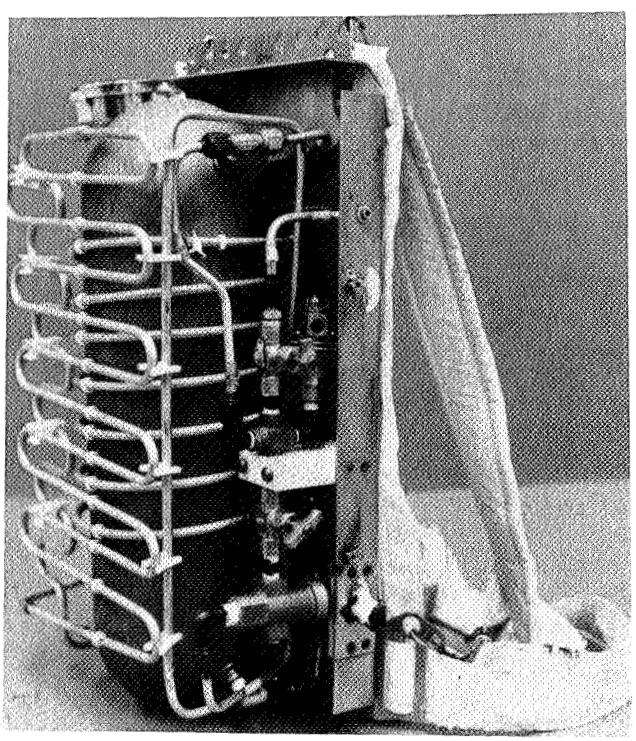

Figure 27.4 *Front view of ELSA with cover removed.*

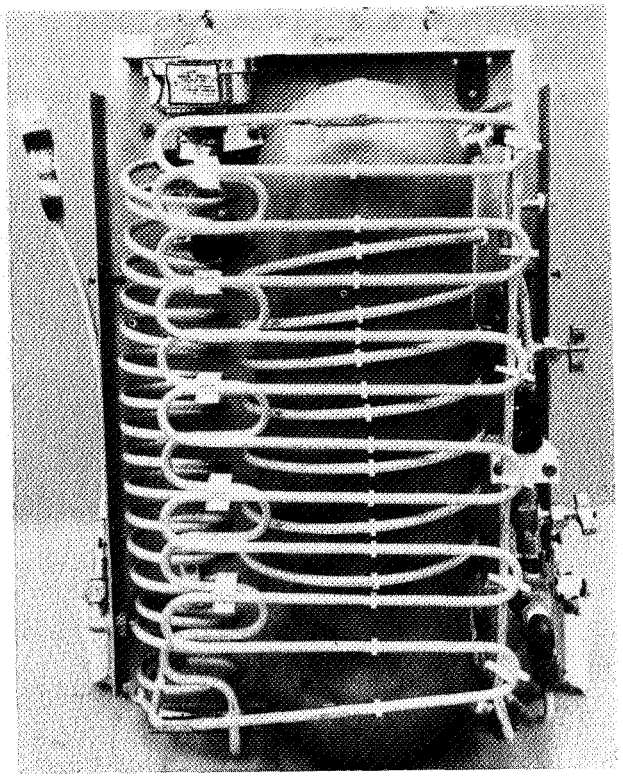

Figure 27.5 *Right side view of ELSA with cover removed.*

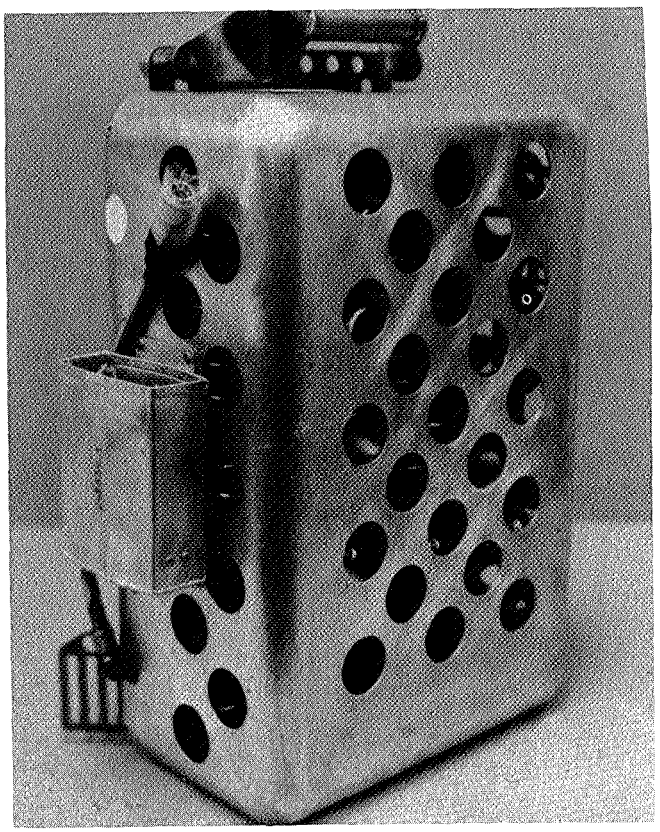

Figure 27.6 *ELSA*

THE PRESENT ENSEMBLE

Since 1966, the ELSA has been modified to remove the flammables, the case is now aluminum instead of plastic (fig. 27.6), and the harness is Beta cloth rather than nylon (fig. 27.7). The original dewars were replaced with dewars designed with superinsulation as a means of maintaining the 16 hr standby time. A problem with outgassing of the superinsulation, however, forced a return to dewars similar to the original ones.

The dacron coveralls have been replaced with a two-piece Beta cloth suit (fig. 27.8) over Roxel treated cotton long underwear. The original plan to use a Beta hood under the helmet proved unsatisfactory due to Beta fibers and any wrinkle in the hood caused discomfort.

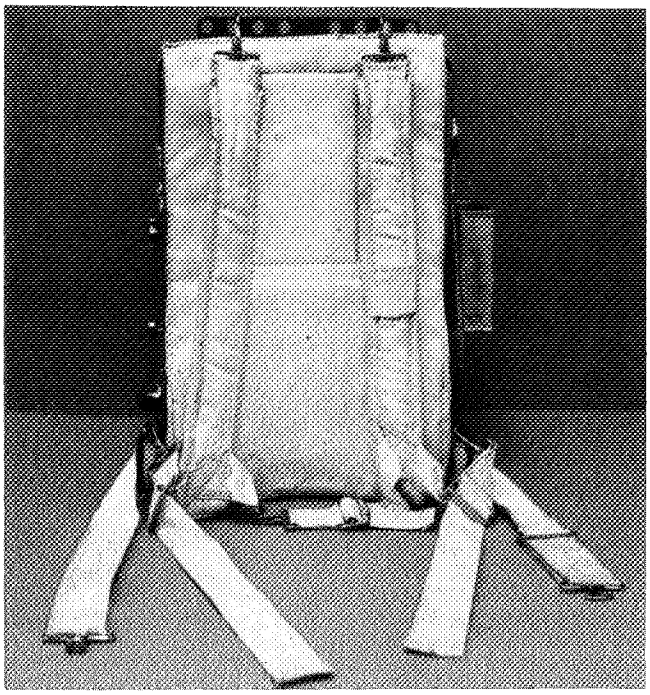

Figure 27.7 *ELSA Beta cloth harness.*

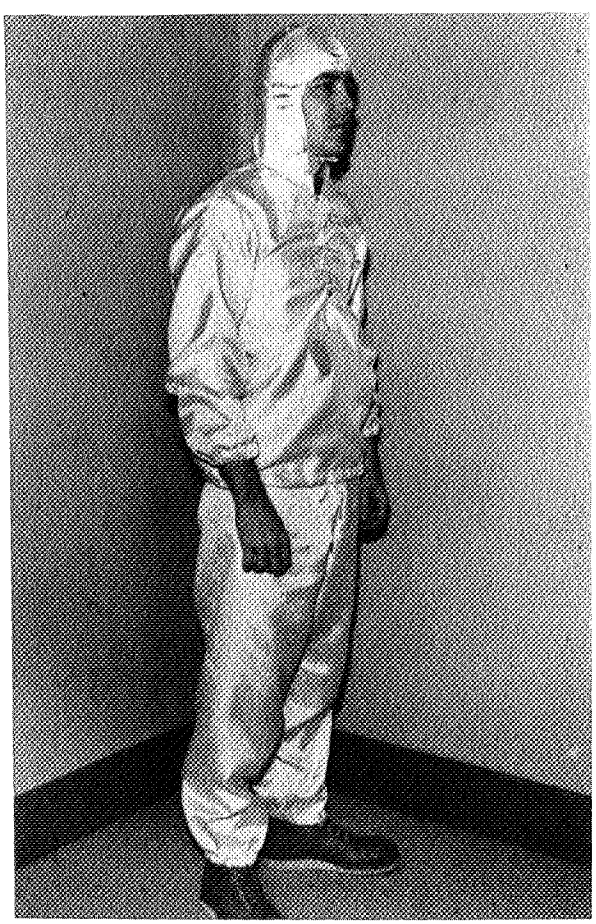

Figure 27.8 *Beta cloth rescue garment.*

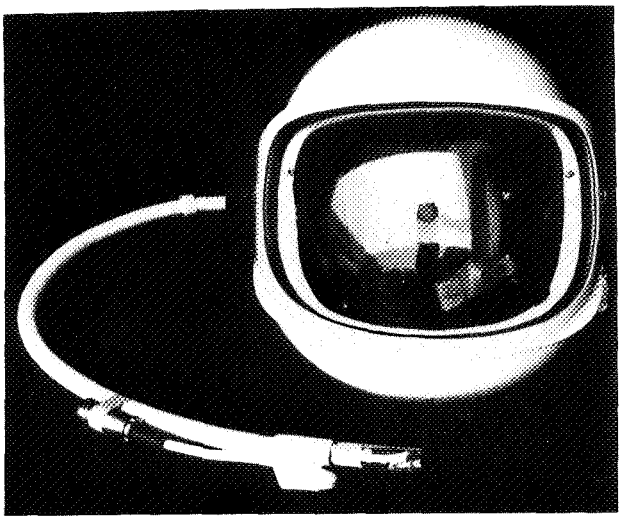

Figure 27.9 *Side view of Robertshaw helmet.*

The most recent change has been the replacement of the helmet, mask, and regulator assembly with a helmet (fig. 27.9 and 27.10) that incorporates all three into a single unit and provides eye protection from smoke and water in the event of fire in the chamber. Efforts to find goggles that would provide a smoke-tight seal with the old helmet and mask were unsuccessful.

The present ensemble consists of the following: (fig. 27.11, 27.12, and 27.13):

1. Full head helmet.
2. ELSA Mark II.
3. Beta cloth suit.
4, Safety boots.
5. FM Handi Talki.

The Kennedy Space Center's philosophy in equipping the altitude chamber rescue team has always been to give them total mobility and flexibility by eliminating the need for a link to the airlock facility itself for any life support function. Thus, they do not have to worry about dragging a long flex hose or having to disconnect from facility oxygen and work with a small, less reliable portable source. The rescue ensemble described here is believed to fulfill these objectives well.

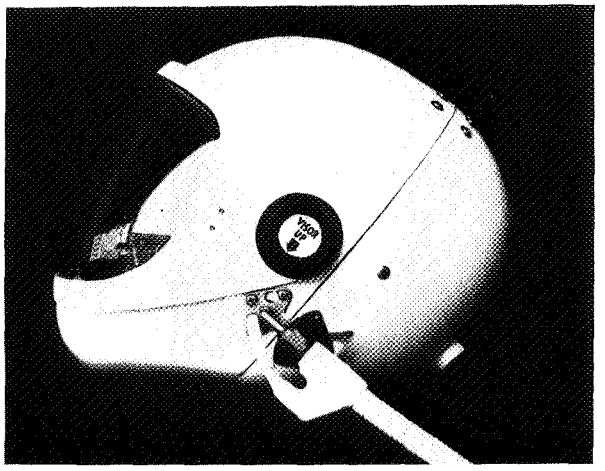

Figure 27.10 *Front view of Robertshaw helmet.*

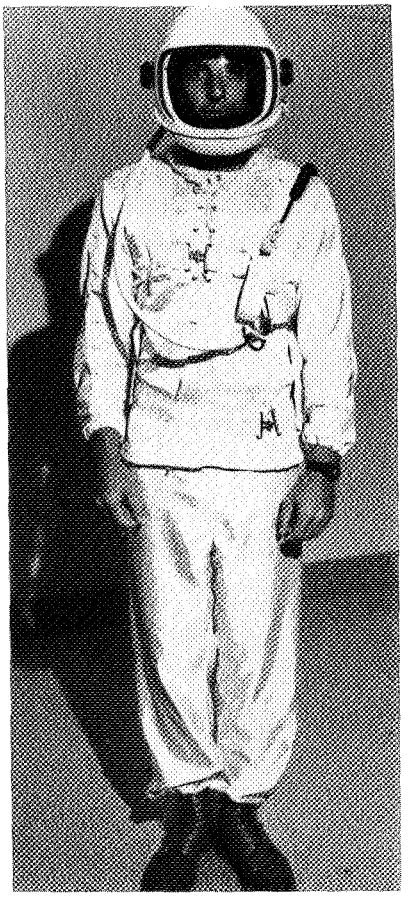

Figure 27.11 *Front view of present rescue ensemble.*

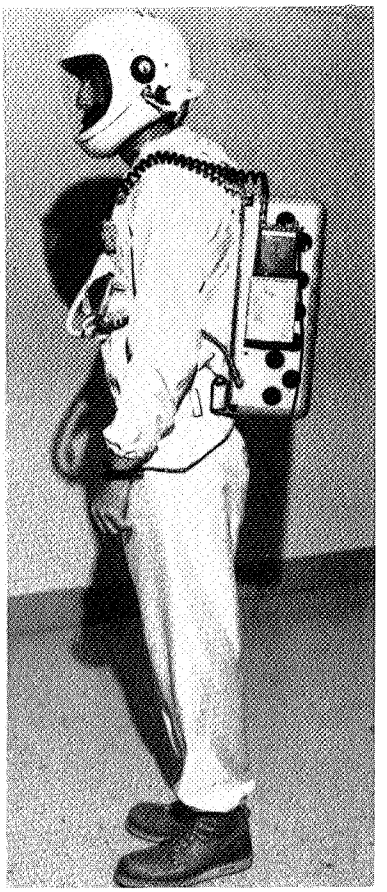

Figure 27.12 *Side view of present rescue ensemble.*

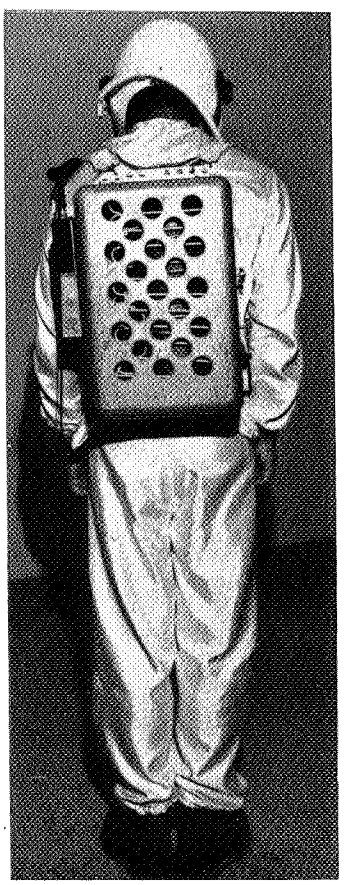

Figure 27.13 *Back view of present rescue ensemble.*

"The aeronautical and space activities of the United States shall be conducted so as to contribute . . . to the expansion of human knowledge of phenomena in the atmosphere and space. The Administration shall provide for the widest practicable and appropriate dissemination of information concerning its activities and the results thereof."

—NATIONAL AERONAUTICS AND SPACE ACT OF 1958

NASA SCIENTIFIC AND TECHNICAL PUBLICATIONS

TECHNICAL REPORTS: Scientific and technical information considered important, complete, and a lasting contribution to existing knowledge.

TECHNICAL NOTES: Information less broad in scope but nevertheless of importance as a contribution to existing knowledge.

TECHNICAL MEMORANDUMS: Information receiving limited distribution because of preliminary data, security classification, or other reasons.

CONTRACTOR REPORTS: Scientific and technical information generated under a NASA contract or grant and considered an important contribution to existing knowledge.

TECHNICAL TRANSLATIONS: Information published in a foreign language considered to merit NASA distribution in English.

SPECIAL PUBLICATIONS: Information derived from or of value to NASA activities. Publications include conference proceedings, monographs, data compilations, handbooks, sourcebooks, and special bibliographies.

TECHNOLOGY UTILIZATION PUBLICATIONS: Information on technology used by NASA that may be of particular interest in commercial and other non-aerospace applications. Publications include Tech Briefs, Technology Utilization Reports and Technology Surveys.

Details on the availability of these publications may be obtained from:

SCIENTIFIC AND TECHNICAL INFORMATION OFFICE

NATIONAL AERONAUTICS AND SPACE ADMINISTRATION

Washington, D.C. 20546